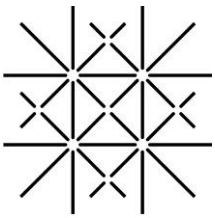

Ruthenium(II) complexes of amino-substituted polypyridine ligands:

Synthesis and photophysical studies with a potential application for molecular switches

Inauguraldissertation

zur

Erlangung der Würde eines Doktors der Philosophie

vorgelegt der

Philosophisch – Naturwissenschaftlichen Fakultät

der Universität Basel

von

Markéta Šmídková

aus der Tschechischen Republik

Basel, 2013

Genehmigt von der Philosophisch-Naturwissenschaftlichen Fakultät auf Antrag von:

Prof. Dr. Edwin C. Constable Prof. Dr. Oliver Wenger

Basel, den 17 September, 2013

Prof. Dr. Jörg Schibler

Dekan der Philosophisch-
Naturwissenschaftlichen Fakultät

creative commons

Namensnennung-Keine kommerzielle Nutzung-Keine Bearbeitung 2.5 Schweiz

---

Sie dürfen:

das Werk vervielfältigen, verbreiten und öffentlich zugänglich machen

Zu den folgenden Bedingungen:

Namensnennung. Sie müssen den Namen des Autors/Rechteinhabers in der von ihm festgelegten Weise nennen (wodurch aber nicht der Eindruck entstehen darf, Sie oder die Nutzung des Werkes durch Sie würden entlohnt).

Keine kommerzielle Nutzung. Dieses Werk darf nicht für kommerzielle Zwecke verwendet werden.

Keine Bearbeitung. Dieses Werk darf nicht bearbeitet oder in anderer Weise verändert werden.

- Im Falle einer Verbreitung müssen Sie anderen die Lizenzbedingungen, unter welche dieses Werk fällt, mitteilen. Am Einfachsten ist es, einen Link auf diese Seite einzubinden.
- Jede der vorgenannten Bedingungen kann aufgehoben werden, sofern Sie die Einwilligung des Rechteinhabers dazu erhalten.
- Diese Lizenz lässt die Urheberpersönlichkeitsrechte unberührt.

Die gesetzlichen Schranken des Urheberrechts bleiben hiervon unberührt.

Die Commons Deed ist eine Zusammenfassung des Lizenzvertrags in allgemeinverständlicher Sprache: http://creativecommons.org/licenses/by-nc-nd/2.5/ch/legalcode.de

Haftungsausschluss:
Die Commons Deed ist kein Lizenzvertrag. Sie ist lediglich ein Referenztext, der den zugrundeliegenden Lizenzvertrag übersichtlich und in allgemeinverständlicher Sprache wiedergibt. Die Deed selbst entfaltet keine juristische Wirkung und erscheint im eigentlichen Lizenzvertrag nicht. Creative Commons ist keine Rechtsanwaltsgesellschaft und leistet keine Rechtsberatung. Die Weitergabe und Verlinkung des Commons Deeds führt zu keinem Mandatsverhältnis.

Quelle: http://creativecommons.org/licenses/by-nc-nd/2.5/ch/ Datum: 3.4.2009

Acknowledgements

First of all, I would like to thank my supervisors, Prof. Dr. Edwin C. Constable and Prof. Dr. Catherine E. Housecroft, for giving me the opportunity to work and study in their research group, to broaden my knowledge in the field of inorganic and coordination chemistry under the guidance of such wonderful scientists, for creating an atmosphere that was both professional and familial, for being motivating and encouraging, as well as helpful and patient, not only in the tough beginnings after arriving from abroad, but also during the whole four years of my stay. My big thanks belong to the Swiss National Fond for sponsoring my stay in Switzerland and also all conferences. Then I would like to thank to Prof. Alberto Credi, University Bologna, and his photochemistry research group for giving me the opportunity to stay in their laboratories and learn from one of the top specialists. I am very grateful to Angelo Lanzilotto and Marek Oszajca for carrying out the photophysical studies of my complexes and teaching me in the process.

From the former and current members of the Constable-Housecroft group I would like to particularly thank Jon Beves for his great help when introducing me to my research topic. I would also like to thank Jason Price, Iain Wright, and Colin Martin for giving me answers to my many chemistry questions. I also thank all of my colleagues who measured MS spectra for me: Gabriel Schneider, Collin Morris, Sven Brauchli, Niamh Murray, Ralph Schmitt, Srba Vujovic, and Imenne Bouamaied, thanks also go to Jonas Schönle for measuring numerous QY and lifetimes in such a short time! Thanks to Colin Martin for teaching me NMR titrations. Thanks to Srba for being such a cool labmate all of the time, and a proud representative of the “Eastern-European minority” in our group. (I’m not, CZ is mid-Europe of course! ☺) Thanks to Cathrin Ertl for taking care of my “Calendar Boys” every month, and thanks to Steffen Müller for being great source of info whenever I needed to know something or find someone. Special thanks belong mainly to Prof. Catherine Housecroft, and also to Niamh Murray, Jennifer Zampese, Colin Martin, and Collin Morris for correcting this thesis.

Big thanks go to friends from the Czech-Slovak community in Switzerland for being around and also thanks to my family for care, support, and staying in touch even though I am far away. Finally, great thanks and admiration go to those few closest people who were and still are around to listen, to help, and to support me, no matter what I do.

Table of Contents

Summary

The goal of this PhD thesis is the synthesis and photophysical studies of new ruthenium(II) complexes of polypyridine ligands with a long amino-substituted side chain with a potential application for molecular switches.

Introduction a short summary of the chemical background and latest investigations on ruthenium(II) complexes of terpyridine ligands and their molecular switching properties.

Chapter 1 describes the synthesis and characterisation of precursors and substituted terpyridine ligands. In this chapter, the original approach of the synthesis of the ruthenium(II) complexes with the long amino-chain via trans-esterification is used.

Chapter 2 shows the synthetic strategy towards ruthenium(II) complexes with a side chain containing a triazole ring and a terminal amino group. Unfortunately such a ruthenium(II) complex was not successfully prepared. However, a useful application was found for its precursor, giving a new series of pytpy ligands with a side amino-chain linked via an ether.

Chapter 3 reports several synthetic strategies towards 4'-(4-pyridyl)-2,2':6',2''-terpyridine ligands with a side amino-chain linked via an ester.

Chapter 4 shows synthesis and characterisation of ruthenium(II) complexes with three or four protonation sites. A series of ruthenium(II) complexes with substituted 4'-phenyl-2,2':6',2''-terpyridine ligands was prepared for a comparison with the Ru(II) complexes bearing pendant pyridyl units.

Chapter 5 shows detailed photophysical properties of the ruthenium complexes from Chapter 4.

Chapter 6 reports acid and base NMR studies of ruthenium complexes and their free ligands with morpholino- and diethylamino-substituted side chains. These studies reveal and clarify that all the Ru(II) complexes with three or four protonation sites were synthesized and isolated already in the mono-protonated form - on the amino group of the side chain.

Chapter 7 describes synthesis and characterisation of pytpy ligands with short (3 and 5 carbon atoms) amino-substituted side chains. Numerous attempts to synthesize ruthenium(II) complexes of these ligands are reported. However, these led only to trace amounts of the desired products.

Conclusion summarises this PhD thesis, achieved results and outlook for further investigation of this topic.

Abbreviations

1D	one dimensional
2D	two dimensional
Ac	acetyl
Ar	aryl
°C	degree Celsius
C	complex
calc.	calculated
cat.	catalytic amount
cm	centimetre
COSY	homonuclear correlation spectroscopy
CV	cyclic voltammetry
D	deuterium
d_n	number of deuterium atoms in solvent
δ	chemical shift [ppm]
DEPT	Distortionless Enhancement by Polarization Transfer (NMR technique)
dm	decimetre
DMF	*N*,*N*-dimethylformamide
DMSO	dimethyl sulfoxide
dppf	1,1'-bis(diphenylphosphino)ferrocene
dppp	1,3-bis(diphenylphosphino)propane
EA	elemental analysis
eq	equivalent
ESI MS	electrospray ionization mass spectroscopy
Et	ethyl
et al.	et alii (and others, from Latin)
eV	electron Volt
Φ	quantum yield (in %), or also QY
g	gram

h	hour
HMBC	heteronuclear multiple bond correlation spectroscopy
HMQC	heteronuclear multiple quantum correlation spectroscopy
Hz	Hertz
IR	infrared spectroscopy (s - strong, m - medium, w - weak, br - broad bands)
J	coupling constant
L	ligand, or litre
λ_{abs}	absorption wavelength
λ_{em}	emission wavelength
λ_{ex}	excitation wavelength
λ_{iso}	*wavelength of the isosbestic point in the absorption spectra (titrations) used as* λ_{ex} during titrations
M	molecular mass, or concentration in mol*L^{-1}
MALDI-TOF	matrix assisted lased desorption/ionisation time of flight mass spectroscopy
Me	methyl
MHz	megahertz
mL	millilitre
MLCT	metal to ligand charge transfer
mmol	millimol
MP	melting point
mV	millivolt
MS	mass spectroscopy
μW	microwave
m/z	mass to charge
ν	frequency in cm^{-1}
nm	nanometre
NMR	nuclear magnetic resonance, signals: s –singlet, d – doublet, t –triplet, m – multiplet, dd – doublet of doublets, ddd – doublet of doublets of doublets, dt – doublet of triplets, td – triplet of doublets, br – broad signal
OTs	tosylate, p-toluenesulfonate
P	precursor

pH	logarithmic measure of the acidity or basicity of an aqueous solution, $\log_{10}(1/a_{H+})$, a_{H+} is the hydrogen ion activity in a solution
Ph	phenyl
p*K*	logarithmic measure of the acid dissociation constant *K*, $\log_{10}(1/K_a)$ (pK_a - water solution)
PPI	1-(2-oxo-2-(pyridin-2-yl)ethyl)pyridin-1-ium iodide, pyridinium iodide salt of 2-acetylpyridine
ppm	parts per million
Phtpy	4'-phenyl-2,2':6',2''-terpyridine
PTSA	p-toluenesulfonic acid
py	pyridine
pytpy	4'-(pyridin-4-yl)-2,2':6',2''-terpyridine
QY	quantum yield
R	alkyl
RT	room temperature
T [°C]	temperature (in degrees of Celsius)
τ	luminescence lifetime
TBAF	tetrabutylammonium fluoride
$TBAPF_6$	tetrabutylammonium hexafluorophosphate
TFA	trifluoroacetic acid
TFA-d	deuterated trifluoroacetic acid (CF_3COOD)
TfOD	deuterated trifluoromethanesulfonic acid (CF_3SO_3D)
THF	tetrahydrofuran
TLC	thin layer chromatography
TMS	trimethylsilyl group
tpy	2,2':6',2''-terpyridine
UV	ultraviolet light
V	volt
vis	visible
vol.	volume
wt%	weight %

Introduction

Ruthenium is a rare transition metal from the platinum group of the periodic table. Ruthenium forms a very wide range of complexes with oligopyridine ligands such as 2,2'-bipyridine (bpy), 1,10-phenanthroline (phen) or 2,2';6,6''-terpyridine (tpy). Terpyridine ligands are tridentate, have three nitrogen donor atoms with the metal coordinated in a perpendicular position to the central nitrogen donor. Ruthenium(II) complexes exhibit an octahedral molecular geometry (Figure 1).

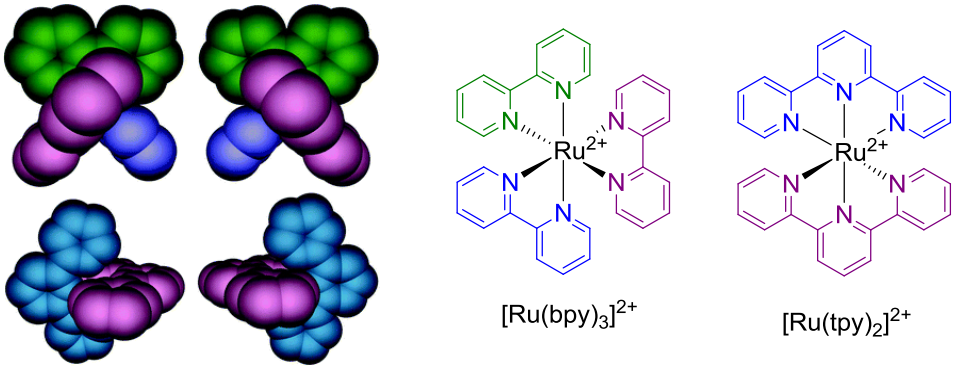

Figure 1: Octahedral ruthenium(II) complexes of bidentate ligands (bpy) and tridentate ligands (tpy)[1]

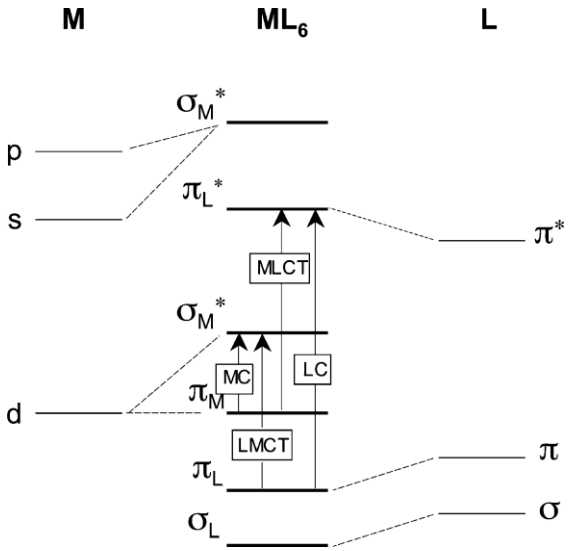

Figure 2: Molecular orbital diagram for octahedral transition metal complexes[2]

Figure 2 displays a molecular orbital diagram for octahedral complexes of transition metals. These contain different types of atomic orbitals: strongly bonding ligand-centred orbital σ_L, bonding ligand-centred orbital π_L, nonbonding metal-centred orbital π_M of t_{2g} symmetry, antibonding metal-centred orbital σ_M^* of e_g symmetry, antibonding ligand-centred orbital π_L^*, strongly antibonding metal-centred orbital σ_M^*. The excited configuration is obtained from the ground state by promoting one electron from occupied to vacant MOs. The arrows indicate the four types of transitions possible based on localized molecular orbital configurations. The transitions are of these types: metal-centred (MC), ligand-centred (LC), ligand-to-metal charge-transfer (LMCT) and metal-to-ligand charge-transfer (MLCT). For octahedral complexes containing Ru(II) (d^6) metal ion, the σ_L, and π_L orbitals are fully occupied and the ground-state configuration is closed-shell since the HOMO π_M $(t_{2g})^6$ is also completely occupied.[2]

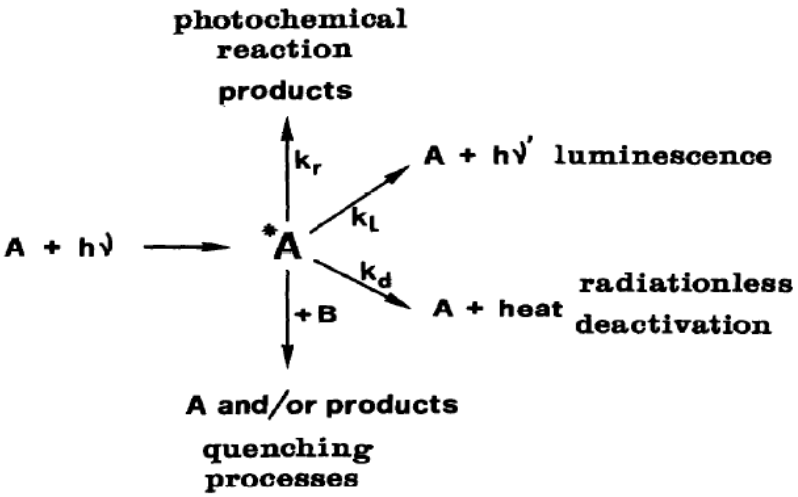

Figure 3: Excited state deactivation processes [3]

In photochemical and photophysical processes (Figure 3), a photon is absorbed by a molecule leading to the formation of an excited state. This exhibits high energy, which must undergo some type of deactivation, such as photochemical reaction, luminescence (light emission), radiationless deactivation (energy excess transform into heat) or quenching (interaction with other species).[3]

Figure 4 compares energy diagrams of $[Ru(bpy)_3]^{2+}$ and $[Ru(tpy)_2]^{2+}$ and explains why $[Ru(tpy)_2]^{2+}$ is not emissive compared to Ru(II) complexes of bpy ligands. $[Ru(bpy)_3]^{2+}$ absorbs electrons (forms the excited state), either through LC or MLCT transitions. Once the electron

density reaches the ^{3}LC or ^{3}MLCT levels, radiationless deactivation to the ^{3}MC (metal-centred) state can occur; however no emission is observed. Emission would be observed, if the decay passed from the ^{3}MLCT to the ground state. This depends on the energy gap (ΔE) between the ^{3}MC or ^{3}MLCT levels. The ^{3}MC level of $[Ru(tpy)_2]^{2+}$ is located below the ^{3}MLCT state, therefore radiationless decay to the ^{3}MC is preferable and as a result $[Ru(tpy)_2]^{2+}$ is not emissive.

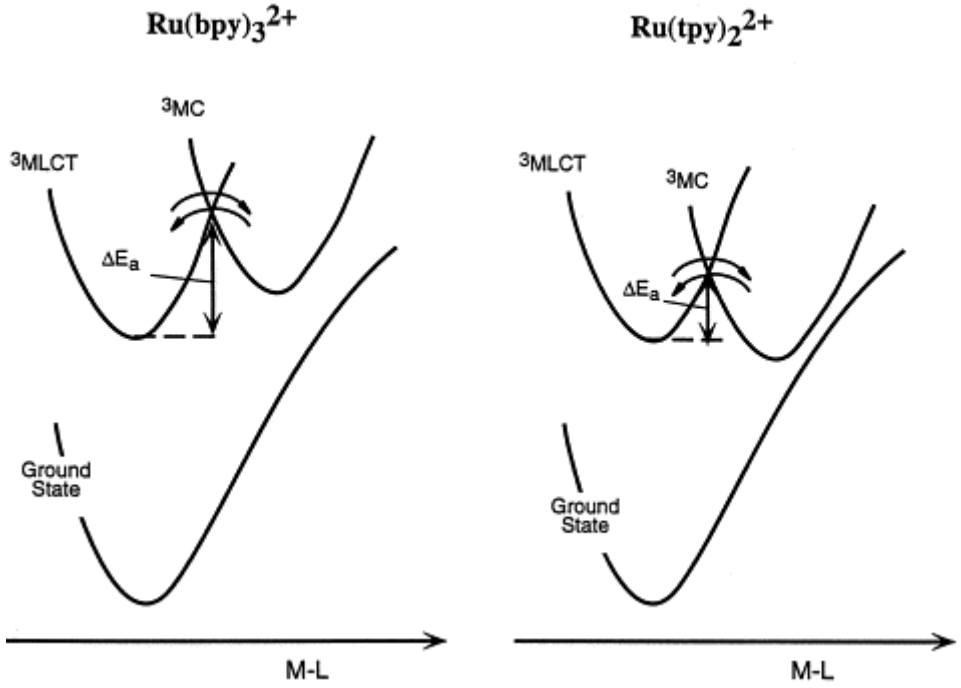

Figure 4: Energy diagrams for $[Ru(bpy)_3]^{2+}$ and $[Ru(tpy)_2]^{2+}$ [2]

However, once the tpy unit is substituted in the 4'-position with an appropriate functional group (such as pyridyl unit), the ^{3}MC level can be shifted in a preferred way. As such Ru(II) complexes $[Ru(pytpy)_2]^{2+}$ are emissive.[4] Each pendant pyridyl position of $[Ru(pytpy)_2]^{2+}$ has a basic nitrogen atom which can be protonated. Therefore, this complex can exist in 3 different protonation states. Furthermore, it was observed that protonation of the pendant pyridyl unit significantly changes the photophysical properties of the Ru(II) complex.[6] Because upon protonation, the pyridyl substituent is changed to an electron-acceptor by lowering its π^* orbital.

The absorption spectrum of $[Ru(pytpy)_2]^{2+}$ consists of two intense bands (LC transitions) in the UV region and a broad moderately intense band in the visible region (^{1}MLCT transitions). Upon acid titration, the ^{1}MLCT band absorption maximum is red-shifted from 489 nm to 505

nm and the absorption intensity increases (bis-protonated form: $[Ru(Hpytpy)_2]^{4+}$). The luminescence spectrum of $[Ru(pytpy)_2]^{2+}$ consists of a low intensity band with an emission maximum at 655 nm (Figure 5). Upon titration this becomes significantly more intense and red shifts to 723 nm indicating formation of the mono-protonated form $[Ru(pytpy)(Hpytpy)]^{3+}$. With the second protonation, the emission intensity increases even more, however a slight blue-shift to 715 nm was observed. The first red-shift is due to the decrease in energy of the π^* orbital of the $(Hpytpy)^+$ unit which stabilises the MLCT levels. The small blue-shift in the second step is explained this way; in the mono-protonated form $[Ru(pytpy)(Hpytpy)]^{3+}$, the electron-accepting character of $(Hpytpy)^+$ is balanced by the enhanced electron-donating character of pytpy to the metal centre. However, such stabilization effects are not possible in the bis-protonated species, because both ligands are protonated.[4]

Certain organic molecules can exhibit properties of so called molecular switches, a functional molecular device which can work as a molecular logic-gate. A molecular switch converts input stimulations into an output signal under the principals of Boolean binary logic.[7, 8, 9] The most common Boolean functions are AND, OR, NOR, XOR, NAND, etc. (Table 1). A half adder is a combinatorial circuit, an ensemble of logic gates in which the output value depends on the 2 inputs.

In. 1	In. 2	Out. 1	Out. 2	Out. 3	Out. 4	Out. 5	Out. 6
0	0	0	0	1	1	0	1
1	0	0	1	1	0	1	0
0	1	0	1	1	0	1	0
1	1	1	1	0	0	0	1
		AND	**OR**	**NAND**	**NOR**	**XOR**	**XNOR**

Table 1: Truth tables of logic gates

Inherent properties of molecules, such as conformation, redox properties, pH sensitivity or photo-induced electron transfer, forms the input and output of such a molecular device. However, not only organic molecules can work this way, but coordination compounds can play a role as in design of such devices. Lately molecular switching properties of $[Ru(pytpy)_2][PF_6]_2$ have been reported.[5] The set consists of a reversible merocyanine-type

photoacid and this Ru(II) complex that works as a pH-controlled three-state luminescence switch. Upon application of light, the photo-acid releases a proton to control the state of the transition metal complex. These two molecular switching devices work together through the exchange of ionic signals and form an “optical-chemical-optical” double signal-transduction mechanism. Upon observing changes in the luminescence spectra for each of the protonation state of the Ru(II) complex, it is possible to construct logic gates (Figure 5). The proton aliquots form 2 inputs for the truth table, and upon setting threshold lines for a certain wavelength it is possible to perform the half-adder functions and obtain outputs. So then by setting the threshold line to 30% at 732 nm we obtain an OR gate, however for the threshold line at 70% at 732 nm we obtain an AND gate. The green threshold at 626 nm gave XNOR gate.

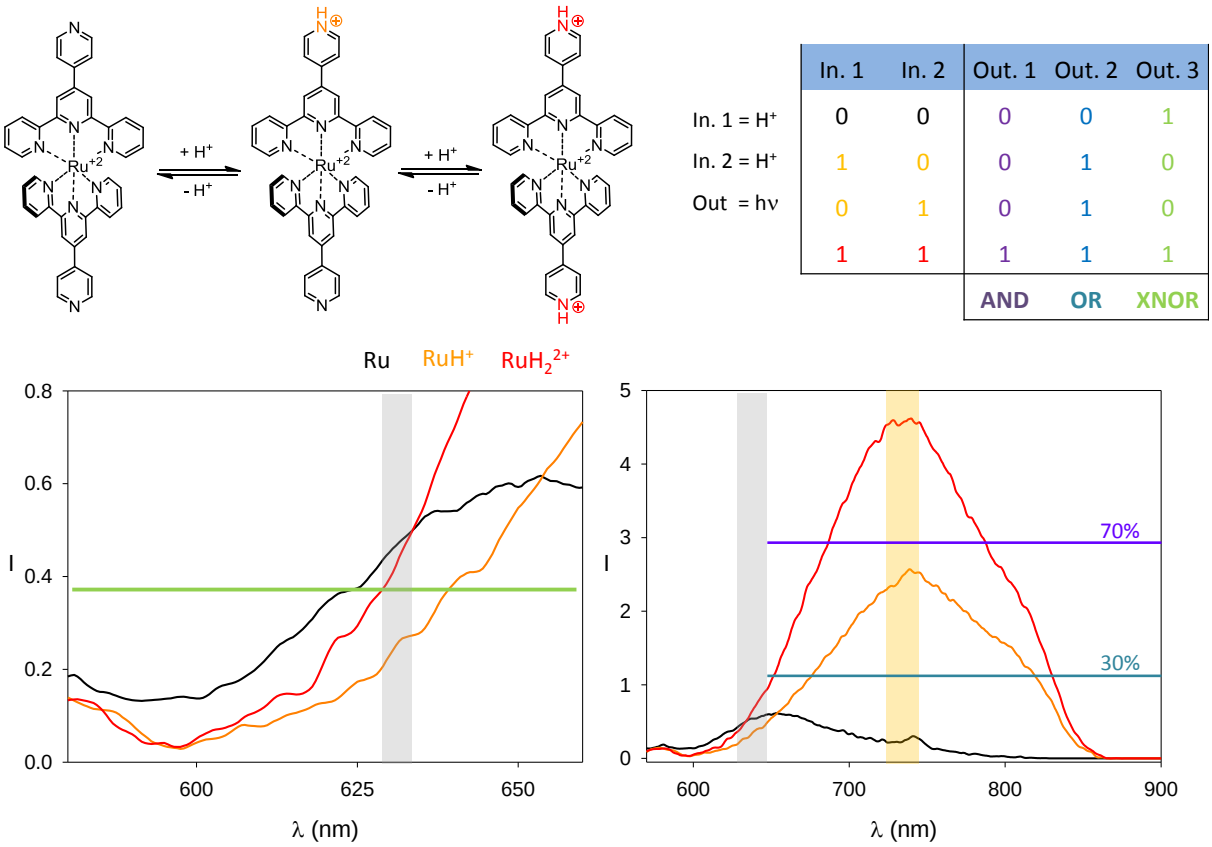

In. 1	In. 2	Out. 1	Out. 2	Out. 3
0	0	0	0	1
1	0	0	1	0
0	1	0	1	0
1	1	1	1	1
		AND	OR	XNOR

Figure 5: Ru(II) complex[Ru(pytpy)$_2$][PF$_6$]$_2$ and its protonated forms, luminescence spectra of the studied complexes, threshold and outputs lines indicated, truth tables for the constructed logic gates

After successful application of Ru(II) complex of the pytpy ligand as a molecular half-adder, we decided to expand on these results and construct a so called full-adder. This would mean

to add a third input to the truth table. This is possible, when such molecule would contain third protonation site. My former co-workers Jonathon Beves and Emma Dunphy designed such molecule and the goal of this thesis is to expand on the initial synthetic results, develop synthetic strategies towards such a ruthenium(II) complex and examine its photophysical properties (Figure 6). The original idea was to synthesize Ru(II) complexs containing pytpy ligands which have linked long side chains with dialkyl-substituted amino groups. The amino group attached to the side chain and the two pendant pyridyl groups bring to the molecule three protonation sites. In the Ru(II) complexes with long side chains (7-12 carbon atoms), there is the possibility of photo-induced electron transfer or proton transfer, intra-molecular via the chain or through space (between the pendant pyridyl unit and the amino group), respectively. However, the Ru(II) complexes with an appropriately short side chain will only have the option of photo-induced electron transfer via the chain (i.e. not through space as the chain is too short). Upon addition of acid aliquots, the side amino unit should be protonated first, followed by protonation of the pendant pyridyl units, allowing the observation of such a complex in 4 protonation states (neutral, mono-, bis- and tris-protonated).

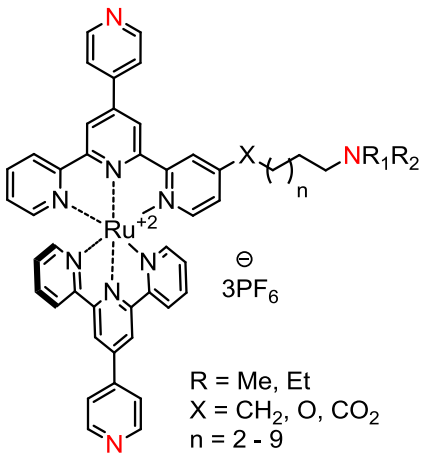

Figure 6: Proposed structure for a Ru(II) complex which would act as a molecular full-adder

Literature

1 Constable, E. C. *Chem. Soc. Rev.*, **2007**, *36*, 246-253.

2 Balzani, V.; Bergamini, G.; Campagna, S.; Puntoriero, F. *Photophysics of Coordination Compounds I*, Springer-Verlag Berlin, **2007**, pp. 280.

3 Balzani, V.; Juris, A.; Barigelleti, F.; Campagna, S.; Belser, P.; Von Zelewsky, A. *Coord. Chem. Rev.*, **1988**, *84*, 85-277.

4 Constable, E. C.; Housecroft, C. E.; Thompson, A. C.; Passaniti, P.; Silvi, S.; Maestri, M. *Inorganica Chimica Acta,* **2007**, *360*, 1102-1110.

5 Silvi, S.; Constable, E. C.; Housecroft, C. E.; Beves, J. E. ; Dunphy, E. L.; Tomasulo, M.; Raymo, F. M.; Credi, A. Chem. Eur. J., **2009**, *15*, 178-185.

6 E.C. Constable and A.M.W. Cargill Thompson, *J. Chem. Soc., Dalton Trans*., **1992**, 1409.

7 *Molecular Switches* (Ed.: B. L. Feringa), Wiley – VCH, Weinheim, **2001**.

8 Credi, A. *Angew. Chem. Int. Ed.,* **2007**, *46*, 5472-5475.

9 Giordiani, S.; Cejas, M. A.; Raymo, F. M. *Tetrahedron*, **2004**, *60*, 10973.

Chapter 1

Synthesis of ruthenium(II) complexes with side amino-chain via trans-esterification strategy

1.1Introduction

The work in this chapter is partly based on the early investigation of $[Ru(pytpy)]^{2+}$ metal complexes and their photophysical and electronic properties.[1] However, the main idea of this project begins in the previously reported molecular switching properties of a ruthenium(II) terpyridine metal complex done by Dr. Jonathon Beves and Dr. Emma Dunphy in collaboration with Prof. Alberto Credi.[2] This work expanded on iron(II) complexes of methyl-substituted pytpy ligand done by Emma Dunphy in her PhD thesis, where the "full adder" idea originally comes from.[3] The aim of this work is to develop such a synthetic route for ruthenium(II) terpyridine metal complexes modified with an attached side chain and explore their expected molecular switching properties.

1.2 Synthesis - results and discussion

1.2.1 Precursors and ligands for ruthenium(II) complexes

The first strategy to synthesize such a ruthenium(II) terpyridine metal complex modified with an attached side chain starts with the previously reported methyl 4'-(pyridin-4-yl)-[2,2':6',2''-terpyridine]-4-carboxylate. Its complexation leads to either a homoleptic or with 4'-(pyridin-4-yl)-2,2':6',2''-terpyridine to a homoleptic metal complex. Further trans-esterification seems an ideal way to get a wide range of side chains with various lengths and bearing a terminal amine, which will bring a third protonation site to each ruthenium(II) complex (Scheme 1.1).

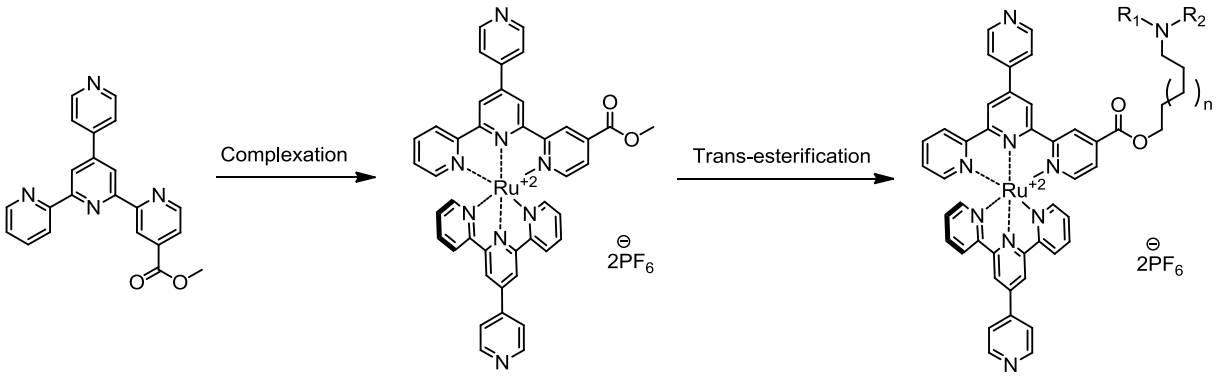

Scheme 1.1: Synthetic strategy towards Ru(II) complexes with a side chain

Lately, the Kröhnke methodology is one of the most popular ways to synthesize in one step symmetric and asymmetric terpyridine ligands with various substituents, where an α,β-unsaturated ketone and a ketone activated as a pyridinium iodide salt react at reflux in a conjugate addition (Michael type) to give a 1,5-diketone, and in the presence of an excess of ammonium acetate in methanol followed by condensation and a ring closure (Scheme 1.2).[4]

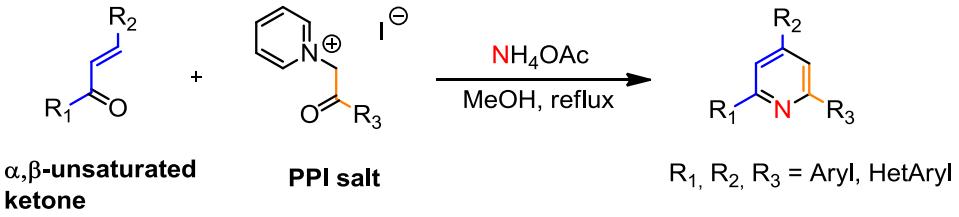

Scheme 1.2: Synthesis of terpyridines via the Kröhnke synthetic method

For the synthesis of the desired methyl ester substituted ligand **L2**, chalcone **P9** was used with an appropriately substituted pyridinium salt **P5** (Scheme 1.3). Formation of the product **L2** was observed during the reflux or upon chilling of the reaction mixture in a freezer. The white precipitate was isolated and washed with cold methanol, which gave analytically pure ligand **L2**.

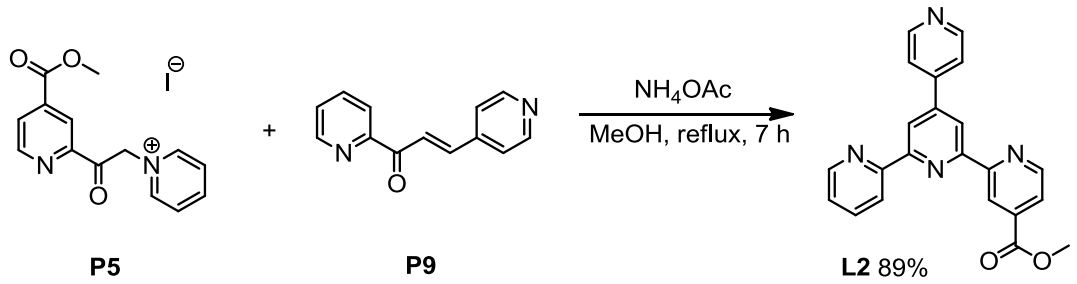

Scheme 1.3: Synthesis of the terpyridine L2 via the Kröhnke synthetic method

Both precursors, PPI salt **P5** and chalcone **P9**, were synthesized according to published procedures. [5, 7] Commercially available methyl isonicotinate was acetylated in the 2- position and was separated with column chromatography from the 2,3- and 2,5-bisacetylated side products. The conversion of methyl 2-acetylisonicotinate **P2** to the corresponding pyridinium salt **P5** was performed as reported in the literature for 2-acetylpyridine. 2-Acetylisonicotinate **P2** reacts at reflux in a presence of 1 equivalent of iodine and pyridine, which serves as a reagent and solvent as well. A reaction time of 1 hour is longer than enough, because the product **P5** is already observed at the beginning of the reflux period (Scheme 1.4).

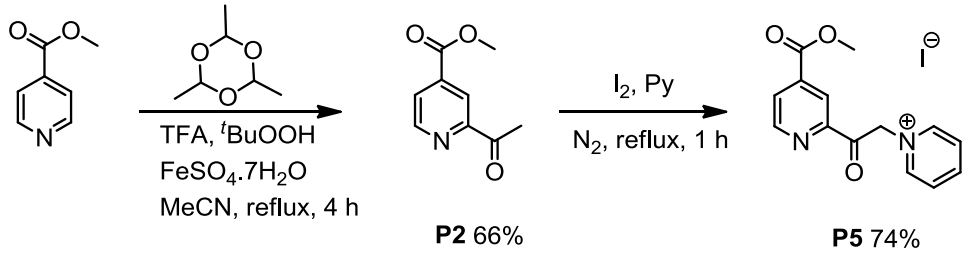

Scheme 1.4: Synthesis of the PPI salt P5

The synthesis of the chalcone **P9** was performed according to the reported procedure of Newkome. It involved microwave irradiation, as shown in the Scheme 1.5. [6] Reactants were dissolved in a suspension of tetrahydrofuran with alumina and irradiated in a domestic microwave oven. The presence of alumina seems to be necessary for the product formation, otherwise the reaction leads to multiple condensation products. A similar condensation product was observed by using classical conditions with KOH in a mixture of solvents ($EtOH/H_2O$). [7] The chalcone **P9** turned out to be unstable upon storage at laboratory temperature, however it is stable in a freezer at -20 °C for a couple of years.

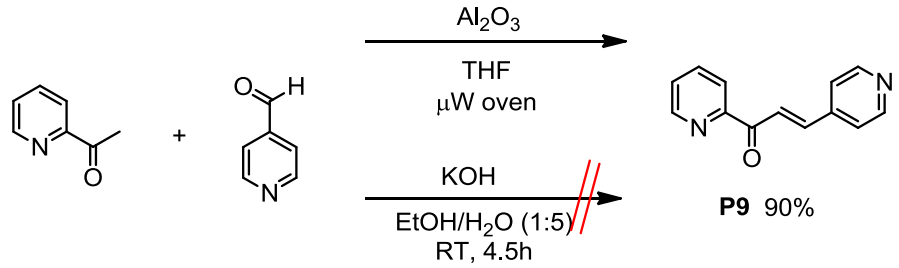

Scheme 1.5: Synthesis of the chalcone P9

In order to prepare the heteroleptic complex with the methyl ester substituted ligand **L2** as mentioned above in Scheme 1.1, it was necessary to prepare another ligand bearing the pendant pyridyl unit as a second protonation site. The second ligand may be functionalized, but it must be tolerant to the further trans-esterification, or it can be just simple pytpy **L3** as shown in a Scheme 1.6. **L3** was prepared following a procedure published by Hanan. [8] This is suitable for the synthesis of various symmetrical 4'-aryl- or heteroaryl substituted terpyridines in moderate to high yields. Condensation of the first equivalent of 2-acetylpyridine with aldehyde under basic conditions of KOH is followed by conjugated addition of the second equivalent of 2-acetylpyridine and a ring closure in a presence of ammonia as a source of nitrogen atom. Among the advantages of this "one pot" method is the fact that the reaction proceeds at room temperature, without an inert atmosphere and the terpyridine product precipitates out from the reaction mixture, due to its insolubility in ethanol. Recrystallisation from MeOH/$CHCl_3$ gives an analytically pure product **L3**.

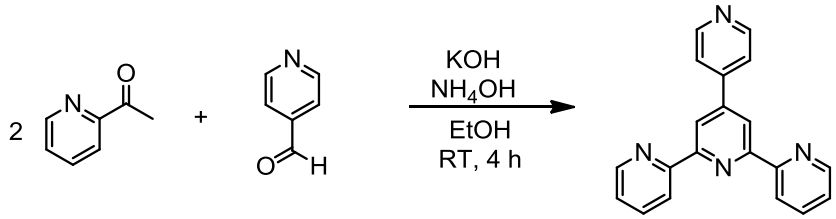

L3 48%

Scheme 1.6: Hanan's synthesis of pytpy ligand L3

Before complexation of **L3**, we decided to synthesize a model heteroleptic Ru(II) complex with 2,2':6',2''-terpyridine **L1**. Potts *et al.* (Scheme 1.7) reported in 1982 a synthetic route of ligand **L1** which involves multiple steps via dithioacetal, followed by reduction of 4'-(methylthio)-2,2':6',2''-terpyridine with $NiCl_2/NaBH_4$ giving the product in 23% overall yield.[9] We tried another method with only two steps (Scheme 1.7), which has been published by Jameson *et al.* in 1991.[10] 2-Acetylpyridine reacts with *N*,*N*-dimethylformamide dimethylacetal in toluene, while azeotropic distillation of methanol moves the reaction in favour of the forming enaminone. In the next step, conjugated addition of the second equivalent of 2-acetylpyridine occurs and a ring closure in a presence of ammonium acetate. A disadvantage of Jameson's method is the complicated work-up of the reaction mixture in the second reaction step, also the long reaction time (3 hours to 2 days) of the azeotropic

distillation in the first step and low yield. However, there has recently been published an elegant method for the enaminone synthesis without any solvent, involving a microwave irradiation and reaction time of only about 10 minutes.[11]

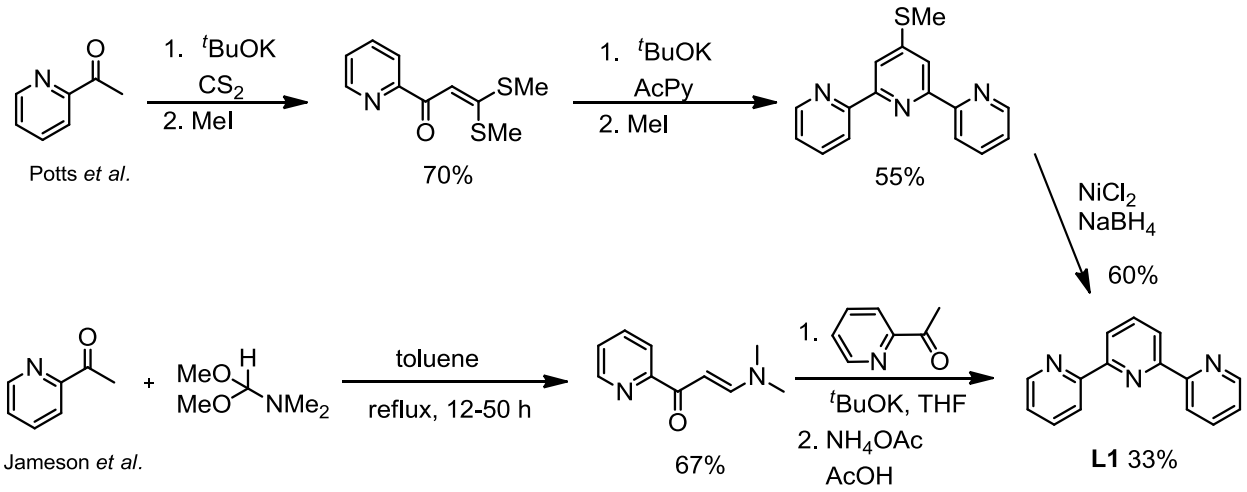

Scheme 1.7: Synthetis of tpy ligand L1

1.2.2 Model ruthenium(II) complexes with tpy and pytpy ligands bearing long amino side-chains

The first step of the **L2** complexation is a conversion of ligands **L1** and **L3** to a ruthenium(III) trichloride complex of the general type [Ru(tpy)Cl_3]. A commonly used method, which gives products in nearly quantitative yields, was reported by Sullivan *et al*. in 1980.[12] As shown in Scheme 1.8, one equivalent of the tpy ligand is suspended in a solution of $RuCl_3$*$3H_2O$ (1 eq.) in ethanol and refluxed for 3 hours. The products **C1** and **C2** precipitated out from the reaction mixture during the reflux as a dark brown or black powder and were used in the next steps without any further purification and analysis.

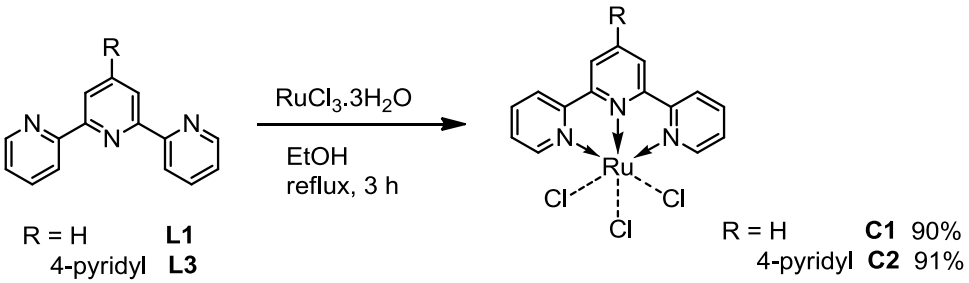

Scheme 1.8: Complexation of ligands L1 and L3 to [Ru(L)Cl_3]

For the complexation of **L2** to prepare the model complex **C3**, conditions involving microwave irradiation (Scheme 1.9) were used because these had previously been successfully applied by Jonathon Beves for the synthesis of a wide range of Ru(II) complexes[1, 2]. **L2** and **C1** were suspended in ethylene glycol, which serves as a solvent and also as a reducing agent for conversion of Ru(III) to Ru(II), and heated at reflux for 2 minutes at the highest setting in the domestic microwave oven. A characteristic colour change of the reaction mixture from brown or black to deep red is typical for the formation of Ru(II) complexes with tpy ligands. **C3** was precipitated out as a PF_6^- salt and also purified with column chromatography on SiO_2. For the separation of Ru(II) complexes, the most common solvent mixtures of MeCN/saturated aqueous KNO_3/H_2O in various polarity ratios were used as eluent, in this case 10:1.5:0.5. The Ru(II) complex **C3** was isolated as a red powder in moderate yields 25-69%. In the ^{1}H NMR spectrum of **C3**, we can observe characteristic shifts for protons A6, D6 and E6 to higher magnetic field in comparison with the free ligand **L1** and **L2**. The signal of the methyl group has also been shifted, but to the lower field (Figure 1.1).

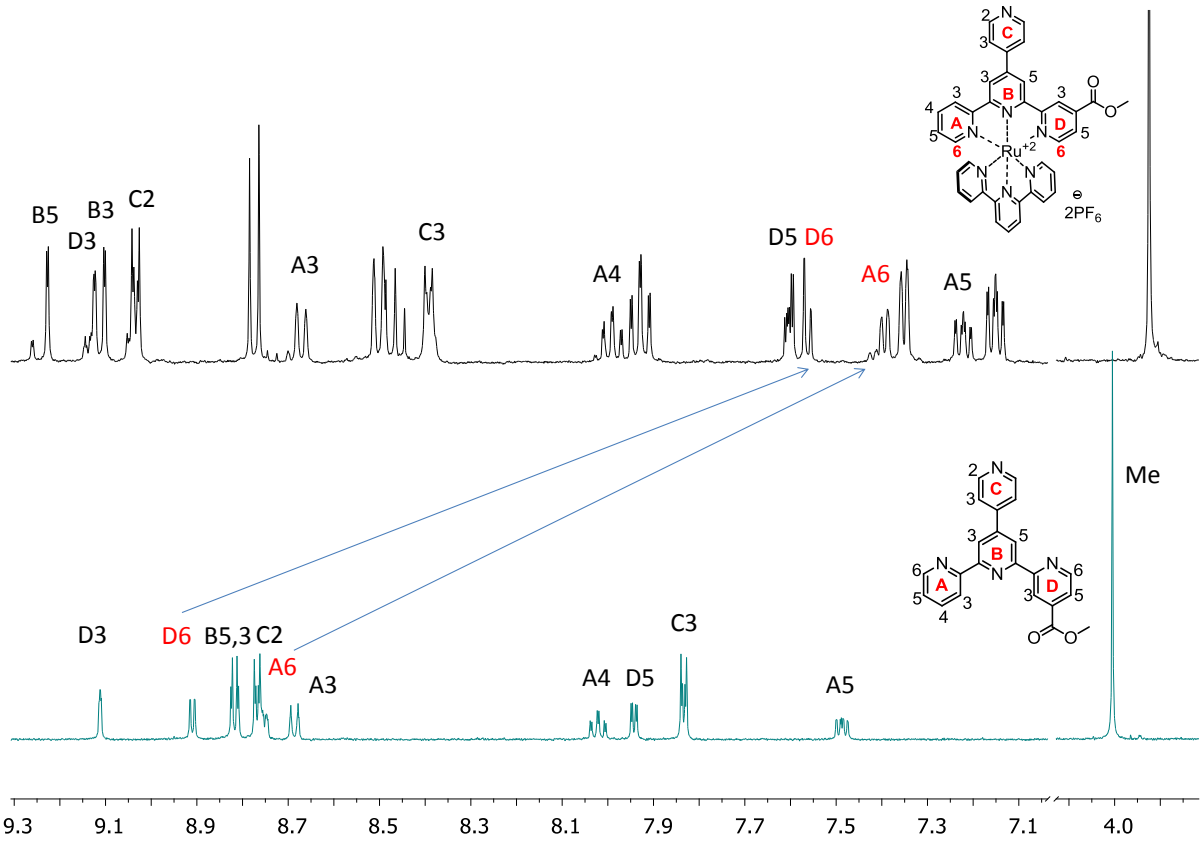

Figure 1.1: ^{1}H NMR (500 MHz, CD_3CN) spectra of the complexed (black) and free ligand L2 (cyan)

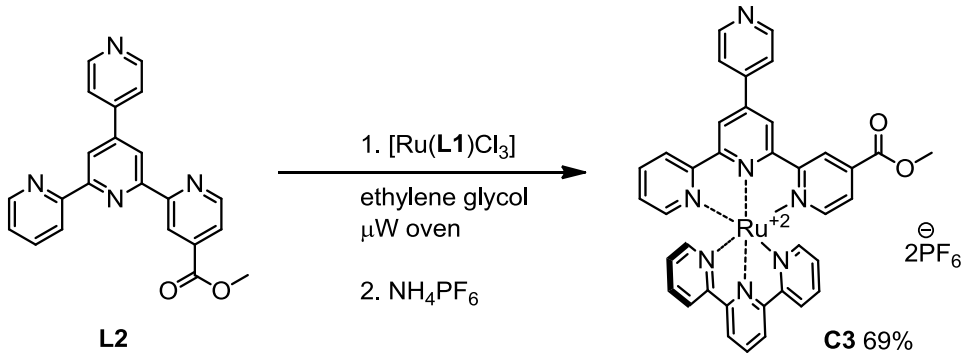

Scheme 1.9: Synthesis of the model complex C3

During the design of the long side chain we followed these main ideas: the chain a) has to bear a hydroxy group at one end to be able to perform trans-esterification, b) has an amino-group at the other end as an additional proton acceptor site of the ruthenium(II) complex, c) has to be long enough to reach the nitrogen of the pendant pyridyl position for a possible proton exchange communication between these groups. According to a computer modelled structure, we found that a suitable amino alcohol has ca. 8 – 13 carbons. To avoid any possible side reactions, it was decided to synthetize amino alcohols with a tertiary amino group. A primary or a secondary amino group might lead during trans-esterification to the formation of dimers between two ligands via an ester and an amide (Scheme 1.10).

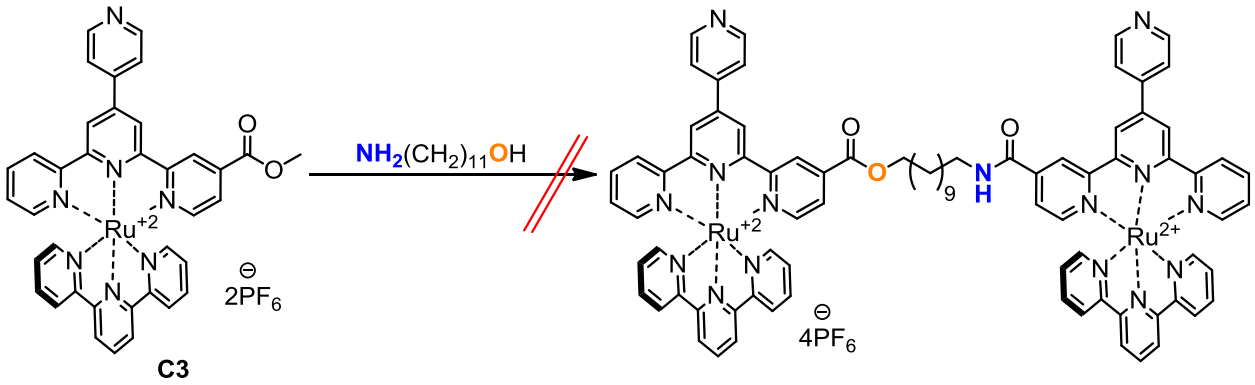

Scheme 1.10: Non-desirable possible side product during trans-esterfication

In 1974 Wetter *et al.* published a very facile two-step synthetic route to such amino alcohols, suitable for various chain lengths (Scheme 1.11).[13] We started with methyl 11-bromoundecanoate, which in the first step reacts with diethylamine, and this works both as a reagent and solvent. Bromine is quantitatively substituted with a diethylamino group. A white precipitate of diethylammonium bromide as a side product is simply filtered off. The

desired product **P12** was purified using vacuum distillation. In the second step, the methyl ester group was reduced by $LiAlH_4$ to a methylene hydroxy group. Sodium sulfate decahydrate was used as a suitable agent for quenching the reaction mixture. A precipitate of LiOH and an excess of sodium sulfate was filtered off and solvent removed under reduced pressure giving the amino alcohol **P16** in an almost quantitative yield. Dodecanol was used for a model reaction.

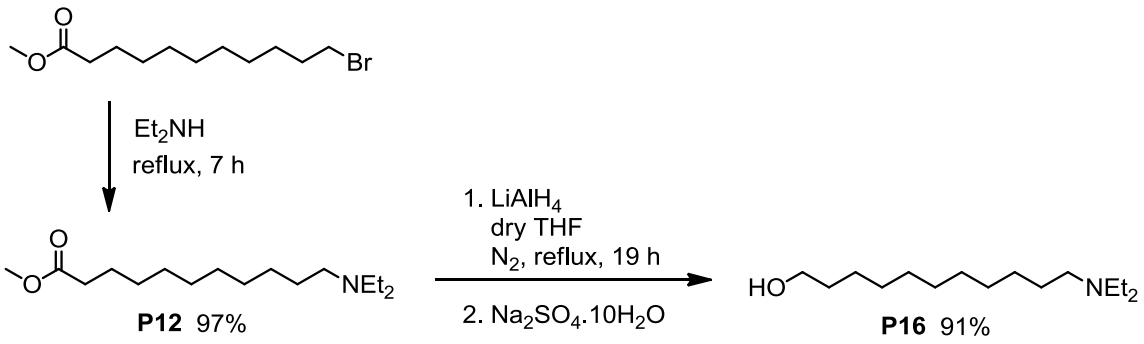

Scheme 1.11: Synthesis of amino alcohol P16 for a side chain

The amino alcohol **P16** was used as a suitable reagent to trans-esterify the methyl ester in the Ru(II) complex **C3** to give a long amino side-chain. Commercially available dodecanol was used as an appropriate model alcohol for comparison with **P16** (Scheme 1.12).

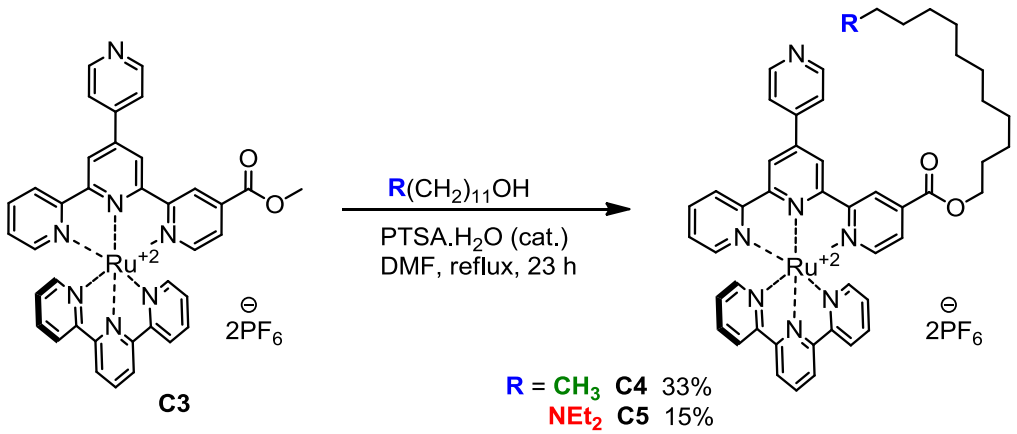

Scheme 1.12: Trans-esterification of the model complex C3

Conditions listed as Input 1 in the Table 1.1 show a first attempt of the trans-esterification shown in Scheme 1.12. Complex **C3** with an excess of dodecanol and a catalytic amount of *p*-toluenesulfonic acid monohydrate were heated in DMF for 26 hours at 120 °C. A

conversion of complex **C3** to the dodecyl substituted complex **C4** was monitored with ^{1}H NMR spectroscopy and with a TLC plate, eluted with a solvent mixture of MeCN/saturated aqueous KNO_3/H_2O = 10:1.5:0.5. Unfortunately only unreacted starting material **C3** was recovered. However heating the reaction mixture at reflux for 23 hours gave the Ru(II) complex **C4** in 33% yield (Table 1.1, Input 2). Trans-esterification of **C3** with the amino alcohol **P16** under the conditions of Input 2 gave the desired product **C5** in a low 15% yield. It was possible to observe that both complexes **C4** and **C5** partly decompose to a free carboxylic acid, which displays a characteristic red band on the start of a TLC plate. We have also applied irradiation in a microwave reactor, but the product seemed to be completely unstable under these conditions (Table 1.1, Input 3).

Input	Place	Temperature / °C	Time / h	Yield /%
1	Fumehood	120	26	0
2	Fumehood	Reflux	23	33
3	μW reactor	200	3/4	0

Table 1.1: Optimisation of synthesis of the complex C4 (Dodecanol, PTSA cat., DMF)

1.2.3 Application to ruthenium(II) complexes with two pytpy ligands

After the successful synthesis and analysis of the model complexes **C3**, **C4** and **C5** bearing only one pendant pyridyl unit, we focused on the synthesis of complex **C7** with ligands **L2** and **L3** bearing two pendant pyridyl units.

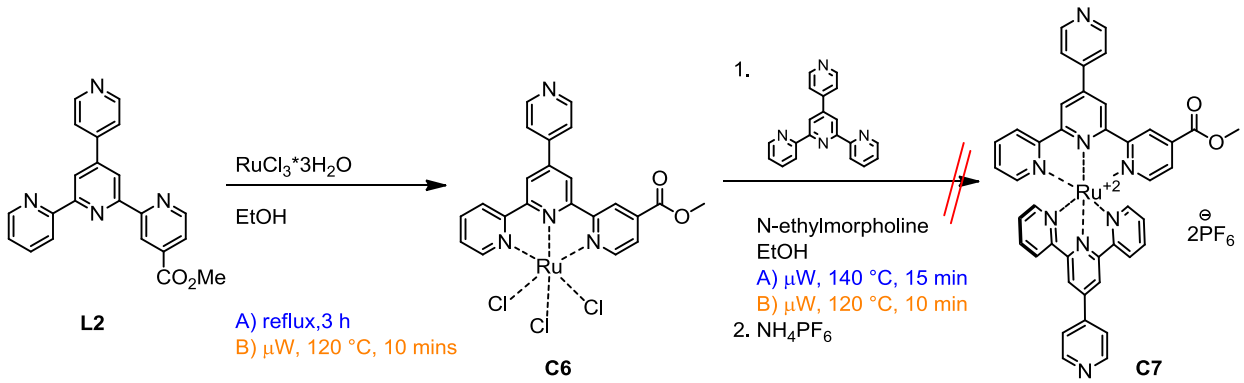

Scheme 1.13: The first attempt to synthetize the complex C7

As the first attempt to synthetize Ru(II) complex **C7**, a microwave reactor was used (Scheme 1.13). Methyl ester ligand **L2** was converted to Ru(III) trichloride complex **C6**. We used either a conventional technique (reflux in ethanol for 3 hours) or microwave irradiation (120 °C for 10 minutes) getting a dark brown precipitate. In the next step, **C6** was heated with ligand **L3** in a microwave reactor in ethanol. *N*-Ethylmorpholine was used as a reducing agent to convert Ru(III) to Ru(II). Unfortunately, in both cases, heating at 140 °C for 15 minutes or at 120 °C for 10 minutes, a black solid soluble only in DMF was isolated.

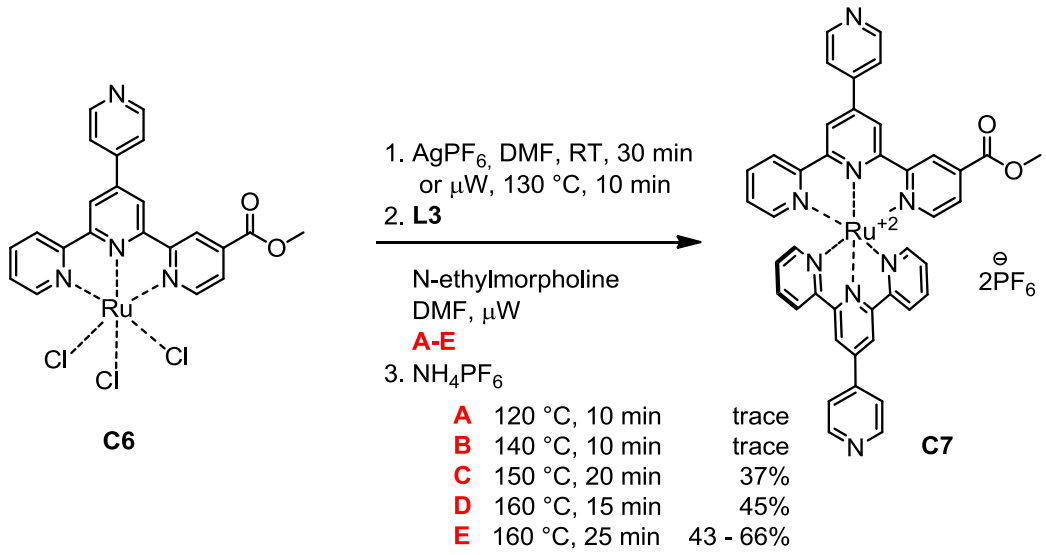

Scheme 1.14: Optimisation of the complex C7 synthesis

One option to improve the conditions in Scheme 1.13 is to increase the reactivity of **C6**. One common way to activate **C6** is a counterion exchange in a presence of $AgBF_4$ or $AgPF_6$. A driving force of this process is a formation of an AgCl precipitate (Scheme 1.14). A black suspension of **C6** in DMF was heated, $AgPF_6$ added and the reaction mixture stirred in the dark, first for 5 minutes at 100 °C and then for 30 minutes at laboratory temperature, or for 10 minutes at 130 °C in a microwave reactor. This process gives a dark brown solution with a characteristic grey-bluish precipitate of AgCl, which was filtered off. This way, activated **C6** was then used for the next step to form a complex with **L3.** The same conditions, heating for 10 minutes at 120 °C or 140 °C (Scheme 1.14, 2A and 2B), gave a slightly reddish reaction mixture and we isolated at least a trace amount of **C7**. These conditions were optimized by increasing the temperature and using a longer reaction time. Heating at 150 °C for 20 minutes gave **C7** in 37% yield (Scheme 1.14, 2C). The best results were obtained with

irradiating at 160 °C for 15-25 minutes giving **C7** in 43-66% yield (Scheme 1.14, 2D-E). However, besides the main product **C7** we also isolated homoleptic Ru(II) complexes with ligands **L2** and **L3** as minor side products.

Scheme 1.15 displays the conversion of the methyl ester complex **C7** to the dodecyl ester **C17** and diethylamino undecyl ester **C18**. Conditions for these reactions were the same as for **C3**, i.e. reflux in DMF for 23 hours in a presence of a catalytic amount of *p*-toluenesulfonic acid monohydrate. In spite of many attempts, both complexes were obtained in quite low yields of 10-30%. In both cases, a free carboxylic acid as a product of ester hydrolysis was also detected.

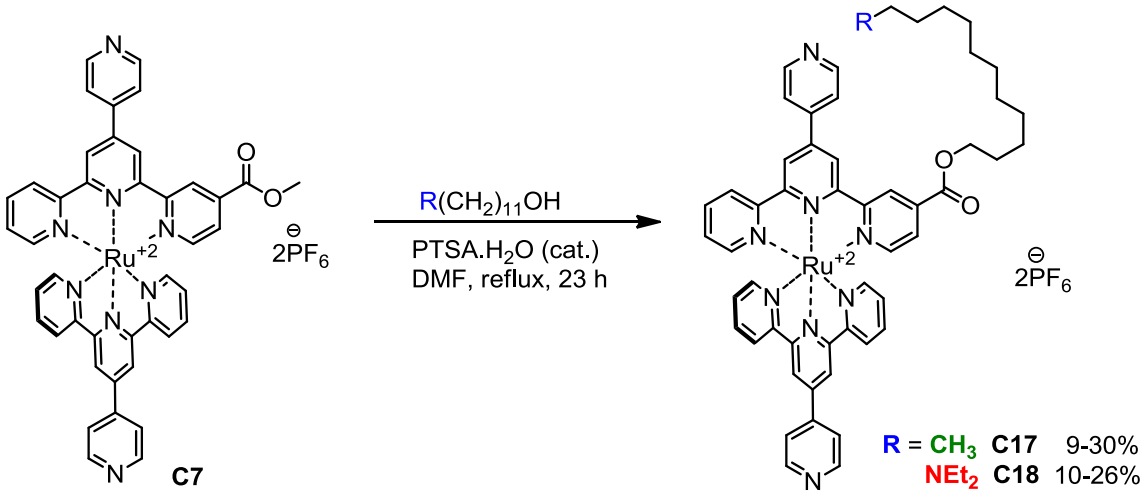

Scheme 1.15: Trans-esterification of the complex C7

In the electrospray mass spectrum of **C7**, peaks with *m/z* = 390.1 (assigned to $[M\text{-}2PF_6]^{2+}$) with 100% intensity and 925.3 (assigned to $[M\text{-}PF_6]^{+}$) with intensity 50% were observed. In cases of **C17** and **C18** only one peak envelope was detected, the base peak with *m/z* = 467.2 or 495.7 which belongs to $[M\text{-}2PF_6]^{2+}$ and has a characteristic distribution of isotopes for ruthenium.

Figure 1.2 compares the ^{1}H NMR spectra of the Ru(II) complexes **C7** (black), **C17** (green) and **C18** (red) measured in CD_3CN. In the aromatic region it is possible to see a characteristic set of proton signals of the coordinated unsubstituted pytpy ligand **L3** and of a ligand substituted with the electron withdrawing CO_2R group. In the aliphatic part, a significant influence of the shielding effect of the long side chain in complexes **C17** and **C18** is observed.

Therefore, the triplet of the methylene group next to the carboxylic group is shifted to δ 4.33 ppm in comparison with the singlet at δ 3.93 ppm for the methyl ester **C7**.

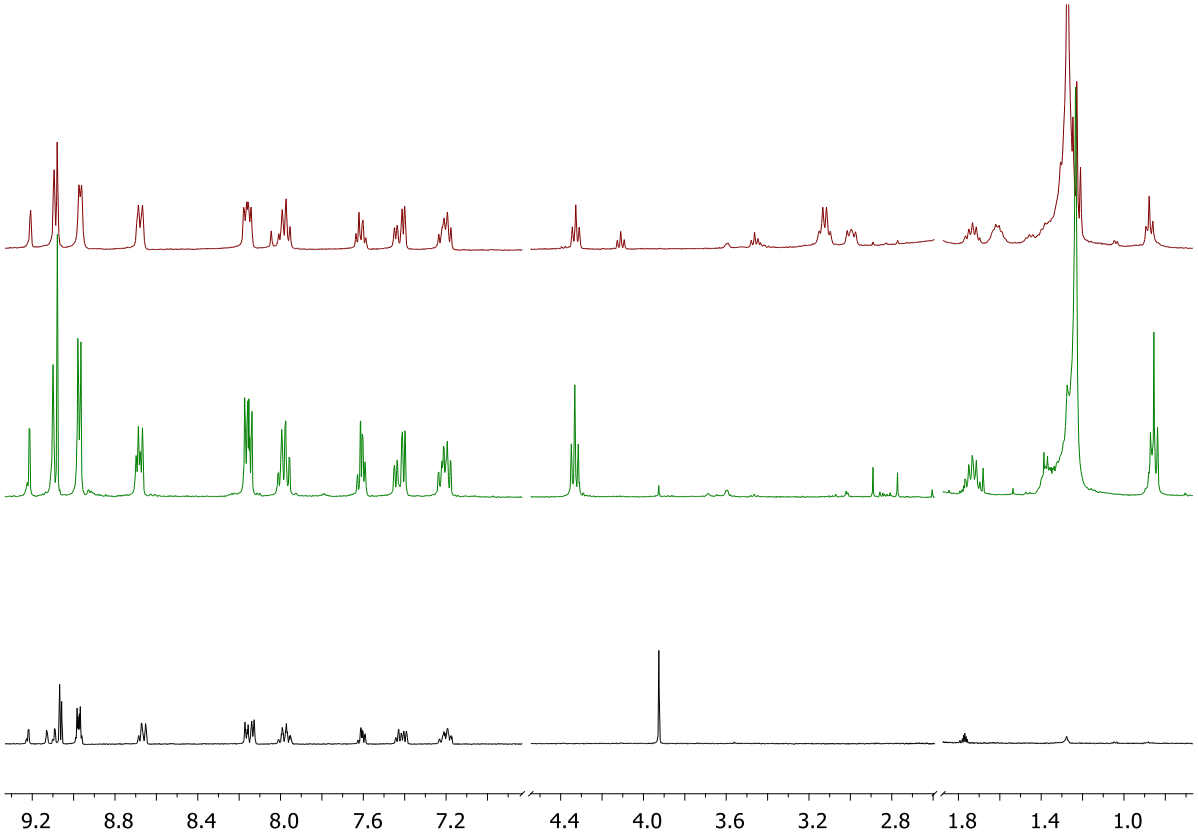

Figure 1.2: ^{1}H NMR (400 MHz, CD_3CN) spectra of complexes C7 (black), C17 (green) and C18 (red)

Previously reported reactions gave the desired Ru(II) complexes **C7**, **C17** and **C18** in very poor yields, therefore we considered all possible side product which could be formed besides the complex with a free carboxylic acid **C17** – a product of the side chain cleavage. We detected the homoleptic Ru(II) complexes of ligands **L2** and **L3**. On a TLC plate and on a chromatographic column, minor bands with a red-purple colour were also seen an the colours are typical for Ru(II) complexes with mono- or bisprotonated pendant pyridyl units, whereas deprotonated forms of Ru(II) complexes have a characteristic orange-red or deep-red colour.

1.2.4 An Alternative route to ruthenium(II) complexes via methylated ligands

Due to the reasons mentioned above, we applied an alternative route to obtain complexes **C17** and **C18** (Scheme 1.16). The idea was based on a four-step strategy. Ligands **L2** and **L3** were methylated on the pendant pyridyl group, so that they are protected against possible side reactions and all reagents are then used selectively and specifically as planned. The N-methylated ligands are then complexed and trans-esterified. A final demethylation removes the protective groups from the pyridyl positions.

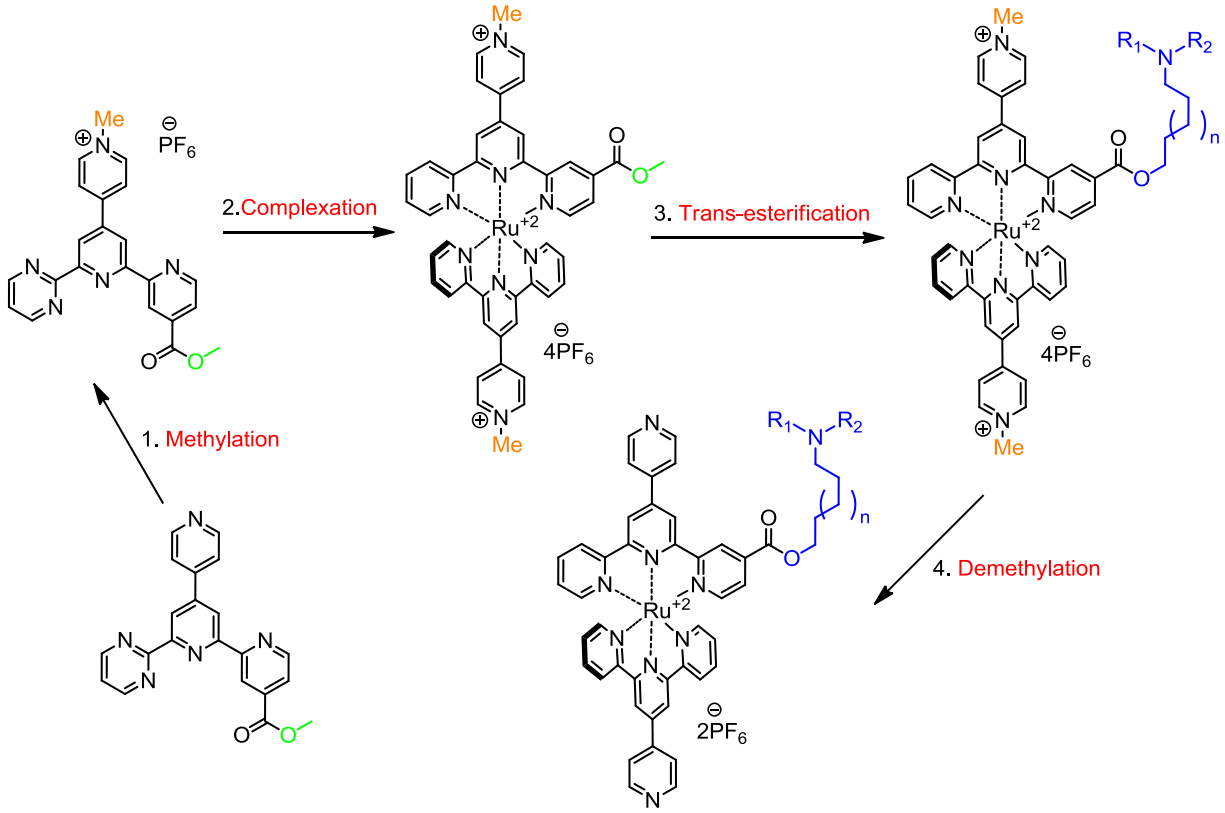

Scheme 1.16: An alternative route to obtain complexes with a long side chain C17 and C18

Ligands **L3** or **L2** were refluxed with an excess of iodomethane in acetonitrile for 7-16 hours.[14] The product precipitated out upon cooling the reaction mixture to room temperature and reducing the volume of solvent to one third. Ammonium hexafluorophosphate was added for a counterion exchange from iodide to hexafluorophosphate, and the colour of the precipitate changed from white to yellow or olive-green, respectively (Scheme 1.17). In the ^{1}H NMR spectra of the methylated ligands, itwas possible to observe a significant chemical shift of the aromatic protons of the pendant

pyridyl unit to lower magnetic field, and this was especially noticeable for the protons in the *meta*-positions.

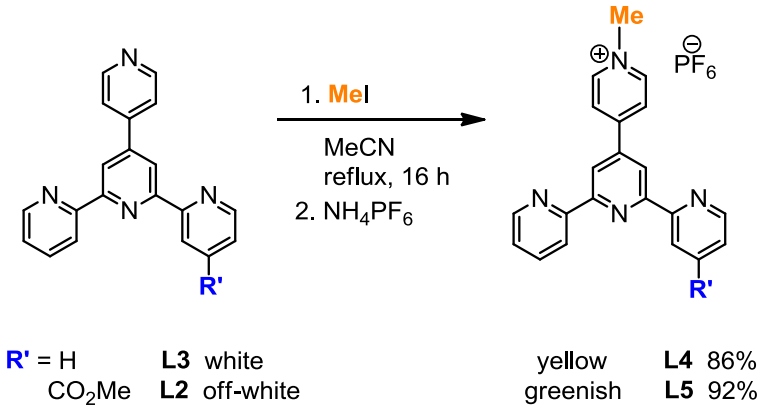

Scheme 1.17: Synthesis of the N-methylated pytpy ligands as an alternative route

Methylated ligand **L5** was then quantitatively converted to the ruthenium(III) complex **C9** and in the next step, **C9** was complexed with the methylated ligand **L4**. Reaction conditions used were those optimized above in Scheme 1.14 for the **C7** synthesis (irradiation in the microwave reactor in EtOH at 160 °C for 20 minutes) giving complex **C10** in 46% yield (Scheme 1.18, green route). The product has a red-purple colour, typical of Ru(II) complexes with a protonated or substituted pendant pyridyl ring. We have also applied a route using activated **C9** with silver hexafluorophosphate, which slightly increased the yield of **C10** to 53% (Scheme 1.18, purple route). The product was purified on silica gel with a very polar solvent mixture of MeCN/saturated aqueous KNO_3/H_2O = 7:2:2.

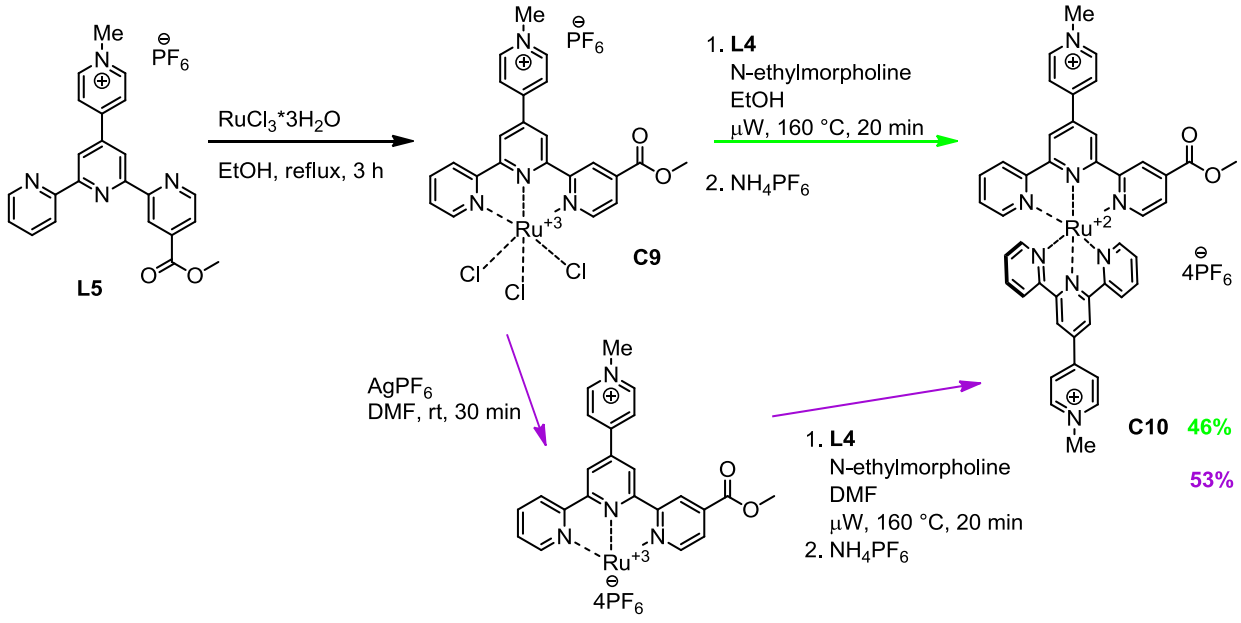

Scheme 1.18: Complexation of methylated ligands L4 and L5 to obtain C10

Figure 1.3 compares the ^{1}H NMR spectra of the Ru(II) complex **C7** and the methylated version **C10**. As for the free ligands **L4** and **L5**, it is also possible in the complexes to observe the significant chemical shift of the *meta*-protons of the pendant pyridyl unit to lower magnetic field.

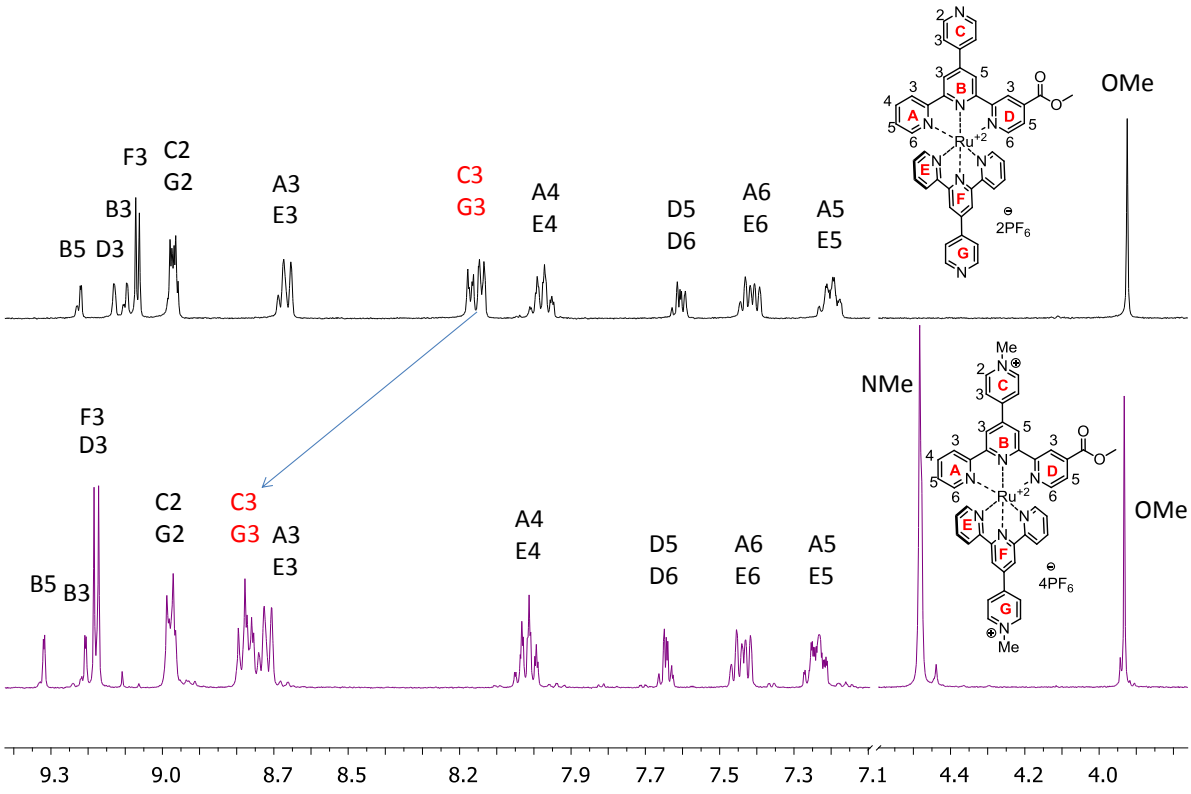

Figure 1.3: ^{1}H NMR (400 MHz, CD_3CN) spectra of complexes C7 (black) and methylated C10 (purple)

In the electrospray mass spectrum of **C10**, it was not possible to detect peaks for $[M\text{-}PF_6]^+$ or $[M\text{-}2PF_6]^{2+}$ characteristic of ruthenium complexes as in case of **C7**, but we found peaks assigned to both the methylated ligands *m/z* 325.2 [**L4**-PF_6]$^+$ and 383.2 [**L5**-PF_6]$^+$ with intensities of 100% or 25%. However, the MALDI TOF MS of **C10** displays all the desired peaks 810.9 $[M\text{-}4PF_6]^+$ (100%), 1099.6 $[M\text{-}2PF_6]^+$.

Trans-esterification of the complex **C10** is the third step of the strategy shown above in Scheme 1.16. To convert the methylated complex **C10** to the product with a long side amino chain, we used the same conditions for these reactions as for **C3** and **C7**, i.e. reflux in DMF for 23 hours in a presence of a catalytic amount of *p*-toluenesulfonic acid monohydrate (Scheme 1.19). The product formation was monitored with TLC plates. Unfortunately, besides the target molecule and unreacted starting **C10** we observed various side products

as well as products of decomposition, which made purification too complicated. Therefore, we gave up on this synthetic strategy and focused on another one.

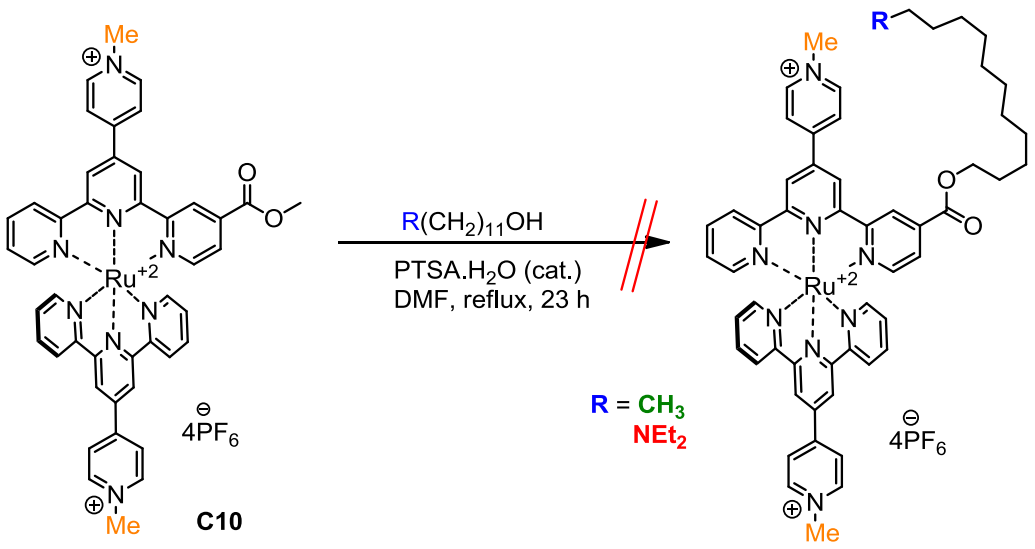

Scheme 1.19: Trans-esterification of the complex C10

1.2.5 Reactivity of methyl ester substituted complex C7 in the presence of methyl 11-bromoundecanoate

Another idea was to investigate the reactivity of **C7** in the presence of methyl 11-bromoundecanoate, and find out which main and side products would be formed. Scheme 1.20 shows the original idea, a product of trans-esterification and intramolecular cyclisation.

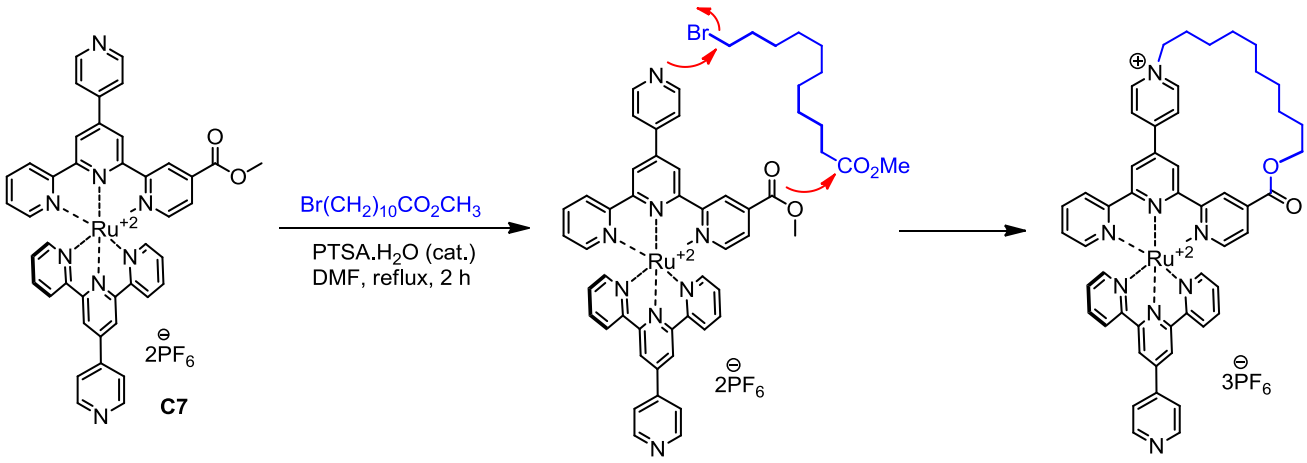

Scheme 1.20: Reaction of C7 with methyl 11-bromoundecanoate

The reaction was monitored with TLC plates, eluting with a solvent mixture of MeCN/saturated aqueous KNO_3/H_2O = 10:1.5:0.5 and was complete in only 2 hours. There were observed only 2 main spots, with almost identical R_f (approx. 0.75) and a red-purple colour, characteristic for Ru(II) complexes with substituted pyridyl positions. A question arose: where would the long chain be connected and how? First we thought it might be 2 complexes with mono- and bis- substituted pyridyl positions. So the reaction mixture was refluxed with another equivalent of methyl 11-bromoundecanoate, to convert the possible mono-substituted product to the bis-substituted one, however nothing changed. The two products were separated on a preparative TLC plate (SiO_2) and characterised with 1D and 2D NMR spectroscopy and ESI MS. After careful comparison of the spectra, we were able to identify both products (Scheme 1.21).

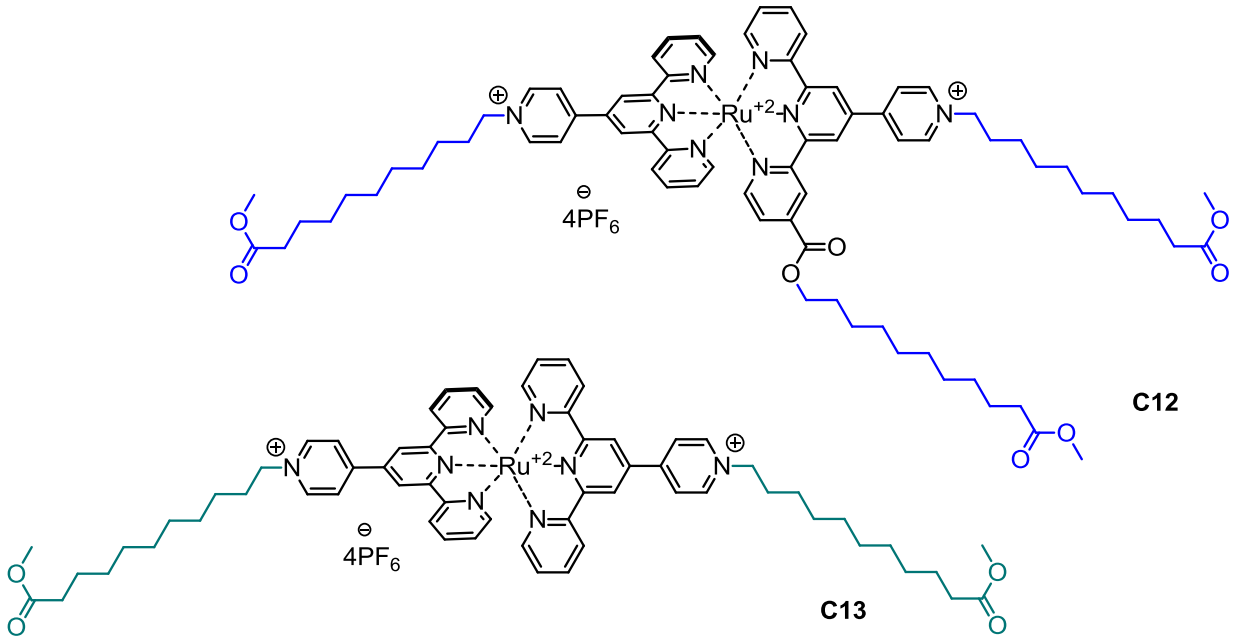

Scheme 1.21: Products of the reaction of C7 with methyl 11-bromoundecanoate

The ^{1}H NMR spectrum of the second product **C13** clearly displays, one set of signals for a symmetrical *N*-substituted pytpy ligand (Figure 1.4). The aliphatic part of the ^{1}H NMR spectra contains all the proton signals of a methyl undecanoate chain, which is linked by the first carbon to the nitrogen of the pyridyl position. This methylene group has chemical shift of δ 4.68 ppm. Formation of this homoleptic Ru(II) complex was supported by the ESI mass spectrum with peaks at 705.3 $[M\text{-}2PF_6]^{2+}$ and 509.3 $[L_1\text{-}PF_6]^+$ with intensities of 29% and

100% respectively. **C13** was presumably formed as a side product due to the presence of an impurity of the homoleptic complex **C8** in the starting **C7**.

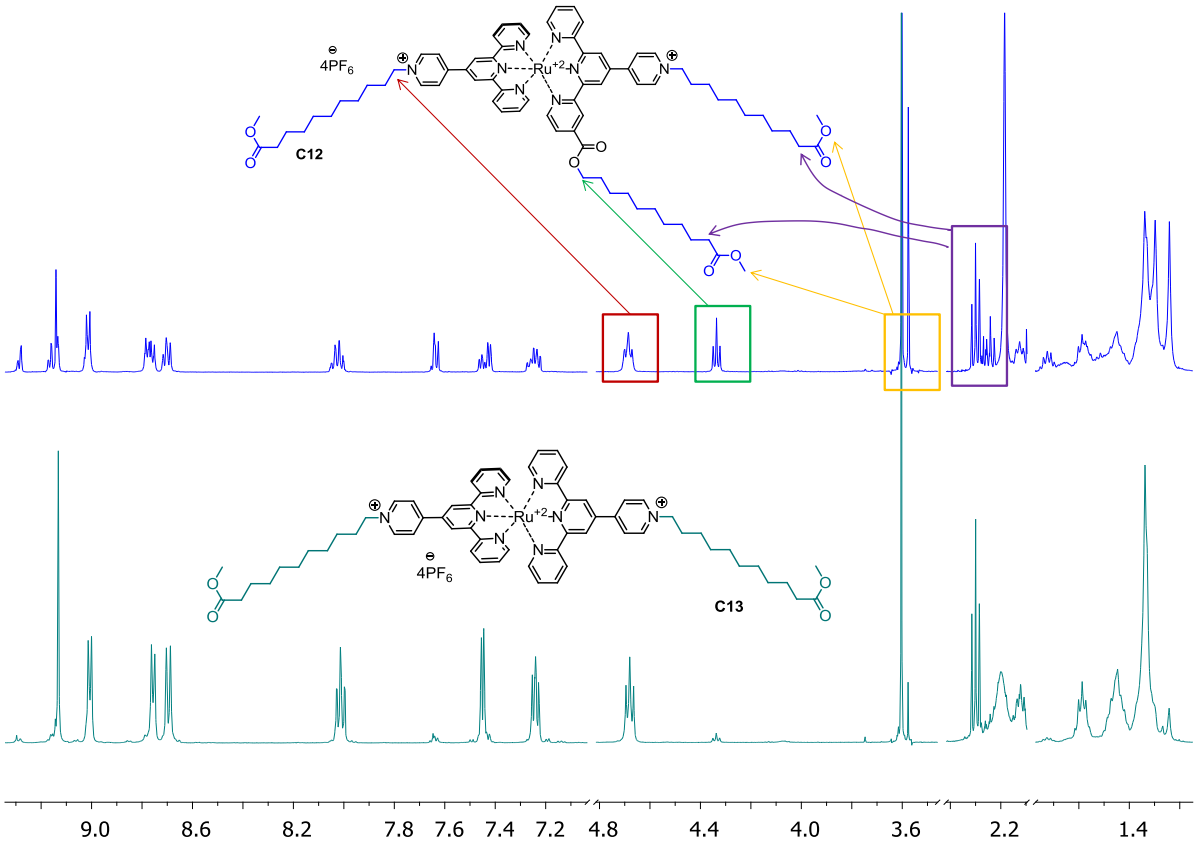

Figure 1.4: Comparison of ^{1}H NMR (500 MHz, CD_3CN) spectra of C12 (blue) and C13 (cyan)

However, the NMR spectrum of **C13** was an important supporting piece of information during the solving of the structure of **C12**. Due to the higher R_f value on a TLC plate and two sets of aromatic signals in ^{1}H NMR spectrum, it was possible to say that **C12** is heteroleptic complex with 3 methyl undecanoate chains. Two of them are linked via a nitrogen atom of the pyridyl ring as in the complex **C13** and one chain is linked via an ester to the atom D4 of the pyridyl ring D. The methylene group linked to this ester has a typical chemical shift of δ 4.34 ppm in the ^{1}H NMR spectrum. In the HMBC 2D NMR spectra characteristic crosspeaks of the carboxyl group with this methylene group were observed and also with protons D3 and D5 (Figure 1.5). Formation of the heteroleptic Ru(II) complex **C12** was confirmed with ESI MS spectra with peaks with *m/z* 751.5 $[L_2\text{-}PF_6]^+$ and 509.3 $[L_1\text{-}PF_6]^+$ with intensities of 60% and 35% respectively. Both suggested structures **C12** and **C13** were confirmed with elemental analysis.

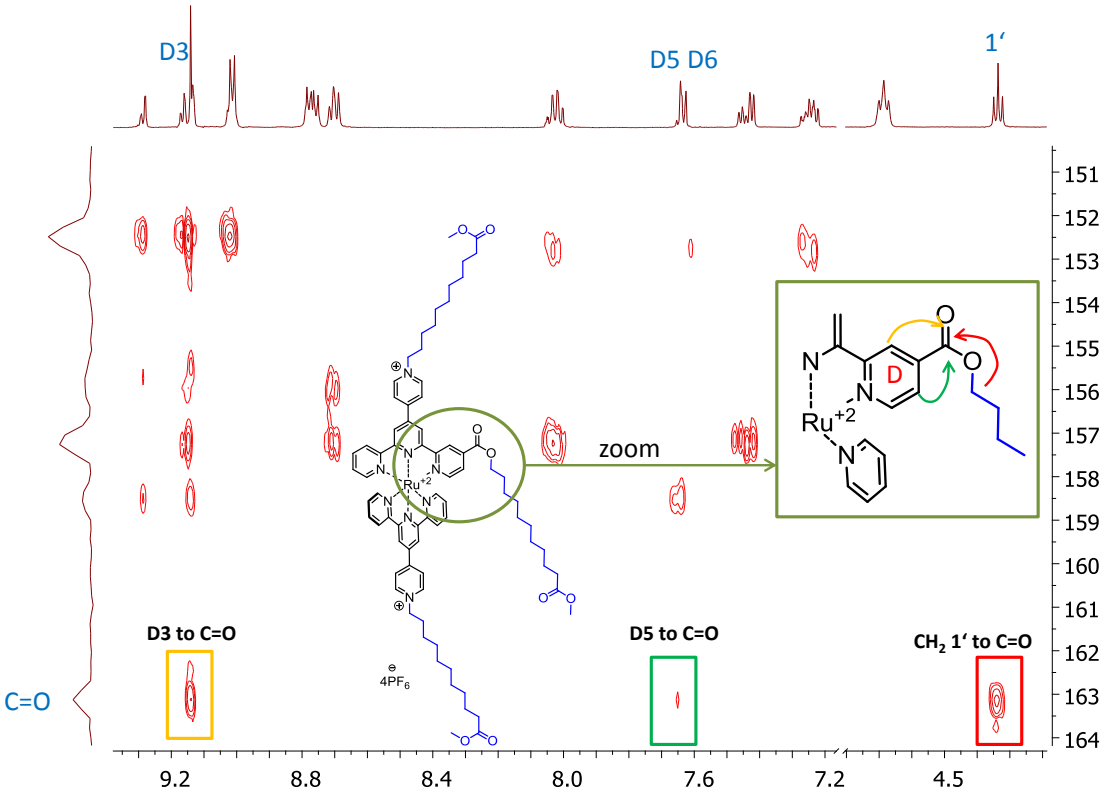

Figure 1.5: HMBC NMR spectrum (500 MHz, CD_3CN) of C12

1.3 Photophysical properties

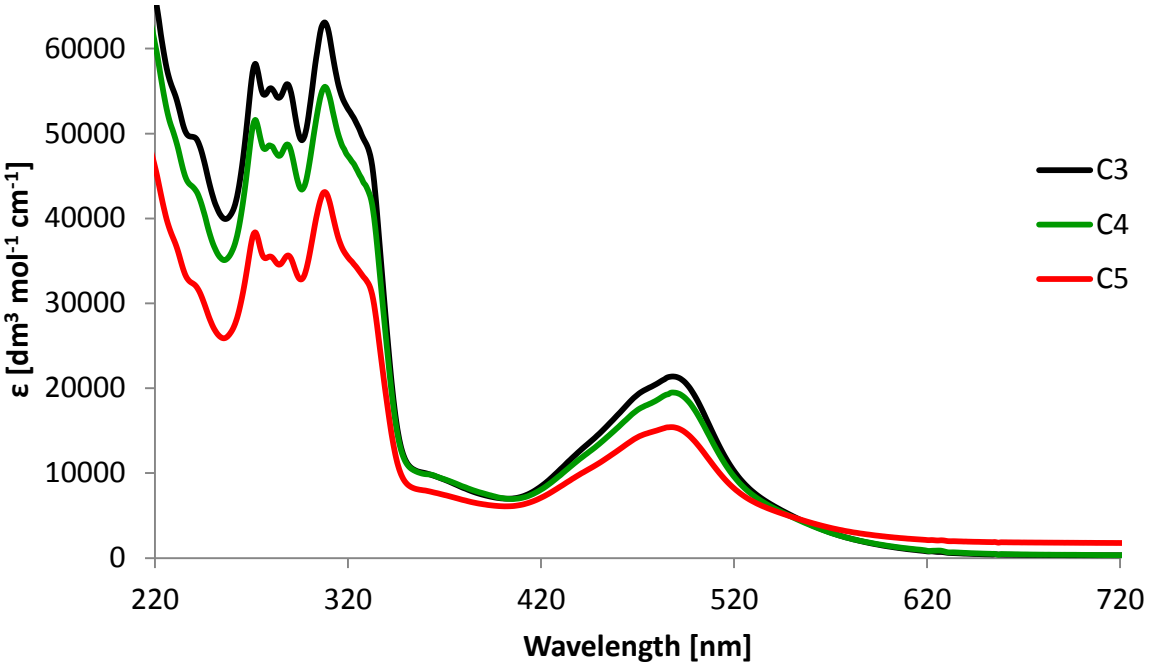

Figure 1.6: Comparison of UV/Vis absorption spectra (CH_3CN, $3 \cdot 10^{-5}$M) of Ru(II) complexes C3, C4 and C5

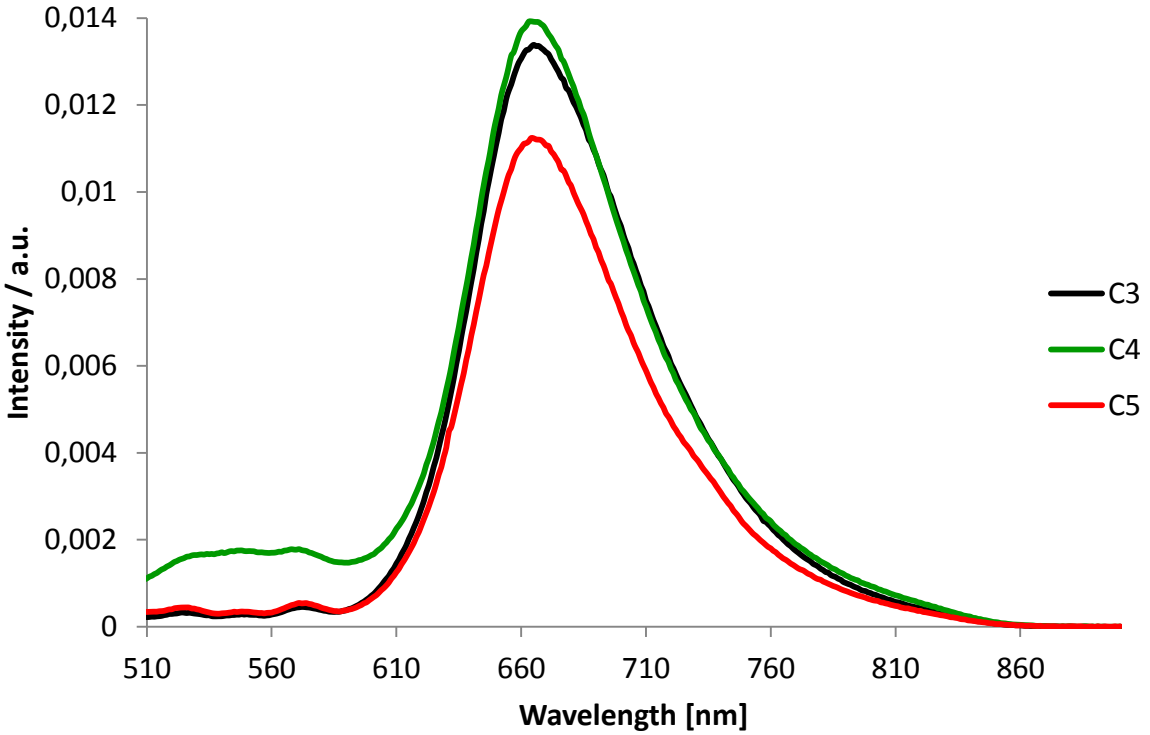

Figure 1.7: Fluorescence spectra (CH_3CN, $3 \cdot 10^{-5}$M) of Ru(II) complexes C3, C4 and C5, λ_{ext} = 488 nm

Figure 1.6 compiles the absorption spectra of ester-substituted Ru(II) complexes **C3-5.** In the UV region of, intense bands around 290 nm and 310 nm were observed. These bands arise from ligand-centred $\pi^* \leftarrow \pi$ transitions. In the visible region, a broad and moderately intense band with a maximum at 464 nm, assigned to the MLCT (metal-to-ligand charge-transfer) excited state, was observed for each of the complexes **C3-5**. The luminescence spectrum (Figure 1.7) of **C3-5** exhibits the typical low energy MLCT phosphorescence band of Ru polypyridine complexes with the emission maximum at 664 nm. The complexes C4 and C5 substituted with the long side amino-chain have longer luminescence lifetime (Table 1.2).

Complex	λ_{MLCT} [nm]	λ_{max}^{em} [nm]	τ [ns]
C3	488	665	9
C4	488	664	26
C5	488	664	16
C7	492	663	3
C16	493	673	13
C17	494	682	21
C10	510	710	197
C12	511	708	248
C13	510	716	194

Table 1.2: Photophysical properties of Ru(II) complexes, λ_{ext} at λ_{MLCT}

Figure 1.8 displays a comparison of the absorption spectra of Ru(II) complexes **C7** and the N-alkylated complexes **C10**, **C12** and **C13**. **C7** has an MLCT band maximum at 492 nm, however the N-alkylated complexes show a strong red-shift to 510 nm and the extinction coefficient has increased. An even more significant red shift (from 663 to ca. 710 nm) and intensity increase due to the N-alkylation is observed in the emission spectra (Figure 1.9). All the N-alkylated Ru(II) complexes **C10**, **C12** and **C13** are stronger emitters and longer lived (Table 1.2). Quantum yield of all reported complexes is lower than 1%. Photophysical properties of **C16-17** are reported in Chapter 5.

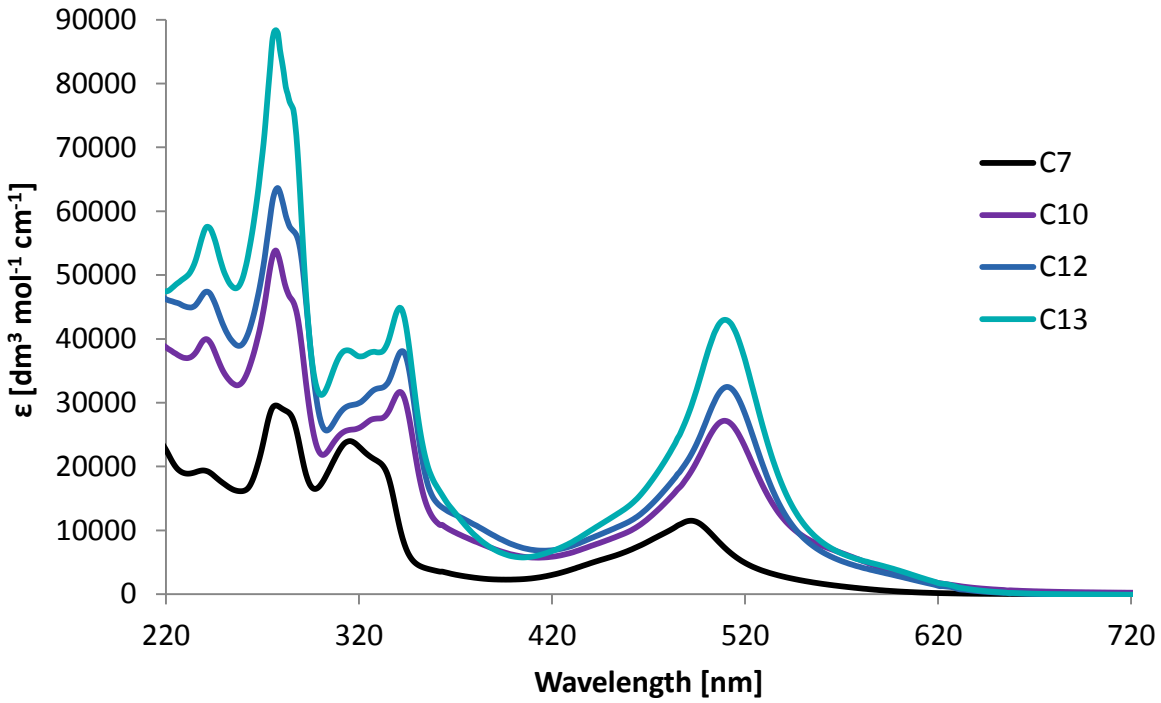

Figure 1.8: Absorption spectra (CH_3CN, $3 \cdot 10^{-5}$M) of complexes C7 (black), methylated C10 (purple), alkylated C12 (blue) and C13 (cyan)

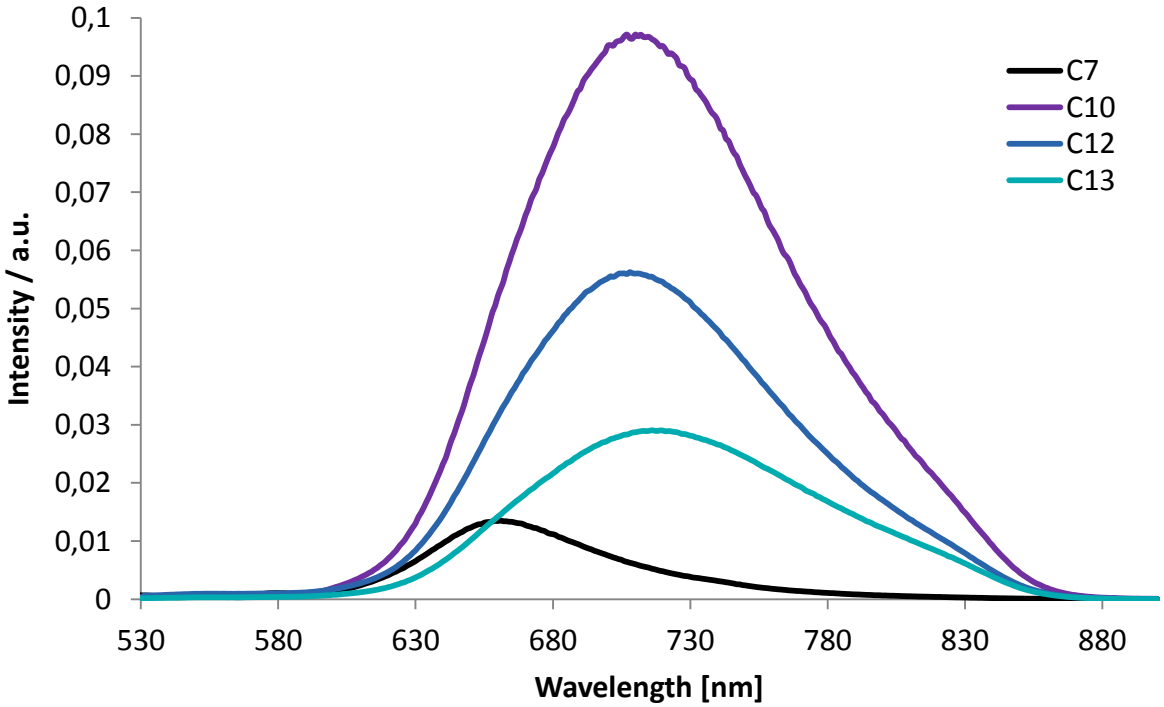

Figure 1.9: Emission spectra (CH_3CN) of complexes C7 (black), methylated C10 (purple), alkylated C12 (blue) and C13 (cyan), solutions ($3 \cdot 10^{-5}$M), λ_{ext} = 492 nm (C10) and 510 nm (C10, C12, C13)

Literature

1. Beves, J. E.; Dunphy, E. L.; Constable, E. C.; Housecroft, C. E.; Kepert, C. J.; Neuburger, M.; Price, D. J.; Schaffner, S. *Dalton Trans,.* **2008**, 386–396.
2. Silvi, S.; Constable, E. C.; Housecroft, C. E.; Beves, J. E. ; Dunphy, E. L.; Tomasulo, M.; Raymo, F. M.; Credi, A. *Chem. Eur. J.,* **2009**, *15*, 178-185**.**
3. Dunphy, E. PhD Thesis, **2009**, University of Basel.
4. Mikel, C.; Potvin, P. G. *Polyhedron,* **2002**, *21*, 49-54.
5. Ishihara, M.; Tsuneya, T.; Shiga, M.; Kawashima, S.; Yamagishi, K.; Yoshida, S.; Sato, H.; Uneyama, K. *J. Agric. Food Chem.,* **1992**, *40*, 1647.
6. Eryazici, I.; Moorefield, C. N.; Durmus, S.; Newkome, G. R. *J. Org. Chem.,* **2006**, *71*, 1009.
7. Zhao, L.-X.; Kim, T. S.; Ahn, S.-H.; Kim, T.-H.; Kim, E.-k.; Cho, W.-J.; Choi, H.; Lee, C.-S.; Kim, J.-A.; Jeong, T. C.; Chang, C.-j.; Lee, E.-S. *Bioorg. Med. Chem. Lett.,* **2001**, *11*, 2659-2662.
8. Wang, J.; Hanan, G. S. *Synlett,* **2005**, *8*, 1251-1254.
9. Potts, K. T.; Cipullo, M. J.; Ralli, P.; Thodoridis, G. *J. Org. Chem*., **1982**, *47*, 3027.
10. Jameson, D. L.; Guise, L. E. *Tetrahedron Letters,* **1991**, *32 (18)*, 1999-2002.
11. Pleier, A. K.; Glas, H.; Grosche, M.; Sirsch, P.; Thiel, W. R. *Synthesis,* **2001**, 55-62.
12. Sulliwan, B. P.; Calvert, J. M.; Meyer, T. J *Inorg. Chem.,* **1980**, *19*, 1404-1407.
13. Wetter, W. P.; De Witt Blanton, C. Jr. *J. Med. Chem.,* **1974**, *17*, 620-624.
14. Constable, E. C.; Housecroft, C. E.; Neuburger, M.; Phillips, D.; Raithby, P.R.; Schofield, E.; Tocher, D.A.; Zehnder, M.; Zimmermann, Y. *J. Chem. Soc., Dalton Trans.,* **2000**, 2219-2228.

Chapter 2

Towards ruthenium(II) complexes with an amino chain containing a triazole ring and pytpy ligands with a side chain linked via an ether

2.1 Introduction

A goal of this chapter was to investigate another synthetic route to obtain Ru(II) complexes of pytpy ligands with an amino side-chain. This time the chain would contain a triazole ring as a spacer and also linkers of various lengths (Figure 2.1). From a retrosynthetic view, these functionalities would allow us to start from precursors of a very wide range and use commonly known reactions (e.g. Sonogashira cross-coupling, "click reaction"). Therefore this will bring to the molecule a side chain with many functional groups and various amino substituents, which all will give us ruthenium complexes with different photophysical and electrochemical properties.

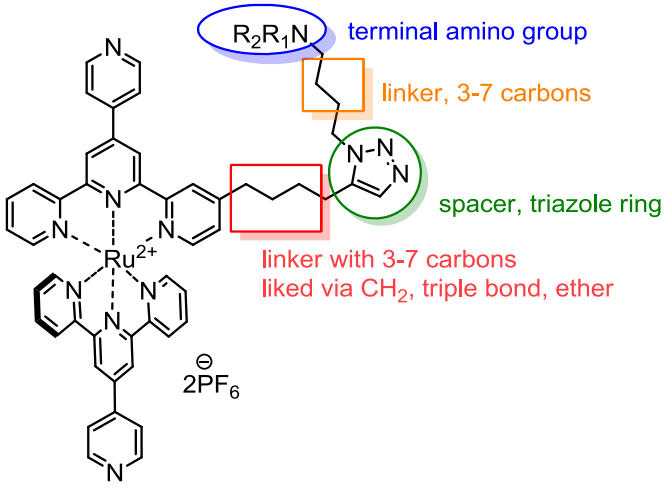

Figure 2.1: Towards the Ru(II) complex with an amino chain containing a triazole ring

2.2 Results and Discussion

2.2.1 Synthetic strategies

It was very clear, that the synthetic paths to such molecules will contain many reaction steps, which will not be easy, therefore it was necessary prepare a careful synthetic plan. We had to also consider in which step the side chain, containing the triazole ring and the terminal tertiary amino group, will be constructed. There were three options: a) create it at the beginning on the pyridine precursor, b) on the ligand, or c) synthesize the chain on a complex. The version B seemed the most promising after considering all potential difficulties of these three possibilities.

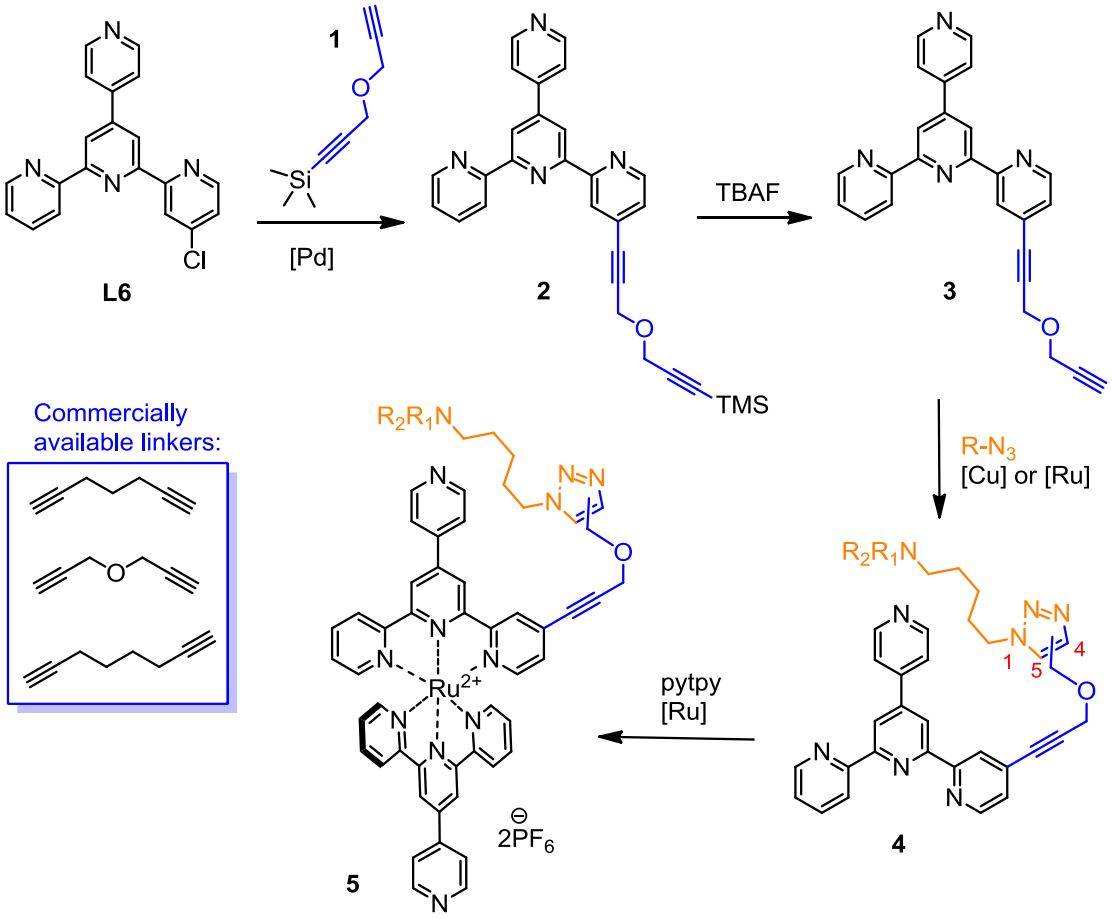

Scheme 2.1: The first synthetic approach via dialkyne towards the side amino chain with triazole

Scheme 2.1 displays the first synthetic strategy via a dialkyne precursor, a linker which would contain two terminal triple bonds. The blue box lists the commercially available ones with 7

and 8 carbons and one which also contains an oxo group. Dialkyne **1**, which has one triple bond protected with a trimethylsilyl group, reacts in the first step with halogen substituted pytpy **L6** in a palladium catalysed Sonogashira cross-coupling reaction. After removal of the TMS protective group, terminal alkyne **3** reacts with the alkylazide in a cycloaddition reaction to give a 1,2,3-triazole **4**, followed by Ru(II) complex **5** formation in the last step. The classic Huisgen 1,3-dipolar cycloaddition gives a mixture of regioisomers **4**. The product formation can be controlled by selection of the catalyst. The copper-catalyzed reaction leads to the 1,4-disubstituted regioisomers. A later developed ruthenium-catalyzed reaction gives the 1,5-disubstituted triazoles.

Due to the fact that the dialkyne linkers could polymerise during the side chain synthesis, we proposed another synthetic route (Scheme 2.2). In this case, 4-chloropytpy **L6** reacts with propargyl alcohol in a palladium catalysed Sonogashira cross-coupling reaction. The synthesized methylene alcohol **6** can then react with a methylene-bromide substituted trizole ring **8** to form the pytpy **4** with the blue "ether-alkyne" linker. Synthesis of the triazole ring **8**, decorated with methylene bromide and a long alkyl amine, starts with nucleophilic substitution of suitable amino alkyl halide or tosylate **7** with alkali azide. Amino alkylazide then reacts with propargyl bromide in a 1,3-dipolar cycloaddition reaction to give a 1,4- or 1,5- substituted 1,2,3-triazole **8**.

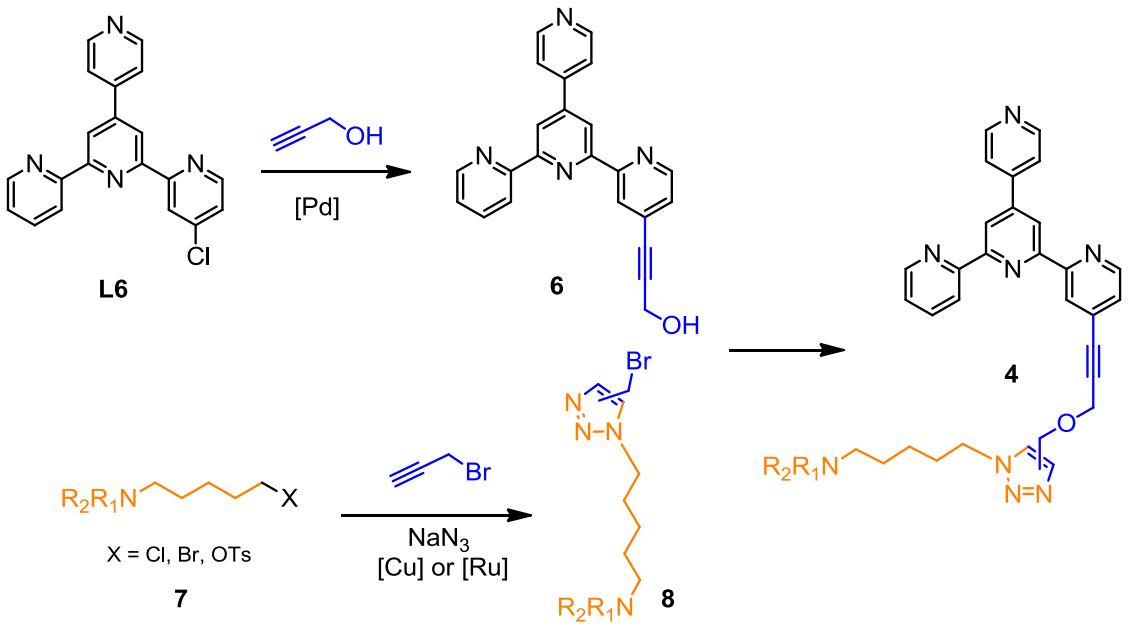

Scheme 2.2: The second synthetic approach via propargyl alcohol towards the triazole side chain

2.2.2 Synthesis of L6 and its alkynylation

4-Chloro substituted tpy **L6** was prepared according to Scheme 2.3. In the first step 4-chloro-2-pyridine carbonitrile was converted to 2-acetyl substituted pyridine **P3.** Addition of methylmagnesium iodide to the nitrile group leads to the formation of an organomagnesium species, which, after acid hydrolysis and neutralisation, is converted to an acetyl group. Purification with a chromatography column (SiO_2, eluted with EtOAc/cyclohexane = 1:2) gives **P3** as pale yellow crystals in high 78% yield as stated in a literature procedure.[1] For the Kröhnke synthetic methodology of pytpy, it was necessary to activate ketone **P3** as its corresponding pyridinium iodide salt **P6**. We used the same procedure as reported in chapter 1 for methyl ester substituted PPI salt **P5**.[2, 3] **P3** was refluxed for 1 hour in pyridine with 1 equivalent of iodine. Product **P6** precipitated out from the reaction mixture as a dark brown powder in nearly quantitative yield and was used for the next step without further purification. Recrystallization attempts of **P6** from hot ethanol containing 5% of activated charcoal led to keto-enol tautomerism, which partly deactivated the PPI salt for the next reaction. In the last step, chalcone **P9** and PPI salt **P6** reacted according to the Kröhnke method and gave **L6** as a grey powder in very high (92%) yield. The product **L6** was confirmed by microanalysis and also from the electrospray mass spectrum which showed peaks at m/z 367.1 for $[M+Na]^+$ and 345.1 for $[M+H]^+$ with intensities of 100% and 86%, respectively.

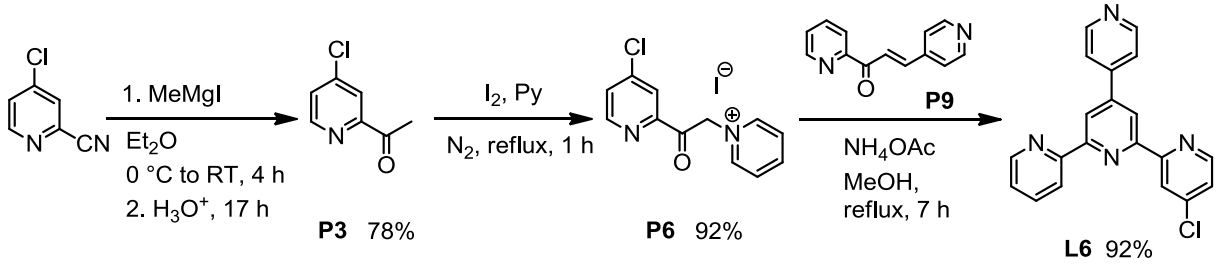

Scheme 2.3: Synthesis of the 4-chloropytpy L6

The Sonogashira cross-coupling reaction was first published by Kenkichi Sonogashira in 1975.[4] It is the formation of a new carbon-carbon bond between a terminal alkyne and an aryl or alkenyl halide. In comparison with the Heck or Suzuki reaction, Sonogashira cross-coupling is revolutionary in affording products under much milder conditions, by using a palladium and copper catalyst simultaneously which increases the reactivity of the reagents

and therefore the reaction can be carried out at ambient temperature. The most commonly used palladium catalysts are $Pd(PPh_3)_2Cl_2$, $Pd(dppp)Cl_2$, and $Pd(dppf)Cl_2$ together with copper(I) iodide as a co-catalyst, where dppp and dppf are diphosphine chelating ligands. Reactions are run under an inert atmosphere, due to the stability of Pd(0) catalysts and with an excess of a base, usually diethylamine or triethylamine, to neutralize the side product - hydrogen halide. Reactivity of aryl chlorides is much lower than of aryl bromides or iodides, therefore our alkynylation of pyterpy chloride **L6** with propargyl alcohol had to be carried out at higher than room temperature (Scheme 2.4., Table 2.1).

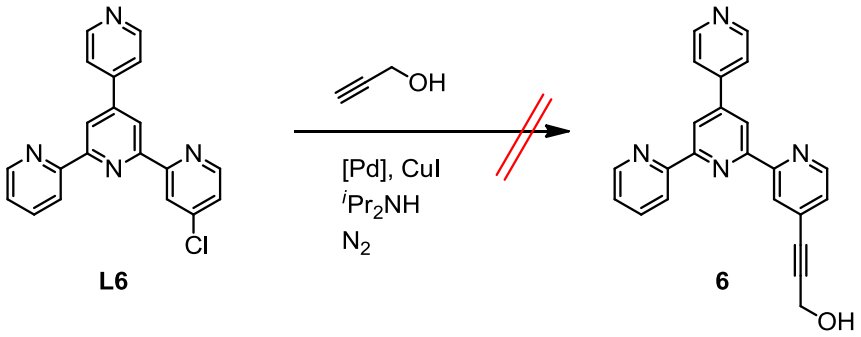

Scheme 2.4: Sonogashira cross-coupling reaction of L6 with propargyl alcohol

Input	μW or hood	T [°C]	Time	[Pd]	Solvent
1	μW	70	45 min	$Pd(PPh_3)_2Cl_2$ (cat.)	THF
2	μW	90	1 h	$Pd(PPh_3)_2Cl_2$ (cat.)	THF
3	hood	100	27 h	$Pd(PPh_3)_2Cl_2$ (cat.)	DMF
4	μW	90	1 h	$Pd(dppf)Cl_2$ (cat.)	THF
5	μW	110	2 h	$Pd(dppf)Cl_2$ (cat.)	toluene
6	μW	140	1.5 h	$Pd(dppf)Cl_2$ (eq.)	toluene
7	hood	110	22 h	$Pd(dppf)Cl_2$ (eq.)	toluene

Table 2.1: Conditions for Sonogashira cross-coupling of L6 with propargyl alcohol

Table 2.1 summarises all applied reaction conditions for alkynylation of **L6** with propargyl alcohol. They vary in reaction temperature, time, palladium catalyst and solvent. There were

also reported conditions for Sonogashira cross-coupling carried out in a microwave reactor, therefore in five cases we applied microwave irradiation and two reactions were done conventionally in a fumehood.[5] As a first attempt, the reaction was done with a catalytic amount of $Pd(PPh_3)_2Cl_2$ in THF and heated in the microwave reactor at 70 °C for 45 minutes (Table 2.1, Input 1). The colour of the reaction mixture turned from brown to dark brown. The reaction was monitored with TLC plates and the product was purified using column chromatography (SiO_2, gradient elution with EtOAc/cyclohexane = 1:2 to 3:1). Two fractions were collected. The first minor one was the product of self condensation of propargyl alcohol and the second major one was recovered starting **L6**, in 70% of the original amount. A ^{1}H NMR spectrum of the second fraction was compared with the ^{1}H NMR spectrum of the starting **L6** and all their signals perfectly overlapped. As a second trial, the reaction temperature was increased to 90 °C and the time extended for one hour. We obtained a product which according to the ^{1}H NMR spectrum was mostly starting **L6**, but we could also observe trace amount of a new aromatic signals.

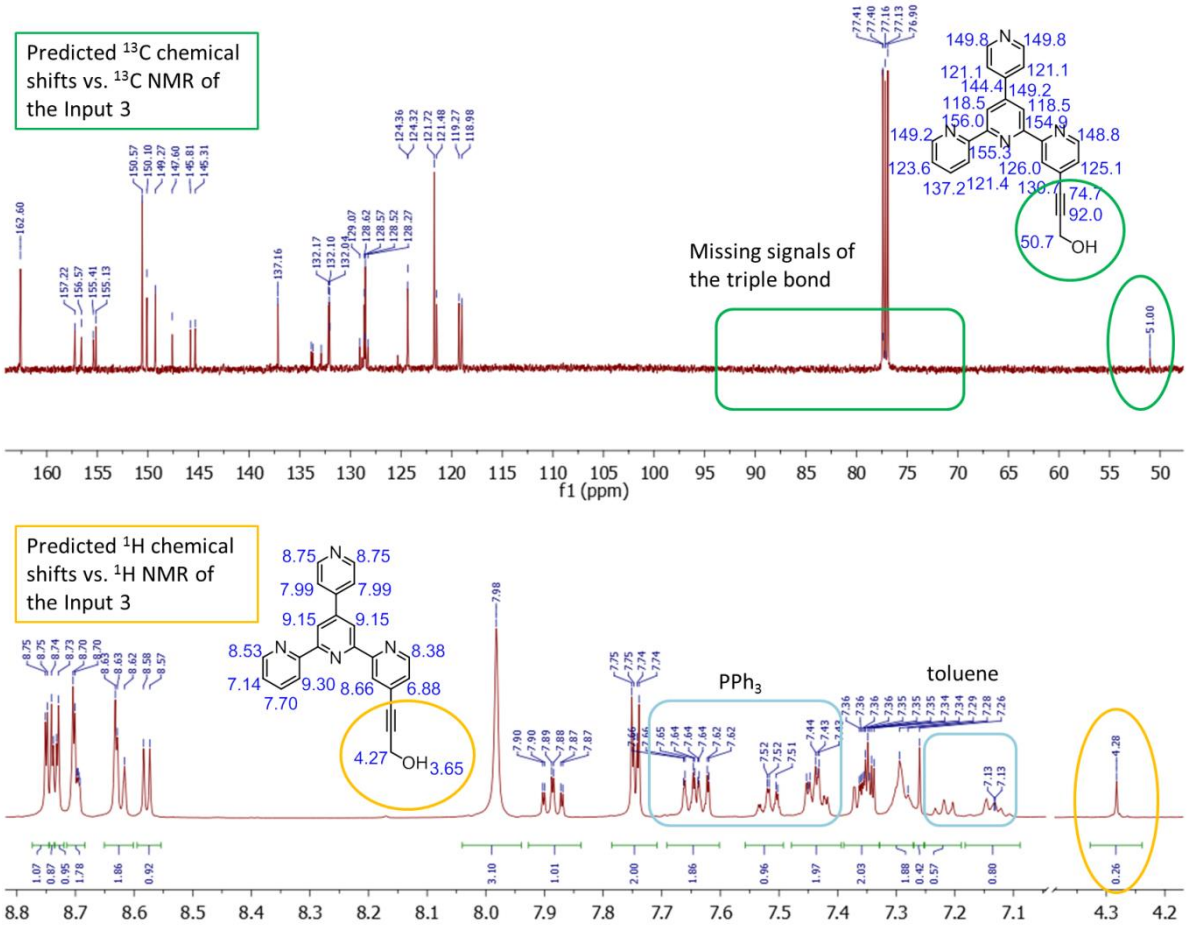

Figure 2.2: ^{13}C NMR (126 MHz, CD_3CN) and ^{1}H NMR (500 MHz, CD_3CN) spectra of the product from the Input 3 vs. predicted chemical shifts of 6

As a third trial the reaction was run in DMF in a fume hood at 100 °C for one day (Table 2.1, Input 3). This time the crude reaction mixture was evaporated, diluted with toluene and extracted with saturated aqueous ammonium chloride to remove copper salts. 1D and 2D NMR spectra were measured. The major signals corresponded to starting **L6**, PPh_3 and solvent but it was also possible to see minor signals of a singlet with a chemical shift δ 4.28 ppm in a ^{1}H NMR spectrum and δ 51 ppm in ^{13}C NMR (Figure 2.2). These signals, according to NMR prediction, could belong to the CH_2 group of the desired molecule **6**. On the contrary, there were missing carbon signals of the triple bond, which were expected between δ 70 – 90 ppm. However, it was hard to tell if they were overlapping with the signal of the solvent at δ 77.16 ppm or if they were missing due to the trace amount of the product. The very low yield did not look promising and alternative methods were therefore tried.

The next four alkynylation attempts were done with $Pd(dppf)Cl_2$ catalyst, which is more efficient for Sonogashira cross-coupling. Input 4 in Table 2.1 is a modification of Input 2. Two equivalents of propargyl alcohol were used instead of 1.1 equivalent and (as already mentioned) a different palladium catalyst. The reaction was monitored with TLC plates (SiO_2, eluting with EtOAc/cyclohexane = 3:1 and EtOAc/MeOH = 10:1). The reaction mixture was purified with extraction from toluene - saturated aqueous NH_4Cl. The ^{1}H NMR spectrum of the product showed again only signals of the recovered **L6** (74% was received back) and a small amount of toluene. Low small intensity singlets at δ 4.28 and 4.60 ppm in the ^{1}H NMR spectrum and a small signal for a CH_2 group with a chemical shift δ 51 ppm in a ^{13}C dept NMR spectrum were observed.

In Input 5 (Table 2.1) 2.4 equivalents of propargyl alcohol and toluene as a solvent were used. The reaction was carried out in the microwave reactor at 110 °C for 2 hours. Starting **L6** was recovered in 68% yield. Once again, low intensity singlets at δ 4.28 and 4.60 ppm in ^{1}H NMR spectrum were observed. The Inputs 6 and 7 in Table 2.1 are modifications of Input 5, but with an equimolar amount of catalyst, because there was a suspicion that the palladium catalyst could have been consumed by coordination to the 4-chloropytpy **L6** in the previous reactions. Input 6 shows that the reaction was run in the microwave reactor at 140 °C for 1.5 hour and Input 7, in a fume hood at 110 °C for 22 hours. Reaction mixtures were extracted from toluene - saturated aqueous NH_4Cl and purified with column chromatography (SiO_2, eluted with EtOAc/MeOH = 10:1). In both cases, several products

were obtained but with unknown structures. Unfortunately the desired product **6** was not obtained, neither was starting **L6** recovered.

2.2.3 Trans-halogenation of L6

Before giving up the alkynylation strategy and finding another linker which would react with 4-chloropytpy **L6** and afford a suitable precursor for building the triazole ring, we decided to try a more reactive substrate for the Sonogashira reaction. Banwell *et al.* reported microwave assisted trans-halogenation of various chloro-, bromo- and trifluoromethanesulfonyloxy- substituted nitrogen-containing heterocyclic systems to corresponding iodo-derivatives by using sodium iodide and acetic anhydride or acetyl chloride as an activating agent.[6] This seemed to be a suitable way to convert **L6** to aryl iodide **9**, which would be a much more reactive substrate, since iodide is a better leaving group than chloride.

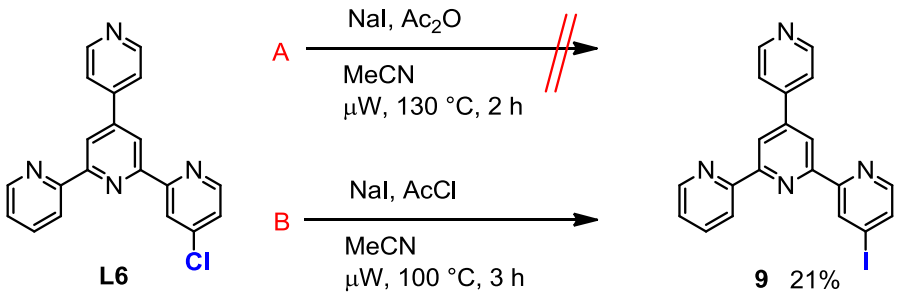

Scheme 2.5: Microwave-assisted trans-halogenation of L6

The first reaction was run under milder conditions (Scheme 2.5, A). **L6** was reacted with 3 equivalents of sodium iodide in acetonitrile in a presence of 2.5 equivalents of acetic anhydride as the activating agent. The brown suspension was heated at 130 °C for 2 hours and colour turned orange. The reaction was monitored with TLC plates and NMR spectroscopy. But after extraction and purification with column chromatography neither product **9** nor starting material was obtained.

Route B in Scheme 2.5 represents more vigorous reaction conditions for less reactive substrates. 4-chloropytpy **L6** with 10 equivalents of sodium iodide and in acetonitrile, activated with 1.5 equivalents of acetyl chloride was heated in a microwave reactor at 100 °C

for 3 hours. The orange reaction mixture was purified with extraction and column chromatography (SiO_2, EtOAc/MeOH = 10:1) to give a grey oil. The NMR spectrum of the product seemed to be identical to that of starting **L6** but sets of signals for both **L6** and **9** in ratio 76:24% were found in ESI MS spectrum. ESI MS shows peaks at m/z 345.1 for $[\mathbf{L6}+H]^+$ and 437.0 for $[\mathbf{9}+H]^+$ with intensities of 100% and 31%, respectively. There were also peaks present corresponding to $[\mathbf{L6}+Na]^+$, $[\mathbf{L6}+K]^+$, $[\mathbf{9}+Na]^+$ and $[\mathbf{9}+K]^+$. As long as the conversion of **L6** to **9** remained non-quantitative, the isolation of the desired molecule **9** could not be achieved.

2.2.4 Ruthenium(II) complexes with L6

Since the trans-halogenation of substrate **L6** does not work as well as reported for other heterocycles in literature,[6] we synthesized its homoleptic and heteroleptic Ru(II) complexes as another option for further alkynylation or alkylation (Scheme 2.6).

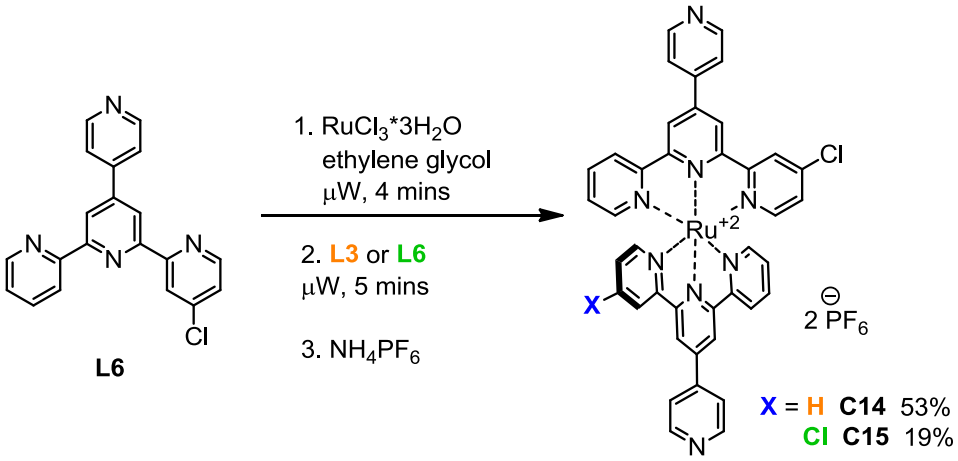

Scheme 2.6: Ruthenium(II) complexes with L6

A mixture of **L6** with $RuCl_3 \cdot 3H_2O$ in ethylene glycol was reacted in a domestic microwave oven at 800W for 4 minutes to form [Ru(**L6**)Cl_3]. Then a second equivalent of **L6** or **L3** was added and the black suspension was heated for 5 minutes more. The product was precipitated out using aqueous ammonium hexafluorophosphate and purified on a chromatography column (eluted with a solvent mixture MeCN/saturated aqueous KNO_3/H_2O = 7:2:2) to give the desired complexes **C14** in 53% and **C15** in 19% yields. Besides the target

molecules, formation of the homoleptic complex **C8** was observed. The second step of complexation was also done in a microwave reactor in ethanol at 150 °C, but a long reaction time of 1 hour or more was needed. For further optimisation one can use silver hexafluorophosphate for activation or a different solvent, such as DMF, which allows one to increase the temperature and therefore shorten the reaction time to 10-20 minutes.

Both complexes were characterised with elemental microanalysis. In the ESI mass spectra of **C14** and of **C15** peaks with characteristic m/z values of 378.1 and 395.1 for $[M\text{-}2PF_6]^{2+}$ (100%) were observed as well as peaks corresponding to the ion $[M\text{-}PF_6]^{+}$ with about 30% intensity.

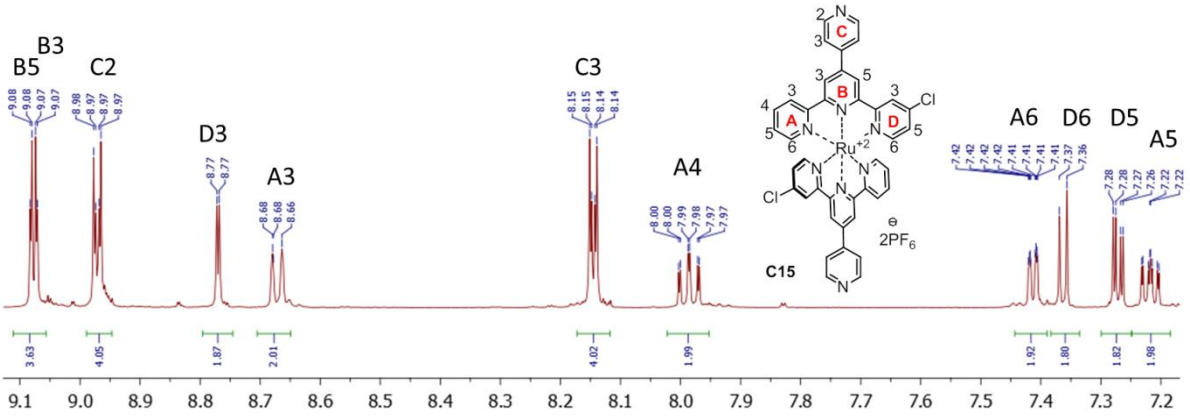

Figure 2.3: ^{1}H NMR (500 MHz, CD_3CN) spectrum of Ru(II) complex C15

Complex	λ_{MLCT} [nm]	λ_{em} (λ_{ex}) [nm]	τ [ns]	QY [%]
C14	490	658 (490)	4	< 1
C15	492	666 (490)	9	< 1

Table 2.2: Photophysical properties of Ru(II) complexes C14 and C15, ($3\cdot10^{-5}$M, CH_3CN)

Table 2.2 summarises the photophysical properties of ruthenium(II) complexes **C14** and **C15** in acetonitrile [$3\cdot10^{-5}$M]. The MLCT absorption maxima were observed at ≅ 490 nm (Figure 2.4), which is a characteristic value for Ru(II) complexes with pytpy ligands. The bands have a higher molar extinction coefficient compared with the methyl ester substituted **C7** (Figure 1.9, Chapter 1). The emission maximum, for excitation wavelength 490 nm, is for both complexes in the characteristic region ~ 660 nm. However both complexes are much less

emissive than **C7** and the emission maximum of the homoleptic complex **C15** is slightly red-shifted in comparison with **C14**.

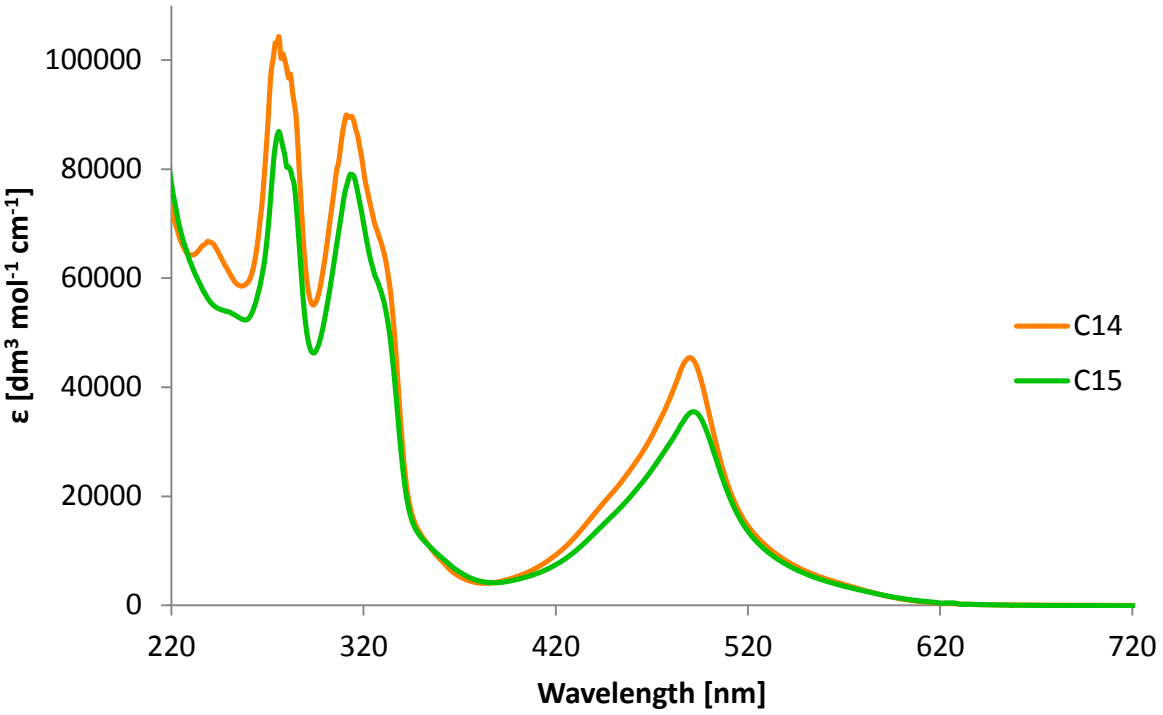

Figure 2.4: Absorption spectrum ($3 \cdot 10^{-5}$M, CH_3CN) of Ru(II) complexes C14 (orange) and C15 (green)

2.3 Pytpy ligands with a side amino-chain linked via an ether

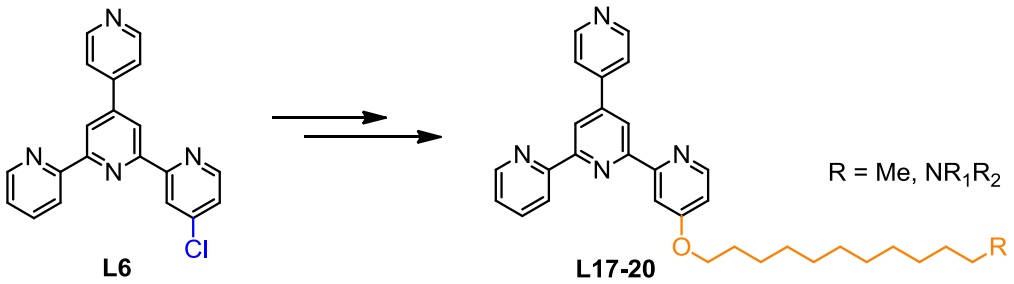

Scheme 2.7: Towards pytpy ligands with an amino-chain linked via an ether unit to the pytpy domain

In section 2.2 we focused on the synthesis of ruthenium(II) complexes with the amino-substituted side chain containing an alkyne unit and a triazole ring. Unfortunately such a ruthenium(II) complex was not successfully prepared. However, a useful application was

found for its precursor, chloro-substituted pytpy ligand **L6**. The chloro group was substituted with an alkoxy or amino-alkoxy group giving a new series of pytpy ligands with a side amino-chain linked via an ether **L17-20** (Scheme 2.7). In this section 2.3, several synthetic strategies will be reported and their results discussed.

2.3.1 Synthetic strategies

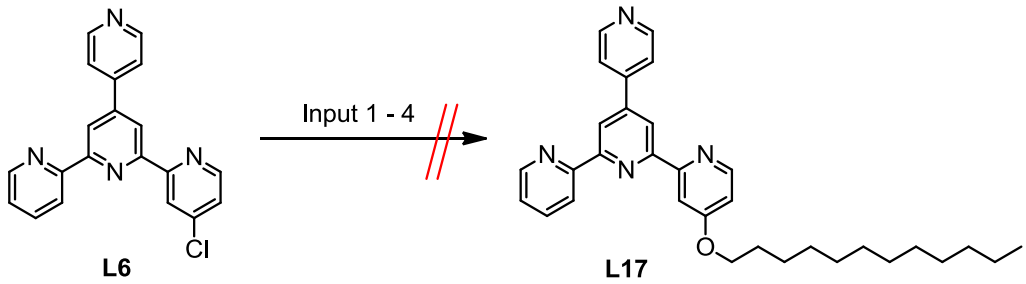

Input	Reaction conditions
1	dodecanol, 2,6-lutidine, toluene, N_2, reflux, 49 h
2	dodecanol, ^{n}BuLi, THF, N_2, 0 °C to RT, 1 h
3	dodecanol, ^{t}BuLi, THF, N_2, 0 °C to RT, 20 h
4	1) AgOTf, toluene, N_2, 80 °C, 40 min 2) dodecanol, toluene, Et_3N, 80 °C, N_2, 20 h

Scheme 2.8: Synthetic strategies towards the dodecyl ether-substituted pytpy L17

A table in Scheme 2.8 summarises four different attempts to synthesize dodecyl oxy-substituted pytpy **L17**, a model alkoxy-substituted pytpy. Dodecanol was used as a suitable commercially available reactant. The first trial to achieve the ether linkage was inspired by work in Chapter 3. Chloro-substituted **L6** was refluxed with dodecanol in toluene in the presence of the base 2,6-lutidine. The reaction process was monitored with ^{1}H NMR spectroscopy. The chemical shift of the first methylene group in ether **L17** was expected to be around δ 4 ppm, considering the fact that in dodecyl ester the chemical shift of this CH_2 group comes at δ 4.44 ppm and in dodecanol at δ 3.69 ppm. However, even after 2 days any signals of the desired product **L17** were not detected, and only peaks of unreacted starting reactants were observed (Input 1 in Scheme 2.8). Another option to synthetize **L17** was via lithium alcoholate (Inputs 2 and 3). Dodecanol was stirred with ^{n}BuLi in dry THF for 15

minutes at 0 °C under an inert atmosphere. This reactive solution of lithium dodecanolate was then stirred for one hour at room temperature with a solution of **L6** in THF. It was possible to see a colour change from bluish to ochre. This reaction was also repeated with ^{t}BuLi and with stirring for 20 hours at room temperature. Reactions were monitored with TLC plates (SiO_2, eluted with EtOAc/MeOH/Et_3N = 60:2:1), and one could observe formation of new bands. However, according to ^{1}H NMR spectra and ESI MS spectra of both crude reaction mixtures, the target molecule **L17** was not prepared. Being aware of the low reactivity of **L6** and difficulties with the conversion to the more reactive aryl iodide, we considered an option to convert **L6** to more reactive trifluoromethanesulfonate, using the formation of silver chloride precipitate is the driving force for the process (Input 4 in Scheme 2.8). A brown suspension of **L6** and silver triflate in toluene was heated at 80 °C for 40 minutes in the dark under an inert atmosphere. Dodecanol and triethylamine were added and the reaction mixture was heated for 20 hours at 80 °C. Though the monitoring with TLC plates looked promising, the ^{1}H NMR spectrum did not reveal any signals of the desired **L17**, and ESI MS spectrometric data were also inconclusive.

There are two options for the synthesis of an aryl-alkyl ether (Scheme 2.9). The first one, discussed in Scheme 2.8, starts with an aryl halide which reacts with alkoxide ion, prepared immediately before the reaction, or generated *in situ* from alcohol. Another common option involves an aryl oxide ion, in our case generated from aryl alcohol **10**, which reacts with an alkylating agent (alkyl halide).

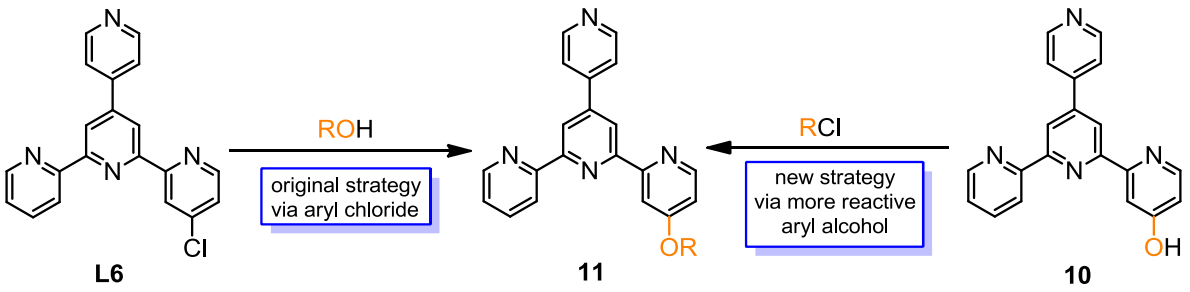

Scheme 2.9: Strategies towards alkoxy-substituted pytpy 11

There were two options for the synthesis of hydroxy-substituted pytpy **10**. One is synthesis from simple precursors, such as 2-acetylpyridine, involving many steps. The other one, worth trying first, involved substituting the chloro group in **L6** by a hydroxyl group. We tried a

conversion method involving trialkylborate (Scheme 2.10). **L6** was stirred with ^{n}BuLi in THF at -80 °C for 3 hours under an inert atmosphere. Triisopropyl borate was added and the reaction mixture was stirred overnight, allowed to slowly warm up to room temperature and the solvent removed in vacuo. For the last step we had two options for quenching of the crude reaction mixture, which currently was in a state of aryl diisopropyl borate. If we used HCl (aq.), we would obtain a pytpy substituted with boronic acid, pytpy-B(OH)$_2$. In addition to this, the nitrogen atoms of the pendant pyridyl positions might be protonated in the presence of HCl. Therefore, a combination MeOH/H_2O_2 (2:1) was used, to directly lead to hydroxy pytpy **10**. The residue from the crude reaction mixture was dissolved in methanol, cooled in an ice bath, and H_2O_2 (30%) was added. The mixture was stirred at 0 °C for 2 hours. Solvent was then evaporated and the residue extracted with DCM - $NaHCO_3$ and water giving a yellow solid after evaporation. In the electrospray mass spectrum, two major peaks were observed. A peak with *m/z* = 326.2 with 37% intensity, which we could assign to $[M]^+$ with M = **10**. However, this was just a minor peak. The other was the base peak with *m/z* = 423.2, which could belong to $[M\text{-}Me]^+$ with M = pytpy-B(O^{i}Pr)$_2$, an intermediate in Scheme 4.4 before quenching of the reaction mixture. However, no isopropyl signals were observed in the ^{1}H NMR spectrum.

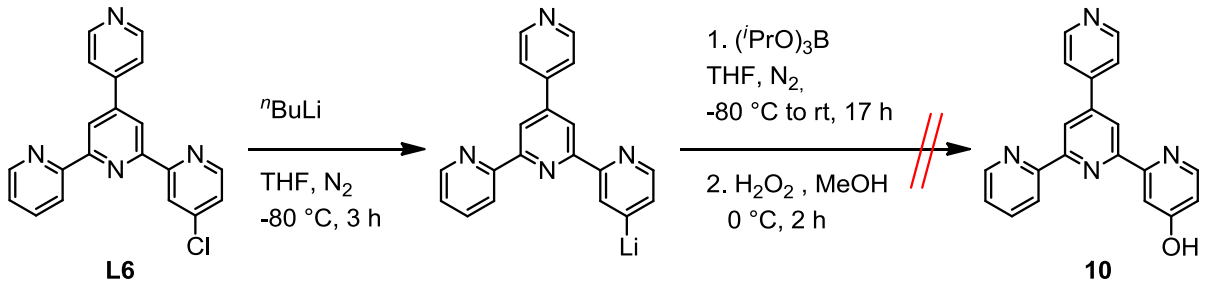

Scheme 2.10: Conversion of L6 to hydroxy-substituted pytpy 10 via trialkylborate

Another option to synthesize compound **10** was reduction of the methyl ester-group of **L2** to the corresponding methylene alcohol **12** (Scheme 2.11).[7] A suspension of **L2** with $LiAlH_4$ in THF was refluxed for 5.5 hours under an inert atmosphere. The reaction mixture was then cooled, placed in an ice bath and stirred overnight with sodium sulfate decahydrate. This was filtered and the yellow solution evaporated to dryness. In the electrospray mass spectrum, a peak with *m/z* = 363.2 (assigned to $[M+Na]^+$) with 75% intensity was observed.

However, the ^{1}H NMR spectrum indicated that the product was very impure. Instead of attempting purification, we focused on finding harsher conditions for the etherification of **L6** (Scheme 2.12).[8]

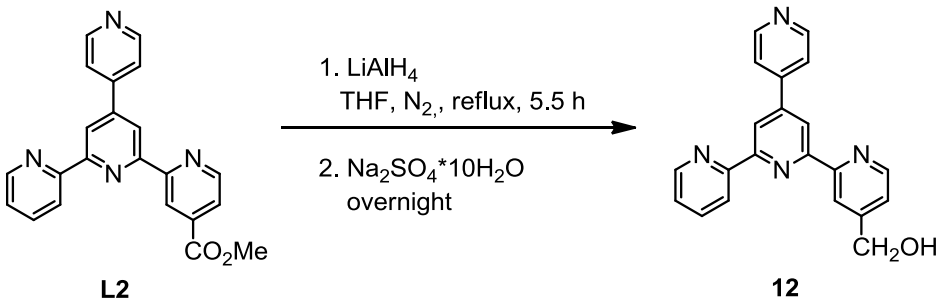

Scheme 2.11: Reduction of the methyl ester group of L2 to methylene alcohol

In 2001, Halcrow *et al.* reported successful harsh conditions of etherification of 4'-chloro-2,2':6',2''-terpyridine, which was a useful inspiration for the etherification of **L6** (Scheme 2.12).[8] Freshly ground potassium hydroxide was suspended in DMSO, to which **L6** and dodecanol were added and heated at 60 °C for 19 hours. This reddish-brown solution was then cooled to room temperature. Addition of ice-cold water gave a brownish mud-like precipitate, which was collected on a frit and washed with water, giving the desired model ligand **L17** as a brown solid in 49% yield.

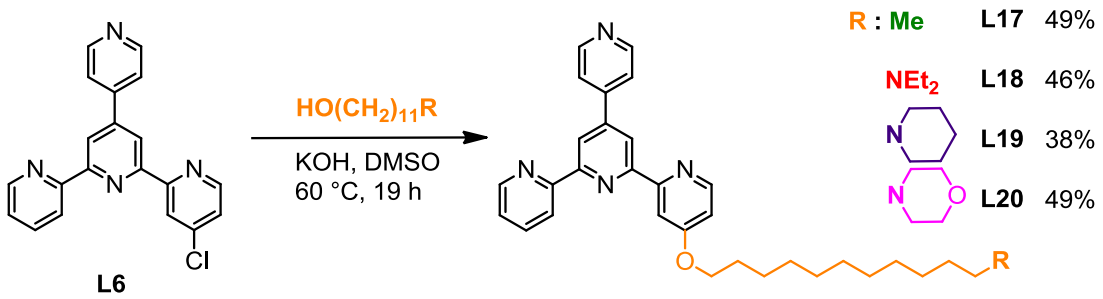

Scheme 2.12: Successful harsher conditions towards alkoxy-substituted pytpy ligands L17-20

The same reaction conditions were applied to the synthesis of amino ethers **L18-20**, where we used amino alcohols **P16-18** with diethyl amine, piperidine or morpholine units (synthesis[7] in Scheme 1.11 and 3.10). During work up, **L18-20** formed as fine precipitates, which were very difficult to separate by filtration. Therefore these products were purified by extraction with chloroform-water. A large amount of water during extraction was necessary

for DMSO removal. However, a certain amount (10-50%) of unreacted alcohol was always detected, no matter which purification technique was used. Even purification on a chromatography column did not help to remove all the alcohol, which tended to elute together with products **L17-20**. However, this fact does not matter for complexation of the ligands, but isolation of pure products was crucial for further analysis. Therefore elemental analysis were not measured for any of **L17-20**.

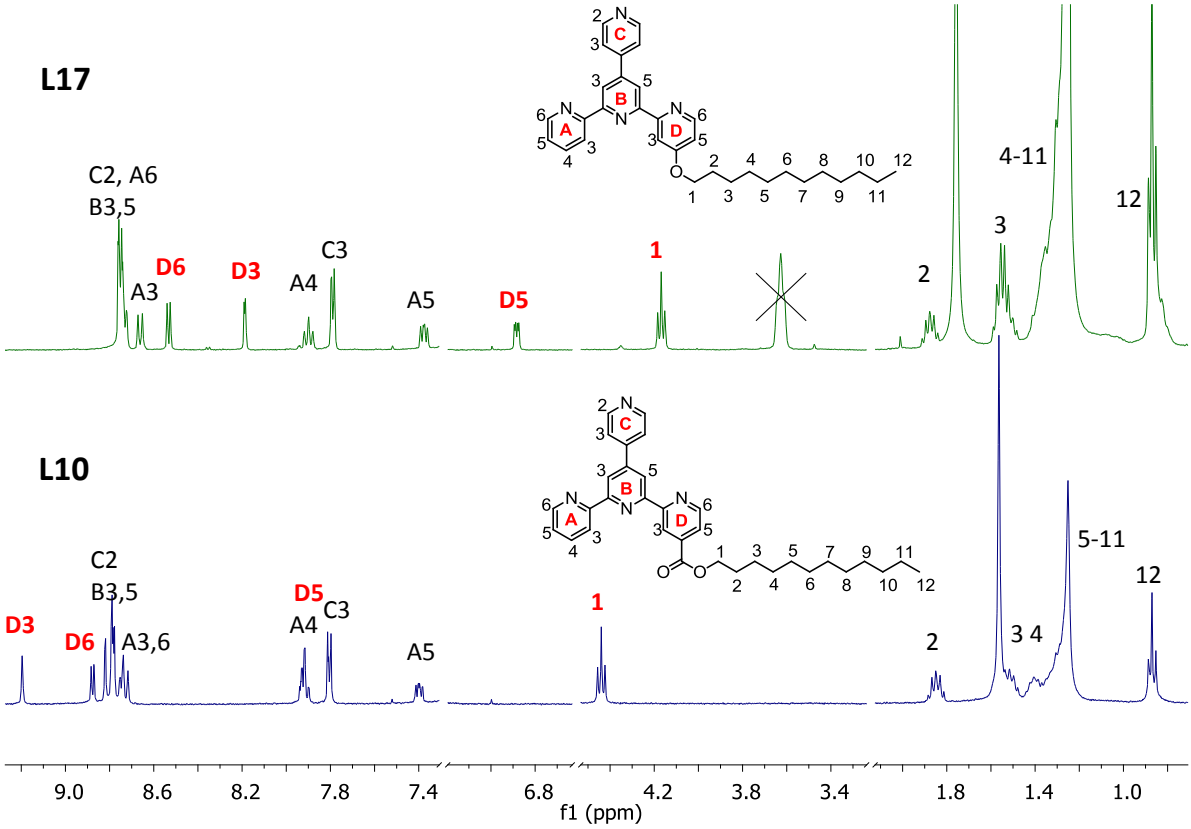

Figure 2.5: ^{1}H NMR (400 MHz, $CDCl_3$) spectra of ester L10 (dark blue) and ether L17 (green)

Figure 2.5 compares the ^{1}H NMR spectra of dodecyl ether-substituted **L17** (green) and dodecyl ester **L10** (blue). In the aromatic region it is possible to observe the characteristic shift of protons of the pyridyl unit **D** to the higher magnetic field, caused by the electron donating effect of the alkoxy group, in comparison to the electron withdrawing effect of the ester group. The same effect is observed in the aliphatic region. Methylene group **1** in the ester group of **L10** has a chemical shift δ 4.43 ppm, and the methylene group **1** in the ether **L17** is shifted to δ 4.15 ppm, as expected. Around δ 3.6 ppm is an impurity peak of unreacted starting dodecanol. In the electrospray mass spectra of **L17-20**, peaks assigned to $[M+Na]^{+}$

with 100% intensity and also peaks assigned to $[M+H]^+$ and $[M+K]^+$ with intensity 20-50% were observed.

Conclusion

We successfully synthesized and fully characterised chloro-substituted pytpy ligand **L6**. Unfortunately we did not manage to fulfil the proposed strategy to prepare the amino-substituted side chain bearing an alkyne and triazole ring. However, another application was found for **L6**, namely the synthesis of ligands with an amino-substituted side chain linked via an ether **L17-20** and also their ruthenium(II) complexes (Section 2.3 and Chapter 5).

Literature

1 Busto, E.; Gotor-Fernández, V.; Gotor, V. *Tetrahedron: Asymmetry*, **2006**, *17*, 1007–1016.

2 Mikel, C.; Potvin, P. G. *Polyhedron*, **2002**, *21*, 49-54.

3 Eryazici, I.; Moorefield, C. N.; Durmus, S.; Newkome, G. R. *J. Org. Chem,*. **2006**, *71*, 1009.

4 Sonogashira, K.; Tohda, Y.; Hagihara, N. *Tetrahedron Lett.,* **1975**, *16*, 4467–4470,

5 Vicente, J.; Gil-Rubio, J.; Barquero, N.; Jones, P.G.; Bautista, D. *Organometallics*, **2008**, *27*, 646-659.

6 Bissember, A. C.; Banwell, M. G. *J. Org. Chem.,* **2009**, *74*, 4893-4895.

7 Wetter, W. P.; De Witt Blanton, C. Jr. *J. Med. Chem,.* **1974**, *17*, 620-624.

8 Liu, X.; McInnes, E. J. L.; Kilner, C. A.; Thornton-Pett, M.; Halcrow, M. A. *Polyhedron,* **2001**, *20*, 2889-2900.

Chapter 3

4'-(4-Pyridyl)-2,2':6',2''-terpyridine ligands with a side amino-chain linked via an ester

3.1 Introduction

In Chapter 1 we focused on the synthesis of ruthenium(II) complexes with pytpy ligands containing a long side amino-chain, which was introduced into the molecule via trans-esterification from methyl ester-substituted complexes. This approach afforded such Ru(II) complexes in quite low yields. Therefore, we decided to investigate a synthetic route in which the long side amino-chain was linked via an ester attached to the pytpy ligand (Scheme 3.1). In this chapter, we report several synthetic strategies and discuss their relative merits.

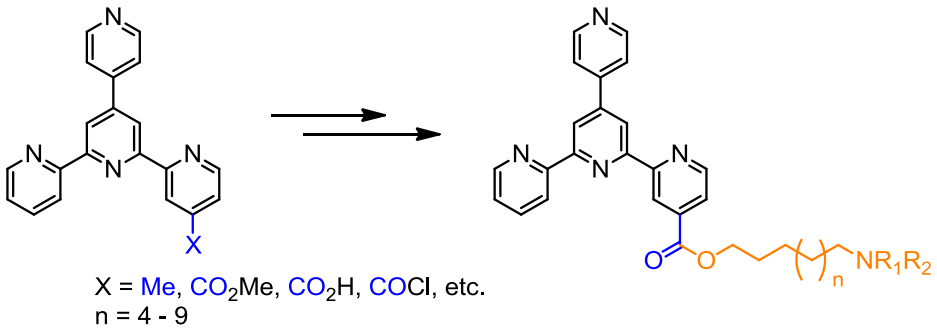

Scheme 3.1: Towards pytpy ligands with an amino-chain linked via an ester

3.2 Results and Discussion

3.2.1 Synthetic strategies

Scheme 3.2 displays all the proposed routes **B-E** to synthetize pytpy ligands with the long side amino-chain linked via an ester **L10-14** along with the original approach **A** from Chapter 1. Route **B** starts from methyl ester substituted pytpy **L2**, which is hydrolysed to a

free carboxylic acid **L8**, a suitable precursor for a wide range of esters and amides. Route **C** represents a "one-pot" esterification of **L8** by an amino-alcohol mediated by DCC.[1, 2] Option **D** is a two-step reaction in which **L8** is converted to the acid chloride of the carboxylic acid and then to an ester.[3, 4, 5] There is also a direct possibility **E**, trans-esterification of the methyl ester substituted pytpy **L2** to **L10-14**. Route **F** represents another option to obtain the carboxylic acid-substituted pytpy **L8**. 4-Picoline is acetylated in the 2-position, then activated as a PPI salt, and with the Kröhnke synthetic method, the methyl substituted pytpy **L7** is obtained. After reaction with an appropriate oxidation agent,[10] this will lead to carboxylic acid **L8**.[6]

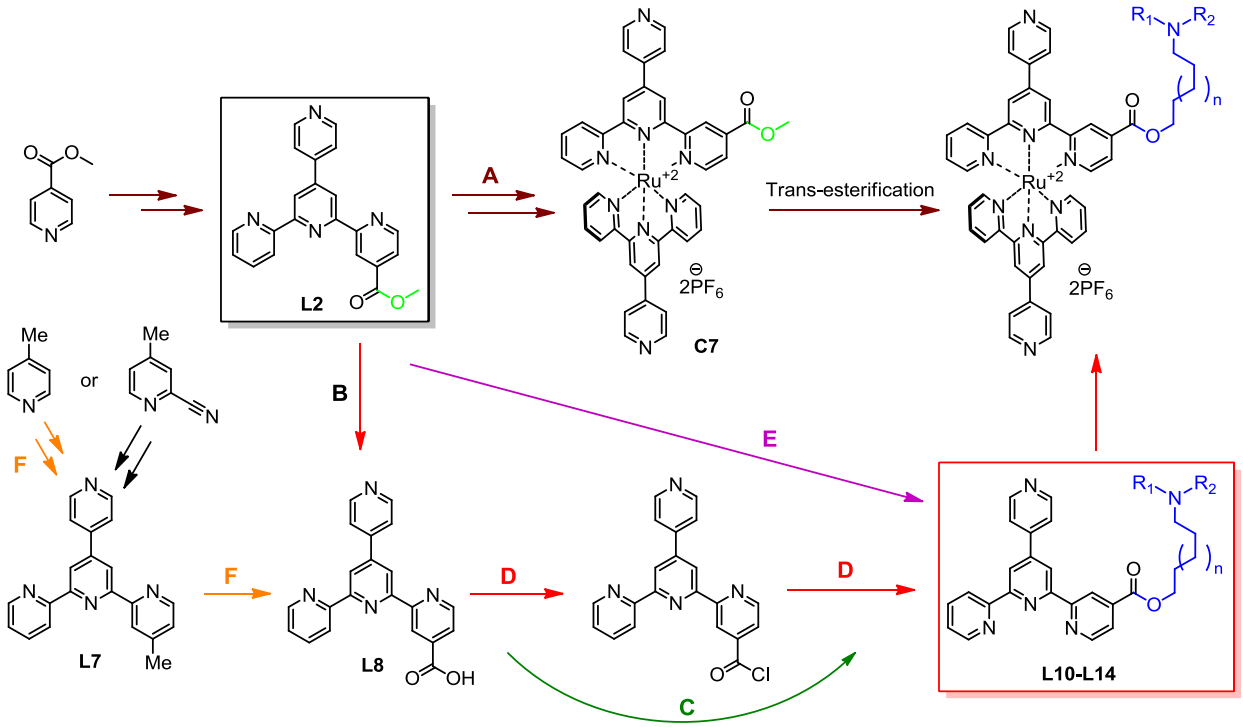

Scheme 3.2: Synthetic strategies towards the pytpy ligands with an amino-chain linked via an ester

3.2.2 Synthesis of the methyl-substituted pytpy L7

Methyl-substituted ligand **L7** was synthesized using strategy **F** (Scheme 3.2). Besides **L2**, **L7** was meant to be another source of carboxylic acid-substituted pytpy **L8**, a suitable precursor for all pytpy ligands with an amino chain linked via an ester **L10-14**. **L7** would be oxidized with strong oxidizing agent (e.g. $KMnO_4$)[10] to **L8** (Scheme 3.2, route **F**).

For the synthesis of **L7**, the same Kröhnke methodology was used as for the methyl ester-substituted ligand **L2** (Scheme 3.3).[7-9] Commercially available 4-picoline was acetylated[7, 8] in

the 2- position and the product **P4** was separated with column chromatography from the 2,3-, 2,5- and 3,5-bisacetylated side products. The formation of the side products was observed on TLC plates (SiO_2, eluted with ethylacetate/cyclohexane = 1:2). **P4** was isolated as yellow needle-like crystals in low 13-24% yields. The yields of **P4** were always so low, in comparison with methyl ester substituted **P2** (66%, Scheme 1.4), due to two facts: 1) methyl is an electron donating group, *ortho*- and *para*-directing, however CO_2Me is an electron withdrawing group and *meta*-directing, 2) in case of CO_2Me group, *ortho*- positions are actually partly sterically hindered in comparison with small size of the methyl group. However, the problem of EDG and EWG groups is the main reason, why the desired **P4** is just the minor product alongside of the bisacetylated side products.

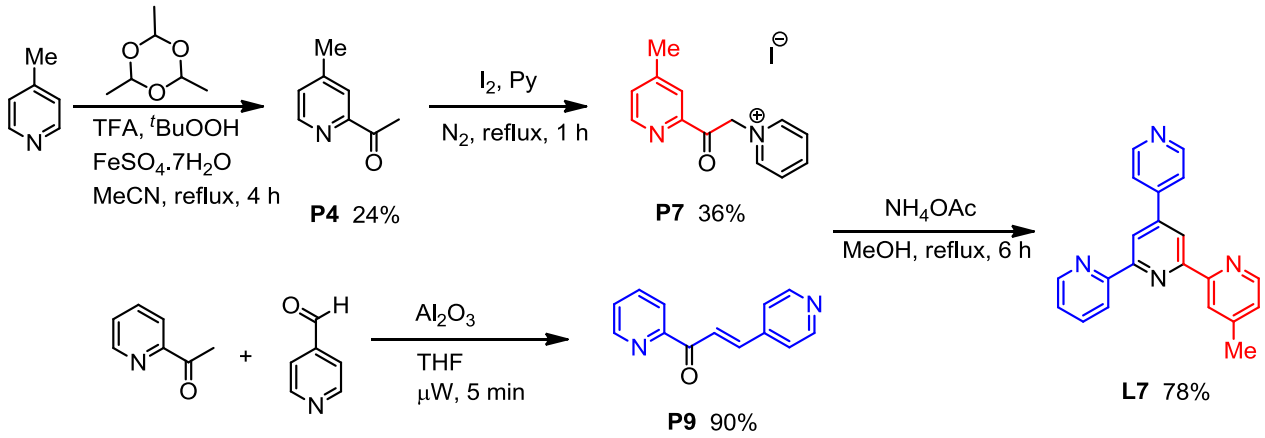

Scheme 3.3: Synthetic approach to obtain L7 via methyl-substituted PPI salt P7

The conversion of 2-acetyl-4-methylpyridine **P4** to the corresponding pyridinium salt **P7** was performed as reported in the literature for 2-acetylpyridine or 2-acetylisonicotinate **P2** (Scheme 3.3).[7] However, the synthesis of the methyl-substituted PPI salt **P7** was not as easy as in the case of the methyl ester-substituted PPI salt **P5** or the chloro-substituted PPI salt **P6** (74% and 92%, respectively) and we obtained **P7** as a black powder in only 9 - 36% yield. Chalcone **P9** (Chapter 1, Scheme 1.5) [9] was used with **P7** for the synthesis of methyl-substituted ligand **L7** via Kröhnke methodology. In the ^1H NMR spectrum of PPI salt **P7** many impurities were observed, which were difficult to separate, and we only obtained impure ligand **L7**, even after recryctallization.

Due to the difficulties with the synthesis and purification of the PPI salt **P7**, preparation of **L7** the other way round seemed to be worth trying (Scheme 3.4). The methyl group would be

introduced into the ligand **L7** via the methyl-substituted enone **P10**, which, when treated with PPI salt **P8** via Kröhnke methodology would give **L7**.

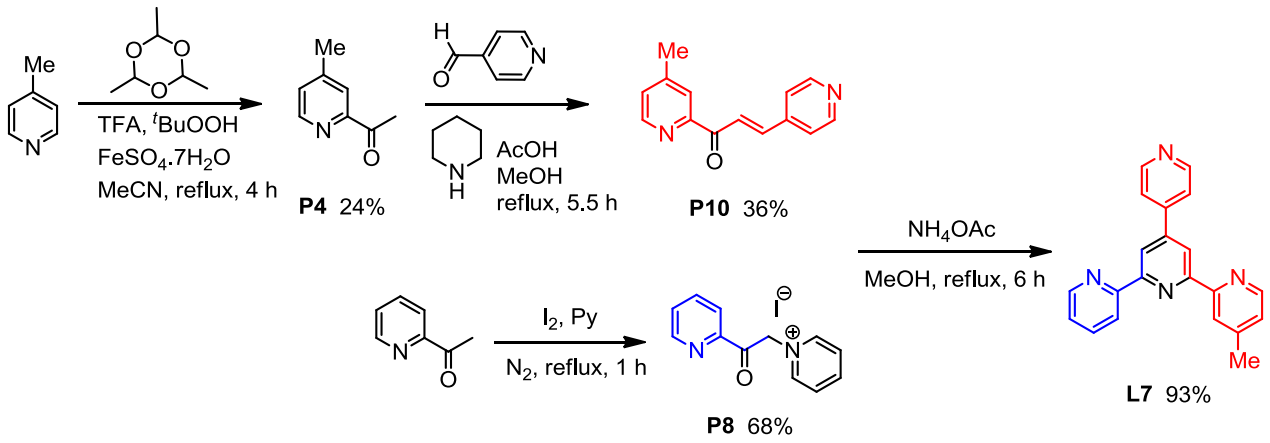

Scheme 3.4: Synthetic approach to obtain L7 via methyl-substituted enone P10

For the synthesis of methyl-substituted enone **P10**, the same microwave assisted reaction conditions were applied as those successfully used for the synthesis of **P9** in the Chapter 1 (Scheme 3.5, green route). In 2006, Newkome reported the synthesis of various substituted azachalcones prepared by the Claisen-Schmidt aldol condensation by using microwave irradiation with a small amount of solvent in the presence of Al_2O_3 as a catalyst and solid support.[9] However, in the case of **P10**, the product was obtained in very low yield (12%) along with unreacted starting aldehyde and ketone. Krebs reported another easy access to azachalcones, involving piperidinium acetate, which affords the product as orange crystals in 30-40% yield.[6] Using this approach, enones **P9** and **P10** were prepared as analytically pure pale orange crystals in 26% and 36% yield, respectively (Scheme 3.5, pink route).

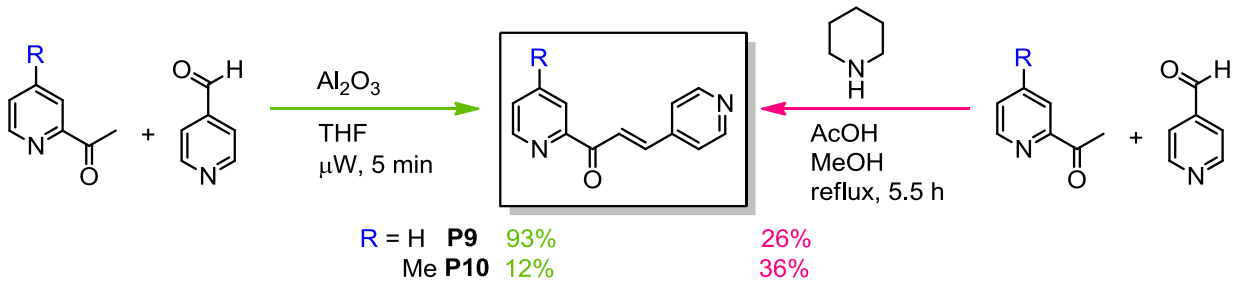

Scheme 3.5: Synthesis of enones P9 and P10 using microwave oven or piperidinium acetate

Figure 3.1 compares the ^{1}H NMR spectra of azachalcones **P9** (red) and **P10** (blue). We could observe two characteristic doublets at δ 8.42 and 7.77 ppm with a large coupling constant ($J_{A,B}$ = 16.1 Hz), typical for a trans double bond. In the ^{1}H NMR spectrum of **P10**, it is possible to observe the influence of the methyl group on the protons labelled **3**, **5** and **6**, which are shifted to lower ppm values in comparison with **P9**. In the electrospray mass spectrum of **P10**, peaks with *m/z* = 225.1 (assigned to $[M+H]^{+}$) with 100% intensity, and 247.0 (assigned to $[M+Na]^{+}$) with intensity 9% were observed.

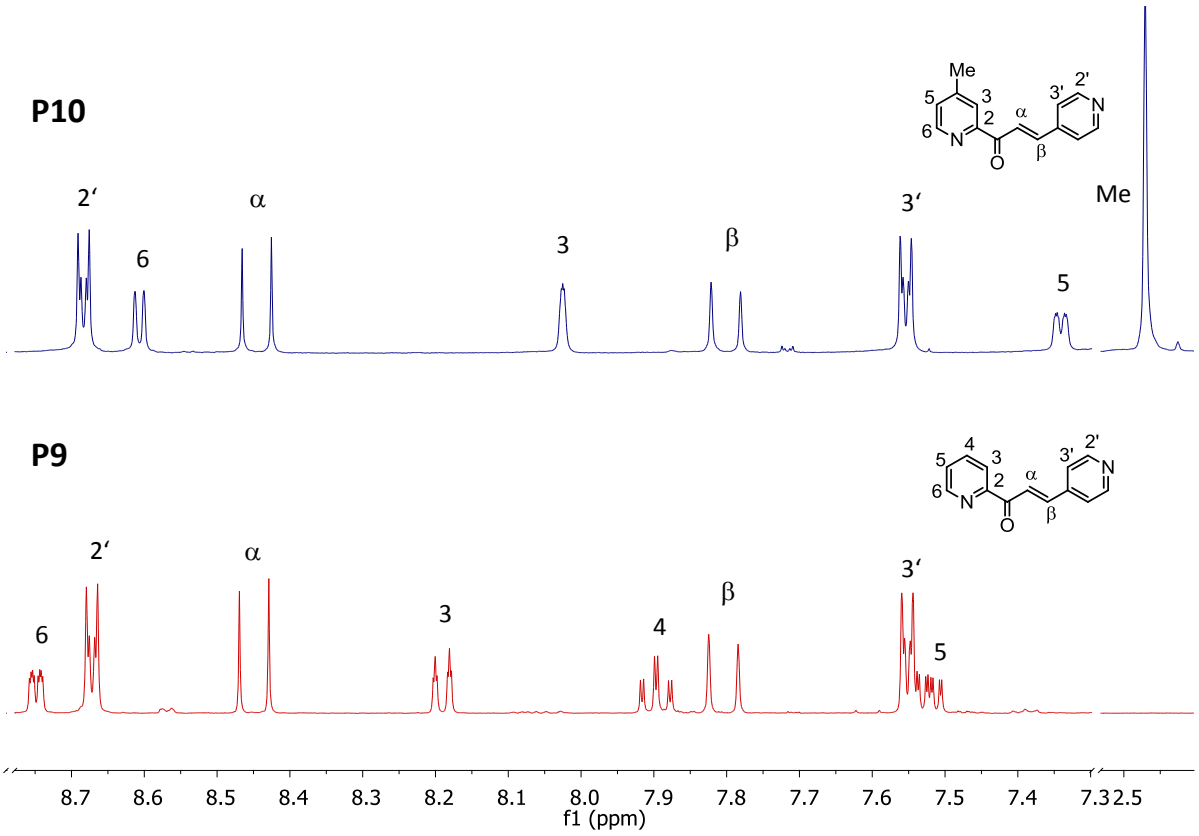

Figure 3.1: Comparison of ^{1}H NMR (400 MHz, $CDCl_3$) spectra of azachalcones P9 (red) and P10 (blue)

Following the reaction of the enone **P10** with Kröhnke's reagent **P8** (consists of pyridinium iodide salt of 2-acetylpyridine) in the presence of an excess of ammonium acetate led to the desired methyl-substituted ligand **L7** (Scheme 3.4). The product precipitated out from the reaction mixture as a pale brown powder in 93% yield. In the MALDI TOF mass spectrum of **L7**, a peak with *m/z* = 324.9 (assigned to $[M]^{+}$) with intensity 78% was observed.

Figure 3.2 shows a comparison of the ^{1}H NMR spectra of the pytpy ligand **L3** (red) and CO_2Me-substituted pytpy **L2** (green), chloro-substituted **L6** (cyan) and Me-substituted **L7** (purple). The influence of the electron-donating and electron-withdrawing substituents on

the chemical shift of protons (red letters) of the pendant pyridyl ring **D** can be observed. The methyl ester substituent of **L2** (green) is typically electron-withdrawing by resonance, therefore all **D**-protons are shifted to higher ppm. However, the methyl substituent of **L7** (purple) is electron-donating by inductive effects, so the **D**-protons are shifted to lower ppm values. The chloro-substituent of ligand **L6** (cyan) is electron-withdrawing inductively but electron-donating through resonance. After combining these two effects, one observes that the **D**-ring protons of **L6** have similar chemical shifts as the **A**-ring protons (Figure 3.2).

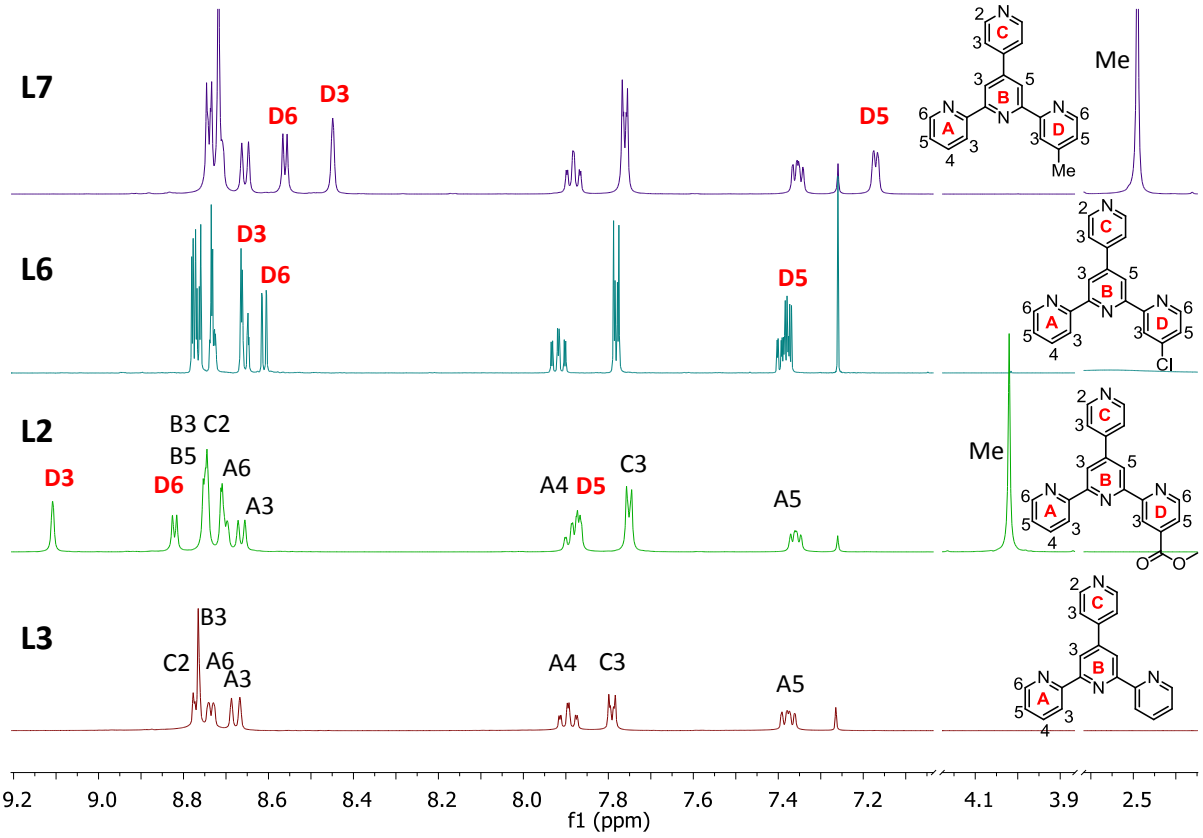

Figure 3.2: Comparison of the ^{1}H NMR (500 MHz, $CDCl_3$) spectra of substituted pytpy ligands L3 (H, red), L2 (CO_2Me, green), L6 (Cl, cyan) and L7 (Me, purple)

We decided not to continue with the further oxidation of **L7** to **L8**, because synthetic routes **B** and **D** (Scheme 3.2) appeared to a better choice. Therefore, we focused on tuning the reaction conditions in routes **B** and **D**. We also had to consider the fact that synthese of precursors **P2**, **P5** and **P9** (Scheme 1.4, 1.5) gave the products in much higher yields (66-93%) in comparison with the synthese of precursors **P4**, **P7** and **P8** (24-36%), which are necessary for the synthese of **L2** and **L7**, respectively.

3.2.3 Synthetic strategies C and D

For synthetic strategy **B** (Scheme 3.2), conversion of the methyl ester-substituted **L2** to the free acid **L8** were used the same reaction conditions as those reported by Krebs (Scheme 3.6).[6] A mixture of **L8** with 1M aqueous NaOH was refluxed overnight in methanol and the pH adjusted with HCl (0.5M) to a value of ≅ 3.5-4.0. A white mud-like precipitate formed, and this was collected on a frit, washed with water and air dried. The product **L8** was isolated as an off-white powder in nearly quantitative yield and used for the next step without any further purification.

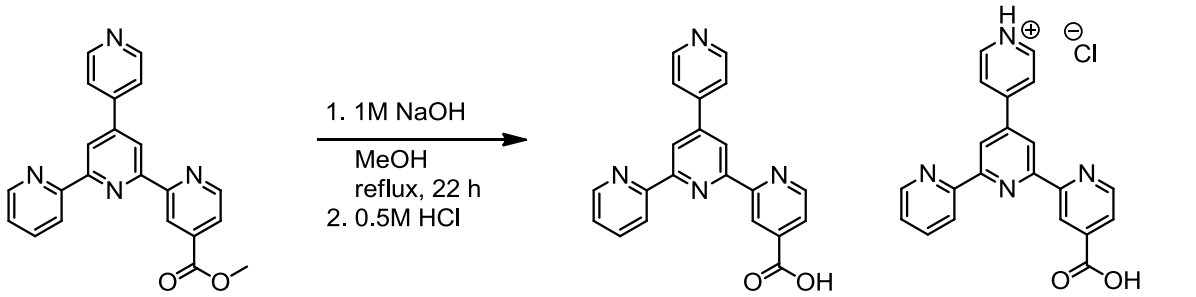

Scheme 3.6: Hydrolysis of the methyl-ester substituted L2 to carboxylic acid L8

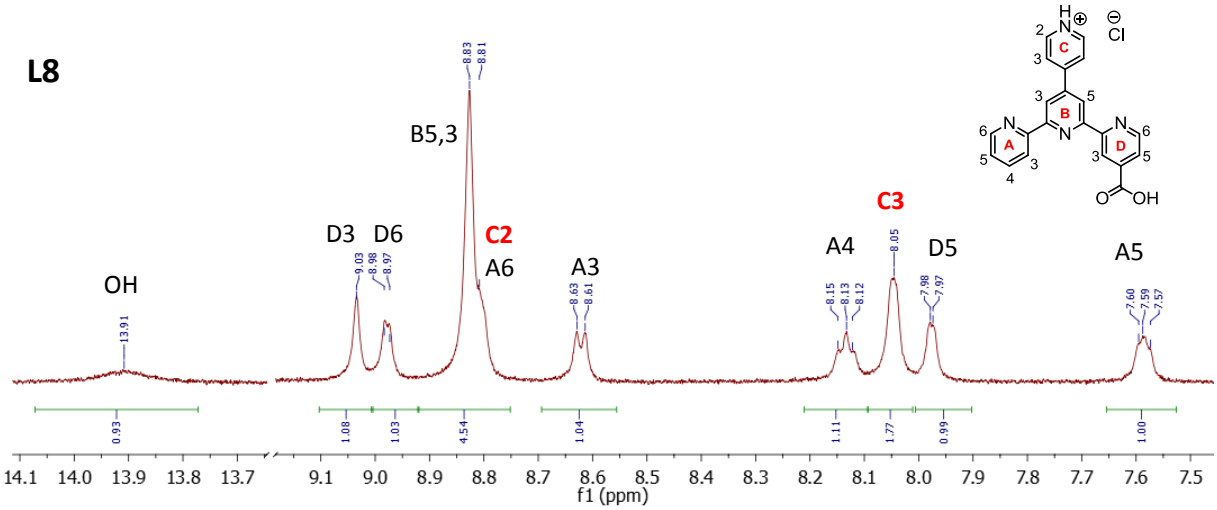

Figure 3.3: ^{1}H NMR (400 MHz, DMSO-d_6) spectrum of L8

An electrospray mass spectrum was recorded and microanalysis measured, and we found that the product **L8** had been isolated in its protonated form with a chloride counterion (Scheme 3.6). In the MALDI TOF mass spectrum of **L8**, a peak with *m/z* = 780.2 (assigned to

[2M]$^+$) with intensity 100% was observed, proving a presence of H^+ and Cl^-. Only a small peak 354.1 (assigned to [M]$^+$ of the neutral form **L8n**) with 5% intensity was found. Results from the elemental analysis were not possible to fit for the expected theoretical values of the neutral form (**L8n**). However, the experimental data from microanalysis fitted well for **L8**. 1D and 2D NMR spectra were measured and we could see that the protonation happens on the pendant pyridyl unit **C** (Figure 3.3). Protons labelled **C2** and **C3** are shifted to lower magnetic field, which is characteristic for N-protonated and N-alkylated pyridyl unit. The ligand **L8** was synthesised several times and we always observed a slightly different chemical shift of protons labelled **C2** and **C3**, according to the amount of the protonated form **L8** vs. the neutral form. Around δ 13.9 ppm is possible to see a broad signal for the proton from the COOH group.

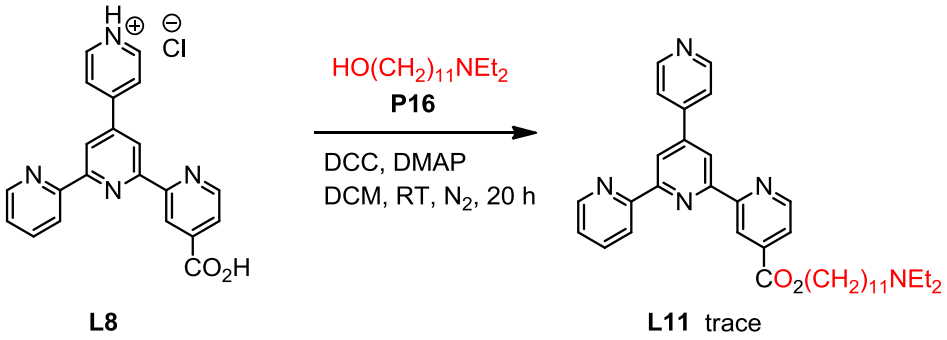

L8 **L11** trace

Scheme 3.7: Steglich reaction – direct one step esterification of carboxylic acids

One option to synthesize the pytpy ligand with a long side amino-chain is a direct esterification of the carboxylic acid substituted ligand **L8** as reported by Steglich (Scheme 3.2, route **C**).[2] This is a one-pot esterification of a carboxylic acid by alcohols, mediated by *N,N'*-dicyclohexylcarbodiimide (DCC) and catalysed by dimethylamidopyridine (DMAP). A side-product is dicyclohexylurea (DCU). Reaction conditions are mild, because the reaction usually takes place at room temperature. Typically, the solvent is dichloromethane (Scheme 3.7).[1] After performing the Steglich reaction with substrate **L8** and measuring the ^{1}H NMR spectrum of the crude reaction mixture, we observed characteristic signals of the side product DCU and signals of unreacted 11-(diethylamino)undecan-1-ol **P16**, but only minor signals which could belong to the desired product **L11**. The DCU was then filtered off as a white powder and the rest was purified using a short chromatography column (Al_2O_3, eluted with EtOAc/cyclohexane = 2:1). Two bands were isolated. The first one was **L11**, however still very impure and in a trace amount. The second main fraction was the symmetrical

unsubstituted pytpy **L3**, a product of decomposition of **L8**. It appears that the failure of the Steglich reaction with substrate **L8** lies in poor solubility in most solvents.

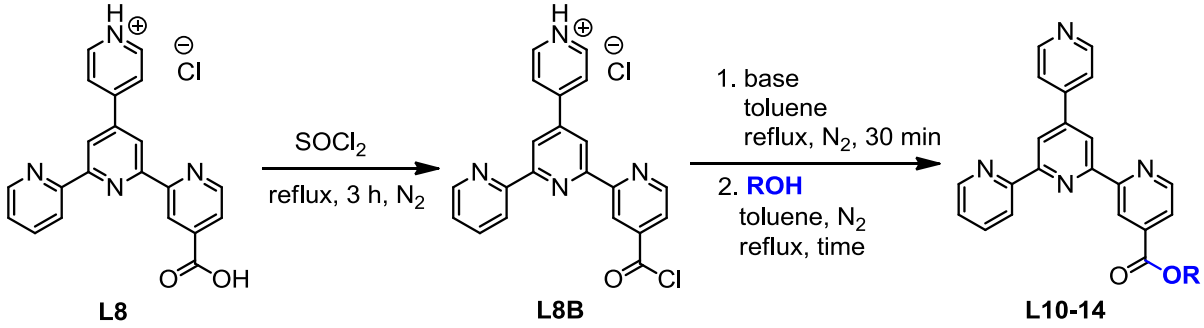

Scheme 3.8: Esterification of L8 via the corresponding acid chloride

Synthetic strategy **C** was abandoned and we focused on strategy **D** (Scheme 3.2). This involves esterification of **L8** which was first converted to the corresponding acid chloride **L8B** (Scheme 3.8).[3] **L8** was refluxed in thionyl chloride for 3 hours under an inert atmosphere and the grey suspension turned to a yellowish solution. The excess of thionyl chloride was evaporated under reduced pressure and the residue dried. The acid chloride **L8B** was obtained as a yellowish powder, assumed to be formed in quantitative yield and immediately used for esterification without any further purification.

L8B was then refluxed with amino alcohol **P16** in toluene for 15 hours under nitrogen (Table 3.1, Input 1). The crude reaction mixture was evaporated, dissolved in chloroform and extracted with saturated aqueous sodium hydrogen carbonate and water. Formation of the target esters **L10-14** was monitored with the ^{1}H NMR spectrum by the presence of the triplet (expected ~ δ 4.4 ppm) of the first CH_2 group next to the carboxyl group. In the ^{1}H NMR spectrum of the crude product of Input 1 (Table 3.1), were observed peaks of solvents, unreacted starting amino alcohol **P16** and a trace amount of the desired **L11**. The poor yield has most likely this reason. The leftover trace amount of $SOCl_2$ and also HCl (formed during the conversion of **L8** to the acid chloride **L8B**) reacted with alcohol **P16** to produce a chloroalkane. Therefore in the next attempts, acid chloride **L8B** was first dried properly on a high vacuum and then refluxed with base (1-5 eq.) and after that with amino alcohols (Table 3.1, Input 2-10).

Input	Base	ROH	Time / h	Yield /%	Product
1	none	$Et_2N(CH_2)_{11}OH$	15	trace	**L11**
2	DMAP	$CH_3(CH_2)_{11}OH$	17	75	**L10**
3	DMAP	$Et_2N(CH_2)_{11}OH$	15	10	**L11**
4	DMAP	$CH_3CH_2(OCH_2CH_2)_3OH$	18	49	**L12**
5	Et_3N	$CH_3(CH_2)_{11}OH$	15	57-69	**L10**
6	Et_3N	$CH_3CH_2(OCH_2CH_2)_3OH$	16	54	**L12**
7	Et_3N	$Et_2N(CH_2)_{11}OH$	15	27-63	**L11**
8	2,6-lutidine	$Et_2N(CH_2)_{11}OH$	21	58	**L11**
9	2,6-lutidine	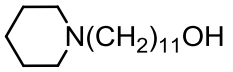	15	41-52	**L13**
10	2,6-lutidine	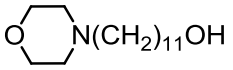	17	34-45	**L14**

Table 3.1: Reaction conditions towards ester-substituted ligands L10-14 (Scheme 3.8)

In Input 2, acid chloride **L8B** was first refluxed for 30 minutes with DMAP and then overnight with commercially available dodecanol, as a model alcohol. The crude reaction mixture was purified by extraction with chloroform – sodium hydrogen carbonate and water. Crystallization from cold ethanol gave analytically pure **L10** as an off-white powder in 75% yield. However, **L11** was received in only 10% yield when these reaction conditions were applied with amino alcohol **P16** (Input 3). When the same reaction conditions were repeated using tetraethyleneglycol monoethyl ether as the alcohol for esterification (Table 3.1, Input 4), **L12** was obtained in 49% yield. The side amino- or ether-chains make crystallisation of the products **L11** and **L12** difficult, therefore they were purified with a short chromatography column (SiO_2, eluted with EtOAc/Et_3N = 9:1 or EtOAc/MeOH/Et_3N = 30:2:1). Triethylamine was used to assist elution of the products on the column, because the R^f values of **L11** and **L12** are very low, and also to avoid their decomposition on SiO_2. In the ^1H NMR spectra we observed signals which were assigned to **L11** and **L12**, but also peaks due to DMAP, which means that DMAP has a similar R^f value as ligands **L11** and **L12**. Therefore Et_3N was used as the base for the next reactions. This strong base has good advantages: an excess can be easily evaporated after the reaction and it is not toxic in contrast to DMAP. Inputs 5 – 7 (Table 3.1) were done with triethylamine as a base and after several attempts, ligands **L10**,

L11 and **L12** were isolated in very good (54 – 69%) yields. However the products **L11** and **L12** were isolated in mixtures with unreacted starting alcohols, usually in a ratio 70:30 to 85:15. This impurity does not matter for the further complexation of the ligands. However the purity of the ligand is important for analysis and characterisation. One option to complete the conversion of esterification was to run the reaction with an excess of Et_3N (5 eq.) (Input 7 in Table 3.1), which increased the average yield of **L11** only slightly. However, starting amino alcohol **P16** was not recovered.

Use of 2,6-lutidine, a sterically hindered mild base, was another option to force the esterification (Table 3.1, Input 8-10). It is possible to remove an excess of 2,6-lutidine under reduced pressure or to separate it on a chromatography column, because its R^f value is very high in comparison with those of the desired ligands. The reaction with amino alcohol **P16** and 2,6-lutidine (5 eq.) was tried 3 times and in all cases product **L11** was isolated in good (57-58%) yields, pure or with only a trace amount of **P16** (Table 3.1, Input 8). Esterification with 2,6-lutidine as a base was realized also with 11-(piperidin-1-yl)undecan-1-ol **P17** and with 11-morpholinoundecan-1-ol **P18**. (Their synthesis[11] is described in section 3.2.4)**.** The ester-substituted ligands bearing a piperidine ring (**L13**) and a morpholine ring (**L14**) were obtained as ochre solids in 52% and 45% yields, respectively (Table 3.1, Input 9 - 10).

All five new ester-substituted ligands **L10**-**14** were characterised with ^1H, ^{13}C, COSY, HMQC and HMBC NMR spectra. In the aromatic part of each ^1H NMR spectrum, it is possible to see the typical distribution of proton peaks of the ester-substituted pytpy, and this is nearly the same as for CO_2Me-substituted **L2** (Compare Figures 3.2 and 3.4). In the aliphatic part of the spectra of the dodecyl ester **L10** and amines **L11** and **L13**-**14** a characteristic triplet of the CH_2 group **1** and a pentet of the CH_2 group **2** were observed with chemical shifts of δ 4.43 ppm and δ 1.83 ppm, respectively. However, methylene protons **1** and **2** of **L12**, shielded by the oxygen atom from the ester and the ether group, resonate at lower field (δ 4.58 and 3.90 ppm, respectively), as well as all protons **4**-**10** of **L12** (δ 3.75 – 3.47 ppm) and methylene groups **14** (δ 3.72 ppm) of the morpholine unit of **L14**. Methylene protons **11** and **13** in the neighbourhood of the amino group (**L11** and **L13**-**14**) absorb typically around δ 2.4 ppm.

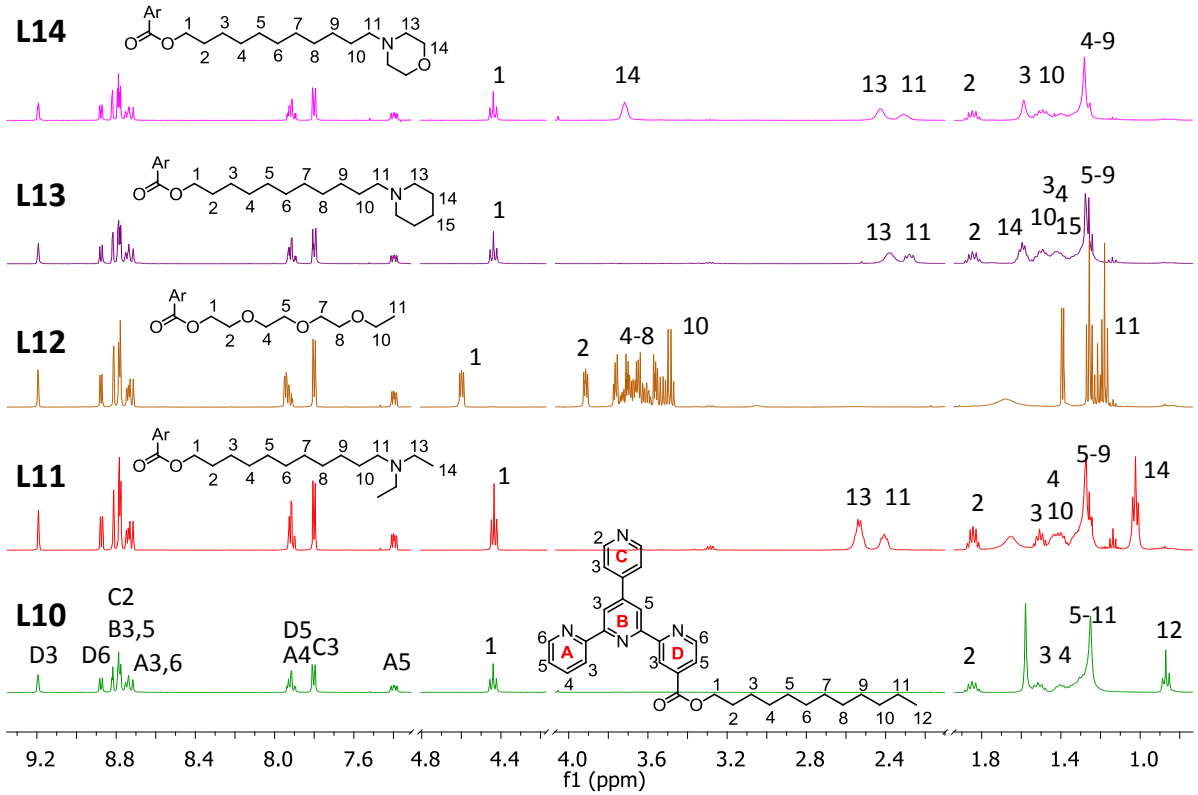

Figure 3.4: Comparison of the ^{1}H NMR (400 MHz, $CDCl_3$) spectra of ester-substituted pytpy ligands L10 (green), L11 (red), L12 (brown), L13 (violet) and L14 (pink)

In the electrospray mass spectra of **L11**, **L13** and **L14** one peak was observed, with *m/z* 580.4, 592.4 and 594.3, respectively (100% intensity), and was assigned to $[M+H]^+$. In the ESI MS of **L10** and **L12** were not only peaks with *m/z* 523.4 and 515.3 (with intensity 45% and 28%, respectively) were assigned to $[M+H]^+$. Extra peaks with *m/z* 561.3 (27%) and 545.4 (100%) for **L10** and with *m/z* 553.2 (27%) and 537.3 (100%) for **L12** were assigned to $[M+K]^+$ and $[M+Na]^+$.

The electronic absorption spectra of acetonitrile solutions of ester-substituted pytpys **L2**, **L10-14**, together with pytpy **L3**, chloro-substituted pytpy **L6** and Me-substituted **L7** are shown in Figure 3.5. The ligands exhibit a series of high energy absorption bands around 240 nm with high extinction coefficients (35 to 60×10^3 dm^3 mol^{-1} cm^{-1}) and around 280 nm with a shoulder at 320 nm with lower extinction coefficients (10 to 30×10^3 dm^3 mol^{-1} cm^{-1}). The bands arise from ligand-centred $\pi^*\leftarrow\pi$ transitions (Table 3.2).

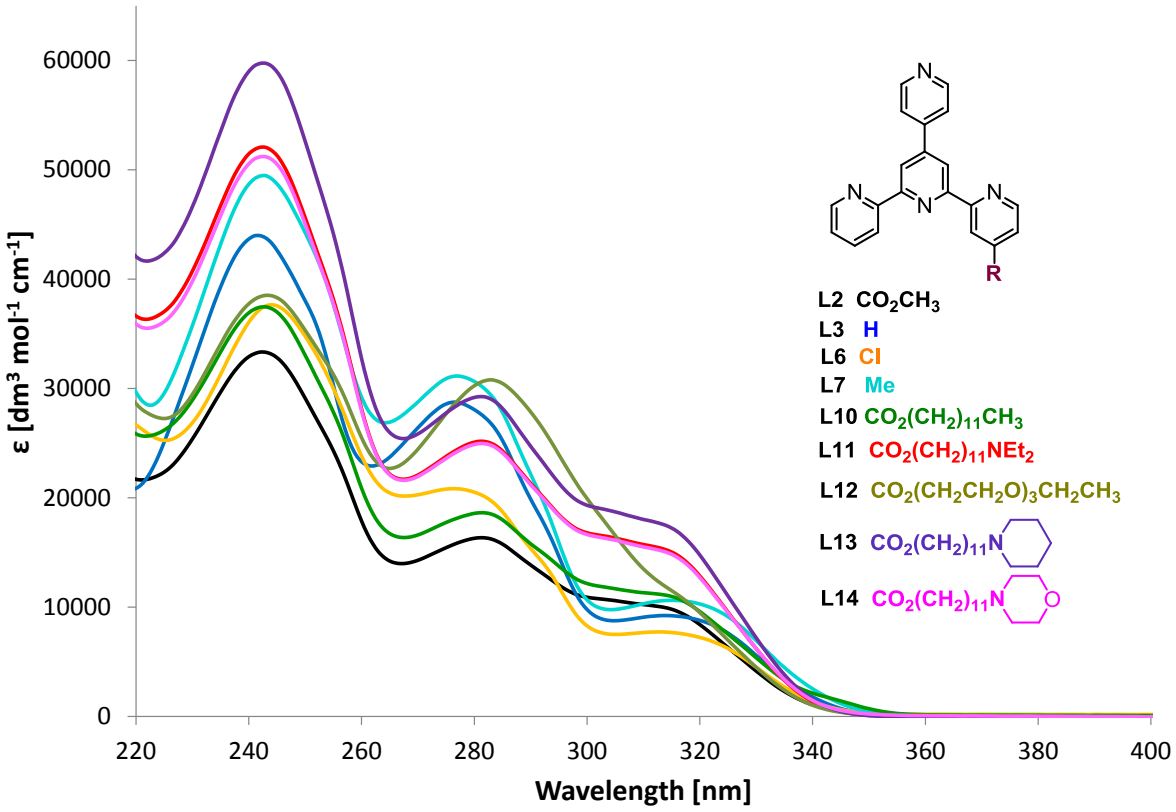

Figure 3.5: UV/Vis absorption spectra (CH_3CN) of 4-substituted pytpy ligands L2 ($4.22 \cdot 10^{-5}$M, black), L3 ($5.97 \cdot 10^{-5}$M, blue), L6 ($4.08 \cdot 10^{-5}$M, orange), L7 ($4.80 \cdot 10^{-5}$M, cyan), L10 ($4.39 \cdot 10^{-5}$M, green), L11 ($3.83 \cdot 10^{-5}$M, red), L12 ($5.76 \cdot 10^{-5}$M, olive-green), L13 ($4.13 \cdot 10^{-5}$M, violet) and L14 ($3.99 \cdot 10^{-5}$M, pink)

Ligand	c / 10^{-5} mol dm^{-3}	λ_{max}/nm ($\varepsilon_{max}/10^3$ dm^{3}mol^{-1}cm^{-1})		
L2	4.22	242 (33.3)	281 (16.3)	316 (9.6 sh)
L3	5.97	242 (44.0)	277 (28.7)	314 (9.1)
L6	4.08	244 (37.6)	276 (20.8)	313 (7.7)
L7	4.80	243 (49.5)	277 (31.1)	315 (10.6)
L10	4.39	243 (37.5)	281 (18.6)	317 (10.6 sh)
L11	3.83	242 (52.1)	281 (25.2)	316 (14.8 sh)
L12	5.76	243 (38.5)	283 (30.8)	
L13	4.13	242 (59.7)	281 (29.2)	316 (16.9 sh)
L14	3.99	243 (51.2)	281 (25.0)	316 (14.5 sh)

Table 3.2: UV/Vis absorption spectra (CH_3CN) of 4-substituted pytpy ligands

3.2.4 Synthesis of amino alcohols P17 and P18

In Scheme 1.11 in Chapter 1 a facile two-step synthetic route to obtain 11-diethylaminoundecanoate **P16** from methyl 11-bromoundecanoate was discussed. This synthetic strategy for a wide range of amino alcohols with various chain-lengths was published by Wetter *et al.* in 1974.[11] In this chapter, we were interested to expand this method to other secondary amines besides diethylamine to obtain several amino alcohols with different chemical properties and afterwards Ru(II) complexes with diverse photophysical properties. A wide range of commercially available secondary amines exists, e.g. Me_2NH, EtMeNH, Pr_2NH, $^{i}Pr_2NH$ or cyclic amines such as pyrrolidine, piperidine and morpholine. We chose $^{i}Pr_2NH$ and piperidine (Scheme 3.9). Reaction conditions were applied the same as for diethylamine (Scheme 1.11). Methyl 11-bromoundecanoate was refluxed overnight with an excess of amine. However, in the case of $^{i}Pr_2NH$ the reaction did not proceed at all and the starting bromo-derivative was recovered in 75% of the original amount. On the contrary, due to too high a reaction temperature, the reaction with piperidine afforded not only the desired product **P13** but the product **P13b** of a double-substitution as the major product. Bromine was replaced by piperidine but also the methyl ester group converted to amide.

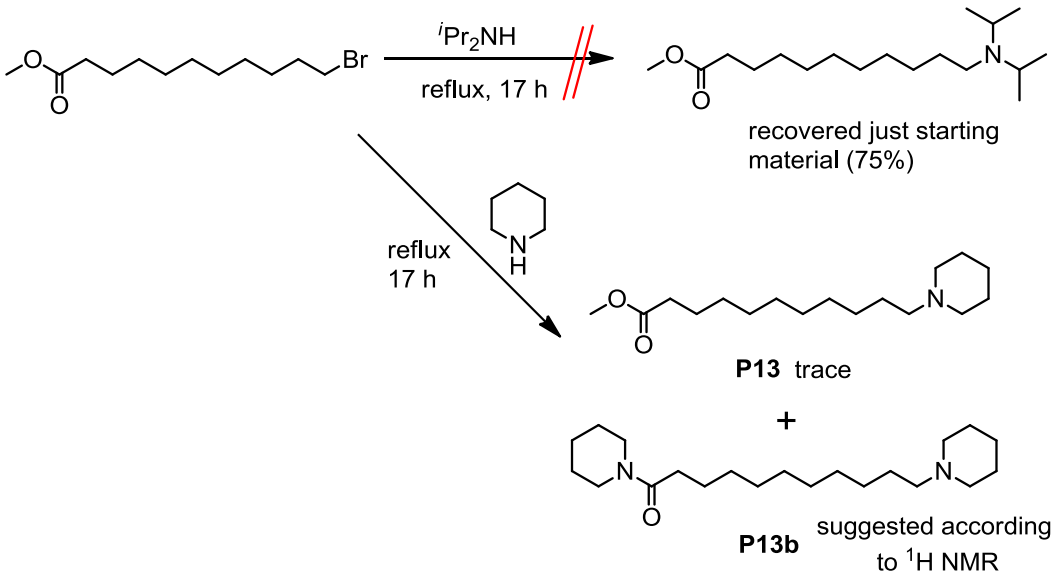

Scheme 3.9: Towards other amino-alcohols besides P16

The reaction with piperidine was repeated several times to optimize the reaction conditions. Stirring at 50-60 °C for 5-6 hours was found as an optimum, yielding **P13** in 92%. The

reaction was repeated also with morpholine to give the corresponding tertiary amine **P14** in 99% yield. **P12**-**14** were purified using vacuum distillation and obtained as yellowish oils. For the next step, the reducing agent $LiAlH_4$ in THF was used for conversion of the methyl ester group of **P13** and **P14** to methylene alcohol, as in the case of **P12** in Chapter 1. Corresponding amino alcohols **P17** and **P18** were obtained as yellowish oils in quantitative yields (Scheme 3.10). Figure 3.6 displays a comparison of their ^{1}H NMR spectra.

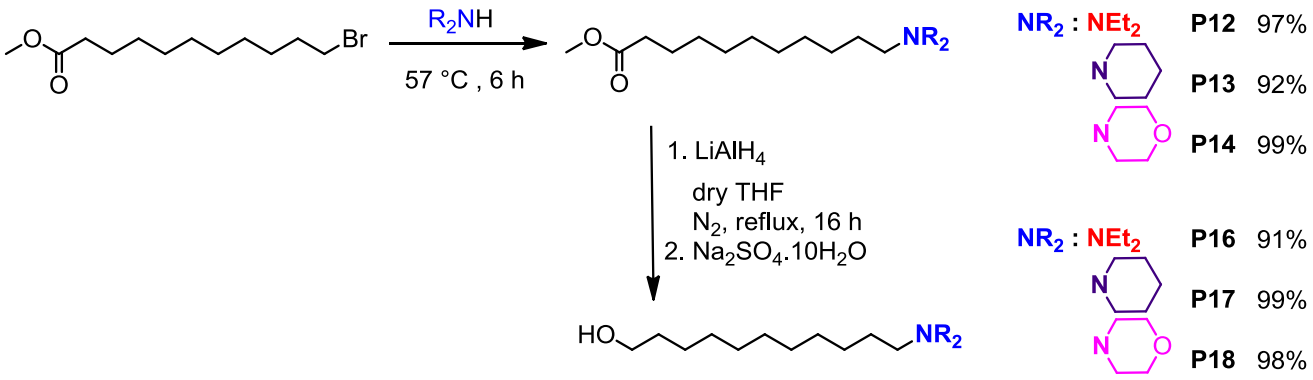

Scheme 3.10: Synthesis of amino alcohols P16-18

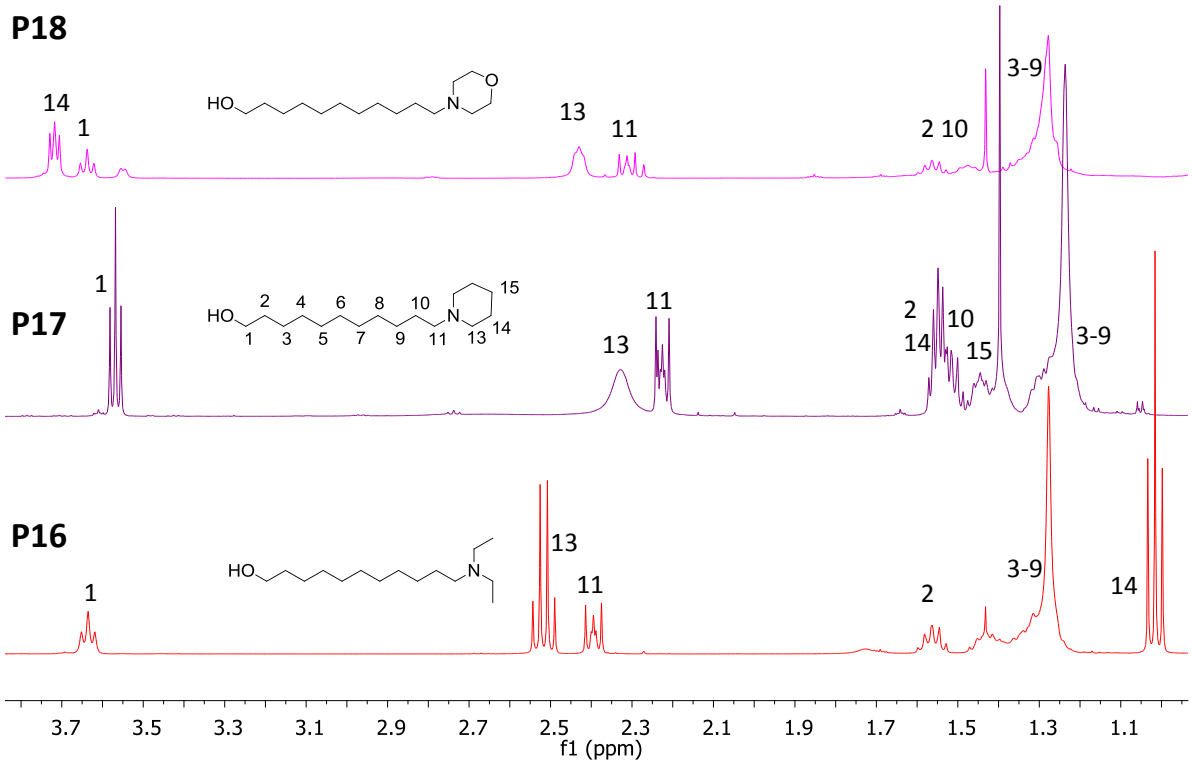

Figure 3.6: Comparison of the ^{1}H NMR (400 MHz, $CDCl_3$) spectra of amino alcohols P16 (red), P17 (violet) and P18 (pink)

Conclusion

In Scheme 3.2 were discussed theoretical possibilities to obtain ester-substituted pytpy ligands **L10-14** with long aliphatic amino chains. After practical experiments, a combination of options **B** (hydrolysis of methyl ester **L2** to **L8**) and **D** (esterification of **L8** via acid chloride) was found to be ideal route. Route **C** (Steglich direct esterification of carboxylic acid **L8**) did not work due to the insolubility of **L8**. In route **F**, methyl-substituted pytpy **L7** was prepared as an alternative source of **L8**, but was not followed up due to low yields during most of the reaction steps. We thought of an alternative **E**, trans-esterification of methyl ester **L2**, but have not tried this since the effective routes **B** and **D** worked so well. Complexation of ligands **L10-14** (Chapter 4) is a more successful alternative to the original idea of complex synthesis by the trans-esterification of **C7** (Chapter 1).

Literature

1 Wiener, H.; Gilon, C. *J. Mol. Catal.,* **1986**, *3*, 45-52.

2 Neises, B.; Steglich, W. *Angew. Chem. Int. Ed.,* **1978**, *17*, 522-524.

3 Uppadine, L. H.; Redman, J. E.; Dent, S. W.; Drew, M. J. B.; Beer, P. D. *Inorg. Chem.,* **2001,** *40,* 2860-2869.

4 Blumhoff, J.; Beckert, R.; Rau, S.; Losse, S.; Matschke, M.; Günther, W.; Görls, H. *Eur. J. Inorg. Chem.,* **2009**, 2162–2169.

5 Song, H.-K.; Park, Y. H.; Han, C.-H.; Jee, J.-G. *J. Ind. Eng. Chem.,* **2009**, *15*, 62–65.

6 Duprez, V.; Krebs, F. C. *Tetrahedron Letters,* **2006**, *47*, 3785–3789.

7 Mikel, C.; Potvin, P. G. *Polyhedron,* **2002**, *21*, 49-54.

8 Ishihara, M.; Tsuneya, T.; Shiga, M.; Kawashima, S.; Yamagishi, K.; Yoshida, S.; Sato, H.; Uneyama, K. *J. Agric. Food Chem.,* **1992**, *40*, 1647.

9 Eryazici, I.; Moorefield, C. N.; Durmus, S.; Newkome, G. R. *J. Org. Chem.,* **2006**, *71*, 1009.

10 Xia, H.; Zhu, Y.; Lu, D.; Li, M.; Zhang, C.; Yang, B.; Ma, Y. *J. Phys. Chem. B,* **2006**, *110*, 18718-18723.

11 Wetter, W. P.; De Witt Blanton, C. Jr. *J. Med. Chem.,* **1974**, *17*, 620-624.

Chapter 4

Ruthenium(II) complexes with three or four protonation sites

4.1 Introduction

In Chapters 2 and 3, ligands with a side amino-chain linked via an ester or an ether **L10-14** and **L17-20** were prepared. In this chapter, ruthenium(II) complexes of these ligands are synthesized (Scheme 4.1). The amino group attached to the side chain and the two pendant pyridyl groups bring to the molecule three (or four, respectively) protonation sites. Several synthetic strategies, analysis and photochemical studies will be reported and their results discussed.

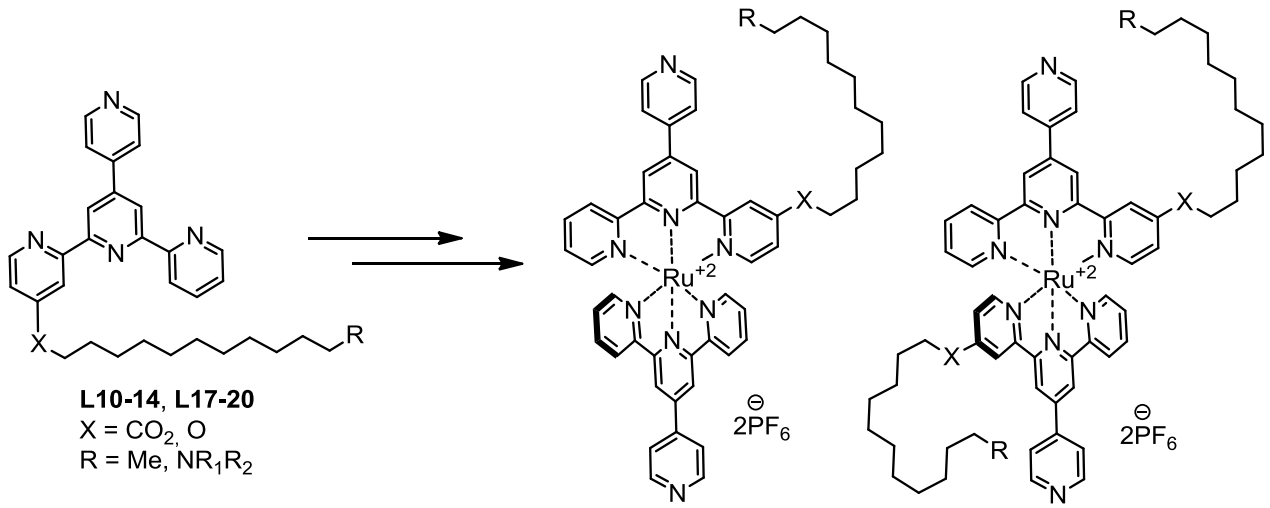

Scheme 4.1: Towards ruthenium(II) complexes with a side chain linked via an ester or via an ether bearing three or four protonation sites

4.2 Results and Discussion

4.2.1 Synthesis of heteroleptic ruthenium(II) complexes with pytpy ligands

We had two options for the synthesis of heteroleptic ruthenium(II) complexes **C17** (a model complex) and **C18** (a complex with a *N*-diethylamino group as the third protonation site). It was important to find out which ligand to use in the first complexation step and which in the second one, i.e. in which order to introduce the symmetrical **L3** and the asymmetrical **L10** and **L11**, respectively.

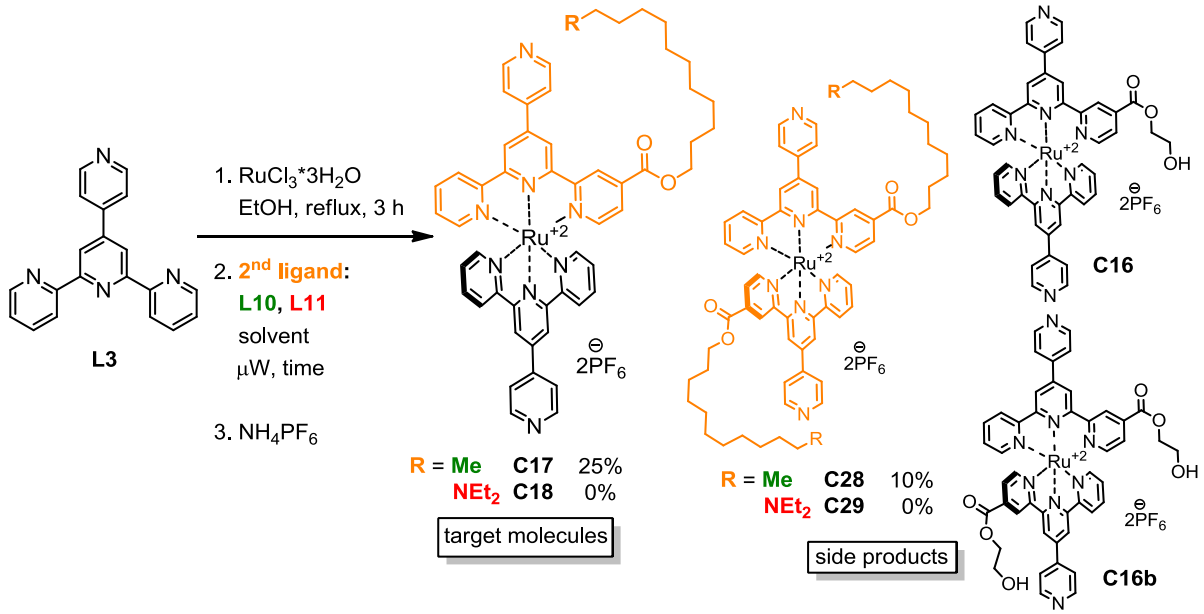

Scheme 4.2: Synthetic strategies in the domestic microwave oven towards the ruthenium(II) complexes with three protonation sites

Input	2nd ligand	Solvent	Time / min	Product /%	Side products	
1	**L10**	ethylene glycol	2.5	**C17** (3%)	-	**C16**, **C16b**, **C8**
2	**L10**	ethylene glycol	1.5	**C17** (25%)	**C28** (10%)	-
3	**L10**	ethylene glycol	2	**C17** (13%)	**C28** (trace)	-
4	**L11**	ethylene glycol	2	**C18** (-)	**C29** (-)	**C16**, **C16b**, **C8**
5	**L10**	AcOH	10	**C17** (trace)	**C28** (trace)	-
6	**L10**	DMF	4	-	-	-

Table 4.1: Reaction conditions for Scheme 4.2

We started with **L3** (Scheme 4.2). **L3** was converted to Ru(**L3**)Cl_3, complex **C2**, according to the procedure reported by Sullivan *et al*. in 1980 (Scheme 1.8 in Chapter 1) and collected as a black powder in a quantitative yield.[1] **C2** and **L10** were suspended in ethylene glycol and irradiated in the domestic microwave oven at 750W for 2.5 minutes (Table 4.1, Input 1). During this period, the black suspension turned to a red solution, which signalled the formation a of Ru(II) complex. Aqueous ammonium hexafluorophosphate was added to precipitate the product as a PF_6^- salt. The red precipitate which formed was collected on Celite®, washed with water and redissolved in acetonitrile. Solvent was removed in vacuo and the red residue purified on a chromatography column (SiO_2, eluted with MeCN/saturated aqueous KNO_3/H_2O = 5:1:1). Three bands were observed. The first, minor one, was the target molecule **C17** in 3% yield. The third fraction, which stayed on the column, was the COOH substituted complex **C21**, a product of decomposition. According to the NMR spectra and ESI MS, it was concluded that the second fraction was a product of transesterification with ethylene glycol **C16**. In the electrospray mass spectrum of **C16**, peaks with *m/z* = 405.1 (assigned to $[M\text{-}2PF_6]^{2+}$) with 100% intensity and 955.2 (assigned to $[M\text{-}PF_6]^{+}$) with intensity 12% were observed. In the ^1H NMR spectrum of **C16**, two triplets with δ 4.39 and 3.79 ppm (assigned to the CH_2 groups of the ester chain) were observed. The aromatic part has a characteristic set of peaks, identical with the dodecyl ester substituted complex **C17**. However, upon a closer comparison, one could observe that all the aromatic peaks are doubled. This gave us a hint that the fraction collected was a mixture of two or more products with the same R_f value on a TLC plate. In the electrospray mass spectrum, another two sets of peaks were assigned, for homoleptic complex **C8** and for another product of trans-esterification with ethylene glycol **C16b** (Scheme 4.2, Table 4.1 Input 1). Peaks with *m/z* = 361.1 and 867.2 (assigned to $[M\text{-}2PF_6]^{2+}$ and $M\text{-}PF_6]^{+}$, respectively) with 38% and 13% intensity were observed for **C8** and a peak with *m/z* = 449.1 (assigned to $[M\text{-}2PF_6]^{2+}$) with 35% intensity was observed for **C16b**.

To avoid the formation of the side products **C16** and **C16b**, the reaction time was shortened to 1.5 and 2 minutes, respectively (Inputs 2 and 3, Table 4.1) and the model complex **C17** was obtained in 25% and 13% yield, respectively. However, the homoleptic complex **C28** was also isolated as a side product, in 10% yield and a trace amount, respectively. These reaction conditions were also used with the *N*-diethylamino-substituted ligand **L11** (Input 4, Table 4.1). The reaction mixture was heated in a domestic microwave oven at 750W until the black

suspension turned red (2 minutes). However, only the products of trans-esterification with ethylene glycol **C16** and **C16b** were obtained. A change of solvent was worth trying (Inputs 5 and 6, Table 4.1). We used acetic acid and the reaction mixture was heated at the highest setting of the microwave oven. However, after 10 minutes the reaction mixture had turned only slightly red and product **C17** was isolated in only a trace amount. The reaction in DMF in the domestic microwave oven did not proceed at all (Input 6, Table 4.1).

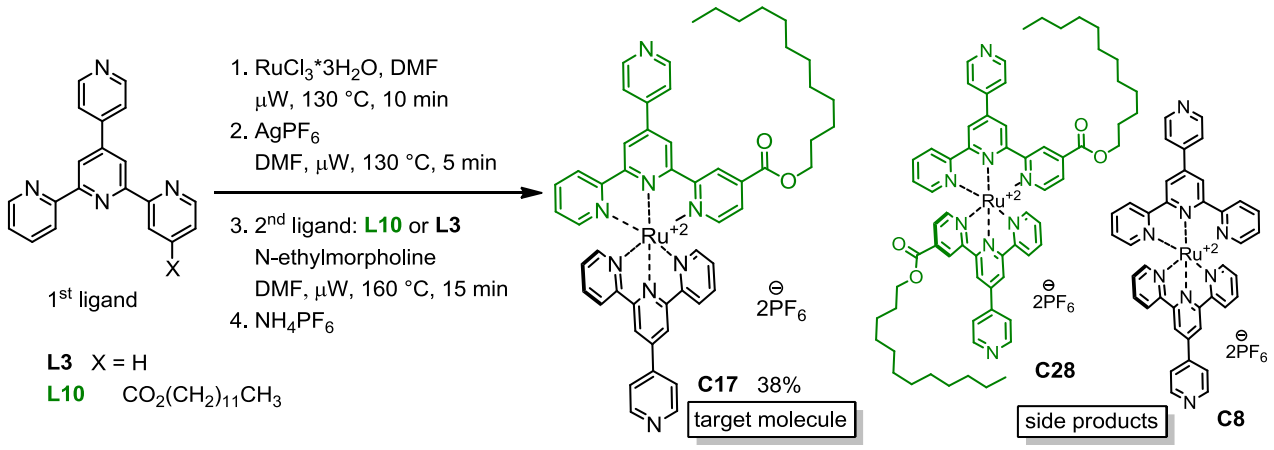

Input	1st ligand	2nd ligand	Product /%	Side product
1	L3	L10	**C17** + **C28** isolated in a mixture	
2	L10	L3	**C17** (38%)	**C28** (trace)

Scheme 4.3: Two options for a microwave reactor towards the model complex C17

Considering the formation of **C16** and **C16b**, for the next reactions we used microwave reactor conditions (Scheme 4.3 and 4.4), which worked well for the synthesis of **C7** in DMF (Scheme 1.14, Chapter 1). These "one-pot" reaction conditions were used with the model complex **C17** and involve four reaction steps, without isolation of intermediates (Scheme 4.3). The first ligand is coordinated as a Ru(**L**)Cl_3 complex, which is then activated with silver hexafluorophosphate. This reacts with the second ligand in a presence of a catalytic amount of *N*-ethylmorpholine, used as a reducing agent for Ru(III) to Ru(II). The product **C17** is then precipitated as a PF_6^- salt. Both options were tried, first to complex **L3** and then **L10** (Input 1, Scheme 4.3) and also the other way round (Input 2, Scheme 4.3). Crude products were purified with column chromatography (SiO_2, eluted with MeCN/saturated aqueous KNO_3/H_2O = 10:1.5:0.5). In the first case, intensely coloured bands of both products (the

target molecule **C17** and the side product **C28**) were observed. However, products were not separated even after two chromatography columns, due to the nearly identical R_f values of the two fractions (Input 1, Scheme 4.3). In the second option, the chromatography separation was much easier, because **C17** was the major fraction (38% yield) and **C28** was isolated in only trace amount (Input 2, Scheme 4.3). In both cases, the homoleptic complex **C8** was also observed as a minor fraction.

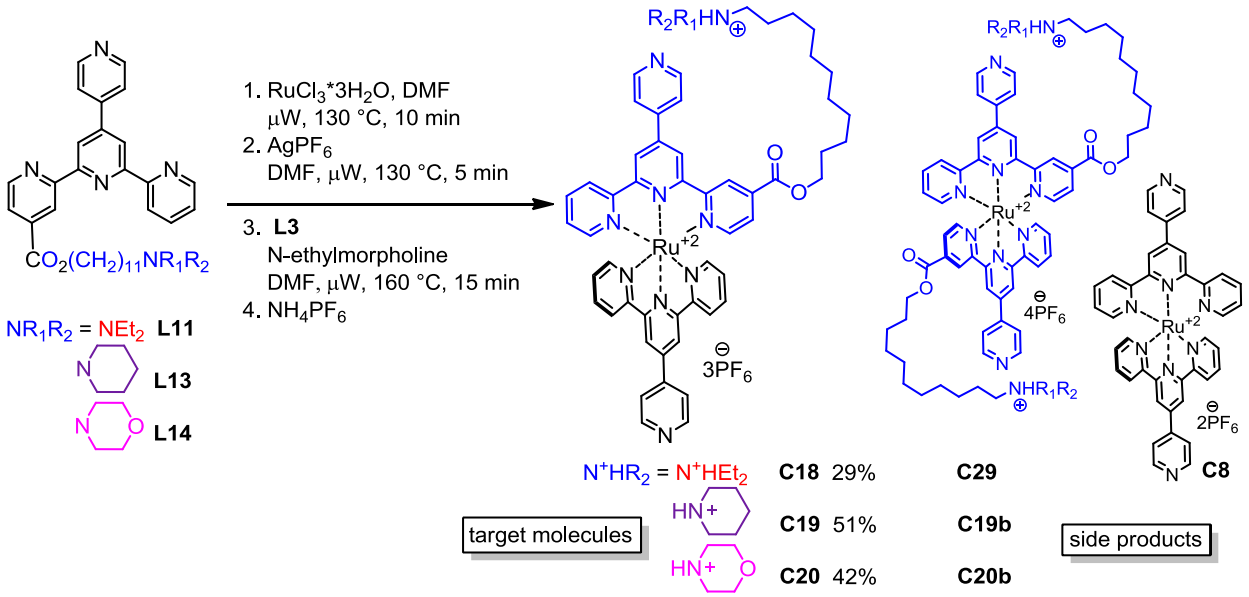

Scheme 4.4: Synthesis of ruthenium(II) complexes C18-20 with three protonation sites

These conditions (Input 2 in Scheme 4.3) were also used for complexation of the ligands with the amino-substituted ester chains **L11** and **L13-14** to synthesize the Ru(II) complexes with three protonation sites **C18-20** in 29%, 51% and 42% yield, respectively (Scheme 4.4). The formation of homoleptic complexes **C8**, **C29**, **C19b** and **C20b** as side products in a trace amount was also observed. The complexes were purified by column chromatography and also with preparative TLC plates (SiO_2, eluted with MeCN/saturated aqueous KNO_3/H_2O = 5:1:1 or 10:1.5:0.5). Although this resulted in a significant loss of material, the purity of the complexes is essential for further photochemistry studies. **C18-20** were characterised with NMR spectroscopy, ESI mass spectrometry and elemental analysis. Upon careful examination of the spectra, we realized that all the complexes **C18-20** are already mono-protonated on the pendant side amino-chain, instead of being in the deprotonated (i.e. neutral) state. The protonation was caused by the presence of NH_4PF_6 during the fourth reaction step and points at the basicity of the amino groups which seems to be even higher than we expected.

The fact, that all complexes **C18-20** are already in the mono-protonated form, was proved with elemental analysis, mass spectrometry and with several NMR spectroscopy studies (Chapter 6).

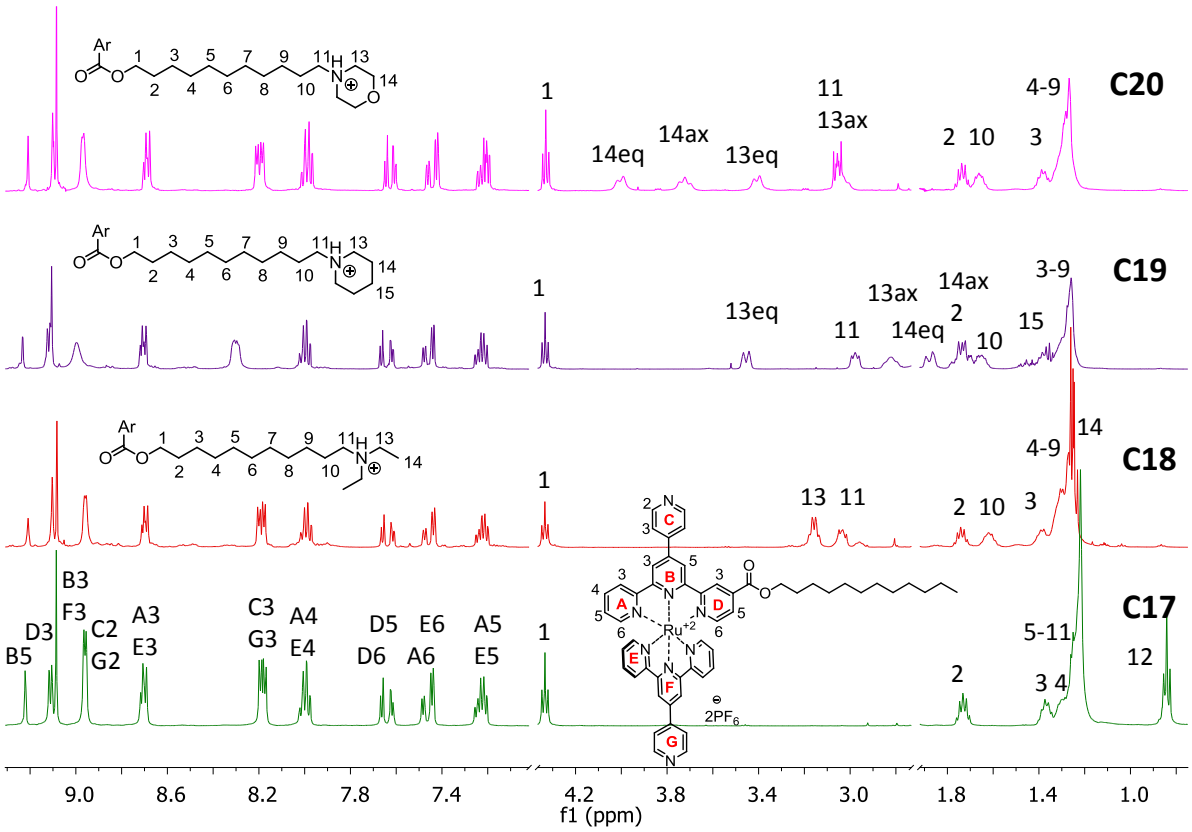

Figure 4.1: ^{1}H NMR (500 MHz, CD_3CN) spectra of ruthenium(II) complexes C17-20 linked via an ester

Figure 4.1 compares the ^{1}H NMR spectra of all four Ru(II) complexes **C17-20**. In the aromatic region it is possible to see the characteristic distribution of peaks for heteroleptic Ru(II) complex with a pytpy ligand substituted in the 4-position with an electron-withdrawing group. Methylene groups **1** and **2** next to the carboxyl group always have a chemical shift δ 4.33 and 1.73 ppm and the methylene groups **3**-**9** are represented with broad signals in the region δ 1.4 - 0.9 ppm. The biggest difference between the ^{1}H NMR spectra of complexes **C18-20** and the free ligands **L11**, **L13-14** (Figure 3.4 in Chapter 3), is in the chemical shift of the methylene groups **11**, **13** and **14**, which are in the closest neighbourhood of the nitrogen atom. The amino group of the ligands **L11**, **L13-14** is in a deprotonated state, therefore the methylene groups **11**, **13** have a chemical shift at about δ 2.35 ppm. However, the methylene groups **11**, **13** of the Ru(II) complex **C18** are shifted to δ 3.10 ppm due to the

protonation of the diethylamino group. In addition to this, **C19** and **C20** have a protonated cyclic amino group. This leads to the fact that each methylene group **13** and **14** has two peaks in the ^{1}H NMR spectrum, because the axial and equatorial protons are non-equivalent (Figure 4.1).

As a next series of heteroleptic ruthenium(II) complexes with three protonation sites, compounds **C23-25** with a side amino-chain linked via an ether unit, and a model complex **C22** substituted with a dodecyl ether were synthesized (Scheme 4.5). Both synthetic approaches (Table 4.2), first to complex the ether-substituted ligands **L17-20** and then pytpy **L3**, or the other way round, were used. The importance of the products' purity and also dealing with the formation of the homoleptic complexes as side products, require several sequential purification steps using column chromatography and preparative TLC plates. This results in only low yields of the desired molecules **C22-25**. In the first case (Inputs 1-4 in Table 4.2), ligands **L17-20** were coordinated first, followed by **L3**. Competitive formation of the homoleptic complexes, resulted in **C22-24** being obtained in only 10-13% yields and **C25** in 31% yield. Reactions with **L17-19** were tried also the other way round (Inputs 5-7 in Table 4.2) and complexes **C22-24** were obtained in slightly higher (21-28%) yields. In this case, formation of the homoleptic complexes was observed in only trace amount, therefore purification of the products was easier.

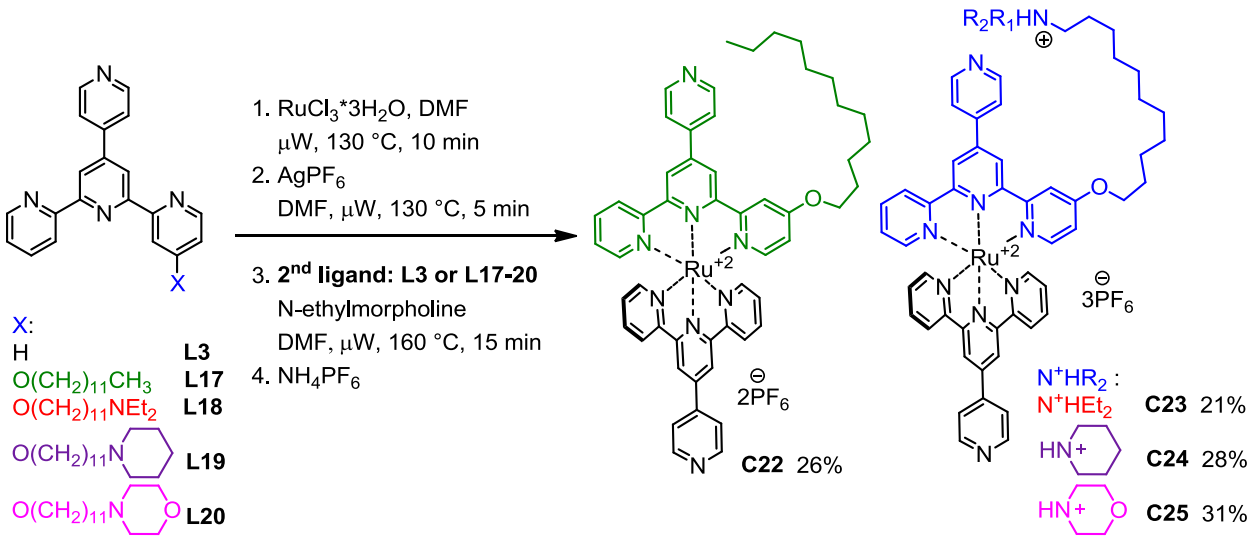

Scheme 4.5: Synthesis of ruthenium(II) complexes C22-25 with three protonation sites

Input	1st ligand	2nd ligand	Product /%
1	L17	L3	C22 (12%)
2	L18	L3	C23 (10%)
3	L19	L3	C24 (13%)
4	L20	L3	C25 (31%)
5	L3	L17	C22 (26%)
6	L3	L18	C23 (21%)
7	L3	L19	C24 (28%)

Table 4.2: Reaction conditions for Scheme 4.5

^{1}H NMR spectra and elemental analysis revealed that complexes **C23-25** were formed in the same state, i.e. protonated on the side amino unit, as we had observed for the complexes **C18-20**. Elemental analysis results for all complexes **C17-20** and **C22-25** were in most cases fitted with addition of 0.5-2 molecules of water or with a leftover amount of NH_4PF_6. The NH_4^+ ion appears at a 1:1:1 non-binomial triplet at δ 6.5 ppm (coupling to 14N, I = 1). In the electrospray mass spectrum of **C22**, peaks with *m/z* = 1051.3 (assigned to $[M\text{-}PF_6]^+$) with 100% intensity and 453.2 (assigned to $[M\text{-}2PF_6]^{2+}$) with intensity 25% were observed. In the electrospray mass spectrum of **C23-25**, the observed peaks were assigned to $[M\text{-}PF_6]^+$, $[M\text{-}2PF_6]^{2+}$ and $[M\text{-}3PF_6]^{3+}$. However, intense peaks assigned to $[M\text{-}PF_6]^+$, $[M\text{-}2PF_6]^{2+}$ for the deprotonated form of **C23-25** were also observed. In the ^{1}H NMR spectrum of **C23-25** (Figure 4.2), a significant change in the aromatic region was noticed, in comparison with the ester-substituted **C17-20** (Figure 4.1). All protons of the pyridyl unit **D** were, due to the electron-donating effect of the alkoxy groups, shifted to higher magnetic field. The distribution of the peaks in the aliphatic region was nearly the same as for the ester-substituted **C17-20**. The only difference is that the methylene group **1** is shifted to δ 4.13 ppm. The chemical shift of the methylene groups **11**, **13** and **14** is consistent with the protonated amino group.

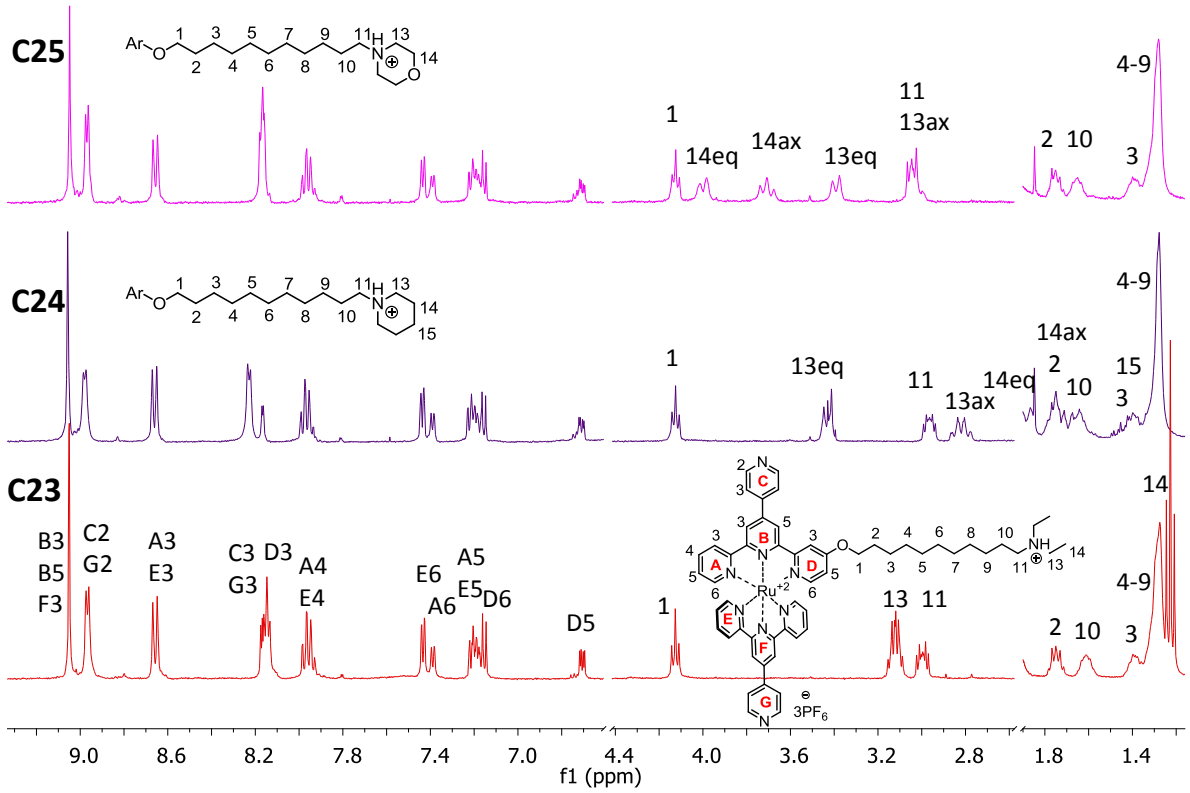

Figure 4.2: ^{1}H NMR (400 MHz, CD_3CN) spectra of Ru(II) complexes C23-25 linked via an ether group

4.2.2 Homoleptic ruthenium(II) complexes with pytpy ligands

As a next series of Ru(II) complexes, homoleptic complexes with ligands **L2**, **L10-11** and **L17-18** were synthesized. $[Ru(DMSO)_4Cl_2]$ is a common suitable reactant for these reactions.[2] In comparison with $RuCl_3 \cdot 3H_2O$, the metal ion in $[Ru(DMSO)_4Cl_2]$ is already in oxidation state +II, so there is no need to include any reducing agents. It is possible to use mild conventional reaction conditions, (reflux in MeOH or EtOH in a fume hood) but this requires a long reaction time. Therefore, we tried irradiation in a microwave reactor in EtOH at 120 °C for 30 minutes (Scheme 4.6). However, after further work-up, only a trace amount of **C27** was obtained. This was confirmed with a MALDI TOF mass spectrum, where a peak with *m/z* = 838.1 (assigned to $[M\text{-}2PF_6]^+$) was observed. It seems that the unprotected pendant pyridyl position of **L2** competes as a site of coordination with the terpyridine unit, and this leads to the formation of non-desired complexes. (Further reactions with $[Ru(DMSO)_4Cl_2]$ are described in Chapter 7.) This also seems to be the case of failure, when **L2** was heated with $RuCl_3 \cdot 3H_2O$ in DMF in the microwave reactor at 160 °C for 15 minutes (Scheme 4.6).

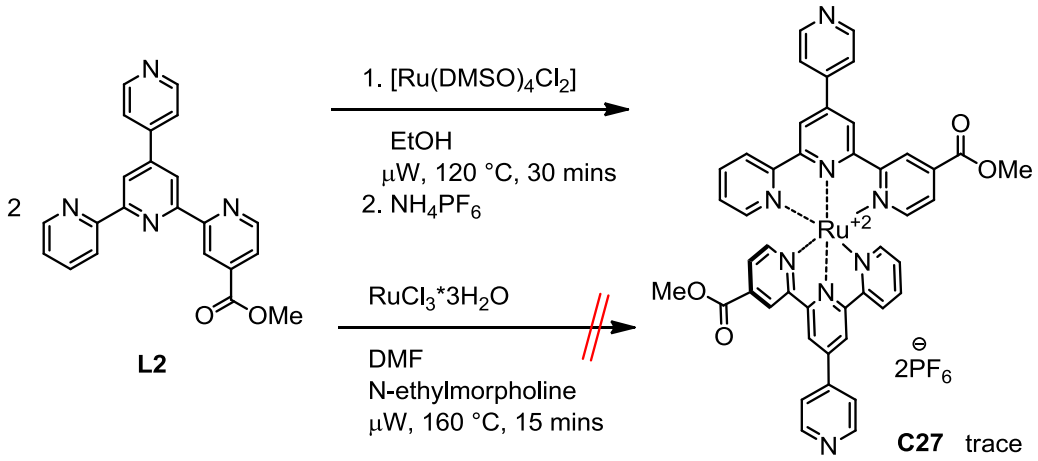

Scheme 4.6: Synthesis of the methyl ester-substituted homoleptic ruthenium(II) complex C27

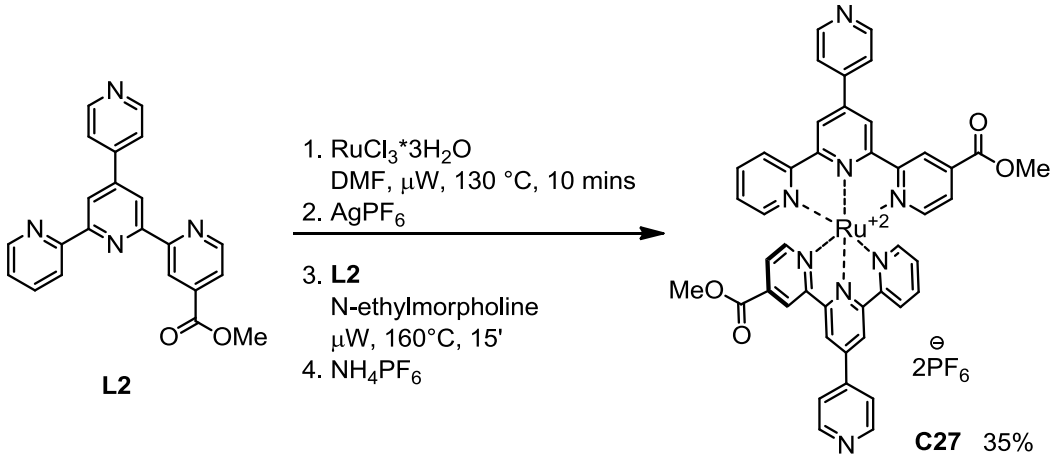

Scheme 4.7: Synthesis of the methyl ester-substituted homoleptic ruthenium(II) complex C27

After these failures, the reaction conditions, which had successfully been used for synthesis of **C17-C20** and **C22-25**, were applied (Scheme 4.7). The first equivalent of **L2** is coordinated as a [Ru(**L2**)Cl_3] complex, which is then activated with silver hexafluorophosphate. This reacts with the second equivalent of **L2** in a presence of a catalytic amount of *N*-ethylmorpholine, used as a reducing agent for Ru(III) to Ru(II). The product **C27** is then precipitated as a PF_6^- salt, purified on a chromatography column (SiO_2, eluted with MeCN/saturated aqueous KNO_3/H_2O = 10:0.5:1.5) and obtained in 35% yield. The homoleptic complex with COOH substituents (a side product of the methyl ester group cleavage) was also observed. In the electrospray mass spectrum of **C27**, peaks with *m/z* = 419.1 (assigned to $[M\text{-}2PF_6]^{2+}$) with 100% intensity and 983.0 (assigned to $[M\text{-}PF_6]^+$) with intensity 12% were observed.

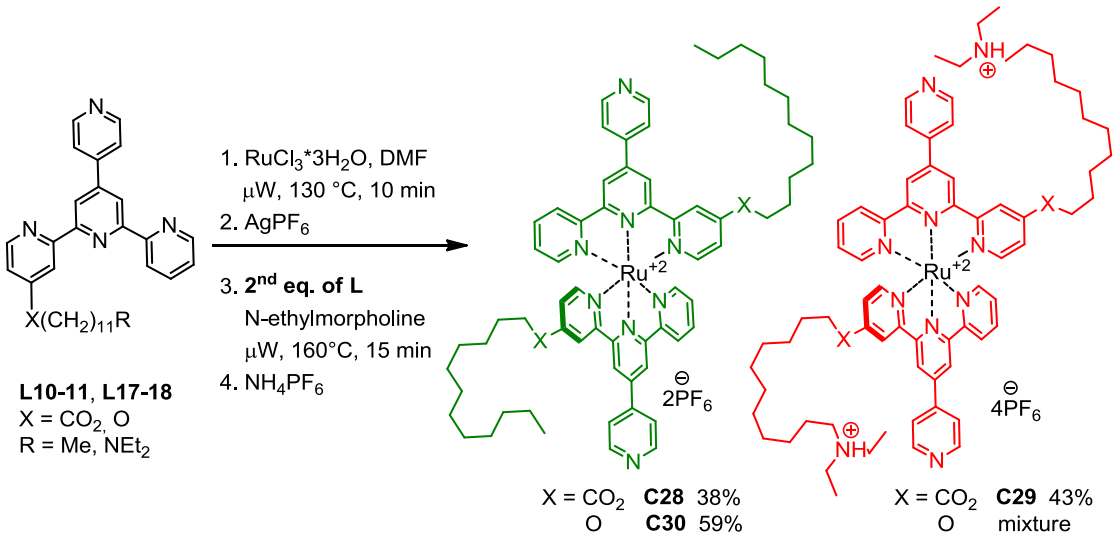

Scheme 4.8: Synthesis of homoleptic ruthenium(II) complexes C28-30

The same conditions were also used for the synthesis of homoleptic Ru(II) complexes containing ligands with a side chain linked via an ester **L10-11** and via an ether **L17-18** (Scheme 4.8). A model complex with two dodecyl ester side chains **C28** was isolated in 38% yield. In the electrospray mass spectrum of **C28**, peaks with *m/z* = 573.2 (assigned to $[M\text{-}2PF_6]^{2+}$) with 100% intensity and 1291.3 (assigned to $[M\text{-}PF_6]^{+}$) with intensity 2% were observed. A model complex with two dodecyl ether side chains **C30** was isolated in a good 59% yield. In the electrospray mass spectrum of **C30**, peaks with *m/z* = 545.2 (assigned to $[M\text{-}2PF_6]^{2+}$) with 100% intensity and 1235.3 (assigned to $[M\text{-}PF_6]^{+}$) with intensity 47% were observed. The ruthenium(II) complex with two diethylamino-substituted side chains linked via an ester (**C29**) was isolated in 37% yield. In the electrospray mass spectrum of **C29**, peaks with *m/z* = 776.3 (assigned to $[M\text{-}2PF_6]^{2+}$) with 43% intensity and 1697.5 (assigned to $[M\text{-}PF_6]^{+}$) with intensity 2% were observed. A homoleptic complex with two diethylamino-substituted side chains linked via an ether group was also synthesized. However purification and isolation of the product failed, because the side products had nearly the same R_f value on the TLC plate as the target molecule.

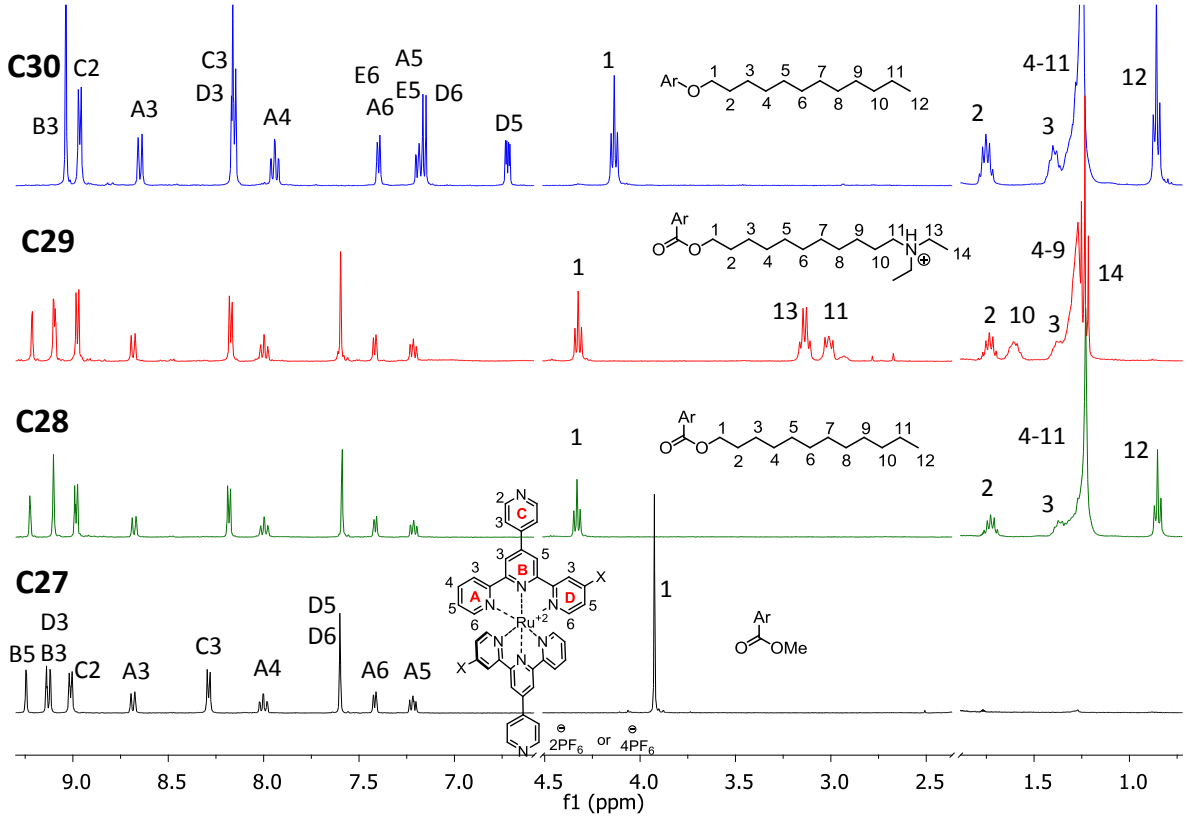

Figure 4.3: ^{1}H NMR (400 MHz, CD_3CN) spectra of the homoleptic ruthenium(II) complexes C27-30

Figure 4.3 shows a comparison of ^{1}H NMR spectra of homoleptic complexes **C27-30**. The aromatic region has one characteristic set of peaks, in comparison with all heteroleptic complexes **C17-20** and **C22-25** (Figures 4.1 and 4.2). A chemical shift of the **D**-ring protons (see Figure 4.3) naturally depends on the electron-withdrawing or electron-donating properties of the **D**-ring substituents. Protons **D5** and **D6** of all complexes **C27-29** are represented with only one peak in the ^{1}H NMR spectrum when measured at 400 MHz (Figure 4.3). However, when these compounds were measured using a 500 MHz spectrometer, the peaks of the protons **D5** and **D6** split up to two characteristic doublets of doublets with chemical shifts δ 7.60 and 7.63 ppm, respectively. In the COSY NMR spectrum of **C28**, a cross-peak for protons **D5** and **D6** and also a small cross-peak for protons **D3** and **D5** was observed. In the HMQC NMR spectrum of **C28**, a characteristic C-H correlation signal for each of **D5** and **D6** group were found (Figure 4.4). **D6** and **D5** are in the ^{13}C NMR spectrum represented with a chemical shift δ 154.6 and 127.4 ppm, respectively.

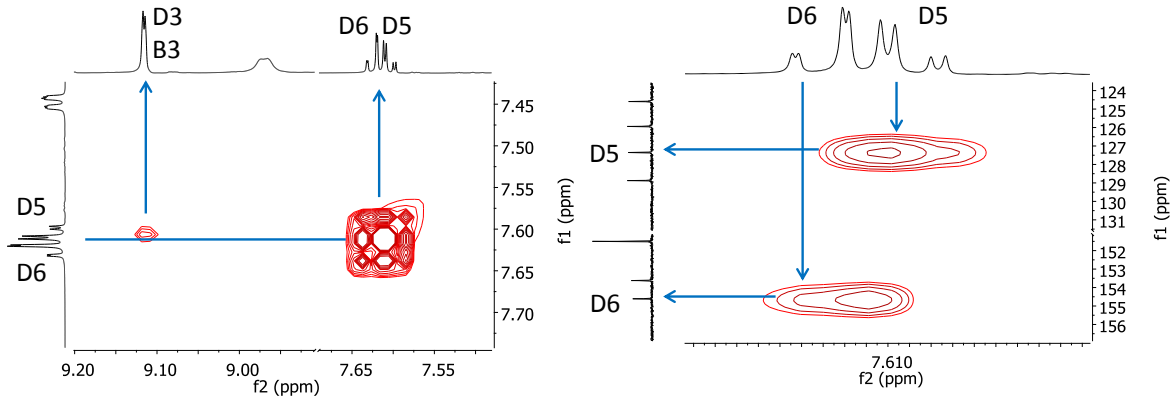

Figure 4.4: Detailed zoom on the COSY and HMQC NMR (500 MHz, CD_3CN) spectra of the homoleptic ruthenium(II) complex C28

4.2.3 Synthesis of ruthenium(II) complexes with 4'-phenyl-2,2':6',2''-terpyridine ligands

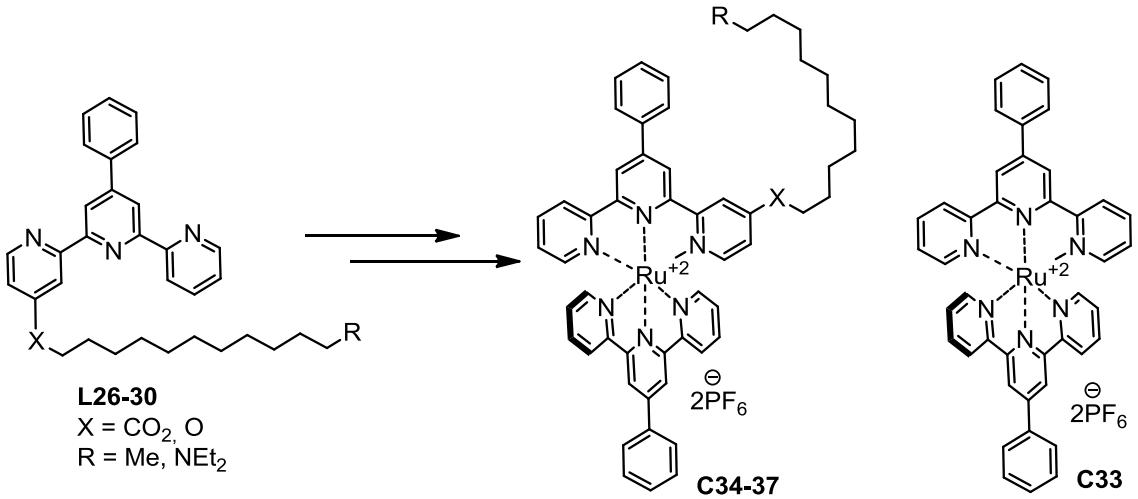

Scheme 4.9: Towards ruthenium(II) complexes with Phtpy ligands with a side amino chain linked via an ester or via an ether group bearing one protonation site

As a next series of Ru(II) complexes, heteroleptic complexes **C34-37** with substituted 4'-phenyl-2,2':6',2''-terpyridine ligands **L26-30** and a homoleptic complex **C33** were synthesized (Scheme 4.9). These compounds were prepared for a comparison with previously synthesized Ru(II) complexes **C17-25** with pendant pyridyl units. Complexes **C35** and **C37** have a side amino chain linked via an ester or via an ether group, respectively. Therefore **C35** and **C37** have just one protonation site in the molecule (the amino group), in comparison with **C18** and **C23** with pytpy ligands, bearing 3 protonation possibilities (one on the side

chain and two on the pendant pyridyl units). Photophysical studies carried out with Phtpy complexes **C33-37** will be a very useful piece of information for a better understanding of the photophysical properties of complexes **C17-25** with pytpy units. We would like to reveal the influence of the side chain, especially of the amino unit of **C35** and **C37**, on the absorption and luminescence properties of the complexes.

For the synthesis of azachalcone **P11** (Scheme 4.10), the same microwave assisted reaction conditions were applied as those Newkome's successfully used for the synthesis of **P9** in the Chapter 1 (Scheme 1.5).[3] However, the Claisen-Schmidt aldol condensation by using microwave irradiation with a small amount of solvent in the presence of Al_2O_3 as a catalyst and solid support, in case of azachalcone **P11** did not work. By using classical conditions with KOH in a mixture of solvents (EtOH/H_2O), azachalcone **P11** was obtained as a yellowish powder in a nearly quantitative yield (97%). Synthesis of PPI salts **P5**, **P6** and **P8** (Kröhnke reagents) were reported in Chapters 1-3 (**P5** – Scheme 1.4, **P6** – Scheme 2.3, **P8** – Scheme 3.4).[5]

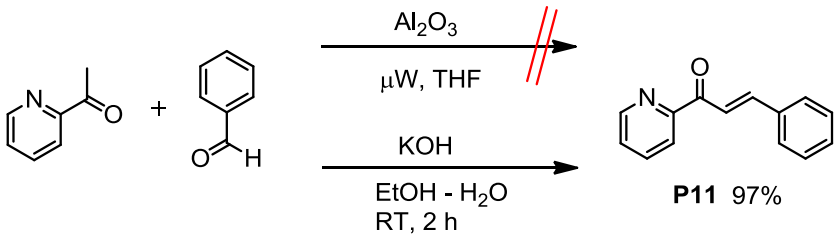

Scheme 4.10: Synthesis of the azachalcone P11

For the synthesis of the 4'-phenyl-2,2':6',2''-terpyridine **L23** (Scheme 4.11), the same Hanan's "one-pot" reaction conditions were applied as those successfully used for the synthesis of **L3** in the Chapter 1 (Scheme 1.6).[6] These conditions, suitable for symmetrical 4-aryl- or heteroaryl substituted terpyridines, involve condensation of the first equivalent of 2-acetylpyridine with aldehyde under basic conditions of KOH, followed by addition of the second equivalent of 2-acetylpyridine and a ring closure in a presence of ammonia as a source of nitrogen atom. However, even after several trials and with a use of freshly distilled benzaldehyde, **L23** was obtained in only 17-21% yields and in a mixture of multiple condensation products. Kröhnke synthetic methodology turned out to be an appropriate option (Scheme 4.12).[5]

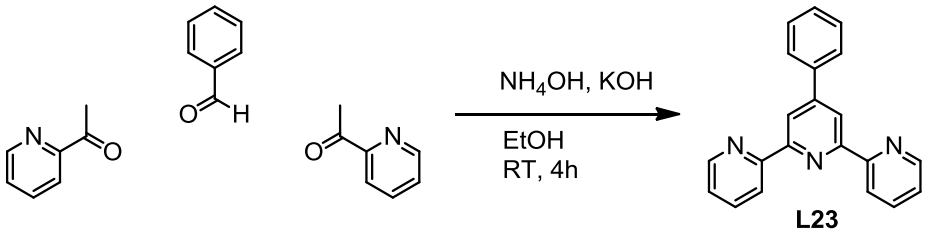

Scheme 4:11: Hanan's synthesis of Phtpy ligand L23

For synthesis of Phtpy ligand **L23** and 4-substituted Phtpy ligands **L24** and **L28** (Scheme 4.12), the same Kröhnke methodology was applied as that succesfully used for the synthesis of pytpy **L2** in the Chapter 1 (Scheme 1.3).[5] For the synthesis of the desired Phtpy ligands **L23**, **L24** and **L28**, azachalcone **P11** was refluxed with an appropriately substituted pyridinium salt (**P8**, **P5** and **P6**) in MeOH for 5-8 hours (Table 4.3, Inputs 1, 3 and 5).

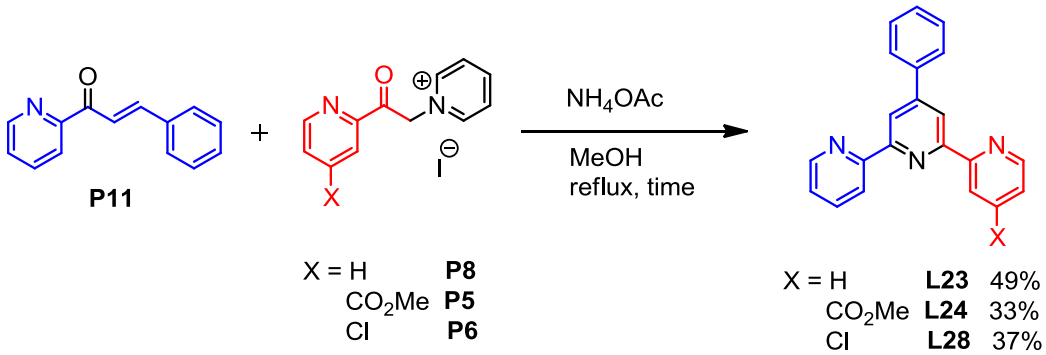

Scheme 4.12: Synthesis of the 4-phenyl-terpyridines L23, L24 and L28 via the Kröhnke synthetic methodology

Input	PPI salt	Time [h]	Product / yield (%)
1	**P8**	8	**L23** (18%)
2	**P8**	19	**L23** (49%)
3	**P5**	5	**L24** (9%)
4	**P5**	16	**L24** (33%)
5	**P6**	7	**L28** (24%)
6	**P6**	23	**L28** (37%)

Table 4.3: Reaction conditions for Scheme 4.12

In comparison with the pytpy ligand **L2**, Phtpy ligands are more soluble in methanol. Therefore, formation of the precipitate of the desired Phtpy ligands was observed during the reflux in only a small amount. Even after reducing the solvent volume or upon chilling of the reaction mixture in a freezer, desired molecules **L23**, **L24** and **L28** were isolated in very low yields (9-24%, Table 4.3, Inputs 1, 3 and 5). To improve the yields of the products **L23**, **L24** and **L28**, the reaction time was prolonged to 16-23 hours and volume of methanol reduced to half. Ligands **L23**, **L24** and **L28** were then obtained in 33-49% yields (Table 4.3, Inputs 2, 4 and 6).

In the electrospray mass spectrum of **L24**, a peak with *m/z* = 368.0 (assigned to $[M+H]^+$) with intensity 100% and also a peak with *m/z* = 390.0 (assigned to $[M+Na]^+$) with intensity 24% were observed. In the electrospray mass spectrum of **L28**, a peak with *m/z* = 366.1 (assigned to $[M+Na]^+$) with intensity 100% and also peaks with *m/z* = 383.1 and 344.1 (assigned to $[M+K]^+$ and $[M+H]^+$, respectively) with intensity 19% and 57%, respectively, were observed.

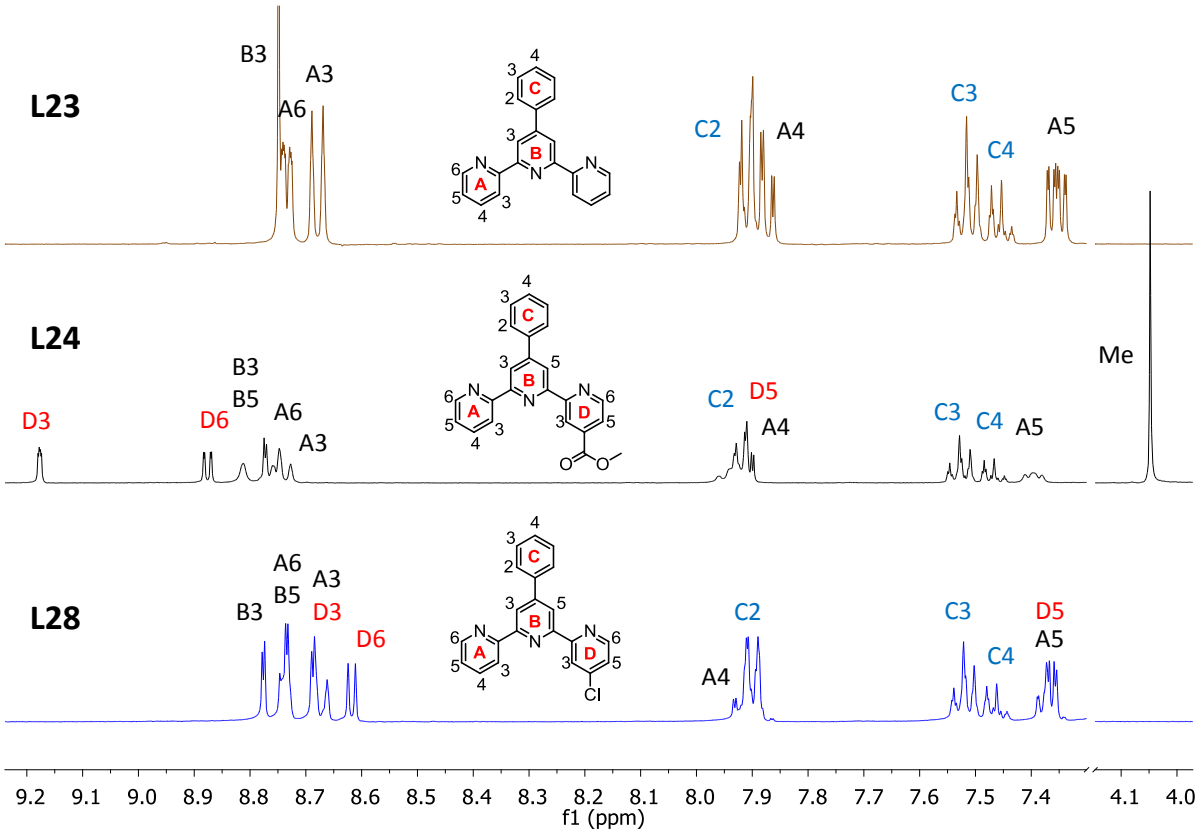

Figure 4.5: ^{1}H NMR spectra (400 MHz, $CDCl_3$) of 4-substituted Phtpy ligands L23 (H, brown), L24 (CO_2Me, black) and L28 (Cl, blue)

Figure 4.5 shows a comparison of the ^{1}H NMR spectra of the Phtpy ligand **L23** (brown) and CO_2Me-substituted Phtpy **L24** (black) and chloro-substituted **L28** (blue). The methyl ester substituent of **L24** (black) is typically electron-withdrawing by resonance, therefore all **D**-protons are shifted to higher ppm. However, the chloro-substituent of ligand **L28** (blue) is electron-withdrawing inductively but electron-donating through resonance. After combining these two effects, one observes that the **D**-ring protons of **L28** have similar chemical shifts as the **A**-ring protons. Protons of the phenyl ring **C** are represented with three multiplets with a chemical shift δ 7.91 ppm (H^{C2}), δ 7.52 ppm (H^{C3}) and δ 7.46 ppm (H^{C4}) (Figure 4.5).

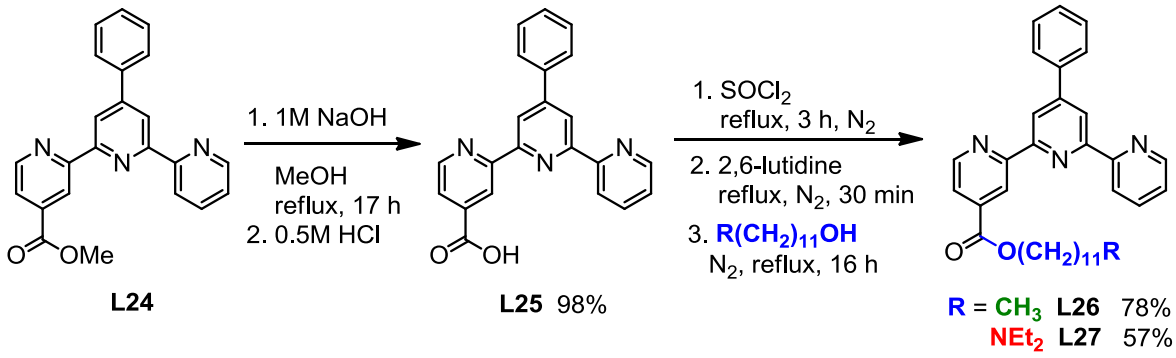

Scheme 4.13: Esterification of L25 via the corresponding acid chloride

For the synthesis of the Phtpy ligands with the side chain linked via an ester group **L26**-**27** (Scheme 4.13), the same reaction conditions were used as those successfully used for the synthesis of **L10**-**11** in Chapter 3 (Scheme 3.6 and 3.8).[7, 8] That is, the intermediates were an –COOH substituted tpy and the corresponding acid chloride. **L24** was refluxed with 1M aqueous NaOH overnight in methanol and the pH was adjusted with HCl (0.5M) to a value of ≅ 3.5-4.0. A grey precipitate formed, and this was collected on a frit, washed with water and air dried. The product **L25** was isolated as a grey powder in nearly quantitative yield and used for the next step without any further purification. In the MALDI TOF mass spectrum of **L25**, a peak with *m/z* = 353.8 (assigned to $[M]^+$) with intensity 93% and also a peak with *m/z* = 309.8 (assigned to $[M\text{-}CO_2]^+$) with intensity 100% were observed. In the ^{1}H NMR spectrum of **L25**, a broad peak at δ 13.9 ppm, assigned to the proton from the COOH group, was observed (Figure 4.6). The chemical shifts of the aromatic protons in rings **A**, **B** and **D** correspond to that of the COOH-substituted pytpy **L8**. The chemical shifts of the **C**-ring protons of **L25** correspond to that of the methyl ester-substituted Phtpy **L24** (Figure 4.5).

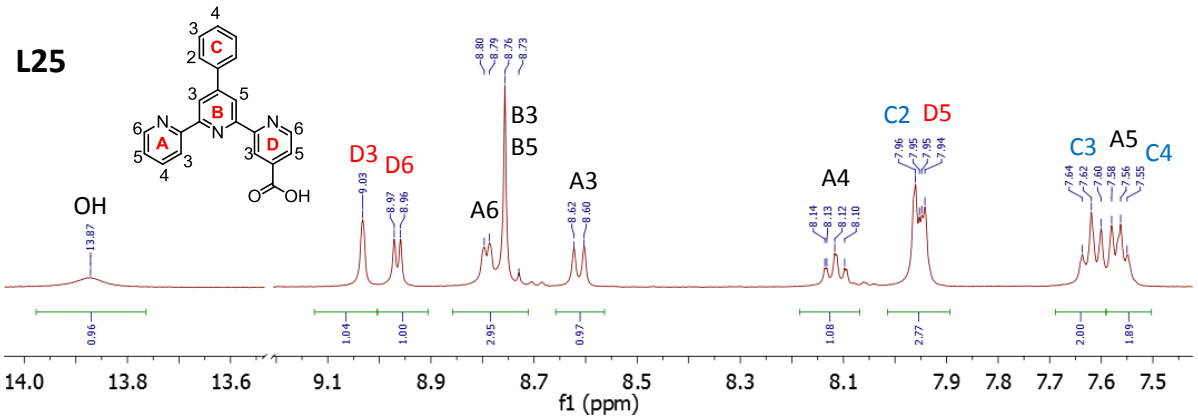

Figure 4.6: ^{1}H NMR spectrum (400 MHz, DMSO-d_6) of COOH-substituted Phtpy ligand L25

L25 was refluxed in thionyl chloride for 3 hours under an inert atmosphere to give a yellowish solution. The excess of thionyl chloride was evaporated under reduced pressure and the residue dried. The acid chloride was obtained as a yellowish powder, assumed to be formed in quantitative yield and immediately used for esterification without any further purification. This was then refluxed with the base 2,6-lutidine in toluene for 30 minutes under nitrogen. Dodecanol (or amino alcohol **P16**, respectively) was added and the reaction mixture was refluxed for 16 hours under nitrogen (Scheme 4.13). The crude reaction mixture was evaporated, dissolved in chloroform and extracted with saturated aqueous sodium hydrogen carbonate and water. Formation of the target esters **L26-27** was monitored by recording the ^{1}H NMR spectrum and looking for the triplet (expected $\sim \delta$ 4.4 ppm) of the first CH_2 group next to the carboxyl group. Dodecyl ester **L26** was purified by crystallisation from cold EtOH and the product was obtained as an analytically pure pale brown powder in 78% yield. Diethylamino-substituted ester **L27** was purified with a short chromatography column (SiO_2, eluted with EtOAc/Et_3N = 99:1) and the product obtained as a yellow oil in 57% yield. In the electrospray mass spectrum of **L26**, a peak with *m/z* = 544.2 (assigned to $[M+Na]^+$) with intensity 100% and also a peak with *m/z* = 522.2 (assigned to $[M+H]^+$) with intensity 66% were observed. In the electrospray mass spectrum of **L27**, a peak with *m/z* = 579.2 (assigned to $[M+H]^+$) with intensity 100% and also a peak with *m/z* = 601.2 (assigned to $[M+Na]^+$) with intensity 4% were observed.

For the synthesis of the alkoxy-substituted Phtpy ligands **L29-30**, the same "harsh reaction conditions" (Scheme 4.14), reported by Halcrow *et al.* in 2001, were applied as those successfully used for the synthesis of **L17**-**20** in Chapter 2 (Scheme 2.12).[9] Freshly ground

potassium hydroxide was suspended in DMSO, to which **L28** and dodecanol (or amino alcohol **P16**, respectively) were added and heated at 60 °C for 16 hours. This reddish-brown solution was then cooled to room temperature. Addition of ice-cold water gave a brown precipitate, which was purified by extraction with chloroform-water. A large amount of water during extraction was necessary for DMSO removal. However, a certain amount (19-56%) of unreacted alcohol was always detected in the isolated products **L29**-**30**, no matter which purification technique was used (crystallisation or column chromatography). Therefore elemental analysis and absorption spectra were not measured for products **L29**-**30**. In the electrospray mass spectrum of **L29**, a peak with *m/z* = 494.4 (assigned to $[M+H]^+$) with intensity 100% and also a peak with *m/z* = 516.3 (assigned to $[M+Na]^+$) with intensity 34% were observed. In the electrospray mass spectrum of **L30**, a peak with *m/z* = 551.4 (assigned to $[M+H]^+$) with intensity 100% and also peaks with *m/z* = 573.2 and 589.2 (assigned to $[M+Na]^+$ and $[M+K]^+$, respectively) with intensity 23% and 7%, respectively were observed.

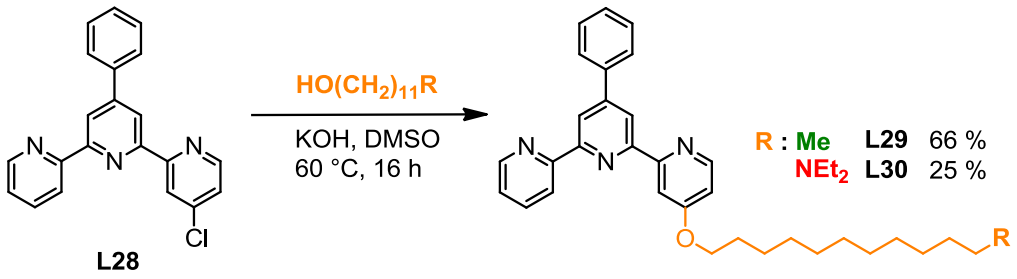

Scheme 4.14: Synthesis of the alkoxy-substituted Phtpy ligands L29-30

Figure 4.7 compares the ^{1}H NMR spectra of the ester-substituted Phtpy ligands **L26** (green) and **L27** (red) and the alkoxy-substituted Phtpy ligands **L29** (cyan) and **L30** (black). The aliphatic part of the ^{1}H NMR spectra of all four Phtpy ligands has nearly the same distribution of peaks as that of the pytpy ligands **L10**-**11** and **L17**-**18** (see Chapter 3, Figure 3.4, Chapter 2, Figure 2.5). The methylene group **1** next to the oxygen atom has a characteristic triplet at δ 4.43 ppm and 4.09 ppm, respectively. Methylene protons **11** and **13** in the neighbourhood of the amino group (**L27** and **L30**) have peaks around δ 2.4 ppm. Multiplets for the CH_2 groups **2** and **3** were observed with chemical shifts of δ 1.83 ppm and δ 1.50 ppm and all protons **4**-**10** resonated around δ 1.30 ppm. Protons of the pyridyl rings **A**, **B** and **D** have, in the aromatic part, the same set of peaks as those of pytpy ligands **L10**-**11**

and **L17**-**18**. However, protons of the phenyl ring **C** are represented with three multiplets in the region δ 7.90 – 7.45 ppm similar to those of the methyl ester-substituted Phtpy **L24** (Figure 4.5).

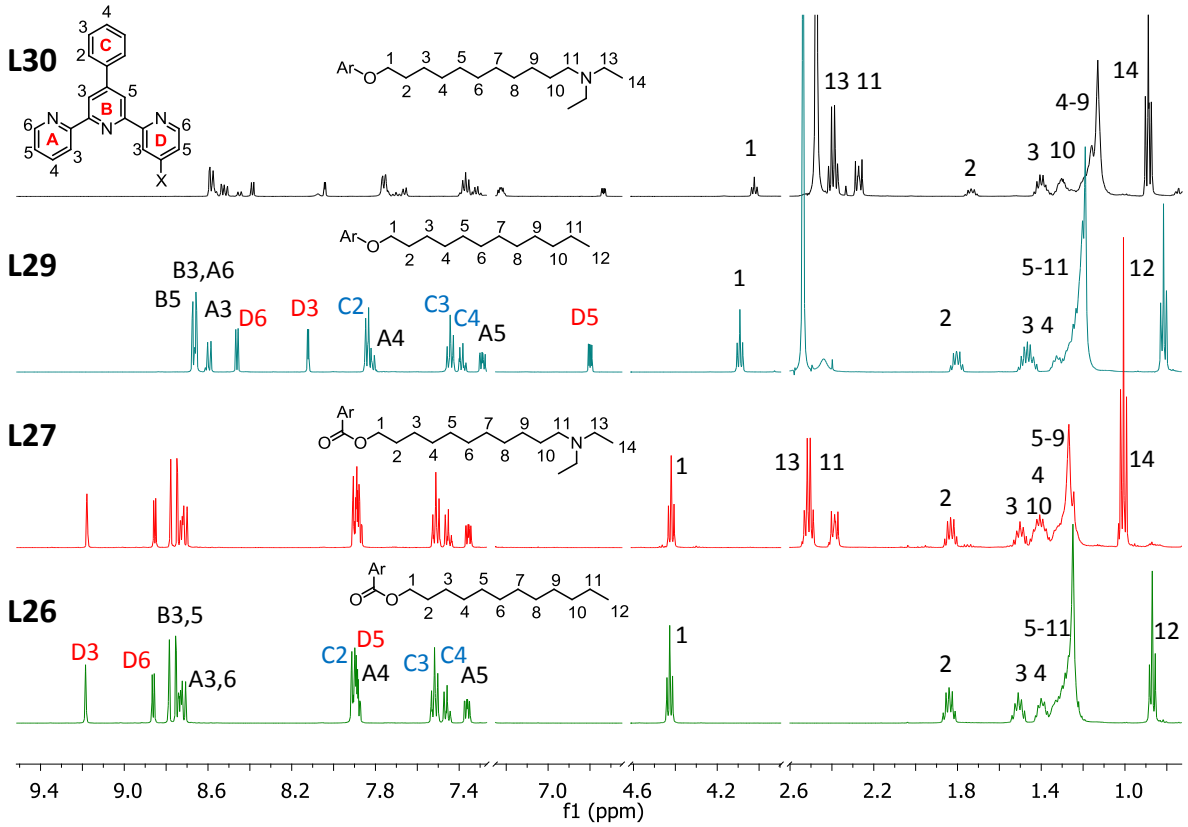

Figure 4.7: ^{1}H NMR spectra (500 MHz, $CDCl_3$) of the ester-substituted Phtpy ligands L26 (green) and L27 (red) and the alkoxy-substituted Phtpy ligands L29 (cyan) and L30 (black)

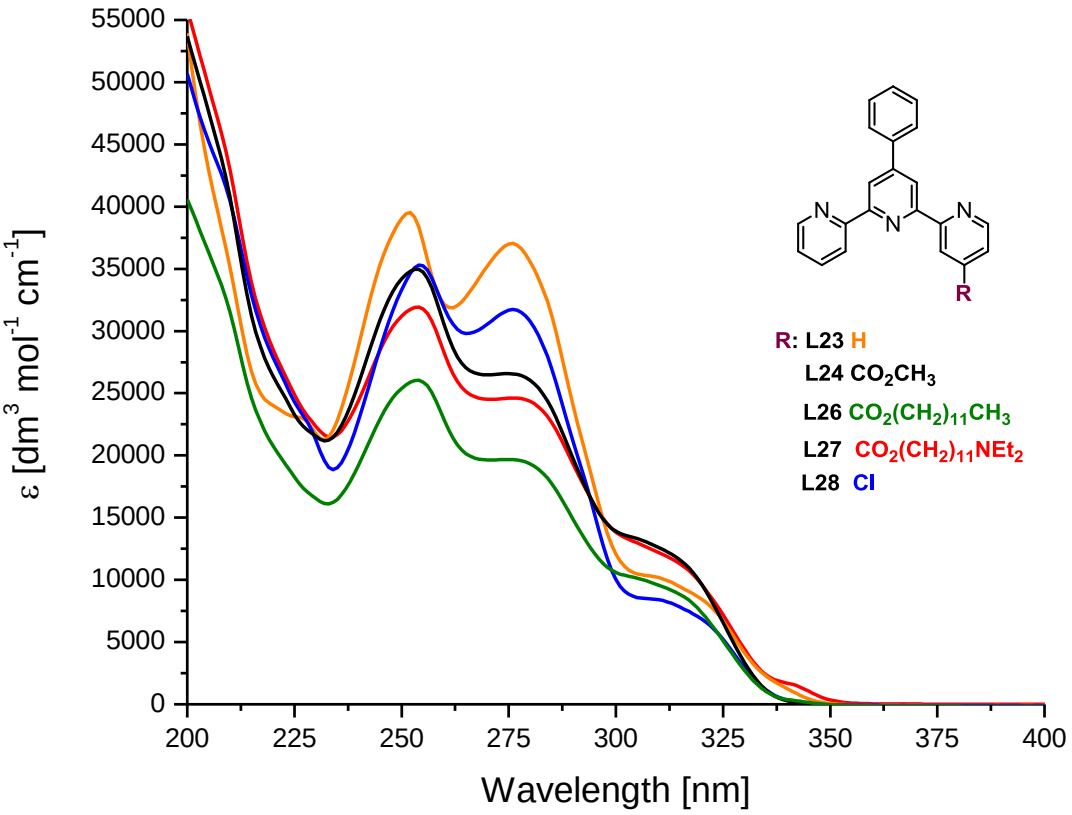

Figure 4.8: UV/Vis absorption spectra (CH_3CN) of the 4-substituted Phtpy ligands L23 ($4.55 \cdot 10^{-5}$M, orange), L24 ($5.97 \cdot 10^{-5}$M, black), L26 ($4.08 \cdot 10^{-5}$M, green), L27 ($4.80 \cdot 10^{-5}$M, red), L28 ($4.39 \cdot 10^{-5}$M, blue)

Ligand	c / 10^{-5} mol dm^{-3}	λ_{max}/nm ($\varepsilon_{max}/10^3$ dm^{3}mol^{-1}cm^{-1})		
L23	4.55	252 (39.5)	276 (37.0)	313 (9.8 sh)
L24	4.44	253 (35.0)	276 (26.6)	310 (12.6 sh)
L26	4.26	254 (26.0)	280 (19.3)	310 (9.2 sh)
L27	3.97	254 (31.9)	280 (24.4)	313 (11.7 sh)
L28	3.88	254 (35.3)	276 (31.7)	313 (8.1 sh)

Table 4.4: UV/Vis absorption spectra (CH_3CN) of the 4-substituted Phtpy ligands

The electronic absorption spectra of acetonitrile solutions of ester-substituted Phtpy ligands **L24**, **L26-27**, together with Phtpy **L23** and chloro-substituted Phtpy **L28** are shown in Figure 4.8. The ligands exhibit a series of high energy absorption bands around 250 nm and around 276 nm with high extinction coefficients (20 to 40×10^3 dm^3 mol^{-1} cm^{-1}) with a shoulder at

about 313 nm with lower extinction coefficients (10×10^3 dm^3 mol^{-1} cm^{-1}). The bands arise from ligand-centred $\pi^*\leftarrow\pi$ transitions (Table 4.4).

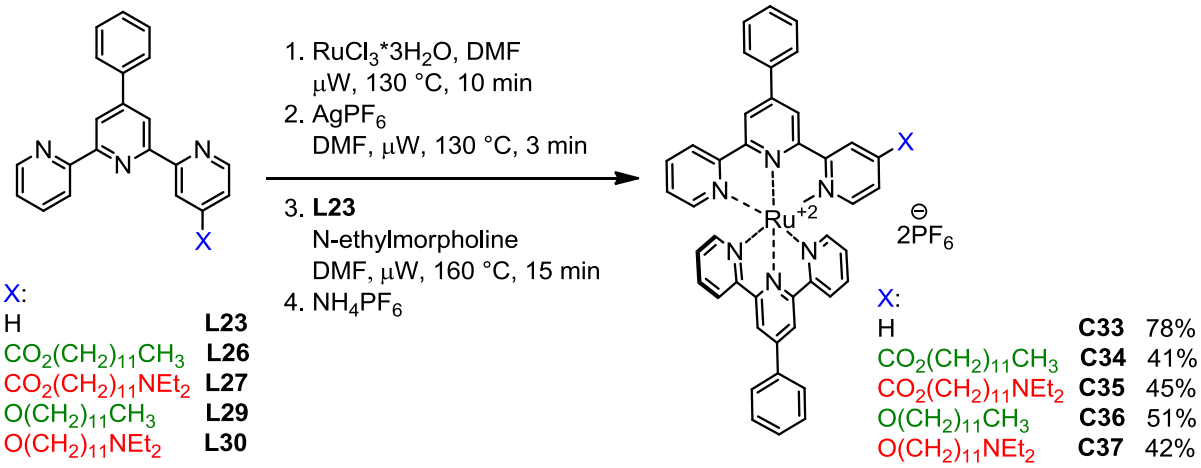

Scheme 4.15: Synthesis of the ruthenium(II) complexes C33-37 with Phtpy ligands

For the synthesis of the homoleptic Ru(II) complex **C33** and heteroleptic Ru(II) complexes with Phtpy ligands **C34-37** (Scheme 4.15), the same four-step "one-pot" reaction conditions were applied as those successfully used for the synthesis of **C17-18** with pytpy ligands (Scheme 4.3 and 4.4). The first ligand (**L23**, **L26-30**) is coordinated as a Ru(**L**)Cl_3 complex, which is then activated with silver hexafluorophosphate. This reacts with the second ligand (**L3**) in a presence of a catalytic amount of *N*-ethylmorpholine, used as a reducing agent to convert Ru(III) to Ru(II). The products **C33-37** are then precipitated as PF_6^- salts. **C33** was purified by crystallisation from MeCN-Et_2O and obtained 78% yield. Complexes **C34-37** were purified by column chromatography (SiO_2, eluted with MeCN/saturated aqueous KNO_3/H_2O = 10:0.5:0.5) and by crystallisation from MeCN-Et_2O. Products **C34-37** were obtained in 41-51% yields. The complex **C37** was isolated in a mixture with side products, which were impossible to separate, therefore **C37** was excluded from further analysis and photophysical measurements.

In the electrospray mass spectrum of the model complexes **C34** and **C36**, peaks with *m/z* = 1077.4 and 1049.4, respectively (assigned to $[M\text{-}PF_6]^+$) with 100% intensity were observed. In the electrospray mass spectrum of **C35**, peaks with *m/z* = 1280.4 and 1134.4 (assigned to the deprotonated form of $[M+H]^+$ and $[M\text{-}PF_6]^+$, respectively) with intensity 100% and 20%, respectively, were observed. Elemental analysis results could only be fitted by allowing for the presence of a small amount of NH_4PF_6, which was consistent with the ^1H NMR spectra.

Figure 4.9 compares the ^{1}H NMR spectra of the ester-substituted complexes Phtpy **C34-35** (green and red) and the dodecyloxy-substituted complex **C36** (blue). The aliphatic part of the spectra of all three complexes is consistent with that of **C17-18** and **C22** with the pytpy ligands (Figure 4.1 and 4.3). Methylene protons **11** and **13** in the neighbourhood of the amino group of the complex **C35** have peaks around δ 3.10 ppm. However protons **11** and **13** of the free ligand **L27** have a chemical shift around δ 2.40 ppm. This is one of the indications that the amino side chain of the complex **C35** is protonated as well as the side chain of **C18**. The chemical shifts of the **D**-ring protons depend on the electronic properties of the **D**-ring substituents. Therefore the **D**-protons of **C34-35** are shifted to lower magnetic field and the **D**-protons of **C36** to higher magnetic field. The **C**-ring protons of the complexed ligand are shifted to higher ppm values (δ 8.30 – 7.80 ppm), in comparison to those of the free ligands **L26-27** (δ 7.90 – 7.45 ppm) (Figure 4.7).

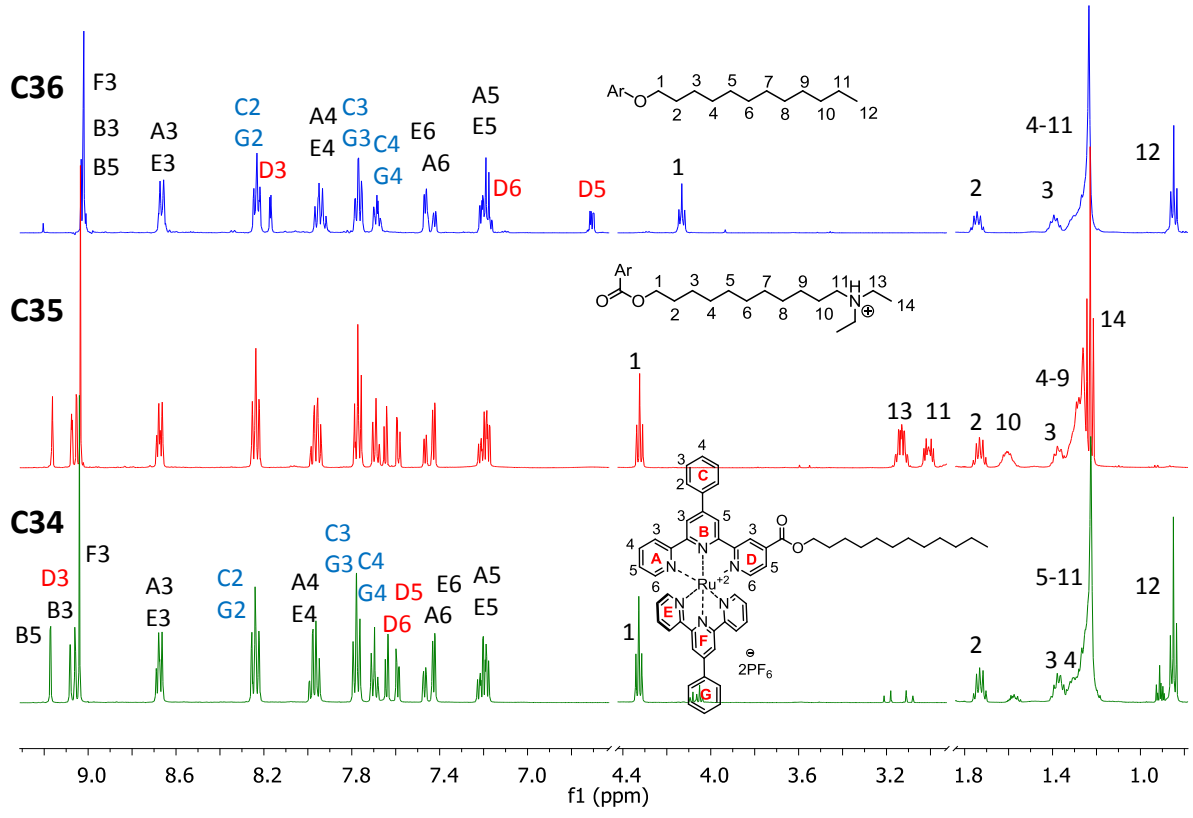

Figure 4.9: ^{1}H NMR spectra (500 MHz, CD_3CN) of ruthenium(II) complexes with Phtpy ligands C34-36

4.2.4 Crystal structure of the homoleptic ruthenium(II) complex C27

Compound		C27
Empirical Formula		$C_{94}H_{75}F_{24}N_{19}O_9P_4Ru_2$
Formula Weight		2396.75
Temperature / K		123
Crystal System		Monoclinic
Space Group		P2/c
Unit cell dimensions:	**a / Å**	9.5096 (7)
	b / Å	11.2463 (8)
	c / Å	25.5889 (15)
	α / °	90
	β / °	108.379 (4)
	γ / °	90
Volume / Å^3		2597.1 (3)
Z		1
Crystal Description		red plate
Crystal Size / mm^3		0.03 × 0.15 × 0.30
Density / Mg m^{-3}		1.531
Absorption Coefficient / mm^{-1}		3.889
Theta range for data collection / °		4.33 to 66.52
Reflections collected		13550
Independent reflections		4533
R(int)		0.0444
Completeness to theta / ° (%)		66.52 (97.4)
Parameters		439
Goodness of fit		1.204
wR_2		0.1986
Final R_1 [I>2sigma(I)]		0.0777

Table 4.5: Crystallographic data summary of the ruthenium(II) complex C27

X-ray quality crystals of the homoleptic ruthenium(II) complex **C27** were grown from a solution of **C27** in acetonitrile by slow evaporation. Crystals grew as red plates. The complex **C27** crystallized in the monoclinic crystal system in the space group P2/c. The R factor is high due to the crystals being very air sensitive, and also slightly twinned. The crystal data is shown in Table 4.5. In the asymmetric unit (Figure 4.10) there is half of the Ru cation, one PF_6^- anion (rotationally disordered with partial occupancies of 54%/46%) and disordered solvent (75% of MeCN (disordered over 2 positions) and 25% H_2O). The rest of the cation is generated by symmetry. The Ru atom is in an octahedral environment and coordinates two

methyl ester-substituted pytpy ligands via the N-donor terpyridine units orthogonally to each other (Figure 4.11). Bond lengths and angles are unexceptional.

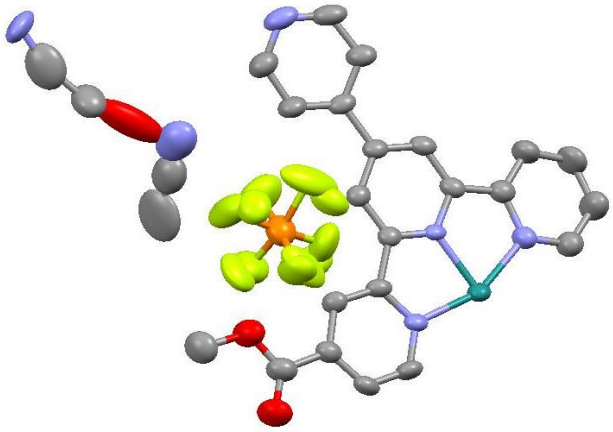

Figure 4.10: The asymmetric unit of the ruthenium(II) complex C27 contains half a cation, one PF_6^- anion (disordered with partial occupancies of 54%/46%) and disordered solvent (75% of MeCN (disordered over 2 positions) and 25% H_2O), H atoms omitted

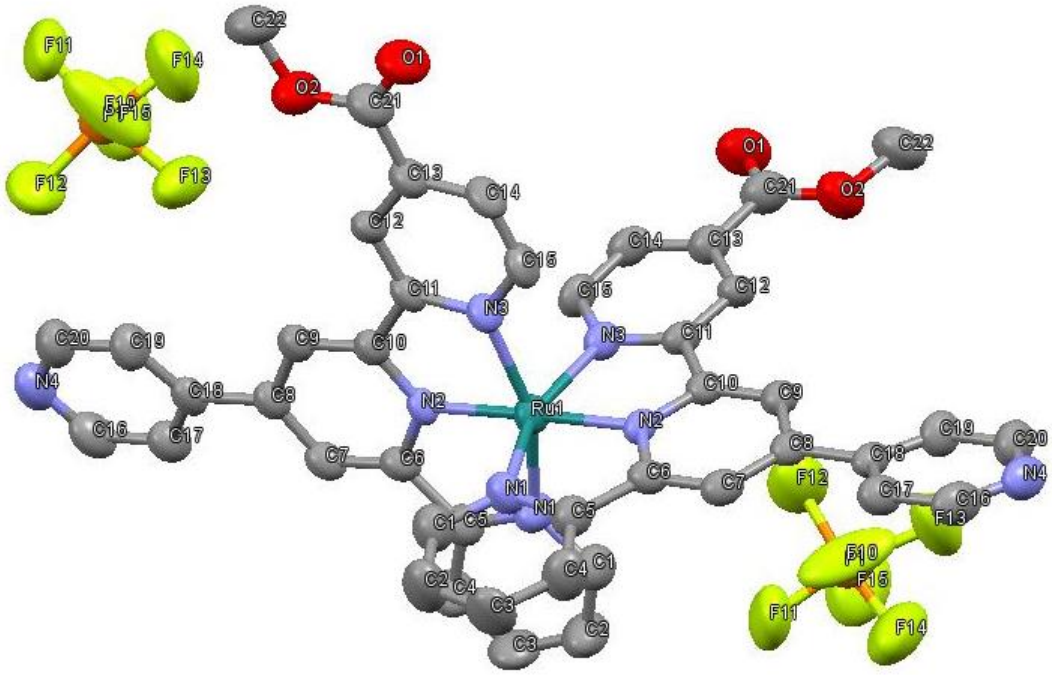

Figure 4.11: An ellipsoid display of the molecular structure of C27 in the X-ray crystal structure of C27·0.75MeCN·0.25H_2O. H atoms, solvent and anion disorder omitted. Selected bond lengths (in Å) and bond angles (in °): Ru1-N1: 2.071(4), Ru1-N2: 1.992(3), Ru1-N3 2.075(3), O1-C21: 1.215(7), O2-C21: 1.325(7), O2-C22: 1.453(7), N1-C1: 1.353(6), C8-C18: 1.493(6), N4-C20: 1.328(8), N2-Ru1-N1: 99.29(14), N1-Ru1-N1: 88.4(2), C21-O2-C22 116.6(5), C1-N1-C5: 118.7(4), C1-N1-Ru1: 127.1(4)

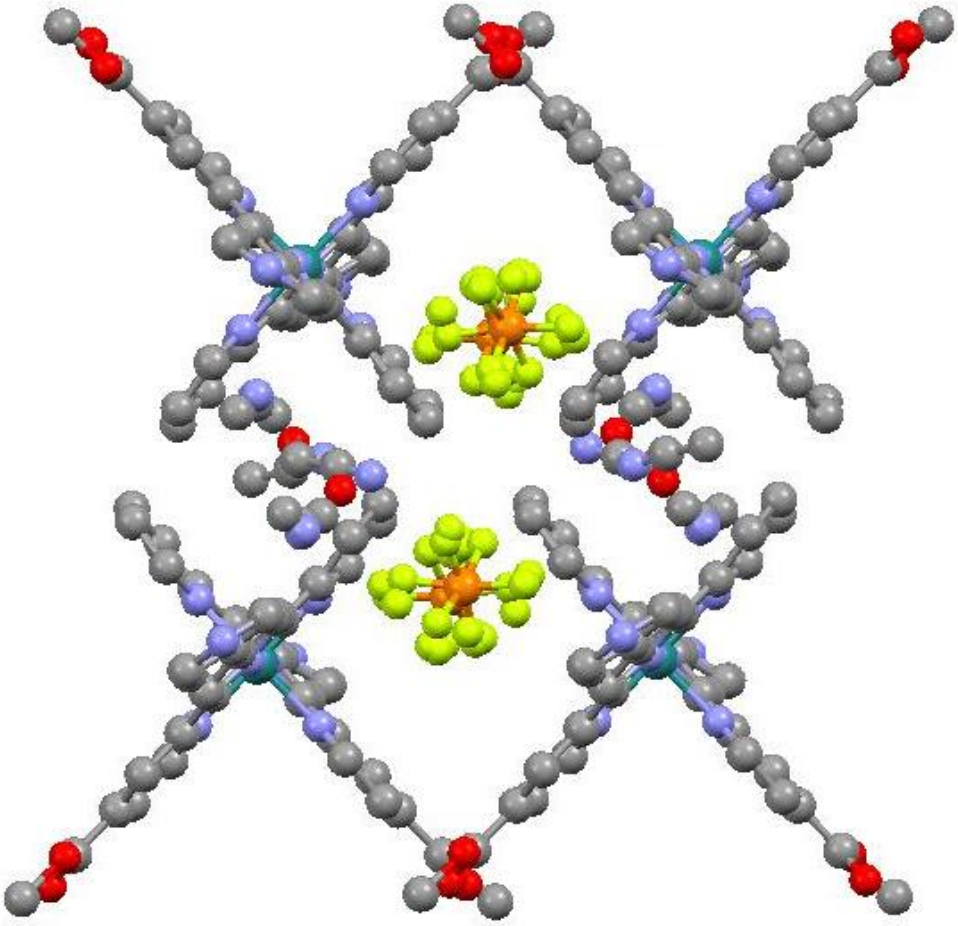

Figure 4.12: Display of packing interactions between molecules of C27, view down c-axis

The methyl ester-substituted pytpy ligands are perpendiculary coordinated to the ruthenium(II) metal center along the c-axis (Figures 4.12 and 4.13). The molecules of the complex **C27** pack together exhibiting two different intermolecular interactions. Therefore the molecules of **C27** form a two dimensional network. “Face to face” π-π interactions (length 3.8 Å) between **B** and **C**-rings of the pytpy units form the first type of chain. H-Bonding between the carboxyl group and the proton A4 of the tpy unit form the second type of chain (Figures 4.14 and 4.15) The H-bonds have a weak character due to the O – H atom distance 2.3 Å . Together these two packing interactions form a net.

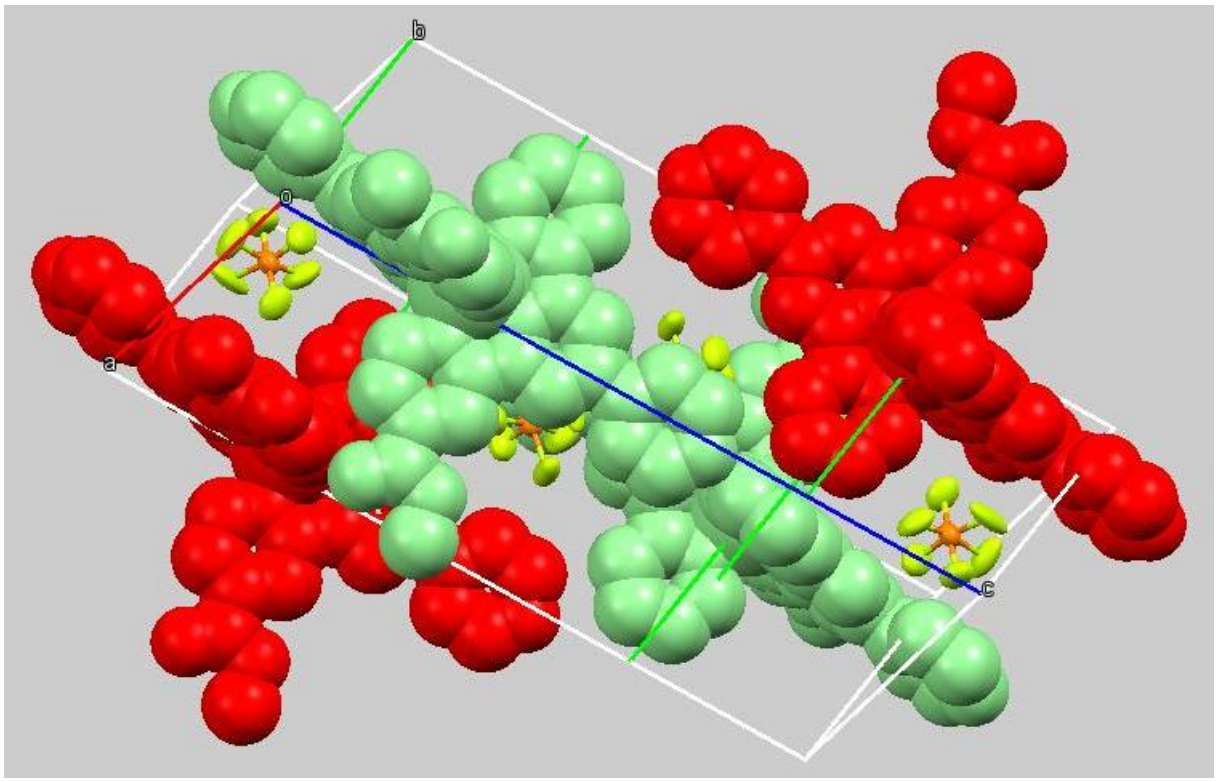

Figure 4.13: C27 - Spacefill display of packing interactions between molecules of C27, viewed along the c-axis

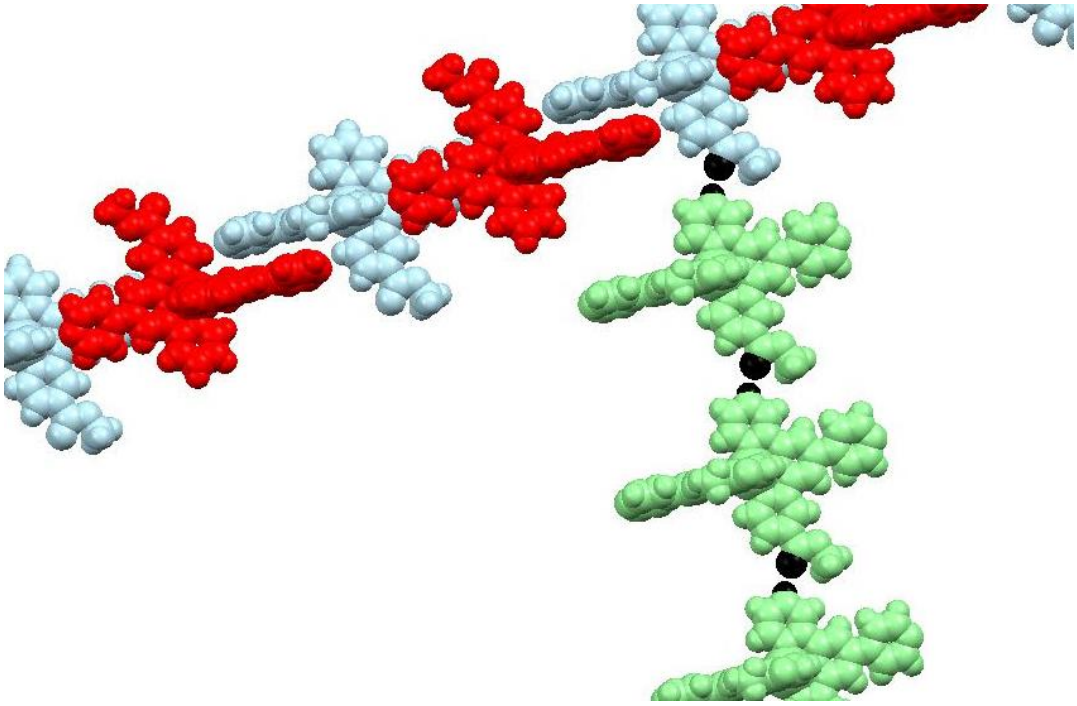

Figure 4.14: "face to face" π-π interactions between pytpy units of C27 form chains (red-blue), H-bonding between the carboxyl group and the proton A4 of the tpy unit form chains orthogonally (black-green)

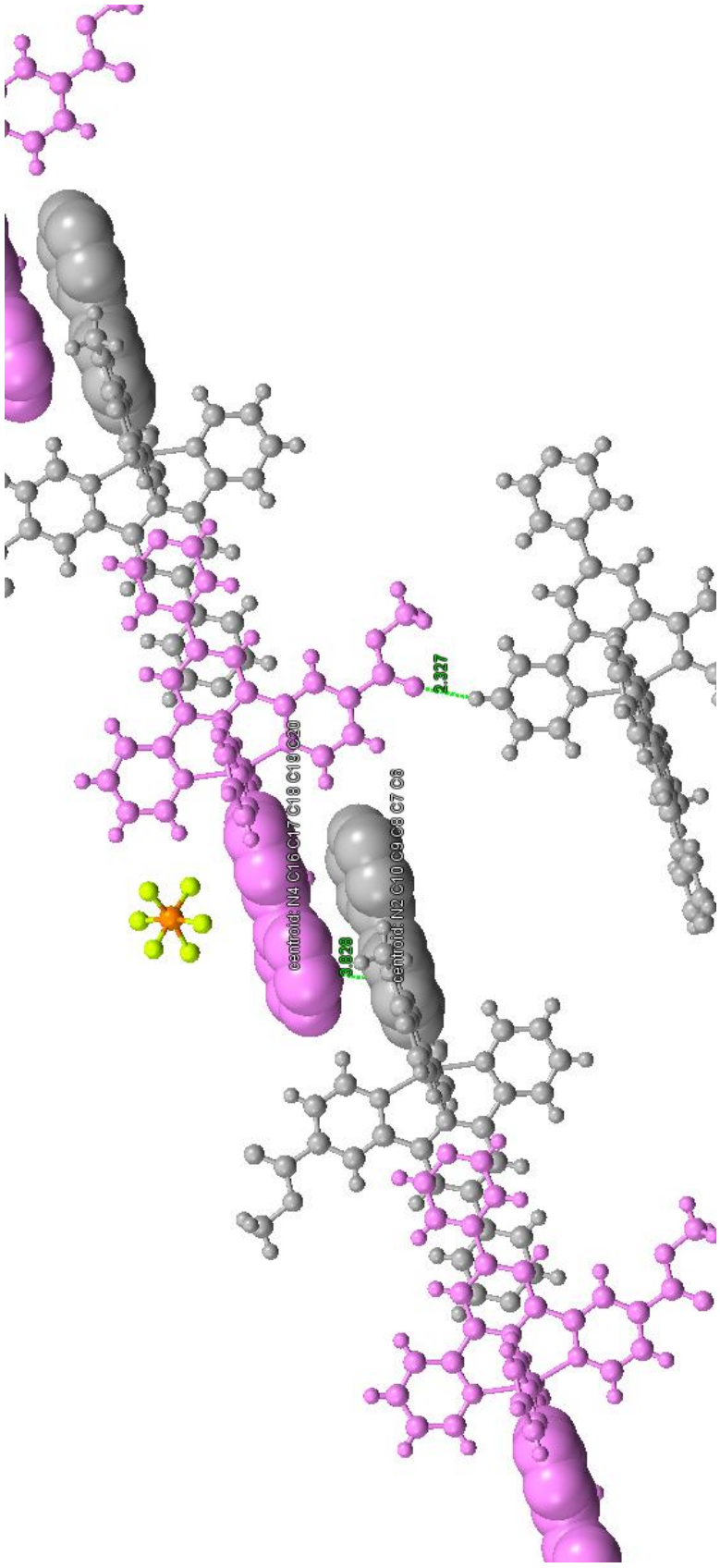

Figure 4.15: the distance between the π-π interacting pytpy units of C27 forming chains is 3.8 Å, weak H-bond interactions (length 2.3 Å) between the carboxyl group and the proton A4 of the tpy unit

Conclusion

Heteroleptic and homoleptic ruthenium(II) complexes with pytpy ligands with an amino-substituted side chain, linked via an ester or an ether group were successfully synthesized. So as to have a model compounds for use in the photophysical studies, ruthenium(II) complexes with Phtpy ligands with the same side chains were also prepared. All complexes were characterised with 1D and 2D NMR spectroscopy, electrospray or MALDI TOF mass spectrometry, infrared spectroscopy, elemental analysis, UV-vis and photoluminescence spectroscopy. Detailed photophysical studies were carried out in a collaboration with the photochemistry research group of Prof. Alberto Credi from the University of Bologna and these results are reported in Chapter 5. NMR titration studies with complexes **C20** and **C29** are reported in Chapter 6.

Literature

1 Sulliwan, B. P.; Calvert, J. M.; Meyer, T. J *Inorg. Chem.,* **1980**, *19*, 1404-1407.

2 Evans, I. P.; Spencer, A.; Wilkinson, G. *J. Chem. Soc., Dalton Trans.,* **1973**, 204-209.

3 Eryazici, I.; Moorefield, C. N.; Durmus, S.; Newkome, G. R. *J. Org. Chem.,* **2006**, *71*, 1009.

4 Zhao, L.-X.; Kim, T. S.; Ahn, S.-H.; Kim, T.-H.; Kim, E.-k.; Cho, W.-J.; Choi, H.; Lee, C.-S.; Kim, J.-A.; Jeong, T. C.; Chang, C.-j.; Lee, E.-S. *Bioorg. Med. Chem. Lett.,* **2001**, *11*, 2659-2662.

5 Mikel, C.; Potvin, P. G. *Polyhedron,* **2002**, 2*1*, 49-54.

6 Wang, J.; Hanan, G. S. *Synlett,* **2005**, *8*, 1251-1254.

7 Duprez, V.; Krebs, F. C. *Tetrahedron Letters,* **2006**, *47*, 3785–3789.

8 Uppadine, L. H.; Redman, J. E.; Dent, S. W.; Drew, M. J. B.; Beer, P. D. *Inorg. Chem.,* **2001,** *40,* 2860-2869.

9 Liu, X.; McInnes, E. J. L.; Kilner, C. A.; Thornton-Pett, M.; Halcrow, M. A. *Polyhedron,* **2001**, *20*, 2889-2900.

Chapter 5

Photophysical studies of ruthenium(II) complexes with a potential application as molecular switches

5.1 Introduction

In Chapter 4, a series of heteroleptic ruthenium(II) complexes with a long amino-substituted side chain linked via an ester **C18**-**20**, or via an ether **C23-25** and the homoleptic ruthenium(II) complex **C29** were synthesized, along with a series of methyl and dodecyl-substituted model Ru(II) complexes (**C7**, **C17**, **C22**, **C27**, **C28** and **C30**). The amino group attached to the side chain and the two pendant pyridyl groups bring three (or four, respectively) protonation sites to the molecule. A series of ruthenium(II) complexes **C33-36** with pendant phenyl units instead of the pendant pyridyl units were synthesized for comparison.

In this chapter, photophysical studies of all these new Ru(II) complexes are reported and discussed. These measurements were carried out by Angelo Lanzilotto (supervised by Dr. Marek Oszajca and Prof. Alberto Credi, as part of a collaboration I am thankful for) in the photochemistry laboratories of Prof. Alberto Credi at the University of Bologna, Italy.[4] It was found that some molecules exhibit unexpected abnormalities during those measurements. Namely, an unusual kinetic effect in the absorption and photoluminescence spectrum during titration of **C20** with TfOH or not enough acid consumed to complete titrations of some complexes (**C29**). Therefore, in Chapter 6, we carried out NMR studies of **C20** and **C29** and of their free ligands **L11** and **L14** with TFA-d or TfOD and with K_2CO_3 and these experiments were monitored with ^{1}H NMR spectrometry. These NMR studies revealed and clarified that all the Ru(II) complexes with three (or four, respectively) protonation sites were synthesized and isolated already in the mono-protonated form - on the amino group of the side chain (Scheme 5.1). This occurred due to the strong basicity of the side-chain amino units, when the complexes were precipitated as PF_6^- salts in the last synthetic step with an aqueous solution of NH_4PF_6. Unfortunately, this fact was discovered nearly at the end of this work,

after all the photophysical studies were carried out. Therefore, there was not enough time to develop a sufficient methodology to convert the mono-protonated Ru(II) complexes to the de-protonated form.

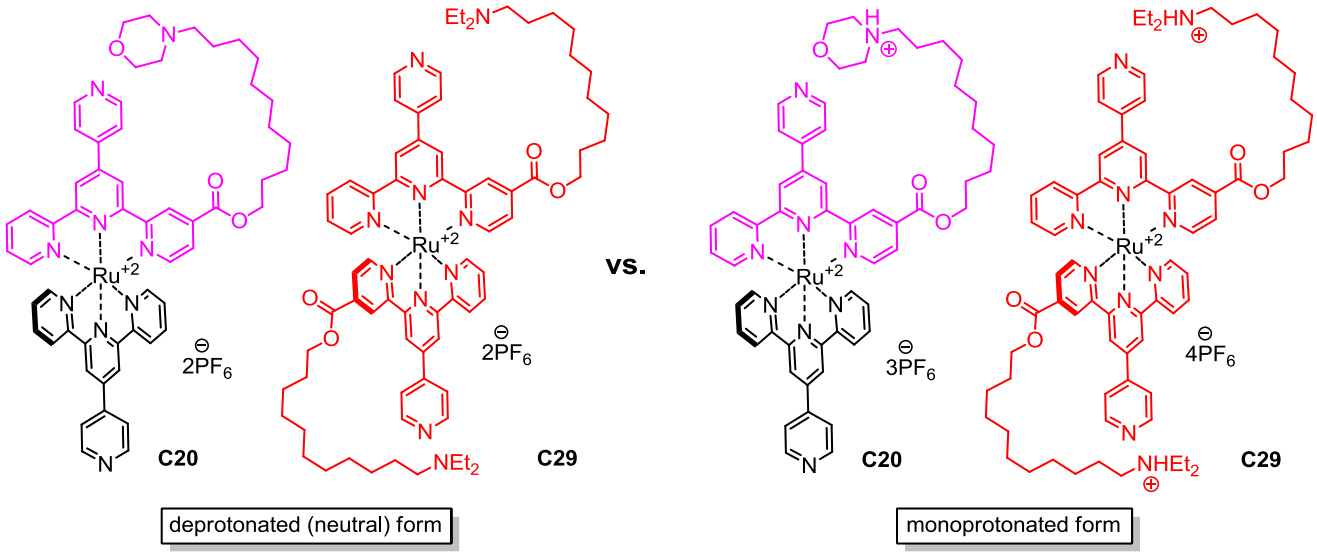

Scheme 5.1: Ruthenium(II) complexes C20 and C29 in the deprotonated (neutral) form (left) and monoprotonated form (right)

5.2 Experimental part

The UV-VIS and photoluminescence measurements were performed using a spectrophotometer Perkin-Elmer Lambda 45 and a Perkin-Elmer LS 50 spectrofluorometer. These measurements were carried out at room temperature with balanced solutions of spectroscopy grade acetonitrile (Fluka) in quartz cells with the optical path length 1 cm. The emission spectra were not corrected for the response of the monochromator/detector ensemble. The measures in rigid matrix were conducted in acetonitrile at 77 K.

The molar absorption coefficient ε was obtained by the interpolation of the data obtained from five solutions (by dilution of the stock solution). The dilution ratios (expressed as mL of the stock solution in mL of acetonitrile) were 0.4 : 2, 0.4 : 1.6, 0.5 : 1.5, 0.7 : 1.7 and 1 : 1. These dilutions correspond to ratios 1:6, 1:5, 1:4, 1:3, 1:2. According to the Lambert-Beer law $A = \varepsilon \times b \times c$, where A is the absorbance, ε the molar absorption coefficient, b the optical path and c is the concentration of the sample, the absorbance values are reported in the plot vs. concentration and this is interpolated by linear regression with the method of least

squares. The slope of the fitted line is used to find the value of the absorption coefficient and its standard deviation.

The quantum yields, expressed in percentage, were calculated by integration of the emission spectra in the range 580-900 nm. A solution of $[Ru(bpy)_3Cl_2]$ in degased acetonitrile was used as a standard, where the quantum yield is 1.25%. The solutions of our Ru(II) complex and of the standard were excited at the wavelength at which their absorbance is equal and less than 0.1 and emission spectra recorded. The excitation and emission slits were open up to 15 nm, because all our Ru(II) complexes with polypyridine ligands are weak emitters. Quantum yields were calculated according to the equation: $\Phi=\Phi_s\cdot(I/I_s)$, where s refers to the standard, Φ is quantum yield, and I is the integrated area under the emission curve.

Luminescence lifetime (τ) measurements were carried out with a time-correlated single-photon counting spectrofluorometer CD900 of Edinburgh Instruments equipped with a Hamamatsu R928 photomultiplier tube cooled to -30 °C. Measurements at room temperature were carried out with solutions in spectrofluorimetric cells and solutions for measurements at 77 K were placed in a capillary tube inserted in a Dewar flask containing liquid nitrogen. The excitation source was a pulsed diode laser at 405 nm. Solutions are required to have absorbance at the working wavelength of the laser lower than 0.1 to prevent photo-degradation of the probe. The decays were recorded with the program F900 provided by the instrument company, as a linear combination of exponential functions and the partial components (τ_1 τ_2 or more) obtained from the decay, and their standard deviations from the fit and non-linear statistical weight of each component. The accuracy of the fit is expressed with χ^2 value (the closer to 1 the better the fit is). The final lifetime is calculated from the partial decay components (τ_1 and τ_2) and their weights w_1 and w_2 according to the equation $\tau = \tau_1 w_1 + \tau_2 w_2$.

The titrations and experiments at variable pH with acid (or base, respectively), monitored with absorption and photoluminescence spectra, were performed by addition of small aliquots of 5×10^{-3} M solution of trifluoromethanesulfonic acid (CF_3SO_3H) (or phosphazene, respectively) in acetonitrile to the solution of a ruthenium(II) complex in a spectrofluorimetric cell. The additions were done via Hamilton microsyringes, until the spectroscopic plateau was reached. Titration curves form isosbestic points in the absorption spectra. The wavelength λ_{iso} of the isosbestic point in the MLCT band of each Ru(II) complex is used as λ_{ex} to monitor luminescence spectral changes.

5.3 Results and discussions

All the ruthenium(II) complexes synthesized in Chapter 4, could be divided into characteristic groups for the photophysical studies according to numerous aspects, e.g. homoleptic and heteroleptic complexes, complexes with pendant pyridyl units or phenyl rings, complexes with a side chain linked via an ester group or an ether group. Then one could also create groups according to the substituents on the side chain, e.g. diethylamino-substituted complexes, piperidine-substituted complexes, etc.

Compound	λ_{abs} [nm]	ε [L cm^{-1} mol^{-1}]	λ_{em} [nm]	QY [%]	τ [ns]	λ_{iso}	τ_{77K} [µs]
C8	489	26000	657	0.008	4	**492**	6
C8-1H	498	26000	751	0.042	98		7
C8-2H	507	32000	743	0.082	138		7
C17	493	20000	673	0.029	13	**487**	
C17-1H	506	24000	720	0.064	81		
C17-2H	508	28000	718	0.087	176		
C18	494	23000	682	0.029	21	**491**	
C18-1H	503	26000	723	0.070	118		
C18-2H	508	32000	717	0.109	176		
C19	494	23000	672	0.033	35	**492**	
C19-1H	502	26000	722	0.095	104		
C19-2H	508	31000	719	0.156	147		
C22	492	23000	681	0.024	9	**496**	
C22-1H	507	28000	730	0.029	23		
C22-2H	510	29000	761	0.042	61		
C23	491	23000	689	0.022	10	**495**	4
C23-1H	504	26000	719	0.021	20		4
C23-2H	511	29000	761	0.027	68		5
C24	491	28000	675	0.019	19	**495**	
C24-1H	501	27000	709	0.011	33		
C24-2H	511	34000	723	0.017	62		
C27	497	28000	662	0.020	6	**493**	
C27-1H	506	33000	716	0.122	124		
C27-2H	509	39000	711	0.165	191		
C28	497	28000	663	0.024	8	**494**	
C28-1H	504	31000	717	0.117	153		

C28-2H	508	38000	708	0.166	188	
C29	498	29000	667	0.236	7	**494**
C29-1H	506	34000	717	0.129	112	
C29-2H	508	39000	709	0.173	185	
C30	493	29000	680	0.025	10	**497**
C30-1H	505	29000	701	0.056	4	
C30-2H	514	36000	786	0.09	5	
C38	490	25000	644	0.004	**2**	
C33	488	24000	644	0.004	3	
C34	494	22000	673	0.015	4	
C35	494	22000	668	0.017	5	
C36	490	25000	652	0.006	3	

Table 5.1: Summary of photophysical properties of ruthenium(II) complexes

5.3.1 Titrations of C17 and C24 with TfOH monitored by absorption and photoluminescence spectra

Titrations of ruthenium(II) complexes with TfOH and monitored by absorption and photoluminescence spectra were performed for all Ru(II) complexes listed in Table 5.1. However, in this chapter results will be discussed for just two of them, dodecyl ester-substituted complex **C17** representing complexes with the side chain linked via an ester group and the complex **C24** with the piperidine-substituted side chain linked via an ether group. Each complex and its corresponding protonation state were given abbreviations. Namely, **C24** for the complex in isolated form (protonated on the side chain), [**C24**-1H]$^{+}$ for the form protonated on one pendant pyridyl unit and [**C17**-2H]$^{2+}$ for the form protonated on both pendant pyridyl units.

Figure 5.1 shows the process of titration of the dodecyl ester-substituted Ru(II) complex **C17** with TfOH monitored by absorption spectra. In the top-right corner is a titration curve displayed for absorption at 507 nm, where one can see that the titration plateau was reached at approx. 2 equivalents of TfOH. In the UV region of **C17** (red curve), 2 intense bands around 280 nm and 320 nm were observed. These bands arise from ligand-centred $\pi^{*}\leftarrow\pi$ transitions. Addition of first equivalent of TfOH caused a decrease of intensity and a red-shift to 340 nm. Due to the second aliquot of TfOH, this band is shifted to 350 nm and

the intensity increased. In the VIS region, a broad and moderately intense band with a maximum at 493 nm, assigned to the MLCT (metal-to-ligand charge-transfer) excited state, was observed. This band steadily increases upon titration and ~~it~~ is red-shifted to 508 nm. Even though **C17** has the attached side chain, the shift of the MLCT band upon the titration corresponds to that of **C8**, reported in early investigations of the homolepetic Ru(II) complexes with pytpy ligands.[1] The MLCT band of [**C17**-2H]$^{2+}$ is red-shifted in comparison with **C17**, because protonation of the pyridyl units makes it an electron-acceptor and therefore the energy of the π^* orbital of the protonated pytpy is lowered and displayed as red-shift (Table 5.2, Figure 5.1).

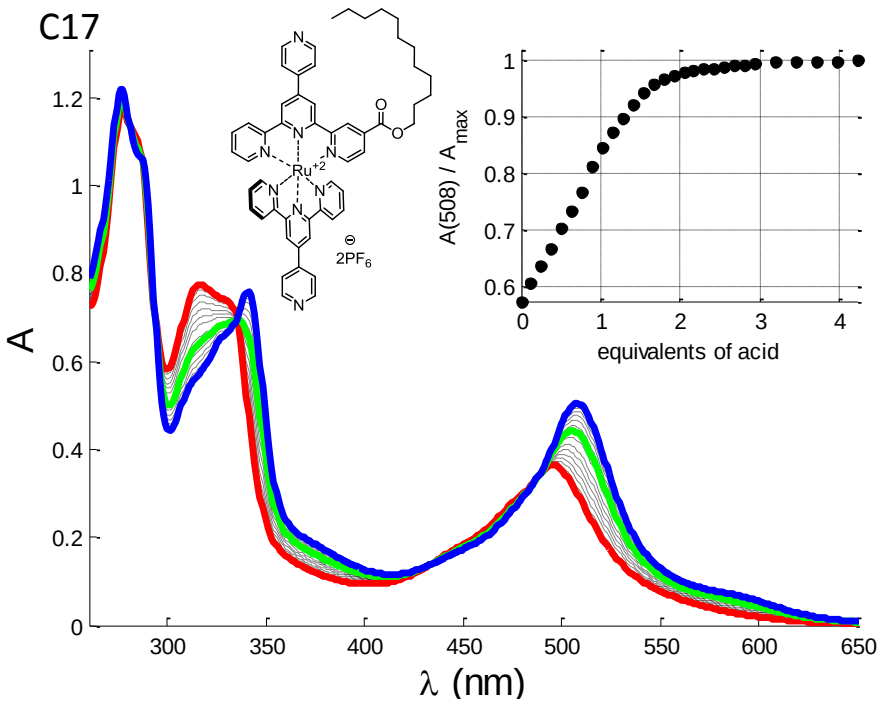

Figure 5.1: Absorption spectral changes of the ruthenium(II) complex C17 (c = 1.80 × 10^{-5} M, MeCN) upon addition of TfOH aliquots (MeCN, RT). The red line is the deprotonated state, the green line is the mono-protonated state and the blue line is the bis-protonated state. The inset shows the normalized titration curve obtained by monitoring the absorbance at 508 nm as a function of acid equivalents.

Compound	λ_{abs} [nm]	ε [L cm^{-1} mol^{-1}]	λ_{em} [nm]	QY [%]	τ [ns]	λ_{iso}
C17	493	20000	673	0.029	13	**487 nm**
C17-1H	506	24000	720	0.068	81	
C17-2H	508	28000	718	0.084	176	

Table 5.2: Photophysical properties of the ruthenium(II) complex C17, (c = 1.80 × 10^{-5} M, MeCN)

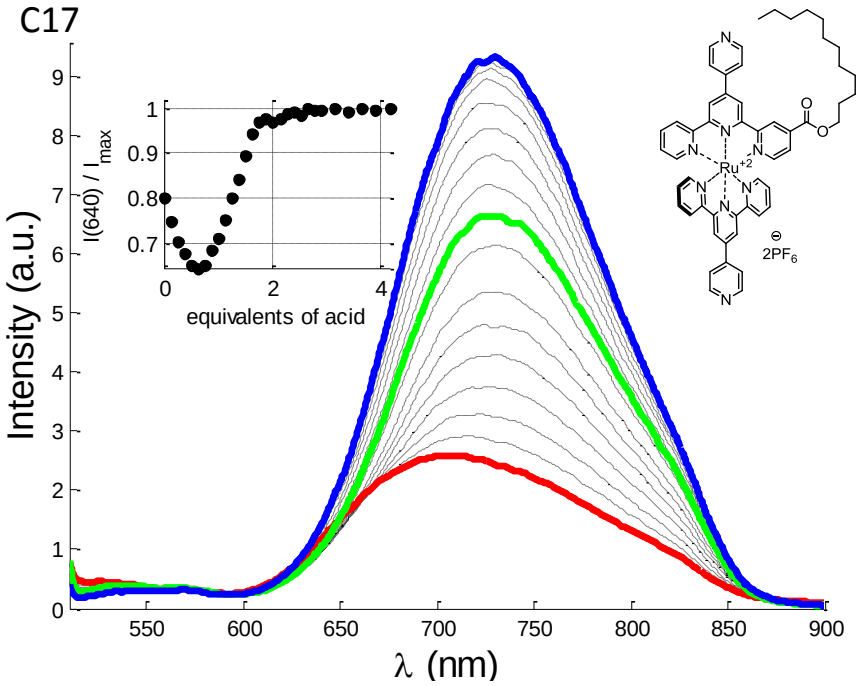

Figure 5.2: Luminescence spectral changes of the ruthenium(II) complex C17 (c = 1.80 × 10^{-5} M, MeCN) upon addition of TfOH aliquots (MeCN, room temperature). Excitation was performed at the isosbestic point at λ_{iso} = 487 nm. The red line is the deprotonated state, the green line is the mono-protonated state and the blue line is the bis-protonated state. The inset shows the normalized titration curve obtained by monitoring the luminescence at 640 nm as a function of acid equivalents.

The luminescence spectrum (Figure 5.2, Table 5.2) of the deprotonated form of **C17** exhibits the typical low energy MLCT phosphorescence band of Ru polypyridine complexes, which is red shifted and longer lived compared to the parent compounds $[Ru(tpy)_2]^{2+}$ and $[Ru(pytpy)_2]^{2+}$ (**C8**) because of the presence of the pendant pytpy unit and the attached dodecyl-substituted side chain. [1, 2] This emission increase of **C17** and **C8** compared to $[Ru(tpy)_2]^{2+}$ is caused by the presence of the pendant pyridyl unit. The emission properties are affected by the thermally activated decay of the ^{3}MLCT states to upper lying ^{3}MC (metal-centred) states which are highly distorted with respect to the ground state and appear with fast radiation decay. The smaller the energy difference between the ^{3}MLCT and ^{3}MC states, the faster the decay is. That is why $[Ru(tpy)_2]^{2+}$ ($\Delta E \cong 1500$ cm^{-1}) is not luminescent.[2] Upon titration of **C17** with TfOH, the intensity of the luminescence band increases and the band is red-shifted to 720 nm until one equivalent of TfOH is added. Upon titration up to 2 eq. of TfOH the emission band intensity increases even more and it is slightly blue-shifted to 718 nm (Figure 5.2). The red shift of the luminescence band of **C17** in the mono-protonated state

[**C17-1H**], along with longer lifetime, is explained by decrease in energy of the π^* orbital of the protonated pytpy, which stabilises the MLCT levels. The thermally activated decay of the lowest ^{3}MLCT state to the short-lived MC state is slowed due to stabilization of the MLCT and destabilization of the MC levels caused by the presence of the electron-accepting pyridyl units. Stabilisation of the MLCT levels is also enhanced by electron donation to the metal by the unprotonated pytpy ligand.[2] However in the bis-protonated form of **C17** [**C17-2H**] both ligands are protonated (electron-accepting), therefore such additional stabilisation is no longer possible, which explains the small blue-shift of the bis protonated form. The further increase of the luminescence lifetime is due to the further destabilisation of the ^{3}MC levels effected by the two bis-protonated ligands.

Figure 5.3 and Table 5.3 show absorption spectral changes of the amino-alkoxy-substituted ruthenium(II) complex **C24** upon addition of TfOH aliquots. The starting form **C24** is represented by the red line and with the structure shown, the mono-protonated form [**C24-1H**] with the green line and the bis-protonated form [**C24-2H**] with the blue curve. The starting form **C24** displays two intense bands around 270 nm and 320 nm in the UV region, assigned to ligand-centred $\pi^* \leftarrow \pi$ transitions, and one broad moderately intense band at 491 nm, assigned to ^{1}MLCT excited state. Upon titration with TfOH, the intensity of the band around 320 nm decreases and a new band around 345 nm appears with the formation of the [**C24-2H**] state.The MLCT band upon titration with 1 eq. of TfOH shifts to 501 nm. With the 2nd aliquot of TfOH the absorption intensity increases, the absorption maximum is even more red-shifted (511 nm) and the absorption band is broadened. The inset in Figure 5.3 displays the titration curve for absorbance at 511 nm as a function of acid aliquots.

Luminescence spectral changes of the ruthenium(II) complex **C24** upon addition of TfOH aliquots are shown in Figure 5.4. Excitation was performed at the wavelength of the MLCT absorption isosbestic point, λ_{iso} = 495 nm. The inset in Figure 5.4 displays the titration curve for photoluminescence monitored at 740 nm as a function of acid aliquots. The emission spectrum of **C24** displays one broad MLCT phosphorescence band with a weak intensity and the emission maximum at 675 nm. Upon titration with 1 eq. of TfOH [**C24-1H**] the emission intensity decreases and is red shifted (709 nm) and longer lived compared to the **C24**. With the 2nd aliquot of TfOH [**C24-2H**] the emission intensity increases and is longer lived, and the maximum is red shifted even more (723 nm) and broadened.

Compound	λ_{abs} [nm]	ε [L cm^{-1} mol^{-1}]	λ_{em} [nm]	QY [%]	τ [ns]	λ_{iso}
C24	491	33000	675	0,019	19	**495 nm**
C24-1H	501	33000	709	0,052	33	
C24-2H	511	42000	723	0,092	62	

Table 5.3: Photophysical properties of the ruthenium(II) complex C24 (c = 1.30 × 10^{-5} M, MeCN)

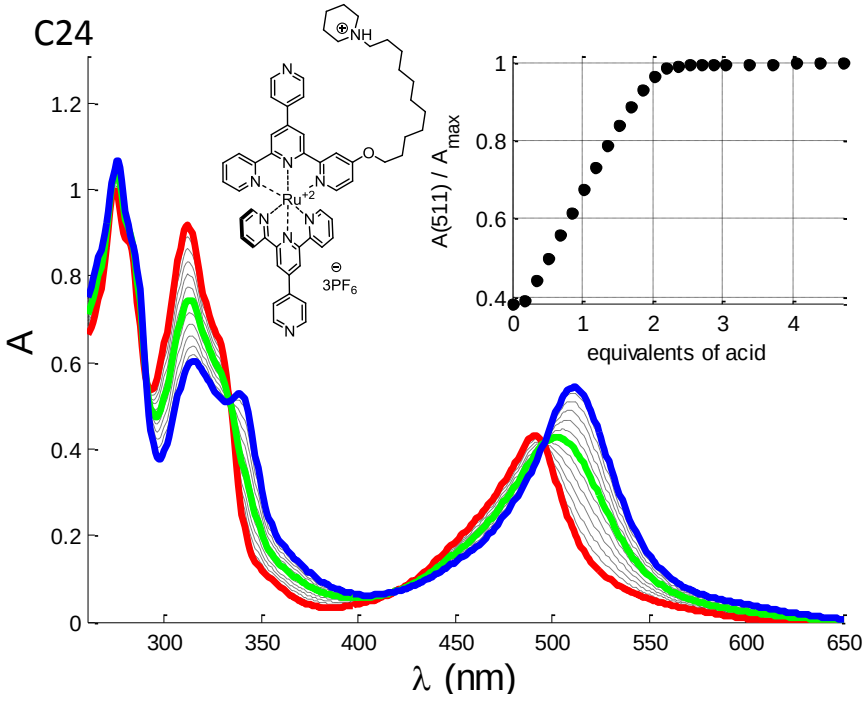

Figure 5.3: Absorption spectral changes of the ruthenium(II) complex C24 (c = 1.30 × 10^{-5} M in MeCN) upon addition of TfOH aliquots (MeCN, RT). Red line: C24, green line: mono-protonated form, blue line: bis-protonated form. The inset shows the normalized titration curve obtained by monitoring the absorbance at 511 nm as a function of acid equivalents.

Titration curves for absorption and emission reach the plateau around 2 eq. of TfOH (Figure 5.3, 5.4). However, in comparison with the model complex **C8**,[1] one does not observe the change of slopes at point of the 1st and at the point of the 2nd aliquot of acid and it is also obvious that the process of the titration monitored with emission spectra is not so monotonous. This indicates that the basicity of the pendant pyridyl units is not equal.

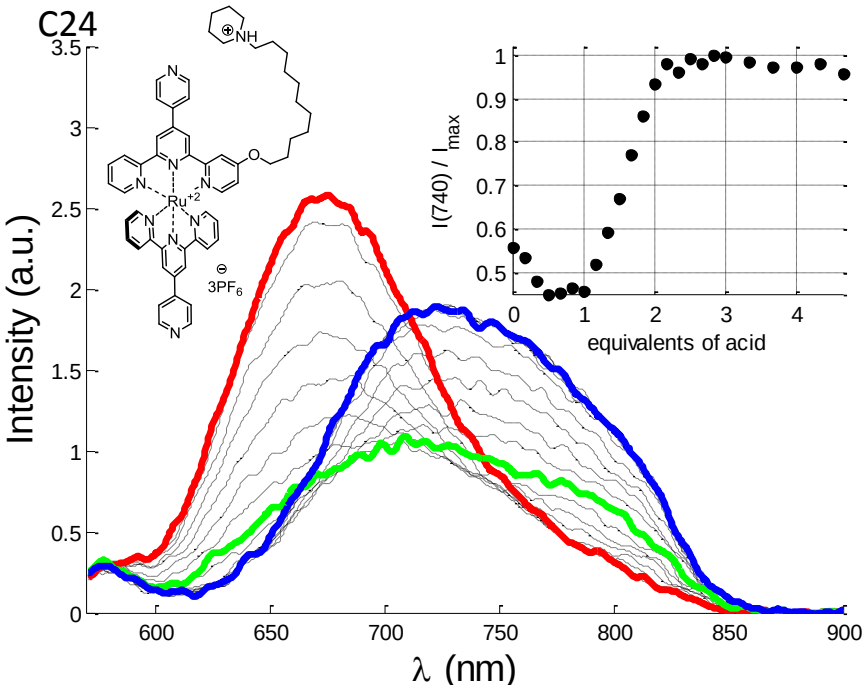

Figure 5.4: Luminescence spectral changes of the ruthenium(II) complex C24 (c = 1.30 × 10^{-5} M in MeCN) upon addition of TfOH aliquots (MeCN, RT), excitation was performed in the isosbestic point at λ_{iso} = 495 nm. Red line is deprotonated state, green line is the mono-protonated state and blue line is the bis-protonated state. The inset shows the normalized titration curve obtained by monitoring the luminescence at 740 nm as a function of acid equivalents.

5.3.2 Model homoleptic ruthenium(II) complexes C8, C33 and C38

In this section, photophysical properties of the model homoleptic ruthenium(II) complexes bearing various substituents in the 4-position of the tpy ligand, will be compared (Table 5.4, Figures 5.5 and 5.6). The complex **C8** contains 2 pyridyl units with an electron-withdrawing character, **C33** has 2 phenyl rings and **C38** is *p*-tolyl-substituted with an electron-donating character (Scheme 5.2).

Compound	λ_{abs} [nm]	ε [L cm^{-1} mol^{-1}]	λ_{em} [nm]	QY [%]	τ [ns]
C8	489	26000	657	0.0078	4
C33	488	24000	644	0.0044	3
C38	490	25000	644	0.0040	2

Table 5.4: Photophysical properties of the model homoleptic ruthenium(II) complexes with different pendant units: C8 (pyridyl), C33 (phenyl), C38 (p-tolyl)

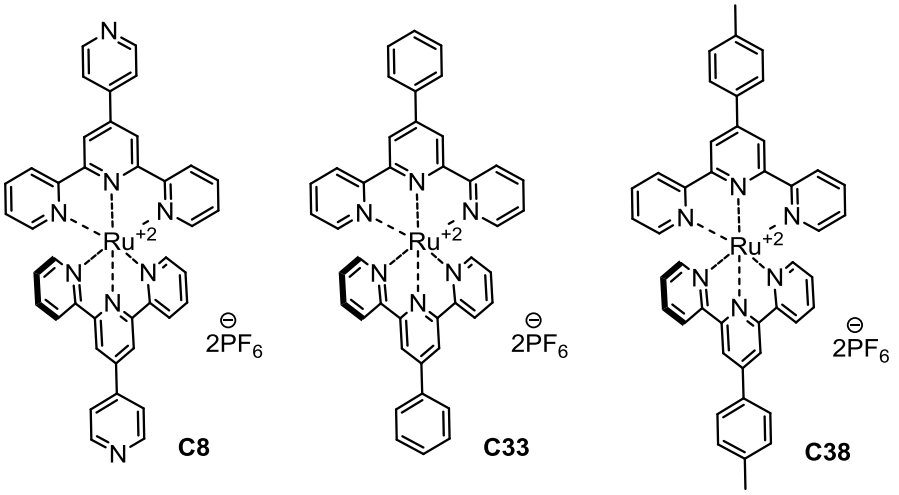

Scheme 5.2: Model homoleptic ruthenium(II) complexes with different substituents in the 4-position of the tpy unit: C8 (pyridyl), C33 (phenyl), C38 (p-tolyl)

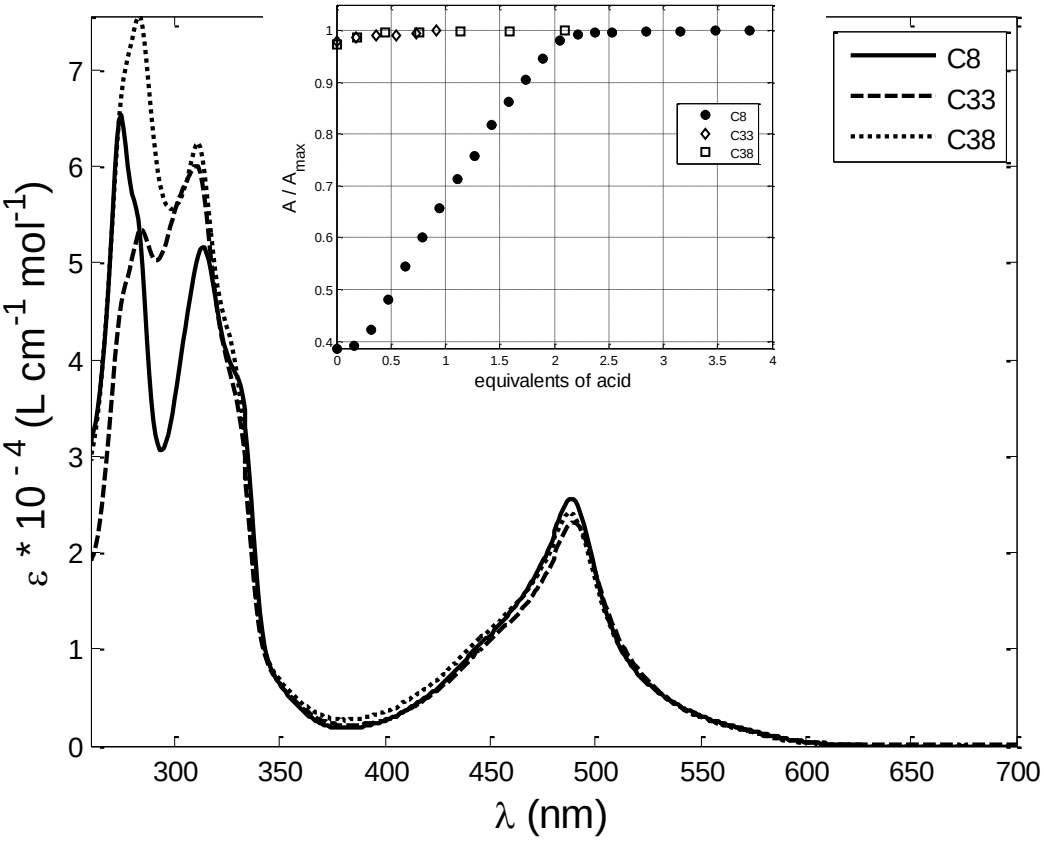

Figure 5.5: Absorption spectra of the ruthenium(II) complexes C8 (c = 2.48 × 10^{-5} M in MeCN), C33 (c = 1.12 × 10^{-5} M in MeCN) and C38 (c = 0.83 × 10^{-5} M in MeCN). The inset shows the normalized titration curve obtained by monitoring the absorbance at 507 nm (C8) 498 nm (C33) and 490 nm (C38) as a function of acid equivalents. Solutions: 1.38 × 10^{-5} M, 0.64 × 10^{-5} M and 1.14 × 10^{-5} M in MeCN, respectively.

Figure 5.5 displays absorption spectra of the three homoleptic ruthenium(II) complexes C8, C33 and C38. The maximum of the MLCT band of all three complexes has almost the same wavelength (488-490 nm) with very similar values of the molar absorption coefficient and nearly the same broadness of the band. However, the effect of the substituent is observed in the UV region. Even the stronger effect of the substituents can be seen in the photoluminescence spectra (Figure 5.6).

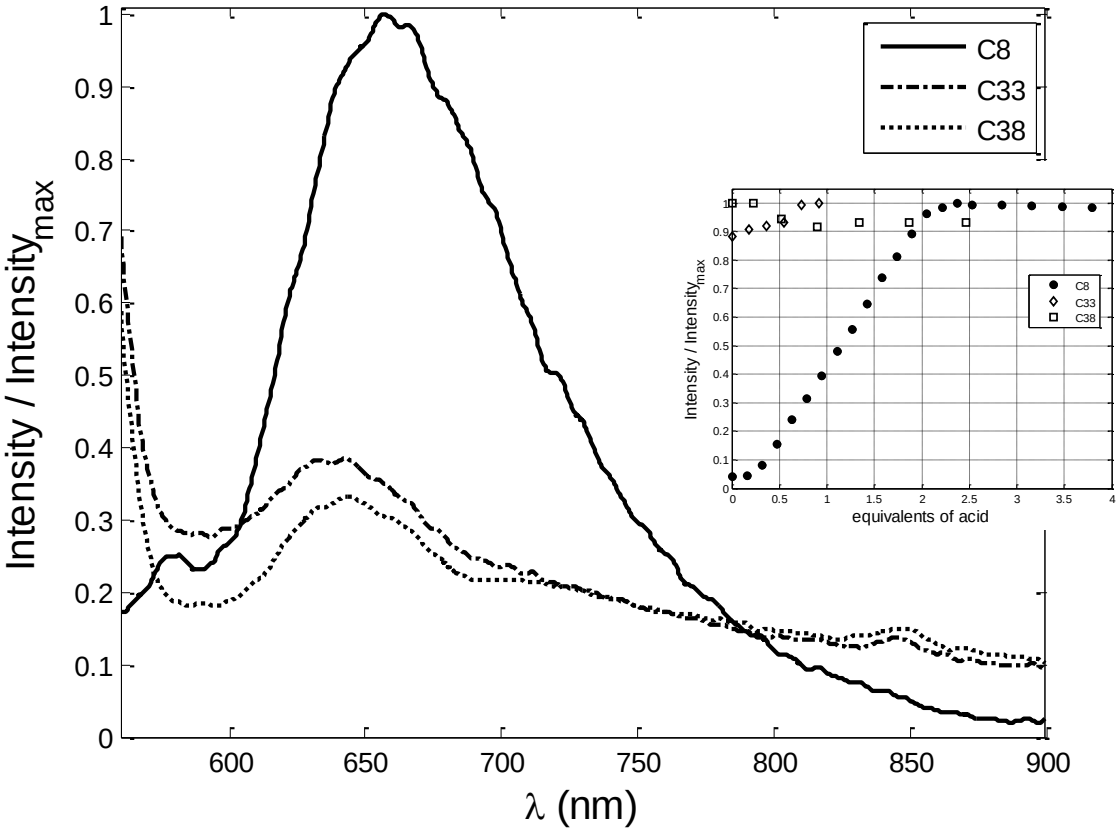

Figure 5.6: Normalized emission spectra of the ruthenium(II) complexes C8 (c = 1.38 × 10^{-5} M in MeCN, λ_{ex} = 492 nm), C33 (c = 0.64 × 10^{-5} M in MeCN, λ_{ex} = 489 nm) and C38 (c = 1.14 × 10^{-5} M in MeCN, λ_{ex} = 490 nm). The inset shows the normalized titration curve obtained by monitoring the photoluminescence at 736 nm (C8) 636 nm (C33) and 647 nm (C38) as a function of acid equivalent.

C8 is much more emissive and the emission maximum at 657 nm is red-shifted compared to that of **C33** and **C38** (both 644 nm), both due to the stabilisation effect of the pendant pyridyl units.[1] **C8** also has about double the luminescence lifetime value and it is about twice longer lived in comparison with **C33** and **C38** (Table 5.4). In the inset of Figures 5.5 and 5.6 are normalized titration curves obtained by monitoring the absorbance at 507 nm (**C8**) or photoluminescence at 736 nm (**C8**), respectively, as a function of TfOH aliquots. The titration

of **C8**, bearing two protonation sites, is consistent with the published data.[1] C33 and C38 naturally do not have any protonation site, therefore their titration curves are approximately constant.

5.3.3 Ruthenium(II) complexes C17-C19 with the side chain linked via an ester group

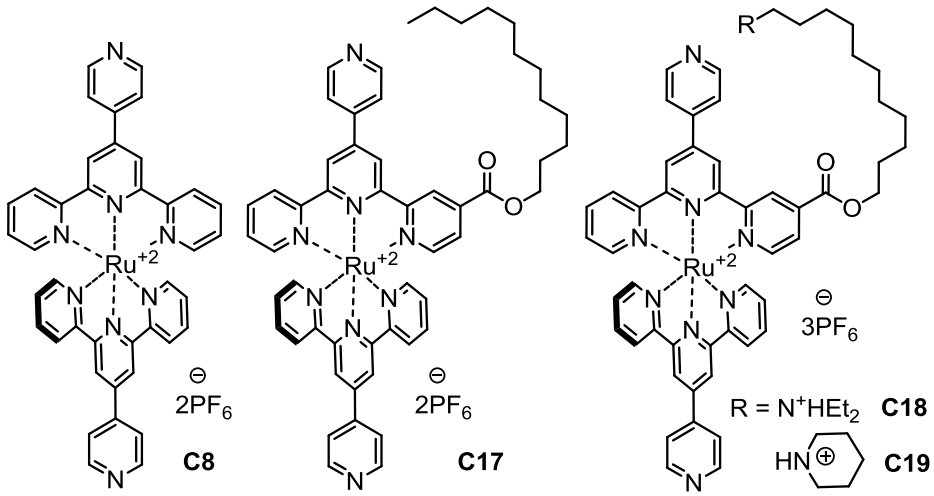

Scheme 5.3: Ruthenium(II) complexes with the side chain linked via an ester group C17-19

In this section, photophysical properties of ruthenium(II) complexes **C18-19** of pytpy ligands with the amino-substituted side chain linked via an ester group, are reported and compared with those of **C8** and the dodecyl ester-substituted complex **C17** (Scheme 5.3). We were interested in the influence of the electron-withdrawing ester group and also the effect of the (protonated) amino unit on the spectroscopic properties of these molecules. Figures 5.7 and 5.10 compile absorption and emission spectra of the Ru(II) complexes **C8**, and **C17-19**. Figures 5.8 and 5.11 compile absorption and emission spectra of the Ru(II) complexes in their mono-protonated form (**C8-1H**, **C17-1H**, **C18-1H** and **C19-1H**). Figures 5.9 and 5.12 compare absorption and emission spectra of the Ru(II) complexes in their bis-protonated form (**C8-2H**, **C17-2H**, **C18-2H** and **C19-2H**). The most important results are summarised in Table 5.5. Figure 5.13 shows the normalized titration curves obtained by monitoring the absorbance at 507 nm (**C8**) and 508 nm (**C17-19**) as a function of acid aliquots and normalized titration curves obtained by monitoring the photoluminescence at 736 nm (**C8**,

λ_{ex} = 492 nm), 729 nm (**C17**, λ_{ex} = 487 nm), 718 nm (**C18**, λ_{ex} = 491 nm) and 716 nm (**C19**, λ_{ex} = 492 nm) as a function of TfOH equivalents. All the titration curves of **C8**, and **C17-19** reach the spectroscopic plateau at approximately 2 equivalents of TfOH.

Compound	λ_{abs} [nm]	ε [L cm^{-1} mol^{-1}]	λ_{em} [nm]	QY [%]	τ [ns]	λ_{iso}
C8	489	26000	657	0.008	4	**492**
C8-1H	498	26000	751	0.042	98	
C8-2H	507	32000	743	0.082	138	
C17	493	20000	673	0.029	13	**487**
C17-1H	506	24000	720	0.064	81	
C17-2H	508	28000	718	0.087	176	
C18	494	23000	682	0.029	21	**491**
C18-1H	503	26000	723	0.070	118	
C18-2H	508	32000	717	0.109	176	
C19	494	23000	672	0.033	35	**492**
C19-1H	502	26000	722	0.095	104	
C19-2H	508	31000	719	0.156	147	

Table 5.5: Photophysical properties of the ruthenium(II) complexes C17-19 and C8

Figure 5.7 compiles the absorption spectra of the Ru(II) complex **C8**, and the ester-substituted complexes **C17-19**. **C8** is represented in the VIS region with a moderately intense MLCT band with the absorption maximum at 489 nm (solid line). However, the MLCT band of the ester-substituted complexes **C17-19** less intense and slightly red-shifted (around 494 nm). Upon first protonation, all complexes are red-shifted (around 498-506 nm) with nearly the same molar extinction coefficient. Upon further protonation, all complexes have the absorption maximum at almost the same wavelength (507-508 nm).

Figure 5.10 displays photoluminescence spectra of the Ru(II) complex **C8**, and the ester-substituted complexes **C17-19**. The emission maximum of the series **C17-19** is shifted to higher energies (672-682 nm) in comparison with **C8** with the emission maximum λ_{em} at 657 nm. Also the ester-substituted complexes are more emissive and longer lived than **C8**. In the diethylamino-substituted complex **C18** the emission band is broader and more red-shifted than **C17** and **C19**. Upon protonation, a strong red-shift of the emission maxima of **C8** to λ_{em} = 751 nm is observed. The ester-substituted complexes are upon first protonation [**C17-19-1H**] shifted to about the same wavelength λ_{em} = 720 nm. The bisprotonated forms [**C17-19-**

2H] are more strongly emissive and longer lived than the mono-protonated forms [**C17-19-1H**], but the emission maxima appears slightly blue-shifted, as that of [**C8-2**] compared to its mono-protonated form [**C8-1**]. This trend was already observed and explained in Section 5.3.1 and is consistent with the reported results for **C8** protonation.[1] Therefore, the effect of the ester-substitution has stronger influence on the luminescence spectra of the starting forms **C17-19**, however upon protonation the pyridyl substituent plays the main role.

Table 5.5 compares quantum yields and luminescence lifetimes of all starting and protonated forms of all complexes. All ester-substituted complexes in the starting forms **C17-19** are stronger emitters than **C8.** However, upon protonation, there are no longer any significant differences.

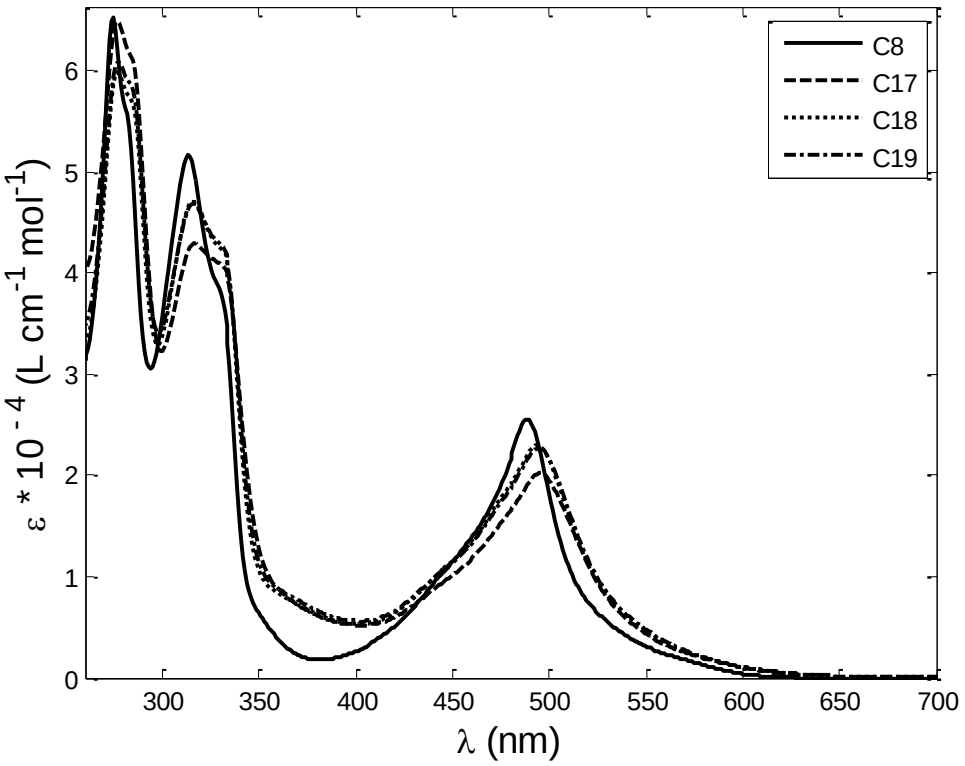

Figure 5.7: Absorption spectra of the ruthenium(II) complexes C8 (c = 2.40× 10^{-5} M, MeCN), C17 (c = 1.80 ×10^{-5} M, MeCN), C18 (c = 2.35 ×10^{-5} M, MeCN) and C19 (c = 2.50 ×10^{-5} M, MeCN).

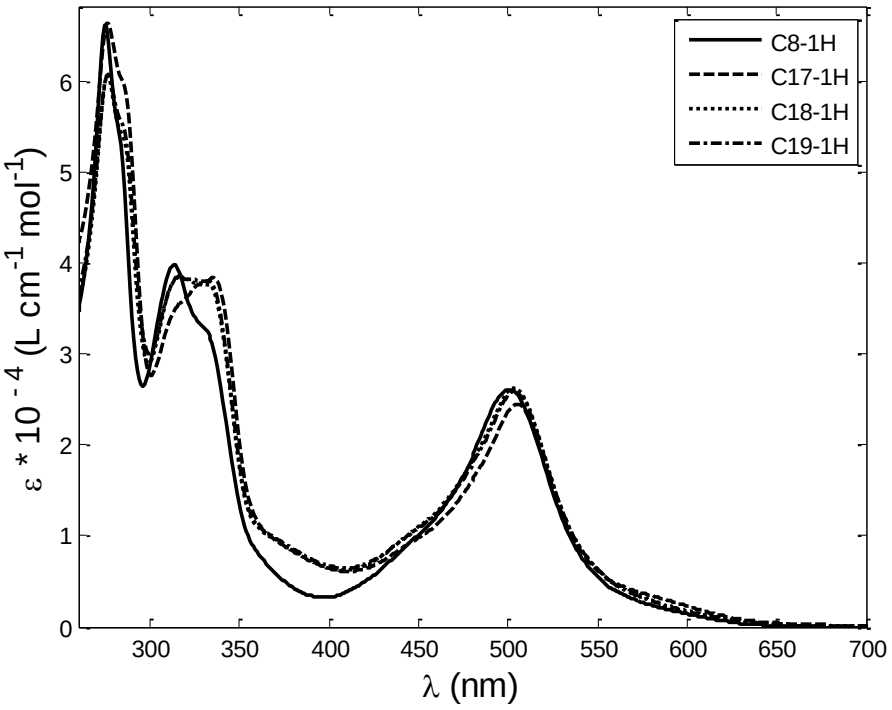

Figure 5.8: Absorption spectra of the ruthenium(II) complexes in their mono-protonated form: C8-1H (c = 2.40 × 10^{-5} M, MeCN), C17-1H (c = 1.80 × 10^{-5} M, MeCN), C18-1H (c = 2.35 × 10^{-5} M, MeCN) and C19-1H (c = 2.50 × 10^{-5} M, MeCN).

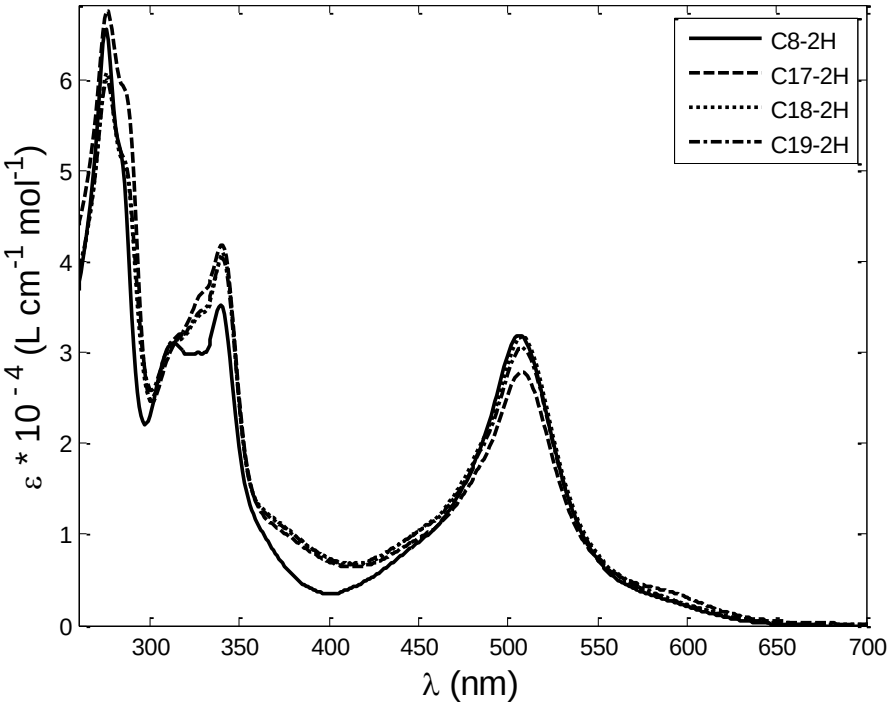

Figure 5.9: Absorption spectra of the ruthenium(II) complexes in their bis-protonated form: C8-2H (c = 2.40 × 10^{-5} M, MeCN), C17-2H (c = 1.80 × 10^{-5} M, MeCN), C18-2H (c = 2.35 × 10^{-5} M, MeCN) and C19-2H (c = 2.50 × 10^{-5} M, MeCN).

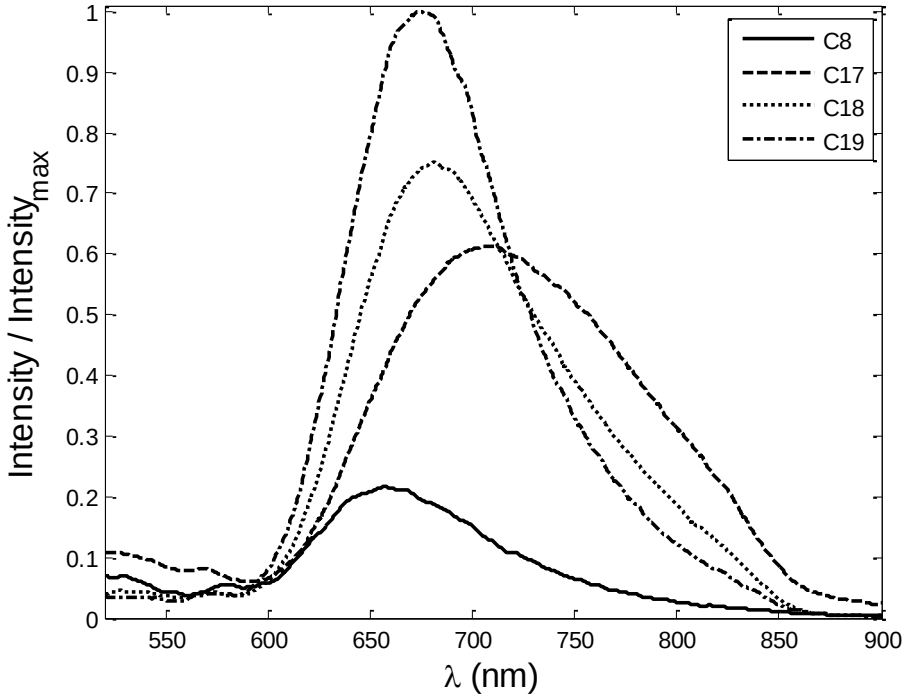

Figure 5.10: Normalized emission spectra of the ruthenium(II) complexes C8 (c = 2.40 × 10^{-5} M in MeCN, λ_{ex} = 492 nm), C17 (c = 1.80 × 10^{-5} M in MeCN, λ_{ex} = 487 nm), C18 (c = 2.35 × 10^{-5} M in MeCN, λ_{ex} = 491 nm) and C19 (c = 2.21 × 10^{-5} M in MeCN, λ_{ex} = 492 nm).

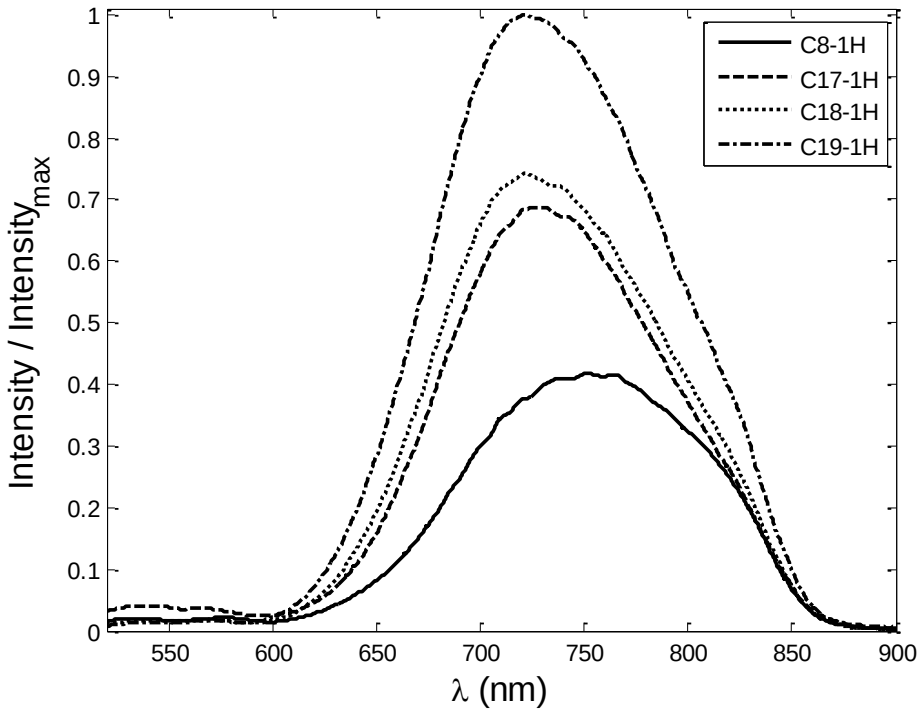

Figure 5.11: Normalized emission spectra of the ruthenium(II) complexes in their mono-protonated form: C8-1H (c = 1.38 × 10^{-5} M in MeCN, λ_{ex} = 492 nm), C17-1H (c = 1.80 × 10^{-5} M in MeCN, λ_{ex} = 487 nm), C18-1H (c = 2.35 × 10^{-5} M in MeCN, λ_{ex} = 491 nm) and C19-1H (c = 2.21 × 10^{-5} M in MeCN, λ_{ex} = 492 nm).

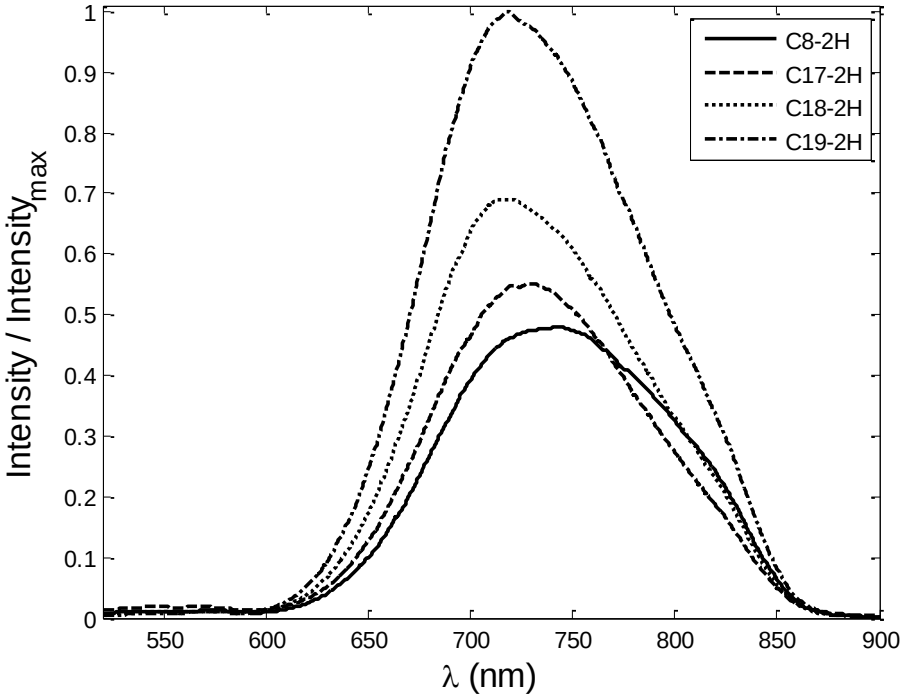

Figure 5.12: Normalized emission spectra of the ruthenium(II) complexes in their bis-protonated form: C8-2H (c = 1.38 × 10^{-5} M in MeCN, λ_{ex} = 492 nm), C17-2H (c = 1.80 × 10^{-5} M in MeCN, λ_{ex} = 487 nm), C18-2H (c = 2.35 × 10^{-5} M in MeCN, λ_{ex} = 491 nm) and C19-2H (c = 2.21 × 10^{-5} M in MeCN, λ_{ex} = 492 nm).

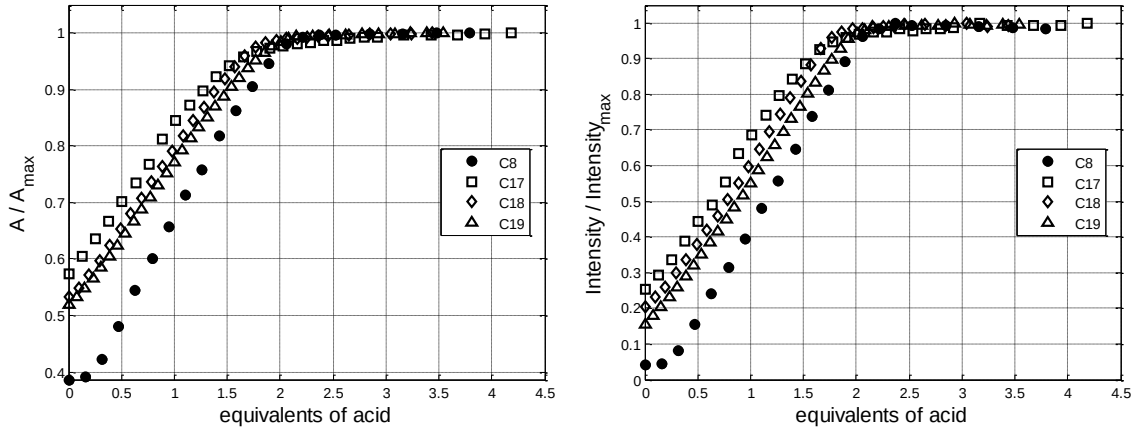

Figure 5.13: Left: normalized titration curves obtained by monitoring the absorbance at 507 nm (C8) and 508 nm (C17-19) as a function of acid equivalents. Right: normalized titration curves obtained by monitoring the photoluminescence at 736 nm (C8, λ_{ex} = 492 nm), 729 nm (C17, λ_{ex} = 487 nm), 718 nm (C18, λ_{ex} = 491 nm) and 716 nm (C19, λ_{ex} = 492 nm) as a function of TfOH equivalents. Solutions: 1.38 × 10^{-5} M, 1.80 × 10^{-5} M, 2.35 × 10^{-5} M and 2.21 × 10^{-5} M in MeCN, respectively.

5.3.4 Ruthenium(II) complexes C22-C24 with the side chain linked via an ether group

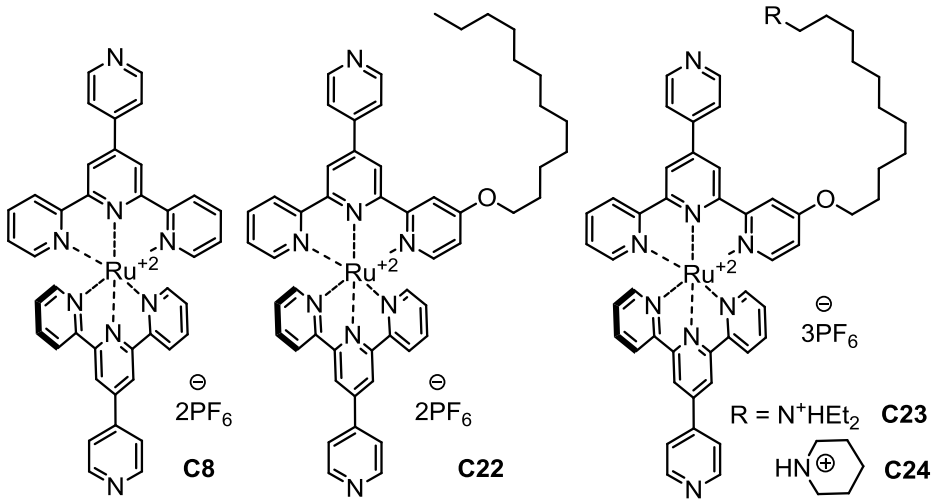

Scheme 5.4: Ruthenium(II) complexes with the side chain linked via an ether group C22-24

In this section, the photophysical properties of ruthenium(II) complexes **C22-24** of pytpy ligands with the amino-substituted side chain linked via an ether group, are reported and compared with those of **C8** and the dodecyloxy-substituted complex **C22** (Scheme 5.4). We were interested to see the influence of the electron-donating ether group and also the effect of the (protonated) amino unit on the spectroscopic properties of these molecules. Figures 5.14 and 5.17 compile absorption and emission spectra of the Ru(II) complexes **C8**, and **C22-24** in their starting forms. Figures 5.15 and 5.18 compile absorption and emission spectra of the Ru(II) complexes in their mono-protonated form (**C8-1H**, **C22-1H**, **C23-1H** and **C24-1H**). Figures 5.16 and 5.19 compare absorption and emission spectra of the Ru(II) complexes in their bis-protonated form (**C8-2H**, **C22-2H**, **C23-2H** and **C24-2H**). The most important results are summarised in Table 5.6. Figure 5.20 shows the normalized titration curves obtained by monitoring the absorbance at 507 nm (**C8**), 510 nm (**C22**) and at 511 nm (**C23-24**) as a function of acid aliquots and normalized titration curves obtained by monitoring the photoluminescence at 736 nm (**C8**, λ_{ex} = 492 nm), 757 nm (**C22**, λ_{ex} = 496 nm), 761 nm (**C23**, λ_{ex} = 495 nm) and 800 nm (**C24**, λ_{ex} = 495 nm) as a function of TfOH equivalents. All the titration curves of **C8** and **C22-24** reach the spectroscopic plateau at approximately 2 equivalents of TFOH.

Compound	λ_{abs} [nm]	ε [L cm^{-1} mol^{-1}]	λ_{em} [nm]	QY [%]	τ [ns]	τ_{77K} [μs]	λ_{iso}
C8	489	26000	657	0.008	4	6	**492**
C8-1H	498	26000	751	0.042	98	7	
C8-2H	507	32000	743	0.082	138	7	
C22	492	23000	681	0.024	9		**496**
C22-1H	507	28000	730	0.029	23		
C22-2H	510	29000	761	0.042	61		
C23	491	23000	689	0.022	10	4	**495**
C23-1H	504	26000	719	0.021	20	4	
C23-2H	511	29000	761	0.027	68	5	
C24	491	28000	675	0.019	19		**495**
C24-1H	501	27000	709	0.011	33		
C24-2H	511	34000	723	0.017	62		

Table 5.6: Photophysical properties of the ruthenium(II) complexes C22-24 and C8

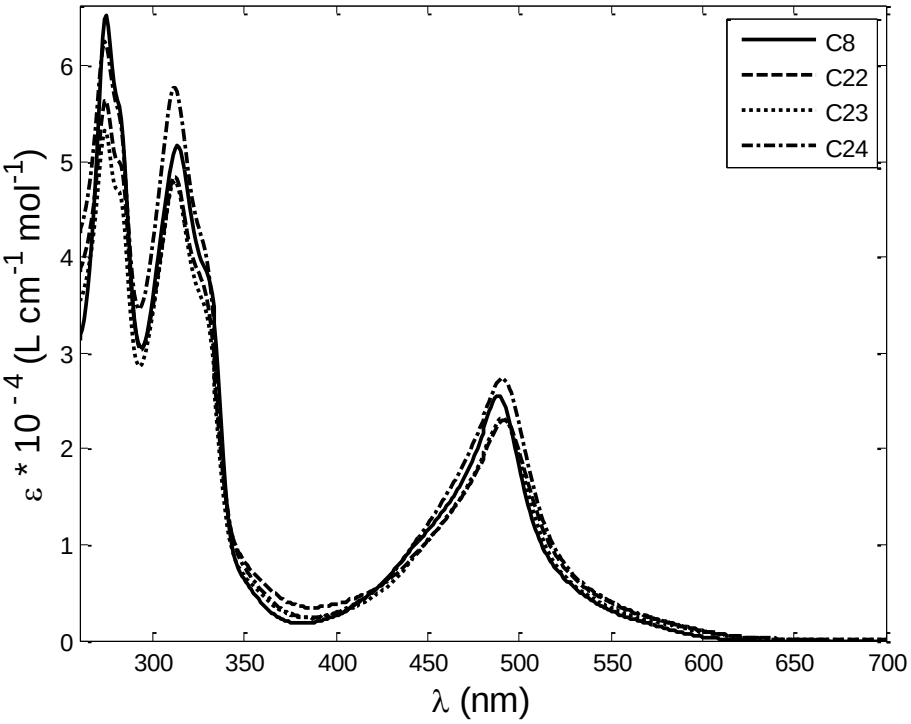

Figure 5.14: Absorption spectra of the ruthenium(II) complexes C8 (c = 2.40× 10^{-5} M, MeCN), C22 (c = 0.80 ×10^{-5} M, MeCN), C23 (c = 0.82 ×10^{-5} M, MeCN) and C24 (c = 2.52 ×10^{-5} M, MeCN).

Figure 5.14 displays absorption spectra of the starting complexes **C8**, and **C22-24**. All ether-substituted complexes **C22-24** have the MLCT band maximum slightly red-shifted to around

wavelength λ_{abs} 491 nm in comparison with **C8**. The piperidine–substituted complex C**24** has the highest value of the molar absorption coefficient. Upon titration with the 1st aliquot of acid, the MLCT band maximum of all complexes was red-shifted. The value of the molar absorption coefficient of **C22-1H** and **C23-1H** increased compared to their starting forms **C22** and **C23**, however the molar absorption coefficient of **C8-1H** stayed the same and the molar absorption coefficient of **C24-1H** decreased compared to **C24**. Upon titration with the 2nd aliquot of TfOH, the absorption maximum of the MLCT band of all complexes was red-shifted even more. The molar absorption coefficient of **C22-2H** and **C23-2H** slightly increased compared to **C22-1H** and **C23-1H**. However, the molar absorption coefficient of **C24-2H** and **C8-2H** increased significantly.

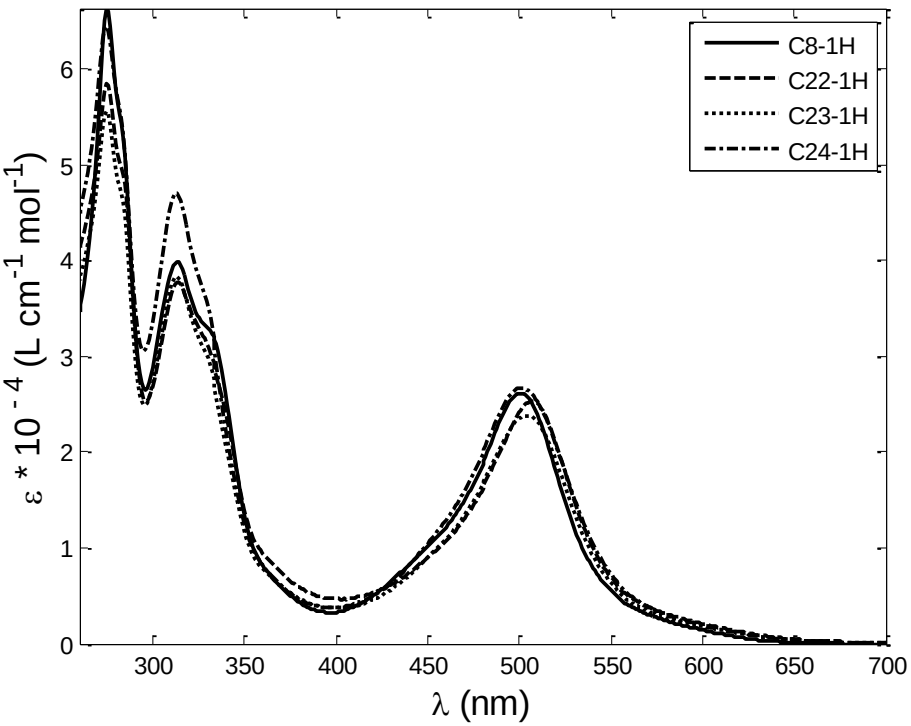

Figure 5.15: Absorption spectra of the ruthenium(II) complexes in their mono-protonated form: C8-1H(c = 2.40× 10^{-5} M, MeCN), C22-1H (c = 0.80 × 10^{-5} M, MeCN), C23 -1H (c = 0.82 × 10^{-5} M, MeCN) and C24-1H (c = 2.52 × 10^{-5} M, MeCN).

Figure 5.17 displays photoluminescence spectra of the starting complexes **C8** and **C22-24**. All ether-substituted complexes **C22-24** have the emission maximum red-shifted to λ_{em} around 675-681 nm compared to **C8** which has the emission maximum at 657 nm. They are also more emissive and longer lived than **C8**. Upon titration with the 1st aliquot of acid, the

emission maxima of all complexes were red-shifted, but not as much as the emission maximum of **C8-1H**. Moreover, the emission intensity of **C22-24-1H** decreased in comparison with **C22-24**. The quantum yields and luminescence lifetimes of **C22-24-1H** are much lower than those of **C8-1H**. Upon titration with the 2nd aliquot of acid, another interesting effect of the alkoxy-substituent is observed. The emission maxima **C22-24-2H** is red-shifted even more compared to the mono-protonated forms **C22-24-1H**. However, emission maxima of **C8-2H** and ester-substituted **C17-19-2H** were slightly blue-shifted in comparison with their mono-protonated forms **C8-1H** and **C17-19-1H.**

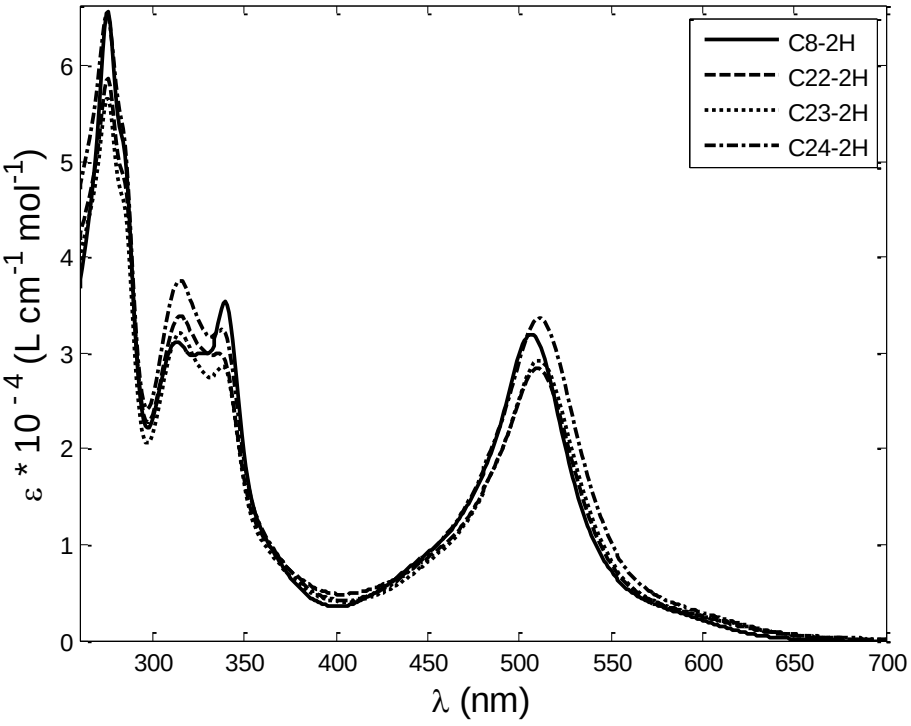

Figure 5.16: Absorption spectra of the ruthenium(II) complexes in their bis-protonated form: C8-2H(c = 2.40× 10^{-5} M, MeCN), C22-2H (c = 0.80 × 10^{-5} M, MeCN), C23 -2H (c = 0.82 × 10^{-5} M, MeCN) and C24-2H (c = 2.52 × 10^{-5} M, MeCN).

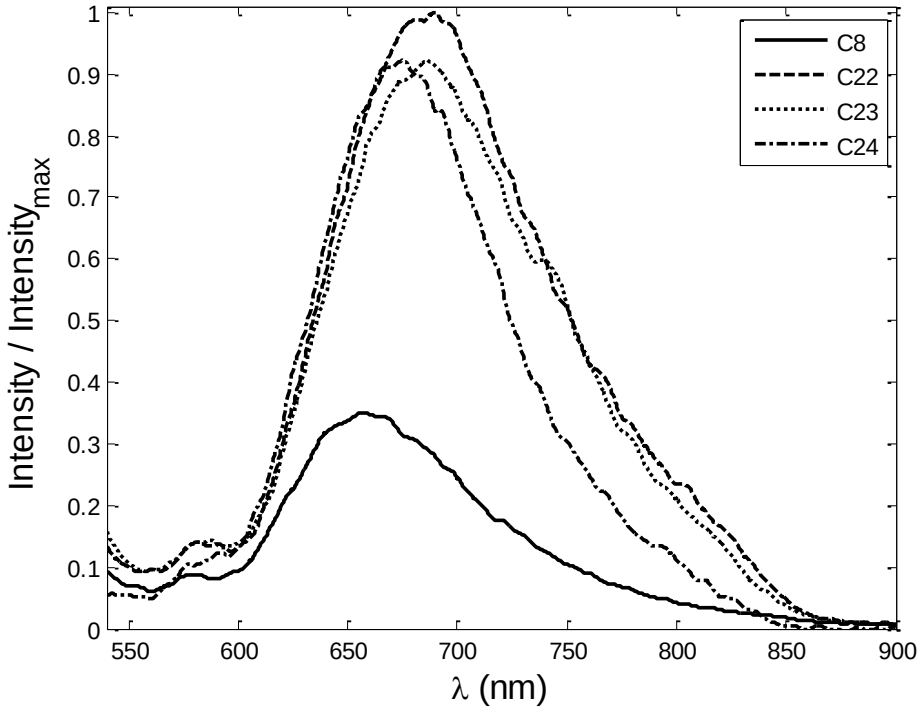

Figure 5.17: Normalized emission spectra of the ruthenium(II) complexes C8 (c = 1.38 × 10^{-5} M in MeCN, λ_{ex} = 492 nm), C22 (c = 0.95 × 10^{-5} M in MeCN, λ_{ex} = 496 nm), C23 (c = 1.07 × 10^{-5} M in MeCN, λ_{ex} = 495 nm) and C24 (c = 1.31 × 10^{-5} M in MeCN, λ_{ex} = 495 nm).

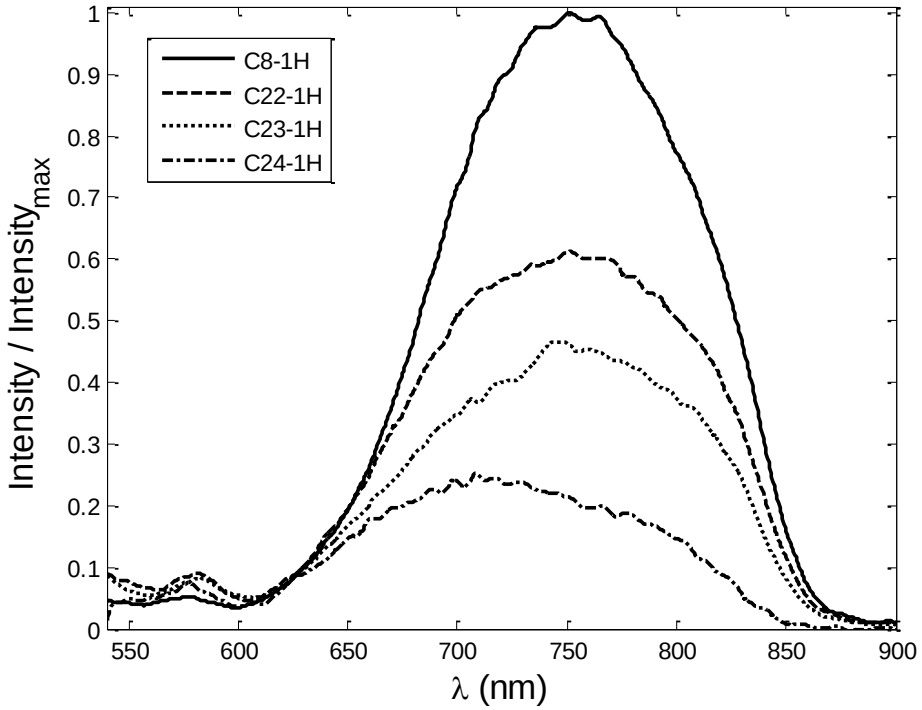

Figure 5.18: Normalized emission spectra of the ruthenium(II) complexes in their mono-protonated form C8-1H (c = 1.38 × 10^{-5} M in MeCN, λ_{ex} = 492 nm), C22-1H (c = 0.95 × 10^{-5} M in MeCN, λ_{ex} = 496 nm), C23-1H (c = 1.07 × 10^{-5} M in MeCN, λ_{ex} = 495 nm) and C24 -1H (c = 1.31 × 10^{-5} M in MeCN, λ_{ex} = 495 nm).

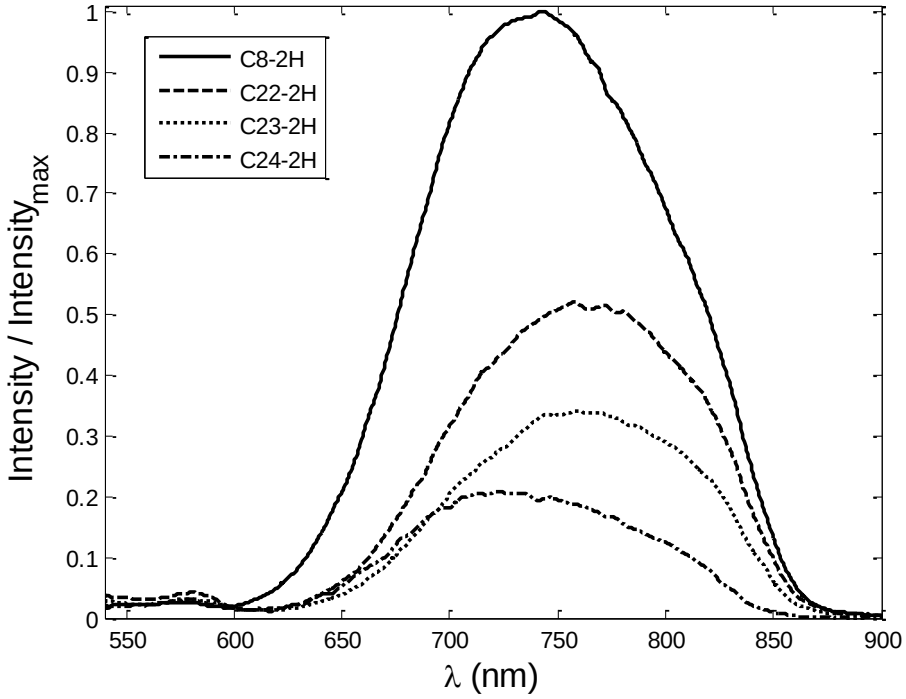

Figure 5.19: Normalized emission spectra of the ruthenium(II) complexes in their bis-protonated form C8-2H (c = 1.38 × 10^{-5} M in MeCN, λ_{ex} = 492 nm), C22-2H (c = 0.95 × 10^{-5} M in MeCN, λ_{ex} = 496 nm), C23-2H (c = 1.07 × 10^{-5} M in MeCN, λ_{ex} = 495 nm) and C24 -2H (c = 1.31 × 10^{-5} M in MeCN, λ_{ex} = 495 nm).

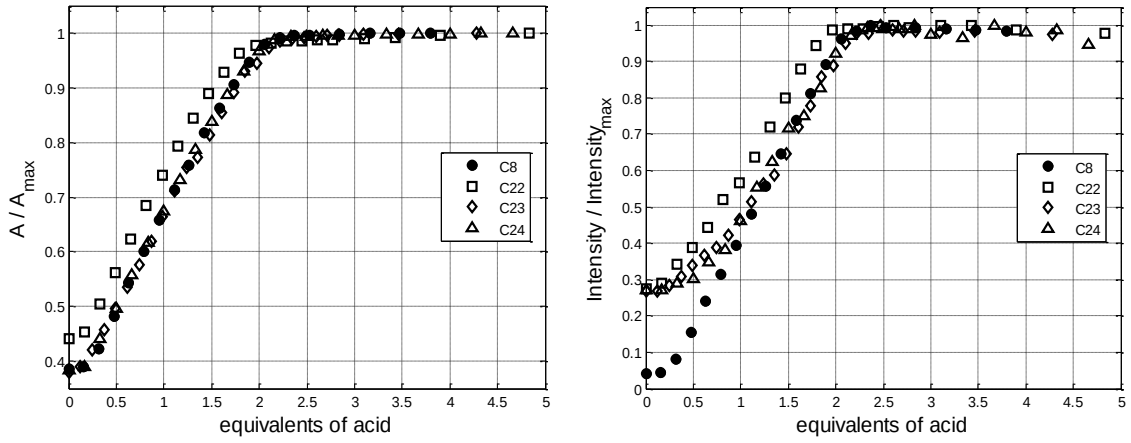

Figure 5.20: Left: Normalized titration curves obtained by monitoring the absorbance at 507 nm (C8), 510 nm (C22) and at 511 nm (C23-24) as a function of acid equivalents. Right: normalized titration curves obtained by monitoring the photoluminescence at 736 nm (C8, λ_{ex} = 492 nm), 757 nm (C22, λ_{ex} = 496 nm), 761 nm (C23, λ_{ex} = 495 nm) and 800 nm (C24, λ_{ex} = 495 nm) as a function of TfOH equivalents. Solutions: 1.38 × 10^{-5} M, 0.95 × 10^{-5} M, 1.07 × 10^{-5} M and 1.31 × 10^{-5} M in MeCN, respectively.

5.3.5 Homoleptic ruthenium(II) complexes C27-C29

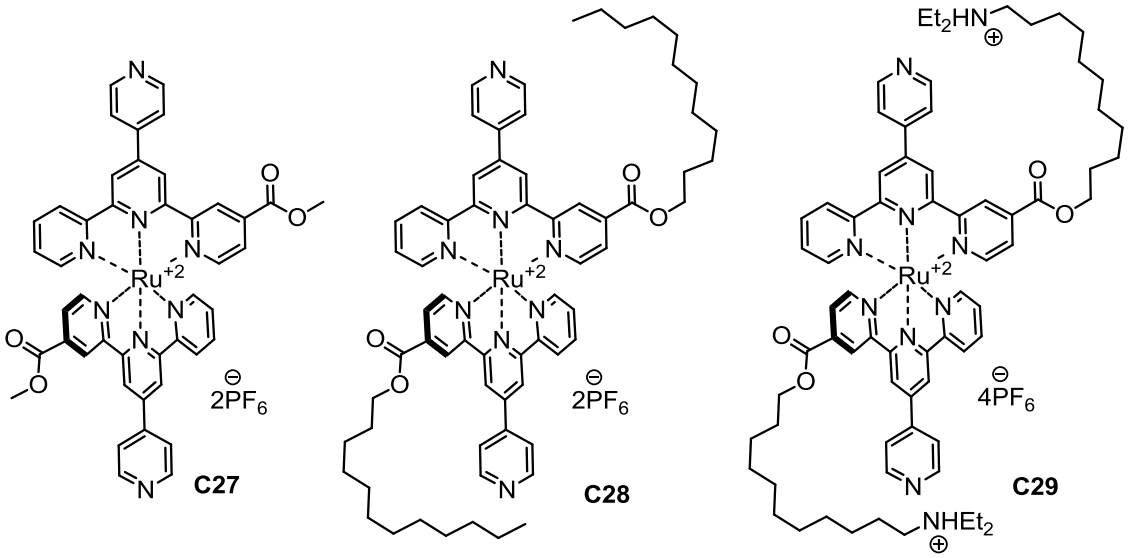

Scheme 5.5: Homoleptic ruthenium(II) complexes C27 - C29

In this section, photophysical properties of the homoleptic ruthenium(II) complex **C29** with pytpy ligands with the diethylamino-substituted side chain linked via an ester group, are reported and compared with those of methyl ester-substituted homoleptic complex **C27** and the dodecyl ester-substituted complex **C28** (Scheme 5.5). We were interested to see the influence of two electron-withdrawing ester groups together with the effect of the (protonated) amino unit on the spectroscopic properties of these molecules, and compare these with spectroscopic properties of the heteroleptic complexes **C17-18**. Figures 5.21 and 5.24 compile absorption and emission spectra of the Ru(II) complexes **C27-29** in their starting forms. Figures 5.22 and 5.25 compare absorption and emission spectra of the Ru(II) complexes in their mono-protonated form (**C27-1H**, **C28-1H** and **C29-1H**). Figures 5.23 and 5.26 compare absorption and emission spectra of the Ru(II) complexes in their bis-protonated form (**C27-2H**, **C28-2H** and **C29-2H**). The most important results are summarised in Table 5.7. Figure 5.27 shows the normalized titration curves obtained by monitoring the absorbance at 507 nm (**C27**), at 509 nm (**C28**) and at 514 (**C29**) as a function of acid aliquots and normalized titration curves obtained by monitoring the photoluminescence at 736 nm (**C27**, λ_{ex} = 492 nm), 709 nm (**C28**, λ_{ex} = 493 nm) and 786 nm (**C29**, λ_{ex} = 497 nm) as a function of TfOH equivalents. All the titration curves of **C27-29** reach the spectroscopic plateau at approximately 2 equivalents of TfOH.

Compound	λ_{abs} [nm]	ε [L cm^{-1} mol^{-1}]	λ_{em} [nm]	QY [%]	τ [ns]	λ_{iso}
C27	497	28000	662	0.020	6	**493**
C27-1H	506	33000	716	0.122	124	
C27-2H	509	39000	711	0.165	191	
C28	497	28000	663	0.024	8	**494**
C28-1H	504	31000	717	0.117	153	
C28-2H	508	38000	708	0.166	188	
C29	498	29000	667	0.236	7	**494**
C29-1H	506	34000	717	0.129	112	
C29-2H	508	39000	709	0.173	185	

Table 5.7: Photophysical properties of the homoleptic ruthenium(II) complexes C27-29

The absorption spectra of all three homoleptic complexes **C27-29** are comparable and exhibit nearly the same absorption maxima in the UV and VIS – region as well as the same molar extinction coefficient (Figure 5.21). This behaviour was also observed during titration of **C27-29** with TfOH. Upon addition of acid, the maxima of the MLCT bands are steadily red-shifted and also the molar extinction coefficient increases (Figures 5.22 and 5.23). Therefore, it is obvious that the main influence leads from the pendant pyridyl units and the two ester substituents, not at all from the side chain substituent. This trend is nearly the same in the emission spectra (Figures 5.24 and 5.26). Upon titration up to 1st eq. of TfOH, the emission intensity increases and a strong red-shift of the emission maxima is observed. The emission intensity increases even more upon the 2nd aliquot of TfOH but the emission maxima of **C27-29-2H** are slightly blue-shifted, as those of **C8-2H** and **C17-19-2H**. Also the quantum yields and luminescence lifetimes for each of the protonation forms are very similar and obey the trend which was also observed for protonation of the heteroleptic complexes **C17-19**. Also the shape and the slopes of the titration curves are nearly identical. Therefore it is obvious that in this case, only the presence of the two ester substituents determines the photophysical properties.

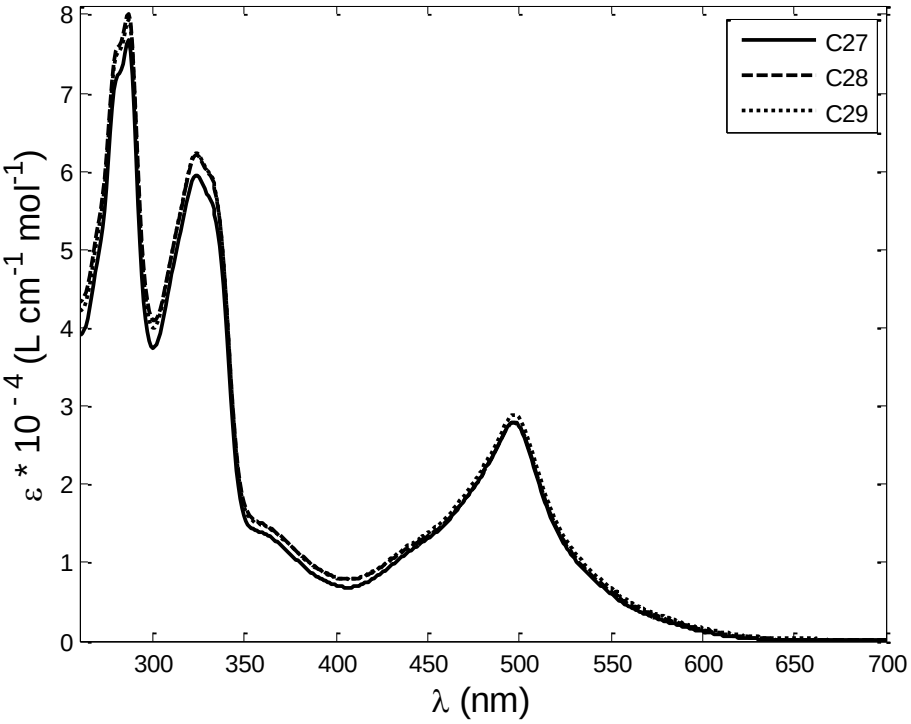

Figure 5.21: Absorption spectra of the Ru(II) complexes C27 (c = 1.10× 10^{-5} M, MeCN), C28 (c = 0.93 × 10^{-5} M, MeCN) and C29 (c = 0.97 × 10^{-5} M, MeCN).

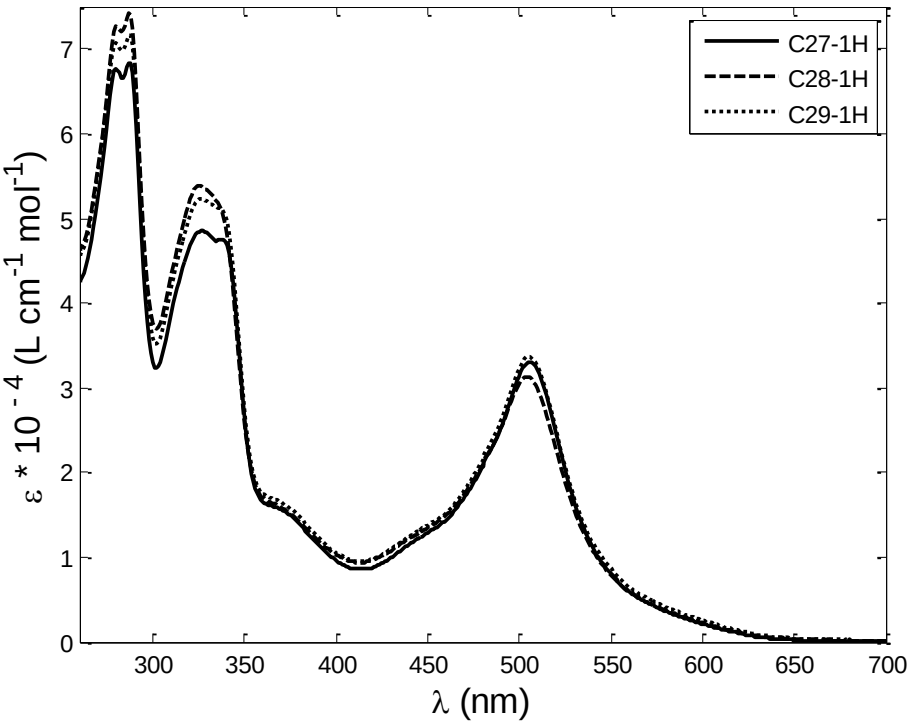

Figure 5.22: Absorption spectra of the Ru(II) complexes in their mono-protonated form C27-1H (c = 1.10× 10^{-5} M, MeCN), C28-1H (c = 0.93 × 10^{-5} M, MeCN) and C29-1H (c = 0.97 × 10^{-5} M, MeCN).

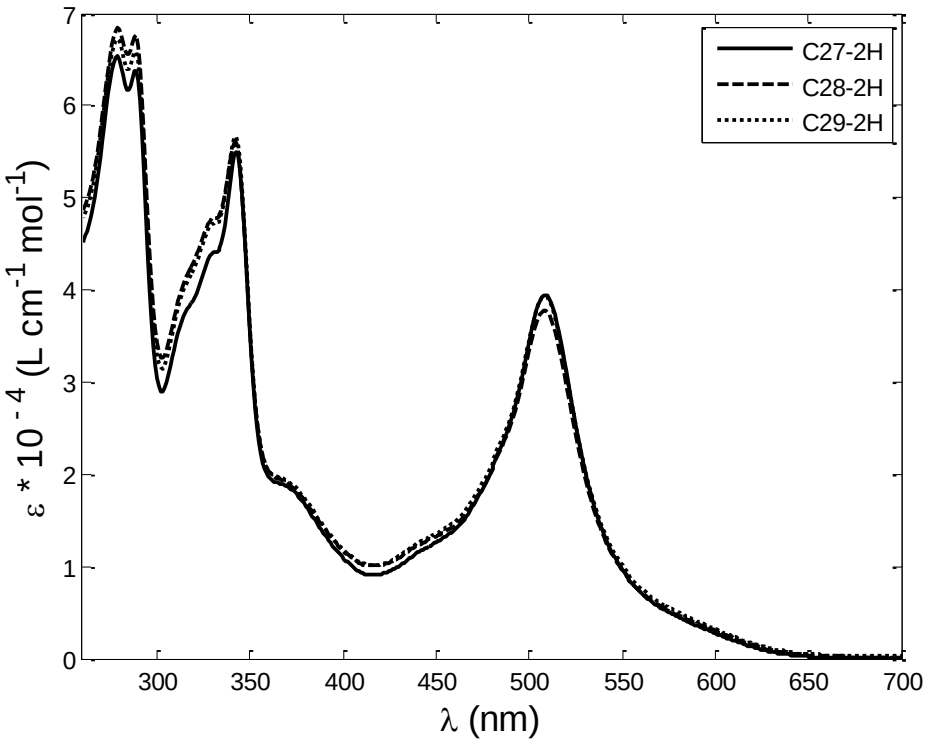

Figure 5.23: Absorption spectra of the Ru(II) complexes in their bis-protonated form C27-2H (c = 1.10×10^{-5} M, MeCN), C28-2H (c = 0.93 ×10^{-5} M, MeCN) and C29-2H (c = 0.97 ×10^{-5} M, MeCN).

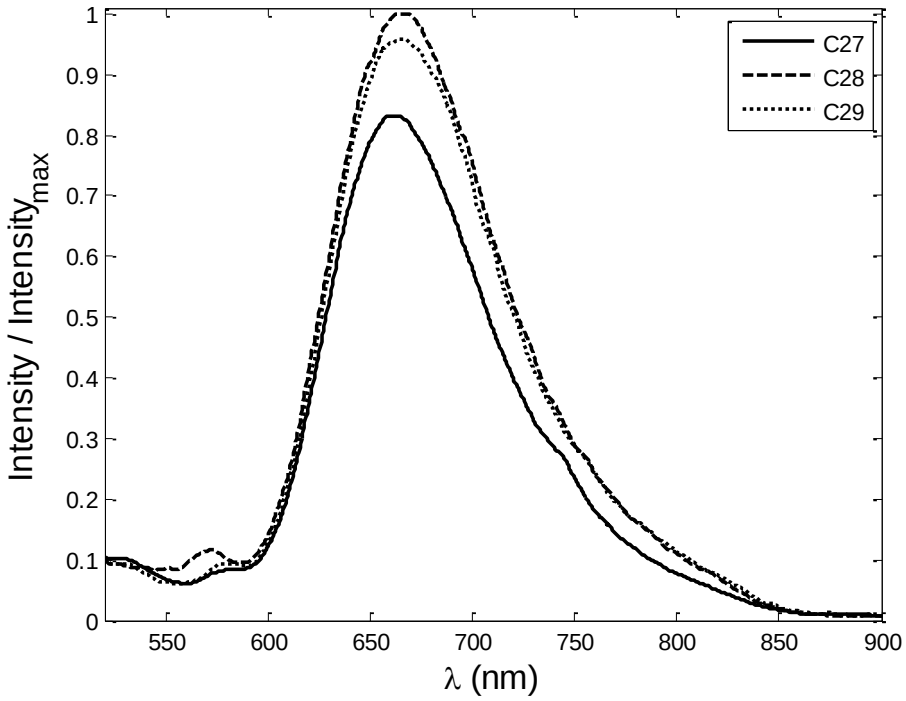

Figure 5.24: Normalized emission spectra of the ruthenium(II) complexes C27 (c = 1.10 × 10^{-5} M in MeCN, λ_{ex} = 493 nm), C28 (c = 1.13 × 10^{-5} M in MeCN, λ_{ex} = 494 nm) and C29 (c = 0.97 × 10^{-5} M in MeCN, λ_{ex} = 494 nm).

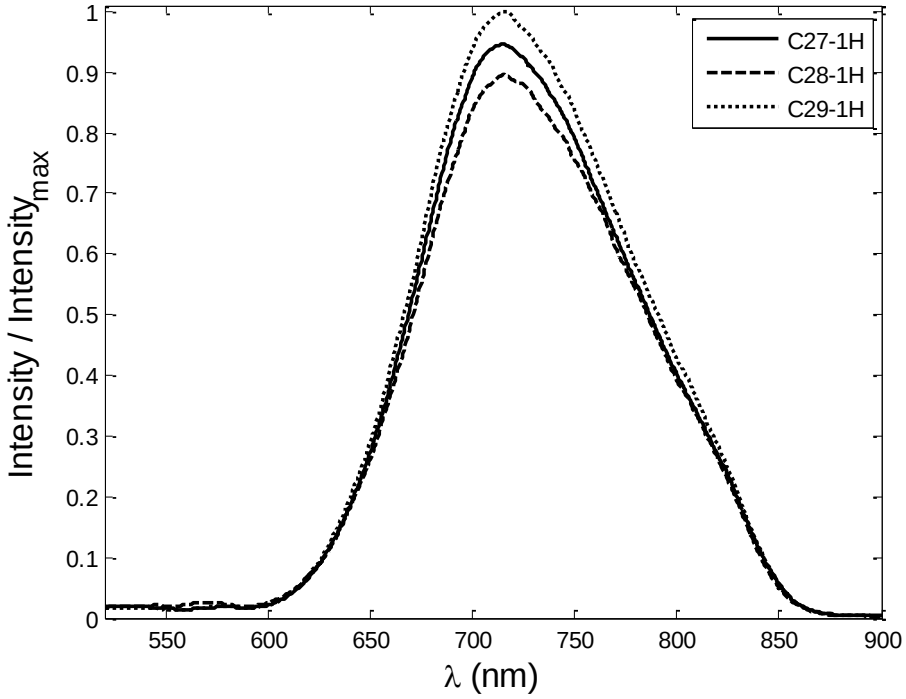

Figure 5.25: Normalized emission spectra of the ruthenium(II) complexes in their mono-protonated forms C27-1H (c = 1.10 × 10^{-5} M in MeCN, λ_{ex} = 493 nm), C28-1H (c = 1.13 × 10^{-5} M in MeCN, λ_{ex} = 494 nm) and C29-1H (c = 0.97 × 10^{-5} M in MeCN, λ_{ex} = 494 nm).

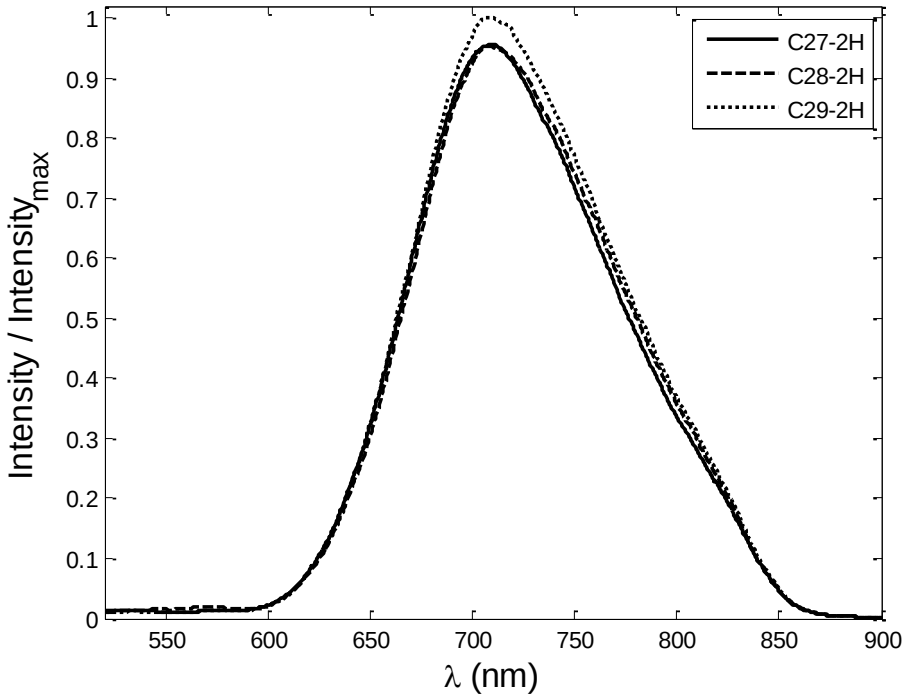

Figure 5.26: Normalized emission spectra of the ruthenium(II) complexes in their bis-protonated forms C27-2H (c = 1.10 × 10^{-5} M in MeCN, λ_{ex} = 493 nm), C28-2H (c = 1.13 × 10^{-5} M in MeCN, λ_{ex} = 494 nm) and C29-2H (c = 0.97 × 10^{-5} M in MeCN, λ_{ex} = 494 nm).

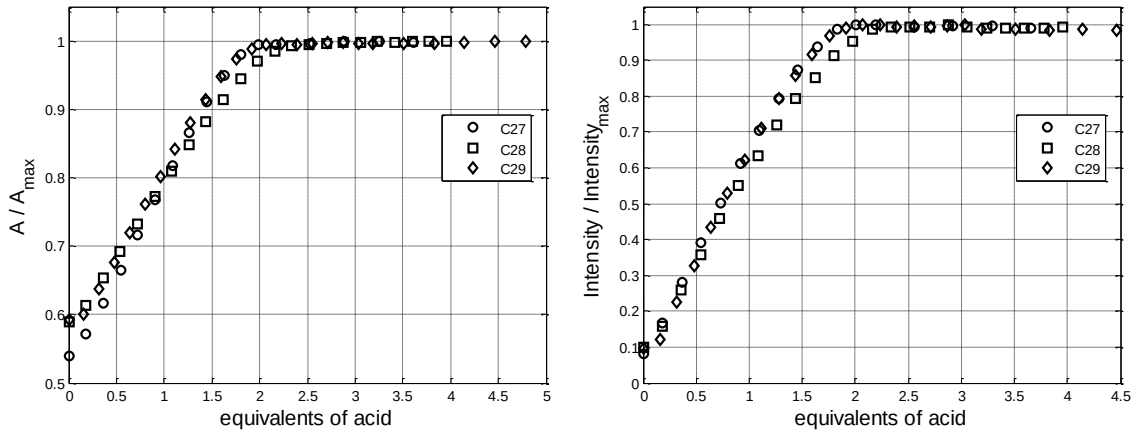

Figure 5.27: Left: Normalized titration curves obtained by monitoring the absorbance at 507 nm (C27), at 509 nm (C28) and at 514 (C29) as a function of acid aliquots. Right: Normalized titration curves obtained by monitoring the photoluminescence at 736 nm (C27, λex = 492 nm), 709 nm (C28, λex = 493 nm) and 786 nm (C29, λex = 497 nm) as a function of TfOH equivalents. All the titration curves of C27-29 reach the spectroscopic plateau at approximately 2 equivalents of TfOH. Solutions: 1.10 × 10^{-5} M, 1.13 × 10^{-5} M and 0.97 × 10^{-5} M in MeCN, respectively.

5.3.6 Ruthenium(II) complexes C33-C36 with Phtpy ligands

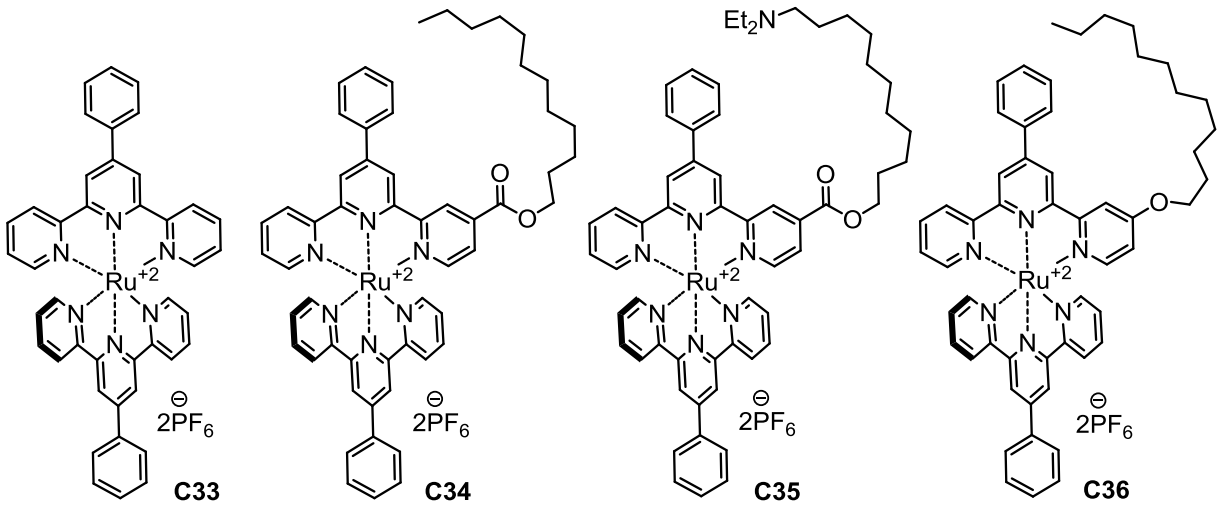

Scheme 5.6: Ruthenium(II) complexes C33-36 of Phtpy ligands

In this section, photophysical properties of the ruthenium(II) complex **C35** of Phtpy ligands with the diethylamino-substituted side chain linked via an ester group, are reported and compared with those of the model complex **C33**, dodecyl ester-substituted complex **C34** and the dodecyl ether-substituted complex **C36** (Scheme 5.6). These complexes were synthesized as model complexes for comparison with the Ru(II) complexes of pytpy ligands **C17-18.** In

comparison with **C18**, **C35** has only one protonation side, on the side chain. We were interested to see if there was any influence of the (protonated) amino unit, other than the reported effect of the electron-withdrawing ester group or the electron-donating effect of the ether group and compare these results with the spectroscopic properties of the heteroleptic complexes of pytpy ligands **C17-18**. Figures 5.28 and 5.29 compile absorption and emission spectra of the Ru(II) complexes **C33-36**. Results are summarised in Table 5.8.

Compound	λ_{abs} [nm]	ε [L cm^{-1} mol^{-1}]	λ_{em} [nm]	QY [%]	τ [ns]
C33	488	24000	644	0.004	3
C34	494	22000	673	0.015	4
C35	494	22000	668	0.017	5
C36	490	25000	652	0.006	3

Table 5.8: Photophysical properties of the ruthenium(II) complexes C33-36 of Phtpy ligands

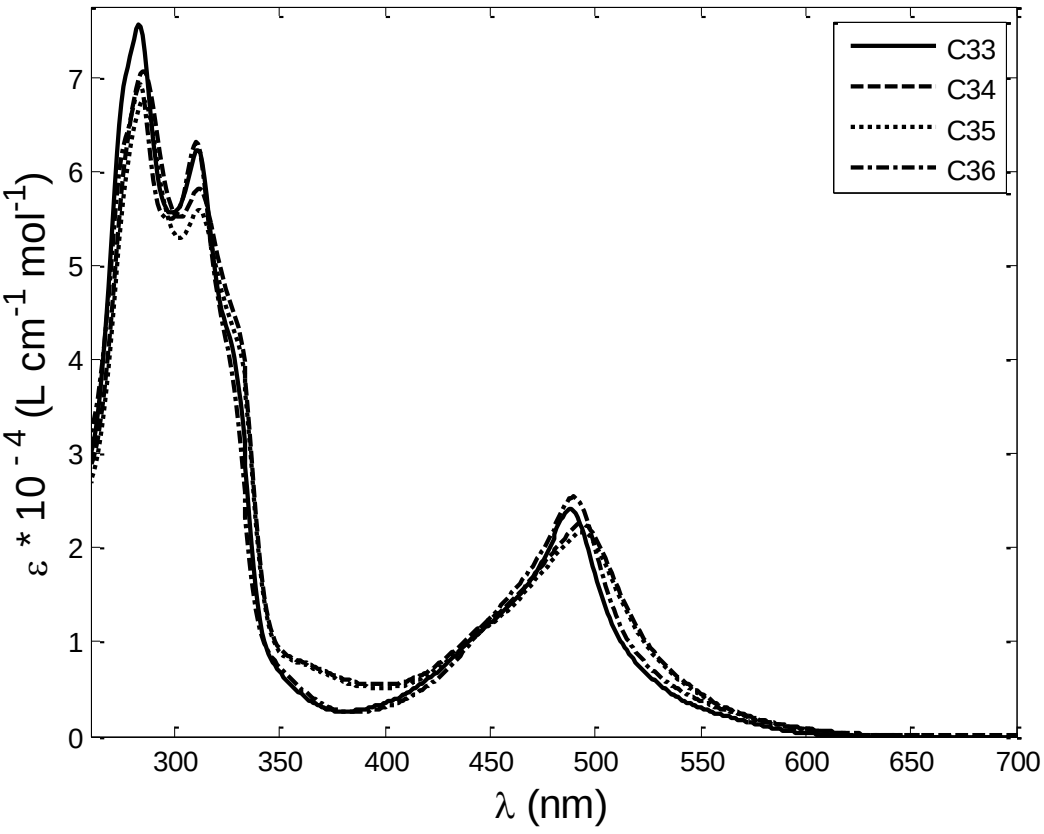

Figure 5.28: Absorption spectra of the Ru(II) complexes C33 (c = 1.12 × 10^{-5} M, MeCN), C34 (c = 1.20 × 10^{-5} M, MeCN), C35 (c = 1.17 × 10^{-5} M, MeCN) and C36 (c = 0.84 × 10^{-5} M, MeCN).

In the absorption spectra of **C33-36** it was observed that functionalizing ~~of~~ the model complex **C33** with an ether group (**C36**) caused a slight red-shift of the MLCT absorption band and even more with the ester group (**C34-35**) (Figure 5.28). The molar extinction coefficient value is similar for all compounds at their λ_{abs}. The substituent effect is also significant in the emission spectra (Figure 2.29). The emission maxima of the ester substituted complexes **C34-35** are more red-shifted than that of the ether-substituted complex **C36.** Actually, complex **C33** is almost not emissive at all, and the presence of the ether group does not cause any change compared with **36** (Table 5.8). Photophysical properties of **C34-35** are comparable, therefore we can conclude that presence of the amino substituent on the long side chain does not cause any differences, however the ester group has the only effect on the spectral changes.

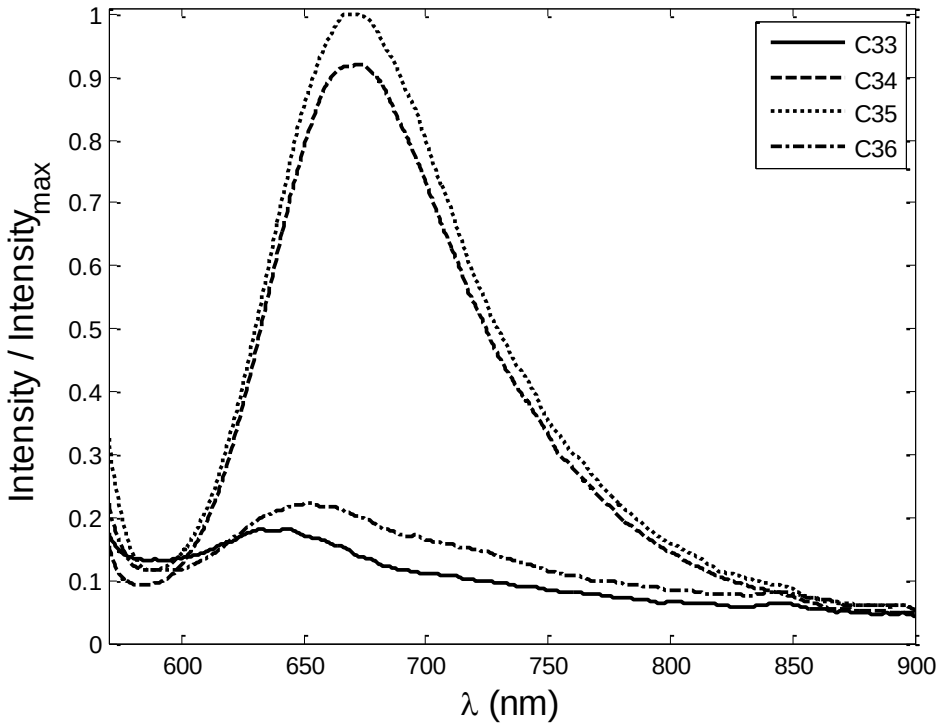

Figure 5.29: Normalized emission spectra of the ruthenium(II) complexes C33 (c = 0.64 × 10^{-5} M in MeCN, λ_{ex} = 489 nm), C34 (c = 0.50 × 10^{-5} M in MeCN, λ_{ex} = 494 nm), C35 (c = 0.46 × 10^{-5} M in MeCN, λ_{ex} = 494 nm) and C36 (c = 0.46 × 10^{-5} M in MeCN, λ_{ex} = 490 nm).

5.3.7 Truth tables

Upon observing changes in the luminescence spectra for each of the protonation state of the dodecyl-oxy-substituted Ru(II) complex **C22**, it is possible to construct logic gates (Figure 5.30). The proton aliquots form 2 inputs for the truth table, and upon setting threshold lines for a certain wavelength it is possible to perform the half-adder functions and obtain outputs. So then by setting the threshold line (violet, at 1 a.u.) at 680 nm we obtain an NAND gate, however for the same threshold line at 730 nm we obtain an AND gate. The red threshold at 762 nm gave an OR gate.

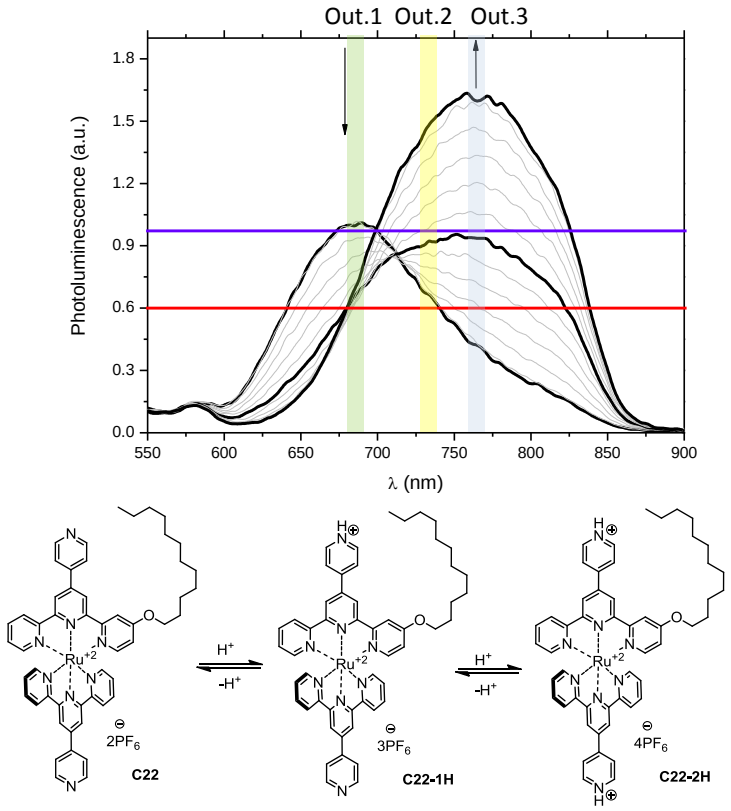

In. 1 = H^+

In. 2 = H^+

Out = hν

In. 1	In. 2	Out. 1	Out. 2	Out. 3
0	0	1	0	0
1	0	0	0	1
0	1	0	0	1
1	1	0	1	1
		NAND	AND	OR

Figure 5.30: Ru(II) complex C22 and its protonated forms, luminescence spectra of the studied complexes, threshold and outputs lines indicated, truth tables for the constructed logic gates

Figure 5.31 shows protonation states of the piperidino-substituted Ru(II) complex **C24** and their corresponding luminescence spectra. The proton aliquots form 3 inputs for the truth table, and upon setting threshold lines for a certain wavelength it is possible to perform the full-adder functions and obtain outputs. The pendant piperidine-unit was protonated already before performing the luminescence measurement, therefore the input 3 is always 1. So then by setting the threshold line (red, at 2 a.u.), at 690 nm we obtain an NAND gate. For the

purple threshold line at 690 nm we obtain an XNOR gate, however at 750 nm we obtain an AND gate.

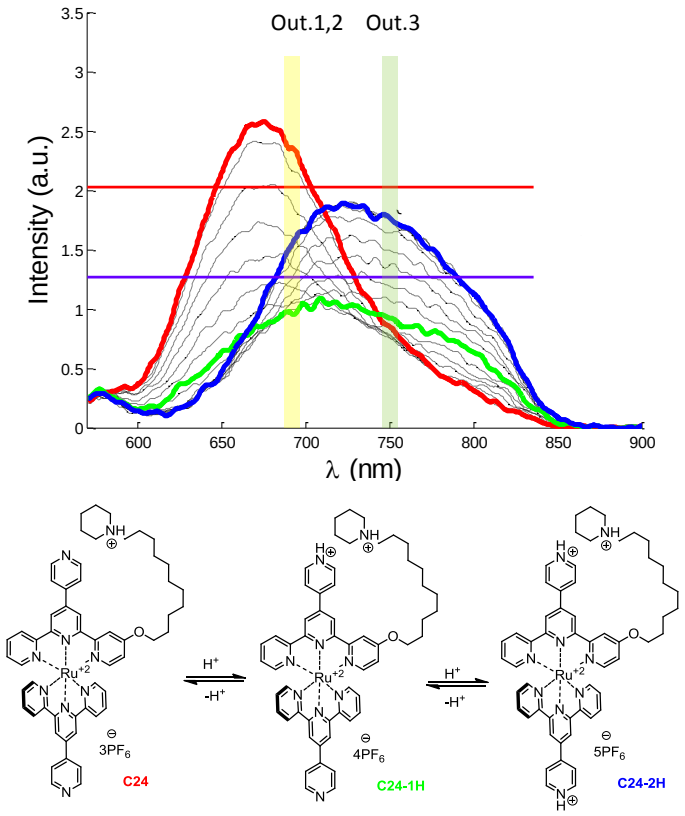

In. 1	In. 2	In. 3	Out. 1	Out. 2	Out. 3
0	0	1	1	1	0
1	0	1	0	0	0
0	1	1	0	0	0
1	1	1	0	1	1
			NAND	XNOR	AND

Figure 5.31: Ru(II) complex C24 and its protonated forms, luminescence spectra of the studied complexes, threshold and outputs lines indicated, truth tables for the constructed logic gates

Conclusion

Ruthenium(II) complexes were analysed in terms of their photophysical properties and compared in groups according to the pendant substituents of the tpy unit, according to the linker group of the side chain and also considering substituents on the side chains. The complexes with the ester linker exhibit similar behaviour in the absorption and emission spectra as reported for the model complex **C8**.[1] Complexes with the ether linker appeared to be very weak emitters. However they exhibit continuous red shift in emission spectra during all acid titration, in contrast to complexes with ester linkers or **C8**. Complexes of Phtpy ligands were found to also be very weak emitters which corresponds with known ruthenium(II) complexes of tpy ligands.[2] Homoleptic ruthenium(II) complexes of ester-

substituted ligands exhibit the best photophysical properties of all the analysed complexes. Unfortunately, we were not able to investigate the actual effect of the amino-substituent on the side chain, due to the fact that such complexes were isolated in their side-chain protonated form.

Literature

1 Constable, E. C.; Housecroft, C. E.; Thompson, A. C.; Passaniti, P.; Silvi, S.; Maestri, M. *Inorganica Chimica Acta* **2007**, *360*, 1102-1110.

2 M. Maestri, N. Armaroli, V. Balzani, E. C. Constable, A. M. W. Thompson, *Inorg. Chem.* **1995**, *34*, 2759-2767.

3 Silvi, S.; Constable, E. C.; Housecroft, C. E.; Beves, J. E. ; Dunphy, E. L.; Tomasulo, M.; Raymo, F. M.; Credi, A. *Chem. Eur. J.* **2009**, *15*, 178-185**.**

4 Lanzilotto, A. MSc Thesis, **2013**, University of Bologna.

Chapter 6

Acid and base NMR studies of ruthenium(II) complexes and their free ligands with an amino-substituted side chain

6.1 Introduction

In Chapter 4, a series of heteroleptic ruthenium(II) complexes with a long amino-substituted side chain linked via an ester **C18**-**20**, via an ether **C23-25** and the homoleptic ruthenium(II) complex **C29** were synthesized, along with a series of methyl and dodecyl-substituted model Ru(II) complexes (**C7**, **C17**, **C22**, **C27**, **C28** and **C30**). The amino group attached to the side chain and the two pendant pyridyl groups bring three protonation sites to the molecule. In Chapter 5, photophysical studies of these Ru(II) complexes were reported and discussed. It was found that some molecules exhibit unexpected abnormalities during those measurements. Namely, an unusual kinetic effect in the absorption and photoluminescence spectrum during titration of **C20** with TfOH or too small amount of acid consumed to complete titrations of some complexes (**C29**).

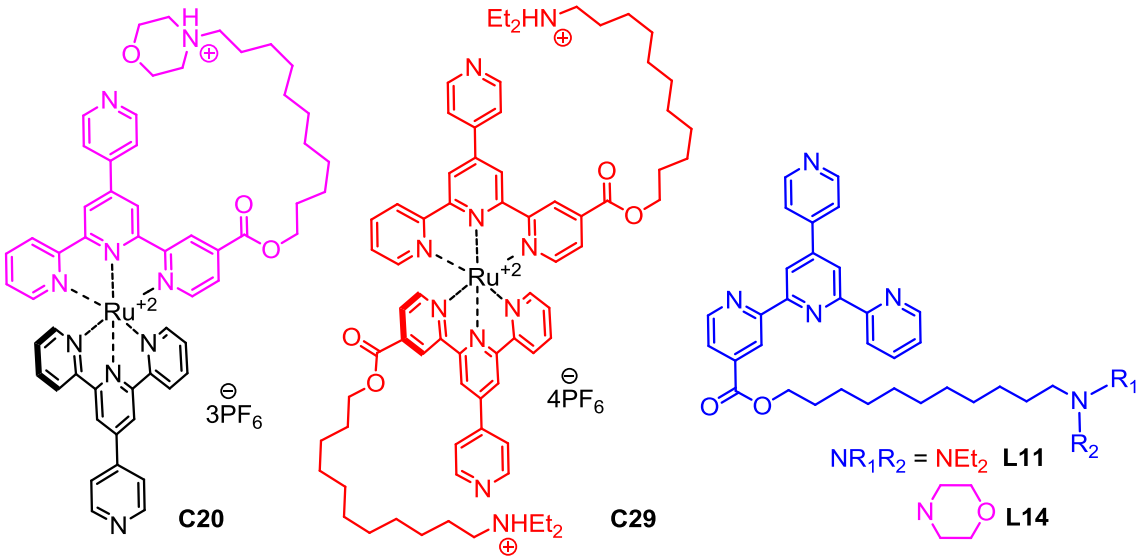

Scheme 6.1: Ruthenium(II) complexes C20 and C29 and their free ligands L11 and L14 used for NMR studies carried out under acidic and basic conditions

Therefore, in this chapter we decided to carry out titrations of **C20** and **C29** with TFA-d and TfOD and to monitor the process of the protonation with ^{1}H NMR spectra. We were investigating which nitrogen atom it is actually possible to protonate, and monitoring the sequence of their protonation. We were also interested to examine the stability of the side amino chains under these acidic conditions and to see if the side chains were cleaved or stayed attached to the Ru(II) complex. The results of these NMR studies are one of the most important and revolutionary piece of information. They reveal and clarify that all the Ru(II) complexes with three protonation sites were synthesized and isolated already in the mono-protonated form - on the amino group of the side chain (Scheme 6.1). Due to this fact, until Section 6.2.3 we talk about the complexes **C20** and **C29** and display them in the deprotonated form (Scheme 6.2).

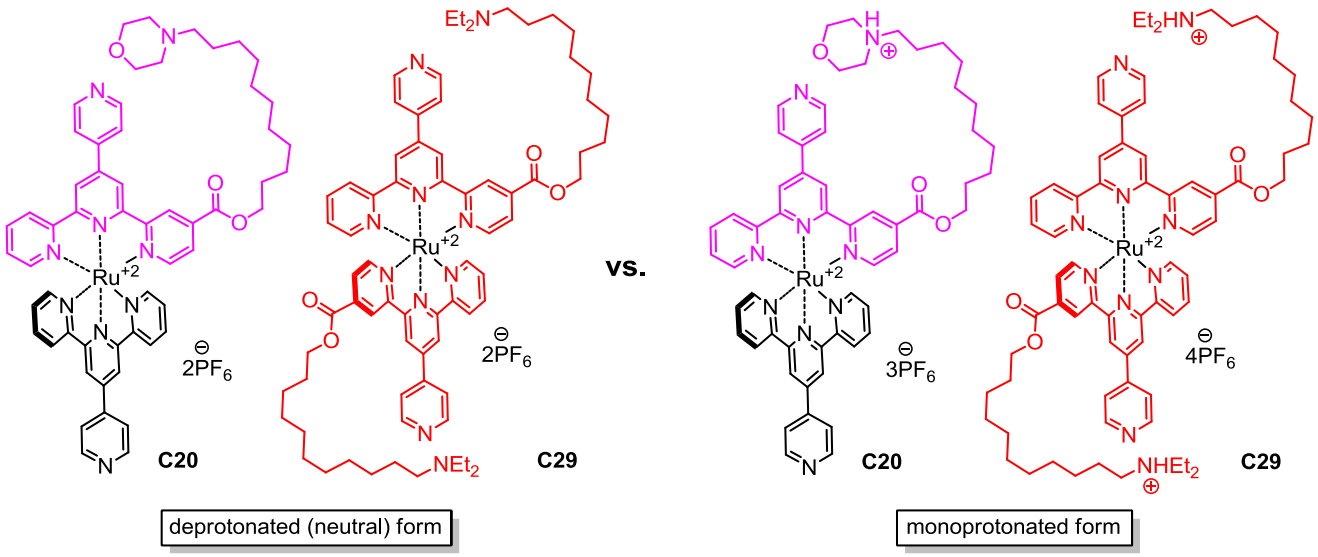

Scheme 6.2: Ruthenium(II) complexes C20 and C29 in the deprotonated (neutral) form (left) and monoprotonated form (right)

6.2 Results and Discussion

6.2.1 NMR titrations of C20 and C29 with TFA-d or TfOD

Homoleptic ruthenium(II) complex **C29** was titrated with TFA-d (CF_3COOD) and the process was monitored with ^{1}H NMR spectra (Figure 6.1). The NMR tube contained a solution of **C29** in CD_3CN (c = 4.34×10^{-3} mol/L, 4 mg in 0.5 mL of CD_3CN). This was titrated in small aliquot dilute TFA-d (c = 21.56×10^{-3} mol/L, 0.6 μL in 0.3 mL of CD_3CN) until 2.8 equivalents of TFA-d

had been added (Table 6.1, Spectra 1-15). Then we continued until 138 equivalents of concentrated TFA-d, when no more change of chemical shifts were observed in the ^{1}H NMR spectrum (Table 6.1, Spectra 16-25).

No. of ^{1}H NMR spectrum	**1**	**2**	**3**	**4**	**5**	**6**	**7**	**8**	**9**	**10**	**11**	**12**	**13**
No. of eq. of TFA-d	0	0.2	0.4	0.6	0.8	1	1.2	1.4	1.6	1.8	2	2.2	2.4
No. of ^{1}H NMR spectrum	**14**	**15**	**16**	**17**	**18**	**19**	**20**	**21**	**22**	**23**	**24**	**25**	
No. of eq. of TFA-d	2.6	2.8	6	9	12	15	21	30	48	75	102	138	

Table 6.1: Titration process of C29 with TFA-d, ^{1}H NMR spectra displayed in Figure 6.1

All ^{1}H NMR spectra of the titration process were stacked together and chemical shifts of all protons compared. We were interested to see which nitrogen atoms of **C29** are being protonated and in which order. The pendant pyridyl positions were expected to be protonated first, then the side chain amino unit. We were also investigating if the side chain under the acidic conditions stayed attached to the ruthenium(II) complex **C29** or if it was cleaved. The protonation process of the pendant pyridyl units was monitored according to chemical shift of the peaks labelled **C2** and **C3** with δ 8.97 ppm and δ 8.20 ppm, respectively. The protonation of the side chain was monitored according to chemical shift of the peaks labelled **13** and **11** with δ 3.15 ppm and δ 3.03 ppm, respectively. Several facts are obvious from the ^{1}H NMR spectra. Both side chains stayed attached to the complex and did not cleave, otherwise one would be able to see a change in the intensity or the chemical shift of the methylene group **1** and also differences in the aromatic region. However, there is not any significant change in any of the aliphatic peaks, but just in the aromatic region (**C2** and **C3** groups shifted to δ 9.07 ppm and δ 8.77 ppm, respectively). This means, that the protonation process was happening only on the pendant pyridyl units and the side chains stayed untouched. This gives rise to a question; are the side chain amino units of **C29** really untouched or were the amino groups already protonated before we even started the titration? This was the subject of the further investigation (Sections 6.2.2 and 6.2.3). In the aromatic region is possible to see the smooth protonation process of the pendant pyridyl units (protons **C2** and **C3**). The protonation has a stronger effect on the pyridyl protons **C3**

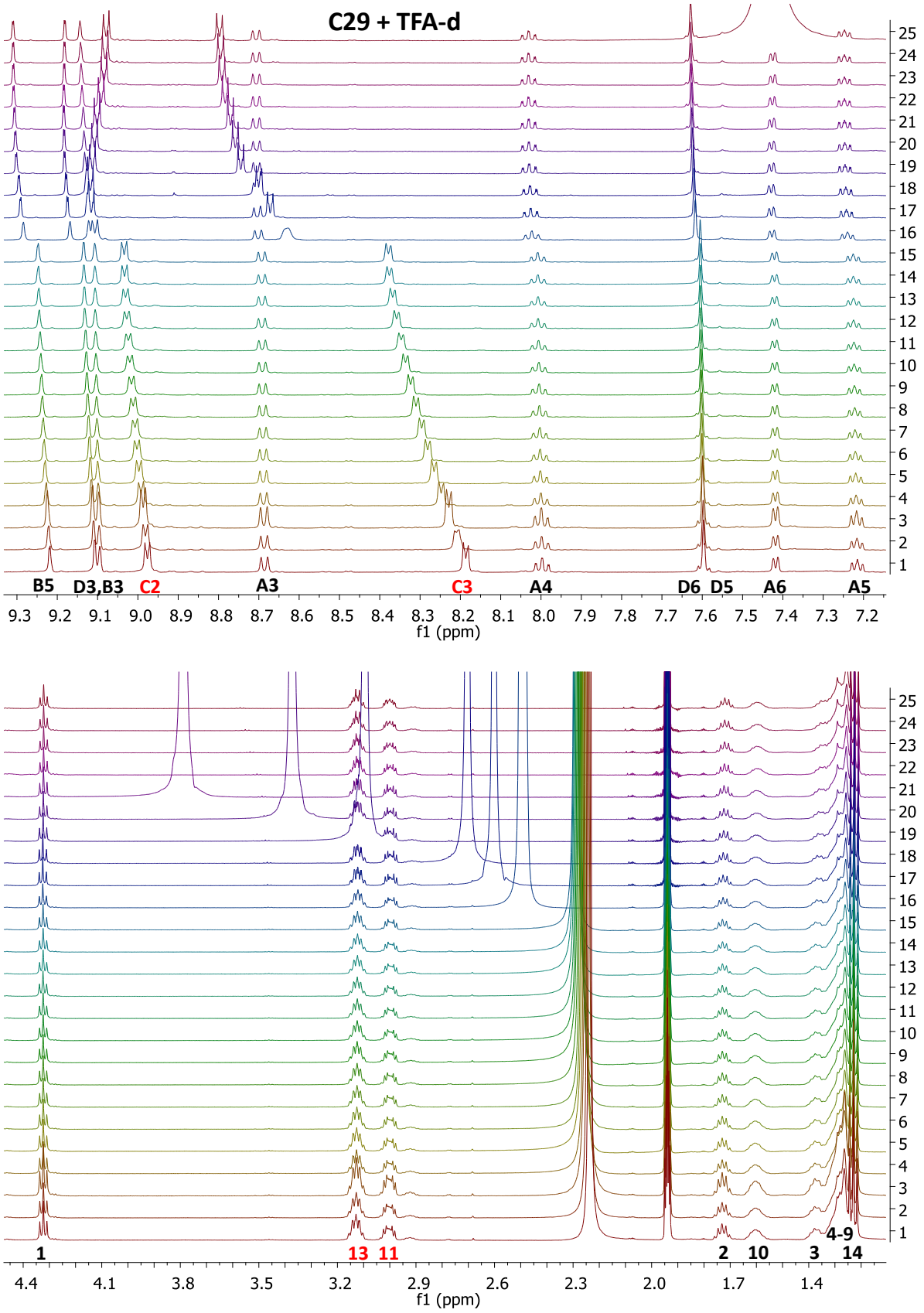

Figure 6.1: Stacked ^{1}H NMR spectra (500 MHz, CD_3CN) of titration of the homoleptic ruthenium(II) complex C29 with TFA-d, aromatic region (top), aliphatic region (bottom)

which are in the *meta*-position. The titration was done with slow increments of TFA-d until 2.8 equivalents, when it looked like the titration process was nearly at an end. Then we continued with larger increments of the acid which caused the big jump in the chemical shifts and showed that the titration had not finished yet (Figure 6.1, Spectrum 15 and 16, aromatic region). The amount of acid needed to complete the titration indicates that TFA-d is strong enough to go from the deprotonated form to the mono-protonated form. However it is too weak to force the protonation process between the equilibrium of the de-, mono- and bis-protonated form towards the preferred final bis-protonated form.

Heteroleptic ruthenium(II) complex **C20** was also titrated with TFA-d (CF_3COOD) at first and the process was monitored with ^1H NMR spectra (Figure 6.2). The NMR tube contained a solution of **C20** in CD_3CN ($c = 4.58\times10^{-3}$ mol/L, 3.3 mg in 0.5 mL of CD_3CN). This was titrated with small increments of diluted TFA-d ($c = 29.74\times10^{-3}$ mol/L, 0.8 μL in 0.3 mL of CD_3CN) until 4 equivalents of TFA-d (Table 6.2, Spectra 1-11). Then we continued until 142 equivalents with concentrated TFA-d, when no more change of chemical shifts were observed in the ^1H NMR spectrum (Table 6.2, Spectra 12-20). The protonation process of the pendant pyridyl units was monitored according to chemical shift of the peaks labelled **C2**, **G2** and **C3**, **G3** at δ 8.97 ppm, δ 8.21 ppm and δ 8.19 ppm, respectively. The protonation of the morpholine unit was monitored according to the chemical shift of the peaks **14**, **13** and **11** between δ 4.00 - 3.04 ppm. At this point, we still believed that **C20** was in its deprotonated form. Therefore, the fact the protons **13** and **14** of the morpholine unit appear non-equivalent and are distributed as axial and equatorial signals in the ^1H NMR spectrum, was accredited to the fact that the ligand was complexed. Also in this case, the protonation process was happening only on the pendant pyridyl units **C** and **G**, and the side chain remained untouched (Figure 6.2).

No. of ^1H NMR spectrum	**1**	**2**	**3**	**4**	**5**	**6**	**7**	**8**	**9**	**10**
No. of eq. of TFA-d	0	0.4	0.8	1.2	1.6	2	2.4	2.8	3.2	3.6
No. of ^1H NMR spectrum	**11**	**12**	**13**	**14**	**15**	**16**	**17**	**18**	**19**	**20**
No. of eq. of TFA-d	4	6	10	14	20	30	46	78	110	142

Table 6.2: Titration process of C20 with TFA-d, ^1H NMR spectra displayed in Figure 6.2

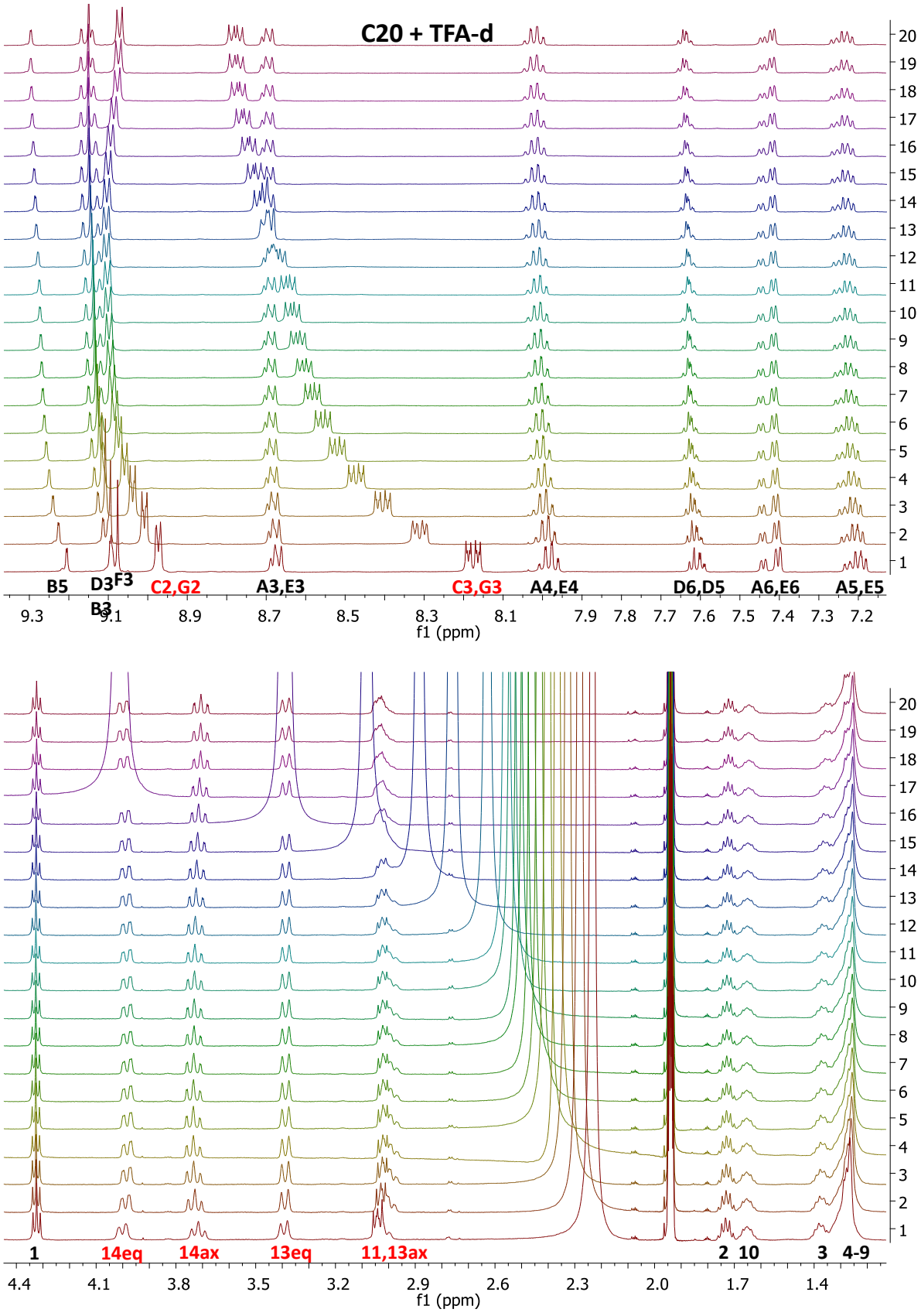

Figure 6.2: Stacked ^{1}H NMR spectra (500 MHz, CD_3CN) of titration of the heteroleptic ruthenium(II) complex C20 with TFA-d, aromatic region (top), aliphatic region (bottom)

To complete the titration of **C20** with TFA-d, a large amount of acid was needed (about 100 eq.). Therefore we decided to repeat this titration of **C20** but with the much stronger deuterated trifluoromethanesulfonic acid (TfOD) (Figure 6.3, Table 6.3). The NMR tube contained a solution of **C20** in CD_3CN (c = 4.72×10^{-3} mol/L, 3.4 mg in 0.5 mL of CD_3CN). This was titrated with small increments of diluted TfOD (c = 30.65×10^{-3} mol/L, 0.8 μL in 0.3 mL of CD_3CN) until 3.5 equivalents of TfOD (Table 6.3, Spectra 1-12). Then we continued until 21.5 equivalents with concentrated TfOD, when the solution in the NMR tube was acid-saturated (Table 6.2, Spectra 13-16). In comparison with Figure 6.2, TfOD is a much stronger acid than TFA-d and one can see that the titration is completed already at around 2.6 equivalents of TfOD (Spectrum 10, Table 6.3). The chemical shift of protons **C2**, **G2** and **C3**, **G3** stayed δ 8.95 ppm and δ 8.80 ppm, respectively. Around 14 equivalents of TfOD, the NMR sample became saturated with the acid and all peaks broadened. No significant change was observed in the aliphatic part of the ^{1}H NMR spectra. Some aliphatic impurities around δ 2.6 ppm were highlighted, but these were not assigned.

No. of ^{1}H NMR spectrum	**1**	**2**	**3**	**4**	**5**	**6**	**7**	**8**
No. of eq. of TfOD	0	0.2	0.4	0.6	0.8	1	1.4	1.8
No. of ^{1}H NMR spectrum	**9**	**10**	**11**	**12**	**13**	**14**	**15**	**16**
No. of eq. of TfOD	2.2	2.6	3	3.5	5.5	9.5	13.5	21.5

Table 6.3: Titration process of C20 with TfOD, ^{1}H NMR spectra displayed in Figure 6.3

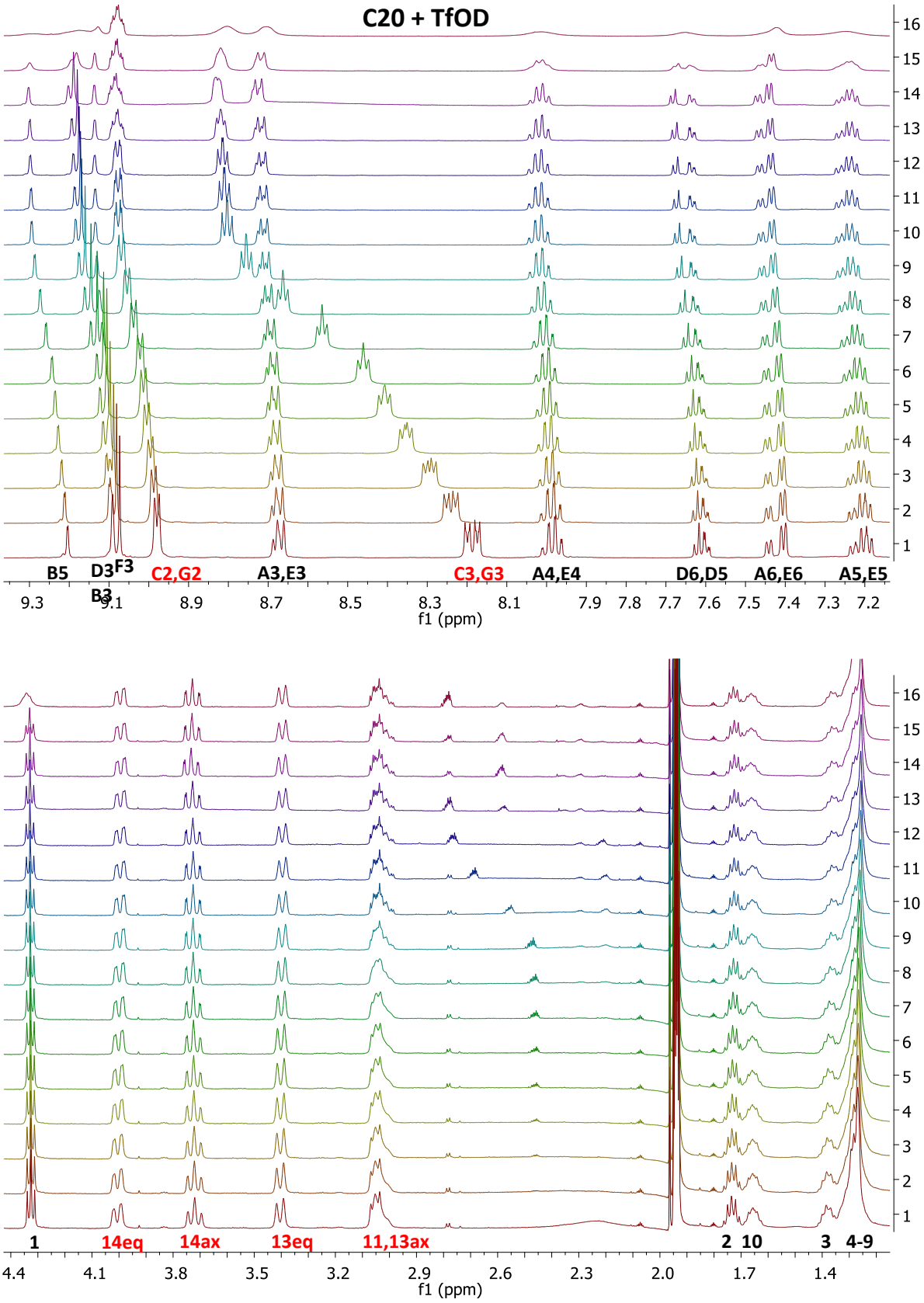

Figure 6.3: Stacked ^{1}H NMR spectra (500 MHz, CD_3CN) of titration of the heteroleptic ruthenium(II) complex C20 with TfOD, aromatic region (top), aliphatic region (bottom)

6.2.2 NMR studies with C20 and C29 under basic conditions

For the next experiment to prove that **C20** and **C29** are in their deprotonated forms, a ^{1}H NMR spectrum of **C20** with an addition of a base was measured. We recorded a ^{1}H NMR spectrum of the isolated complex **C20** (Figure 6.4, red) and then ^{1}H NMR spectrum of this same complex but with an addition of a small amount of K_2CO_3 (tip of spatula) (Figure 6.4, cyan). Under an ideal situation, these two spectra should exactly overlap. When comparing these two spectra, we observed only a small change in a chemical shift of the protons **C3**, **G3** and the rest of peaks stayed exactly the same (see also Figure 6.5, red and green).

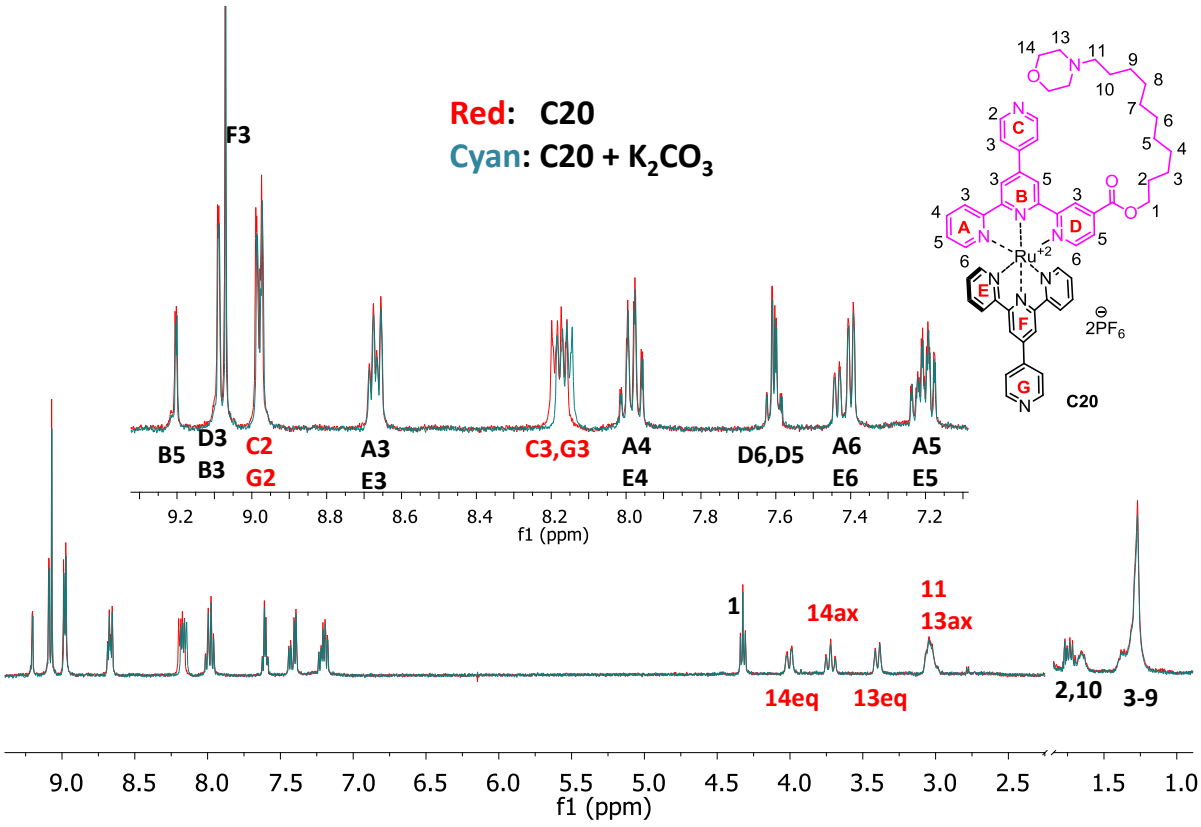

Figure 6.4: ^{1}H NMR spectrum (400 MHz, CD_3CN) of the heteroleptic ruthenium(II) complex C20 (red) overlapped with C20 +addition of K_2CO_3 (cyan)

However, when a second aliquot of K_2CO_3 was added, a significant change in the aliphatic region of **C20** was observed. All peaks of protons **14**, **13** and **11** shifted to the lower ppm values and the distribution to axial and equatorial signals started disappearing (Figure 6.5, cyan). When a large excess of K_2CO_3 was added (Figure 6.5, purple), the peaks of protons **14**, **13** and **11** were shifted even more to the lower ppm values and were represented by only 3

peaks with nearly the same chemical shift values as the protons **14**, **13** and **11** of the free ligand **L14**, in which the protons **14**, **13** and **11** are equivalent (see Figure 3.4 in Chapter 3, pink). We can say that the side chain has stayed attached to the molecule **C20**, because the peak of the methylene group **1** has not been shifted. This discovery brought us to the only possible conclusion, that the amino unit of the side chain of the starting **C20** was protonated and upon addition of K_2CO_3, was deprotonated.

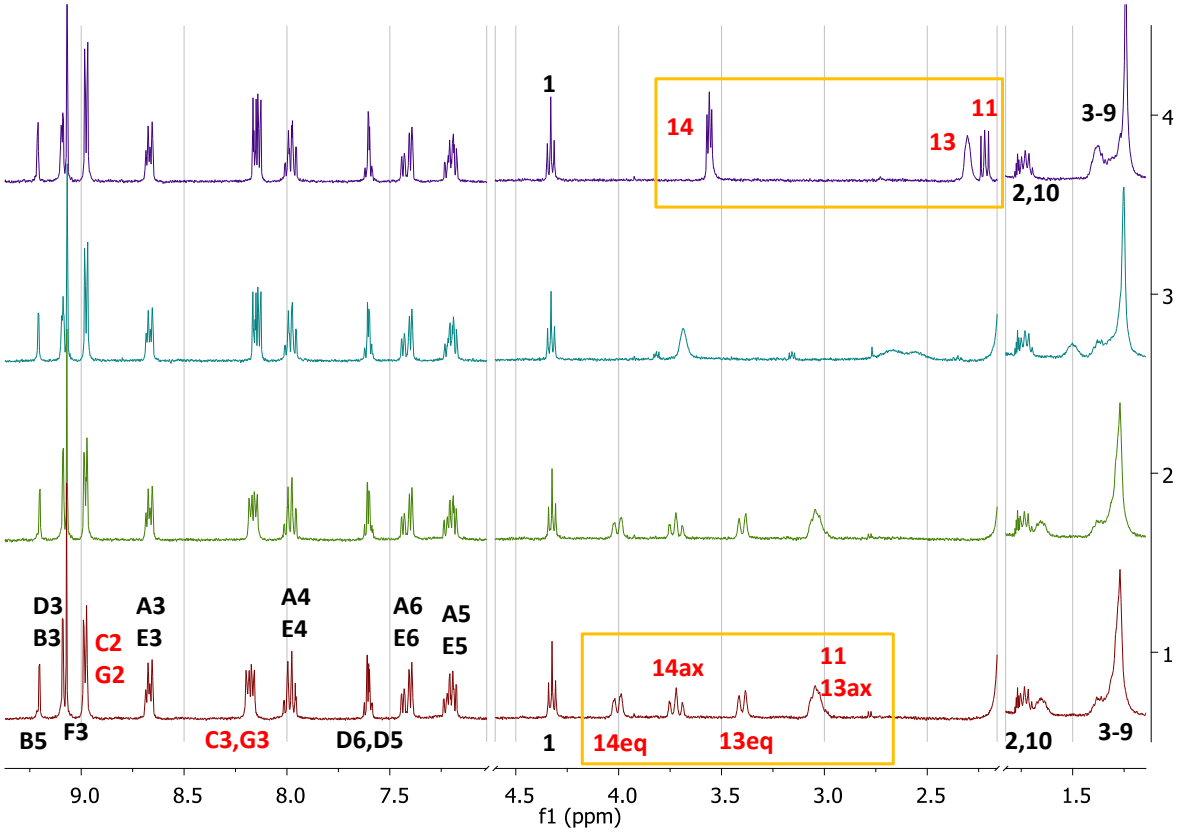

Figure 6.5: ^{1}H NMR spectra (400 MHz, CD_3CN) of the heteroleptic ruthenium(II) complex C20 (red) and with a sequent addition of K_2CO_3 (green, cyan) and with an excess of K_2CO_3 (purple)

After this, we were curious to try this experiment with the homoleptic ruthenium(II) complex **C29** containing diethylamino-substituted side chains. We measured a number of ^{1}H NMR spectra with small, sequential increments of K_2CO_3 (Figure 6.6, olive, green, blue) and with an excess of K_2CO_3 (Figure 6.6, purple). We observed that all the typical protons of the amino group **14**, **13**, **11** and **10** were also shifted to the lower ppm values as were those in **C20**, with nearly the same ppm values as the protons of the free, neutral ligand **L11** (see Figure 3.4 in Chapter 3, red).

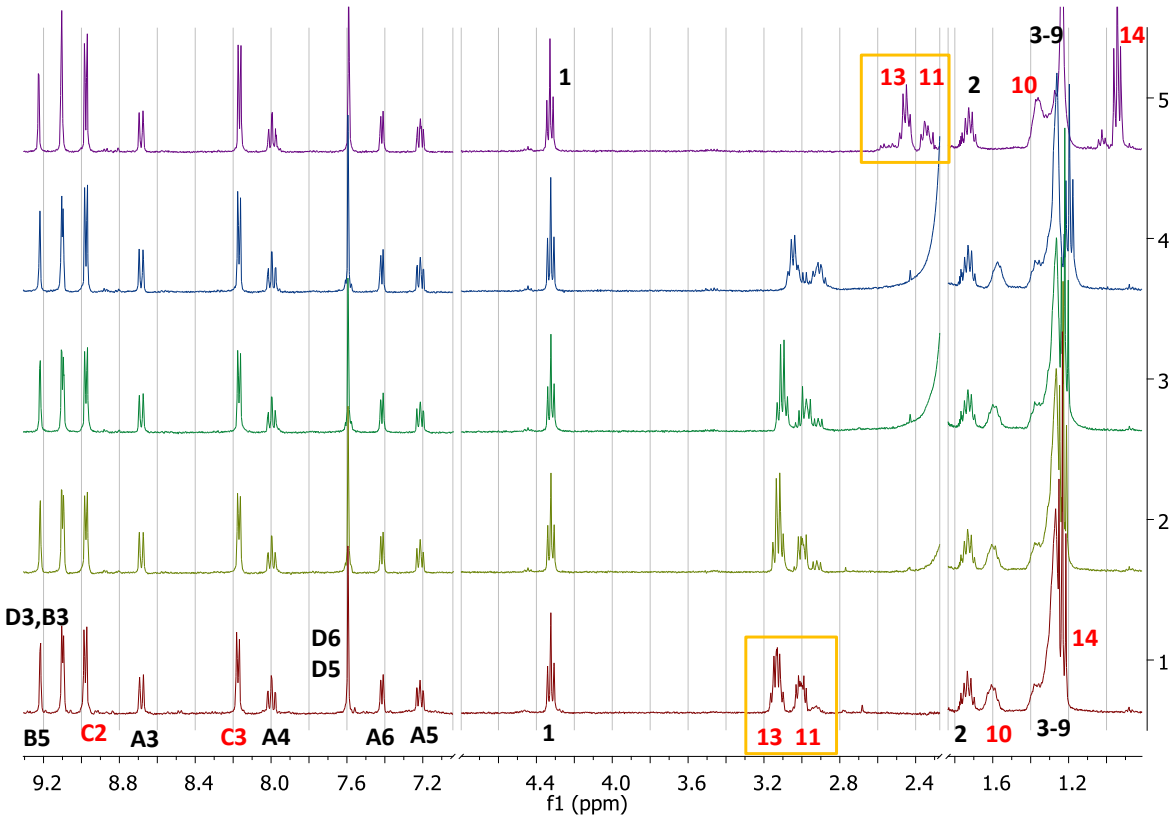

Figure 6.6: ^{1}H NMR spectra (400 MHz, CD_3CN) of the homoleptic ruthenium(II) complex C29 (red) and with sequential addition of K_2CO_3 (olive, green, blue) and with an excess of K_2CO_3 (purple)

6.2.3 NMR studies of the free ligands L11 and L14 with amino-substituted side chain under acidic conditions and their data fitting

As the next experiment, to prove that **C20** and **C29** are in their monoprotonated forms, we measured ^{1}H NMR spectrum of the morpholine-substituted free ligand **L14** in CD_3CN (Figure 6.7, pink) and then also one ^{1}H NMR spectrum with the addition of an excess of TfOD (Figure 6.7, blue). We monitored the chemical shift of **L14** in its protonated form and compared the spectrum with the ^{1}H NMR spectrum of **C20**. Since an excess of TfOD was used, we expected that all nitrogen atoms of the ligand **L14** would be protonated. In the aromatic region, a typical set of peaks of fully protonated pytpy ligand is observed. The pytpy protonation is obvious due to the fact that protons **D6**, **A6** and **C2** are represented by triplets (in comparison with **L14** in the neutral form when these protons are doublets of doublets) and also all pytpy protons are shifted to higher ppm values. In the aliphatic region it is clearly possible to see that the morpholine unit was also protonated.

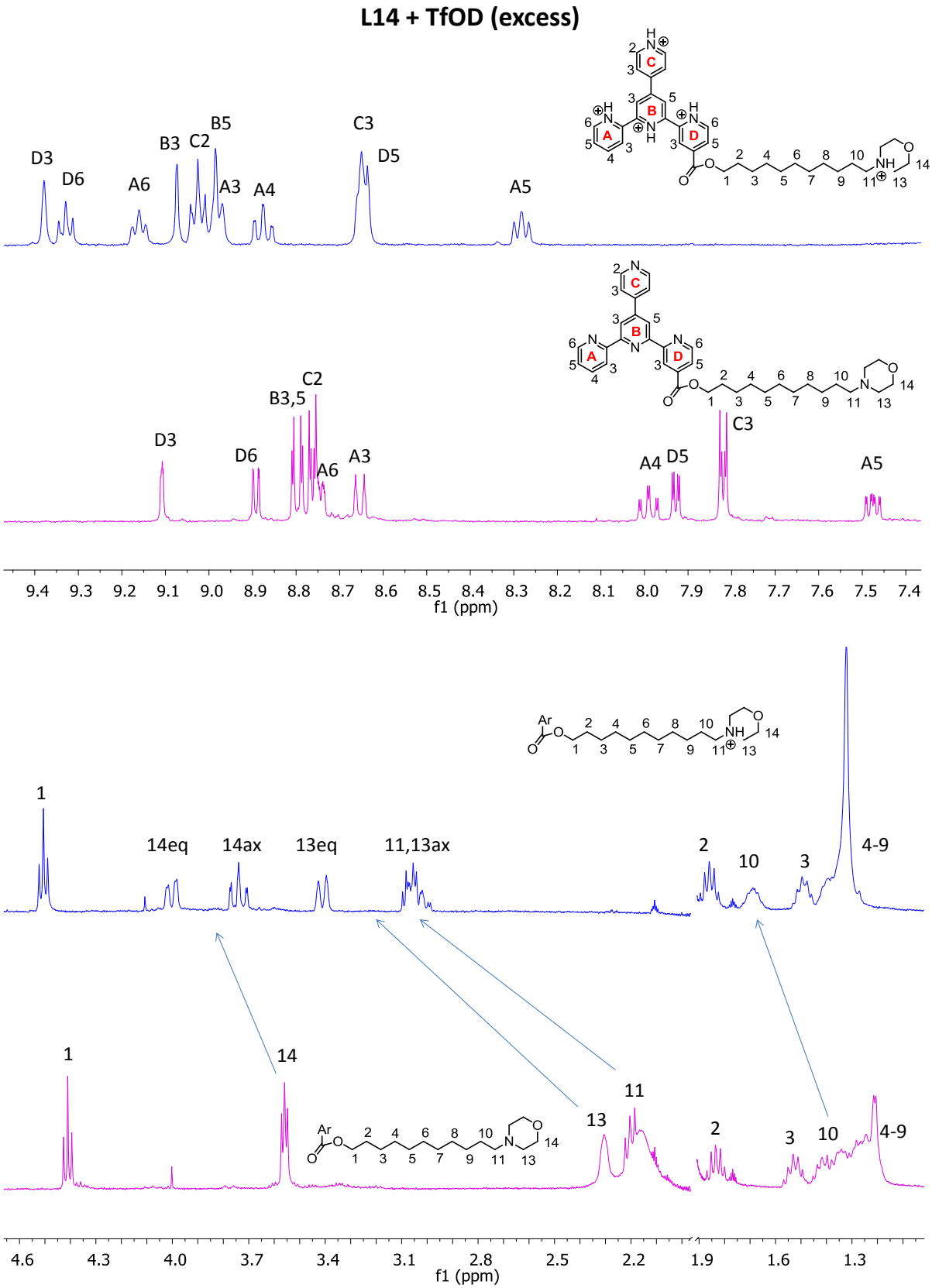

Figure 6.7: ^{1}H NMR spectra (400 MHz, CD_3CN) of the free ligand L14 (pink) and with an addition of TfOD (excess, blue)

All the typical protons of the amino group **14**, **13**, **11** and **10** were shifted to the higher ppm values as those in **C20** and signals of the methylene groups **14** and **13** were split to axial and equatorial peaks as for non-equivalent protons. Figure 6.8 displays COSY-NMR spectrum of the protonated form of **L14**. There are intense interactions between the axial and equatorial protons **14** and between protons **11** and **13**. We also observed weak interactions between the equatorial proton **14** and the axial proton **13**, but not the other way round - between the equatorial proton **13** and any proton **14**.

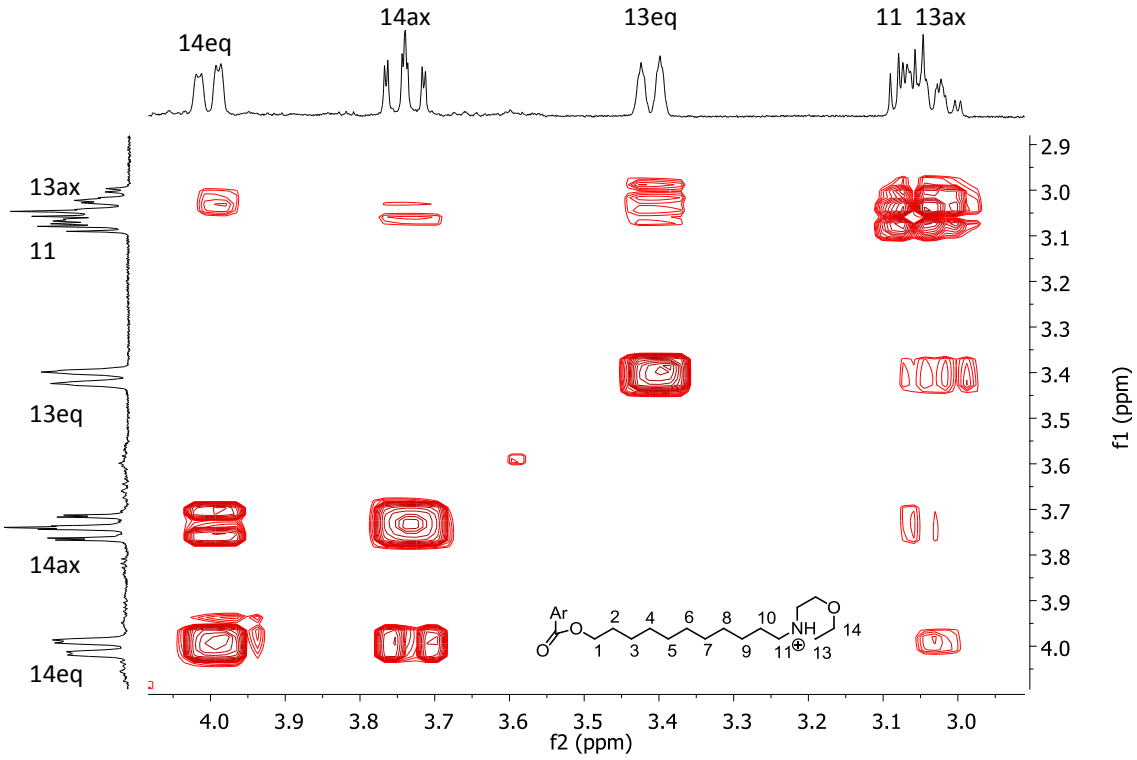

Figure 6.8: COSY NMR spectrum (500 MHz, CD_3CN) of the protonated ligand L14, zoom of the aliphatic region with morpholine unit

After this latest discovery, that the complexes **C20** and **C29** were already isolated in the monoprotonated form which was proved *via* several experiments in this chapter, we were also interested in a detailed ^{1}H NMR titration of the ligands **L11** and **L14** with TFA-D or TfOD. We believe that the protonation of the side chain of **C20** and **C29** had to have happened during the work-up of these complexes, most likely in the presence of aqueous ammonium hexafluorophosphate. This indicates a very strong basicity of the side chains' amino units. Therefore, for the titration of **L11** and **L14** we decided to use the weaker acid, TFA-d, to monitor the protonation of the side chain and calculate a pK value of this process. In case of

the use of the stronger acid (TfOD), this protonation could happen immediately within even the first tenth of an equivalent of TfOD.

The morpholine-substituted ligand **L14** was titrated with TFA-d (CF_3COOD) and the process was monitored with ^1H NMR spectra (Figure 6.9). The NMR tube contained a solution of **L14** in CD_3CN (c = 5.16×10^{-3} mol/L, 1.6 mg in 0.5 mL of CD_3CN). This was titrated with 0.1 equivalent increments of diluted TFA-d (c = 33.51×10^{-3} mol/L, 0.8 μL in 0.3 mL of CD_3CN) until 0.8 equivalents of TFA-d (Table 6.4, Spectra 1-9). Then we continued with 0.2 eq. increments until 2 equivalents (Table 6.4, Spectra 10-15).

No. of ^1H NMR spectrum	**1**	**2**	**3**	**4**	**5**	**6**	**7**	**8**
No. of eq. of TFA-d	0	0.1	0.2	0.3	0.4	0.5	0.6	0.7
No. of ^1H NMR spectrum	**9**	**10**	**11**	**12**	**13**	**14**	**15**	
No. of eq. of TFA-d	0.8	1	1.2	1.4	1.6	1.8	2	

Table 6.4: Titration process of L14 with TFA-d, ^1H NMR spectra displayed in Figure 6.9

In the aromatic part of the ^1H NMR spectra no significant change was observed until 1 equivalent of TFA-d was added (Figure 6.9, Spectrum 10). However, in the aliphatic region, protons **10**, **11**, **13** and **14** started steadily shifting to higher ppm values from the beginning of the titration. After the addition of 1 eq. of TFA-d these protons stopped shifting to the higher ppm values, and the protons **13** and **14** started to split to the typical set of four signals for axial and equatorial protons. After the addition of 1 eq. of TFA-d, protons in the aromatic region started to shift, most significantly protons **C2** and **C3**, indicating that protonation happens at this site next. Altogether this proves that protonation happens first on the side chain, showing that this is the most basic nitrogen atom. The titration was stopped after the addition of 2 eq. of TFA-d because we were mainly interested in the first part, the protonation of the side chain.

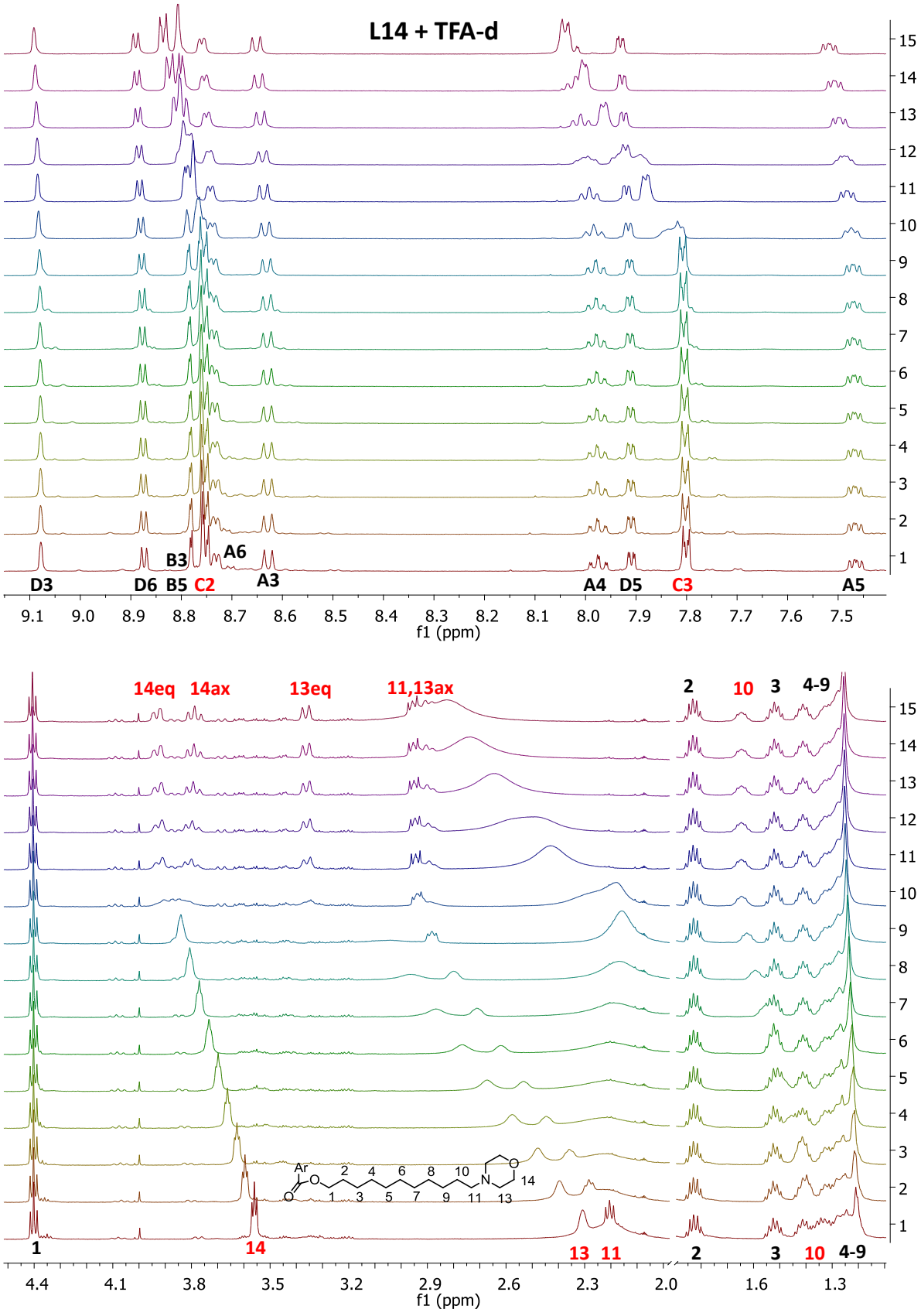

Figure 6.9: Stacked ^{1}H NMR spectra (500 MHz, CD_3CN) of titration of the morpholine-substituted ligand L14 with TFA-d, aromatic region (top), aliphatic region (bottom)

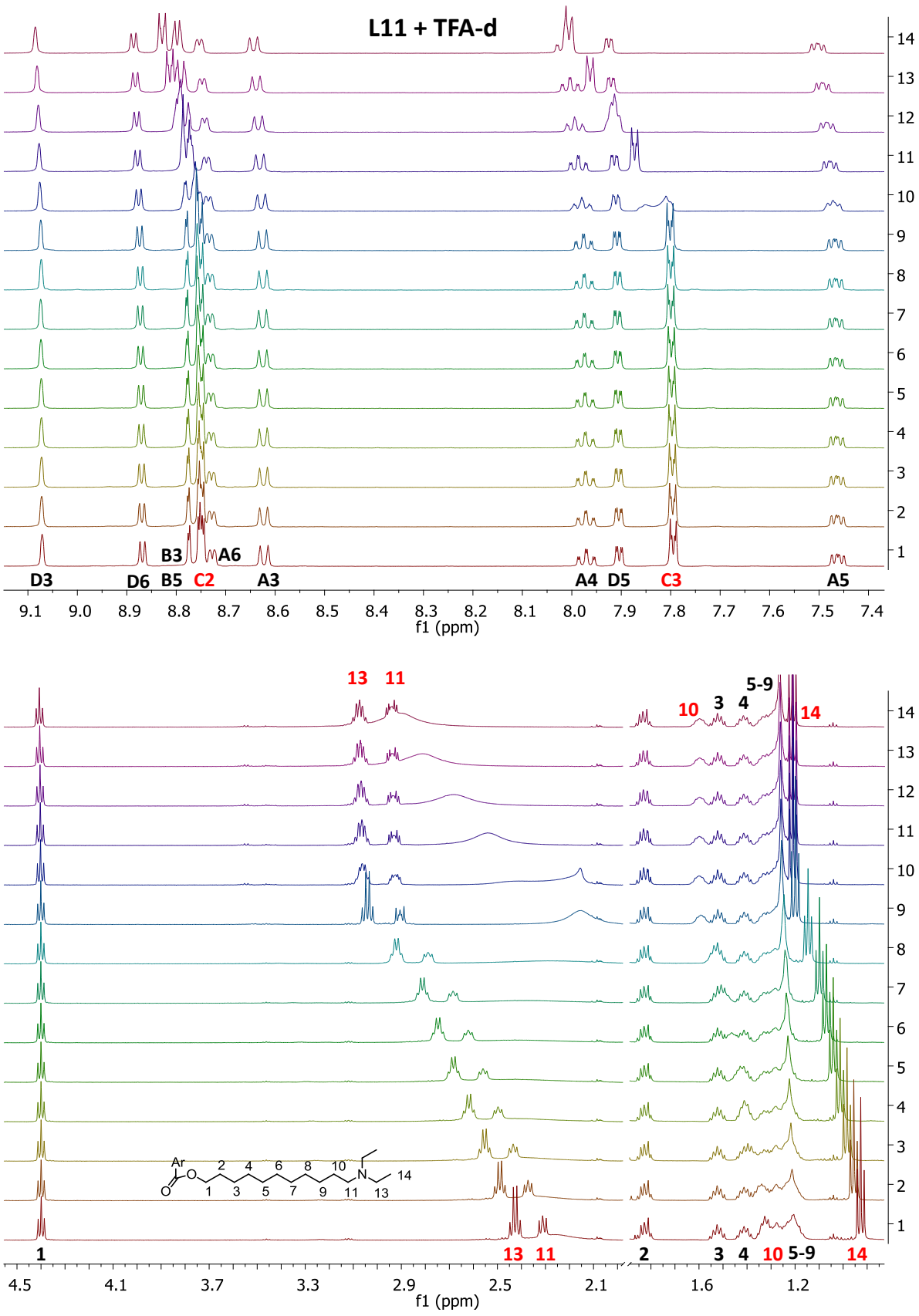

Figure 6.10: Stacked ^{1}H NMR spectra (500 MHz, CD_3CN) of titration of the diethyamino-substituted ligand L11 with TFA-d, aromatic region (top), aliphatic region (bottom)

The diethylamino-substituted ligand **L11** was titrated with TFA-d (CF_3COOD) and the process was monitored with ^1H NMR spectra (Figure 6.10). The NMR tube contained a solution of **L11** in CD_3CN (c = 5.16×10^{-3} mol/L, 1.5 mg in 0.5 mL of CD_3CN). This was titrated with 0.1 equivalent increments of diluted TFA-d (c = 33.51×10^{-3} mol/L, 0.8 μL in 0.3 mL of CD_3CN) until 0.6 equivalents of TFA-d (Table 6.5, Spectra 1-7). Then we continued with 0.2 eq. increments until 2 equivalents (Table 6.5, Spectra 8-14).

No. of ^1H NMR spectrum	**1**	**2**	**3**	**4**	**5**	**6**	**7**	**8**	**9**	**10**	**11**	**12**	**13**	**14**
No. of eq. of TFA-d	0	0.1	0.2	0.3	0.4	0.5	0.6	0.8	1	1.2	1.4	1.6	1.8	2

Table 6.5: Titration process of L11 with TFA-d, ^1H NMR spectra displayed in Figure 6.10

As for **L14**, in the aromatic part of the ^1H NMR spectra no significant change was observed until 1 equivalent of TFA-d was used (Figure 6.10, Spectrum 9). However, in the aliphatic region, protons **10**, **11**, **13** and **14** started steadily shifting to higher ppm values from the beginning of the titration. At the point of 1 eq. of TFA-d (Figure 6.10, Spectrum 9), protons in the aromatic region started to shift, most significantly protons **C2** and **C3**, which indicates that the protonation happens next on the nitrogen atom of the pendant pyridyl unit **C**. These titrations of ligands **L11** and **L14** prove that the protonation happens first on the side chains, which means that the most basic nitrogen atom is located there. As for **L14**, this titration was also stopped at 2 eq. of TFA-d, because we were mainly interested in the first part, the protonation of the side chain.

The protonation processes of the complexes **C20** and **C29** and of the ligands **L11** and **L14** were evaluated from non-linear least squares fitting of the chemical shift of proton **C3** (**C20** and **C29**), **11** (**L14**) or **13** (**L11**) to appropriate equations by using WinEQNMR2 (by Michael J. Hynes)[1]. The equilibrium constants were calculated for a logarithmic fitting process. As an input pK values of conjugate acids of the appropriate amines were used: Et_3N (9.11), piperidine (11.22), morpholine (8.36), pyridine (5.25). In this case, we neglected the fact that these are tabulated for water. The output of this fit was then used as the input for a linear fit to determine the equilibrium constants of the protonation process.

[**L11**] + [H^+] ⇔ [**L11**…H] pK = 7.92 (pK of the side chain)

[**L14**] + [H^+] ⇔ [**L14**…H] pK = 8.85 (pK of the side chain)

[**C20**] + [H^+] ⇔ [**C20**…H] pK = 5.06 (pK of the pendant pyridyl unit)

[**C29**] + [H^+] ⇔ [**C29**…H] pK = 4.54 (pK of the pendant pyridyl unit)

After all, when considering the tabulated and the calculated pK values, it is clear why the side chain was protonated first and then the pendant pyridyl units. The regression of the linear fit of protonation of the side chain of the ligand **L11** is shown in Figure 6.11.

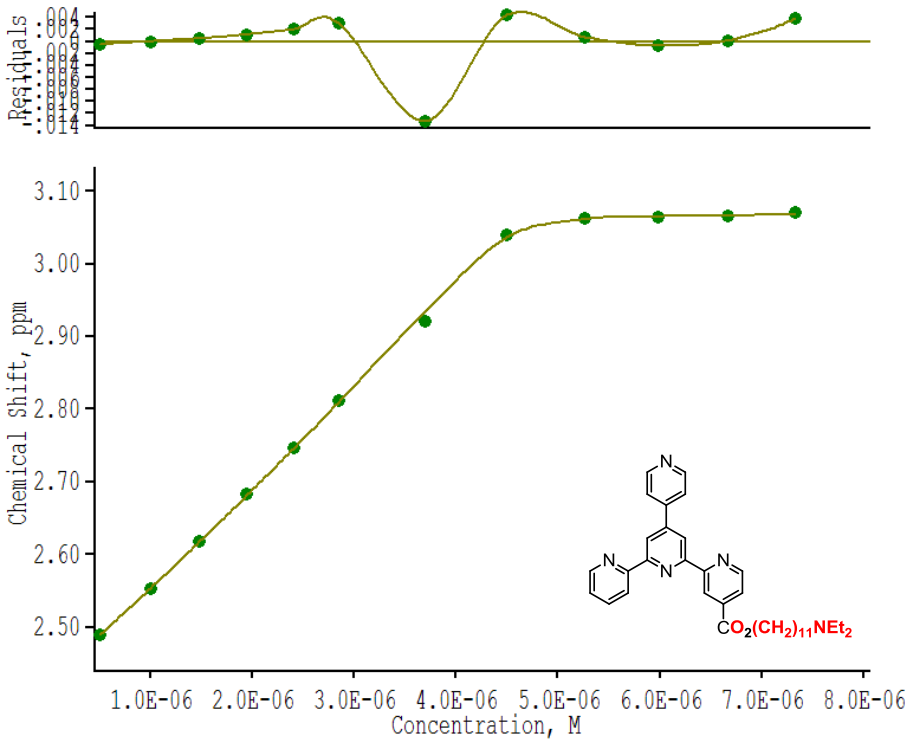

Figure 6.11: Regression of the linear fit of the diethyamino-substituted ligand L11 (protonation of its side chain unit)

Conclusion

In this chapter, NMR studies of ruthenium(II) complexes **C20** and **C29** and of their free ligands **L11** and **L14** under acidic and basic conditions were carried out and the processes were monitored with ^{1}H NMR spectra. We were investigating which nitrogen atoms are possible to protonate, and in which sequence. We were also interested in examining the stability of the side amino chains under these acidic conditions and found that the side chains stayed attached to the Ru(II) complex. The results of these NMR studies reveal and clarify that all the Ru(II) complexes with three protonation sites were synthesized and isolated already in the mono-protonated form - on the amino group of the side chains (which most likely happened during the work-up with ammonium hexafluorophosphate). Therefore, the only protonation happening during the NMR titrations of the Ru(II) complexes was on the pendant pyridyl units. The ligands **L11** and **L14** were titrated with TFA-d to monitor the side chain protonation and prove that this amino unit is protonated first. From these processes we calculated pK values which points at basicity of the side chain amines.

Literature

1 Hynes, M. J. *J. Chem. Soc., Dalton Trans.*, **1993**, 311.

Chapter 7

Ruthenium(II) complexes with a short amino-substituted side chain containing three or five carbons

7.1 Introduction

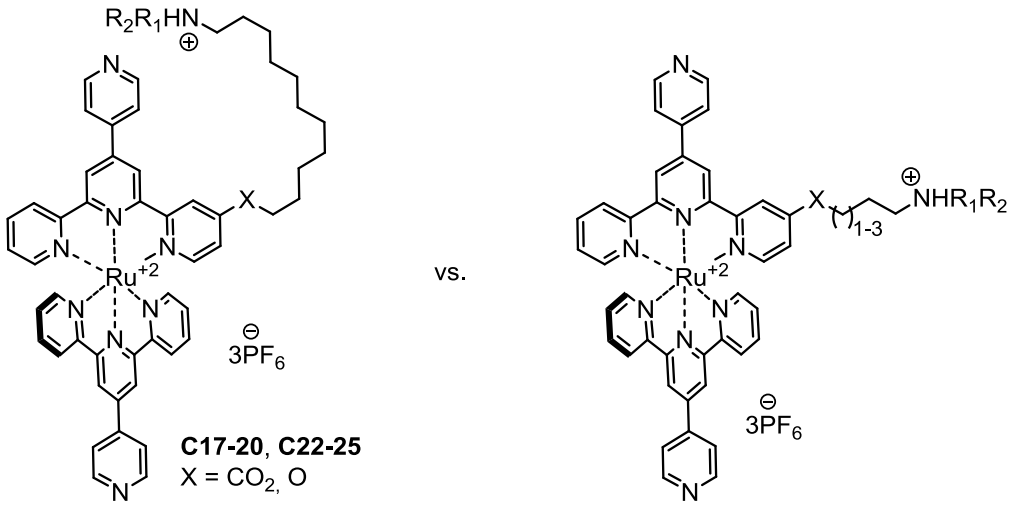

Scheme 7.1: Towards ruthenium(II) complexes with a long or short side chain linked via an ester group or via an ether group bearing three protonation sites

In Chapter 2 and 3, pytpy ligands with long (11 carbon atoms) side amino-chains linked via an ester or an ether group **L10-14** and **L17-20** were prepared. In Chapter 4, ruthenium(II) complexes of these ligands were synthesized (**C17-20** and **C22-25**). The amino group attached to the side chain and the two pendant pyridyl groups bring to the molecule three protonation sites. In this chapter, synthetic strategies towards ligands with short side amino-chains (3 – 5 carbon atoms) and towards ruthenium(II) complexes of these ligands are reported (Scheme 7.1). Such ruthenium(II) complexes are very interesting and useful materials for further photophysical studies. In the Ru(II) complexes with long side chains, there is the possibility of a photo-induced electron transfer or a proton transfer, intra-molecular via the chain or via space (between the pendant pyridyl unit and the amino group), respectively. However, the Ru(II) complexes with an appropriately short side chain (3

– 5 carbons) will only have the option of photo-induced electron transfer via the chain (i.e. not through space as the chain is too short). All photophysical studies are carried out with highly diluted solutions so prevent any inter-molecular communication options.

7.2 Results and Discussion

7.2.1 Towards heteroleptic ruthenium(II) complexes of pytpy ligands with an amino-substituted 3-carbon-side chain

For the synthesis of the pytpy ligands with the short side chain linked via an ester group **1** (Scheme 7.2), the same reaction conditions as those successfully used for the synthesis of **L10**-**14** in Chapter 3 (Scheme 3.8) were applied.[1]

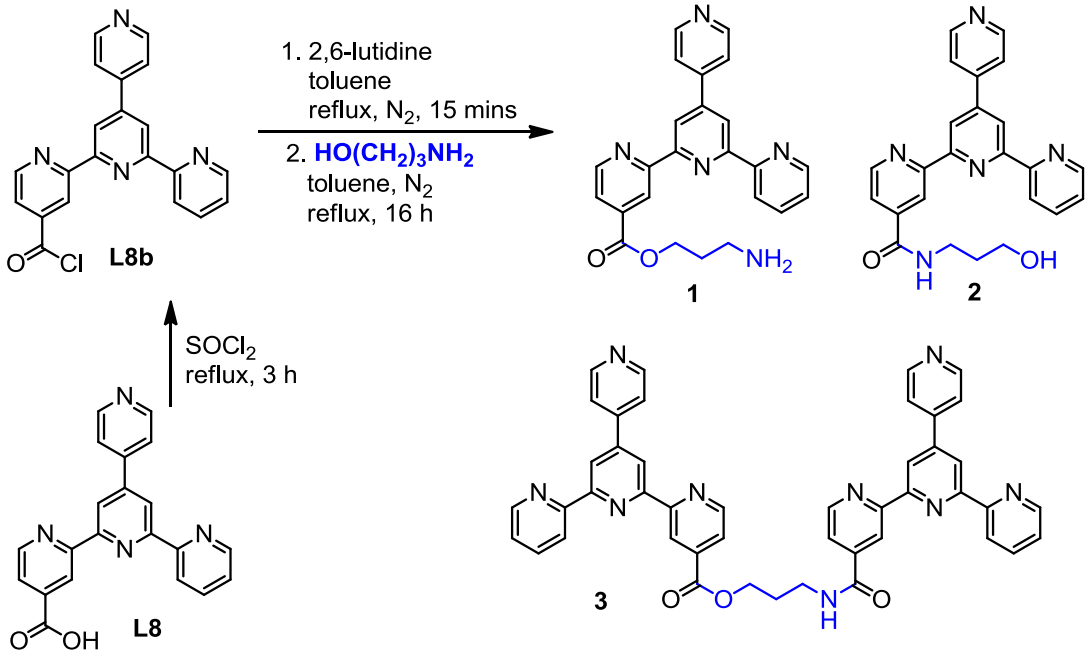

Scheme 7.2: Synthesis of a pytpy ligand with a 3-carbon-side chain linked via an ester group

The precursor was the COOH-substituted pytpy (**L8**) and this was prepared according to the procedure reported by Krebs (Chapter 3, Scheme 3.6)[2] and was converted to the corresponding acid chloride **L8b**. **L8** was refluxed in thionyl chloride for 3 hours under an inert atmosphere to give a yellowish solution. The excess of thionyl chloride was evaporated under reduced pressure and the residue was dried. The acid chloride **L8b** was obtained as a

yellowish powder, and was assumed to be formed in quantitative yield. It was immediately used for esterification without any further purification (Scheme 7.2). It was refluxed with the base 2,6-lutidine in toluene for 15 minutes under nitrogen. Commercially available 3-aminopropan-1-ol was added and the reaction mixture was refluxed for 16 hours under nitrogen. The crude reaction mixture was evaporated, dissolved in chloroform and extracted with saturated aqueous sodium hydrogen carbonate and water. Formation of the target ester **1** was monitored by recording the ^{1}H NMR spectrum and looking for the triplet (expected ~ δ 4.5 ppm) of the first CH_2 group next to the carboxyl group. The residue was purified with a short chromatography column (SiO_2, eluted with EtOAc/MeOH/Et_3N = 60:2:1 and 30:2:1) and two oily fractions (**A** and **B**) were obtained. The identity of fraction **A** was not clarified. However, in the electrospray mass spectrum of fraction **B**, two intense peaks were observed. The first peak with *m/z* = 434.1 with intensity 60% was assigned to $[M+Na]^+$ of the ligand **1**. The second peak with *m/z* = 770.2 with intensity 95% was assigned to $[M+Na]^+$ of the molecule **3**. As the product of a "double substitution", **3** was expected because the acid chloride **L8b** is a very reactive species and the starting 3-aminopropan-1-ol offers both options (formation of the ester or the amide). Therefore, with the same probability, we expect also the presence of the amide **2** in fraction **B**.

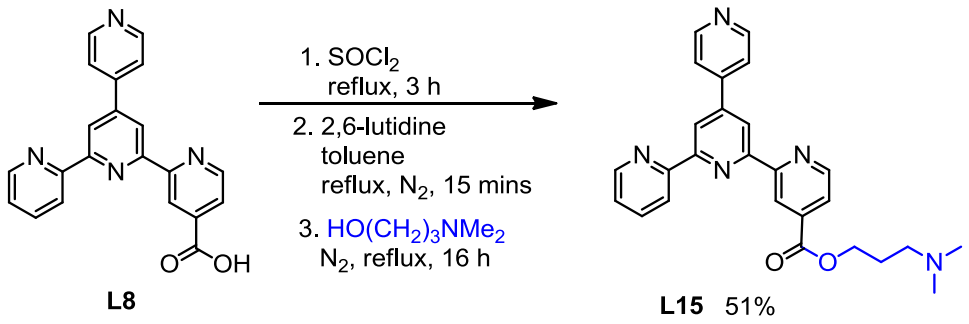

Scheme 7.3: Synthesis of a pytpy ligand L15 with a 3-carbon-side chain linked via an ester group

The esterification attempt with 3-aminopropan-1-ol was abandoned, and for the next reaction commercially available 3-dimethylamino-1-propanol was used instead (Scheme 7.3). The product was purified by crystallisation from a mixture of cold ethanol-cyclohexane. **L15** was obtained as a pale brown powder in 51% yield. In the electrospray mass spectrum of **L15**, peaks with *m/z* = 440.2 and *m/z* = 462.1 (assigned to $[M+H]^+$ and $[M+Na]^+$, respectively) with intensities of only 8% and 4%, respectively, were observed. However, a peak with *m/z* =

391.1 with intensity 100% was observed, which was assigned to $[M\text{-}CH_2CH_2NMe_2+Na]^+$. This fact points to the fragility of the short side chain when exposed to a "stress situation", which would also explain the complications during all further complexation attempts. However, the identity of **L15** was confirmed with elemental analysis and with 1D and 2D NMR spectra. The ^{1}H NMR spectrum and the electronic absorption spectrum of **L15** will be discussed together with those of ligands **L16** and **L21-22** (Section 7.2.2).

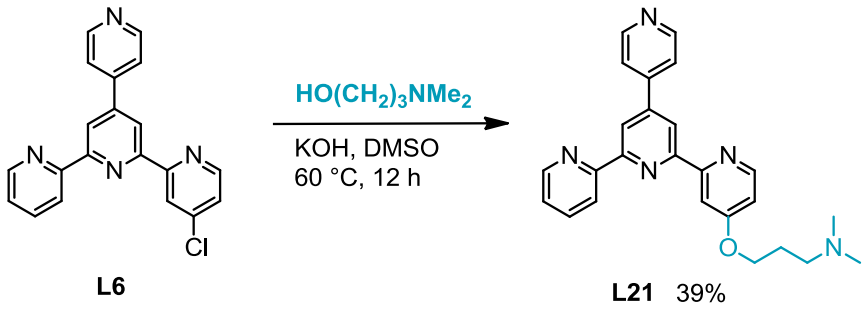

Scheme 7.4: Synthesis of a pytpy ligand L21 with a 3-carbon-side chain linked via an ether group

For the synthesis of the alkoxy-substituted pytpy ligand **L21**, the same harsh reaction conditions (Scheme 7.4), reported by Halcrow *et al.* in 2001, were applied as those that had been successfully used for the synthesis of **L17**-**20** in Chapter 2 (Scheme 2.12).[3] Freshly ground potassium hydroxide was suspended in DMSO, and **L6** and 3-dimethylamino-1-propanol were added and the mixture was heated at 60 °C for 12 hours. This reddish-brown solution was then cooled to room temperature. Addition of ice-cold water gave a brown precipitate, which was purified by extraction with chloroform-water. A large amount of water during extraction was necessary for DMSO removal. **L21** was isolated nearly pure in 39% yield, but there was a trace amount of unreacted starting amino alcohol. This was an improvement on the situation with the alkoxy-substituted ligands **L17**-**20**, where a certain amount (19-56%) of unreacted alcohol was always detected in the isolated products. However, because of the impurity in **L21**, elemental analysis and absorption spectra were not measured. In the electrospray mass spectrum of **L21**, a peak with *m/z* = 412.2 (assigned to $[M+H]^+$) with intensity 100% and also a peak with *m/z* = 434.2 (assigned to $[M+Na]^+$) with intensity 47% were observed. The ^{1}H NMR spectrum of **L21** will be discussed together with those of ligands **L15-16** and **L22** (Section 7.2.2).

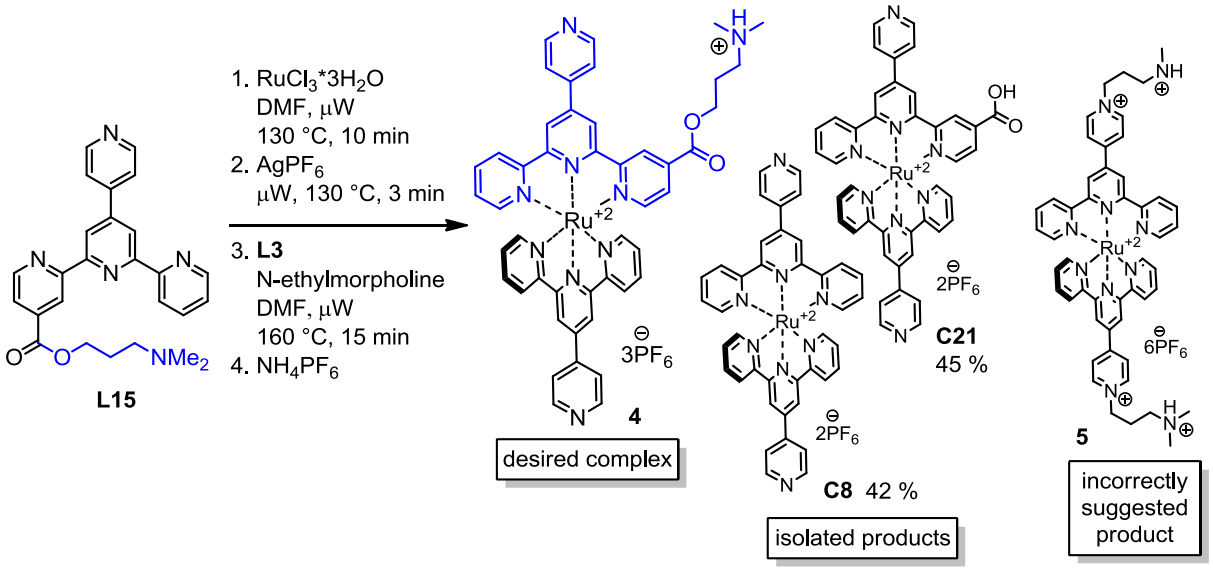

Scheme 7.5: Towards the ruthenium(II) complex of the ligand L15

For the synthesis of the heteroleptic Ru(II) complex **4** containing pytpy ligand **L15** (Scheme 7.5), the same four-step "one-pot" microwave-assisted reaction conditions were applied as those successfully used for the synthesis of **C18-20**, i.e. the complexes containing the pytpy ligands with the long side chains (Chapter 4, Scheme 4.4). The first ligand (**L21**) is coordinated to form the [Ru(**L21**)Cl_3] complex, which is then activated with silver hexafluorophosphate. The complex reacts with the second ligand (**L3**) in a presence of a catalytic amount of *N*-ethylmorpholine, used as a reducing agent to convert Ru(III) to Ru(II). The product is then precipitated as a PF_6^- salt and purified by column chromatography (SiO_2, eluted with MeCN/saturated aqueous KNO_3/H_2O = 7:1:0.5) and by crystallisation from MeCN-Et_2O. Two main fractions (**A** and **B**) were collected and their ^{1}H NMR spectra recorded. However, neither of them was the desired complex **4**. The structure of **B** (according to the very low R_f value on a TLC plate, due to the NMR spectrum and ESI MS spectrum) was assigned as the product of ester hydrolysis **C21**. In the ^{1}H NMR spectrum of fraction **A**, a set of only 7 peaks in the aromatic region and 4 peaks in the aliphatic part were observed. After realizing that the ester chain had cleaved, we concluded that the product had structure **5** (Scheme 7.5). However, this idea was incorrect. If the pendant pyridyl positions were alkylated, the protons of the pendant pyridyl unit would be shifted to the higher ppm values (δ 8.6 – 9.0 ppm) and the first alkyl CH_2 group next to the pyridyl nitrogen atom would appear around δ 4.7 ppm (instead of being around δ 3.5 ppm) (see complex **C13** in Figure 1.4, Chapter 1). The structure of fraction **A** was finally assigned to compound **C8**,

when it was realized that its ^{1}H NMR spectrum matched exactly with the ^{1}H NMR spectrum of the previously synthesized **C8**. The four aliphatic signals the ^{1}H NMR spectrum, mentioned above, were assumed to belong to the protons of the cleaved side chain. The identities of fractions **A** and **B** were also confirmed with ESI MS spectrum and we noted that they had the same R_f values on a TLC plate as formerly prepared complexes **C8** and **C21**. The synthesis in Scheme 7.5 was also carried out the other way round (complex with **L3** first and then **L15**). However, even this trial failed and only products of decomposition (**C8** and **C21**) were obtained.

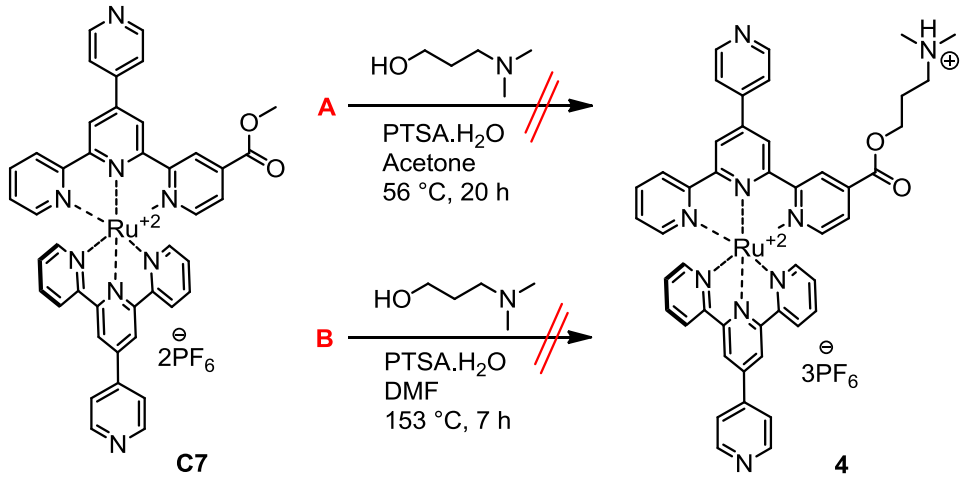

Scheme 7.6: Towards the ruthenium(II) complex 4 via trans-esterification

As a next option to obtain the ester-substituted ruthenium(II) complex **4** with the short side chain, we tried trans-esterification of the methyl ester-substituted complex **C7** with 3-dimethylamino-1-propanol (Scheme 7.6). The same reaction conditions were applied as those successfully used for the synthesis of **C17-18** (Chapter 1, Scheme 1.15), i.e. reflux in DMF in a presence of a catalytic amount of p-toluenesulfonic acid monohydrate (Scheme 7.6, **B**). Milder conditions, i.e. reflux in acetone for 20 hours, were also tried (Scheme 7.6, route **A**). Reactions were monitored with TLC plates (SiO_2, eluted with MeCN/saturated aqueous KNO_3/H_2O = 10:0.5:1.5) and ^{1}H NMR spectra. However, only products resulting from a decomposition to **C8** and **C21** were observed.

We tried also to synthesize the heteroleptic ruthenium(II) complex **6** of the alkoxy-substituted pytpy ligand **L21** (Scheme 7.7). The same reaction conditions were applied as

those used for the synthesis of **C18-20** of the pytpy ligands with the long side chain (Chapter 4, Scheme 4.4). However, this attempt also failed.

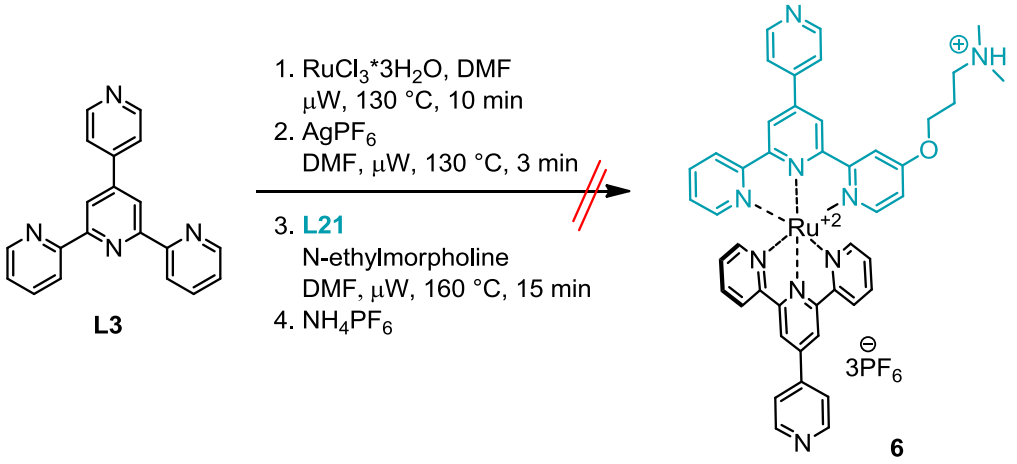

Scheme 7.7: Towards the ruthenium(II) complex of the ligand L21

7.2.2 Towards heteroleptic ruthenium(II) complexes of pytpy ligands with an amino-substituted 5-carbon-side chain

The synthetic attempts towards ruthenium(II) complexes with the 3-carbon-side chain were abandoned, due to the hydrolysis liability of this short side ester chain during all the reaction conditions tested. As the next option, we decided to synthesize pytpy ligands with a 5-carbon side chain and investigate their robustness during synthesis of their ruthenium(II) complexes.

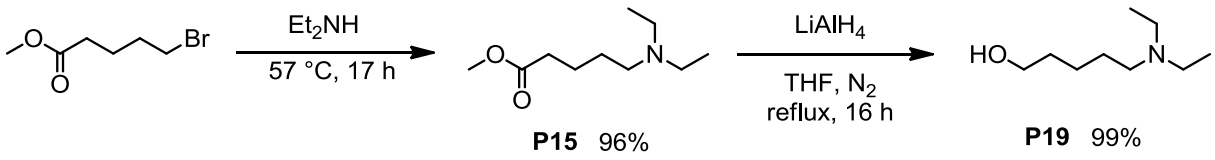

Scheme 7.8: Synthesis of the amino alcohol with a 5-carbon-chain P19

For synthesis of 5-diethylamino-1-pentanol **P19** (Scheme 7.8), the same reaction conditions were applied as those successfully used for the synthesis of 11-diethylamino-1-undecanol **P16** (Chapter 1, Scheme 1.11).This reaction strategy, reported by Wetter *et al.* in 1974, is a very facile two-step synthetic route to such amino alcohols, and is suitable for various chain lengths.[4] We started with methyl 5-bromovalerate, which in the first step reacts with diethylamine. The latter functions both as a reagent and solvent. The bromo group is

quantitatively substituted with a diethylamino group. The white precipitate of diethylammonium bromide as a side product is simply removed by filtration. The desired product **P15** was purified using vacuum distillation. In the second step, the methyl ester group was reduced by $LiAlH_4$ to a methylene hydroxy group. Sodium sulfate decahydrate was used as a suitable agent for quenching the reaction mixture. A precipitate of LiOH and an excess of sodium sulfate was removed by filtration, and the solvent removed under reduced pressure giving the amino alcohol **P19** as a yellowish oil in quantitative yield.

For the synthesis of the pytpy ligands with a 5-carbon chain linked via an ester group **L16** (Scheme 7.9), the same reaction conditions as those successfully used for the synthesis of pytpy ligands with the long side chains **L10**-**14** (Chapter 3, Scheme 3.8) or for **L15** with a 3-carbon chain (Scheme 7.3), were applied.[1,2] **L16** was purified using column chromatography (SiO_2, eluted with EtOAc/MeOH/Et_3N = 60:3:1 and 30:3:1) and was obtained as a pale brown solid in 51% yield. In the electrospray mass spectrum of **L16**, a peak with *m/z* = 496.3 (assigned to $[M+H]^+$) with intensity 100% and also peaks with *m/z* = 518.3 and 534.3 (assigned to $[M+Na]^+$ and $[M+K]^+$, respectively) both with intensity 5% were observed.

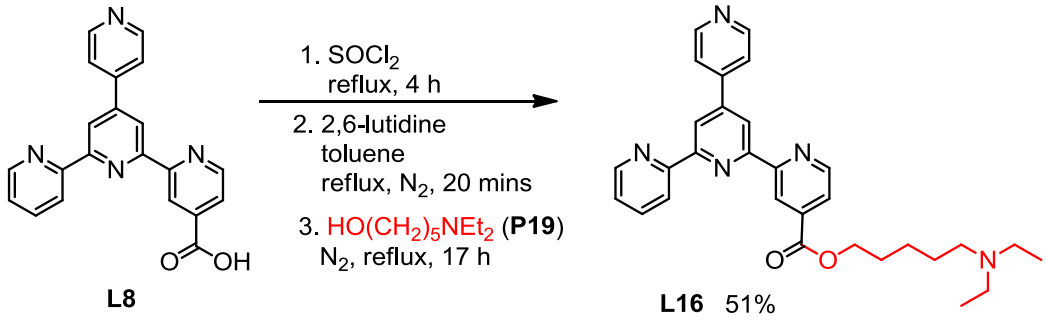

Scheme 7.9: Synthesis of the pytpy ligand L16 with a 5-carbon-side chain linked via an ester group

For the synthesis of the alkoxy-substituted pytpy ligand **L22**, the same harsh reaction conditions (Scheme 7.10), reported by Halcrow *et al.*, were applied as those successfully used for the synthesis of **L17**-**20** in Chapter 2 (Scheme 2.12) or for the synthesis of **L21** (Scheme 7.4).[3] Freshly ground potassium hydroxide was suspended in DMSO, and **L6** and 5-diethylamino-1-pentanol were added; the mixture was heated at 60 °C for 17 hours. The reddish-brown solution was then cooled to room temperature. Addition of ice-cold water gave a brown precipitate, which was purified by extraction with chloroform-water. A large amount of water during extraction was necessary to remove all the DMSO. **L22** was isolated

virtually pure in 52% yield, but a small amount of unreacted starting amino alcohol remained with the product and could not be separated. Consequently, elemental analysis and an absorption spectrum were not recorded for **L22**. In the electrospray mass spectrum of **L22**, a peak with *m/z* = 468.3 (assigned to $[M+H]^+$) with intensity 100% and also peaks with *m/z* = 490.2 and 506.2 (assigned to $[M+Na]^+$ and $[M+K]^+$, respectively) with intensity 12% and 5%, respectively, were observed.

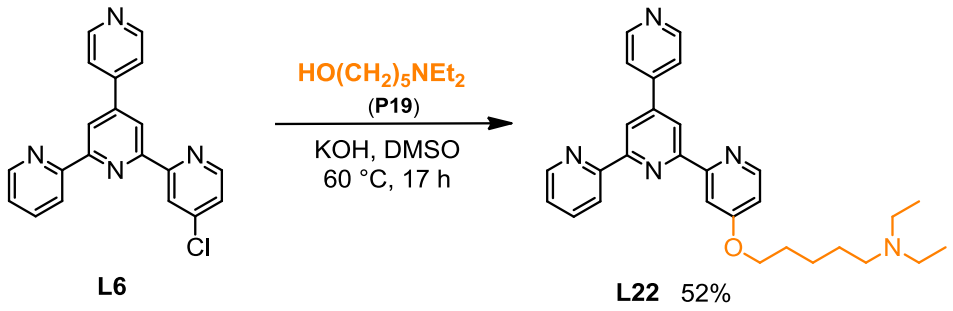

Scheme 7.10: Synthesis of the pytpy ligand L22 with a 5-carbon-side chain linked via an ether group

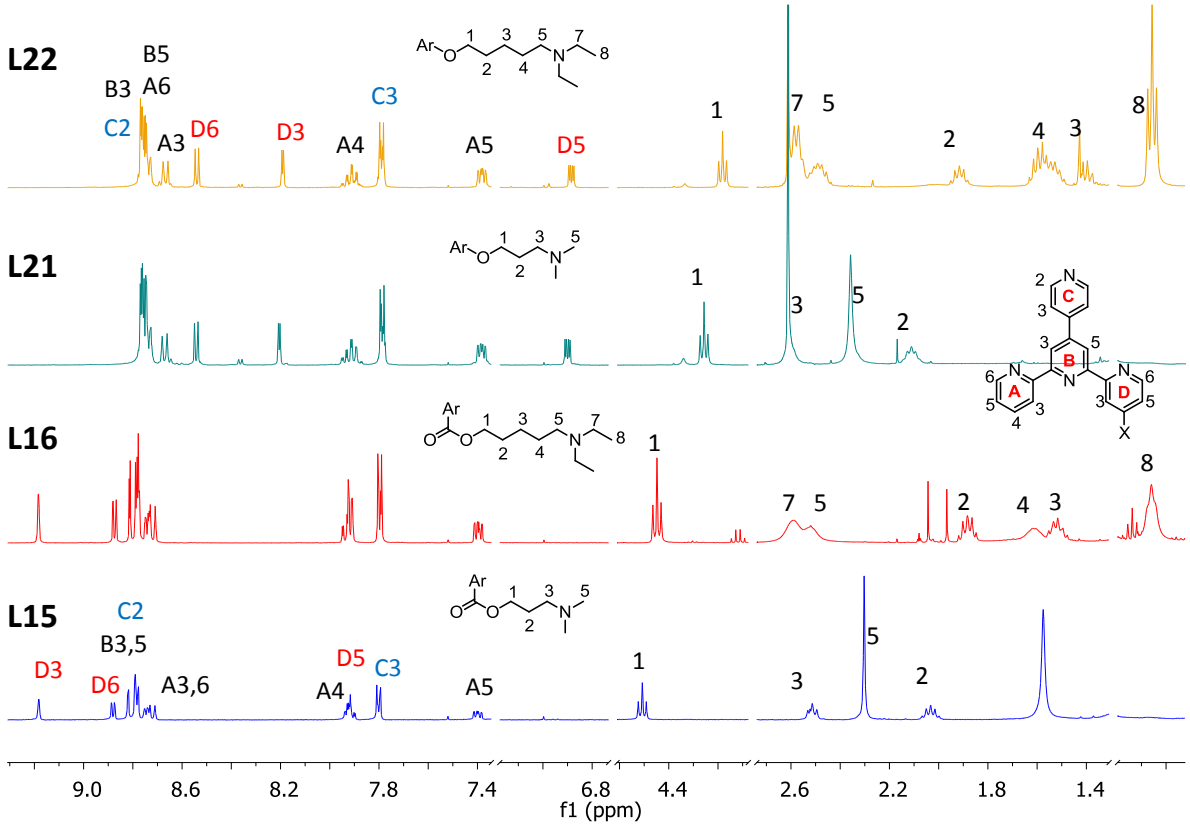

Figure 7.1: ^{1}H NMR spectra (400 MHz, $CDCl_3$) of the ester-substituted pytpy ligands L15 (blue) and L16 (red) and the alkoxy-substituted pytpy ligands L21 (cyan) and L22 (orange)

All four new short-chain-substituted pytpy ligands **L15**-**16** and **L21**-**22** were characterised with ^{1}H and ^{13}C NMR spectra using COSY, HMQC and HMBC methods. In the aromatic part of ^{1}H NMR spectra of ligands **L15**-**16**, it is possible to see the typical distribution of peaks of the ester-substituted pytpy, and this is nearly the same as observed for **L11**. (Compare Figures 7.1 and 3.4 in Chapter 3.) In the aromatic part of ^{1}H NMR spectra of ligands **L21**-**22**, it is possible to see the typical distribution of peaks of the ether-substituted pytpy, and this looks very much like the spectrum of the dodecyloxy-substituted **L17**. (Compare Figures 7.1 and 2.5 in Chapter 2). However, there are some significant differences in the aliphatic part of the spectra of all 4 ligands, in comparison with the ligands with the long diethylamino-substituted chain linked via an ester group **L11** or via an ether group **L18**. The first methylene group **1** in the ester chain of **L15** has a chemical shift δ 4.51 ppm (δ 4.43 ppm in **L11** or in **L16**). The first methylene group **1** in the ether chain of **L21** has a chemical shift δ 4.21 ppm (δ 4.14 ppm in **L18** or in **L22**). The methylene group **2** of **L15** or of **L21** is shifted to δ 2.08 ppm, but in **L16** or in **L22** it appears typically at δ 1.87 ppm (as in **L11** or **L18**). The methylene group **3** of **L15** and **L21** has a typical peak around δ 2.5 ppm, as well as methylene groups **5** and **7** of **L16** and **L22**. The methylene group **3** of **L21** overlaps with the signal arising from residual DMSO, but the existence of the methylene group **3** of **L21** was confirmed with a COSY NMR spectrum. The methyl groups **5** of **L15** and **L21** are represented with a singlet around δ 2.3 ppm.

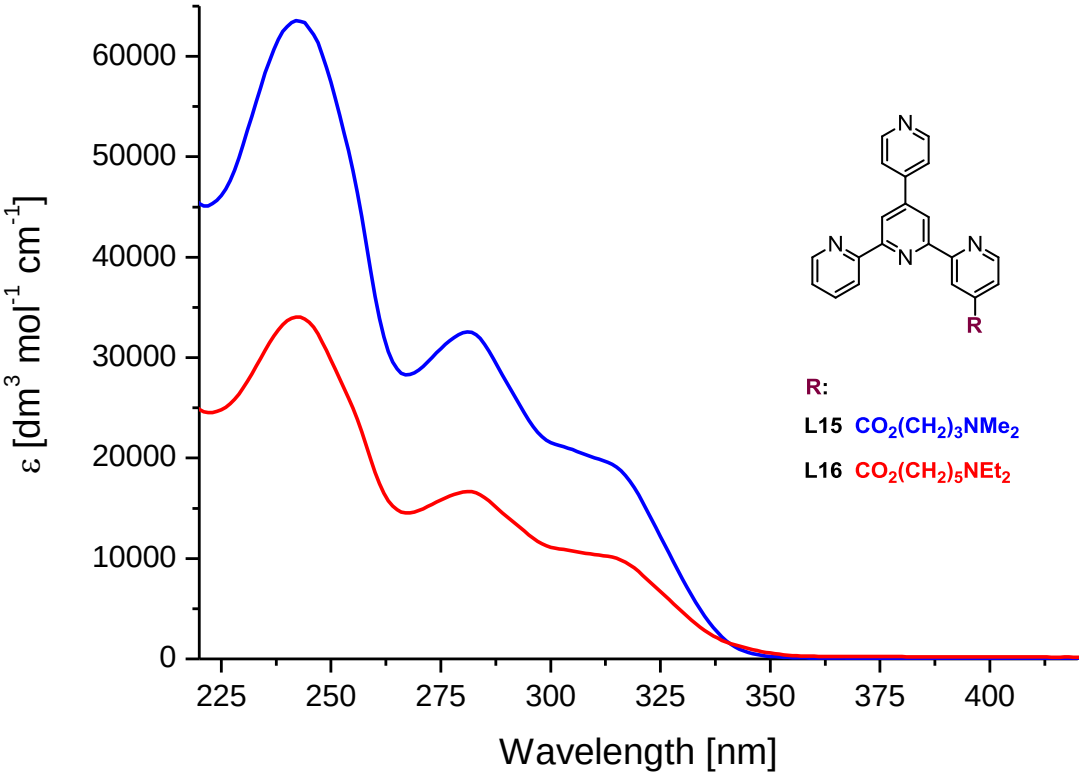

Figure 7.2: UV/Vis absorption spectra (CH_3CN) of the ester-substituted pytpy ligands L15 ($6.07 \cdot 10^{-5}$ M, blue), L16 ($5.38 \cdot 10^{-5}$ M, red)

Ligand	c / 10^{-5} mol dm^{-3}	λ_{max}/nm ($\varepsilon_{max}/10^3$ dm^3 mol^{-1} cm^{-1})		
L15	6.07	242 (63.6)	281 (32.8)	316 (18.7 sh)
L16	5.38	242 (34.0)	281 (16.7)	316 (9.8 sh)

Table 7.1: UV/Vis absorption spectra (CH_3CN) of the pytpy ligands L15 and L16 (Figure 7.2)

The electronic absorption spectra of acetonitrile solutions of the 3- and 5-carbon chain ester-substituted pytpy ligands **L15** and **L16** are shown in Figure 7.2. The ligands exhibit high energy absorption bands at 242 nm with high extinction coefficients (34.0 and 63.3×10^3 dm^3 mol^{-1} cm^{-1}) and at 281 nm with a shoulder at about 316 nm with lower extinction coefficients (10 to 33×10^3 dm^3 mol^{-1} cm^{-1}). The bands arise from ligand-centred $\pi^* \leftarrow \pi$ transitions (Table 7.1).

We also tried to synthesize the heteroleptic ruthenium(II) complex **7** of the alkoxy-substituted pytpy ligand **L22** (Scheme 7.11). The same reaction conditions were applied as those used for the synthesis of **C23-25** of the pytpy ligands with the long side chain (Chapter 4, Scheme 4.5). However, this attempt also failed just like the attempt with the ligand **L21** (Scheme 7.7). At first, the ^{1}H NMR spectrum of the crude reaction mixture looked promising for the presence of the product **7**. It was possible to see the characteristic triplet with δ 4.15 ppm (typical of the methylene group **1** of the side chain) and two multiplets around δ 3 ppm (typical of the methylene groups **5** and **7** which are closest to the protonated amine of the side chain). Three fractions were collected from the chromatography column. But one fraction was again the side product **C8** and the other two were products of decomposition, of the side-chain cleavage.

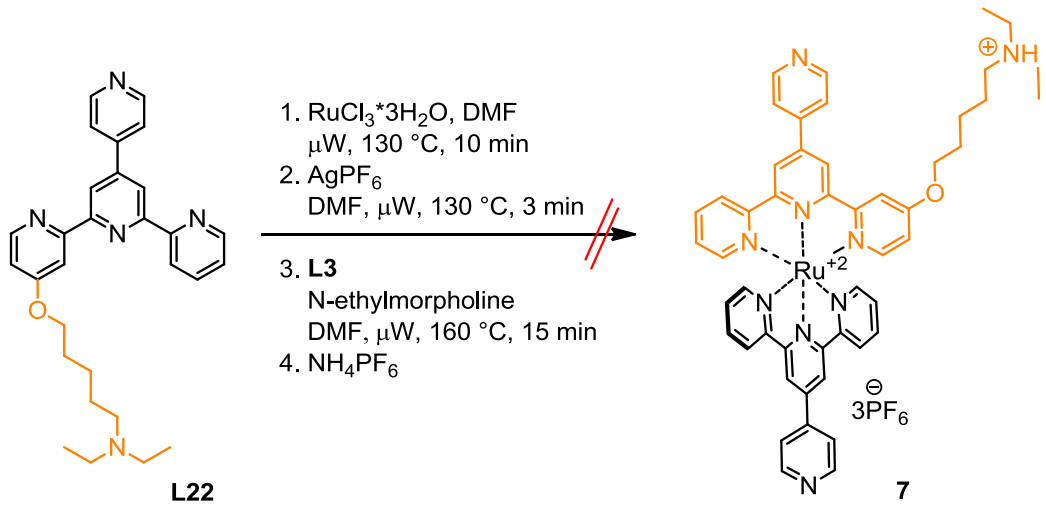

Scheme 7.11: Towards the ruthenium(II) complex of the ligand L22

7.2.3 Synthesis of ruthenium(II) complexes with a short side chain via a combination of mild and "harsh microwave-assisted" reaction conditions

All the following attempts to make ruthenium(II) complexes with short amino-substituted side chains were carried out using milder reaction conditions or a combination of harsher and mild reaction conditions.

Classical harsh conditions towards ruthenium(II) complexes via $RuCl_3 \cdot 3H_2O$ or $[Ru(tpy)Cl_3]$ require the use of boiling ethylene glycol or DMF to achieve reduction of Ru(III) to Ru(II) in situ.[5] In 2004, Ziessel *et al.* reported a useful precursor *cis*-[Ru(2,2':6',2''-

terpyridine)(DMSO)Cl_2] for the synthesis of various heteroleptic terpyridine complexes under mild conditions.[6] These reaction conditions were first tried out with the model ligand **L10** (Scheme 7.12).

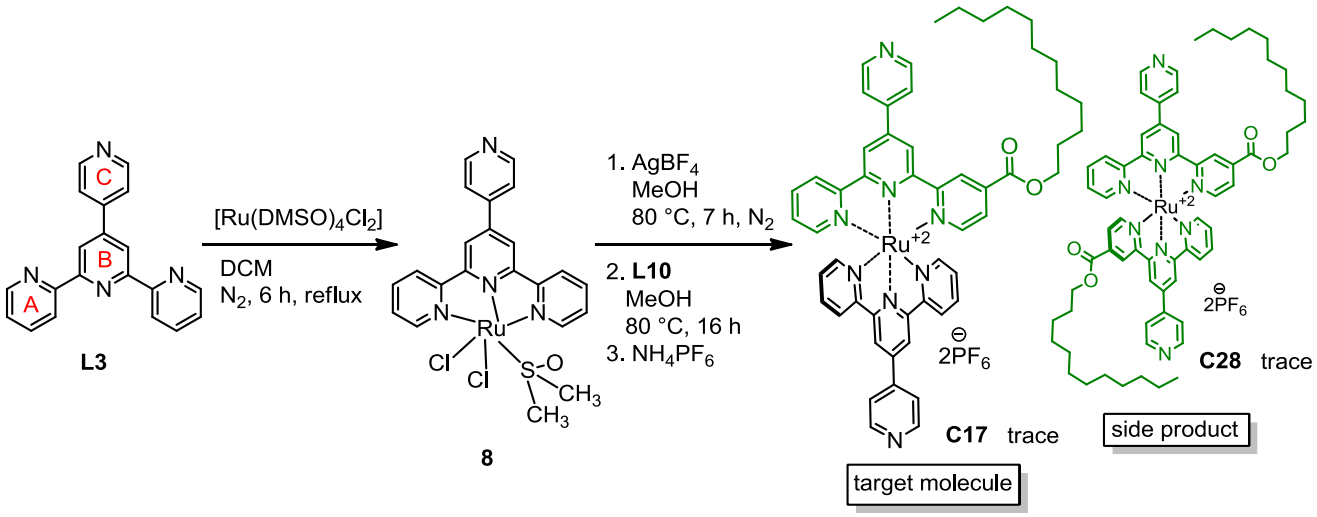

Scheme 7.12: Towards the model Ru(II) complex C17 via mild reaction conditions with [Ru(L3)(DMSO)Cl_2] complex 8

A suspension of **L3** and [Ru(DMSO)$_4$$Cl_2$] in dry degassed CH_2Cl_2 was heated to reflux for 6 hours. The brown solution was then concentrated until a brown precipitate of **8** formed. This was then collected on a frit and washed with Et_2O. A mixture of **8** and $AgBF_4$ in degassed dry MeOH was heated at 80 °C for 7 hours. The precipitate of AgCl was removed by filtration and the red solution was allowed to react with **L10** for 16 hours at 80 °C. After this, aqueous ammonium hexafluorophosphate was added and the reddish-brown product precipitated as a PF_6^- salt. However, **C17** was isolated in only a trace amount, along with a trace amount of the homoleptic complex **C28**. The main reason for this failure was found to be in the starting ligand **L3**. In contrast to compounds used in the reported procedure,[6] **L3** has the extra pendant pyridyl unit **C**, which competes with the tpy unit during reaction with the [Ru(DMSO)$_4$$Cl_2$] complex. This can lead to various side products, which are possible to see in the ^{1}H NMR spectrum of **8**. One can distinguish in the ^{1}H NMR spectrum between the free and coordinated pendant pyridyl unit **C** and between the free and coordinated tpy unit. The coordinated pyridyl unit has the protons **C** shifted to the higher ppm and coordinated tpy unit has the protons **B** shifted slightly to the lower ppm (due to the orientation of the **A**-rings and its nitrogen atoms in the free ligand versus the complexed form).

The first reaction step from Scheme 7.12 was repeated, but with pytpy ligand **L4** which has the pendant pyridyl unit protected with a methyl group (Scheme 7.13). ^{1}H NMR and COSY spectra were measured and it was possible to see that all the aromatic proton signals were shifted by about 0.04 ppm to higher magnetic field. Only the singlet of the methyl group stayed at δ 4.43 ppm. However, the singlet of the two methyl groups of the coordinated DMSO (expected to be at δ 3.3 - 3.6 ppm)[6] was not observed. This methodology was abandoned, due to doubts about its reproducibility.

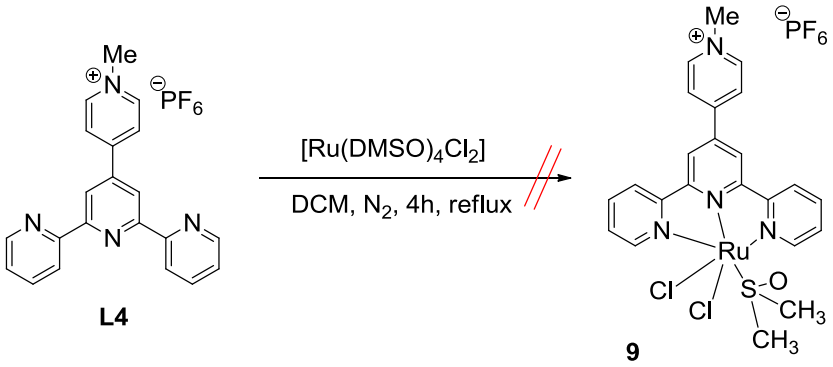

Scheme 7.13: Synthesis of the [Ru(L4)(DMSO)Cl$_2$] complex 9 with a protected pendant pyridyl position

As a next trial to synthesize complexes containing ligands with short side chains, we tried a combination of harsh microwave-assisted conditions with a milder heating in a fume-hood (Scheme 7.14). [Ru(pytpy)Cl$_3$] (**C2**) was first heated in a microwave reactor with $AgPF_6$ in EtOH at 130 °C for 5 minutes and then overnight with ligand **L22**. According to the ^{1}H NMR spectrum, the desired complex **7** was not achieved, but the spectrum was consistent with a complex **10** containing two **L22** ligands coordinated to the metal centre with both the tpy unit and pyridyl unit. However, **10** looks a very unlikely as a product, because **10** is only 4-coordinate. The positive news about this reaction is that the side chain of **L22** was not cleaved and all its signals were in the ^{1}H NMR observed The amino group of the chain was protonated because of the third reaction step with aqueous ammonium hexafluorophosphate.

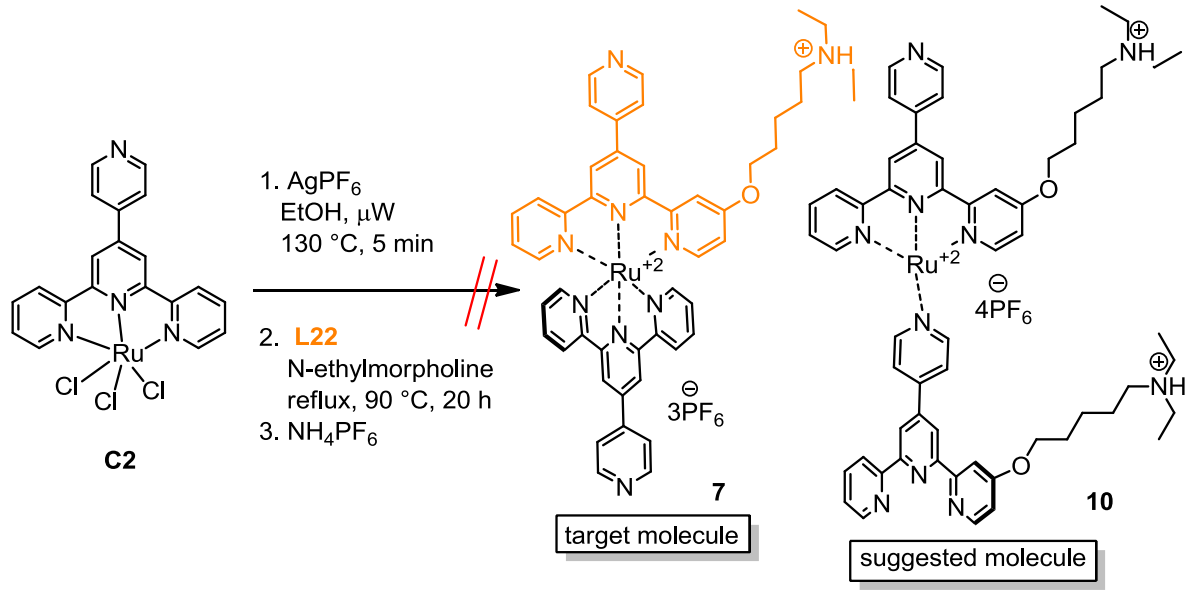

Scheme 7.14: Another trial towards the Ru(II) complex 7, but via a combination of microwave-assisted and milder reaction conditions

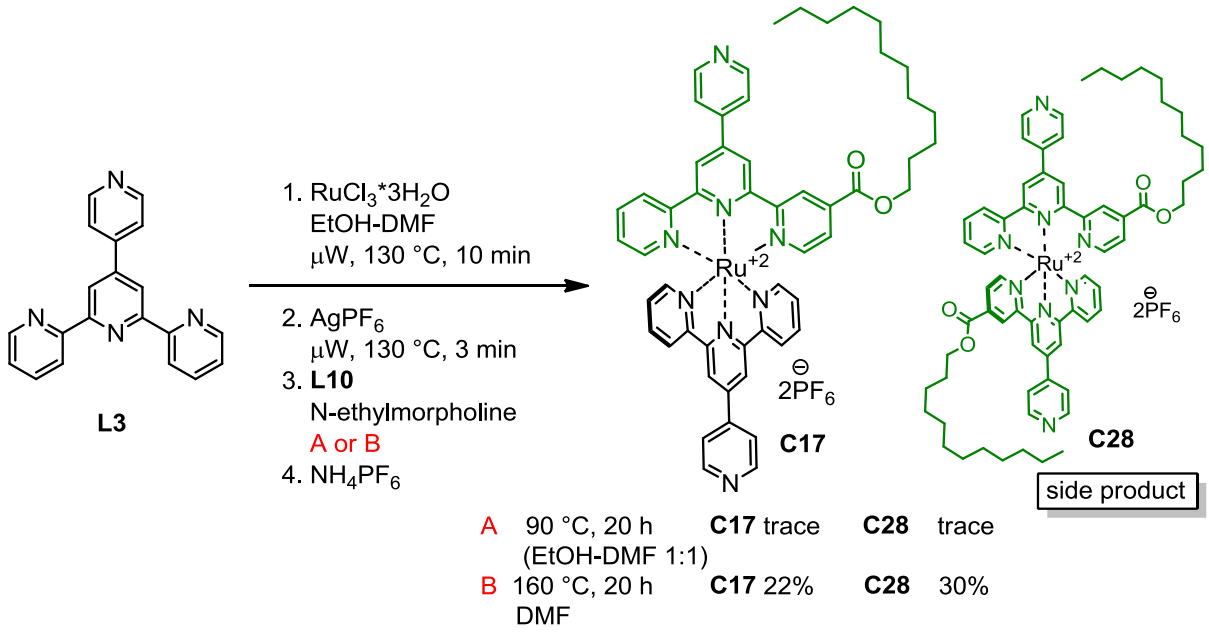

Scheme 7.15: Towards the model Ru(II) complex C17, but via a combination of microwave-assisted and milder reaction conditions

The reaction conditions from Scheme 7.14 were tried again but this time with a mixture of solvents EtOH-DMF (1:1). These reaction conditions were tested using model ligand **L10** (Scheme 7.15). In the third reaction step, the reaction mixture was heated at 90 °C for 20 hours and turned slightly purple. **C17** was isolated in only a trace amount, along with a trace amount of the homoleptic complex **C28** (Scheme 7.15, **A**). In the option **B** (Scheme 7.15),

only DMF was used as a solvent. In the third step, the reaction mixture was heated to reflux for 20 hours and turned red. This was purified with a chromatography column (SiO_2, eluted with a solvent mixture of MeCN/saturated aqueous KNO_3/H_2O = 10:1.5:0.5). **C17** was isolated in 22% yield, along with the homoleptic complex **C28** in 30% yield (Scheme 7.15, **B**). The reaction conditions **B** from Scheme 7.15 were then tried with **L22** with the 5-carbon side chain linked via an ether group (Scheme 7.16). The ^{1}H NMR spectrum of the crude reaction mixture looked promising and the first band on the chromatography column was collected (SiO_2, eluted with a solvent mixture of MeCN/saturated aqueous KNO_3/H_2O = 10:0.5:1.5). However, according to the ^{1}H NMR spectrum after the column, the product seemed to be decomposing. In the electrospray mass spectrum of the product **7**, peaks with *m/z* = 1024.3 and with *m/z* = 439.6 (assigned to $[M\text{-}2PF_6]^{2+}$ of the complex **7** in the neutral form) both with 11% intensity were observed. However, there were also present two intense peaks with a typical Ru isotope pattern at *m/z* = 882.1 and *m/z* = 368.6 with intensity 100% and 82%, respectively. These were assigned to an ion formed after side-chain cleavage, i.e. $[M\text{-}PF_6\text{-}(CH_2)_5NEt_2]^+$ and $[M\text{-}2PF_6\text{-}(CH_2)_5NEt_2]^{2+}$, respectively.

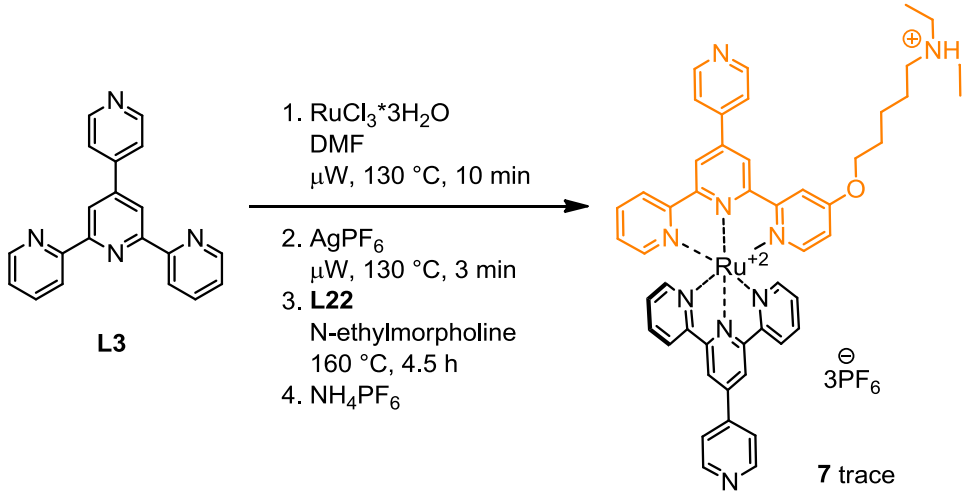

Scheme 7.16: Application of the milder reaction conditions from Scheme 7.15 on synthesis of the complex 7

Scheme 7.17 shows another trial, this time using milder reaction conditions. A mixture of **L3** and $RuCl_3 \cdot 3H_2O$ in EtOH was irradiated in a microwave reactor at 130 °C for 10 minutes. The mixture was then refluxed with $AgBF_4$ in acetone for 2 hours. This was then filtered, solvent evaporated and the brown residue refluxed with **L16** in EtOH for 16 hours. However, after a

work-up, only a brown-orange solid was obtained, which according to the ^{1}H NMR spectrum, seemed to be just protonated starting **L16**.

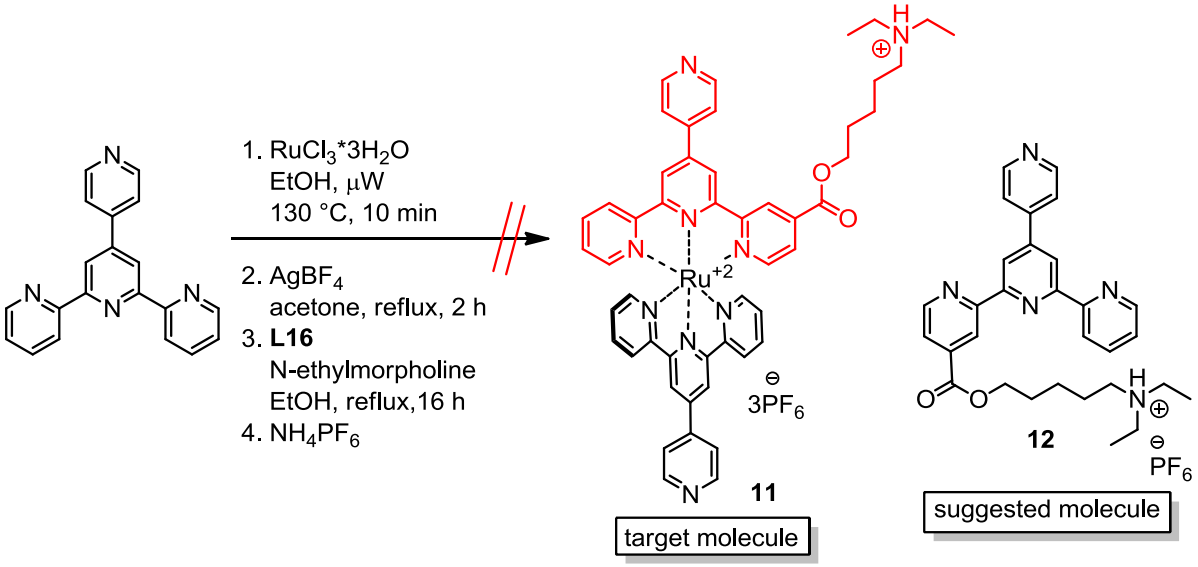

Scheme 7.17: Towards the Ru(II) complex 11 via a combination of microwave-assisted and milder reaction conditions

Scheme 7.18 shows the last trial towards the heteroleptic Ru(II) complexes with a short side chain, via the COOH-substituted complex **C21** and esterification of its corresponding acid chloride. For the synthesis of the heteroleptic Ru(II) complex **C21** of the COOH-substituted pytpy ligand **L8** (Scheme 7.5), the same four-step "one-pot" microwave-assisted reaction conditions were applied as those successfully used for the synthesis of **C18-20** of the pytpy ligands with the long side chain (Chapter 4, Scheme 4.4). The product **C21** was purified using a chromatography column (SiO_2, eluted with a solvent mixture of MeCN/saturated aqueous KNO_3/H_2O = 7:2:2) and obtained in 51% yield. In the electrospray mass spectrum of **C21**, a peak with *m/z* = 911.2 (assigned to $[M\text{-}PF_6]^+$) with 96% intensity and a peak with *m/z* = 383.1 (assigned to $[M\text{-}2PF_6]^{2+}$) with 51% intensity were observed. For esterification of **C21** (Scheme 7.18, **A**), the same reaction conditions as those successfully used for the synthesis of pytpy ligand **L16** (Scheme 7.9) were applied. In the case **B** in Scheme 7.18, a small amount of MeCN as solvent was used to support the solubility of **C21** in thionyl chloride. However, neither the NMR nor mass spectrum revealed the presence of the desired complex **11**.

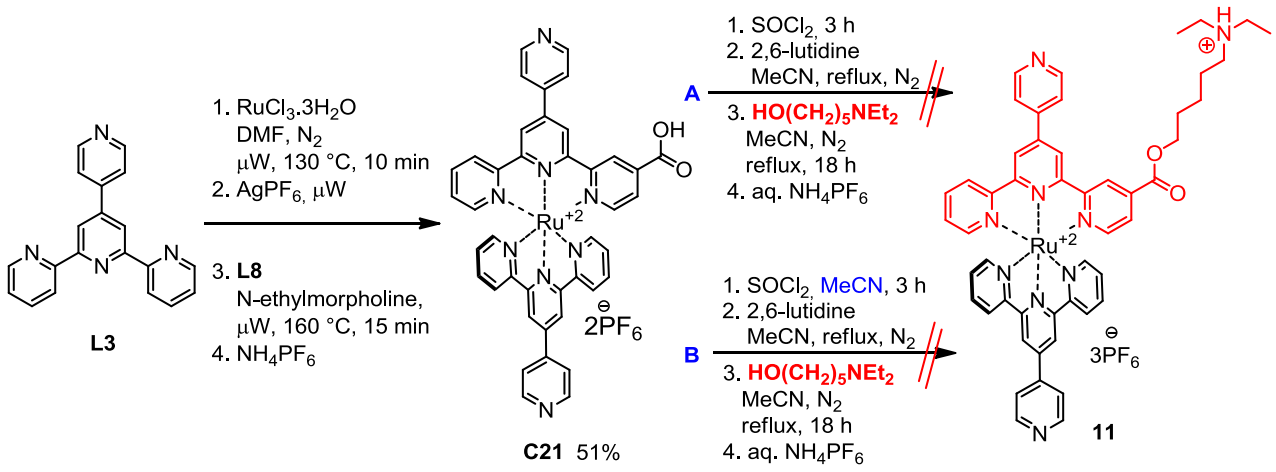

Scheme 7.18: Towards complex 11 via –COOH-substituted Ru(II) complex C21 and corresponding acid chloride

We also tried to synthesize the homoleptic ruthenium(II) complex **C27** using mild conditions. A mixture of **L2** and $[Ru(DMSO)_4Cl_2]$ in methanol were refluxed for 5 hours, until the reaction mixture turned from ochre to reddish colour (Scheme 7.19, **A**). However, after work-up, **C27** was obtained in only a trace amount. Conditions **B** in Scheme 7.19 involve refluxing the reaction mixture in MeOH for 21 hours. With conditions **C**, the reaction mixture was refluxed in DMF for 7 hours. However, **C27** was still obtained in only a trace amount. After these failures, we abandoned any further synthetic attempts towards ruthenium(II) complexes with short side chains.

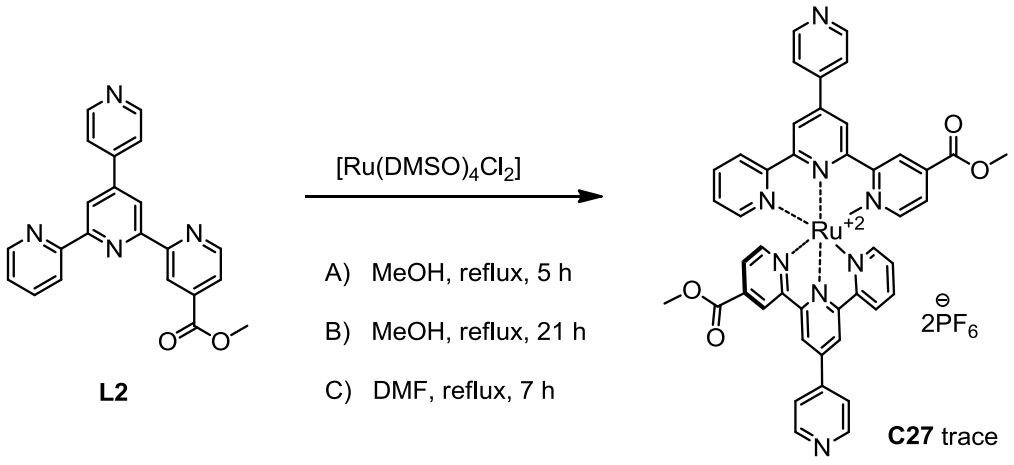

Scheme 7.19: Synthesis of the model homoleptic Ru(II) complex C27 using $[Ru(DMSO)_4Cl_2]$

Conclusion

In this chapter, pytpy ligands with short (3 and 5 carbon atoms) amino-substituted side chains linked via an ester group **L15-16** or an ether group **L21-22** were synthesized. All four ligands were characterised with 1D and 2D NMR spectroscopies, electrospray ionisation mass spectrometry and infrared spectroscopy. **L15-16** were also characterised with elemental analysis and UV-vis absorption spectroscopy. Numerous attempts to synthesize ruthenium(II) complexes of these ligands failed and led only to trace amounts of the desired products or to products of decomposition (side chain cleavage). Several reactions under mild conditions were applied. One worked well for the synthesis of the model complex **C17**, but similar reaction conditions failed when applied to complexation of the ligands with short side chains. These results point to the lability of the short side chain during exposure to acidic or basic conditions.

Literature

1 Uppadine, L. H.; Redman, J. E.; Dent, S. W.; Drew, M. J. B.; Beer, P. D. *Inorg. Chem.,* **2001,** *40,* 2860-2869.

2 Duprez, V.; Krebs, F. C. *Tetrahedron Letters,* **2006**, *47*, 3785–3789.

3 Liu, X.; McInnes, E. J. L.; Kilner, C. A.; Thornton-Pett, M.; Halcrow, M. A. *Polyhedron,* **2001**, *20*, 2889-2900.

4 Wetter, W. P.; De Witt Blanton, C. Jr. *J. Med. Chem.,* **1974**, *17*, 620-624.

5 Calvert, I. M.; Meyer, T. J. *Inorg. Chem*., **1980**, *19*, 1404.

6 Ziessel, R.; Grosshenny, V.; Muriel, H.; Stroh, C. *Inorg. Chem.,* **2004**, *43*, 4262-4271.

Conclusions

In this PhD thesis, numerous synthetic strategies towards new ruthenium(II) complexes of polypyridine ligands with a long amino-substituted side chain are reported. The first approach involves the complexation of methyl 4'-(pyridin-4-yl)-[2,2':6',2''-terpyridine]-4-carboxylate (**L2**) followed by trans-esterification of the methyl ester group with a long side chain. However this reaction gives the desired complexes in very poor yields, along with the complex with a free carboxylic acid – a product of the side chain cleavage. Owing to these reasons, an alternative route to obtain long side chain-substituted complexes was developed: trans-esterification of N-methylated complexes (protected against possible side reactions) followed by a final demethylation to remove the protecting group. However, the trans-esterification step again was the problematic one, therefore this strategy was abandoned.

Another synthetic route to obtain Ru(II) complexes of 4'-(pyridin-4-yl)-2,2':6',2''-terpyridine ligands (pytpy) substituted in 4-position with an amino side-chain involved Sonogashira cross-coupling and "click reaction". This allowed a wide range of reactants to be used as starting materials and gave access to several different funcitonal groups. The precursor, chloro-substituted pytpy ligand **L6**, successfully synthesized, but all further alkynylation attempts failed. **L6** was transhalogenated to the more reactive iodo-derivative. Unfortunately, the conversion proceeded in only 30%. However, another application was found for **L6**, namely the synthesis of ligands with an amino-substituted side chain linked via an ether group (**L17-20**).

The next attempted route to obtain Ru(II) complexes of pytpy ligands with an amino side-chain appended the side chain to the ligand first and subsequently formed the complex. Four different ways to synthetize pytpy ligands with the long amino side-chain linked via an ester **L10-14** were tried. Hydrolysis of **L2** to free carboxylic acid **L8**, followed by esterification via the corresponding acid chloride was successful whereas direct Steglich esterification of carboxylic acid **L8** did not work due to the insolubility of **L8**. Further complexation of ligands **L10-14** was the more successful alternative to the original idea of complex synthesis by the trans-esterification of **C7.** Heteroleptic and homoleptic ruthenium(II) complexes with pytpy

ligands with an amino-substituted side chain (diethylamine, piperidine and morpholine), linked via an ester or an ether group were successfully synthesized. In order to have model compounds for use in the photophysical studies, ruthenium(II) complexes with 4'-phenyl-2,2':6',2''-terpyridine ligands (Phtpy) substituted in 4-possition with the same side chains were also prepared. Pytpy ligands with short (3 and 5 carbon atoms) amino-substituted side chains linked via an ester group (**L15-16**) or an ether group (**L21-22**) were synthesized and characterised. Numerous attempts to synthesize ruthenium(II) complexes of these ligands failed and led only to trace amounts of the desired products or to decomposition (i.e., side chain cleavage). Several reactions under mild conditions were attempted. One worked well for the synthesis of the model complex **C17**, but similar reaction conditions failed when applied to complexation of the ligands with short side chains. These results point to the lability of the short side chain during exposure to acidic or basic conditions.

All complexes were characterised with 1D and 2D NMR spectroscopy, electrospray or MALDI TOF mass spectrometry, infrared spectroscopy, elemental analysis, UV-vis and photoluminescence spectroscopy. Detailed photophysical of the new ruthenium(II) complexes were carried out in collaboration with the photochemistry research group of Prof. Alberto Credi from the University of Bologna in Italy. Ruthenium(II) complexes were analysed in terms of their photophysical properties and compared in groups according to the pendant substituents of the tpy unit, the linker group of the side chain and also considering substituents on the side chains. The complexes with the ester linker exhibit similar behaviour in the absorption and emission spectra as reported for the model complex **C8**. Complexes with the ether linker are very weak emitters. However they exhibit a continuous red shift in their emission spectra during titration with acid, in contrast to complexes with ester linkers or **C8**. Complexes of Phtpy ligands were also found to be very weak emitters, which corresponds with known ruthenium(II) complexes of tpy ligands. Homoleptic ruthenium(II) complexes of ester-substituted ligands exhibit are the strongest emitters of all the analysed complexes.

Unfortunately, the actual effect of the amino-substituent on the side chain was not investigated, due to the fact that such complexes were isolated already in their side-chain protonated form. Unfortunately, this fact was discovered nearly at the end of this work, after all the photophysical studies were carried out. Therefore, there was not enough time to develop a sufficient methodology to convert the mono-protonated Ru(II) complexes to

the de-protonated form and examine the complexes in terms of the originally suggested full-adder. It was also found that some molecules exhibit unexpected anomalies during photophysical measurements. Namely, an unusual kinetic effect in the absorption and photoluminescence spectra during titration of **C20** with TfOH or too small amount of acid consumed to complete titrations of some complexes (**C29**).

Therefore, NMR studies of ruthenium(II) complexes **C20** and **C29** and of their free ligands **L11** and **L14** under acidic and basic conditions were carried out and the processes monitored by ^{1}H NMR spectroscopy. Protonation possibilities of the nitrogen atoms were investigated and the stability of the side amino chains under these acidic conditions was examined. It was observed that the side chains stay attached to the Ru(II) complex. The results of these NMR studies reveal and confirm that all Ru(II) complexes with three protonation sites were synthesized and isolated in the mono-protonated form - on the amino group of the side chains (which most likely occurred during the work-up with ammonium hexafluorophosphate). Therefore, the only protonation happening during the NMR titrations of the Ru(II) complexes was on the pendant pyridyl units. The ligands **L11** and **L14** were titrated with TFA-d to monitor the side chain protonation and prove that this amino unit is protonated first. From these processes we calculated pK values which points at basicity of the side chain amines.

In this PhD thesis, 25 new substituted pytpy or Phtpy ligands and 30 new Ru(II) complexes of these ligands were synthesized and characterised.

Moving forward, it would be interesting to investigate the influence of other side chain linkers, such as amide or carbonyl groups, and develop a sufficient technique to complex the pytpy ligands bearing a short side chain (**L15-16** and **L21-22**).

Experimental

General Experimental

^{1}H, ^{13}C, COSY, HMQC, HMBC, NOESY NMR spectra were recorded on Bruker AM 400 or DRX 500 spectrometers. The chemical shifts were referenced to residual solvent peaks with respect to δ(TMS) = 0 ppm.

Infrared spectra were recorded on a Shimadzu FTIR 8400 S Fourier-transform spectrophotometer with Golden Gate accessory for solid samples.

Solution UV/vis spectroscopic measurements (carried out in Basel) were recorded using an Agilent 8453 spectrophotometer or a Varian Cary 5000 spectrophotometer. Emission spectra were recorded on a Shimadzu 5301PC spectrofluorophotometer (carried out in Basel).

Electrospray ionization (ESI) mass spectra were measured using a Bruker esquire 3000^{plus} mass spectrometer. MALDI (Matrix-assisted laser desorption/ionization) spectra were recorded on Voyager-DE-Pro or Bruker Microflex with p-nitroaniline or 2,5-dihydroxybenzoic acid as matrixes.

The microanalyses were performed with a Vario Micro Cube microanalyser by Sylvie Mittelheisser.

Microwave reactions were carried out in a Biotage InitiatorTM 8 reactor. Absolute solvents were used for all reactions (Sigma-Aldrich or ACROS crown capped bottles).

Fluka silica 60 and Merck alumina 90 were used for column chromatography.

NH_4PF_6 was purchased from Alfa Aesar or ACROS Organics and used without further purification. Starting materials were purchased from ACROS Organics, Sigma-Aldrich, or Fluorochem and were used without further purification. Deuterated solvents for NMR were purchased from Cambridge Isotope Laboratories, Inc.

Precursors

(E)-3-(dimethylamino)-1-(pyridin-2-yl)prop-2-en-1-one (P1)

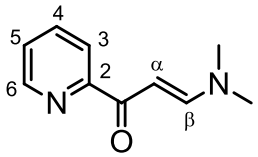

A solution of 2-acetylpyridine (20 g, 0.165 mol) and *N*,*N*-dimethylformamide dimethyl acetal (24 g, 0.201 mol) in toluene (100 mL) was heated to reflux. Methanol formed was removed by azeotropic distillation on a Dean-Stark apparatus. The reaction mixture was heated until no more methanol distilled over (ca. 50 hours). Toluene was removed in vacuo. The product was crystallized out by addition of cyclohexane. The yellow crystals of (19.42 g, 110.20 mmol, 67%) were collected by filtration on a glass frit and air dried. The NMR data match those published.[1]

^{1}H NMR (400 MHz, $CDCl_3$, TMS) δ/ppm 8.61 (ddd, *J* = 4.8, 1.6, 0.8 Hz, 1H, H^6), 8.13 (d, *J* = 7.9 Hz, 1H, H^3), 7.90 (d, *J* = 12.7 Hz, 1H, H^β), 7.78 (td, *J* = 7.7, 1.8 Hz, 1H, H^4), 7.34 (ddd, *J* = 7.5, 4.8, 1.3 Hz, 1H, H^5), 6.43 (d, *J* = 12.7 Hz, 1H, H^α), 3.16 (s, 3H, H^{Me}), 2.98 (s, 3H, H^{Me}), 1.91 (s, 0H).

Methyl 2-acetylisonicotinate (P2)

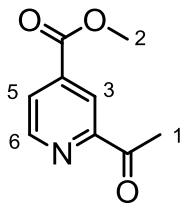

Methyl isonicotinate (41 g, 0.30 mol) was added to a solution of an excess of paraldehyde (200 g, 6.66 mol) in acetonitrile (700 mL). To this solution iron(II) sulfate heptahydrate (1.4 g, 5 mmol), trifluoroacetic acic (35 g, 0.31 mol) and tert-butyl hydroperoxide (70% in water, 75 g, 0.83 mol) were added and the reaction mixture was heated for 4 hours at reflux. Solvent was then removed under reduced pressure. The residue was neutralized with saturated aqueous sodium carbonate (500 mL) and extracted with toluene. The organic phase was washed with brine, dried over magnesium sulfate, filtered through a glass frit and solvent evaporated. The

crude mixture containing mono- and bisacetylated isonicotinate was purified with column chromatography (SiO_2, EtOAc/hexane = 1:2), which afforded the product as yellow solid (22.4 g, 0.12 mol, 42%). The NMR data match those published.[2]

^{1}H NMR (400 MHz, $CDCl_3$, TMS) δ/ppm 8.82 (dd, *J* = 4.9, 0.7 Hz, 1H, H^6), 8.54 (dd, *J* = 1.4, 0.7 Hz, 1H, H^3), 8.01 (dd, *J* = 4.9, 1.6 Hz, 1H, H^5), 3.97 (s, 3H, H^{Me2}), 2.74 (s, 3H, H^{Me1}).

1-(4-Chloropyridin-2-yl)ethanone (P3)

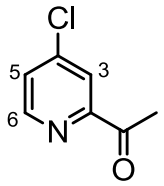

A 50mL round bottom flask was heated with a heatgun and cooled down on a Schlenk line. 4-Chloro-2-pyridine carbonitrile (1 g, 7.22 mmol) ground to a powder was added, the flask sealed with a septum and flushed with nitrogen. Dry diethyl ether (20 mL) was added with a syringe via a septum and the reaction mixture cooled to 0 °C in an ice bath. Methylmagnesium iodide (3M in Et_2O, 5.99 g, 36 mmol) was added dropwise via a syringe. The resulting yellow solution was stirred for 4 hours at room temperature and turned greenish. This was poured onto saturated aqueous ammonium chloride (30 mL) while cooling in an ice bath. The colour changed to ochre and the pH was adjusted with concentrated HCl to pH=1. The ochre solution was stirred overnight at room temperature, then neutralized with ammonium hydroxide (32%), stirred 2 hours and extracted with diethyl ether. The organic phase was dried over sodium sulfate, filtered and solvent evaporated to give a yellow oil. Purification with column chromatography (SiO_2, EtOAc/hexane = 1:2) afforded product as yellow crystals (0.87 g, 5.61 mmol, 78%). The NMR data match those published.[3]

^{1}H NMR (400 MHz, $CDCl_3$, TMS) δ/ppm 8.58 (d, *J* = 5.2 Hz, 1H, H^6), 8.04 (d, *J* = 2.0 Hz, 1H, H^3), 7.47 (dd, *J* = 5.2, 2.1 Hz, 1H, H^5), 2.72 (s, 3H, H^{Me}).

1-(4-Methylpyridin-2-yl)ethanone (P4)

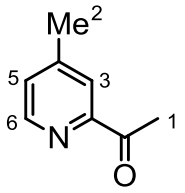

4-Picoline (7.6 g, 82 mmol) was added to a solution of an excess of paraldehyde (54 g, 0.41 mol) in acetonitrile (150 mL). To this solution iron(II) sulfate heptahydrate (0.38 g, 1.3 mmol), trifluoroacetic acid (9.5 g, 83 mmol) and tert-butyl hydroperoxide (80% in water, 15.8 g, 0.12 mol) were added and the reaction mixture was heated for 4 hours at reflux. Solvent was removed under reduced pressure. The residue was neutralized with saturated aqueous sodium carbonate (150 mL) and extracted with toluene (5times 150 mL). The organic phase was dried over sodium sulfate, filtered through a glass frit and solvent evaporated to give a black oil. The residue was purified with column chromatography (SiO_2, EtOAc/hexane = 1:2), which afforded the product as yellow oil (2.62 g, 19.38 mmol, 24%). The NMR data match those published.[4]

^{1}H NMR (400 MHz, $CDCl_3$, TMS) δ/ppm 8.53 (m, 1H, H^6), 7.87 (s, 1H, H^3), 7.28 (m, 1H, H^5), 2.71 (s, 3H, H^{Me1}), 2.42 (s, 3H, H^{Me2}).

1-(2-(4-(Methoxycarbonyl)pyridin-2-yl)-2-oxoethyl)pyridin-1-ium iodide (P5)

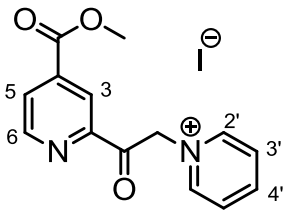

Iodine (14 g, 56 mmol) was dissolved in dry pyridine (67 mL) and the solution heated at 100 °C for 15 minutes under a nitrogen atmosphere. Then methyl 2-acetylisonicotinate **P2** (10 g, 56 mmol) was added in a single portion and the resulting brown mixture was heated for 1 hour at reflux. A brown precipitate formed on cooling, which was collected on a glass frit, washed with chloroform and diethylether. This was suspended in hot ethanol containing 5 (w/w)% of activated charcole, heated to reflux and filtered hot under reduced pressure. The orange filtrate was partly evaporated and left in a freezer to crystallize. The yellow-ochre crystals

(7.7 g, 20 mmol, 36%) were collected on a glass frit, washed with cold ethanol and air dried. The NMR data match those published.[5]

^{1}H NMR (400 MHz, DMSO-d_6) δ/ppm 9.08 (dd, *J* = 5.0, 0.8 Hz, 1H, H^6), 8.98 (dd, *J* = 6.7, 1.2 Hz, 2H, $H^{2'}$), 8.72 (tt, *J* = 7.9, 1.3 Hz, 1H, $H^{4'}$), 8.34 (dd, *J* = 1.6, 0.8 Hz, 1H, H^3), 8.27 (dd, *J* = 7.8, 6.7 Hz, 2H, $H^{3'}$), 8.23 (dt, *J* = 7.1, 3.6 Hz, 1H, H^5), 6.50 (s, 2H, H^{CH_2}), 3.94 (s, 3H, H^{CH_3}).

1-(2-(4-Chloropyridin-2-yl)-2-oxoethyl)pyridin-1-ium iodide (P6)

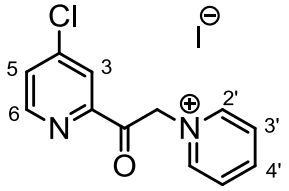

Iodine (1.16 g, 4.58 mmol) was dissolved in dry pyridine (16 mL) and the solution was heated at 100 °C for 15 minutes under a nitrogen atmosphere. Then 1-(4-chloropyridin-2-yl)ethanone **P3** (0.71 g, 4.58 mmol) was added in a single portion and the resulting brown mixture was heated for 1 hour at reflux. A brown microcrystalline powder (1.52 g, 4.22 mmol, 92%) formed on cooling and was collected on a glass frit, washed with chloroform, diethyl ether and air dried.

^{1}H NMR (400 MHz, DMSO-d_6) δ/ppm 8.99 (dd, *J* = 6.7, 1.3 Hz, 2H, $H^{2'}$),8.87 (dd, *J* = 5.3, 0.6 Hz, 1H, H^6), 8.74 (tt, *J* = 7.9, 1.3 Hz, 1H, $H^{4'}$),8.29 (dd, *J* = 7.8, 6.8 Hz, 2H, $H^{3'}$),8.11 (dd, *J* = 2.1, 0.6 Hz, 1H, H^3), 8.01 (dd, *J* = 5.3, 2.1 Hz, 1H, H^5), 6.49 (s, 2H, H^{CH_2}). **^{13}C {^{1}H} NMR** (126 MHz, DMSO-d_6) δ/ppm 190.5 ($C^{C=O}$), 151.9 (C^2), 151.1 (C^6), 146.4 ($C^{4'}$), 146.4 ($C^{2'}$), 144.8 (C^4), 128.8 (C^5), 127.8 ($C^{3'}$), 121.2 (C^3), 26.6 (C^{CH_2}). **MP** 223 °C. **ESI MS** (MeOH/$CHCl_3$): *m/z* 233.44 $[M\text{-}I]^+$ (100%, calc. 233.05). **IR** (solid, ν/cm^{-1}) 3105 (w), 1725 (m), 1643 (w), 1553 (w), 1518 (w), 1533 (m), 1440 (w), 1383 (w), 1294 (m), 1276 (m), 1229 (w), 1190 (w), 974 (w), 875 (w), 830 (s), 799 (w), 772 (w), 699 (w), 618 (w), 555 (s). **EA** found: C, 40.04; H, 2.76; N, 8.27%. $C_{12}H_{10}ClIN_2O$ requires C, 39.97; H, 2.80; N, 7.77%.

1-(2-(4-Methylpyridin-2-yl)-2-oxoethyl)pyridin-1-ium iodide (P7)

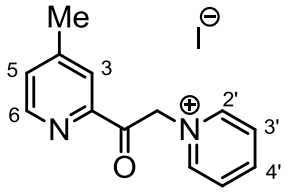

Iodine (2.04 g, 8.01 mmol) was dissolved in dry pyridine (12 mL) and the solution was heated at 100 °C for 15 minutes under a nitrogen atmosphere. Then 1-(4-methylpyridin-2-yl)ethanone **P4** (1.08 g, 8.01 mmol) was added in a single portion and the resulting black mixture was heated for 1 hour at reflux. A dark brown powder (0.97 g, 2.85 mmol, 36%) formed on cooling and was collected on a glass frit, washed with a mixture of chloroform and ethanol, diethylether and air dried. Analytical data match those published.[5]

ESI MS: *m/z* 213.1 $[M\text{-}I]^+$

1-(2-Oxo-2-(pyridin-2-yl)ethyl)pyridin-1-ium iodide (P8)

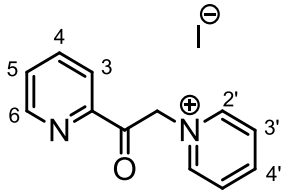

Iodine (3.05 g, 12 mmol) was dissolved in dry pyridine (67 mL) and the solution was heated at 100 °C for 15 minutes under a nitrogen atmosphere. Then 2-acetylpyridine (1.45 g, 12 mmol) was added in a single portion and the resulting brown mixture was heated for 1 hour at reflux. Grey needle-like crystals (2.65 g, 8.15 mmol, 68%) formed on cooling, and were collected on a glass frit, washed with chloroform, diethylether and air dried. The NMR data match those published.[5]

^{1}H NMR (400 MHz, DMSO-d_6) δ/ppm 9.02 (dd, *J* = 6.7, 1.2 Hz, 2H, $H^{2'}$), 8.88 (ddd, *J* = 6.4, 3.2, 2.4 Hz, 1H, H^6), 8.74 (tt, *J* = 8.0, 1.2 Hz, 1H, $H^{4'}$), 8.29 (dd, *J* = 7.7, 6.7 Hz, 2H, $H^{3'}$), 8.15 (td, *J* = 7.7, 1.7 Hz, 1H, H^4), 8.09 (dt, *J* = 7.8, 1.1 Hz, 1H, H^3), 7.85 (ddd, *J* = 7.5, 4.8, 1.4 Hz, 1H, H^5), 6.52 (s, 2H, H^{CH_2}).

(E)-1-(pyridin-2-yl)-3-(pyridin-4-yl)prop-2-en-1-one (P9)

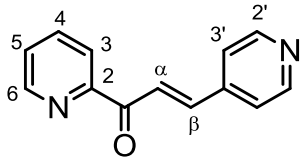

2-Acetylpyridine (3.60 g, 30 mmol) and pyridine-4-carboxaldehyde (3.21 g, 30 mmol) were added to a 100mL round bottom flask containing alumina (30 g) and tetrahydrofuran (30 mL). The mixture was heated in a domestic microwave oven (second lowest setting, 300 W) for approx. 5 minutes until it turned yellow. The alumina was filtered off on a glass frit, and washed with chloroform (500 mL). Solvent was reduced to approx. 5 mL and 5 mL of ethanol were added and the yellow solution was left in a freezer overnight to crystallize. The resulting yellow needle-like crystals (5.81 g, 27.63 mmol, 93%) were collected on a glass frit and washed with cold diethyl ether. The NMR data match those published.[5]

^{1}H NMR (400 MHz, $CDCl_3$, TMS) δ/ppm 8.75 (d, *J* = 4.8 Hz, 1H, H^6), 8.67 (dd, *J* = 4.5, 1.6 Hz, 2H, $H^{2'}$), 8.45 (d, *J* = 16.1 Hz, 1H, H^{α}), 8.19 (dt, *J* = 7.9, 1.0 Hz, 1H, H^3), 7.90 (td, *J* = 7.7, 1.7 Hz, 1H, H^4), 7.80 (d, *J* = 16.1 Hz, 1H, H^{β}), 7.55 (dd, *J* = 4.7, 1.5 Hz, 2H, $H^{3'}$), 7.52 (m, 1H, H^5).

(E)-1-(4-methylpyridin-2-yl)-3-(pyridin-4-yl)prop-2-en-1-one (P10)

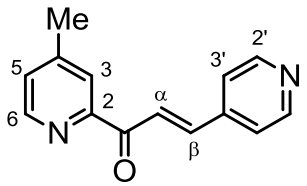

1-(4-Methylpyridin-2-yl)ethanone **P4** (2.02 g, 14.95 mmol) and pyridine-4-carboxaldehyde (1.60 g, 14.95 mmol) were mixed with methanol (26 mL) in a 50mL round bottom flask. Piperidine (1.40 g, 16.45 mmol) and acetic acid (0.99 g, 16.45 mmol) were added to this yellow reaction mixture, which was heated at reflux for 6.5 hours and the colour turned red. This solution was cooled to room temperature, solvent concentrated in vacuo and the residue left for 3 days in a freezer to crystallize. The orange needle-like crystals (1.19 g, 5.31 mmol, 36%) were collected on a glass frit, washed with cold water and air dried.

^{1}H NMR (500 MHz, $CDCl_3$, TMS) δ/ppm 8.65 (dd, *J* = 4.4, 1.7 Hz, 2H, $H^{2'}$), 8.58 (d, *J* = 4.9 Hz, 1H, H^{6}), 8.42 (d, *J* = 16.1 Hz, 1H, H^{α}), 7.99 (s, 1H, H^{3}), 7.77 (d, *J* = 16.1 Hz, 1H, H^{β}), 7.53 (m, 2H, $H^{3'}$), 7.31 (d, *J* = 4.9 Hz, 1H, H^{5}), 2.44 (s, 3H, H^{Me}). **^{13}C {^{1}H} NMR** (126 MHz, $CDCl_3$) δ/ppm 189.5 ($C^{C=O}$), 153.5 (C^{2}), 150.6 ($C^{2'}$), 148.9 (C^{6}), 148.7 (C^{4}), 142.5 ($C^{4'}$), 141.2 (C^{α}), 128.3 (C^{5}), 125.5 (C^{β}), 124.0 (C^{3}), 122.4 ($C^{3'}$), 21.24 (C^{Me}). **ESI MS** (MeOH/$CHCl_3$): *m/z* 247.0 $[M+Na]^+$ (9%, calc. 247.1), 225.0 $[M+H]^+$ (100%, calc. 225.1). **IR** (solid, ν/cm^{-1}) 3405 (w), 2948 (w), 1678 (s), 1615 (s), 1591 (s), 1568 (m), 1548 (s), 1410 (m), 1382 (m), 1338 (w), 1309 (m), 1285 (m), 1258 (w), 1229 (m), 1156 (m), 1043 (m), 985 (s), 961 (m), 858 (s), 837 (m), 804 (s), 775 (m), 652 (w), 560 (s), 539 (s). **EA** found: C, 67.64; H, 5.75; N, 11.38%. $C_{14}H_{12}N_2O{\cdot}1.3H_2O$ requires C, 67.89; H, 5.94; N, 11.31%.

(E)-3-phenyl-1-(pyridin-2-yl)prop-2-en-1-one (P11)

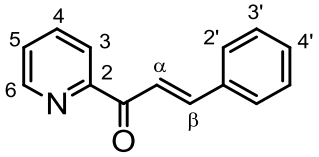

2-Acetylpyridine (2.42 g, 20 mmol) and freshly distilled benzaldehyde (2.12 g, 20 mmol) were dissolved in ethanol (70 mL). Potassium hydroxide (2.24 g, 40 mmol) dissolved in 50 mL of water was added to the solution, which slowly turned yellow. Water was added in 10mL portions to the reaction mixture until a milky precipitate formed (approx. 300 mL). The suspension was stirred at the room temperature for 4 hours. A yellowish precipitate formed and was collected on a glass frit, washed with water (100 mL) and air dried. The product was isolated as a pale yellow powder (4.08 g, 19.50 mmol, 97%). The NMR data match those published.[6]

^{1}H NMR (500 MHz, $CDCl_3$, TMS) δ/ppm 8.77 (ddd, *J* = 4.7, 1.7, 0.9 Hz, 1H, H^{6}), 8.33 (d, *J* = 16.0 Hz, 1H, H^{α}), 8.22 (dt, *J* = 7.9, 1.1 Hz, 1H, H^{3}), 7.97 (d, *J* = 16.0, 1H, H^{β}), 7.90 (td, *J* = 7.7, 1.7 Hz, 1H, H^{4}), 7.76 (m, 2H, $H^{2'}$), 7.52 (ddd, *J* = 7.6, 4.8, 1.2 Hz, 1H, H^{5}), 7.44 (m, 3H, $H^{2'+4'}$).

Methyl 11-(diethylamino)undecanoate (P12)

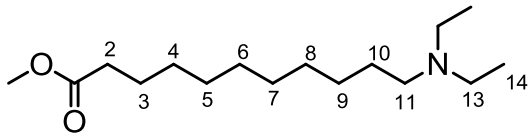

A mixture of methyl 11-bromoundecanoate (0.50 g, 1.79 mmol) and diethylamine (0.79 g, 10.75 mmol) was heated at 55 °C for 18 hours. The white precipitate of diethylamonium bromide was filtered off on a glass frit and washed with diethyl ether. The solvent and an excess of diethylamine was removed in vacuo to give an orange oil. The crude material was purified by vacuum distillation (80 °C, 0.05 mbar) to give the product as a yellowish oil (0.47 g, 1.73 mmol, 97%). The NMR data match those published.[7]

^{1}H NMR (400 MHz, $CDCl_3$, TMS) δ/ppm 3.66 (s, 3H, H^{Me}), 2.60 (m, 4H, H^{13}), 2.47 (m, 2H, H^{11}), 2.29 (t, *J* = 7.6 Hz, 2H, H^2), 1.61 (m, 2H, H^3), 1.48 (m, 2H, H^{10}), 1.27 (s, 12H, H^{4-9}), 1.07 (t, *J* = 7.1 Hz, 6H, H^{14}).

Methyl 11-(piperidin-1-yl)undecanoate (P13)

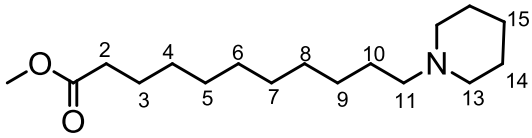

A mixture of methyl 11-bromoundecanoate (1.49 g, 5.35 mmol) and piperidine (3.64 g, 42.76 mmol) was heated at 55 °C for 7 hours. The white precipitate of piperidinium bromide was filtered off on a glass frit and washed with diethyl ether. The solvent was removed in vacuo to give an orange oil. The crude material was purified by vacuum distillation (85 °C, $9\cdot10^{-3}$ mbar) to give a product as a yellowish oil (1.40 g, 4.94 mmol, 92%). The NMR data match those published. [7]

^{1}H NMR (400 MHz, $CDCl_3$, TMS) δ/ppm 3.66 (s, 3H, H^{Me}), 2.35 (br s, 4H, H^{13}), 2.27 (m, 4H, H^{2+11}), 1.59 (m, 6H, H^{3+14}), 1.44 (m, 4H, H^{10+15}), 1.27 (m, 12H, H^{4-9}).

Methyl 11-morpholinoundecanoate (P14)

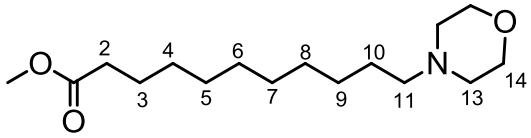

A mixture of methyl 11-bromoundecanoate (0.50 g, 1.79 mmol) and morpholine (1.23 g, 14.17 mmol) was heated at 55 °C for 6 hours. The white precipitate of morpholinium bromide was filtered off on a glass frit and washed with diethyl ether. The solvent was removed in vacuo to give orange oil. The crude material was purified by vacuum distillation (120 °C, $1.5 \cdot 10^{-2}$ mbar) to give a product as a yellow oil (0.51 g, 1.79 mmol, 99%).

^{1}H NMR (500 MHz, $CDCl_3$, TMS) δ/ppm 3.70 (t, *J* = 4.7 Hz, 4H, H^{14}), 3.64 (s, 3H, H^{Me}), 2.41 (m, 4H, H^{13}), 2.28 (m, 4H, H^{2+11}), 1.59 (m, 2H, H^{3}), 1.45 (m, 2H, H^{10}), 1.27 (m, 12H, H^{4-9}). **^{13}C {^{1}H} NMR** (126 MHz, $CDCl_3$) δ/ppm 165.5 ($C^{C=O}$), 67.1 (C^{14}), 59.4 (C^{11}), 53.9 (C^{13}), 51.6 (C^{Me}), 34.2 (C^{2}), 29.7, 29.6, 29.5, 29.3, 29.2 (C^{4-8}), 27.6 (C^{9}), 26.7 (C^{10}), 25.1 (C^{3}). **ESI MS** (MeOH/$CHCl_3$): m/z 308.2 $[M+Na]^+$ (5%, calc. 308.2), 286.2 $[M+H]^+$ (100%, calc. 286.2). **IR** (solid, ν/cm^{-1}) 2925 (s), 2852 (m), 2803 (w), 1739 (s), 1455 (m), 1439 (m), 1356 (w), 1272 (w), 1255 (w), 1167 (m), 1136 (m), 1117 (s), 1007 (m), 866 (s), 725 (w), 512 (s). **EA** found: C, 66.91; H, 10.75; N, 4.98%. $C_{16}H_{31}NO_3$ requires C, 67.33; H, 10.95; N, 4.91%.

Methyl 5-(diethylamino)pentanoate (P15)

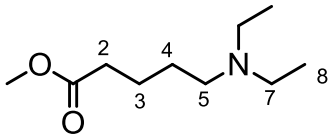

A mixture of methyl 5-bromovalerate (2.73 g, 13.98 mmol) and diethylamine (8.18 g, 111.81 mmol) was heated at 55 °C for 17 hours. The white precipitate of diethylamonium bromide was filtered off on a glass frit and washed with tetrahydrofuran. The solvent and an excess of diethylamine was removed in vacuo to give orange oil. The crude material was purified by vacuum distillation (47 °C, 0.02 mbar) to give a product as colorless oil (2.51 g, 13.40 mmol, 96%). The NMR data match those published. [7]

^{1}H NMR (400 MHz, $CDCl_3$, TMS) δ/ppm 3.66 (s, 3H, H^{Me}), 2.50 (q, *J* = 7.2 Hz, 4H, H^{7}), 2.42 (m, 2H, H^{5}), 2.33 (t, *J* = 7.4 Hz, 2H, H^{2}), 1.63 (m, 2H, H^{3}), 1.47 (m, 2H, H^{4}), 1.00 (t, *J* = 7.2 Hz, 6H, H^{8}).

11-(Diethylamino)undecan-1-ol (P16)

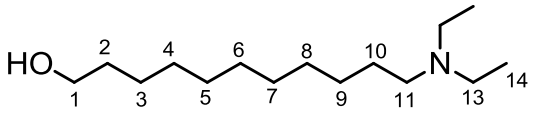

Methyl 11-(diethylamino)undecanoate **P12** (0.94 g, 3.47 mmol) in 2 mL of dry tetrahydrofuran was added dropwise with a syringe via a septum to a mixture of lithium aluminium hydride (1.06 g, 27.79 mmol) in dry tetrahydrofuran (8 mL) in a two necked round bottom flask, while stirring under an inert atmosphere. The reaction mixture was refluxed for 19 hours and cooled to room temperature. An excess of the lithium aluminium hydride was quenched by careful addition of sodium sulfate decahydrate, while stirred in an ice bath until the reaction mixture turned white. The white precipitate of lithium hydroxide was filtered off on a glass frit and washed with diethyl ether. The organic phase was dried over magnesium sulfate, filtered and solvent evaporated in vacuo to give the product as a colourless oil (0.77 g, 3.17 mmol, 91%). The NMR data match those published. [7]

^{1}H NMR (400 MHz, $CDCl_3$, TMS) δ/ppm 3.64 (t, *J* = 6.6 Hz, 2H, H^1), 2.52 (q, *J* = 7.2 Hz, 4H, H^{13}), 2.39 (m, 2H, H^{11}), 1.56 (m, 2H, H^2), 1.30 (m, 16H, $H^{3\text{-}9}$), 1.02 (t, *J* = 7.2 Hz, 6H, H^{14}).

11-(Piperidin-1-yl)undecan-1-ol (P17)

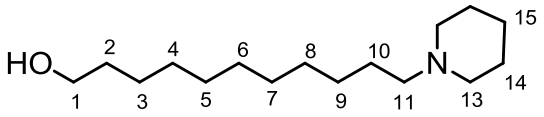

Methyl 11-(piperidin-1-yl)undecanoate **P13** (1.40 g, 4.94 mmol) in 4 mL of dry tetrahydrofuran was added dropwise with a syringe via a septum to a mixture of lithium aluminium hydride (0.77 g, 24.70 mmol) in dry tetrahydrofuran (16 mL) in a two necked round bottom flask, while stirring under an inert atmosphere. The reaction mixture was refluxed for 19 hours and cooled to room temperature. An excess of the lithium aluminium hydride was quenched by careful addition of sodium sulfate decahydrate, while stirred in an ice bath until the reaction mixture turned white. The white precipitate of lithium hydroxide was filtered off on a glass frit and washed with diethyl ether. The organic phase was dried over magnesium sulfate, filtered and

solvent evaporated in vacuo to give the product as a pale yellow solid (1.25 g, 4.89 mmol, 99%). The NMR data match those published. [7]

^{1}H NMR (500 MHz, $CDCl_3$, TMS) δ/ppm 3.57 (t, *J* = 6.7 Hz, 2H, H^{1}), 2.33 (br s, 4H, H^{13}), 2.23 (m, 2H, H^{11}), 1.53 (m, 6H, H^{2+14}), 1.45 (m, 2H, H^{10}), 1.41 (m, 2H, H^{15}), 1.27 (m, 14H, H^{3-9}). **^{13}C {^{1}H} NMR** (126 MHz, $CDCl_3$) δ/ppm 62.7 (C^{1}), 59.8 (C^{11}), 54.7 (C^{13}), 32.9 (C^{2}), 30.4, 29.7, 29.6 (C^{5-8}), 29.5 (C^{4}), 27.9 (C^{9}), 26.9 (C^{10}), 25.9 (C^{3+14}), 24.6 (C^{15}).

11-morpholinoundecan-1-ol (P18)

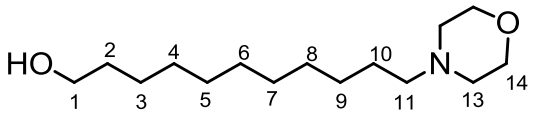

Methyl 11-morpholinoundecanoate **P14** (0.92 g, 3.22 mmol) in 3 mL of dry tetrahydrofuran was added dropwise with a syringe via a septum to a mixture of lithium aluminium hydride (0.62 g, 16.12 mmol) in dry tetrahydrofuran (13 mL) in a two necked round bottom flask, while stirring under an inert atmosphere. The reaction mixture was refluxed for 19 hours and cooled to room temperature. An excess of the lithium aluminium hydride was quenched by careful addition of sodium sulfate decahydrate, while stirred in an ice bath until the reaction mixture turned white. The white precipitate of lithium hydroxide was filtered off on a glass frit and washed with tetrahydrofuran. The organic phase was dried over magnesium sulfate, filtered and solvent evaporated in vacuo to give the product as a pale yellow solid (0.82 g, 3.19 mmol, 98%). The NMR data match those published. [7]

^{1}H NMR (500 MHz, $CDCl_3$, TMS) δ/ppm 3.83 (br s, 4H, H^{14}), 3.57 (m, 2H, H^{1}), 2.62 (br s, 4H, H^{13}), 2.50 (m, 2H, H^{11}), 1.58 (m, 4H, H^{2+10}), 1.30 (m, 14H, H^{3-9}).

5-(Diethylamino)pentan-1-ol (P19)

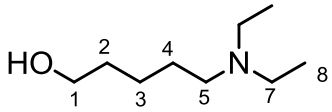

Methyl 5-(diethylamino)pentanoate **P15** (2.00 g, 10.68 mmol) in 5 mL of dry tetrahydrofuran was added dropwise with a syringe via a septum to a mixture of lithium aluminium hydride

(2.03 g, 53.40 mmol) in dry tetrahydrofuran (35 mL) in a 100mL two necked round bottom flask, while stirring under an inert atmosphere. The reaction mixture was refluxed for 16 hours and cooled to room temperature. This was poured to a 500mL round bottom flask and an excess of the lithium aluminium hydride was quenched by careful addition of sodium sulfate decahydrate, while stirred in an ice bath until the reaction mixture turned white. The white precipitate of lithium hydroxide was filtered off on a glass frit and washed with diethyl ether. The organic phase was dried over magnesium sulfate, filtered and solvent evaporated in vacuo to give the product as a yellowish oil (1.65 g, 10.36 mmol, 99%). The NMR data match those published. [7]

^{1}H NMR (400 MHz, $CDCl_3$, TMS) δ/ppm 3.64 (t, *J* = 6.4 Hz, 2H, H^1), 2.53 (q, *J* = 7.2 Hz, 4H, H^7), 2.43 (dd, *J* = 8.2, 6.5 Hz, 2H, H^5), 1.59 (m, 2H, H^2), 1.49 (m, 2H, H^4), 1.38 (m, 2H, H^3), 1.02 (t, *J* = 7.2 Hz, 6H, H^8).

Ligands

2,2':6',2''-Terpyridine (L1)

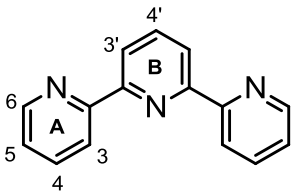

A nitrogen flushed 500 mL round-bottomed flask was charged with potassium tert-butoxide (10.04 g, 90.0 mmol) in 220 mL of dry tetrahydrofuran. To this solution 2-acetylpyridine (5.45 g, 45.0 mmol) was added and the reaction mixture was allowed to stir for 2 hours. Ketone **P1** (7.88 g, 45.0 mmol) was added in a single portion. The yellow solution, which gradually turned deep red, was allowed to stir for 20 hours at room temperature. Then the solution was slowly treated with an excess of ammonium acetate (35.0 g, 0.45 mol) and acetic acid (113 mL). The mixture produced fumes and the colour changed to dark orange-brown and it was left to stir

overnight. Tetrahydrofuran and acetic acid were partly removed in vacuo and the black-oil residue was treated with water (220 mL). Sodium carbonate was added slowly until the reaction mixture stopped producing bubbles. This was extracted with dichloromethane (5 times 200 mL). The organic phase was dried over anhydrous sodium sulfate and solvent removed in vacuo to give black oil. This was purified on a short column of alumina, eluted with toluene and solvent removed in vacuo, which afforded the product (3.30 g, 14.15 mmol, 32%) as a pale brown solid. The NMR data match those published.[1]

^{1}H NMR (400 MHz, $CDCl_3$, TMS) δ/ppm 8.71 (ddd, *J* = 4.8, 1.8, 0.9 Hz, 2H, H^{A6}), 8.63 (dt, *J* = 8.0, 1.0 Hz, 2H, H^{A3}), 8.46 (d, *J* = 7.8 Hz, 2H, H^{B3}), 7.96 (t, *J* = 7.8 Hz, 1H, H^{B4}), 7.86 (td, *J* = 7.7, 1.8 Hz, 2H, H^{A4}), 7.33 (ddd, *J* = 7.5, 4.8, 1.2 Hz, 2H, H^{A5}).

Methyl 4'-(pyridin-4-yl)-[2,2':6',2''-terpyridine]-4-carboxylate (L2)

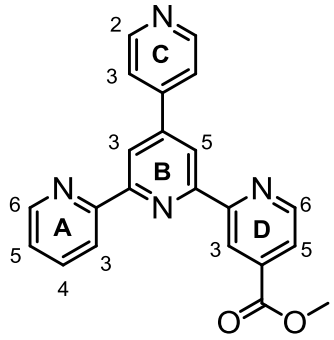

An excess of ammonium acetate (13 g, 160 mmol) was dissolved in methanol (150 mL). Chalcone **P9** (0.92 g, 4.38 mmol) and PPI salt **P5** (2.01 g, 5.25 mmol) were added and this brown suspension was heated at reflux for 7 hours and the solids slowly dissolved. The white precipitate which formed was collected on a glass frit, washed with cold methanol and diethyl ether, and air dried to give the product as a white powder (1.43 g, 3.88 mmol, 89%).

^{1}H NMR (500 MHz, $CDCl_3$, TMS) δ/ppm 9.15 (dd, *J* = 1.6, 0.9 Hz, 1H, H^{D3}), 8.86 (dd, *J* = 5.0, 0.9 Hz, 1H, H^{D6}), 8.78 (d, *J* = 1.7 Hz, 1H, H^{B3}), 8.76 (m, 3H, H^{C2+B5}), 8.72 (m, 2H, H^{A6+A3}), 7.92 (m, 2H, H^{A4+D5}), 7.80 (dd, *J* = 4.5, 1.7 Hz, 2H, H^{C3}), 7.39 (ddd, *J* = 7.5, 4.8, 1.3 Hz, 1H, H^{A5}), 4.04 (s, 3H, H^{Me}). **^{13}C {^{1}H} NMR** (126 MHz, $CDCl_3$) δ/ppm 165.9 ($C^{C=O}$), 156.9 (C^{D2}), 156.7 (C^{B2}), 155.6 (C^{B6}), 155.5 (C^{A2}), 150.6 (C^{C2}), 150.0 (C^{D6}), 149.3 (C^{A6}), 147.6 (C^{B4}), 145.9 (C^{C4}), 138.5 (C^{D4}), 137.2 (C^{A4}), 124.3 (C^{A5}), 123.2 (C^{D5}), 121.7 (C^{C3}), 121.6 (C^{A3}), 120.7 (C^{D3}), 119.1 (C^{B3}), 118.9 (C^{B5}), 53.0 (C^{Me}).

MP 216-217 °C (from MeOH). **ESI MS** (MeOH/$CHCl_3$): *m/z* 391.1 $[M+Na]^+$ (100%, calc. 391.1), 369.2 $[M+H]^+$ (16%, calc. 369.1). **IR** (solid, ν/cm^{-1}) 3020 (w), 2961 (w), 1731 (s), 1583 (m), 1559 (m), 1538 (m), 1533 (m), 1475 (m), 1436 (m), 1378 (m), 1309 (w), 1292 (w), 1270 (m), 1263 (w), 1218 (m), 1211 (m), 1130 (w), 973 (w), 895 (w), 821 (m), 795 (s), 770 (s), 736 (w), 682 (m), 669 (m), 660 (m), 618 (m), 533 (m). **UV/VIS** λ_{max}/nm (4.22×10^{-5} mol dm^{-3}, MeCN) 242 (ε / dm^3 mol^{-1} cm^{-1} 33000), 281 (16000), 316 (10000 sh). **EA** found: C, 70.96; H, 4.44; N, 15.19%. $C_{22}H_{16}N_4O_2\cdot0.25H_2O$ requires C, 70.86; H, 4.46; N, 15.02%.

4'-(Pyridin-4-yl)-2,2':6',2''-terpyridine (L3)

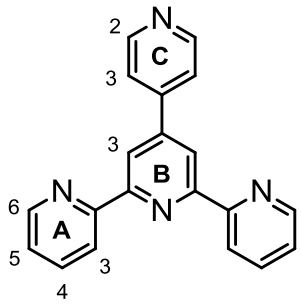

2-Acetylpyridine (4.89 g, 40.40 mmol) was mixed with a solution of pyridine-4-carboxaldehyde (2.16 g, 20.20 mmol) in ethanol (100 mL). Potassium hydroxide pellets (2.72 g, 48.50 mmol) and aqueous ammonia (30%, 0.86 g, 50.5 mmol) were added to the solution, which was allowed to stir for 4 hours at room temperature. The off-white solid, which formed, was collected by filtration and washed with ethanol. This was suspended in hot methanol and chloroform added until all the solid dissolved. Upon cooling in a freezer, white needle-like crystals (2.97 g, 9.58 mmol, 48%) were collected by filtration and washed with ethanol. The NMR data match those published.[8]

^{1}H NMR (400 MHz, $CDCl_3$, TMS) δ/ppm 8.77 (m, 4H, H^{B3+C2}), 8.73 (m, 2H, H^{A6}), 8.67 (d, *J* = 8.0 Hz, 2H, H^{A3}), 7.89 (td, *J* = 7.7, 1.8 Hz, 2H, H^{A4}), 7.82 (dd, *J* = 4.6, 1.7 Hz, 2H, H^{C3}), 7.38 (ddd, *J* = 7.5, 4.8, 1.1 Hz, 2H, H^{A5}). **UV/VIS** λ_{max}/nm (5.97×10^{-5} mol dm^{-3}, MeCN) 242 (ε / dm^3 mol^{-1} cm^{-1} 44000), 277 (29000), 314 (9000).

Ligand (L4)

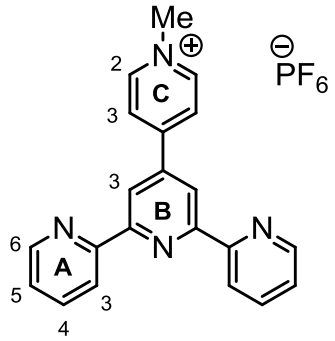

An excess of methyl iodide (2.74 g, 19.28 mmol) was added to a suspension of **L3** (0.50 g, 1.61 mmol) in acetonitrile (150 mL) and the reaction mixture was heated at reflux for 7 hours, while **L3** slowly dissolved and a yellow precipitate formed. This was then cooled to the room temperature and 2/3 of solvent removed in vacuo. An aqueous solution of ammonium hexafluorophosphate was added to this solution with the dark yellow precipitate, which turned bright yellow and was left in a freezer, then collected on a frit, washed with water, ethanol and diethyl ether and air dried to give the product as a yellow powder (0.62 g, 1.31 mmol, 81%). The NMR data match those published.[9]

^{1}H NMR (500 MHz, DMSO-d_6) δ/ppm 9.15 (d, J = 6.3 Hz, 2H, H^{C2}), 8.89 (s, 2H, H^{B3}), 8.79 (d, J = 4.2 Hz, 2H, H^{A6}), 8.76 (d, J = 6.4 Hz, 2H, H^{C3}), 8.69 (d, J = 7.9 Hz, 2H, H^{A3}), 8.07 (t, J = 7.6 Hz, 2H, H^{A4}), 7.58 (m, 2H, H^{A5}), 4.44 (s, 3H, H^{NMe}).

Ligand (L5)

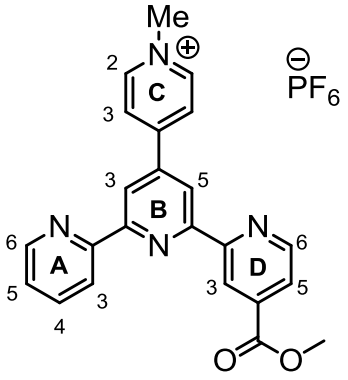

An excess of methyl iodide (2.74 g, 19.28 mmol) was added to a white suspension of **L2** (0.59 g, 1.61 mmol) in acetonitrile (130 mL) and the reaction mixture was heated at reflux for 13 hours,

while **L2** slowly dissolved. This was then cooled to room temperature and 2/3 of solvent removed in vacuo, giving a precipitate. The dark yellow suspension was mixed with an aqueous solution of ammonium hexafluorophosphate. The rest of the acetonitrile was removed in vacuo from the green solution, while an olive-green precipitate formed. This was collected on a frit, washed with water, ethanol and diethyl ether and air dried to give the product as a pale olive-green powder (0.79 g, 1.50 mmol, 93%).

^{1}H NMR (500 MHz, DMSO-d_6) δ/ppm 9.16 (d, J = 6.7 Hz, 2H, H^{C2}), 9.00 (m, 2H, H^{D3+D6}), 8.94 (s, 1H, H^{B3}), 8.93 (s, 1H, H^{B5}), 8.80 (m, 3H, H^{A6+C3}), 8.60 (d, J = 7.9 Hz, 1H, H^{A3}), 8.13 (td, J = 7.8, 1.6 Hz, 1H, H^{A4}), 8.01 (dd, J = 4.7, 1.5 Hz, 1H, H^{D5}), 7.61 (ddd, J = 7.7, 4.8, 1.2 Hz, 1H, H^{A5}), 4.43 (s, 1H, H^{NMe}), 4.00 (s, 1H, H^{OMe}). **^{13}C {^{1}H} NMR** (126 MHz, DMSO-d_6) δ/ppm 165.1 ($C^{C=O}$), 156.7 (C^{B2}), 156.5 (C^{B6}), 155.5 (C^{D2}), 154.1 (C^{A2}), 150.0 (C^{C4}), 150.8 (C^{D6}), 149.5 (C^{A6}), 142.0 (C^{C2}), 144.0 (C^{B4}), 138.5 (C^{D4}), 137.9 (C^{A4}), 125.6 (C^{C3}), 125.2 (C^{A5}), 123.6 (C^{D5}), 121.1 (C^{A3}), 119.6 (C^{D3}), 118.9, 119.4 (C^{B3}), 119.1 (C^{B5}), 53.1 (C^{OMe}), 47.6 (C^{NMe}). **MP** 225 °C. **ESI MS** (MeOH/$CHCl_3$): m/z 383.2 $[M\text{-}PF_6]^+$ (100%, calc. 383.2). **IR** (solid, ν/cm^{-1}) 3105 (w), 1725 (m), 1643 (w), 1553 (w), 1518 (w), 1440 (w), 1383 (w), 1294 (m), 1276 (m), 1230 (w), 1191 (w), 975 (w), 876 (m), 830 (s), 799 (s), 772 (m), 699 (m), 618 (w), 555 (s). **UV/VIS** λ_{max}/nm (3.93×10^{-5} mol dm^{-3}, MeCN) 255 (ε/dm^3 mol^{-1} cm^{-1} 30000), 276 (24000 sh), 333 (4000 sh). **EA** found: C, 48.33; H, 3.86; N, 9.93%. $C_{23}H_{19}N_4O_2P\cdot2.5H_2O$ requires C, 48.17; H, 4.22; N, 9.77%.

4-Chloro-4'-(pyridin-4-yl)-2,2':6',2''-terpyridine (L6)

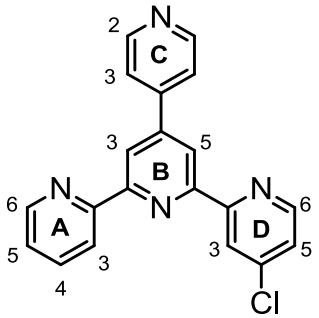

An excess of ammonium acetate (6.0 g, 77.92 mmol) was dissolved in methanol (60 mL). Chalcone **P9** (0.73 g, 3.46 mmol) and PPI salt **P6** (1.40 g, 3.88 mmol) were added and this black suspension was heated at reflux for 6 hours, while all slowly dissolved. Then the reaction

mixture was cooled to room temperature and placed in the freezer overnight. The brown precipitate which formed was collected on a glass frit, washed with cold methanol and diethyl ether and air dried to give the product as a brown powder (1.10 g, 3.19 mmol, 92%). **^{1}H NMR** (500 MHz, $CDCl_3$, TMS) δ/ppm 8.78 (d, *J* = 1.7 Hz, 1H, H^{B3}), 8.77 (dd, *J* = 4.4, 1.7 Hz, 2H, H^{C2}), 8.73 (m, 2H, H^{A6+B5}), 8.66 (m, 2H, H^{A3+D3}), 8.61 (dd, *J* = 5.2, 0.5 Hz, 1H, H^{D6}), 7.92 (td, *J* = 7.9, 1.8 Hz, 1H, H^{A4}), 7.78 (dd, *J* = 4.5, 1.7 Hz, 2H, H^{C3}), 7.39 (m, 2H, H^{A5+D5}). **^{13}C {^{1}H} NMR** (126 MHz, $CDCl_3$) δ/ppm 157.3 (C^{D2}), 156.7 (C^{B2}), 155.5 (C^{A2}), 155.2 (C^{B6}), 150.6 (C^{C2}), 150.2 (C^{D6}), 149.4 (C^{A6}), 147.7 (C^{B4}), 146.0 (C^{C4}), 145.4 (C^{D4}), 137.3 (C^{A4}), 124.4 (C^{A5+D5}), 121.9 (C^{C3}), 121.8 (C^{D3}), 121.6 (C^{A3}), 119.4 (C^{B3}), 119.1 (C^{B5}). **MP** at 210 °C decomposes. **ESI MS** ($MeOH/CHCl_3$): *m/z* 367.1 $[M+Na]^+$ (100%, calc. 367.1), 345.1 $[M+H]^+$ (86%, calc. 345.1). **IR** (solid, ν/cm^{-1}) 3051 (w), 1705 (s), 1584 (m), 1568 (s), 1554 (s), 1533 (s), 1464 (m), 1323 (w), 1261 (w), 1230 (w), 1064 (w), 988 (m), 875 (m), 815 (s), 788 (s), 733 (s), 673 (m), 659 (m), 619 (s), 582 (m). **UV/VIS** λ_{max}/nm (4.08×10^{-5} mol dm^{-3}, MeCN) 244 (ε / dm^3 mol^{-1} cm^{-1} 38000), 276 (21000), 313 (8000). **EA** found: C, 63.05; H, 3.75; N, 15.04%. $C_{20}H_{13}ClN_4 \cdot 2H_2O$ requires C, 63.08; H, 4.50; N, 14.71%.

4-Methyl-4'-(pyridin-4-yl)-2,2':6',2''-terpyridine (L7)

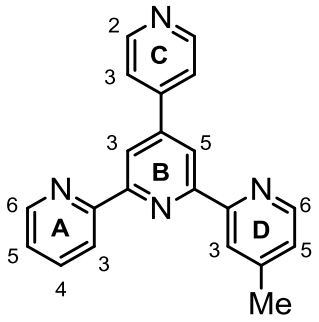

An excess of ammonium acetate (1.52 g, 19.71 mmol) was dissolved in methanol (13 mL). Chalcone **P10** (0.17 g, 0.76 mmol) and PPI salt **P8** (0.30 g, 0.91 mmol) were added and this brown suspension was heated to reflux for 6 hours, while all slowly dissolved. Then the reaction mixture was cooled to room temperature, filtered on a glass frit and the brown filtrate placed in the freezer overnight. The pale brown precipitate which formed was collected on a glass frit, washed with cold methanol and diethyl ether and air dried to give the product as a pale brown powder (0.20 g, 0.62 mmol, 93%).

^{1}H NMR (500 MHz, $CDCl_3$, TMS) δ/ppm 8.74 (dd, *J* = 4.5, 1.7 Hz, 2H, H^{C2}), 8.72 (m, 3H, $H^{B3+B5+A6}$), 8.66 (dt, *J* = 8.0, 1.1 Hz, 1H, H^{A3}), 8.56 (d, *J* = 4.9 Hz, 1H, H^{D6}), 8.45 (br s, 1H, H^{D3}), 7.88 (td, *J* = 7.7, 1.8 Hz, 1H, H^{A4}), 7.76 (dd, *J* = 4.5, 1.7 Hz, 1H, H^{C3}), 7.35 (ddd, *J* = 7.4, 4.7, 1.2 Hz, 1H, H^{A5}), 7.17 (m, 1H, H^{D5}), 2.49 (s, 3H, H^{Me}). **^{13}C {^{1}H} NMR** (126 MHz, $CDCl_3$) δ/ppm 156.7 (C^{B6}), 156.4 (C^{B2}), 155.8 (C^{A2}), 155.6 (C^{D2}), 150.6 (C^{C2}), 149.3 (C^{A6}), 149.1 (C^{D6}), 148.2 (C^{D4}), 147.5 (C^{B4}), 146.1 (C^{C4}), 137.1 (C^{A4}), 125.2 (C^{D5}), 124.2 (C^{A5}), 122.2 (C^{D3}), 121.8 (C^{C3}), 121.5 (C^{A3}), 118.9, 118.7 (C^{B3+B5}), 21.5 (C^{Me}). **MP** 173-174 °C (from MeOH). **MALDI TOF MS**: *m/z* 324.90 $[M]^+$ (78%, calc. 324.2). **IR** (solid, ν/cm^{-1}) 3052 (w), 2877 (w), 1747 (w), 1711 (w), 1582 (m), 1564 (w), 1469 (w), 1412 (w), 1379 (m), 1327 (m), 1227 (w), 1063 (w), 995 (m), 890 (w), 820 (s), 876 (s), 691 (m), 668 (s), 660 (m), 619 (s). **UV/VIS** λ_{max}/nm (4.80×10^{-5} mol dm^{-3}, MeCN) 243 (ε / dm^3 mol^{-1} cm^{-1} 50000), 277 (31000), 315 (11000). **EA** found: C, 76.91; H, 4.93; N, 17.54%. $C_{21}H_{16}N_4 \cdot 1/4H_2O$ requires C, 76.69; H, 5.06; N, 17.04%.

4'-(Pyridin-4-yl)-[2,2':6',2''-terpyridine]-4-carboxylic acid (L8)

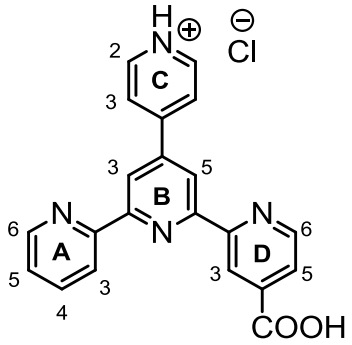

Methyl 4'-(pyridin-4-yl)-[2,2':6',2''-terpyridine]-4-carboxylate **L2** (0.15 g, 0.41 mmol) was suspended in hot methanol (4.5 mL). Then aqueous sodium hydroxide (1M, 0.81 mL, 0.81 mmol) was added and the reaction mixture was heated at reflux for 20 hours, while the milky white suspension turned to pale brown solution. This was cooled to room temperature and acidified with hydrochloric acid (0.5M) to pH~4. The white precipitate which formed was collected on a glass frit, washed thoroughly with water and air dried to give the product as an off-white powder (0.14 g, 0.40 mmol, 97%).

^{1}H NMR (500 MHz, DMSO-d_6) δ/ppm 13.93 (br s, 1H, OH), 9.04 (dd, *J* = 1.5, 0.8 Hz, 1H, H^{D3}), 9.02 (d, *J* = 6.5 Hz, 2H, H^{C2}), 8.98 (dd, *J* = 4.9, 0.8 Hz, 1H, H^{D6}), 8.91 (d, *J* = 1.6 Hz, 1H, H^{B3}), 8.90 (d, *J* =

1.7 Hz, 1H, H^{B5}), 8.83 (dd, *J* = 4.8, 0.8 Hz, 1H, H^{A6}), 8.67 (d, *J* = 7.9 Hz, 1H, H^{A3}), 8.48 (d, *J* = 5.0 Hz, 2H, H^{C3}), 8.20 (td, *J* = 7.8, 1.6 Hz, 1H, H^{A4}), 7.99 (dd, *J* = 4.9, 1.6 Hz, 1H, H^{D5}), 7.65 (dd, *J* = 7.4, 4.9 Hz, 1H, H^{A5}). **^{13}C {^{1}H} NMR** (126 MHz, DMSO-d_6) δ/ppm 166.5 ($C^{C=O}$), 156.1 (C^{B2+B6}), 155.9 (C^{D2}), 154.1 (C^{A2}), 151.3 (C^{C4}), 151.1 (C^{D6}), 149.5 (C^{A6}), 146.0 (C^{B4}), 145.5 (C^{C2}), 140.2 (C^{D4}), 139.2 (C^{A4}), 125.7 (C^{A5}), 124.7 (C^{C3}), 124.3 (C^{D5}), 121.9 (C^{A3}), 120.4 (C^{D3}), 119.8 (C^{B3+B5}). **MP** >350 °C. **MALDI TOF MS**: *m/z* 780.2 $[2M]^+$ (100%, calc. 780.2), 354.9 $[M]^+$ (5%, 354.1, neutral form). **IR** (solid, ν/cm^{-1}) 3378 (s), 1703 (m), 1586 (m), 1557 (m), 1468 (w), 1383 (w), 1287 (w), 1218 (w), 1069 (w), 829 (m), 791 (w), 770 (w), 667 (m), 629 (m), 567 (s), 519 (s). **EA** found: C, 59.50; H, 4.22; N, 13.59%. $C_{21}H_{15}ClN_4O_2 \cdot 2H_2O$ requires C, 59.09; H, 4.49; N, 13.13%.

Ligand (L9)

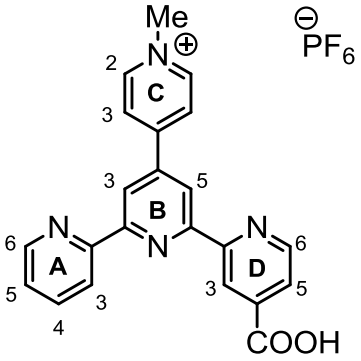

Ligand **L5** (0.22 g, 0.41 mmol) was suspended in hot methanol (3 mL). Then aqueous sodium hydroxide (1M, 0.81 mL, 0.81 mmol) was added and the reaction mixture was heated at reflux for 22 hours, while the greenish suspension turned to dark red-brown solution. This was cooled to the room temperature and acidified with hydrochloric acid (0.5M) to pH~4. The brown precipitate which formed was collected on a glass frit, washed thoroughly with water, suspended in an aqueous solution of ammonium hexafluorophosphate, collected again on a frit, washed with water and air dried to give the product as a brown powder (73 mg, 0.14 mmol, 35%).

^{1}H NMR (500 MHz, DMSO-d_6) δ/ppm 9.14 (br s, 2H, H^{C2}), 8.88 (m, 4H, $H^{A6+B3+B5+D3}$), 8.74 (m, 3H, H^{C3+D6}), 8.56 (m, 1H, H^{A3}), 8.07 (m, 1H, H^{A4}), 7.93 (br s, 1H, H^{D5}), 7.56 (m, 1H, H^{A5}), 4.42 (s, 3H, H^{Me}). **^{13}C {^{1}H} NMR** (126 MHz, DMSO-d_6) δ/ppm 166.8 ($C^{C=O}$), 150.1 (C^{D6}), 150.8 (C^{A6}), 146.8 (C^{C2}), 138.2 (C^{A4}), 125.8 (C^{C3}), 125.4 (C^{A5}), 124.2 (C^{D5}), 121.4 (C^{A3}), 119.4 (C^{D3}), 120.4 (C^{B3+B5}),

48.0 (C^{NMe}), (C^{q} were not observed due to the poor solubility of the ligand). **MP** at 210 °C decomposes. **MALDI TOF MS**: *m/z* 368.8 $[M\text{-}PF_6]^+$ (84%, calc. 369.1), 324.7 $[M\text{-}PF_6\text{-}CO_2]^+$ (24%, calc. 324.8). **IR** (solid, ν/cm^{-1}) 3073 (s), 1717 (m), 1588 (m), 1548 (m), 1369 (m), 1225 (w), 1076 (m), 835 (s), 784 (m), 775 (m), 663 (m).

Dodecyl 4'-(pyridin-4-yl)-[2,2':6',2''-terpyridine]-4-carboxylate (L10)

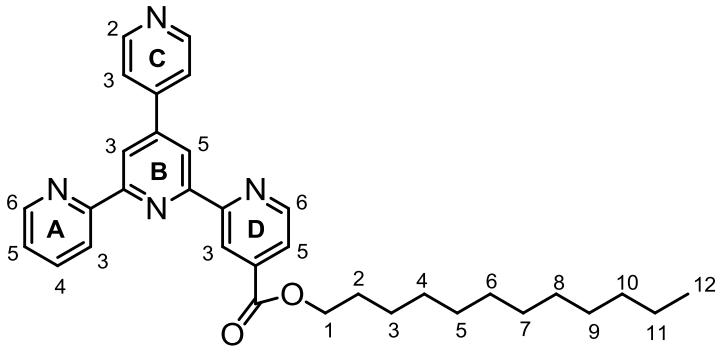

4'-(Pyridin-4-yl)-[2,2':6',2''-terpyridine]-4-carboxylic acid **L8** (0.11 g, 0.31 mmol) was refluxed in an excess of thionyl chloride (14 mL) under an inert atmosphere for 4 hours, and it became a yellow solution. This was cooled to room temperature and thionyl chloride evaporated to give 4'-(pyridin-4-yl)-[2,2':6',2''-terpyridine]-4-carbonyl chloride as a yellow powder, which was used in the next step without further purification and characterization. This was refluxed with triethylamine (63 mg, 0.62 mmol) in toluene (9 mL) under an inert atmosphere for 30 minutes to give a greenish suspension. Then dodecanol (0.12 g, 0.62 mmol) was added. The reaction mixture turned dark brown and was refluxed for 15 hours. Then solvent was removed in vacuo and the brown residue dissolved in chloroform and extracted with an aqueous solution of sodium hydrogencarbonate and then with water. The organic phase was dried over sodium sulfate, filtered and evaporated to give a dark brown solid, which was recrystallized from cold mixture of ethanol - diethyl ether to afford the product as an off-white powder (0.12 g, 0.23 mmol, 75%).

^{1}H NMR (500 MHz, $CDCl_3$, TMS) δ/ppm 9.17 (d, *J* = 1.5 Hz, 1H, H^{D3}), 8.86 (d, *J* = 4.9 Hz, 1H, H^{D6}), 8.79 (d, *J* = 1.8 Hz, 1H, H^{B3}), 8.77 (d, *J* = 1.8 Hz, 1H), 8.76 (m, 3H, H^{C2+B5}), 8.73 (m, 1H, H^{A6}), 8.72 (d, *J* = 7.8 Hz, 1H, H^{A3}), 7.91 (m, 2H, H^{D5+A4}), 7.78 (dd, *J* = 4.5, 1.6 Hz, 2H, H^{C3}), 7.38 (m, 1H, H^{A5}), 4.43 (t, *J* = 6.6 Hz, 2H, H^1), 1.84 (m, 2H, H^2), 1.51 (m, 2H, H^3), 1.40 (m, 2H, H^4), 1.29 (m, 14H, H^{5-}

^{11}), 0.86 (t, *J* = 6.9 Hz, 3H, H^{12}). **^{13}C {^{1}H} NMR** (126 MHz, $CDCl_3$) δ/ppm 165.5 ($C^{C=O}$), 157.0 (C^{D2}), 156.7 (C^{B2}), 155.7 (C^{B6}), 155.6 (C^{A2}), 150.7 (C^{C2}), 150.0 (C^{D6}), 149.3 (C^{A6}), 147.7 (C^{C4}), 145.9 (C^{B4}), 139.0 (C^{D4}), 137.2 (C^{A4}), 124.4 (C^{A5}), 123.2 (C^{D5}), 121.8 (C^{C3}), 121.6 (C^{A3}), 120.9 (C^{D3}), 119.2 (C^{B5}), 118.9 (C^{B3}), 66.1 (C^{1}), 32.0 (C^{10}), 29.8, 29.7, 29.5 (C^{5-9}), 29.4 (C^{4}), 28.8 (C^{2}), 26.2 (C^{3}), 22.8 (C^{11}), 14.3 (C^{12}). **MP** 97-98 °C (from EtOH-Et_2O). **ESI MS** (MeOH/CH_2Cl_2): *m/z* 561.3 $[M+K]^+$ (27%, calc. 561.3), 545.4 $[M+Na]^+$ (100%, calc. 545.4), 523.4 $[M+H]^+$ (45%, calc. 523.3). **IR** (solid, ν/cm^{-1}) 3063 (w), 2951 (w), 2914 (s), 2850 (m), 1733 (s), 1584 (s), 1560 (m), 1533 (m), 1471 (m), 1381 (m), 1347 (w), 1290 (m), 1285 (m), 1269 (s), 1217 (m), 1210 (m), 1134 (w), 1127 (w), 1105 (w), 964 (w), 890 (w), 816 (s), 788 (s), 770 (s), 730 (s), 716 (m), 684 (s), 669 (m), 660 (s), 621 (m), 519 (s). **UV/VIS** λ_{max}/nm (4.39×10^{-5} mol dm^{-3}, MeCN) 243 (ε / dm^3 mol^{-1} cm^{-1} 38000), 281 (19000), 317 (11000 sh). **EA** found: C, 75.09; H, 7.25; N, 10.81%. $C_{33}H_{38}N_4O_2\cdot0.5H_2O$ requires C, 74.55; H, 7.39; N, 10.54%.

11-(Diethylamino)undecyl 4'-(pyridin-4-yl)-[2,2':6',2''-terpyridine]-4-carboxylate (L11)

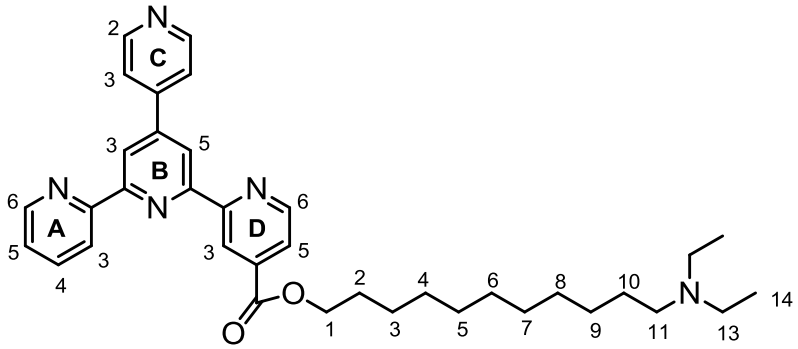

4'-(Pyridin-4-yl)-[2,2':6',2''-terpyridine]-4-carboxylic acid **L8** (0.11 g, 0.31 mmol) was refluxed in an excess of thionyl chloride (14 mL) under an inert atmosphere for 4 hours, and it became a yellow solution. This was cooled to room temperature and thionyl chloride evaporated to give 4'-(pyridin-4-yl)-[2,2':6',2''-terpyridine]-4-carbonyl chloride as a yellow powder, which was used in the next step without further purification and characterization. This was refluxed with triethylamine (63 mg, 0.62 mmol) in toluene (9 mL) under an inert atmosphere for 30 minutes to give a greenish suspension. Then 11-(diethylamino)undecan-1-ol **P16** (0.12 g, 0.47 mmol) was added. The reaction mixture turned dark brown and was refluxed for 15 hours. Then solvent was removed in vacuo and the brown residue dissolved in chloroform and extracted

with an aqueous solution of sodium hydrogencarbonate and then with water. The organic phase was dried over sodium sulfate, filtered and evaporated to give a dark brown solid, which was purified with column chromatography (SiO_2, eluted with EtOAc/MeOH/Et_3N = 30:2:1) and afforded the product as a pale brown solid (0.11 g, 0.19 mmol, 63%).

^{1}H NMR (500 MHz, $CDCl_3$, TMS) δ/ppm 9.17 (dd, *J* = 1.6, 0.9 Hz, 1H, H^{D3}), 8.85 (dd, *J* = 5.0, 0.9 Hz, 1H, H^{D6}), 8.79 (d, *J* = 1.7 Hz, 1H, H^{B3}), 8.76 (m, 3H, H^{B5+C2}), 8.72 (ddd, *J* = 4.8, 1.8, 0.9 Hz, 1H, H^{A6}), 8.70 (dt, *J* = 8.0, 1.1 Hz, 1H, H^{A3}), 7.89 (m, 2H, H^{A4+D5}), 7.78 (dd, *J* = 4.5, 1.7 Hz, 2H, H^{C3}), 7.38 (ddd, *J* = 7.5, 4.7, 1.2 Hz, 1H, H^{A5}), 4.42 (t, *J* = 6.7 Hz, 2H, H^1), 2.53 (q, *J* = 7.1 Hz, 4H, H^{13}), 2.40 (m, 2H, H^{11}), 1.83 (m, 2H, H^2), 1.50 (m, 2H, H^3), 1.39 (m, 4H, H^{4+10}), 1.28 (m, 10H, H^{5-9}), 1.01 (t, *J* = 7.2 Hz, 6H, H^{14}). **^{13}C {^{1}H} NMR** (126 MHz, $CDCl_3$) δ/ppm 165.5 ($C^{C=O}$), 157.0 (C^{D2}), 156.7 (C^{B2}), 155.7 (C^{B6}), 155.6 (C^{A2}), 150.7 (C^{C2}), 150.0 (C^{D6}), 149.3 (C^{A6}), 147.7 (C^{C4}), 145.9 (C^{B4}), 139.0 (C^{D4}), 137.2 (C^{A4}), 124.4 (C^{A5}), 123.2 (C^{D5}), 121.8 (C^{C3}), 121.6 (C^{A3}), 120.9 (C^{D3}), 119.2 (C^{B5}), 118.9 (C^{B3}), 66.2 (C^1), 53.0 (C^{11}), 46.9 (C^{13}), 29.7 (C^{5-8}), 29.4 (C^4), 28.8 (C^2), 27.8 (C^9), 26.9 (C^{10}), 26.2 (C^3), 11.6 (C^{14}). **ESI MS** (MeOH/CH_2Cl_2): *m/z* 580.4 $[M+H]^+$ (100%, calc. 580.4). **IR** (solid, ν/cm^{-1}) 3060 (w), 2921 (s), 2853 (m), 2798 (w), 1725 (s), 1592 (m), 1584 (s), 1560 (m), 1533 (m), 1470 (m), 1380 (s), 1324 (w), 1287 (m), 1268 (s), 1217 (s), 1209 (s), 1131 (m), 1096 (w), 987 (w), 896 (w), 815 (s), 788 (s), 769 (s), 730 (s), 684 (m), 660 (s), 621 (s), 507 (s). **UV/VIS** λ_{max}/nm (3.83×10^{-5} mol dm^{-3}, MeCN) 242 (ε / dm^3 mol^{-1} cm^{-1} 52000), 281 (25000), 316 (15000 sh). **EA** found: C, 74.26; H, 7.94; N, 11.89%. $C_{36}H_{45}N_5O_2$ requires C, 74.58; H, 7.82; N, 12.08%.

2-(2-(2-Ethoxyethoxy)ethoxy)ethyl 4'-(pyridin-4-yl)-[2,2':6',2''-terpyridine]-4-carboxylate (L12)

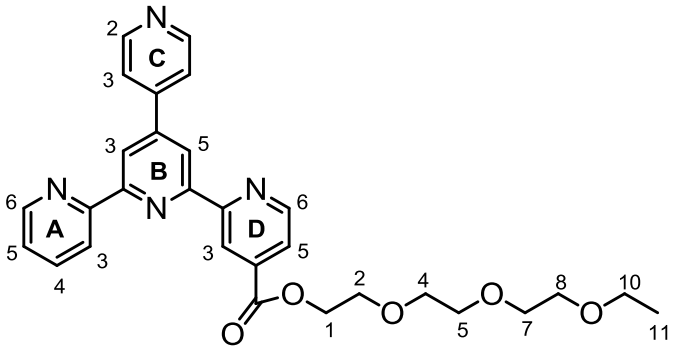

4'-(Pyridin-4-yl)-[2,2':6',2''-terpyridine]-4-carboxylic acid **L8** (0.11 g, 0.31 mmol) was refluxed in an excess of thionyl chloride (14 mL) under an inert atmosphere for 4 hours, and it became a yellow solution. This was cooled to the room temperature and thionyl chloride evaporated to give 4'-(pyridin-4-yl)-[2,2':6',2''-terpyridine]-4-carbonyl chloride as a yellow powder, which was used in the next step without further purification and characterization. This was refluxed with triethylamine (63 mg, 0.62 mmol) in toluene (8 mL) under an inert atmosphere for 30 minutes to give a greenish suspension. Then triethylene glycol monoethyl ether (87 mg, 0.47 mmol) was added. The reaction mixture turned dark brown and was refluxed for 16 hours. Then solvent was removed in vacuo and the brown residue dissolved in chloroform and extracted with an aqueous solution of sodium hydrogencarbonate and then with water. The organic phase was dried over sodium sulfate, filtered and evaporated to give a dark brown solid, which was purified with column chromatography (SiO_2, eluted with EtOAc/MeOH/Et_3N = 30:2:1) and afforded the product as a pale brown solid (87 mg, 0.17 mmol, 54%).

^{1}H NMR (500 MHz, $CDCl_3$, TMS) δ/ppm 9.15 (dd, *J* = 1.6, 0.9 Hz, 1H, H^{D3}), 8.84 (dd, *J* = 5.0, 0.9 Hz, 1H, H^{D6}), 8.77 (d, *J* = 1.7 Hz, 1H, H^{B3}), 8.76 (dd, *J* = 4.5, 1.7 Hz, 2H, H^{C2}), 8.74 (d, *J* = 1.7 Hz, 1H, H^{B5}), 8.71 (ddd, *J* = 4.8, 1.8, 0.9 Hz, 1H, H^{A6}), 8.68 (dt, *J* = 7.9, 1.1 Hz, 1H, H^{A3}), 7.90 (m, 2H, H^{D5+A4}), 7.79 (dd, *J* = 4.5, 1.7 Hz, 2H, H^{C3}), 7.37 (ddd, *J* = 7.5, 4.8, 1.2 Hz, 1H, H^{A5}), 4.58 (m, 2H, H^1), 3.90 (m, 2H, H^2), 3.75 (m, 2H, H^4), 3.68 (m, 2H, H^5), 3.63 (m, 3H, H^7), 3.54 (m, 2H, H^8), 3.47 (q, *J* = 7.0 Hz, 2H, H^{10}), 1.16 (t, *J* = 7.0 Hz, 3H, H^{11}). **^{13}C {^{1}H} NMR** (126 MHz, $CDCl_3$) δ/ppm 165.4 ($C^{C=O}$), 156.9 (C^{D2}), 156.7 (C^{B2}), 155.7 (C^{B6}), 155.5 (C^{A2}), 150.4 (C^{C2}), 150.0 (C^{D6}), 149.3 (C^{A6}), 147.5 (C^{C4}), 146.2 (C^{B4}), 138.6 (C^{D4}), 137.3 (C^{A4}), 124.4 (C^{A5}), 123.3 (C^{D5}), 121.9 (C^{C3}), 121.6 (C^{A3}), 120.9 (C^{D3}), 119.2 (C^{B3}), 118.9 (C^{B5}), 70.9 (C^4), 70.8 (C^5), 70.7 (C^7), 69.9 (C^8), 69.1 (C^2), 66.7 (C^{10}), 65.1 (C^1), 15.2 (C^{11}). **ESI MS** (MeOH/$CHCl_3$): *m/z* 553.2 $[M+K]^+$ (27%, calc. 553.2), 537.3 $[M+Na]^+$ (100%, calc. 537.2), 515.3 $[M+H]^+$ (28%, calc. 515.2). **IR** (solid, ν/cm^{-1}) 3413 (m), 3059 (w), 2966 (w), 2860 (m), 1723 (s), 1649 (s), 1583 (s), 1562 (s), 1535 (m), 1470 (m), 1447 (w), 1381 (s), 1348 (m), 1288 (m), 1268 (s), 1236 (w), 1209 (m), 1100 (s), 1078 (s), 1066 (m), 1033 (m), 945 (w), 815 (s), 789 (s), 769 (s), 730 (s), 621 (s), 588 (m), 522 (m). **UV/VIS** λ_{max}/nm (5.76×10^{-5} mol dm^{-3}, MeCN) 243 (ε / dm^3 mol^{-1} cm^{-1} 39000), 283 (31000). **EA** found: C, 65.51; H, 5.53; N, 11.06%. $C_{29}H_{30}N_4O_5\cdot0.75H_2O$ requires C, 65.40; H, 6.06; N, 10.52%.

11-(Piperidin-1-yl)undecyl 4'-(pyridin-4-yl)-[2,2':6',2''-terpyridine]-4-carboxylate (L13)

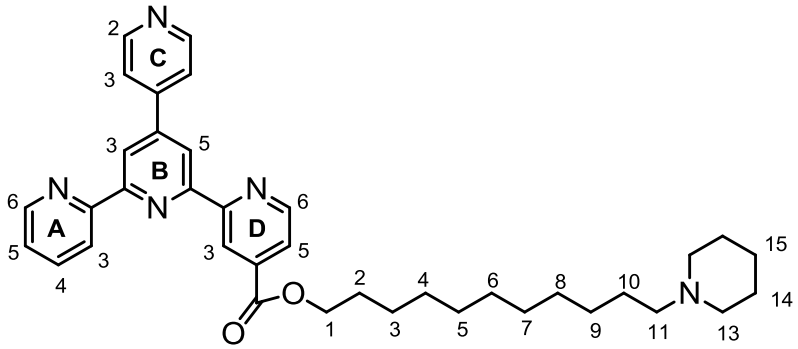

4'-(Pyridin-4-yl)-[2,2':6',2''-terpyridine]-4-carboxylic acid **L8** (0.52 g, 1.47 mmol) was refluxed in an excess of thionyl chloride (50 mL) under an inert atmosphere for 3 hours, and it became a yellow solution. This was cooled to the room temperature and thionyl chloride evaporated to give 4'-(pyridin-4-yl)-[2,2':6',2''-terpyridine]-4-carbonyl chloride as a yellow powder, which was used in the next step without further purification and characterization. This was refluxed with 2,6-lutidine (0.79 g, 7.34 mmol) in toluene (30 mL) under an inert atmosphere for 30 minutes to give a greenish suspension. Then 11-(piperidin-1-yl)undecan-1-ol **P17** (0.56 g, 2.20 mmol) was added. The reaction mixture turned dark brown and was refluxed for 17 hours. Then solvent was removed in vacuo and the brown residue dissolved in chloroform and extracted with aqueous sodium hydrogencarbonate and then with water. The organic phase was dried over sodium sulfate, filtered and evaporated to give a dark brown solid, which was purified with column chromatography (SiO_2, eluted with EtOAc/MeOH/Et_3N = 60:2:1) and afforded the product as a pale brown solid (0.45 g, 0.75 mmol, 52%).

^{1}H NMR (500 MHz, $CDCl_3$, TMS) δ/ppm 9.13 (s, 1H, H^{D3}), 8.82 (dd, *J* = 4.9, 0.9 Hz, 1H, H^{D6}), 8.76 (d, *J* = 1.7 Hz, 1H, H^{B3}), 8.74 (dd, *J* = 4.4, 1.7 Hz, 2H, H^{C2}), 8.72 (d, *J* = 1.7 Hz, 1H, H^{B5}), 8.70 (m, 1H, H^{A6}), 8.66 (d, *J* = 7.9 Hz, 1H, H^{A3}), 7.87 (m, 2H, H^{A4+D5}), 7.75 (dd, *J* = 4.5, 1.7 Hz, 2H, H^{C3}), 7.35 (ddd, *J* = 7.5, 4.8, 1.3 Hz, 1H, H^{A5}), 4.40 (t, *J* = 6.7 Hz, 2H, H^{1}), 2.36 (m, 4H, H^{13}), 2.26 (m, 2H, H^{11}), 1.81 (m, 2H, H^{2}), 1.56 (m, 4H, H^{14}), 1.47 (m, 4H, H^{3+10}), 1.38 (m, 4H, H^{4+15}), 1.25 (m, 10H, H^{5-9}).
^{13}C {^{1}H} NMR (126 MHz, $CDCl_3$) δ/ppm 165.4 ($C^{C=O}$), 156.9 (C^{D2}), 156.6 (C^{B2}), 155.6 (C^{B6}), 155.5 (C^{A2}), 150.8 (C^{C2}), 150.0 (C^{D6}), 149.3 (C^{A6}), 147.6 (C^{C4}), 145.8 (C^{B4}), 138.9 (C^{D4}), 137.1 (C^{A4}), 124.3 (C^{A5}), 123.1 (C^{D5}), 121.7 (C^{C3}), 121.5 (C^{A3}), 120.8 (C^{D3}), 119.1 (C^{B3}), 118.8 (C^{B5}), 66.10 (C^{1}), 59.6 (C^{11}), 54.7 (C^{13}), 29.7 (C^{5-8}), 29.4 (C^{4}), 28.7 (C^{2}), 27.8 (C^{9}), 26.8 (C^{10}), 26.1 (C^{3}), 25.9 (C^{14}), 24.4

(C^{15}). **MP** 90-91 °C. **ESI MS** (MeOH/$CHCl_3$): *m/z* 592.4 $[M+H]^+$ (100%, calc. 592.4). **IR** (solid, ν/cm^{-1}) 3060 (w), 2922 (s), 2851 (m), 1725 (s), 1676 (w), 1592 (m), 1583 (s), 1560 (m), 1533 (m), 1470 (m), 1380 (s), 1348 (w), 1324 (m), 1287 (m), 1268 (s), 1210 (s), 1127 (m), 1100 (m), 987 (w), 896 (w), 815 (s), 788 (s), 767 (s), 684 (m), 668 (s), 660 (s), 621 (m), 504 (s). **UV/VIS** λ_{max}/nm (4.13×10^{-5} mol dm^{-3}, MeCN) 242 (ε / dm^3 mol^{-1} cm^{-1} 60000), 281 (29000), 316 (17000 sh). **EA** found: C, 70.95; H, 7.02; N, 11.44%. $C_{37}H_{45}N_5O_2 \cdot 1/3CHCl_3$ requires C, 71.04; H, 7.24; N, 11.10%.

11-Morpholinoundecyl 4'-(pyridin-4-yl)-[2,2':6',2''-terpyridine]-4-carboxylate (L14)

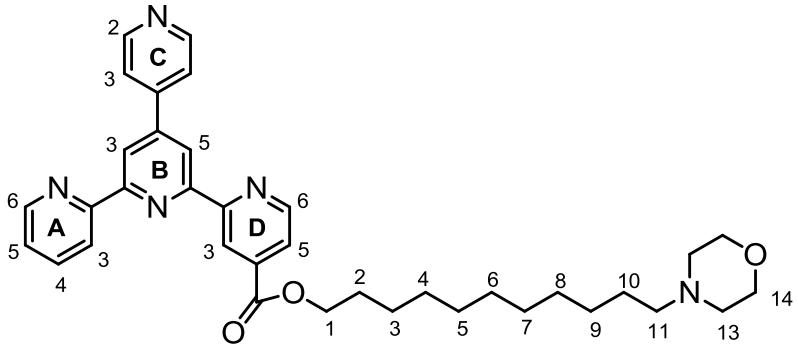

4'-(Pyridin-4-yl)-[2,2':6',2''-terpyridine]-4-carboxylic acid **L8** (0.30 g, 0.85 mmol) was refluxed in an excess of thionyl chloride (25 mL) under an inert atmosphere for 3 hours, and it became a yellow solution. This was cooled to the room temperature and thionyl chloride evaporated to give 4'-(pyridin-4-yl)-[2,2':6',2''-terpyridine]-4-carbonyl chloride as a yellow powder, which was used in the next step without further purification and characterization. This was refluxed with 2,6-lutidine (0.45 g, 4.23 mmol) in toluene (24 mL) under an inert atmosphere for 15 minutes to give a greenish suspension. Then 11-morpholinoundecan-1-ol **P18** (0.33 g, 1.27 mmol) was added. The reaction mixture turned dark brown and was refluxed for 17 hours. Then solvent was removed in vacuo and the brown residue dissolved in chloroform and extracted with an aqueous solution of sodium hydrogencarbonate and then with water. The organic phase was dried over sodium sulfate, filtered and evaporated to give a dark brown solid, which was purified with column chromatography (SiO_2, eluted with EtOAc/MeOH/Et_3N = 60:2:1) and afforded the product as a pale brown solid (0.24 g, 0.41 mmol, 45%).

^{1}H NMR (500 MHz, $CDCl_3$, TMS) δ/ppm 9.19 (dd, *J* = 1.6, 0.8 Hz, 1H, H^{D3}), 8.88 (dd, *J* = 5.0, 0.9 Hz, 1H, H^{D6}), 8.82 (d, *J* = 1.7 Hz, 1H, H^{B3}), 8.79 (m, 3H, H^{B5+C2}), 8.73 (m, 2H, H^{A3+A6}), 7.92 (m, 2H,

H^{A4+D5}), 7.80 (dd, *J* = 4.5, 1.7 Hz, 2H, H^{C3}), 7.40 (ddd, *J* = 7.5, 4.8, 1.2 Hz, 1H, H^{A5}), 4.44 (t, *J* = 6.7 Hz, 2H, H^{1}), 3.72 (br s, 4H, H^{14}), 2.43 (br s, 4H, H^{13}), 2.31 (br s, 2H, H^{11}), 1.85 (m, 2H, H^{2}), 1.50 (m, 2H, H^{3}), 1.41 (m, 2H, H^{10}), 1.27 (m, 12H, H^{4-9}). **^{13}C {^{1}H} NMR** (126 MHz, $CDCl_3$) δ/ppm δ/ppm 165.5 ($C^{C=O}$), 157.0 (C^{D2}), 156.6 (C^{B2}), 155.6 (C^{A2+B2}), 150.7 (C^{C2}), 150.1 (C^{D6}), 149.3 (C^{A6}), 147.6 (C^{B4}), 146.0 (C^{C4}), 139.0 (C^{D4}), 137.1 (C^{A4}), 124.4 (C^{A5}), 123.2 (C^{D5}), 121.8 (C^{C3}), 121.5 (C^{A3}), 120.9 (C^{D3}), 119.1 (C^{B3}), 118.9 (C^{B5}), 66.6 (C^{14}), 66.2 (C^{1}), 59.2 (C^{11}), 53.6 (C^{13}), 29.7, 29.6 (C^{4-8}), 28.9 (C^{2}), 27.4 (C^{9}), 26.2 (C^{10}), 26.1 (C^{3}). **MP** 89-90 °C. **ESI MS** (MeOH/$CHCl_3$): *m/z* 616.3 $[M+Na]^+$ (12%, calc. 616.3), 594.3 $[M+H]^+$ (100%, calc. 594.3). **IR** (solid, ν/cm^{-1}) 3060 (w), 2921 (s), 2852 (m), 1725 (s), 1660 (m), 1584 (s), 1560 (m), 1533 (m), 1467 (m), 1457 (m), 1380 (s), 1287 (m), 1268 (s), 1209 (s), 1116 (s), 1100 (m), 987 (w), 896 (w), 860 (s), 814 (m), 788 (s), 767 (s), 730 (s), 683 (m), 660 (s), 621 (m). **UV/VIS** λ_{max}/nm (3.99×10^{-5} mol dm^{-3}, MeCN) 243 (ε / dm^3 mol^{-1} cm^{-1} 51000), 281 (25000), 316 (15000 sh). **EA** found: C, 70.67; H, 6.78; N, 11.48%. $C_{36}H_{43}N_5O_3\cdot0.2CHCl_3$ requires C, 70.40; H, 7.05; N, 11.34%.

3-(Dimethylamino)propyl 4'-(pyridin-4-yl)-[2,2':6',2''-terpyridine]-4-carboxylate (L15)

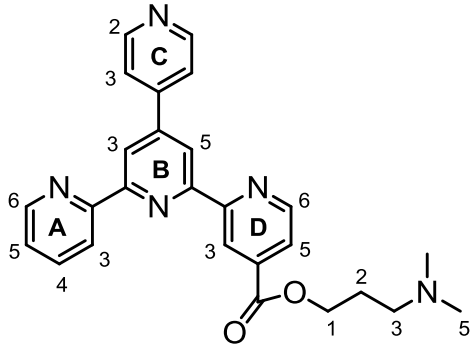

4'-(Pyridin-4-yl)-[2,2':6',2''-terpyridine]-4-carboxylic acid **L8** (0.40 g, 0.85 mmol) was refluxed in an excess of thionyl chloride (40 mL) under an inert atmosphere for 3 hours, and it became a yellow solution. This was cooled to room temperature and thionyl chloride evaporated to give 4'-(pyridin-4-yl)-[2,2':6',2''-terpyridine]-4-carbonyl chloride as a yellow powder, which was used in the next step without further purification and characterization. This was refluxed with 2,6-lutidine (0.61 g, 5.64 mmol) in toluene (23 mL) under an inert atmosphere for 30 minutes to give a greenish suspension. Then 3-dimethylamino-1-propanol (0.18 g, 1.69 mmol) was added.

The reaction mixture turned dark brown and was refluxed for 16 hours. Then solvent was removed in vacuo and the brown residue dissolved in chloroform and extracted with an aqueous solution of sodium hydrogencarbonate and then with water. The organic phase was dried over sodium sulfate, filtered and evaporated to give a dark brown solid, which was recrystallized from a mixture of cold ethanol – cyclohexane. This yielded the product as a pale brown powder (0.25 g, 0.57 mmol, 51%).

^{1}H NMR (500 MHz, $CDCl_3$, TMS) δ/ppm 9.16 (dd, *J* = 1.6, 0.9 Hz, 1H, H^{D3}), 8.87 (d, *J* = 4.9, 0.9 Hz, 1H, H^{D6}), 8.80 (d, *J* = 1.7 Hz, 1H, H^{B3}), 8.77 (m, 3H, H^{C2+B5}), 8.73 (ddd, *J* = 4.8, 1.8, 0.9 Hz, 1H, H^{A6}), 8.70 (dt, *J* = 7.9, 1.1 Hz, 1H, H^{A3}), 7.91 (m, 2H, H^{A4+D5}), 7.78 (dd, *J* = 4.5, 1.7 Hz, 2H, H^{C3}), 7.39 (ddd, *J* = 7.5, 4.8, 1.2 Hz, 1H, H^{A5}), 4.51 (t, *J* = 6.5 Hz, 2H, H^{1}), 2.59 (t, 2H, H^{3}), 2.36 (s, 6H, H^{5}), 2.08 (m, 2H, H^{2}). **^{13}C {^{1}H} NMR** (126 MHz, $CDCl_3$) δ/ppm 165.4 ($C^{C=O}$), 157.0 (C^{D2}), 156.8 (C^{B2}), 155.7 (C^{B6}), 155.6 (C^{A2}), 150.8 (C^{C2}), 150.1 (C^{D6}), 149.4 (C^{A6}), 147.7 (C^{C4}), 145.9 (C^{B4}), 138.8 (C^{D4}), 137.2 (C^{A4}), 124.4 (C^{A5}), 123.2 (C^{D5}), 121.8 (C^{C3}), 121.6 (C^{A3}), 120.8 (C^{D3}), 119.2 (C^{B3}), 119.0 (C^{B5}), 64.2 (C^{1}), 56.2 (C^{3}), 45.3 (C^{4}), 26.7 (C^{2}). **MP** 118-120 °C (from EtOH-cyclohexane). **ESI MS** (MeOH/$CHCl_3$): *m/z* 478.1 $[M+K]^+$ (8%, calc. 478.2), 462.1 $[M+Na]^+$ (4%, calc. 462.2), 440.2 $[M+H]^+$ (3%, calc. 440.2). **IR** (solid, ν/cm^{-1}) 3066 (w), 2957 (w), 2759 (w), 1720 (s), 1583 (m), 1538 (s), 1532 (m), 1471 (m), 1436 (w), 1380 (s), 1287 (w), 1266 (m), 1209 (m), 1132 (w), 1096 (w), 1038 (w), 895 (w), 814 (m), 788 (s), 769 (s), 730 (s), 684 (m), 668 (s), 660 (s), 619 (m). **UV/VIS** λ_{max}/nm (6.07×10^{-5} mol dm^{-3}, MeCN) 242 (ε / dm^3 mol^{-1} cm^{-1} 64000), 281 (33000), 316 (19000 sh). **EA** found: C, 65.33; H, 5.25; N, 14.95%. $C_{26}H_{25}N_5O_2\cdot0.35CHCl_3$ requires C, 65.76; H, 5.31; N, 14.55%.

5-(Diethylamino)pentyl 4'-(pyridin-4-yl)-[2,2':6',2''-terpyridine]-4-carboxylate (L16)

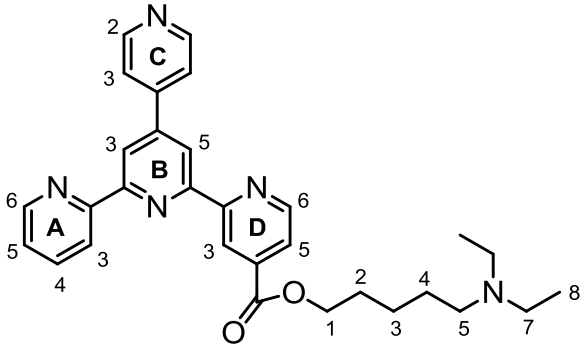

4'-(Pyridin-4-yl)-[2,2':6',2''-terpyridine]-4-carboxylic acid **L8** (0.20 g, 0.56 mmol) was refluxed in an excess of thionyl chloride (15 mL) under an inert atmosphere for 4 hours, and it became a yellow solution. This was cooled to the room temperature and thionyl chloride evaporated to give 4'-(pyridin-4-yl)-[2,2':6',2''-terpyridine]-4-carbonyl chloride as a yellow powder, which was used in the next step without further purification and characterization. This was refluxed with 2,6-lutidine (0.30 g, 2.82 mmol) in toluene (10 mL) under an inert atmosphere for 20 minutes to give a greenish suspension. Then 5-diethylamino-1-pentanol **P19** (0.14 g, 0.85 mmol) was added. The reaction mixture turned dark brown and was refluxed for 17 hours. Then solvent was removed in vacuo and the brown residue dissolved in chloroform and extracted with an aqueous solution of sodium hydrogencarbonate and then with water. The organic phase was dried over sodium sulfate, filtered and evaporated to give a dark brown solid, which was purified with column chromatography (SiO_2, eluted with EtOAc/MeOH/Et_3N = 60:3:1 and 30:3:1) and afforded the product as a pale brown solid (0.14 g, 0.29 mmol, 51%).

^{1}H NMR (500 MHz, $CDCl_3$, TMS) δ/ppm 9.16 (dd, *J* = 1.7, 0.9 Hz, 1H, H^{D3}), 8.84 (dd, *J* = 5.0, 0.9 Hz, 1H, H^{D6}), 8.79 (d, *J* = 1.7 Hz, 1H, H^{B3}), 8.76 (dd, *J* = 4.4, 1.7 Hz, 2H, H^{C2}), 8.75 (d, *J* = 1.7 Hz, 1H, H^{B5}), 8.72 (m, 1H, H^{A6}), 8.69 (dt, *J* = 8.0, 1.1 Hz, 1H, H^{A3}), 7.90 (m, 2H, H^{A4+D5}), 7.78 (dd, *J* = 4.4, 1.7 Hz, 2H, H^{C3}), 7.37 (ddd, *J* = 7.5, 4.7, 1.2 Hz, 1H, H^{A5}), 4.43 (t, *J* = 6.7 Hz, 2H, H^1), 2.53 (q, *J* = 7.1 Hz, 4H, H^7), 2.47 (m, 2H, H^5), 1.87 (m, 2H, H^2), 1.56 (m, 2H, H^4), 1.50 (m, 2H, H^3), 1.01 (t, *J* = 7.2 Hz, 3H, H^8). **^{13}C {^{1}H} NMR** (126 MHz, $CDCl_3$) δ/ppm 165.5 ($C^{C=O}$), 157.0 (C^{D2}), 156.7 (C^{A2}), 155.7 (C^{B6}), 155.6 (C^{B2}), 150.7 (C^{C2}), 150.0 (C^{D6}), 149.3 (C^{A6}), 147.7 (C^{C4}), 145.9 (C^{B4}), 138.9 (C^{D4}), 137.2 (C^{A4}), 124.4 (C^{A5}), 123.2 (C^{D5}), 121.8 (C^{C3}), 121.6 (C^{A3}), 120.9 (C^{D3}), 119.2 (C^{B3}), 118.9 (C^{B5}), 66.0 (C^1), 52.9 (C^5), 47.0 (C^7), 28.8 (C^2), 26.8 (C^4), 24.2 (C^3), 11.7 (C^8). **ESI MS** (MeOH/$CHCl_3$): *m/z* 534.3 $[M+K]^+$ (4%, calc. 534.3), 518.3 $[M+Na]^+$ (5%, calc. 518.3), 496.3 $[M+H]^+$ (100%, calc. 496.3). **IR** (solid, ν/cm^{-1}) 3060 (w), 2964 (m), 2926 (s), 2860 (m), 2795 (m), 1723 (s), 1592 (m), 1583 (s), 1560 (m), 1534 (m), 1470 (m), 1434 (m), 1381 (s), 1348 (w), 1324 (w), 1287 (m), 1267 (s), 1208 (s), 1130 (m), 1095 (m), 1086 (w), 1077 (w), 1067 (w), 987 (w), 968 (w), 896 (w), 814 (s), 788 (s), 768 (s), 769 (s), 749 (m), 742 (m), 730 (s), 714 (m), 684 (m), 668 (s), 660 (s), 620 (s). **UV/VIS** λ_{max}/nm (5.38×10^{-5} mol dm^{-3}, MeCN) 242 (ε / dm^3 mol^{-1} cm^{-1} 34000), 281 (17000), 316

(10000 sh). **EA** found: C, 72.38; H, 6.90; N, 13.59%. $C_{30}H_{33}N_5O_2$ requires C, 72.70; H, 6.71; N, 14.13%.

4-(Dodecyloxy)-4'-(pyridin-4-yl)-2,2':6',2''-terpyridine (L17)

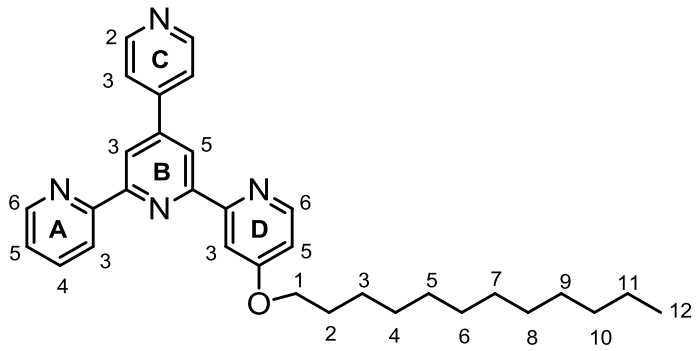

A white suspension of freshly ground potassium hydroxide (122 mg, 2.17 mmol) and dodecanol (81 mg, 0.44 mmol) in dimethyl sulfoxide (3 mL) was stirred at 50 °C for 30 minutes. 4-Chloro-4'-(pyridin-4-yl)-2,2':6',2''-terpyridine **L6** (80 mg, 0.22 mmol) was added and the reddish-brown suspension was heated at 65 °C for 19 hours. This was cooled to room temperature and cold water (10 mL) was added. The fine orange-brown precipitate which formed was collected on a filter paper, washed with cold water and air dried to give the product as a brown solid (53 mg, 0.11 mmol, 49%).

^{1}H NMR (500 MHz, $CDCl_3$, TMS) δ/ppm 8.76 (m, 5H, $H^{A6+B3+B5+C2}$), 8.67 (d, *J* = 7.9 Hz, 1H, H^{A3}), 8.54 (d, *J* = 5.7 Hz, 1H, H^{D6}), 8.19 (d, *J* = 2.6 Hz, 1H, H^{D3}), 7.90 (t, *J* = 7.0 Hz, 1H, H^{A4}), 7.79 (d, *J* = 5.3 Hz, 2H, H^{C3}), 7.38 (m, 1H, H^{A5}), 6.89 (d, *J* = 3.2 Hz, 1H, H^{D5}), 4.17 (t, *J* = 6.4 Hz, 2H, H^1), 1.89 (m, 2H, H^2), 1.55 (m, 2H, H^3), 1.29 (m, 16H, H^{4-11}), 0.88 (t, *J* = 6.5 Hz, 3H, H^{12}). **^{13}C {^{1}H} NMR** (126 MHz, $CDCl_3$) δ/ppm 166.4 (C^{D4}), 157.7(C^{D2}), 156.6 (C^{B2}), 156.4 (C^{B6}), 156.0 (C^{A2}), 150.7 (C^{C2+D6}), 149.4 (C^{A6}), 147.7 (C^{B4}), 146.2 (C^{C4}), 137.2 (C^{A4}), 124.3 (C^{A5}), 121.8 (C^{C3}), 121.5 (C^{A3}), 119.1 (C^{B5}), 118.9 (C^{B3}), 110.7 (C^{D5}), 108.1 (C^{D3}), 68.3 (C^1), 32.1 (C^{10}), 29.8, 29.7, 29.6 (C^{5-9}), 29.5 (C^4), 28.8 (C^2), 26.2 (C^3), 22.9 (C^{11}), 14.3 (C^{12}). **ESI MS** (MeOH/CH_2Cl_2): *m/z* 517.3 $[M+Na]^+$ (100%, calc. 517.2), 495.3 $[M+H]^+$ (23%, calc. 495.3). **IR** (solid, ν/cm^{-1}) 2915 (s), 2849 (m), 1585 (s), 1567 (m), 1471 (m), 1386 (m), 1303 (w), 1195 (w), 1092 (m), 1064 (s), 1044 (s), 1023 (s), 1006 (s), 999 (s), 988 (s), 972 (m), 907 (m), 897 (m), 877 (m), 798 (m), 670 (m), 617 (m), 557 (m). **UV/VIS** λ_{max} / nm (3.03×10^{-5} mol dm^{-3}, MeCN) 242 (ε/ dm^3 mol^{-1} cm^{-1} 55 000), 281 (30 000), 315 (13 000).

N,N-Diethyl-11-((4'-(pyridin-4-yl)-[2,2':6',2''-terpyridin]-4-yl)oxy)undecan-1-amine L18)

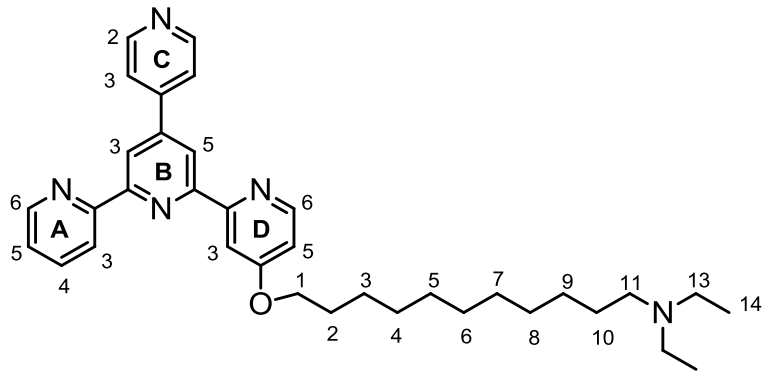

A white suspension of freshly ground potassium hydroxide (0.33 g, 5.80 mmol) and 11-(diethylamino)undecan-1-ol **P16** (0.28 g, 1.16 mmol) in dimethyl sulfoxide (7 mL) was stirred at 50 °C for 30 minutes. 4-Chloro-4'-(pyridin-4-yl)-2,2':6',2''-terpyridine **L6** (0.20 g, 0.58 mmol) was added and the dark brown suspension was heated at 65 °C for 16 hours. This was cooled to room temperature and cold water (10 mL) was added. The fine orange-brown precipitate which formed was dissolved in chloroform (100 mL) and thoroughly extracted with water (four times 100 mL) to remove all dimethyl sulfoxide. The organic phase was dried over sodium sulfate, filtered and solvent evaporated to give the product as a brown oil (0.15 g, 0.26 mmol, 46%).

^{1}H NMR (500 MHz, $CDCl_3$, TMS) δ/ppm 8.72 (d, *J* = 1.6 Hz, 2H, H^{C2}), 8.71 (d, *J* = 1.7 Hz, 1H, H^{B3}), 8.70 (d, *J* = 1.7 Hz, 1H, H^{B5}), 8.69 (ddd, *J* = 4.8, 1.7, 1.0 Hz, 1H, H^{A6}), 8.62 (dt, *J* = 7.9, 1.0 Hz, 1H, H^{A3}), 8.49 (d, *J* = 5.6 Hz, 1H, H^{D6}), 8.15 (d, *J* = 2.5 Hz, 1H, H^{D3}), 7.86 (td, *J* = 7.6, 1.8 Hz, 1H, H^{A4}), 7.76 (dd, *J* = 4.5, 1.7 Hz, 2H, H^{C3}), 7.34 (ddd, *J* = 7.5, 4.8, 1.2 Hz, 1H, H^{A5}), 6.85 (dd, *J* = 5.6, 2.6 Hz, 1H, H^{D5}), 4.13 (t, *J* = 6.5 Hz, 2H, H^{1}), 2.49 (q, *J* = 7.2 Hz, 4H, H^{13}), 2.37 (m, 2H, H^{11}), 1.85 (m, 2H, H^{2}), 1.40 (m, 2H, H^{3}), 1.39 (m, 2H, H^{10}), 1.25 (m, 12H, H^{4-9}), 0.98 (t, *J* = 7.2 Hz, 6H, H^{14}). **^{13}C {^{1}H} NMR** (126 MHz, $CDCl_3$) δ/ppm 166.3 (C^{D4}), 157.4 (C^{D2}), 156.3 (C^{B2+B6}), 155.7 (C^{A2}), 150.5 (C^{C2+D6}), 149.2 (C^{A6}), 147.4 (C^{B4}), 146.0 (C^{C4}), 137.1 (C^{A4}), 124.2 (C^{A5}), 121.8 (C^{C3}), 121.5 (C^{A3}), 118.9 (C^{B5}), 118.8 (C^{B3}), 110.6 (C^{D5}), 108.0 (C^{D3}), 68.2 (C^{1}), 53.0 (C^{11}), 46.9 (C^{13}), 29.7, 29.6 (C^{5-7}), 29.5 (C^{8}), 29.4 (C^{4}), 29.1 (C^{2}), 27.8 (C^{9}), 26.8 (C^{10}),26.1 (C^{3}), 11.6 (C^{14}). **ESI MS** (MeOH/$CHCl_3$): *m/z* 590.3 $[M+K]^+$ (32%, calc. 590.4), 574.4 $[M+Na]^+$ (56%, calc. 574.4), 552.4 $[M+H]^+$ (100%, calc. 552.4). **IR** (solid, ν/cm^{-1}) 2966 (w), 2922 (s), 2852 (m), 2797 (w), 1663 (w), 1583 (s), 1565 (s), 1556 (m), 1539 (m), 1468 (m), 1383 (s), 1297 (m), 1202 (m), 1125 (w), 1061 (m), 987 (m), 867 (w), 817

(m), 790 (s), 659 (m), 618 (s), 502 (m). **UV/VIS** λ_{max} / nm (3.00×10^{-5} mol dm^{-3}, MeCN) 241 (ε/ dm^3 mol^{-1} cm^{-1} 58 000), 281 (27 000), 314 (12 000).

4-((11-(Piperidin-1-yl)undecyl)oxy)-4'-(pyridin-4-yl)-2,2':6',2''-terpyridine (L19)

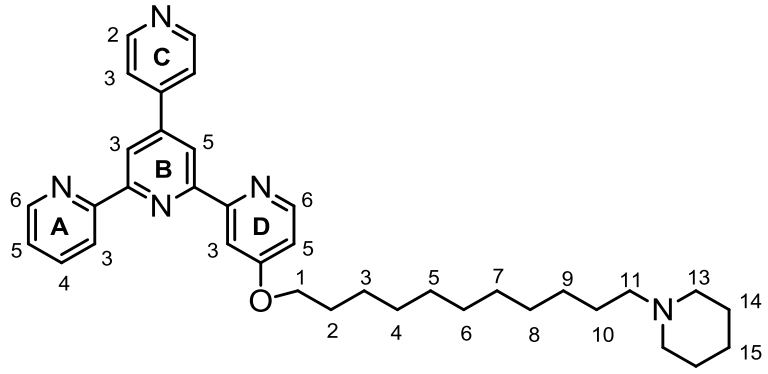

A white suspension of freshly ground potassium hydroxide (0.24 g, 4.35 mmol) and 11-(piperidin-1-yl)undecan-1-ol **P17** (0.13 g, 0.52 mmol) in dimethyl sulfoxide (5 mL) was stirred at 50 °C for 30 minutes. 4-Chloro-4'-(pyridin-4-yl)-2,2':6',2''-terpyridine **L6** (0.15 g, 0.44 mmol) was added and the reddish-brown suspension was heated at 65 °C for 18 hours. This was cooled to room temperature and cold water (15 mL) was added. The fine orange-brown precipitate which formed was dissolved in chloroform (100 mL) and thoroughly extracted with water (four times 100 mL) to remove all dimethyl sulfoxide. The organic phase was dried over sodium sulfate, filtered and solvent evaporated to give the product as a brown oil (94 mg, 0.17 mmol, 38%).

^{1}H NMR (500 MHz, $CDCl_3$, TMS) δ/ppm 8.75 (dd, *J* = 1.6, 1.0 Hz, 2H, H^{C2}), 8.74 (d, *J* = 1.7 Hz, 1H, H^{B3}), 8.73 (d, *J* = 1.7 Hz, 1H, H^{B5}), 8.72 (ddd, *J* = 4.8, 1.8, 1.0 Hz, 1H, H^{A6}), 8.65 (dt, *J* = 8.0, 1.1 Hz, 1H, H^{A3}), 8.52 (d, *J* = 5.6 Hz, 1H, H^{D6}), 8.17 (d, *J* = 2.5 Hz, 1H, H^{D3}), 7.89 (td, *J* = 7.7, 1.8 Hz, 1H, H^{A4}), 7.78 (dd, *J* = 4.4, 1.7 Hz, 2H, H^{C3}), 7.37 (ddd, *J* = 7.6, 4.8, 1.2 Hz, 1H, H^{A5}), 6.87 (dd, *J* = 5.6, 2.6 Hz, 1H, H^{D5}), 4.15 (t, *J* = 6.5 Hz, 2H, H^1), 2.37 (m, 4H, H^{13}), 2.25 (m, 2H, H^{11}), 1.86 (m, 2H, H^2), 1.56 (m, 4H, H^{14}), 1.48 (m, 4H, H^{3+10}), 1.35 (m, 2H, H^{15}), 1.29 (m, 12H, H^{4-9}). **^{13}C {^{1}H} NMR** (126 MHz, $CDCl_3$) δ/ppm 166.4 (C^{D4}), 157.5 (C^{D2}), 156.4 (C^{B2+B6}), 155.8 (C^{A2}), 150.6 (C^{C2}), 150.6 (C^{D6}), 149.3 (C^{A6}), 147.5 (C^{B4}), 146.1 (C^{C4}), 137.1 (C^{A4}), 124.3 (C^{A5}), 121.8 (C^{C3}), 121.5 (C^{A3}), 119.0 (C^{B5}), 118.8 (C^{B3}), 110.6 (C^{D5}), 108.0 (C^{D3}), 68.3 (C^1), 59.8 (C^{11}), 54.7 (C^{13}), 29.7, 29.6, 29.5 (C^{5-8}),

29.4 (C^4), 29.2 (C^2), 27.9 (C^9), 27.1 (C^{10}), 26.0 (C^3), 25.9 (C^{14}), 24.6 (C^{15}). **ESI MS** (MeOH/$CHCl_3$): *m/z* 602.3 $[M+K]^+$ (15%, calc. 602.3), 586.3 $[M+Na]^+$ (100%, calc. 586.4), 564.4 $[M+H]^+$ (46%, calc. 564.4). **IR** (solid, ν/cm^{-1}) 2923 (s), 2911 (s), 2849 (s), 2812 (w), 2782 (w), 1665 (w), 1582 (s), 1564 (s), 1537 (m), 1470 (m), 1381 (m), 1299 (m), 1267 (w), 1197 (m), 1057 (m), 1038 (s), 1023 (s), 1016 (s), 988 (m), 952 (w), 824 (m), 793 (m), 668 (m), 618 (s), 503 (s). **UV/VIS** λ_{max} / nm (2.48×10^{-5} mol dm^{-3}, MeCN) 243 (ε/ dm^3 mol^{-1} cm^{-1} 65 000), 281 (37 000), 314 (14 000 sh).

4-(11-((4'-(Pyridin-4-yl)-[2,2':6',2''-terpyridin]-4-yl)oxy)undecyl)morpholine (L20)

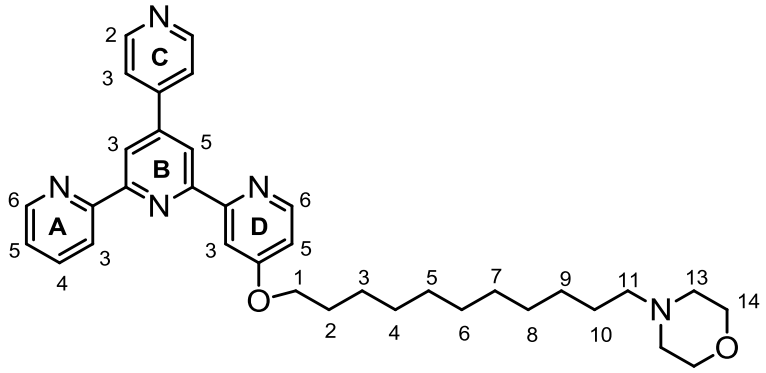

A white suspension of freshly ground potassium hydroxide (0.24 g, 4.35 mmol) and 11-morpholinoundecan-1-ol **P18** (0.13 g, 0.52 mmol) in dimethyl sulfoxide (5 mL) was stirred at 50 °C for 30 minutes. 4-Chloro-4'-(pyridin-4-yl)-2,2':6',2''-terpyridine **L6** (0.15 g, 0.44 mmol) was added and the reddish-brown suspension was heated at 65 °C for 18 hours. This was cooled to room temperature and cold water (15 mL) was added. The fine orange-brown precipitate which formed was dissolved in chloroform (100 mL) and thoroughly extracted with water (four times 100 mL) to remove all dimethyl sulfoxide. The organic phase was dried over sodium sulfate, filtered and solvent evaporated to give the product as a brown oil (0.12 g, 0.21 mmol, 49%).

^{1}H NMR (500 MHz, $CDCl_3$, TMS) δ/ppm 8.72 (dd, *J* = 1.7, 0.8 Hz, 2H, H^{C2}), 8.71 (d, *J* = 1.7 Hz, 1H, H^{B3}), 8.70 (d, *J* = 1.7 Hz, 1H, H^{B5}), 8.69 (m, 1H, H^{A6}), 8.62 (dt, *J* = 8.0, 1.1 Hz, 1H, H^{A3}), 8.49 (d, *J* = 5.6 Hz, 1H, H^{D6}), 8.14 (d, *J* = 2.5 Hz, 1H, H^{D3}), 7.86 (td, *J* = 7.7, 1.8 Hz, 1H, H^{A4}), 7.76 (dd, *J* = 4.5, 1.7 Hz, 2H, H^{C3}), 7.34 (ddd, *J* = 7.5, 4.8, 1.2 Hz, 1H, H^{A5}), 6.85 (dd, *J* = 5.7, 2.6 Hz, 1H, H^{D5}), 4.13 (t, *J* = 6.5 Hz, 2H, H^1), 3.69 (m, 4H, H^{14}), 2.39 (m, 4H, H^{13}), 2.27 (m, 2H, H^{11}), 1.84 (m, 2H, H^2), 1.51 (m, 2H, H^3), 1.44 (m, 2H, H^{10}), 1.27 (m, 12H, H^{4-9}). **^{13}C {^{1}H} NMR** (126 MHz, $CDCl_3$) δ/ppm 166.3

(C^{D4}), 157.4 (C^{D2}), 156.3 (C^{B2+B6}), 155.7 (C^{A2}), 150.5 (C^{C2+D6}), 149.2 (C^{A6}), 147.4 (C^{B4}), 146.0 (C^{B4}), 137.1 (C^{A4}), 124.2 (C^{A5}), 121.8 (C^{C3}), 121.5 (C^{A3}), 118.9 (C^{B5}), 118.8 (C^{B3}), 110.5 (C^{D5}), 108.0 (C^{D3}), 68.2 (C^{1}), 67.0 (C^{14}), 59.3 (C^{11}), 53.8 (C^{13}), 29.7, 29.6 (C^{5-8}), 29.5 (C^{4}), 29.1 (C^{2}), 27.6 (C^{9}), 26.5 (C^{10}), 26.1 (C^{3}). **ESI MS** (MeOH/$CHCl_3$): *m/z* 604.3 $[M+K]^+$ (41%, calc. 604.3), 588.4 $[M+Na]^+$ (100%, calc. 588.3), 566.4 $[M+H]^+$ (6%, calc. 566.8). **IR** (solid, ν/cm^{-1}) 2921 (m), 2911 (s), 2894 (m), 2849 (m), 2809 (m), 1582 (s), 1560 (m), 1474 (m), 1382 (m), 1299 (m), 1198 (w), 1135 (m), 1127 (m), 1112 (s), 1076 (m), 1070 (m), 1038 (m), 1031 (m), 1007 (m), 910 (m), 883 (m), 864 (s), 822 (m), 806 (m), 792 (s), 745 (m), 715 (m), 616 (s). **UV/VIS** λ_{max} / nm (5.30×10^{-5} mol dm^{-3}, MeCN) 242 (ε/ dm^3 mol^{-1} cm^{-1} 48 000), 281 (23 000 sh), 314 (10 000).

N,N-Dimethyl-3-((4'-(pyridin-4-yl)-[2,2':6',2''-terpyridin]-4-yl)oxy)propan-1-amine (L21)

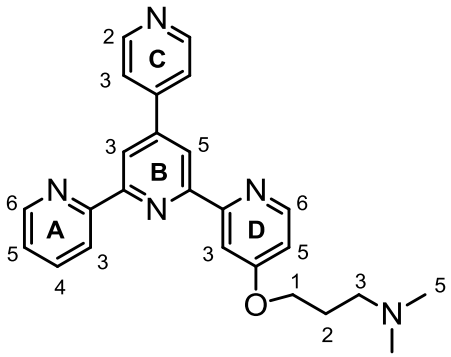

A white suspension of freshly ground potassium hydroxide (0.33 g, 5.80 mmol) and 3-dimethylamino-1-propanol (0.07 g, 0.70 mmol) in dimethyl sulfoxide (6 mL) was stirred at 50 °C for 30 minutes. 4-Chloro-4'-(pyridin-4-yl)-2,2':6',2''-terpyridine **L6** (0.20 g, 0.58 mmol) was added and the dark brown suspension was heated at 60 °C for 12 hours. This was cooled to room temperature and cold water (15 mL) was added. The fine orange-brown precipitate which formed was dissolved in chloroform (100 mL) and thoroughly extracted with water (four times 100 mL) to remove all dimethyl sulfoxide. The organic phase was dried over sodium sulfate, filtered and solvent evaporated to give the product as a brown oil (93 mg, 0.23 mmol, 39%).

^{1}H NMR (500 MHz, $CDCl_3$, TMS) δ/ppm 8.71 (m, 5H, $H^{C2+B3+B5+A6}$), 8.63 (dt, *J* = 8.0, 1.1 Hz, 1H, H^{A3}), 8.50 (d, *J* = 5.6 Hz, 1H, H^{D6}), 8.16 (d, *J* = 2.6 Hz, 1H, H^{D3}), 7.87 (td, *J* = 7.7, 1.8 Hz, 1H, H^{A4}), 7.75 (m, 2H, H^{C3}), 7.35 (ddd, *J* = 7.5, 4.8, 1.2 Hz, 1H, H^{A5}), 6.87 (dd, *J* = 5.7, 2.6 Hz, 1H, H^{A5}), 4.21 (t, *J* = 6.3 Hz, 2H, H^{1}), 2.53 (t, *J* = 7.2 Hz, 2H, H^{3}), 2.29 (s, 6H, H^{5}), 2.04 (m, 2H, H^{2}). **^{13}C {^{1}H} NMR**

(126 MHz, $CDCl_3$) δ/ppm 166.2 (C^{D4}), 157.4 (C^{D2}), 156.4 (C^{B2}), 156.3 (C^{B6}), 155.7 (C^{A2}), 150.6 (C^{C2}), 150.5 (C^{D6}), 149.3 (C^{A6}), 147.4 (C^{C4}), 146.0 (C^{B4}), 137.1 (C^{A4}), 124.2 (C^{A5}), 121.8 (C^{C3}), 121.5 (C^{A3}), 118.9 (C^{B5}), 118.8 (C^{B3}), 110.6 (C^{D5}), 108.0 (C^{D3}), 66.3 (C^{1}), 56.2 (C^{3}), 45.5 (C^{4}), 27.3 (C^{2}). **ESI MS** (MeOH/$CHCl_3$): *m/z* 450.1 $[M+K]^+$ (6%, calc. 450.2), 434.2 $[M+Na]^+$ (47%, calc. 434.2), 412.2 $[M+H]^+$ (100%, calc. 412.2). **IR** (solid, ν/cm^{-1}) 2949 (m), 2858 (w), 2765 (w), 1582 (s), 1560 (s), 1537 (m), 1448 (m), 1412 (w), 1383 (s), 1352 (w), 1297 (m), 1272 (w), 1258 (w), 1198 (w), 1040 (m), 1031 (m), 1008 (m), 968 (w), 882 (w), 822 (m), 790 (s), 745 (m), 668 (m), 659 (m), 618 (s). **UV/VIS** λ_{max} / nm (4.86×10^{-5} mol dm^{-3}, MeCN) 242 (ε/ dm^3 mol^{-1} cm^{-1} 28 000), 281 (13 000 sh), 314 (6 000).

N,N-Diethyl-5-((4'-(pyridin-4-yl)-[2,2':6',2''-terpyridin]-4-yl)oxy)pentan-1-amine (L22)

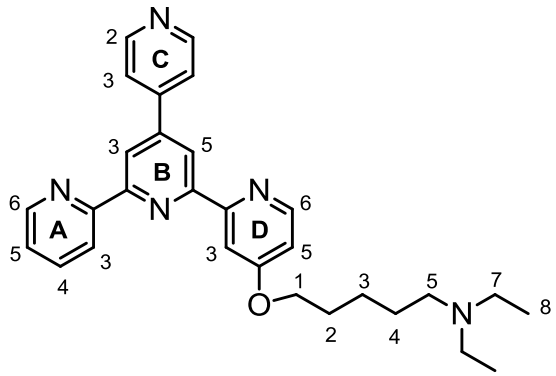

A white suspension of freshly ground potassium hydroxide (0.33 g, 5.80 mmol) and 5-diethylamino-1-pentanol **P19** (0.19 g, 1.16 mmol) in dimethyl sulfoxide (7 mL) was stirred at 50 °C for 30 minutes. 4-Chloro-4'-(pyridin-4-yl)-2,2':6',2''-terpyridine **L6** (0.20 g, 0.58 mmol) was added and the dark brown suspension was heated at 60 °C for 17 hours. This was cooled to room temperature and cold water (15 mL) was added. The fine orange-brown precipitate which formed was dissolved in chloroform (100 mL) and thoroughly extracted with water (four times 100 mL) to remove all dimethyl sulfoxide. The organic phase was dried over sodium sulfate, filtered and solvent evaporated to give the product as a brown oil (0.14 g, 0.30 mmol, 52%).

^{1}H NMR (500 MHz, $CDCl_3$, TMS) δ/ppm 8.72 (m, 3H, H^{C2+B3}), 8.70 (m, 2H, H^{A6+B5}), 8.63 (dt, *J* = 8.0, 1.0 Hz, 1H, H^{A3}), 8.50 (d, *J* = 5.6 Hz, 1H, H^{A6}), 8.15 (d, *J* = 2.5 Hz, 1H, H^{A3}), 7.87 (m, 1H, H^{A4}), 7.75 (dd, *J* = 4.5, 1.7 Hz, 2H, H^{C3}), 7.34 (ddd, *J* = 7.5, 4.8, 1.2 Hz, 1H, H^{A5}), 6.85 (dd, *J* = 5.6, 2.6 Hz, 1H,

H^{D5}), 4.14 (t, *J* = 6.4 Hz, 2H, H^{1}), 2.52 (q, *J* = 7.1 Hz, 4H, H^{7}), 2.46 (m, 2H, H^{5}), 1.88 (m, 2H, H^{2}), 1.55 (m, 4H, H^{3+4}), 1.01 (t, *J* = 7.2 Hz, 3H, H^{8}). **^{13}C {^{1}H} NMR** (126 MHz, $CDCl_3$) δ/ppm 166.3 (C^{D4}), 157.4 (C^{D2}), 156.4 (C^{B2+B6}), 155.8 (C^{A2}), 150.6 (C^{C2}), 150.5 (C^{D6}), 149.3 (C^{A6}), 147.4 (C^{C4}), 146.0 (C^{B4}), 137.1 (C^{A4}), 124.2 (C^{A5}), 121.8 (C^{C3}), 121.5 (C^{A3}), 118.9 (C^{B5}), 118.8 (C^{B3}), 110.6 (C^{D5}), 108.0 (C^{D3}), 68.1 (C^{1}), 52.9 (C^{5}), 50.0 (C^{7}), 29.1 (C^{2}), 26.5 (C^{4}), 24.2 (C^{3}), 11.7 (C^{8}). **ESI MS** (MeOH/$CHCl_3$): *m/z* 506.2 $[M+K]^+$ (5%, calc. 506.2), 490.2 $[M+Na]^+$ (12%, calc. 490.3), 468.3 $[M+H]^+$ (100%, calc. 468.2). **IR** (solid, ν/cm^{-1}) 2964 (w), 2930 (m), 2859 (w), 2794 (w), 1582 (s), 1564 (s), 1537 (m), 1467 (m), 1448 (w), 1383 (m), 1298 (m), 1265 (w), 1197 (m), 1067 (m), 1040 (m), 1033 (m), 1025 (m), 988 (m), 884 (w), 864 (s), 823 (m), 793 (s), 744 (m), 618 (s). **UV/VIS** λ_{max} / nm (8.55×10^{-5} mol dm^{-3}, MeCN) 244 (ε/ dm^3 mol^{-1} cm^{-1} 45 000), 281 (25 000 sh), 315 (11 000).

4'-Phenyl-2,2':6',2''-terpyridine (L23)

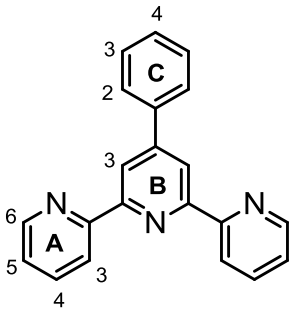

An excess of ammonium acetate (7.36 g, 95.58 mmol) was dissolved in methanol (70 mL). Chalcone **P11** (1.00 g, 4.78 mmol) and PPI salt **P8** (1.83 g, 5.74 mmol) were added and this brown suspension was heated at reflux for 19 hours, while all slowly dissolved. Then the reaction mixture was cooled to room temperature and placed to the freezer overnight. The pale brown precipitate which formed was collected on a glass frit, washed with cold methanol and air dried to give the product as a pale brown powder (0.73 g, 2.35 mmol, 49%). The NMR data match those published. [8]

^{1}H NMR (400 MHz, $CDCl_3$, TMS) δ/ppm 8.75 (s, 2H, H^{B3}), 8.73 (ddd, *J* = 4.8, 1.9, 1.0 Hz, 2H, H^{A6}), 8.68 (dt, *J* = 7.9, 1.1 Hz, 2H, H^{A3}), 7.91 (d, *J* = 7.9 Hz, 2H, H^{C2}), 7.87 (td, *J* = 7.8, 1.8 Hz, 2H, H^{A4}),

7.52 (m, 2H, H^{C3}), 7.46 (m, 1H, H^{C4}), 7.35 (ddd, *J* = 7.5, 4.8, 1.2 Hz, 2H, H^{A5}). **UV/VIS** λ_{max}/nm (4.55×10^{-5} mol dm^{-3}, MeCN) 252 (ε/dm^3 mol^{-1} cm^{-1} 40000), 276 (37000), 313 (10000 sh).

Methyl 4'-phenyl-[2,2':6',2''-terpyridine]-4-carboxylate (L24)

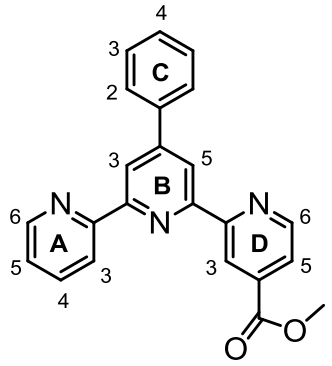

An excess of ammonium acetate (9.60 g, 124.68 mmol) was dissolved in methanol (110 mL). Chalcone **P11** (1.00 g, 4.76 mmol) and PPI salt **P5** (2.21 g, 5.71 mmol) were added and the brown solution was heated at reflux for 16 hours, during which time a brown precipitate formed. Then the reaction mixture was cooled to room temperature and placed to the freezer overnight. The brown precipitate was collected on a glass frit, washed with cold methanol and air dried to give the product as a pale brown powder (0.56 g, 1.53 mmol, 33%).

^{1}H NMR (500 MHz, $CDCl_3$, TMS) δ/ppm 9.16 (dd, *J* = 1.7, 0.9 Hz, 1H, H^{D3}), 8.86 (dd, *J* = 5.0, 0.9 Hz, 1H, H^{D6}), 8.78 (d, *J* = 1.7 Hz, 1H, H^{B3}), 8.75 (d, *J* = 1.7 Hz, 1H, H^{B5}), 8.74 (ddd, *J* = 4.7, 1.9, 1.0 Hz, 1H, H^{A6}), 8.72 (dt, *J* = 7.9, 1.1 Hz, 1H, H^{A3}), 7.90 (m, 4H, $H^{A4+C2+D5}$), 7.52 (m, 2H, H^{C3}), 7.47 (m, 1H, H^{C4}),7.37 (ddd, *J* = 7.5, 4.8, 1.2 Hz, 1H, H^{A5}), 4.04 (s, 3H, H^{Me}). **^{13}C {^{1}H} NMR** (126 MHz, $CDCl_3$) δ/ppm 166.1 ($C^{C=O}$), 157.6 (C^{D2}), 156.2 (C^{A2}), 156.1 (C^{B2}), 155.3 (C^{B6}), 150.6 (C^{B4}), 150.0 (C^{D6}), 149.2 (C^{A6}), 138.5 (C^{C1}), 138.4 (C^{D4}), 137.2 (C^{A4}), 129.3 (C^{C4}), 129.1 ($C^{C3,5}$), 127.5 ($C^{C2,6}$), 124.1 (C^{A5}), 122.9 (C^{D5}), 121.7 (C^{A3}), 120.8 (C^{D3}), 119.5 (C^{B5}), 119.3 (C^{B3}), 52.9 (C^{Me}). **MP** 197-198 °C (from MeOH). **ESI MS** (MeOH/$CHCl_3$): *m/z* 390.0 $[M+Na]^+$ (24%, calc. 390.1), 368.0 $[M+H]^+$ (100%, calc. 368.1). **IR** (solid, ν/cm^{-1}) 3051 (w), 2969 (w), 1723 (s), 1583 (m), 1548 (m), 1467 (w), 1432 (m), 1378 (s), 1268 (s), 1218 (s), 1132 (w), 1099 (w), 989 (m), 887 (w), 800 (m), 775 (m), 764 (s), 754 (s), 731 (s), 707 (s), 694 (s), 681 (s), 662 (s), 620 (s), 517 (s). **UV/VIS** λ_{max}/nm

(4.44×10^{-5} mol dm^{-3}, MeCN) 253 (ε/dm^3 mol^{-1} cm^{-1} 35000), 276 (27000 sh), 310 (13000 sh). **EA** found: C, 74.41; H, 4.67; N, 11.22%. $C_{23}H_{17}N_3O_2 \cdot 0.25H_2O$ requires C, 74.28; H, 4.74; N, 11.30%.

4'-Phenyl-[2,2':6',2''-terpyridine]-4-carboxylic acid (L25)

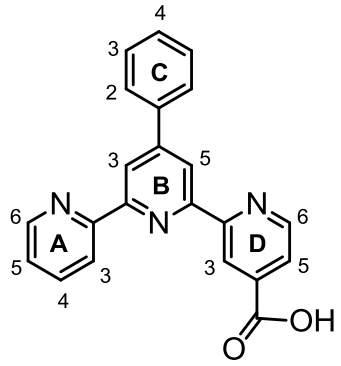

Methyl 4'-phenyl-[2,2':6',2''-terpyridine]-4-carboxylate **L24** (0.30 g, 0.82 mmol) was suspended in hot methanol (6 mL). Then aqueous solution of sodium hydroxide (1M, 1.63 mL, 1.63 mmol) was added and the reaction mixture was heated to reflux for 18 hours, while the greenish suspension dissolved and turned to a brown solution. This was cooled to room temperature and acidified with hydrochloric acid (0.5M) to pH~4. The off-white precipitate which formed was collected on a glass frit, washed thoroughly with water and air dried to give the product as a grey powder (0.28 g, 0.80 mmol, 98%).

^{1}H NMR (500 MHz, DMSO-d_6) δ/ppm 13.87 (br s, 1H, OH), 9.03 (dd, J = 1.6, 0.8 Hz, 1H, H^{D3}), 8.95 (dd, J = 4.9, 0.8 Hz, 1H, H^{D6}), 8.79 (ddd, J = 4.8, 1.7, 0.9 Hz, 1H, H^{A6}), 8.75 (s, 2H, H^{B3+B5}), 8.62 (d, J = 7.9 Hz, 1H, H^{A3}), 8.13 (td, J = 7.7, 1.8 Hz, 1H, H^{A4}), 7.95 (m, 3H, H^{C2+D5}), 7.61 (m, 2H, H^{C3}), 7.57 (m, 2H, H^{A5+C4}). **^{13}C {^{1}H} NMR** (126 MHz, DMSO-d_6) δ/ppm 168.7 (C^{D4}), 156.0 (C^{B2}), 155.4 (C^{B6}), 154.9 (C^{A2}), 154.5 (C^{D2}), 150.7 (C^{D6}), 150.2 (C^{B4}), 149.2 (C^{A6}), 138.2 (C^{A4}), 137.8 (C^{C1}), 129.7 (C^{C4}), 129.5 (C^{C3}), 127.0 (C^{C2}), 124.8 (C^{A5}), 123.5 (C^{D5}), 121.0 (C^{A3}), 119.7 (C^{D3}), 119.7 (C^{B5}), 118.4 (C^{B3}). **MP** 321-322 °C. **MALDI TOF MS**: *m/z* 353.8 $[M]^+$ (93%, calc. 353.1), 309.8 $[M\text{-}CO_2]^+$ (100%, calc. 309.2). **IR** (solid, ν/cm^{-1}) 3061 (w), 2378 (m), 1708 (s), 1591 (m), 1549 (m), 1464 (w), 1381 (s), 1346 (w), 1296 (m), 1282 (m), 1268 (s), 1255 (m), 1217 (m), 1206 (m), 1076 (w), 1010 (w), 989 (w), 882 (m), 863 (m), 830 (w), 758 (m), 752 (m), 744 (m), 732(m), 702 (m), 688 (m), 662 (m),

619 (m). **EA** found: C, 71.53; H, 4.34; N, 11.53%. $C_{33}H_{39}N_3O{\cdot}H_2O$ requires C, 71.15; H, 4.61; N, 11.31%.

Dodecyl 4'-phenyl-[2,2':6',2''-terpyridine]-4-carboxylate (L26)

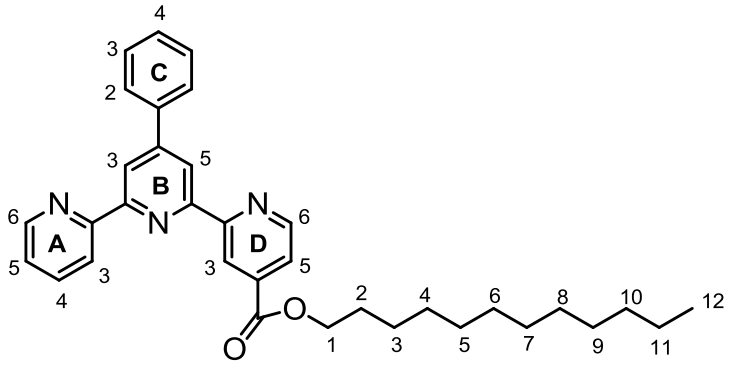

4'-Phenyl-[2,2':6',2''-terpyridine]-4-carboxylic acid **L25** (0.15 g, 0.41 mmol) was refluxed in an excess of thionyl chloride (13 mL) under an inert atmosphere for 4 hours, and it became a yellow solution. This was cooled to room temperature and thionyl chloride evaporated to give 4'-phenyl-[2,2':6',2''-terpyridine]-4-carbonyl chloride as a yellow powder, which was used in the next step without further purification and characterization. This was refluxed with 2,6-lutidine (0.22 g, 2.07 mmol) in toluene (12 mL) under an inert atmosphere for 20 minutes to give a greenish suspension. Then dodecanol (0.15 g, 0.83 mmol) was added. The reaction mixture turned dark brown and was refluxed for 17 hours. Then solvent was removed in vacuo and the brown residue dissolved in chloroform and extracted with an aqueous solution of sodium hydrogencarbonate and then with water. The organic phase was dried over sodium sulfate, filtered and evaporated to give a dark brown solid, which was recrystallized from a mixture of cold ethanol - diethyl ether to afford the product as a pale brown powder (0.17 g, 0.32 mmol, 78%).

^{1}H NMR (500 MHz, $CDCl_3$, TMS) δ/ppm 9.18 (br s, 1H, H^{D3}), 8.86 (dd, *J* = 4.9, 0.9 Hz, 1H, H^{D6}), 8.78 (d, *J* = 1.7 Hz, 1H, H^{B3}), 8.75 (d, *J* = 1.7 Hz, 1H, H^{B5}), 8.72 (m, 2H, H^{A6+A3}), 7.90 (m, 4H, $H^{A4+C2+D5}$), 7.52 (m, 2H, H^{C3}), 7.46 (m, 1H, H^{C4}),7.36 (ddd, *J* = 7.5, 4.8, 1.3 Hz, 1H, H^{A5}), 4.43 (t, *J* = 6.6 Hz, 2H, H^1), 1.84 (m, 2H, H^2), 1.51 (m, 2H, H^3), 1.40 (m, 2H, H^4), 1.28 (m, 14H, H^{5-11}), 0.87 (t, *J* = 6.9 Hz, 3H, H^{12}). **^{13}C {^{1}H} NMR** (126 MHz, $CDCl_3$) δ/ppm 165.6 ($C^{C=O}$), 157.5 (C^{D2}), 156.2 (C^{A2}),

156.1 (C^{B2}), 155.3 (C^{B6}), 150.6 (C^{B4}), 150.0 (C^{D6}), 149.3 (C^{A6}), 138.9 (C^{D4}), 138.5 (C^{C1}), 137.1 (C^{A4}), 129.2 (C^{C4}), 129.1 (C^{C3}), 127.5 (C^{C2}), 124.1 (C^{A5}), 122.9 (C^{D5}), 121.6 (C^{A3}), 120.9 (C^{D3}), 119.4 (C^{B5}), 119.2 (C^{B3}), 66.1 (C^{1}), 32.0 (C^{10}), 29.8, 29.7, 29.5 (C^{5-9}), 29.5 (C^{4}), 28.8 (C^{2}), 26.2 (C^{3}),22.8 (C^{11}), 14.3 (C^{12}). **MP** 79 °C (from EtOH-Et_2O). **ESI MS** (MeOH/$CHCl_3$): *m/z* 544.2 $[M+Na]^+$ (100%, calc. 544.3), 522.2 $[M+H]^+$ (66%, calc. 522.3). **IR** (solid, ν/cm^{-1}) 2916 (s), 2850 (m), 1733 (s), 1583 (s), 1551 (m), 1466 (m), 1431 (m), 1379 (s), 1282 (m), 1270 (s), 1217 (s), 1136 (w), 1105 (m), 995 (w), 893 (s), 856 (m), 797 (s), 761 (s), 745 (s), 734 (s), 709 (s), 692 (m), 682 (m), 663 (s), 620 (s). **UV/VIS** λ_{max}/nm (4.26×10^{-5} mol dm^{-3}, MeCN) 254 (ε/dm^3 mol^{-1} cm^{-1} 26000), 280 (19000), 310 (9000 sh). **EA** found: C, 78.90; H, 7.61; N, 8.36%. $C_{34}H_{39}N_3O_2$ requires C, 78.28; H, 7.54; N, 8.05%.

11-(Diethylamino)undecyl 4'-phenyl-[2,2':6',2''-terpyridine]-4-carboxylate (L27)

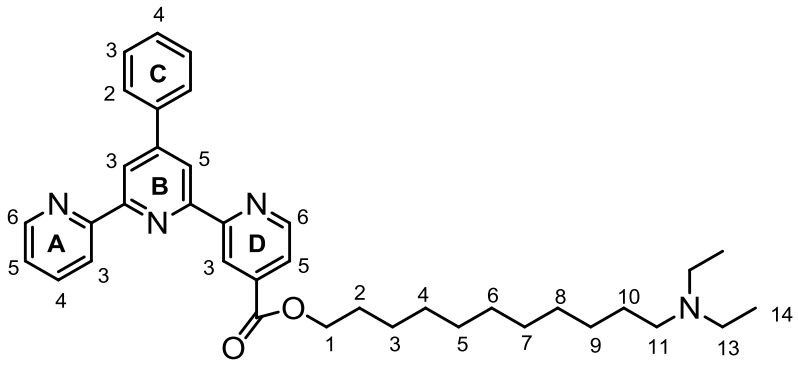

4'-Phenyl-[2,2':6',2''-terpyridine]-4-carboxylic acid **L25** (0.18 g, 0.50 mmol) was refluxed in an excess of thionyl chloride (12 mL) under an inert atmosphere for 4 hours, and it became a yellow solution. This was cooled to room temperature and thionyl chloride evaporated to give 4'-phenyl-[2,2':6',2''-terpyridine]-4-carbonyl chloride as a yellow powder, which was used in the next step without further purification and characterization. This was refluxed with 2,6-lutidine (0.27 g, 2.49 mmol) in toluene (13 mL) under an inert atmosphere for 30 minutes to give a greenish suspension. Then 11-(diethylamino)undecan-1-ol **P16** (0.24 g, 1.00 mmol) was added. The reaction mixture turned dark brown and was refluxed for 16 hours. Then solvent was removed in vacuo and the brown residue dissolved in chloroform and extracted with an aqueous solution of sodium hydrogencarbonate and then with water. The organic phase was dried over sodium sulfate, filtered and evaporated to give a dark brown solid, which was

purified with column chromatography (SiO_2, eluted with EtOAc/Et_3N = 99:1) and afforded the product as a yellow oil (0.16 g, 0.28 mmol, 57%).

^{1}H NMR (500 MHz, $CDCl_3$, TMS) δ/ppm 9.18 (dd, *J* = 1.7, 0.9 Hz, 1H, H^{D3}), 8.85 (dd, *J* = 4.9, 0.9 Hz, 1H, H^{D6}), 8.78 (d, *J* = 1.7 Hz, 1H, H^{B3}), 8.75 (d, *J* = 1.7 Hz, 1H, H^{B5}), 8.72 (m, 2H, H^{A3+A6}), 7.89 (m, 4H, $H^{A4+C2+D5}$), 7.51 (m, 2H, H^{C3}), 7.45 (m, 1H, H^{C4}), 7.36 (ddd, *J* = 7.5, 4.7, 1.2 Hz, 1H, H^{A5}), 4.42 (t, *J* = 6.7 Hz, 2H, H^1), 2.51 (m, 4H, H^{13}), 2.39 (dd, *J* = 8.9, 6.7 Hz, 2H, H^{11}), 1.84 (m, 2H, H^2), 1.50 (m, 2H, H^3), 1.41 (m, 4H, H^{4+10}), 1.23 (m, 10H, H^{5-9}), 1.01 (t, *J* = 7.2 Hz, 6H, H^{14}). **^{13}C {^{1}H} NMR** (126 MHz, $CDCl_3$) δ/ppm 165.6 ($C^{C=O}$), 157.5 (C^{D2}), 156.2 (C^{B2}), 156.1 (C^{A2}), 155.3 (C^{B6}), 150.6 (C^{B4}), 150.0 (C^{D6}), 149.3 (C^{A6}), 138.9 (C^{D4}), 138.5 (C^{C1}), 137.1 (C^{A4}), 129.2 (C^{C4}), 129.1 (C^{C3}), 127.4 (C^{C2}), 124.0 (C^{A5}), 122.9 (C^{D5}), 121.6 (C^{A3}), 120.9 (C^{D3}), 119.4 (C^{B3}), 119.2 (C^{B5}), 66.1 (C^1), 53.1 (C^{11}), 47.0 (C^{13}), 29.8, 29.7 (C^{5-8}), 29.4 (C^4), 28.8 (C^2), 27.8 (C^9), 27.0 (C^{10}),26.2 (C^3), 11.7 (C^{14}). **ESI MS** (MeOH/$CHCl_3$): *m/z* 601.2 $[M+Na]^+$ (4%, calc. 601.4), 579.2 $[M+H]^+$ (100%, calc. 579.4). **IR** (solid, ν/cm^{-1}) 2965 (w), 2919 (s), 2851 (m), 2792 (w), 1721 (s), 1584 (m), 1550 (m), 1466 (m), 1430 (m), 1379 (s), 1345 (w), 1283 (s), 1266 (s), 1214 (s), 1133 (m), 1101 (m), 1077 (m), 891 (m), 796 (m), 763 (s), 751 (s), 745 (s), 731 (s), 709 (s), 699 (s), 682 (s), 663 (s), 621 (s). **UV/VIS** λ_{max}/nm (3.97×10^{-5} mol dm^{-3}, MeCN) 254 (ε/dm^3 mol^{-1} cm^{-1} 32000), 280 (24000 sh), 313 (12000 sh). **EA** found: C, 75.52; H, 8.15; N, 9.29%. $C_{37}H_{46}N_4O_2\cdot0.5H_2O$ requires C, 75.60; H, 8.06; N, 9.53%.

4-Chloro-4'-phenyl-2,2':6',2''-terpyridine (L28)

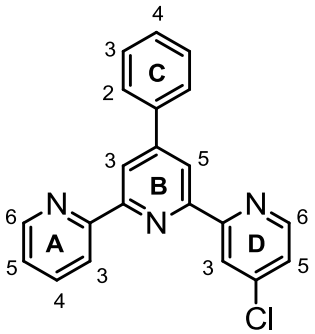

An excess of ammonium acetate (4.09 g, 53.16 mmol) was dissolved in methanol (30 mL). Chalcone **P11** (0.48 g, 2.31 mmol) and PPI salt **P6** (1.00 g, 2.77 mmol) were added and this brown suspension was heated at reflux for 23 hours, while all slowly dissolved. Then the

reaction mixture was cooled to room temperature and placed to the freezer overnight. The pale brown precipitate which formed was collected on a glass frit, washed with cold methanol and diethyl ether, and air dried to give the product as a pale brown powder (0.30 g, 0.87 mmol, 37%).

^{1}H NMR (500 MHz, $CDCl_3$, TMS) δ/ppm 8.77 (d, *J* = 1.7 Hz, 1H, H^{B3}), 8.74 (m, 2H, H^{A6+B5}), 8.67 (m, 2H, H^{D3+A3}), 8.60 (d, *J* = 5.2 Hz, 1H, H^{D6}), 7.90 (m, 3H, $H^{A4+C2+C6}$), 7.51 (m, 2H, H^{C3+C5}), 7.47 (m, 1H, H^{C4}),7.36 (m, 2H, H^{A5+D5}). **^{13}C {^{1}H} NMR** (126 MHz, $CDCl_3$) δ/ppm 157.9 (C^{D2}), 156.2 (C^{A2}), 156.1 (C^{B2}), 154.7 (C^{B6}), 150.6 (C^{B4}), 150.1 (C^{D6}), 149.3 (C^{A6}), 145.2 (C^{D4}), 138.4 (C^{C1}), 137.1 (C^{A4}), 129.3 (C^{C4}), 129.1 ($C^{C3,5}$), 127.5 ($C^{C2,6}$), 124.1 ($C^{A5, D5}$), 121.8 (C^{D3}), 121.5 (C^{A3}), 119.6 (C^{B3}), 119.3 (C^{B5}). **MP** 161-162 °C (from MeOH). **ESI MS** (MeOH/$CHCl_3$): *m/z* 383.1 $[M+K]^+$ (19%, calc. 382.1), 366.1 $[M+Na]^+$ (100%, calc. 366.1), 344.1 $[M+H]^+$ (57%, calc. 344.1). **IR** (solid, ν/cm^{-1}) 3056 (w), 2914 (w), 2853 (w), 1582 (m), 1566 (m), 1549 (m), 1464 (m), 1373 (m), 1341 (w), 1074 (w), 887 (m), 873 (w), 831 (m), 796 (m), 764 (s), 730 (s), 684 (m), 662 (m), 619 (s), 565 (s), 557 (m). **UV/VIS** λ_{max}/nm (3.88×10^{-5} mol dm^{-3}, MeCN) 254 (ε/dm^3 mol^{-1} cm^{-1} 35000), 276 (32000), 313 (8000 sh). **EA** found: C, 70.54; H, 4.06; N, 12.08%. $C_{21}H_{14}ClN_3{\cdot}0.75H_2O$ requires C, 70.59; H, 4.37; N, 11.76%.

4-(Dodecyloxy)-4'-phenyl-2,2':6',2''-terpyridine (L29)

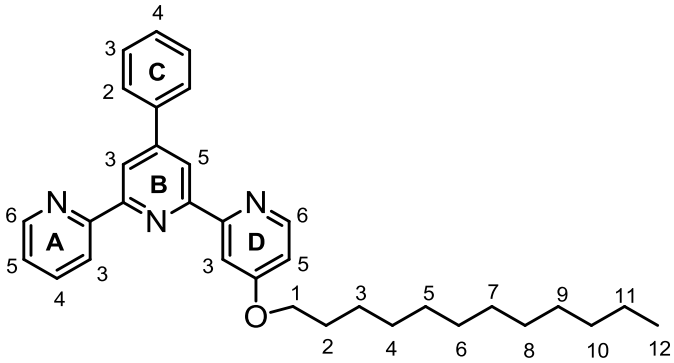

A white suspension of freshly ground potassium hydroxide (78 mg, 1.40 mmol) and dodecanol (52 mg, 0.28 mmol) in dimethyl sulfoxide (2 mL) was stirred at 50 °C for 15 minutes. 4-Chloro-4'-phenyl-2,2':6',2''-terpyridine **L28** (48 mg, 0.14 mmol) was added and the reddish-brown suspension was heated at 60 °C for 16 hours. This was cooled to room temperature and cold

water (10 mL) was added. The fine orange-brown precipitate which formed was dissolved in chloroform (100 mL) and thoroughly extracted with water (four times 100 mL) to remove all dimethyl sulfoxide. The organic phase was dried over sodium sulfate, filtered and solvent evaporated to give the product as a brown solid (46 mg, 0.09 mmol, 66%).

^{1}H NMR (500 MHz, $CDCl_3$, TMS) δ/ppm 8.67 (d, *J* = 1.8 Hz, 1H, H^{B5}), 8.66 (m, 2H, H^{A6+B3}), 8.59 (dt, *J* = 7.9, 1.1 Hz, 1H, H^{A3}), 8.46 (d, *J* = 5.6 Hz, 1H, H^{D6}), 8.12 (d, *J* = 2.5 Hz, 1H, H^{D3}), 7.83 (m, 3H, H^{A4+C2}), 7.45 (m, 2H, H^{C3}), 7.39 (m, 1H, H^{C4}), 7.29 (ddd, *J* = 7.5, 4.8, 1.2 Hz, 1H, H^{A5}), 6.80 (dd, *J* = 5.6, 2.6 Hz, 1H, H^{D5}), 4.09 (t, *J* = 6.5 Hz, 2H, H^{1}), 1.80 (m, 2H, H^{2}), 1.47 (m, 2H, H^{3}), 1.25 (m, 16H, H^{4-11}), 0.87 (t, *J* = 6.9 Hz, 3H, H^{12}). **^{13}C {^{1}H} NMR** (126 MHz, $CDCl_3$) δ/ppm 166.1 (C^{D4}), 157.8 (C^{D2}), 156.1 (C^{A2}), 155.8 (C^{B2+B6}), 150.3 (C^{D6}), 150.2 (C^{B4}), 149.1 (C^{A6}), 138.4 (C^{C1}), 136.9 (C^{A4}), 129.0 (C^{C4}), 128.9 (C^{C3}), 127.3 (C^{C2}), 123.8 (C^{A5}), 121.3 (C^{A3}), 119.0 (C^{B3}), 118.9 (C^{B5}), 110.3 (C^{D5}), 107.7 (C^{D3}), 68.1 (C^{1}), 31.9 (C^{10}), 29.7, 29.6, 29.5 (C^{6-9}), 29.5 (C^{4}), 29.3 (C^{5}), 29.0 (C^{2}), 26.0 (C^{3}),22.7 (C^{11}), 14.1 (C^{12}). **ESI MS** (MeOH/$CHCl_3$): *m/z* 516.3 $[M+Na]^+$ (34%, calc. 516.3), 494.4 $[M+H]^+$ (100%, calc. 494.3). **IR** (solid, ν/cm^{-1}) 3063 (w), 2918 (s), 2848 (m), 1584 (s), 1562 (s), 1551 (m), 1467 (m), 1453 (m), 1382 (m), 1297 (s), 1195 (m), 1115 (w), 1029 (s), 1004 (m), 880 (m), 797 (s), 765 (s), 756 (s), 733 (m), 722 (m), 698 (s), 688 (s), 661 (m), 619 (s). **UV/VIS** λ_{max} / nm (4.05×10^{-5} mol dm^{-3}, MeCN) 255 (ε/ dm^3 mol^{-1} cm^{-1} 75 000), 278 (63 000 sh), 309 (20 000).

N,N-Diethyl-11-((4'-phenyl-[2,2':6',2''-terpyridin]-4-yl)oxy)undecan-1-amine (L30)

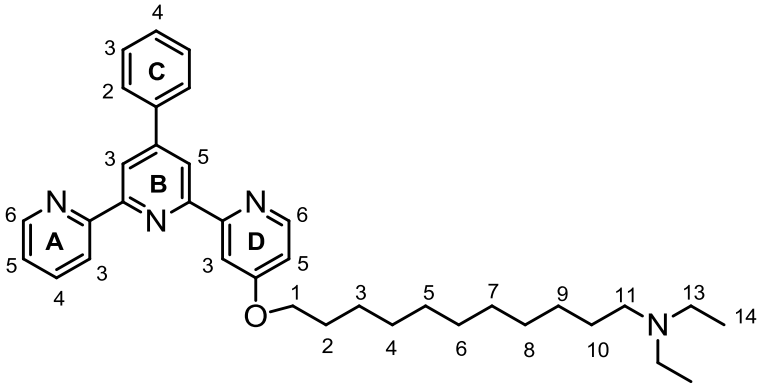

A white suspension of freshly ground potassium hydroxide (0.16 g, 2.91 mmol) and 11-(diethylamino)undecan-1-ol **P16** (0.14 g, 0.58 mmol) in dimethyl sulfoxide (7 mL) was stirred at 50 °C for 15 minutes. 4-Chloro-4'-phenyl-2,2':6',2''-terpyridine **L28** (0.10 g, 0.29 mmol) was

added and the reddish-brown suspension was heated at 65 °C for 16 hours. This was cooled to room temperature and cold water (10 mL) was added. The fine orange-brown precipitate, which formed, was dissolved in chloroform (100 mL) and thoroughly extracted with water (four times 100 mL) to remove all dimethyl sulfoxide. The organic phase was dried over sodium sulfate, filtered and solvent evaporated to give the product as a brown solid (39 mg, 0.07 mmol, 25%).

^{1}H NMR (500 MHz, $CDCl_3$, TMS) δ/ppm 8.59 (d, *J* = 2.0 Hz, 1H, H^{B3}), 8.56 (m, 2H, H^{B5+A6}), 8.51 (dt, *J* = 7.8, 1.1 Hz, 1H, H^{A3}), 8.39 (d, *J* = 5.6 Hz, 1H, H^{D6}), 8.04 (d, *J* = 2.5 Hz, 1H, H^{D3}), 7.76 (m, 3H, H^{A4+C2}), 7.36 (m, 2H, H^{C3}), 7.33 (m, 1H, H^{C4}), 7.23 (m, 1H, H^{A5}), 6.74 (dd, *J* = 5.6, 2.5 Hz, 1H, H^{D5}), 4.02 (t, *J* = 6.5 Hz, 2H, H^{1}), 2.39 (q, *J* = 7.1, 4H, H^{13}), 2.27 (m, 2H, H^{11}), 1.74 (m, 2H, H^{2}), 1.40 (m, 2H, H^{3}), 1.30 (m, 2H, H^{10}), 1.16 (m, 12H, H^{4-9}), 0.89 (t, *J* = 7.2, 6H, H^{14}). **^{13}C {^{1}H} NMR** (126 MHz, $CDCl_3$) δ/ppm 166.0 (C^{D4}), 157.6 (C^{D2}), 155.9 (C^{A2}), 155.6 (C^{B2+B6}), 150.2 (C^{D6}), 149.9 (C^{B4}), 148.9 (C^{A6}), 138.1 (C^{C1}), 136.7 (C^{A4}), 129.0 (C^{C4}), 128.7 (C^{C3}), 127.1 (C^{C2}), 123.7 (C^{A5}), 121.2 (C^{A3}), 118.9 (C^{B5}), 118.7 (C^{B3}), 110.1 (C^{D5}), 107.6 (C^{D3}), 67.9 (C^{1}), 52.7 (C^{11}), 46.5 (C^{13}), 29.4, 29.3 (C^{5-8}), 29.3 (C^{4}), 28.8 (C^{2}), 27.5 (C^{9}), 26.5 (C^{10}),25.8 (C^{3}), 11.3 (C^{14}). **ESI MS** (MeOH/$CHCl_3$): *m/z* 589.2 $[M+K]^+$ (7%, calc. 589.3), 573.2 $[M+Na]^+$ (23%, calc. 573.4), 551.2 $[M+H]^+$ (100%, calc. 551.4). **IR** (solid, ν/cm^{-1}) 2921 (s), 2852 (m), 1583 (s), 1565 (m), 1551 (m), 1466 (m), 1455 (m), 1383 (m), 1298 (m), 1196 (w), 1059 (m), 1043 (m), 989 (m), 884 (w), 794 (m), 766 (m), 694 (m), 620 (s). **UV/VIS** λ_{max} / nm (3.63×10^{-5} mol dm^{-3}, MeCN) 255 (ε/ dm^3 mol^{-1} cm^{-1} 71 000), 278 (53 000 sh), 312 (17 000 sh).

Complexes

[Ru(**L1**)]Cl_3 **(C1)**

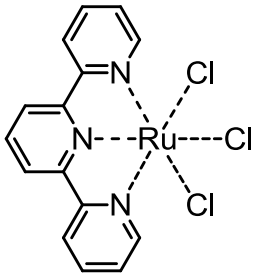

2,2':6',2''-Terpyridine **L1** (0.59 g, 2.53 mmol) and $RuCl_3 \cdot 3H_2O$ (0.66 g, 2.53 mmol) were suspended in ethanol (250 mL). The black reaction mixture was heated to reflux for 3.5 hours, while all reactants dissolved. The brown solid which formed was filtered off, washed with ethanol and diethyl ether and air dried to give a dark brown powder (1.0 g, 2.23 mmol, 90%). The product was submitted for the next step without further purification and characterization.

[Ru(**L3**)]Cl_3 **(C2)**

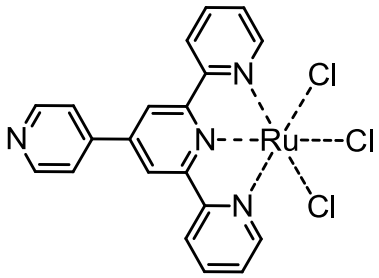

Terpyridine **L3** (0.60 g, 1.94 mmol) and $RuCl_3 \cdot 3H_2O$ (0.51 g, 1.94 mmol) were suspended in ethanol (200 mL). The black reaction mixture was heated to reflux for 3.5 hours, while all reactants dissolved. The black solid which formed was filtered off, washed with ethanol and diethyl ether and air dried to give a black powder (0.91 g, 1.76 mmol, 91%). The product was submitted for the next step without further purification and characterization.

[Ru(**L2**)(**L1**)][PF_6]$_2$ **(C3)**

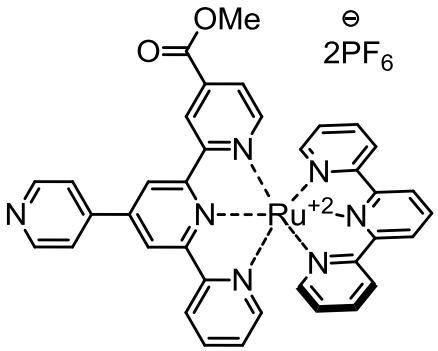

The ligand **L2** (0.20 g, 0.54 mmol) and the Ru(III) complex **C1** (0.24 g, 0.54 mmol) were suspended in ethylene glycol (20 mL) in a 50mL round bottomed flask and this dark brown suspension was treated in a domestic microwave oven at the highest setting for 2 minutes. The resulting dark red solution was poured into 250 mL of aqueous ammonium hexafluorophosphate to give a fine red precipitate, which was collected on Celite® and washed with cold water (500 mL), cold ethanol (20 mL) and diethyl ether (20 mL). The residue was redissolved in acetonitrile and solvent removed in vacuo to give a dark red solid, which was purified by column chromatography (SiO_2, eluted with MeCN/saturated aqueous KNO_3/H_2O = 10:1.5:0.5). The first red band was collected, aqueous ammonium hexafluorophosphate added and solvent evaporated until a red precipitate formed. This was collected on Celite® and washed thoroughly with cold water (500 mL), cold ethanol (15 mL) and diethyl ether (10 mL). The red residue was redissolved in acetonitrile and solvent removed in vacuo to give the product as a dark red powder (0.37 g, 0.37 mmol, 69%).

^{1}H NMR (500 MHz, CD_3CN) δ/ppm 9.21 (s, 1H, H^{B5}), 9.14 (s, 1H, H^{D3}), 9.10 (s, 1H, H^{B3}), 8.93 (d, *J* = 5.2 Hz, 2H, H^{C2}), 8.81 (d, *J* = 8.1 Hz, 2H, H^{F3}), 8.72 (d, *J* = 8.2 Hz, 1H, H^{A3}), 8.54 (d, *J* = 8.1 Hz, 2H, H^{E3}), 8.48 (t, *J* = 8.1 Hz, 1H, H^{F4}), 8.18 (d, *J* = 5.0 Hz, 2H, H^{C3}), 8.00 (t, *J* = 8.0 Hz, 1H, H^{A4}), 7.95 (t, *J* = 7.8 Hz, 2H, H^{E4}), 7.62 (m, 2H, H^{D5+D6}), 7.43 (d, *J* = 5.4 Hz, 3H, H^{A6+E6}), 7.24 (m, 1H, H^{A5}), 7.19 (m, 2H, H^{E5}), 3.93 (s, 3H, H^{Me}). **^{13}C {^{1}H} NMR** (101 MHz, CD_3CN) δ/ppm 164.8 ($C^{C=O}$), 160.2 (C^{D2}), 158.9 (C^{E2}), 158.8 (C^{A2}), 157.0 (C^{B2}), 156.5 (C^{B6}), 156.1 (C^{F2}), 154.5 (C^{D6}), 153.6 (C^{E6}), 153.5 (C^{A6}), 152.0 (C^{C2}), 146.4 (C^{B4}), 145.0 (C^{C4}), 139.6 (C^{A4}), 139.4 (C^{D4+E4}), 137.5 (C^{F4}), 128.8 (C^{A5}), 128.5 (C^{E5}), 127.3 (C^{D5}), 125.8 (C^{A3}), 125.6 (C^{E3}), 124.9 (C^{F3}), 124.5 (C^{D3}), 123.3 (C^{B5}), 123.1 (C^{B3+C3}), 54.0 (C^{Me}). **ESI MS** (MeCN): *m/z* 848.1 $[M\text{-}PF_6]^+$ (100%, calc. 848.1), 351.5 $[M\text{-}2PF_6]^{2+}$ (94%, 351.6). **IR**

(solid, ν/cm^{-1}) 3060 (w), 1731 (m), 1599 (m), 1448 (m), 1441 (w), 1406 (w), 1389 (w), 1311 (m), 1266 (m), 1246 (w), 1240 (w), 1120 (w), 1029 (w), 878 (w), 830 (s), 827 (s), 822 (s), 816 (s), 800 (m), 785 (m), 760 (m), 751 (m), 739 (m), 726 (m), 705 (w), 690 (w), 645 (w), 638 (w), 601 (w). **EA** found: C, 44.45; H, 3.12; N, 10.31%. $C_{37}H_{27}F_{12}N_7O_2P_2Ru$ requires C, 44.77; H, 2.74; N, 9.88%. **UV/VIS** λ_{max}/nm (3.02 x 10^{-5}mol dm^{-3}, MeCN) 271 (ε/dm^3 mol^{-1} cm^{-1} 58000), 286 (54000), 306 (62000), 327 (50000, sh), 488 (21000). **Luminescence** (MeCN, 3.02 x 10^{-5}mol dm^{-3}, λ_{ex} = 488 nm): λ_{em} = 665 nm.

[Ru(**L10**)(**L1**)][PF_6]$_2$ **(C4)**

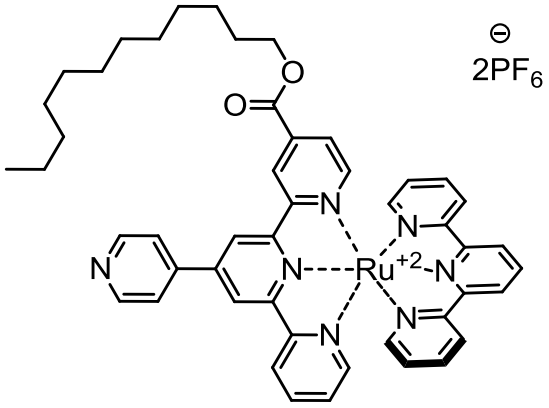

The ruthenium(II) complex **C3** (0.20 g, 0.20 mmol) was dissolved in *N*,*N*-dimethylformamide (2.5 mL). Dodecanol (0.19 g, 1.01 mmol) and a catalytic amount of *p*-toluenesulfonic acid monohydrate (3.8 mg, 0.02 mmol) were added. The red reaction mixture was heated at reflux for 21 hours and the formation of the product was monitored by thin layer chromatography (SiO_2, eluted with MeCN/saturated aqueous KNO_3/H_2O = 10:1.5:0.5). Solvent was removed in vacuo and the crude product was purified by flash column chromatography (SiO_2, eluted with MeCN/saturated aqueous KNO_3/H_2O = 10:1.5:0.5). The first red band was collected, aqueous ammonium hexafluorophosphate added and solvent evaporated until a red precipitate formed. This was collected on Celite® and washed thoroughly with cold water (250 mL) and diethyl ether (10 mL). The red residue was redissolved in acetonitrile and solvent removed in vacuo to give the product as a dark red powder (76 mg, 0.07 mmol, 33%).

^{1}H NMR (400 MHz, CD_3CN) δ/ppm 9.19 (s, 1H, H^{B5}), 9.07 (m, 2H, H^{B3+D3}), 8.97 (d, J = 3.7 Hz, 2H, H^{C2}), 8.77 (d, J = 8.2 Hz, 2H, H^{F3}), 8.67 (d, J = 8.1 Hz, 1H, H^{A3}), 8.50 (d, J = 8.1 Hz, 2H, H^{E3}), 8.46 (t,

J = 8.2 Hz, 1H, H^{F3}), 8.18 (d, J = 3.9 Hz, 2H, H^{C3}), 7.98 (td, J = 8.0, 1.4 Hz, 1H, H^{A4}), 7.93 (td, J = 8.0, 1.4 Hz, 2H, H^{E4}), 7.59 (dd, J = 5.8, 1.6 Hz, 1H, H^{D5}), 7.55 (d, J = 5.8 Hz, 1H, H^{D6}), 7.38 (m, 3H, H^{A6+E6}), 7.21 (m, 1H, H^{A5}), 7.16 (ddd, J = 7.0, 5.6, 1.2 Hz, 2H, H^{E5}), 4.33 (t, J = 6.7 Hz, 2H, H^{1}), 1.73 (m, 2H, H^{2}), 1.30 (m, 18H, $H^{3\text{-}11}$), 0.86 (t, J = 6.9 Hz, 3H, H^{12}). **MALDI TOF MS**: *m/z* 1170.4 $[M\text{-}Na]^+$ (100%, calc. 1170.2), 1025.4 $[M\text{-}PF_6\text{+}Na]^+$ (77%, 1025.3). **UV/VIS** λ_{max}/nm (3.49 x 10^{-5}mol dm^{-3}, MeCN) 272 (ε/dm^3 mol^{-1} cm^{-1} 51000), 281 (48000), 306 (54000), 326 (45000, sh), 488 (19000). **Luminescence** (MeCN, 3.49 x 10^{-5}mol dm^{-3}, λ_{ex} = 488 nm): λ_{em} = 664 nm.

$[Ru(H\mathbf{L11})(\mathbf{L1})][PF_6]_3$ **(C5)**

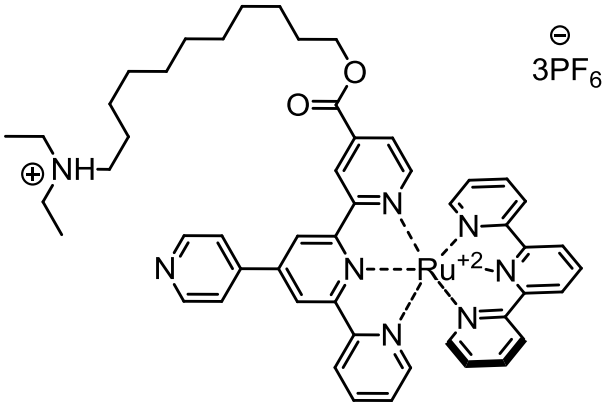

The ruthenium(II) complex **C3** (0.15 g, 0.15 mmol) was dissolved in *N*,*N*-dimethylformamide (2 mL). 11-(Diethylamino)undecan-1-ol **P16** (0.37 g, 1.51 mmol) and a catalytic amount of *p*-toluenesulfonic acid monohydrate (3.0 mg, 0.015 mmol) were added. The red reaction mixture was heated at reflux for 23 hours and the formation of the product was monitored by thin layer chromatography (SiO_2, eluted with MeCN/saturated aqueous KNO_3/H_2O = 10:1.5:0.5). Solvent was removed in vacuo and the crude product was purified by flash column chromatography (SiO_2, eluted with MeCN/saturated aqueous KNO_3/H_2O = 10:1.5:0.5). The first red band was collected, aqueous ammonium hexafluorophosphate added and solvent evaporated until a red precipitate formed. This was collected on Celite® and washed thoroughly with cold water (150 mL) and diethyl ether (10 mL). The red residue was redissolved in acetonitrile and solvent removed in vacuo to give the product as a dark red powder (30 mg, 0.02 mmol, 15%).

^{1}H NMR (500 MHz, CD_3CN) δ/ppm 9.19 (d, *J* = 1.3 Hz, 1H, H^{B5}), 9.08 (br s, 2H, H^{B3+D3}), 8.96 (d, *J* = 4.5 Hz, 2H, H^{C2}), 8.78 (d, *J* = 8.2 Hz, 2H, H^{F3}), 8.68 (d, *J* = 8.0 Hz, 1H, H^{A3}), 8.51 (d, *J* = 8.1 Hz, 2H,

H^{E3}), 8.46 (m, 1H, H^{F4}), 8.18 (d, *J* = 6.0 Hz, 2H, H^{C3}), 7.98 (td, *J* = 8.0, 1.4 Hz, 1H, H^{A4}), 7.93 (td, *J* = 8.1, 1.4 Hz, 2H, H^{E4}), 7.59 (dd, *J* = 5.8, 1.7 Hz, 1H, H^{D5}), 7.57 (d, *J* = 5.8 Hz, 1H, H^{D6}), 7.39 (m, 3H, H^{A6+E6}), 7.22 (m, 1H, H^{A5}), 7.17 (m, 2H, H^{E5}), 4.33 (t, *J* = 6.8 Hz, 2H, H^{1}), 3.14 (q, *J* = 7.0 Hz, 4H, H^{13}), 3.02 (br s, 2H, H^{11}), 1.74 (m, 2H, H^{2}), 1.63 (m, 2H, H^{10}), 1.39 (m, 2H, H^{3}), 1.27 (m, 12H, H^{4-9}), 1.24 (t, *J* = 7.3 Hz, 6H, H^{14}). **^{13}C {^{1}H} NMR** (126 MHz, CD_3CN) δ/ppm 164.3 ($C^{C=O}$), 160.1 (C^{D2}), 158.9 (C^{E2}), 158.8 (C^{A2}), 157.0 (C^{B2}), 156.5 (C^{B6}), 156.1 (C^{F2}), 154.5 (C^{D6}), 153.6 (C^{E6}), 153.5 (C^{A6}), 151.9 (C^{C2}), 146.3 (C^{B4}), 145.3 (C^{C4}), 139.9 (C^{D4}), 139.4 (C^{A4+E4}), 137.4 (C^{F4}), 128.8 (C^{A5}), 128.5 (C^{E5}), 127.3 (C^{D5}), 125.8 (C^{A3}), 125.6 (C^{E3}), 124.9 (C^{F3}), 124.4 (C^{D3}), 123.3 (C^{B5}), 123.2 (C^{C3}), 123.1 (C^{B3}), 67.5 (C^{1}), 53.0 (C^{11}), 48.4 (C^{13}), 30.3, 30.2, 30.1 (C^{5-7}), 29.9 (C^{4}), 29.7 (C^{8}), 29.2 (C^{2}), 27.0 (C^{9}), 26.5 (C^{3}), 24.4 (C^{10}), 9.1 (C^{14}). **ESI MS** (MeCN) monoprotonated form: *m/z* 1205.5 $[M\text{-}PF_6]^+$ (3%, calc. 1205.3), 530.2 $[M\text{-}2PF_6]^{2+}$ (83%, 530.2), deprotonated form: *m/z* 1205.5 $[M+H]^+$ (3%, 1205.3), 1059.3 $[M\text{-}PF_6]^+$ (36%, 1059.3). **IR** (solid, ν/cm^{-1}) 3632 (w), 3120 (w), 2927 (m), 2850 (m), 1722 (m), 1716 (m), 1600 (m), 1449 (m), 1407 (w), 1390 (w), 1265 (m), 1248 (m), 1241 (m), 1166 (w), 1117 (w), 1030 (w), 824 (s), 822 (s), 785 (s), 765 (s), 739 (m), 725 (m), 690 (w), 668 (w), 657 (w), 644 (m), 601 (m). **EA** found: C, 45.87; H, 4.74; N, 8.95%. $C_{51}H_{57}F_{18}N_8O_2P_3Ru$ requires C, 45.37; H, 4.26; N, 8.30%. **UV/VIS** λ_{max}/nm (3.32 x 10^{-5}mol dm^{-3}, MeCN) 271 (ε/dm^3 mol^{-1} cm^{-1} 37000), 283 (35000), 306 (42000), 327 (33000, sh), 488 (15000). **Luminescence** (MeCN, 3.32 x 10^{-5}mol dm^{-3}, λ_{ex} = 488 nm): λ_{em} = 664 nm.

[Ru(**L3**)]Cl_3 **(C6)**

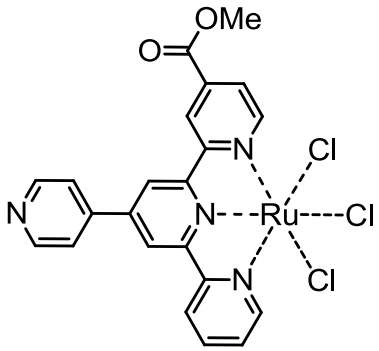

Terpyridine **L2** (0.30 g, 0.81 mmol) and $RuCl_3 \cdot 3H_2O$ (0.21 g, 0.81 mmol) were suspended in ethanol (150 mL). The brown reaction mixture was heated to reflux for 3.5 hours, while all

reactants dissolved. The brown solid which formed was filtered off, washed with ethanol and diethyl ether and air dried to give a dark brown powder (0.44 g, 1.76 mmol, 93%). The product was submitted for the next step without further purification and characterization.

[Ru(**L2**)(**L3**)][PF_6]$_2$ **(C7)**

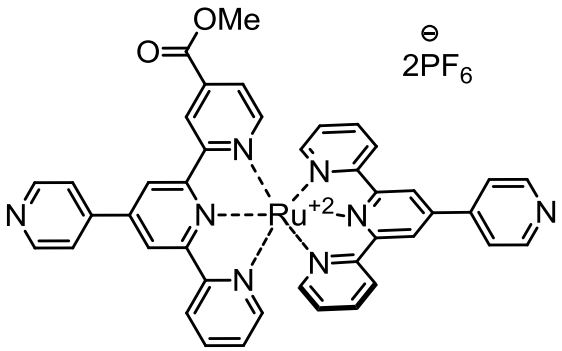

The ruthenium(II) complex **C6** (56 mg, 0.11 mmol) was suspended in dry *N*,*N*-dimethylformamide (5 mL) in a 10mL round bottomed flask. Silver hexafluorophosphate (122 mg, 0.48 mmol) was added and the black suspension was stirred for 10 minutes at 100 °C and then 30 minutes at laboratory temperature under an inert atmosphere in darkness. This dark brown solution was filtered on Celite® to remove silver chloride, then washed with *N*,*N*-dimethylformamide (5 mL) and solvent mostly removed in vacuo. The black residue was transferred into a 2mL microwave reactor vial and dissolved in dry *N*,*N*-dimethylformamide (2 mL). The ligand **L3** (30 mg, 0.11 mmol) and *N*-ethylmorpholine (3 drops) were added and the reaction mixture was treated in a microwave reactor at 160 °C for 15 minutes. The resulting dark red solution was poured into 250 mL of aqueous ammonium hexafluorophosphate to give a fine red precipitate, which was collected on Celite® and washed with cold water (250 mL) and diethyl ether (20 mL). The residue was redissolved in acetonitrile and solvent removed in vacuo to give a dark red solid, which was purified with column chromatography (SiO_2, eluted with MeCN/saturated aqueous KNO_3/H_2O = 7:2:2). The first red band was collected, aqueous ammonium hexafluorophosphate added and solvent evaporated until a red precipitate formed. This was collected on Celite® and washed thoroughly with cold water (250 mL), cold ethanol (15 mL) and diethyl ether (15 mL). The red residue was redissolved in acetonitrile and solvent removed in vacuo to give the product as a dark red powder (47 mg, 0.044 mmol, 45%).

^{1}H NMR (400 MHz, CD_3CN) δ/ppm 9.22 (d, *J* = 1.2 Hz, 1H, H^{B5}), 9.13 (s, 1H, H^{D3}), 9.10 (d, *J* = 1.2 Hz, 1H, H^{B3}), 9.07 (s, 1H, H^{F3}), 9.06 (s, 1H, H^{F5}),8.97 (dd, *J* = 4.3, 1.9 Hz, 4H, H^{C2+G2}), 8.67 (m, 3H, H^{A3+E3}), 8.17 (m, 2H, H^{C3}), 8.14 (d, *J* = 4.8, 2H, H^{G3}), 8.00 (m, 3H, H^{A4+E4}), 7.61 (m, 2H, H^{D6+D5}), 7.43 (m, 2H, H^{E6+A6}), 7.20 (m, 3H, H^{A5+E5}), 3.92 (s, 3H, H^1). **ESI MS** (MeCN): *m/z* 925.3 $[M\text{-}PF_6]^+$ (50%, calc. 925.1), 390.1 $[M\text{-}2PF_6]^{2+}$ (100%, 390.1). **IR** (solid, ν/cm^{-1}) 3645 (w), 3067 (w), 1731 (m), 1700 (m), 1597 (m), 1474 (w), 1406 (m), 1343 (w), 1312 (m), 1268 (m), 1248 (w), 1246 (w), 1237 (w), 1163 (w), 1125 (w), 1029 (w), 830 (s), 822 (s), 798 (m), 785 (m), 766 (m), 752 (m), 741 (w), 730 (w), 637 (w), 602 (w). **UV/VIS** λ_{max}/nm (1 x 10^{-5}mol dm^{-3}, MeCN) 239 (ε/dm^3 mol^{-1} cm^{-1} 19000), 277 (28000), 315 (25000), 492 (11000). **Luminescence** (MeCN, 1 x 10^{-5}mol dm^{-3}, λ_{ex} = 492 nm): λ_{em} = 661 nm.

$[Ru(\mathbf{L3})_2][PF_6]_2$ **(C8)**

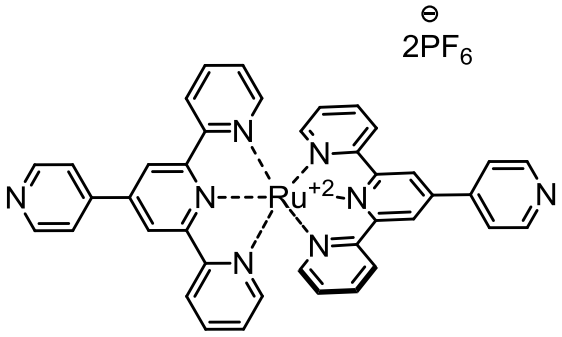

The ruthenium(II) complex **C8** is formed as a side product during synthesis of **C7**, **C17**-**C20**, **C22**-**25**.

^{1}H NMR (400 MHz, CD_3CN) δ/ppm 9.06 (s, 4H, H^{B3}), 8.97 (dd, *J* = 4.4, 1.7 Hz, 4H, H^{C2}), 8.66 (dd, *J* = 8.0, 0.9 Hz, 4H, H^{A3}), 8.13 (dd, *J* = 4.4, 1.7 Hz, 4H, H^{C3}), 7.97 (td, *J* = 8.0, 1.5 Hz, 4H, H^{A4}), 7.42 (ddd, *J* = 5.6, 1.3, 0.6 Hz, 4H, H^{A6}), 7.20 (ddd, *J* = 7.5, 5.6, 1.3 Hz, 4H, H^{A5}). **UV/VIS** λ_{max}/nm (2.48 x 10^{-5}mol dm^{-3}, MeCN) 275 (ε/dm^3 mol^{-1} cm^{-1} 65000), 313 (52000), 489 (26000). **Luminescence** (MeCN, 1.38 x 10^{-5}mol dm^{-3}, λ_{ex} = 492 nm): λem = 657 nm.

[Ru(**L3**)]Cl_3 **(C9)**

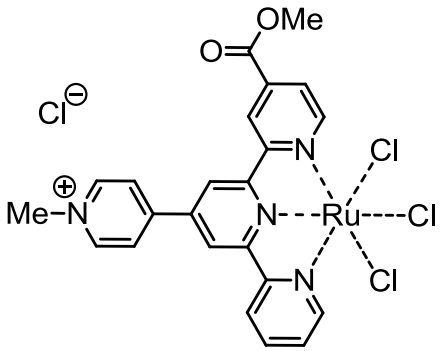

Terpyridine **L5** (0.50 g, 0.95 mmol) and $RuCl_3 \cdot 3H_2O$ (0.25 g, 0.95 mmol) were suspended in ethanol (125 mL). The brown reaction mixture was heated to reflux for 3 hours, while all reactants dissolved. The black solid which formed was filtered off, washed with ethanol and diethyl ether and air dried to give a black powder (0.52 g, 0.83 mmol, 75%). The product was submitted for the next step without further purification and characterization.

[Ru(**L5**)(**L4**)][PF_6]$_4$ **(C10)**

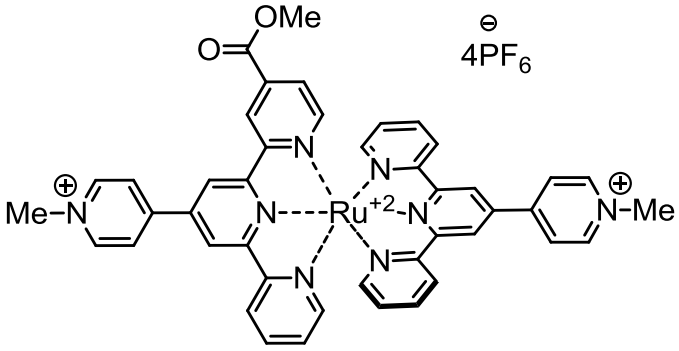

The ruthenium(II) complex **C9** (74 mg, 0.10 mmol) was suspended in dry *N*,*N*-dimethylformamide (4 mL) in a 10mL round bottomed flask. Silver hexafluorophosphate (102 mg, 0.40 mmol) was added and the black suspension was stirred for 10 minutes at 100 °C and then 30 minutes at laboratory temperature under an inert atmosphere in darkness. This dark brown solution was filtered on Celite® to remove silver chloride, then washed with *N*,*N*-dimethylformamide (5 mL) and solvent mostly removed in vacuo. The black residue was transferred into a 2mL microwave reactor vial and dissolved in dry *N*,*N*-dimethylformamide (2 mL). The ligand **L4** (47 mg, 0.10 mmol) and *N*-ethylmorpholine (3 drops) were added and the

reaction mixture was treated in a microwave reactor at 160 °C for 20 minutes. The resulting dark red-purple solution was poured into 250 mL of aqueous ammonium hexafluorophosphate to give a fine red precipitate, which was collected on Celite® and washed with cold water (250 mL) and diethyl ether (20 mL). The residue was redissolved in acetonitrile and solvent removed in vacuo to give a dark purple-black solid, which was purified with column chromatography (SiO_2, eluted with MeCN/saturated aqueous KNO_3/H_2O = 7:2:2). The first red-purple band was collected, aqueous ammonium hexafluorophosphate added and solvent evaporated until a red-purple precipitate formed. This was collected on Celite® and washed thoroughly with cold water (250 mL), cold ethanol (15 mL) and diethyl ether (15 mL). The residue was redissolved in acetonitrile and solvent removed in vacuo to give the product as a dark red-purple powder (73 mg, 0.053 mmol, 53%).

^{1}H NMR (500 MHz, CD_3CN) δ/ppm 9.32 (d, *J* = 1.4 Hz, 1H, H^{B5}), 9.20 (d, *J* = 1.4 Hz, 1H, H^{B3}), 9.17 (m, 3H, H^{D3+F3}), 8.97 (m, 4H, H^{C2+G2}), 8.78 (m, 4H, H^{C3+G3}), 8.72 (m, 3H, H^{A3+E3}), 8.02 (m, 3H, H^{A4+E4}), 7.67 (dd, *J* = 5.8, 0.6 Hz, 1H, H^{D6}), 7.63 (dd, *J* = 5.8, 1.7 Hz, 1H, H^{D5}), 7.46 (m, 3H, H^{A6+E6}), 7.25 (m, 3H, H^{A5+E5}), 4.48 (m, 6H, H^{NMe}), 3.93 (s, 3H, H^{OMe}). **^{13}C {^{1}H} NMR** (126 MHz, CD_3CN) δ/ppm 164.7 ($C^{C=O}$), 159.6 (C^{D2}), 158.4 (C^{E2}), 158.3 (C^{A2}), 157.1 (C^{B2}), 157.0 (C^{F2}), 156.6 (C^{B6}), 154.7 (C^{D6}), 153.7 (C^{E6}), 153.6 (C^{A6}), 153.3 (C^{C2+G2}), 147.3 (C^{C3+G3}), 142.5 (C^{F4}), 142.2 (C^{B4}), 140.0 (C^{D4}), 139.8 (C^{A4}), 139.7 (C^{E4}), 129.5 (C^{A5+E5}), 127.6 (C^{D5}), 126.1 (C^{E3}), 126.0 (C^{A3}), 124.8 (C^{D3}), 123.9 (C^{B5}), 123.6 (C^{B3}), 123.4 (C^{F3}), 54.1 (C^{OMe}), 49.3 (C^{NMe}). **MALDI TOF MS** (DCM-MeCN): *m/z* 1099.6 $[M\text{-}2PF_6]^+$ (25%, calc. 1100.1), 954.2 $[M\text{-}3PF_6]^+$ (46%, calc. 955.2), 810.9 $[M\text{-}4PF_6]^+$ (100%, calc. 810.2), 325.3 $[L4]^+$ (100%, 325.1). **IR** (solid, ν/cm^{-1}) 3107 (w), 1739 (m), 1640 (m), 1635 (m), 1622 (w), 1616 (w), 1605 (w), 1527 (w), 1469 (w), 1422 (m), 1419 (m), 1364 (m), 1340 (m), 1317 (m), 1293 (m), 1273 (m), 1250 (w), 1190 (w), 1030 (w), 822 (s), 786 (m), 767 (m), 752 (m), 740 (m), 733 (m), 723 (w), 711 (w), 652 (w), 618 (w), 600 (w). **UV/VIS** λ_{max}/nm (2.88 x 10^{-5}mol dm^{-3}, MeCN) 241 ($\varepsilon/dm^3\ mol^{-1}\ cm^{-1}$ 39000), 277 (53000), 341 (33000), 510 (26000). **Luminescence** (MeCN, 2.88 x 10^{-5}mol dm^{-3}, λ_{ex} = 510 nm): λ_{em} = 710 nm.

[Ru(**L9**)(**L4**)][PF_6]$_4$ **(C11)**

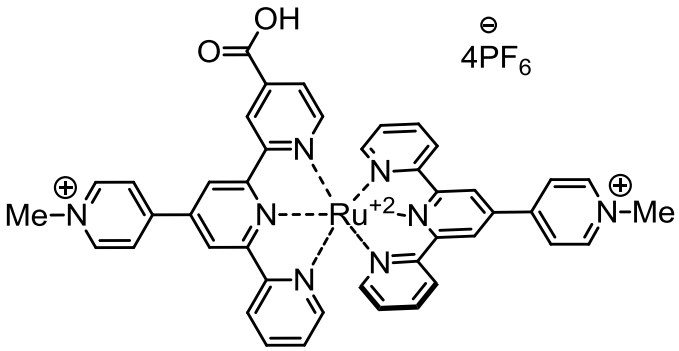

The ruthenium(II) complex **C11** is formed as a side product during synthesis of the complex **C10**. The second red-purple band was collected, aqueous ammonium hexafluorophosphate added and solvent evaporated until a red-purple precipitate formed. This was collected on Celite® and washed with cold water (250 mL), cold ethanol (15 mL) and diethyl ether (15 mL). The residue was redissolved in acetonitrile and solvent removed in vacuo to give the product as a dark red-purple powder (23 mg, 0.016 mmol, 17%).

^{1}H NMR (500 MHz, CD_3CN) δ/ppm 9.34 (s, 1H, H^{B5}), 9.19 (m, 4H, $H^{D3+B3+F3}$), 8.97 (m, 4H, H^{C2+G2}), 8.81 (m, 2H, H^{C3}), 8.78 (m, 2H, H^{G3}), 8.71 (m, 3H, H^{A3+E3}), 8.00 (m, 3H, H^{A4+E4}), 7.60 (m, 1H, H^{D6}), 7.52 (m, 1H, H^{D5}), 7.45 (m, 3H, H^{A6+E6}), 7.25 (m, 3H, H^{A5+E5}), 4.46 (m, 6H, H^{NMe}). **^{13}C {^{1}H} NMR** (126 MHz, CD_3CN) δ/ppm 164.5 ($C^{C=O}$), 158.8 (C^{D2}), 158.3 (C^{E2+A2}), 157.0 (C^{B2}), 156.9 (C^{F2+B6}), 153.9 (C^{D6}), 153.7 (C^{E6}), 153.6 (C^{A6}), 153.3 (C^{C2+G2}), 147.3 (C^{C3+G3}), 142.2 (C^{F4+B4}), 140.0 (C^{D4}), 139.6 (C^{A4+E4}), 129.0 (C^{A5+E5}), 128.2 (C^{D5}), 126.0 (C^{E3+A3}), 123.6 (C^{D3}), 123.4 ($C^{F3+ B3}$), 123.3 (C^{B5}), 49.2 (C^{NMe}). **ESI MS** (MeCN): *m/z* 369.2 $[L9]^+$ (60%, calc. 369.1), 325.2 $[L4]^+$ (100%, 325.1). **IR** (solid, ν/cm^{-1}) 3089 (w), 1720 (m), 1641 (s), 1635 (m), 1616 (w), 1605 (w), 1527 (w), 1486 (w), 1471 (w), 1422 (m), 1419 (m), 1409 (w), 1360 (w), 1339 (w), 1321 (w), 1293 (w), 1243 (w), 1228 (w), 1193 (w), 1163 (w), 1091 (w), 1023 (w), 820 (s), 805 (s), 785 (s), 777 (s), 750 (m), 736 (m), 730 (m), 709 (m), 697 (w), 683 (w), 653 (w), 602 (m). **EA** found: C, 34.52; H, 2.61; N, 9.05%. $C_{43}H_{34}F_{24}N_8O_2P_4Ru{\cdot}NH_4PF_6{\cdot}1.5MeCN$ requires C, 34.52; H, 2.68; N, 9.19%. **UV/VIS** λ_{max}/nm (1.45 x 10^{-5}mol dm^{-3}, MeCN) 241 (ε/dm^3 mol^{-1} cm^{-1} 40000), 277 (58000), 343 (31000), 511 (28000). **Luminescence** (MeCN, 1.45 x 10^{-5}mol dm^{-3}, λ_{ex} = 510 nm): λ_{em} = 725 nm.

Complex **C12**

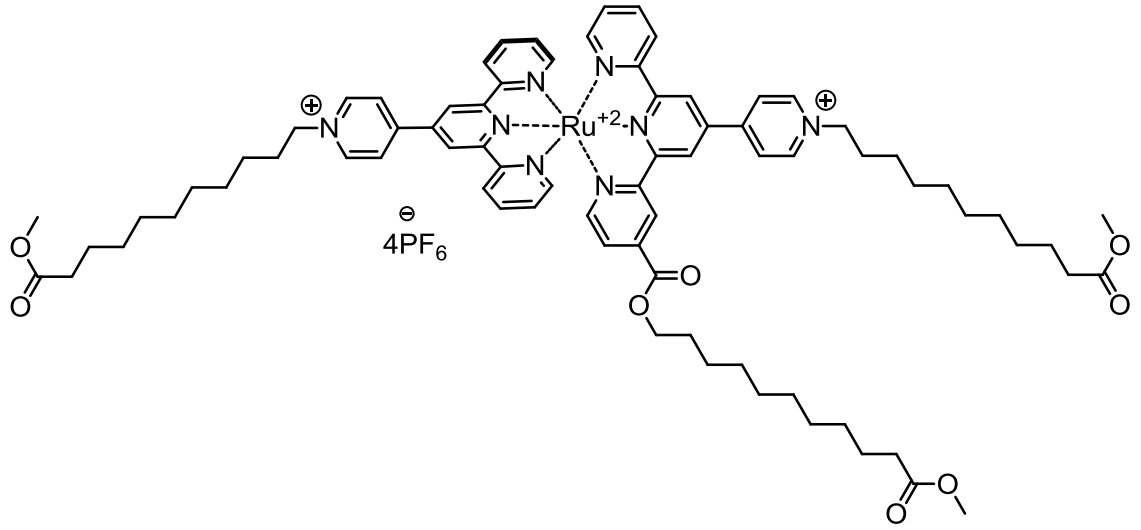

The ruthenium(II) complex **C7** (50 mg, 0.047 mmol) was dissolved in *N*,*N*-dimethylformamide (2.5 mL). Methyl 11-bromoundecanoate (0.13 g, 0.47 mmol) and a catalytic amount of *p*-toluenesulfonic acid monohydrate (4.4 mg, 0.02 mmol) were added. The red reaction mixture was heated at reflux for 2 hours and the formation of the product was monitored by thin layer chromatography (SiO_2, eluted with MeCN/saturated aqueous KNO_3/H_2O = 10:1.5:0.5). Solvent was removed in vacuo and the crude product was purified on a preparative TLC plate (SiO_2, eluted with MeCN/saturated aqueous KNO_3/H_2O = 10:1.5:0.5). The first wine-red band was collected, aqueous ammonium hexafluorophosphate added and solvent evaporated until a precipitate formed. This was collected on Celite® and washed thoroughly with cold water (250 mL) and diethyl ether (10 mL). The residue was redissolved in acetonitrile and solvent removed in vacuo to give the product as a dark red powder (11 mg, 0.006 mmol, 12%).

^{1}H NMR (500 MHz, CD_3CN) δ/ppm 9.28 (d, *J* = 1.3 Hz, 1H, H^{B5}), 9.16 (d, *J* = 1.3 Hz, 1H, H^{B3}), 9.14 (m, 3H, H^{D3+F3}), 9.02 (m, 4H, H^{C2+G2}), 8.78 (m, 4H, H^{C3+G3}), 8.69 (m, 3H, H^{A3+E3}), 8.03 (m, 3H, H^{A4+E4}), 7.64 (m, 2H, H^{D6+D5}), 7.46 (m, *J* = 4.9 Hz, 1H, H^{A6}), 7.42 (m, *J* = 5.6 Hz, 2H, H^{E6}),7.26 (m, 3H, H^{A5+E5}), 4.69 (t, *J* = 7.2 Hz, 4H, H^{1}), 4.34 (t, *J* = 6.7 Hz, 2H, $H^{1'}$), 3.60 (s, 6H, H^{Me}), 3.58 (s, 3H, $H^{Me'}$), 2.30 (t, *J* = 7.6 Hz, 4H, H^{10}), 2.25 (m, *2*H, $H^{10'}$), 2.18 (m, 4H, H^{2}), 1.74 (m, 2H, $H^{2'}$),1.59 (m, 4H, H^{9}), 1.40 (m, 38H, $H^{3\text{-}8,\ 3'\text{-}9'}$). **ESI MS** (MeCN): *m/z* 751.5 $[L_2\text{-}PF_6]^+$ (60%, calc. 751.4), 509.3 $[L_1\text{-}PF_6]^+$ (35%, 509.2). **EA** found: C, 41.00; H, 4.98; N, 5.68%. $C_{89}H_{96}F_{24}N_8O_8P_4Ru{\cdot}2NH_4PF_6{\cdot}$requires C, 40.77; H, 4.62; N, 6.17%. **UV/VIS** λ_{max}/nm (3.09 x 10^{-5}mol dm^{-3}, MeCN) 241 (ε/dm^3 mol^{-1} cm^{-1}

46000), 278 (63000), 342 (39000), 511 (32000). **Luminescence** (MeCN, 3.09 x 10^{-5}mol dm^{-3}, λ_{ex} = 510 nm): λ_{em} = 708 nm.

Complex **C13**

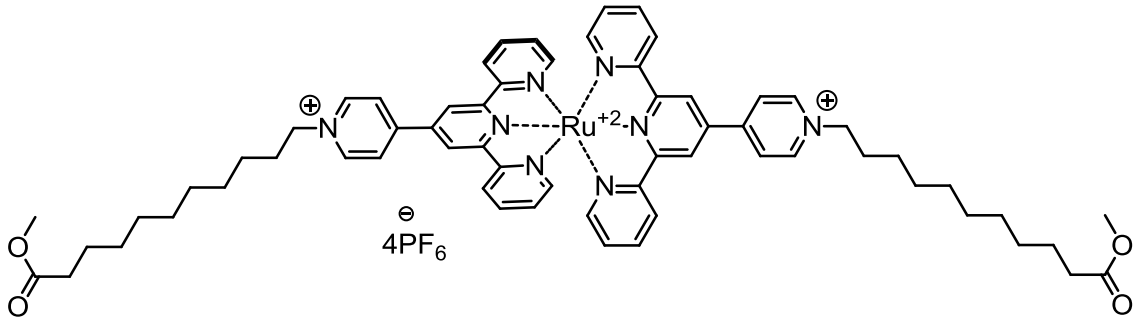

The ruthenium(II) complex **C13** is formed as a side product during synthesis of the complex **C12.** The second wine-red band was collected, aqueous ammonium hexafluorophosphate added and solvent evaporated until a precipitate formed. This was collected on Celite® and washed thoroughly with cold water (250 mL) and diethyl ether (10 mL). The residue was redissolved in acetonitrile and solvent removed in vacuo to give the product as a dark red powder (19 mg, 0.011 mmol, 24%).

^{1}H NMR (500 MHz, CD_3CN) δ/ppm 9.13 (s, 4H, H^{B3}), 9.01(d, *J* = 6.6 Hz, 4H, H^{C2}), 9.01(d, *J* = 6.6 Hz, 4H, H^{C3}), 8.70 (d, *J* = 8.1 Hz, 4H, H^{A3}), 8.01 (td, *J* = 7.9, 1.4 Hz, 4H, H^{A4}), 7.45 (dd, *J* = 5.6, 1.0 Hz, 4H, H^{A6}), 7.25 (m, 4H, H^{A5}), 4.68 (t, *J* = 7.5 Hz, 4H, H^{1}), 3.60 (s, 6H, H^{Me}), 2.30 (t, *J* = 7.5 Hz, 4H, H^{10}), 2.20 (m, 4H, H^{2}), 1.59 (m, 4H, H^{9}), 1.40 (m, 24H, H^{3-8}). **^{13}C {^{1}H} NMR** (126 MHz, CD_3CN) δ/ppm 174.9 ($C^{C=O}$), 158.4 (C^{A2}), 156.9 (C^{B2}), 153.7 (C^{A6}), 153.6 (C^{C2}), 146.3 (C^{C3}), 142.1 (C^{B4}), 139.6 (C^{A4}), 129.1 (C^{A5}), 126.1 (C^{A3}), 123.3 (C^{B3}), 62.8 (C^{1}), 51.9 (C^{Me}), 34.5 (C^{10}), 31.9 (C^{2}), 31.9 (C^{4-8}), 26.5 (C^{3}), 25.5 (C^{9}). **ESI MS** (MeCN): *m/z* 705.3 $[L_2\text{-}PF_6]^+$ (29%, calc. 705.3), 509.3 $[L\text{-}PF_6]^+$ (100%, 509.2). **EA** found: C, 39.41; H, 4.45; N, 6.85%. $C_{64}H_{74}F_{24}N_8O_4P_4Ru{\cdot}1.5NH_4PF_6{\cdot}$requires C, 39.53; H, 4.15; N, 6.84%. **UV/VIS** λ_{max}/nm (3.23 x 10^{-5}mol dm^{-3}, MeCN) 241 (ε/dm^3 mol^{-1} cm^{-1} 56000), 278 (88000), 342 (44000), 511 (42000). **Luminescence** (MeCN, 3.23 x 10^{-5}mol dm^{-3}, λ_{ex} = 510 nm): λ_{em} = 708 nm.

[Ru(**L6**)(**L3**)][PF_6]$_2$ **(C14)**

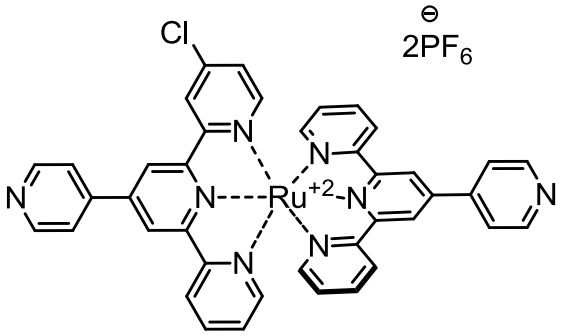

The ligand **L6** (50 mg, 0.15 mmol) and $RuCl_3.3H_2O$ (38 mg, 0.15 mmol) were suspended in ethylene glycol (8 mL) in a 25mL round bottomed flask and this dark brown suspension was treated in a domestic microwave oven at the highest setting for 4 minutes. The ligand **L3** (45 mg, 0.15 mmol) was added and the reaction mixture was threated in a domestic microwave oven at the highest setting for 4 minutes. The resulting dark red solution was poured into 250 mL of aqueous ammonium hexafluorophosphate to give a fine red precipitate, which was collected on Celite® and washed with cold water (200 mL), cold ethanol (20 mL) and diethyl ether (20 mL). The residue was redissolved in acetonitrile and solvent removed in vacuo to give a dark red solid, which was purified by column chromatography (SiO_2, eluted with MeCN/saturated aqueous KNO_3/H_2O = 7:2:2). The second red band was collected, aqueous ammonium hexafluorophosphate added and solvent evaporated until a red precipitate formed. This was collected on Celite® and washed thoroughly with cold water (500 mL), cold ethanol (15 mL) and diethyl ether (10 mL). The red residue was redissolved in acetonitrile and solvent removed in vacuo to give the product as a dark red powder (80 mg, 0.076 mmol, 53%).

^{1}H NMR (400 MHz, CD_3CN) δ/ppm 9.08 (s, 1H, H^{B5}), 9.07 (s, 1H, H^{B3}), 9.07 (s, 2H, H^{F3}), 8.99 (m, 4H, H^{C2+G2}), 8.77 (dd, *J* = 2.3, 0.5 Hz, 1H, H^{D3}), 8.67 (m, 3H, H^{A3+E3}), 8.17 (m, 4H, H^{C3+G3}), 7.98 (m, 3H, H^{A4+E4}), 7.44 (m, 2H, H^{E6+A6}), 7.37 (dd, *J* = 6.1, 0.5 Hz, 1H, H^{D6}), 7.26 (dd, *J* = 6.1, 2.2 Hz, 1H, H^{D5}), 7.21 (m, 3H, H^{A5+E5}). **ESI MS** (MeCN): *m/z* 901.2 $[M\text{-}PF_6]^+$ (28%, calc. 901.1), 378.1 $[M\text{-}2PF_6]^{2+}$ (100%, 378.1). **IR** (solid, ν/cm^{-1}) 3645 (w), 3073 (w), 1597 (m), 1530 (w), 1477 (w), 1464 (w), 1429 (m), 1407 (m), 1386 (w), 1355 (w), 1288 (w), 1245 (w), 1233 (w), 1164 (w), 1029 (m), 968 (w), 878 (w), 830 (s), 820 (s), 785 (s), 749 (s), 741 (m), 733 (m), 723 (m), 711 (m), 694 (w), 680 (w), 663 (w), 652 (m), 636 (m), 626 (w), 601 (m). **EA** found: C, 44.44; H, 2.97; N, 10.65%.

$C_{40}H_{27}ClF_{12}N_8P_2Ru{\cdot}2H_2O$ requires C, 44.39; H, 2.89; N, 10.35%. **UV/VIS** λ_{max}/nm (3.35 x 10^{-5}mol dm^{-3}, MeCN) 239 (ε/dm^3 mol^{-1} cm^{-1} 66000), 276 (103000), 312 (90000), 490 (44000). **Luminescence** (MeCN, 3.35 x 10^{-5}mol dm^{-3}, λ_{ex} = 490 nm): λ_{em} = 658 nm.

$[Ru(\mathbf{L6})_2][PF_6]_2$ **(C15)**

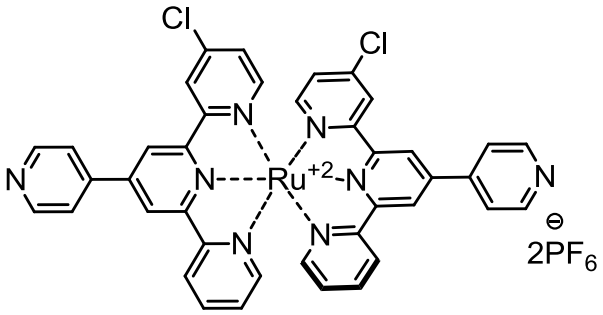

The ligand **L6** (50 mg, 0.15 mmol) and $RuCl_3.3H_2O$ (38 mg, 0.15 mmol) were suspended in ethylene glycol (8 mL) in a 25mL round bottomed flask and this dark brown suspension was treated in a domestic microwave oven at the highest setting for 4 minutes. The second aliquot of **L6** (50 mg, 0.15 mmol) was added and the reaction mixture was threated in a domestic microwave oven at the highest setting for 4 minutes. The resulting dark red solution was poured into 250 mL of aqueous ammonium hexafluorophosphate to give a fine red precipitate, which was collected on Celite® and washed with cold water (200 mL), cold ethanol (20 mL) and diethyl ether (20 mL). The residue was redissolved in acetonitrile and solvent removed in vacuo to give a dark red solid, which was purified by column chromatography (SiO_2, eluted with MeCN/saturated aqueous KNO_3/H_2O = 7:2:2). The second red band was collected, aqueous ammonium hexafluorophosphate added and solvent evaporated until a red precipitate formed. This was collected on Celite® and washed thoroughly with cold water (500 mL), cold ethanol (15 mL) and diethyl ether (10 mL). The red residue was redissolved in acetonitrile and solvent removed in vacuo to give the product as a dark red powder (30 mg, 0.028 mmol, 19%).

^{1}H NMR (400 MHz, CD_3CN) δ/ppm 9.08 (d, *J* = 1.4, 2H, H^{B5}), 9.07 (d, *J* = 1.4, 2H, H^{B3}), 8.97 (dd, *J* = 4.4, 1.7 Hz, 2H, H^{C2}), 8.77 (d, *J* = 2 Hz, 2H, H^{D3}), 8.67 (m, 2H, H^{A3}), 8.15 (dd, *J* = 4.4, 1.7 Hz, 4H, H^{C3}), 8.01 (m, 2H, H^{A4}), 7.41 (ddd, *J* = 5.8, 1.4, 0.7 Hz, 2H, H^{A6}), 7.36 (dd, *J* = 6.1 Hz, 2H, H^{D6}), 7.27 (dd, *J* = 6.1, 2.2Hz, 2H, H^{D5}), 7.22 (ddd, *J* = 7.5, 5.6, 1.3 Hz, 2H, H^{A5}). **ESI MS** (MeCN): *m/z* 935.1

$[M\text{-}PF_6]^+$ (13%, calc. 935.0), 395.1 $[M\text{-}2PF_6]^{2+}$ (100%, 395.1). **UV/VIS** λ_{max}/nm (3.24 x 10^{-5}mol dm^{-3}, MeCN) 276 (ε/dm^3 mol^{-1} cm^{-1} 86000), 313 (80000), 492 (34000). **Luminescence** (MeCN, 3.24 x 10^{-5}mol dm^{-3}, λ_{ex} = 492 nm): λ_{em} = 666 nm.

[Ru(**pytpy-$CO_2(CH_2)_2OH$**)(**L3**)][PF_6]$_2$ **(C16)**

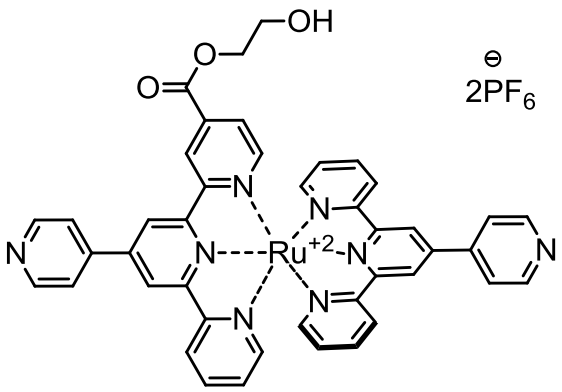

C16 formed as a trans-esterification-product during reactions when ethylene glycol was used as a solvent.

^{1}H NMR (400 MHz, CD_3CN) δ/ppm 9.25 (dd, *J* = 5.2, 1.4 Hz, 1H, H^{B5}), 9.15 (s, 1H, H^{D3}), 9.10 (dd, *J* = 4.3, 1.4 Hz, 1H, H^{B3}), 9.07 (s, 1H, H^{F3}), 9.06 (s, 1H, H^{F5}),8.99 (m, 4H, H^{C2+G2}), 8.65 (m, 3H, H^{A3+E3}), 8.17 (m, 4H, H^{C3+G3}), 8.00 (m, 3H, H^{A4+E4}), 7.60 (m, 2H, H^{D6+D5}), 7.41 (m, 2H, H^{E6+A6}), 7.20 (m, 3H, H^{A5+E5}), 4.42 (m, 2H, H^1), 3.79 (m, 2H, H^2). **ESI MS** (MeCN): *m/z* 955.2 $[M\text{-}PF_6]^+$ (12%, calc. 955.2), 405.1 $[M\text{-}2PF_6]^{2+}$ (100%, 405.1). **IR** (solid, ν/cm^{-1}) 3388 (w), 3097 (w), 2930 (w), 1722 (m), 1717 (m), 1703 (w), 1599 (m), 1407 (m), 1362 (w), 1267 (m), 1247 (m), 1235 (w), 1164 (w), 1129 (m), 1073 (w), 1030 (w), 820 (s), 785 (s), 752 (m), 739 (m), 717 (w), 601 (m). **EA** found: C, 41.95; H, 3.29; N, 9.22%. $C_{40}H_{27}F_{12}N_8P_2Ru\cdot 2H_2O\cdot 0.5NH_4PF_6$ requires C, 42.43; H, 3.15; N, 9.78%. **UV/VIS** λ_{max}/nm (1.82 x 10^{-5}mol dm^{-3}, MeCN) 238 (ε/dm^3 mol^{-1} cm^{-1} 46000), 278 (66000), 316 (54000), 493 (26000). **Luminescence** (MeCN, 1.82 x 10^{-5}mol dm^{-3}, λ_{ex} = 493 nm): λ_{em} = 662 nm.

[Ru(**L10**)(**L3**)][PF_6]$_2$ **(C17)**

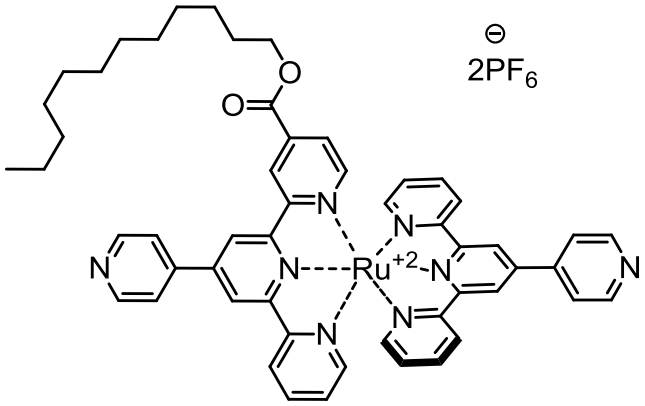

L10 (50 mg, 0.10 mmol) and $RuCl_3.3H_2O$ (25 mg, 0.10 mmol) were suspended in dry *N*,*N*-dimethylformamide (5 mL) in a microwave reactor vial. The reaction mixture was treated in a microwave reactor at 130 °C for 10 minutes. Silver hexafluorophosphate (73 mg, 0.29 mmol) was added and the black suspension was heated in a microwave reactor at 130 °C for 3 minutes. The ligand **L3** (30 mg, 0.10 mmol) and *N*-ethylmorpholine (3 drops) were added and the reaction mixture was treated in a microwave reactor at 160 °C for 15 minutes. The resulting dark red solution was poured into 250 mL of aqueous ammonium hexafluorophosphate to give a fine red precipitate, which was collected on Celite® and washed with cold water (250 mL) and diethyl ether (20 mL). The residue was redissolved in acetonitrile and solvent removed in vacuo to give a dark red solid, which was purified with column chromatography (SiO_2, eluted with MeCN/saturated aqueous KNO_3/H_2O = 5:1:1). The second red band was collected, aqueous ammonium hexafluorophosphate added and solvent evaporated until a red precipitate formed. This was collected on Celite® and washed thoroughly with cold water (250 mL), cold ethanol (15 mL) and diethyl ether (15 mL). The residue was redissolved in acetonitrile and solvent removed in vacuo to give the product as a red powder (44 mg, 0.036 mmol, 38%).

^{1}H NMR (500 MHz, CD_3CN) δ/ppm 9.21 (d, *J* = 1.4 Hz, 1H, H^{B5}), 9.11 (d, *J* = 1.7 Hz, 1H, H^{D3}), 9.09 (d, *J* = 1.4 Hz, 1H, H^{B3}), 9.08 (s, 2H, H^{F3}), 8.97 (dd, *J* = 5.5, 1.3 Hz, 4H, H^{C2+G2}), 8.67 (dd, *J* = 8.1, 4.9 Hz, 3H, H^{A3+E3}), 8.17 (dd, *J* = 4.6, 1.4 Hz, 2H, H^{C3}), 8.15 (dd, *J* = 4.6, 1.4 Hz, 2H, H^{G3}), 8.00 (m, 3H, H^{A4+E4}), 7.62 (d, *J* = 5.8 Hz, 1H, H^{D6}), 7.60 (dd, *J* = 5.8, 1.8 Hz, 1H, H^{D5}), 7.48 (dd, *J* = 5.6, 1.4 Hz, 1H, H^{A6}), 7.44 (dd, *J* = 5.7, 1.4 Hz, 2H, H^{E6}), 7.23 (m, 3H, H^{A5+E5}), 4.33 (t, *J* = 6.6 Hz, 2H, H^1), 1.73 (m, 2H, H^2), 1.38 (m, 2H, H^3), 1.25 (m, 16H, H^{4-11}), 0.84 (t, *J* = 6.9 Hz, 3H, H^{12}). **^{13}C {^{1}H} NMR**

(126 MHz, CD_3CN) δ/ppm 164.3 ($C^{C=O}$), 160.1 (C^{D2}), 158.8 (C^{E2}), 158.7 (C^{A2}), 156.9 (C^{B2}), 156.7 (C^{F2}), 156.4 (C^{B6}), 154.5 (C^{D6}), 153.7 (C^{E6}), 153.5 (C^{A6}), 151.8 (C^{G2}), 151.7 (C^{C2}), 146.7 (C^{F4}), 146.6 (C^{B4}), 145.3 (C^{C4+G4}), 140.1 (C^{D4}), 139.5 (C^{A4}), 139.4 (C^{E4}), 128.8 (C^{A5}), 128.7 (C^{E5}), 127.3 (C^{D5}), 125.9 (C^{A3+E3}), 124.5 (C^{D3}), 123.4 (C^{B5}), 123.2 (C^{C3}), 123.1 (C^{B3+G3}), 122.9 (C^{F3}), 67.5 (C^{1}), 32.6 (C^{10}), 30.3, 30.2, 30.0 (C^{5-9}), 29.9 (C^{4}), 29.2 (C^{2}), 26.5 (C^{3}), 23.4 (C^{11}), 14.4 (C^{12}). **ESI MS**: *m/z* 1079.3 $[M\text{-}PF_6]^+$ (5%, calc. 1079.3), 467.2 $[M\text{-}2PF_6]^{2+}$ (100%, 467.2). **IR** (solid, ν/cm^{-1}) 3105 (w), 2918 (m), 2851 (m), 1729 (m), 1596 (m), 1543 (m), 1476 (w), 1459 (w), 1428 (w), 1406 (m), 1343 (w), 1307 (w), 1291 (w), 1261 (m), 1246 (w), 1166 (w), 1124 (w), 1113 (w), 1030 (w), 976 (w), 830 (s), 817 (s), 803 (s), 785 (m), 765 (m), 751 (m), 740 (m), 730 (m), 722 (m), 713 (w), 708 (w), 696 (w), 684 (w), 636 (w). **EA** found: C, 46.22; H, 4.19; N, 8.11%. $C_{53}H_{52}F_{12}N_8O_2P_2Ru{\cdot}HPF_6$ requires C, 46.46; H, 3.90; N, 8.18%. **UV/VIS** λ_{max}/nm (1.80 x 10^{-5}mol dm^{-3}, MeCN) 277 (ε/dm^3 mol^{-1} cm^{-1} 65000), 316 (43000), 493 (20000). **Luminescence** (MeCN, 1.80 x 10^{-5}mol dm^{-3}, λ_{ex} = 487 nm): λ_{em} = 673 nm.

[Ru(H**L11**)(**L3**)][PF_6]$_3$ **(C18)**

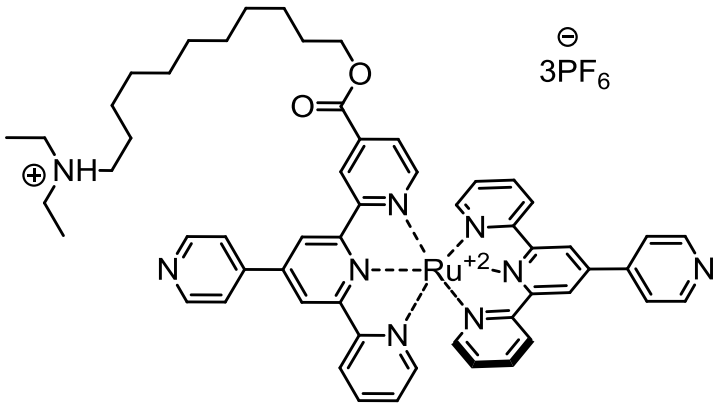

L11 (56 mg, 0.10 mmol) and $RuCl_3.3H_2O$ (25 mg, 0.10 mmol) were suspended in dry *N*,*N*-dimethylformamide (5 mL) in a microwave reactor vial. The reaction mixture was treated in a microwave reactor at 130 °C for 10 minutes. Silver hexafluorophosphate (73 mg, 0.29 mmol) was added and the black suspension was heated in a microwave reactor at 130 °C for 3 minutes. The ligand **L3** (30 mg, 0.10 mmol) and *N*-ethylmorpholine (3 drops) were added and the reaction mixture was treated in a microwave reactor at 160 °C for 15 minutes. The resulting dark red solution was poured into 250 mL of aqueous ammonium hexafluorophosphate to give

a fine red precipitate, which was collected on Celite® and washed with cold water (250 mL) and diethyl ether (20 mL). The residue was redissolved in acetonitrile and solvent removed in vacuo to give a dark red solid, which was purified with column chromatography (SiO_2, eluted with MeCN/saturated aqueous KNO_3/H_2O = 10:1.5:0.5). The second red band was collected, aqueous ammonium hexafluorophosphate added and solvent evaporated until a red precipitate formed. This was collected on Celite® and washed thoroughly with cold water (250 mL), cold ethanol (15 mL) and diethyl ether (15 mL). The residue was redissolved in acetonitrile and solvent removed in vacuo to give the product as a red powder (39 mg, 0.027 mmol, 29%).

^{1}H NMR (500 MHz, CD_3CN) δ/ppm 9.21 (d, *J* = 1.5 Hz, 1H, H^{B5}), 9.10 (m, 2H, H^{B3+D3}), 9.08 (s, 2H, H^{F3}), 8.96 (dd, *J* = 5.0, 0.9 Hz, 4H, H^{C2+G2}), 8.70 (m, 3H, H^{A3+E3}), 8.20 (dd, *J* = 4.4, 1.7 Hz, 2H, H^{C3}), 8.18 (dd, *J* = 4.4, 1.8 Hz, 2H, H^{G3}), 7.99 (m, 3H, H^{A4+E4}), 7.66 (d, *J* = 5.8 Hz, 1H, H^{D6}), 7.62 (dd, *J* = 5.8, 1.7 Hz, 1H, H^{D5}), 7.48 (dd, *J* = 5.7, 1.4 Hz, 1H, H^{A6}), 7.43 (m, 2H, H^{E6}), 7.23 (m, 3H, H^{A5+E5}), 4.33 (t, *J* = 6.7 Hz, 2H, H^1), 3.16 (m, 4H, H^{13}), 3.04 (m, 2H, H^{11}), 1.75 (m, 2H, H^2), 1.61 (m, 2H, H^{10}), 1.39 (m, 2H, H^3), 1.26 (m, 18H, H^{4-9+14}). **^{13}C {^{1}H} NMR** (126 MHz, CD_3CN) δ/ppm 164.3 ($C^{C=O}$), 160.1 (C^{D2}), 158.8 (C^{E2}), 158.7 (C^{A2}), 156.9 (C^{B2}), 156.7 (C^{F2}), 156.4 (C^{B6}), 154.5 (C^{D6}), 153.7 (C^{E6}), 153.5 (C^{A6}), 151.8 (C^{G2+C2}), 146.7 (C^{F4}), 146.5 (C^{B4}), 145.4 (C^{C4+G4}), 140.0 (C^{D4}), 139.5 (C^{A4}), 139.4 (C^{E4}), 128.8 (C^{A5}), 128.7 (C^{E5}), 127.3 (C^{D5}), 125.9 (C^{A3+E3}), 124.5 (C^{D3}), 123.4 (C^{B5}), 123.3 (C^{C3}), 123.2 (C^{B3}), 123.1 (C^{G3}), 123.0 (C^{F3}), 67.5 (C^1), 53.1 (C^{11}), 48.6 (C^{13}), 30.2, 30.1, 30.0 (C^{5-7}), 29.9 (C^4), 29.7 (C^8), 29.2 (C^2), 27.0 (C^9), 26.6 (C^3), 24.5 (C^{10}), 9.2 (C^{14}). **ESI MS** (MeCN) deprotonated form: *m/z* 495.7 $[M\text{-}2PF_6]^{2+}$ (100%, calc. 495.7), 480.7 $[M\text{-}2PF_6\text{-}Me]^{2+}$ (94%, 480.8). **IR** (solid, ν/cm^{-1}) 2928 (m), 2854 (w), 1725 (m), 1600 (m), 1464 (w), 1407 (m), 1264 (m), 1233 (w), 1164 (w), 1117 (w), 1031 (w), 819 (s), 785 (m), 752 (m), 740 (m), 730 (m), 601 (w). **EA** found: C, 44.15; H, 4.15; N, 8.32%. $C_{56}H_{60}F_{18}N_9O_2P_3Ru{\cdot}0.5NH_4PF_6$ requires C, 44.58; H, 4.14; N, 8.82%. **UV/VIS** λ_{max}/nm (2.35 x 10^{-5}mol dm^{-3}, MeCN) 277 (ε/dm^3 mol^{-1} cm^{-1} 60000), 316 (47000), 494 (23000). **Luminescence** (MeCN, 2.35 x 10^{-5}mol dm^{-3}, λ_{ex} = 491 nm): λ_{em} = 682 nm.

[Ru(H**L13**)(**L3**)][PF_6]$_3$ **(C19)**

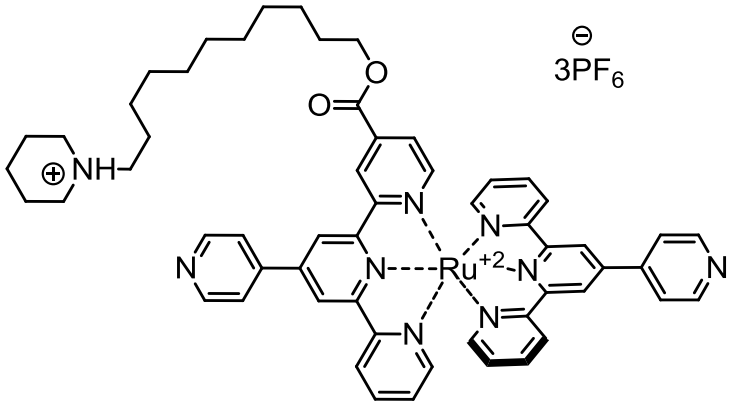

L13 (50 mg, 0.08 mmol) and $RuCl_3.3H_2O$ (22 mg, 0.08 mmol) were suspended in dry *N*,*N*-dimethylformamide (5 mL) in a microwave reactor vial. The reaction mixture was treated in a microwave reactor at 130 °C for 10 minutes. Silver hexafluorophosphate (64 mg, 0.25 mmol) was added and the black suspension was heated in a microwave reactor at 130 °C for 3 minutes. The ligand **L3** (26 mg, 0.08 mmol) and *N*-ethylmorpholine (3 drops) were added and the reaction mixture was treated in a microwave reactor at 160 °C for 15 minutes. The resulting dark red solution was poured into 250 mL of aqueous ammonium hexafluorophosphate to give a fine red precipitate, which was collected on Celite® and washed with cold water (250 mL) and diethyl ether (20 mL). The residue was redissolved in acetonitrile and solvent removed in vacuo to give a dark red solid, which was purified with column chromatography (SiO_2, eluted with MeCN/saturated aqueous KNO_3/H_2O = 5:1:1). The second red band was collected, aqueous ammonium hexafluorophosphate added and solvent evaporated until a red precipitate formed. This was collected on Celite® and washed thoroughly with cold water (250 mL), cold ethanol (15 mL) and diethyl ether (15 mL). The residue was redissolved in acetonitrile and solvent removed in vacuo to give the product as a red powder (61 mg, 0.042 mmol, 51%).

^{1}H NMR (500 MHz, CD_3CN) δ/ppm 9.23 (d, *J* = 1.4 Hz, 1H, H^{B5}), 9.12 (d, *J* = 1.4 Hz, 1H, H^{B3}), 9.11 (d, *J* = 1.7 Hz, 1H, H^{D3}), 9.11 (s, 2H, H^{F3}), 9.01 (br s, 4H, H^{C2+G2}), 8.70 (m, 3H, H^{A3+E3}), 8.31 (m, 4H, H^{C3+G3}), 8.00 (m, 3H, H^{A4+E4}), 7.66 (d, *J* = 5.9 Hz, 1H, H^{D6}), 7.62 (dd, *J* = 5.8, 1.7 Hz, 1H, H^{D5}), 7.48 (d, *J* = 4.9 Hz, 1H, H^{A6}), 7.44 (dd, *J* = 5.6, 0.7 Hz, 2H, H^{E6}), 7.23 (m, 3H, H^{A5+E5}), 4.33 (t, *J* = 6.7 Hz, 2H, H^1), 3.45 (d, *J* = 12.4 Hz, 2H, H^{13eq}), 2.98 (t, *J* = 8.3 Hz, 2H, H^{11}), 2.83 (m, 2H, H^{13ax}), 1.88 (d, *J* = 14.2 Hz, 2H, H^{14eq}), 1.73 (m, 4H, H^{2+14ax}), 1.65 (m, 2H, H^{10}), 1.44 (m, 2H, H^{15}), 1.37 (m, 2H, H^3),

1.27 (m, 12H, H^{4-9}). **^{13}C {^{1}H} NMR** (126 MHz, CD_3CN) δ/ppm 164.3 ($C^{C=O}$), 160.0 (C^{D2}), 158.8 (C^{E2}), 158.7 (C^{A2}), 156.9 (C^{B2}), 156.7 (C^{F2}), 156.4 (C^{B6}), 154.5 (C^{D6}), 153.7 (C^{E6}), 153.5 (C^{A6}), 150.4 (C^{C2}), 150.3 (C^{G2}), 147.1 (C^{F4+B4}), 146.1 (C^{G4}), 145.9 (C^{C4}), 140.1 (C^{D4}), 139.5 (C^{A4}), 139.4 (C^{E4}), 128.9 (C^{A5}), 128.8 (C^{E5}), 127.4 (C^{D5}), 125.9 (C^{A3+E3}), 124.5 (C^{D3}), 123.9 (C^{C3+G3}), 123.5 (C^{B5}), 123.3 (C^{B3}), 123.1 (C^{F3}), 67.6 (C^{1}), 58.1 (C^{11}) , 54.3 (C^{13}), 30.2, 30.1, 30.0 (C^{5-7}), 29.9 (C^{4}), 29.6 (C^{8}), 29.2 (C^{2}), 27.0 (C^{9}), 26.5 (C^{3}), 24.5 (C^{10}), 23.8 (C^{14}), 22.2 (C^{15}). **ESI MS** (MeCN) monoprotonated form: *m/z* 1294.2 $[M\text{-}PF_6]^+$ (7%, calc. 1294.3), 574.7 $[M\text{-}2PF_6]^{2+}$ (23%, 574.7), deprotonated form: *m/z* 1294.2 $[M+H]^+$ (7%, calc. 1294.3), 1148.3 $[M\text{-}PF_6]^+$ (5%, 1148.4), 501.7 $[M\text{-}2PF_6]^{2+}$ (85%, 501.7). **IR** (solid, ν/cm^{-1}) 3323 (w), 2930 (m), 2853 (w), 1722 (m), 1712 (m), 1635 (w), 1602 (m), 1464 (w), 1409 (m), 1307 (w), 1293 (w), 1264 (m), 1237 (w), 1167 (w), 1121 (w), 1031 (m), 817 (s), 785 (s), 773 (s), 768 (s), 753 (s), 740 (m), 730 (m), 718 (w), 714 (w), 698 (w). **EA** found: C, 41.83; H, 4.09; N, 8.33%. $C_{57}H_{60}F_{18}N_9O_2P_3Ru{\cdot}H_2O{\cdot}NH_4PF_6$ requires C, 42.26; H, 4.11; N, 8.65%. **UV/VIS** λ_{max}/nm (2.50 x 10^{-5}mol dm^{-3}, MeCN) 277 ($\varepsilon/dm^3\ mol^{-1}\ cm^{-1}$ 61000), 316 (47000), 494 (23000). **Luminescence** (MeCN, 2.21 x 10^{-5}mol dm^{-3}, λ_{ex} = 492 nm): λ_{em} = 672 nm.

[Ru(H**L14**)(**L3**)][PF_6]$_3$ **(C20)**

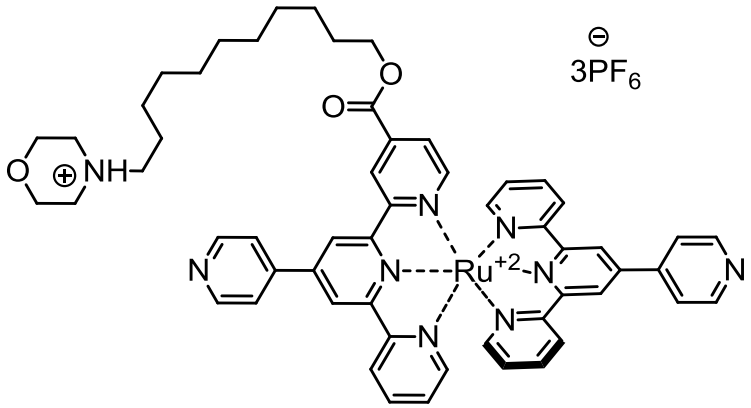

L14 (50 mg, 0.08 mmol) and $RuCl_3.3H_2O$ (22 mg, 0.08 mmol) were suspended in dry *N*,*N*-dimethylformamide (5 mL) in a microwave reactor vial. The reaction mixture was treated in a microwave reactor at 130 °C for 10 minutes. Silver hexafluorophosphate (64 mg, 0.25 mmol) was added and the black suspension was heated in a microwave reactor at 130 °C for 3 minutes. The ligand **L3** (26 mg, 0.08 mmol) and *N*-ethylmorpholine (3 drops) were added and the reaction mixture was treated in a microwave reactor at 160 °C for 15 minutes. The resulting

dark red solution was poured into 250 mL of aqueous ammonium hexafluorophosphate to give a fine red precipitate, which was collected on Celite® and washed with cold water (250 mL) and diethyl ether (20 mL). The residue was redissolved in acetonitrile and solvent removed in vacuo to give a dark red solid, which was purified with column chromatography (SiO_2, eluted with MeCN/saturated aqueous KNO_3/H_2O = 5:1:1). The second red band was collected, aqueous ammonium hexafluorophosphate added and solvent evaporated until a red precipitate formed. This was collected on Celite® and washed thoroughly with cold water (250 mL), cold ethanol (15 mL) and diethyl ether (15 mL). The residue was redissolved in acetonitrile and solvent removed in vacuo to give the product as a red powder (40 mg, 0.028 mmol, 33%).

^{1}H NMR (500 MHz, CD_3CN) δ/ppm 9.21 (d, *J* = 1.5 Hz, 1H, H^{B5}), 9.10 (m, 2H, H^{B3+D3}), 9.08 (s, 2H, H^{F3}), 8.97 (d, *J* = 5.2 Hz, 4H, H^{C2+G2}), 8.69 (m, 3H, H^{A3+E3}), 8.21 (dd, *J* = 4.4, 1.7 Hz, 2H, H^{C3}), 8.19 (dd, *J* = 4.5, 1.6 Hz, 2H, H^{G3}), 7.98 (m, 3H, H^{A4+E4}), 7.64 (d, *J* = 5.8 Hz, 1H, H^{D6}), 7.61 (dd, *J* = 5.8, 1.7 Hz, 1H, H^{D5}), 7.46 (dd, *J* = 5.6, 0.7 Hz, 1H, H^{A6}), 7.42 (dd, *J* = 5.6, 1.4 Hz, 2H, H^{E6}), 7.20 (m, 3H, H^{A5+E5}), 4.33 (t, *J* = 6.7 Hz, 2H, H^1), 4.00 (d, *J* = 13.3 Hz, 2H, H^{14eq}), 3.72 (t, *J* = 12.0 Hz, 2H, H^{14ax}), 3.41 (d, *J* = 12.8 Hz, 2H, H^{13eq}), 3.04 (m, 4H, $H^{11+13ax}$), 1.74 (m, 2H, H^2), 1.67 (m, 2H, H^{10}), 1.38 (m, 2H, H^3), 1.27 (m, 12H, H^{4-9}). **^{13}C {^{1}H} NMR** (126 MHz, CD_3CN) δ/ppm 164.3 ($C^{C=O}$), 160.1 (C^{D2}), 158.8 (C^{E2}), 158.7 (C^{A2}), 156.9 (C^{B2}), 156.7 (C^{F2}), 156.4 (C^{B6}), 154.5 (C^{D6}), 153.7 (C^{E6}), 153.5 (C^{A6}), 151.6 (C^{G2+C2}), 146.7 (C^{F4}), 146.5 (C^{B4}), 145.4 (C^{C4+G4}), 140.0 (C^{D4}), 139.5 (C^{A4}), 139.4 (C^{E4}), 128.8 (C^{A5}), 128.7 (C^{E5}), 127.3 (C^{D5}), 125.8 (C^{A3+E3}), 124.5 (C^{D3}), 123.4 (C^{B5}), 123.3 (C^{B3}), 123.2 (C^{C3+G3}), 123.0 (C^{F3}), 67.6 (C^1), 64.6 (C^{14}), 58.5 (C^{11}) , 53.1 (C^{13}), 30.2, 30.1, 30.0 (C^{5-7}), 29.9 (C^4), 29.6 (C^8), 29.2 (C^2), 26.9 (C^9), 26.6 (C^3), 24.1 (C^{10}). **ESI MS** (MeCN) monoprotonated form: *m/z* 575.7 $[M\text{-}2PF_6]^{2+}$ (3%, calc. 575.7), deprotonated form: *m/z* 1150.3 $[M\text{-}PF_6]^+$ (7%, 1150.3), 502.7 $[M\text{-}2PF_6]^{2+}$ (100%, 502.7). **IR** (solid, ν/cm^{-1}) 3096 (w), 2927 (m), 2850 (w), 1722 (m), 1700 (m), 1637 (w), 1597 (w), 1464 (w), 1407 (m), 1394 (w), 1388 (w), 1307 (w), 1293 (w), 1263 (m), 1246 (w), 1237 (w), 1165 (w), 1119 (w), 1029 (m), 817 (s), 802 (s), 783 (s), 767 (s), 753 (s), 740 (s), 729 (m), 719 (w), 711 (w), 686 (w), 609 (w), 601 (w). **EA** found: C, 43.49; H, 4.22; N, 8.77%. $C_{56}H_{58}F_{18}N_9O_3P_3Ru{\cdot}5H_2O$ requires C, 43.93; H, 4.48; N, 8.23%. **UV/VIS** λ_{max}/nm (1 x 10^{-5}mol dm^{-3}, MeCN) 278 (ε/dm^3 mol^{-1} cm^{-1} 75000), 316 (61000), 494 (29000). **Luminescence** (MeCN, 1 x 10^{-5}mol dm^{-3}, λ_{ex} = 494 nm): λ_{em} = 662 nm.

[Ru(**L8**)(**L3**)][PF_6]$_2$ **(C21)**

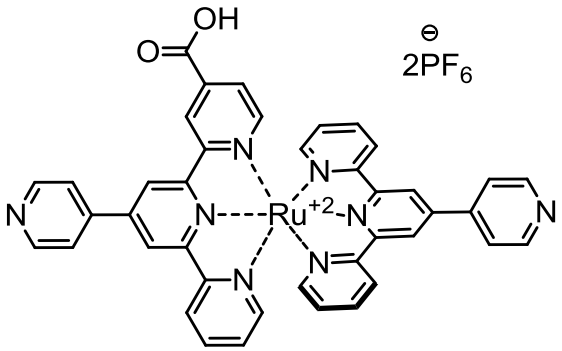

L8 (57 mg, 0.16 mmol) and $RuCl_3.3H_2O$ (42 mg, 0.16 mmol) were suspended in dry *N*,*N*-dimethylformamide (5 mL) in a microwave reactor vial. The reaction mixture was treated in a microwave reactor at 130 °C for 10 minutes. Silver hexafluorophosphate (122 mg, 0.48 mmol) was added and the black suspension was heated in a microwave reactor at 130 °C for 3 minutes. The ligand **L3** (50 mg, 0.16 mmol) and *N*-ethylmorpholine (3 drops) were added and the reaction mixture was treated in a microwave reactor at 160 °C for 15 minutes. The resulting dark red solution was poured into 250 mL of aqueous ammonium hexafluorophosphate to give a fine red precipitate, which was collected on Celite® and washed with cold water (250 mL) and diethyl ether (20 mL). The residue was redissolved in acetonitrile and solvent removed in vacuo to give a dark red solid, which was purified with column chromatography (SiO_2, eluted with MeCN/saturated aqueous KNO_3/H_2O = 7:2:2). The second red band was collected, aqueous ammonium hexafluorophosphate added and solvent evaporated until a red precipitate formed. This was collected on Celite® and washed thoroughly with cold water (250 mL), cold ethanol (15 mL) and diethyl ether (15 mL). The residue was redissolved in acetonitrile and solvent removed in vacuo to give the product as a red powder (87 mg, 0.082 mmol, 51%).

^{1}H NMR (500 MHz, CD_3CN) δ/ppm 9.21 (d, *J* = 1.4 Hz, 1H, H^{B5}), 9.12 (br s, 1H, H^{D3}), 9.08 (d, *J* = 1.4 Hz, 1H, H^{B3}), 9.07 (s, 2H, H^{F3}), 8.96 (m, 4H, H^{C2+G2}), 8.67 (m, 3H, H^{A3+E3}), 8.17 (dd, *J* = 4.4, 1.6 Hz, 2H, H^{C3}), 8.14 (dd, *J* = 4.4, 1.6 Hz, 2H, H^{G3}), 7.98 (m, 3H, H^{A4+E4}), 7.61 (s, 2H, H^{D5+D6}), 7.44 (ddd, *J* = 5.6, 1.4, 0.6 Hz, 1H, H^{A6}), 7.41 (ddd, *J* = 5.6, 1.4, 0.6 Hz, 2H, H^{E6}), 7.20 (m, 3H, H^{A5+E5}). **^{13}C {^{1}H} NMR** (126 MHz, CD_3CN) δ/ppm 164.4 ($C^{C=O}$), 154.3 (C^{D6}), 153.6 (C^{E6}), 153.4 (C^{A6}), 151.9 (C^{C2+G2}), 139.4 (C^{A4+E4}), 128.6 (C^{A5+E5}), 127.5 (C^{D5}), 125.7 (C^{A3+E3}), 124.8 (C^{D3}), 123.3 (C^{B5}), 123.0 ($C^{B3+C3+G3}$), 122.9 (C^{F3}), (C^q were not recorded due to the poor solubility of the complex). **ESI MS**

(MeCN): *m/z* 911.2 $[M\text{-}PF_6]^+$ (96%, calc. 911.1), 383.1 $[M\text{-}2PF_6]^{2+}$ (51%, 383.1). **IR** (solid, ν/cm^{-1}) 3221 (m), 3076 (m), 1763 (m), 1598 (w), 1364 (s), 1354 (s), 1343 (s), 1244 (m), 1233 (m), 1229 (m), 1221 (m), 1213 (m), 1187 (m), 1161 (w), 1143 (w), 823 (s), 786 (m), 715 (w).

$[Ru(\mathbf{L17})(\mathbf{L3})][PF_6]_2$ **(C22)**

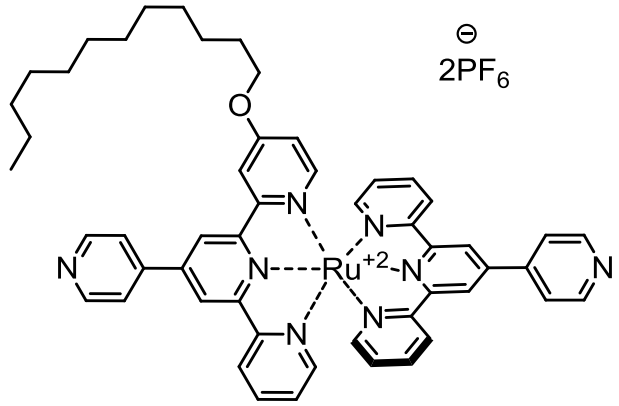

L17 (87 mg, 0.16 mmol) and $RuCl_3.3H_2O$ (42 mg, 0.18 mmol) were suspended in dry *N*,*N*-dimethylformamide (5 mL) in a microwave reactor vial. The reaction mixture was treated in a microwave reactor at 130 °C for 10 minutes. Silver hexafluorophosphate (134 mg, 0.53 mmol) was added and the black suspension was heated in a microwave reactor at 130 °C for 3 minutes. The ligand **L3** (55 mg, 0.18 mmol) and *N*-ethylmorpholine (3 drops) were added and the reaction mixture was treated in a microwave reactor at 160 °C for 15 minutes. The resulting dark red solution was poured into 250 mL of aqueous ammonium hexafluorophosphate to give a fine red precipitate, which was collected on Celite® and washed with cold water (250 mL) and diethyl ether (20 mL). The residue was redissolved in acetonitrile and solvent removed in vacuo to give a dark red solid, which was purified with column chromatography (SiO_2, eluted with MeCN/saturated aqueous KNO_3/H_2O = 10:0.5:1.5). The second red band was collected, aqueous ammonium hexafluorophosphate added and solvent evaporated until a red precipitate formed. This was collected on Celite® and washed thoroughly with cold water (250 mL), cold ethanol (15 mL) and diethyl ether (15 mL). The residue was redissolved in acetonitrile and solvent removed in vacuo to give the product as a red powder (54 mg, 0.045 mmol, 26%).

^{1}H NMR (500 MHz, CD_3CN) δ/ppm 9.06 (s, 4H, $H^{B3+B5+F3}$), 8.97 (m, 4H, H^{C2+G2}), 8.67 (d, *J* = 8.2 Hz, 3H, H^{A3+E3}), 8.20 (m, 5H, $H^{C3+D3+G3}$), 7.96 (m, 3H, H^{A4+E4}), 7.45 (d, *J* = 4.9 Hz, 2H, H^{E6}), 7.40 (d, *J* =

4.9 Hz, 1H, H^{A6}), 7.21 (m, 3H, H^{A5+E5}), 7.16 (d, *J* = 6.6 Hz, 1H, H^{D6}), 6.72 (dd, *J* = 6.5, 2.7 Hz, 1H, H^{D5}), 4.13 (t, *J* = 6.6 Hz, 2H, H^{1}), 1.74 (m, 2H, H^{2}), 1.39 (m, 2H, H^{3}), 1.27 (m, 16H, H^{4-11}), 0.85 (t, *J* = 6.9 Hz, 2H, H^{12}). **^{13}C {^{1}H} NMR** (126 MHz, CD_3CN) δ/ppm 167.9 (C^{D4}), 159.8 (C^{D2}), 158.9 (C^{A2+E2}), 156.8 (C^{F2}), 156.7 (C^{B2+B6}), 154.0 (C^{D6}), 153.6 (C^{A6}), 153.4 (C^{E6}), 151.4 (C^{C2+G2}), 146.1 (C^{F4}), 145.9 (C^{B4}), 145.8 (C^{C4+G4}), 139.1 (C^{E4}), 139.0 (C^{A4}), 128.6 (C^{A5+E5}), 125.7 (C^{A3}), 125.6 (C^{E3}), 123.2 (C^{C3+G3}), 122.9 (C^{B5}), 122.8 (C^{B3+F3}), 114.7 (C^{D5}), 113.3 (C^{D3}), 70.8 (C^{1}), 32.6 (C^{10}), 30.3, 30.2, 30.0 (C^{5-9}), 29.8 (C^{4}), 29.3 (C^{2}), 26.3 (C^{3}), 23.4 (C^{11}), 14.4 (C^{12}). **ESI MS** (MeCN): *m/z* 1051.3 $[M\text{-}PF_6]^+$ (100%, calc. 1051.3), 453.2 $[M\text{-}2PF_6]^{2+}$ (25%, 453.2). **IR** (solid, ν/cm^{-1}) 3322 (w), 2924 (m), 2847 (w), 1984 (w), 1608 (m), 1597 (m), 1428 (m), 1406 (m), 1385 (w), 1355 (w), 1317 (w), 1290 (w), 1225 (w), 1218 (w), 1029 (m), 876 (m), 831 (s), 817 (s), 804 (s), 780 (s), 750 (m), 740 (m), 735 (m), 721 (w), 601 (w). **EA** found: C, 45.24; H, 4.18; N, 9.22%. $C_{52}H_{52}F_{12}N_8OP_2Ru{\cdot}0.5H_2O{\cdot}NH_4PF_6$ requires C, 45.65; H, 4.20; N, 9.21%. **UV/VIS** λ_{max}/nm (0.80 x 10^{-5}mol dm^{-3}, MeCN) 274 (ε/dm^3 mol^{-1} cm^{-1} 56000), 312 (48000), 492 (23000). **Luminescence** (MeCN, 0.95 x 10^{-5}mol dm^{-3}, λ_{ex} = 496 nm): λ_{em} = 681 nm.

[Ru(H**L18**)(**L3**)][PF_6]$_3$ **(C23)**

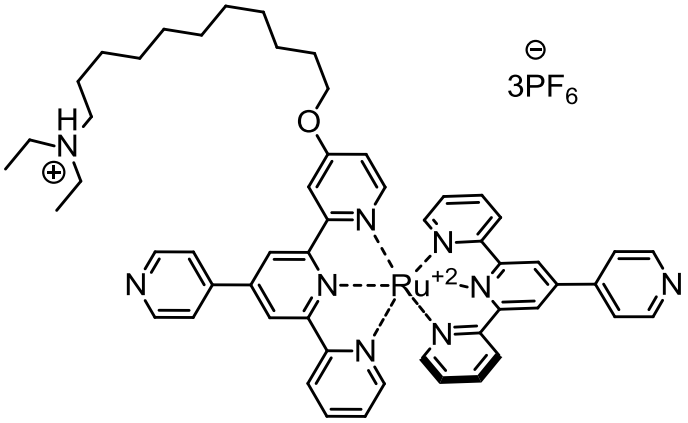

L18 (52 mg, 0.10 mmol) and $RuCl_3.3H_2O$ (25 mg, 0.10 mmol) were suspended in dry *N*,*N*-dimethylformamide (5 mL) in a microwave reactor vial. The reaction mixture was treated in a microwave reactor at 130 °C for 10 minutes. Silver hexafluorophosphate (72 mg, 0.28 mmol) was added and the black suspension was heated in a microwave reactor at 130 °C for 3 minutes. The ligand **L3** (29 mg, 0.10 mmol) and *N*-ethylmorpholine (3 drops) were added and

the reaction mixture was treated in a microwave reactor at 160 °C for 15 minutes. The resulting dark red solution was poured into 250 mL of aqueous ammonium hexafluorophosphate to give a fine red precipitate, which was collected on Celite® and washed with cold water (250 mL) and diethyl ether (20 mL). The residue was redissolved in acetonitrile and solvent removed in vacuo to give a dark red solid, which was purified with column chromatography (SiO_2, eluted with MeCN/saturated aqueous KNO_3/H_2O = 10:0.5:1.5). The second red band was collected, aqueous ammonium hexafluorophosphate added and solvent evaporated until a red precipitate formed. This was collected on Celite® and washed thoroughly with cold water (250 mL), cold ethanol (15 mL) and diethyl ether (15 mL). The residue was redissolved in acetonitrile and solvent removed in vacuo to give the product as a red powder (27 mg, 0.019 mmol, 21%).

^{1}H NMR (500 MHz, CD_3CN) δ/ppm 9.06 (s, 4H, $H^{B3+B5+F3}$), 8.97 (m, 4H, H^{C2+G2}), 8.68 (d, *J* = 8.1 Hz, 3H, H^{A3+E3}), 8.18 (m, 5H, $H^{C3+D3+G3}$), 7.96 (m, 3H, H^{A4+E4}), 7.46 (d, *J* = 5.5 Hz, 2H, H^{E6}), 7.41 (d, *J* = 5.5 Hz, 1H, H^{A6}), 7.20 (m, 3H, $H^{A5+E5+D6}$), 6.72 (dd, *J* = 6.6, 2.7 Hz, 1H, H^{D5}), 4.14 (t, *J* = 6.6 Hz, 1H, H^1), 3.12 (m, 4H, H^{13}), 3.00 (m, 2H, H^{11}), 1.75 (m, 2H, H^2), 1.61 (m, 2H, H^{10}), 1.39 (m, 2H, H^3), 1.30 (m, 12H, H^{4-9}), 1.23 (t, *J* = 7.3 Hz, 6H, H^{14}). **^{13}C {^{1}H} NMR** (126 MHz, CD_3CN) δ/ppm 167.9 (C^{D4}), 159.8 (C^{D2}), 158.9 (C^{A2+E2}), 156.8 (C^{F2}), 156.7 (C^{B2+B6}), 154.0 (C^{D6}), 153.5 (C^{A6}), 153.4 (C^{E6}), 151.8 (C^{C2+G2}), 146.3 (C^{B4}), 146.0 (C^{F4}), 145.4 (C^{C4+G4}), 139.1 (C^{E4}), 139.0 (C^{A4}), 128.6 (C^{A5+E5}), 125.7 (C^{A3}), 125.6 (C^{E3}), 122.7 ($C^{C3+G3+B3+B5+F3}$), 114.7 (C^{D5}), 113.2 (C^{D3}), 67.5 (C^1), 52.9 (C^{11}), 48.2 (C^{13}), 30.2, 30.1, 30.0 (C^{5-7}), 29.9 (C^4), 29.7 (C^8), 29.3 (C^2), 27.1 (C^9), 26.4 (C^3), 24.4 (C^{10}), 9.0 (C^{14}). **ESI MS** (MeCN) monoprotonated form: *m/z* 1254.3 $[M\text{-}PF_6]^+$ (2%, calc. 1254.3), 554.7 $[M\text{-}2PF_6]^{2+}$ (11%, 554.7), 321.5 $[M\text{-}3PF_6]^{3+}$ (13%, 321.5), deprotonated form: *m/z* 1254.3 $[M+H]^+$ (2%, 1254.3), 1108.3 $[M\text{-}PF_6]^+$ (5%, 1108.4), 481.7 $[M\text{-}2PF_6]^{2+}$ (100%, 481.7). **IR** (solid, ν/cm^{-1}) 3409 (w), 2929 (m), 2855 (w), 1980 (w), 1639 (w), 1598 (m), 1575 (w), 1486 (w), 1464 (w), 1456 (w), 1441 (w), 1429 (w), 1409 (m), 1393 (w), 1387 (w), 1316 (w), 1292 (w), 1258 (w), 1227 (w), 1218 (w), 1162 (w), 1029 (m), 993 (w), 818 (s), 800 (s), 783 (s), 750 (m), 740 (m), 734 (m), 719 (w), 704 (w), 659 (w), 602 (w). **EA** found: C, 44.81; H, 4.23; N, 9.03%. $C_{55}H_{60}F_{18}N_9O_2P_3Ru{\cdot}0.5NH_4PF_6$ requires C, 44.62; H, 4.22; N, 8.99%. **UV/VIS** λ_{max}/nm (0.82 x 10^{-5}mol dm^{-3}, MeCN) 274 (ε/dm^3 mol^{-1} cm^{-1} 53000), 312 (48000), 491 (23000). **Luminescence** (MeCN, 1.07 x 10^{-5}mol dm^{-3}, λ_{ex} = 495 nm): λ_{em} = 689 nm.

[Ru(H**L19**)(**L3**)][PF_6]$_3$ **(C24)**

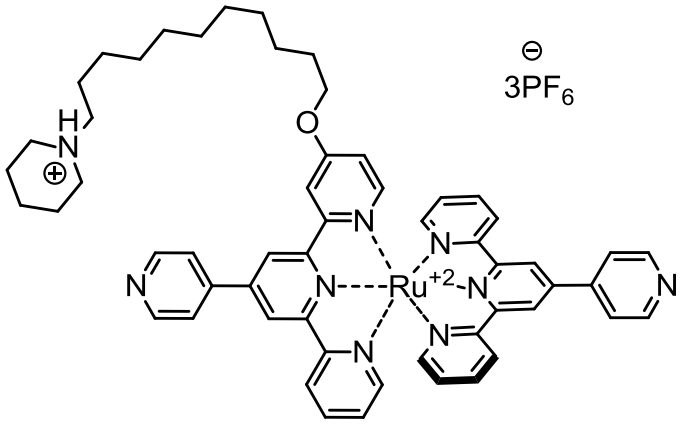

L19 (50 mg, 0.09 mmol) and $RuCl_3.3H_2O$ (23 mg, 0.09 mmol) were suspended in dry *N*,*N*-dimethylformamide (5 mL) in a microwave reactor vial. The reaction mixture was treated in a microwave reactor at 130 °C for 10 minutes. Silver hexafluorophosphate (67 mg, 0.27 mmol) was added and the black suspension was heated in a microwave reactor at 130 °C for 3 minutes. The ligand **L3** (26 mg, 0.08 mmol) and *N*-ethylmorpholine (3 drops) were added and the reaction mixture was treated in a microwave reactor at 160 °C for 15 minutes. The resulting dark red solution was poured into 250 mL of aqueous ammonium hexafluorophosphate to give a fine red precipitate, which was collected on Celite® and washed with cold water (250 mL) and diethyl ether (20 mL). The residue was redissolved in acetonitrile and solvent removed in vacuo to give a dark red solid, which was purified with column chromatography (SiO_2, eluted with MeCN/saturated aqueous KNO_3/H_2O = 10:0.5:1.5). The second red band was collected, aqueous ammonium hexafluorophosphate added and solvent evaporated until a red precipitate formed. This was collected on Celite® and washed thoroughly with cold water (250 mL), cold ethanol (15 mL) and diethyl ether (15 mL). The residue was redissolved in acetonitrile and solvent removed in vacuo to give the product as a red powder (35 mg, 0.025 mmol, 31%).

^{1}H NMR (500 MHz, CD_3CN) δ/ppm 9.06 (m, 4H, $H^{B3+B5+F3}$), 8.97 (d, *J* = 4.5 Hz, 4H, H^{C2+G2}), 8.66 (d, *J* = 8.1 Hz, 3H, H^{A3+E3}), 8.18 (m, 5H, $H^{C3+D3+G3}$), 7.96 (m, 3H, H^{A4+E4}), 7.44 (d, *J* = 4.9 Hz, 2H, H^{E6}), 7.39 (d, *J* = 5.5 Hz, 1H, H^{A6}), 7.20 (m, 3H, H^{A5+E5}), 7.16 (d, *J* = 6.5 Hz, 1H, H^{D6}), 6.71 (dd, *J* = 6.5, 2.7 Hz, 1H, H^{D5}), 4.13 (t, *J* = 6.6 Hz, 2H, H^{1}), 3.43 (d, *J* = 11.6 Hz, 2H, H^{13eq}), 2.95 (m, 2H, H^{11}), 2.78 (t, *J* = 12.3 Hz, 2H, H^{13ax}), 1.85 (d, *J* = 15.1 Hz, 2H, H^{14eq}), 1.74 (dd, *J* = 13.5, 9.5 Hz, 4H, H^{2+14ax}),

1.66 (m, 2H, H^{10}), 1.42 (m, 4H, H^{3+15}), 1.27 (m, 12H, H^{4-9}). **^{13}C {^{1}H} NMR** (126 MHz, CD_3CN) δ/ppm 167.9 (C^{D4}), 159.9 (C^{D2}), 158.9 (C^{A2+E2}), 156.7 ($C^{B2+B6+F2}$), 154.0 (C^{D6}), 153.5 (C^{A6}), 153.4 (C^{E6}), 152.1 (C^{C2+G2}), 146.4 (C^{B4}), 146.1 (C^{F4}), 145.1 (C^{C4+G4}), 139.1 (C^{E4}), 138.9 (C^{A4}), 128.6 (C^{A5}), 128.5 (C^{E5}), 125.6 (C^{A3+E3}), 123.0 (C^{C3+G3}), 122.9 (C^{F3}), 122.8 (C^{B3+B5}), 114.7 (C^{D5}), 113.2 (C^{D3}), 70.8 (C^{1}), 58.2 (C^{11}), 54.3 (C^{13}), 30.2, 30.1, 30.0 (C^{5-7}), 29.9 (C^{4}), 29.7 (C^{8}), 29.3 (C^{2}), 27.1 (C^{9}), 26.4 (C^{3}), 24.6 (C^{10}), 23.8 (C^{14}), 22.2 (C^{15}). **ESI MS** (MeCN) monoprotonated form: *m/z* 1266.3 $[M\text{-}PF_6]^+$ (15%, calc. 1266.3), 560.7 $[M\text{-}2PF_6]^{2+}$ (48%, 560.7), 325.5 $[M\text{-}3PF_6]^{3+}$ (18%, 325.5), deprotonated form: *m/z* 1266.3 $[M+H]^+$ (15%, 1266.3), 1120.3 $[M\text{-}PF_6]^+$ (3%, 1120.4), 487.7 $[M\text{-}2PF_6]^{2+}$ (35%, 487.7). **IR** (solid, ν/cm^{-1}) 3635 (w), 2925 (m), 2851 (w), 1636 (w), 1602 (m), 1464 (w), 1458 (w), 1429 (w), 1409 (m), 1393 (w), 1318 (w), 1291 (w), 1229 (w), 1218 (w), 1029 (m), 819 (s), 779 (s), 752 (m), 739 (m), 734 (m), 713 (w). **EA** found: C, 41.87; H, 4.13; N, 8.46%. $C_{56}H_{60}F_{18}N_9O_2P_3Ru{\cdot}H_2O{\cdot}NH_4PF_6$ requires C, 42.25; H, 4.18; N, 8.80%. **UV/VIS** λ_{max}/nm (2.25 x 10^{-5}mol dm^{-3}, MeCN) 274 (ε/dm^3 mol^{-1} cm^{-1} 63000), 312 (58000), 491 (28000). **Luminescence** (MeCN, 1.31 x 10^{-5}mol dm^{-3}, λ_{ex} = 495 nm): λ_{em} = 675 nm.

[Ru(H**L20**)(**L3**)][PF_6]$_3$ **(C25)**

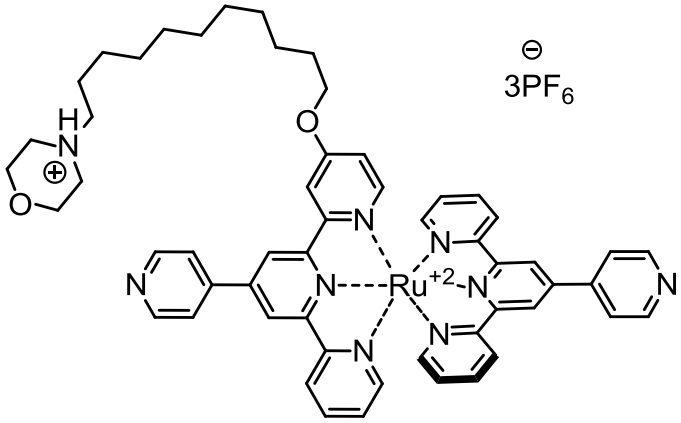

L20 (48 mg, 0.08 mmol) and $RuCl_3.3H_2O$ (22 mg, 0.08 mmol) were suspended in dry *N*,*N*-dimethylformamide (5 mL) in a microwave reactor vial. The reaction mixture was treated in a microwave reactor at 130 °C for 10 minutes. Silver hexafluorophosphate (64 mg, 0.25 mmol) was added and the black suspension was heated in a microwave reactor at 130 °C for 3 minutes. The ligand **L3** (26 mg, 0.08 mmol) and *N*-ethylmorpholine (3 drops) were added and

the reaction mixture was treated in a microwave reactor at 160 °C for 15 minutes. The resulting dark red solution was poured into 250 mL of aqueous ammonium hexafluorophosphate to give a fine red precipitate, which was collected on Celite® and washed with cold water (250 mL) and diethyl ether (20 mL). The residue was redissolved in acetonitrile and solvent removed in vacuo to give a dark red solid, which was purified with column chromatography (SiO_2, eluted with MeCN/saturated aqueous KNO_3/H_2O = 10:0.5:1.5). The second red band was collected, aqueous ammonium hexafluorophosphate added and solvent evaporated until a red precipitate formed. This was collected on Celite® and washed thoroughly with cold water (250 mL), cold ethanol (15 mL) and diethyl ether (15 mL). The residue was redissolved in acetonitrile and solvent removed in vacuo to give the product as a red powder (37 mg, 0.026 mmol, 31%).

^{1}H NMR (500 MHz, CD_3CN) δ/ppm 9.08 (m, 4H, $H^{B3+B5+F3}$), 9.03 (br m, 4H, H^{C2+G2}), 8.67 (dd, *J* = 8.1, 0.6 Hz, 3H, H^{A3+E3}), 8.36 (br s, 4H, H^{C3+G3}), 8.17 (d, *J* = 2.6 Hz, 1H, H^{D33}), 7.97 (m, 3H, H^{A4+E4}), 7.45 (d, *J* = 5.6 Hz, 2H, H^{E6}), 7.40 (d, *J* = 4.9 Hz, 1H, H^{A6}), 7.21 (m, 3H, H^{A5+E5}), 7.17 (d, *J* = 6.5 Hz, 1H, H^{D6}), 6.72 (dd, *J* = 6.5, 2.7 Hz, 1H, H^{D5}), 4.13 (t, *J* = 6.5 Hz, 2H, H^1), 3.99 (d, *J* = 12.0 Hz, 2H, H^{14eq}), 3.71 (t, *J* = 12.4 Hz, 2H, H^{14ax}), 3.39 (d, *J* = 12.5 Hz, 2H, H^{13eq}), 3.03 (m, 4H, $H^{11+13ax}$), 1.74 (m, 2H, H^2), 1.65 (m, 2H, H^{10}), 1.40 (m, 2H, H^3), 1.28 (m, 12H, H^{4-9}). **^{13}C {^{1}H} NMR** (126 MHz, CD_3CN) δ/ppm 168.0 (C^{D4}), 159.9 (C^{D2}), 158.8 (C^{A2+E2}), 156.8 ($C^{B2+B6+F2}$), 154.0 (C^{D6}), 153.6 (C^{A6}), 153.5 (C^{E6}), 148.6 (C^{B4+F4}), 147.5 (C^{C4+G4}), 139.2 (C^{E4}), 139.1 (C^{A4}), 128.7 (C^{A5+E5}), 125.8 (C^{A3+E3}), 124.4 (C^{C3+G3}), 123.0 ($C^{B3+B5+F3}$), 114.8 (C^{D5}), 113.3 (C^{D3}), 70.8 (C^1),63.5 (C^{14}), 58.4 (C^{11}), 53.0 (C^{13}), 30.2, 30.1, 30.0 (C^{5-7}), 29.9 (C^4), 29.6 (C^8), 29.2 (C^2), 26.8 (C^9), 26.3 (C^3), 24.0 (C^{10}), (C^{C2+G2} not recorded). **ESI MS** (MeCN) monoprotonated form: *m/z* 1268.1 $[M\text{-}PF_6]^+$ (3%, calc. 1268.3), 561.6 $[M\text{-}2PF_6]^+$ (5%, 561.7), 326.1 $[M\text{-}3PF_6]^{3+}$ (3%, 326.1), deprotonated form: *m/z* 1268.1 $[M+H]^+$ (3%, 1268.3), 1122.3 $[M\text{-}PF_6]^+$ (8%, 1122.3), 488.7 $[M\text{-}2PF_6]^{2+}$ (100%, 488.7). **IR** (solid, ν/cm^{-1}) 3314 (m), 2925 (w), 2854 (w), 1634 (w), 1605 (m), 1426 (m), 1413 (m), 1318 (w), 1229 (w), 1029 (m), 810 (s), 797 (s), 787 (s), 771 (s), 754 (m), 740 (m), 720 (m), 700 (m), 704 (w), 693 (w), 658 (w), 647 (w), 609 (w), 601 (w). **EA** found: C, 27.80; H, 3.40; N, 7.88%. $C_{55}H_{58}F_{18}N_9O_2P_3Ru{\cdot}2H_2O{\cdot}5.5NH_4PF_6$ requires C, 28.16; H, 3.61; N, 8.66%. **UV/VIS** λ_{max}/nm (1 x 10^{-5}mol dm^{-3}, MeCN) 241 (ε/dm^3 mol^{-1} cm^{-1} 38000), 274 (53000), 312 (50000), 492 (25000). **Luminescence** (MeCN, 1 x 10^{-5}mol dm^{-3}, λ_{ex} = 492 nm): λ_{em} = 665 nm.

[Ru(H**L22**)(**L3**)][PF_6]$_3$ **(C26)**

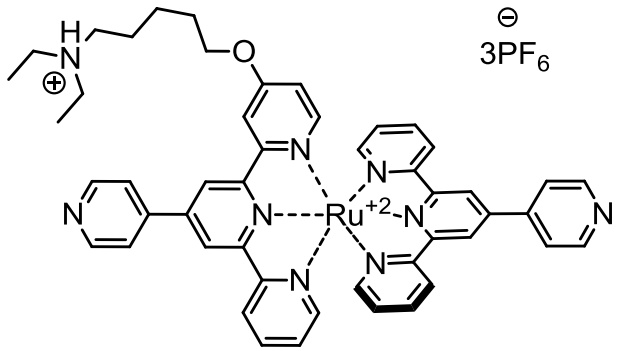

L3 (22 mg, 0.07 mmol) and $RuCl_3.3H_2O$ (22 mg, 0.08 mmol) were suspended in dry *N*,*N*-dimethylformamide (5 mL) in a microwave reactor vial. The reaction mixture was treated in a microwave reactor at 130 °C for 10 minutes. Silver hexafluorophosphate (60 mg, 0.23 mmol) was added and the black suspension was heated in a microwave reactor at 130 °C for 3 minutes. The ligand **L21** (37 mg, 0.07 mmol) and *N*-ethylmorpholine (3 drops) were added and the reaction mixture was treated in a microwave reactor at 160 °C for 15 minutes. The resulting dark red solution was poured into 250 mL of aqueous ammonium hexafluorophosphate to give a fine red precipitate, which was collected on Celite® and washed with cold water (250 mL) and diethyl ether (20 mL). The residue was redissolved in acetonitrile and solvent removed in vacuo to give a dark red solid, which was purified with column chromatography (SiO_2, eluted with MeCN/saturated aqueous KNO_3/H_2O = 10:0.5:1.5). The second red band was collected, aqueous ammonium hexafluorophosphate added and solvent evaporated until a red precipitate formed. This was collected on Celite® and washed thoroughly with cold water (250 mL), cold ethanol (15 mL) and diethyl ether (15 mL). The residue was redissolved in acetonitrile and solvent removed in vacuo to give the product as a red powder in a trace amounth.

ESI MS (MeCN) deprotonated form: *m/z* 1024.3 $[M\text{-}PF_6]^+$ (12%, calc. 1024.3), 882.1 $[M\text{-}PF_6\text{-}(CH_2)_5NEt_2]^+$ (100%, 882.1), 439.7 $[M\text{-}2PF_6]^{2+}$ (16%, 439.7), 368.6 $[M\text{-}2PF_6\text{-}(CH_2)_5NEt_2]^{2+}$ (82%, calc. 368.6).

$[Ru(\mathbf{L2})_2][PF_6]_2$ **(C27)**

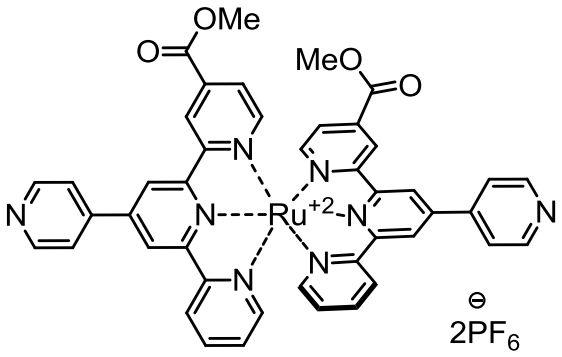

L2 (50 mg, 0.14 mmol) and $RuCl_3.3H_2O$ (36 mg, 0.14 mmol) were suspended in dry *N*,*N*-dimethylformamide (5 mL) in a microwave reactor vial. The reaction mixture was treated in a microwave reactor at 130 °C for 10 minutes. Silver hexafluorophosphate (103 mg, 0.41 mmol) was added and the black suspension was heated in a microwave reactor at 130 °C for 3 minutes. The ligand **L2** (50 mg, 0.14 mmol) and *N*-ethylmorpholine (3 drops) were added and the reaction mixture was treated in a microwave reactor at 160 °C for 15 minutes. The resulting dark red solution was poured into 250 mL of aqueous ammonium hexafluorophosphate to give a fine red precipitate, which was collected on Celite® and washed with cold water (250 mL) and diethyl ether (20 mL). The residue was redissolved in acetonitrile and solvent removed in vacuo to give a dark red solid, which was purified with column chromatography (SiO_2, eluted with MeCN/saturated aqueous KNO_3/H_2O = 10:0.5:1.5). The first red band was collected, aqueous ammonium hexafluorophosphate added and solvent evaporated until a red precipitate formed. This was collected on Celite® and washed thoroughly with cold water (250 mL), cold ethanol (15 mL) and diethyl ether (15 mL). The residue was redissolved in acetonitrile and solvent removed in vacuo to give the product as a red powder (54 mg, 0.048 mmol, 35%).

^{1}H NMR (500 MHz, CD_3CN) δ/ppm 9.25 (d, *J* = 1.2 Hz, 2H, H^{B5}), 9.15 (dd, *J* = 1.6, 0.7 Hz, 2H, H^{D3}), 9.13 (d, *J* = 1.2 Hz, 2H, H^{B3}), 8.98 (br s, 4H, H^{C2}), 8.71 (d, *J* = 7.9 Hz, 2H, H^{A3}), 8.26 (d, *J* = 5.3 Hz, 4H, H^{C3}), 8.01 (m, 2H, H^{A4}), 7.63 (dd, *J* = 5.8, 0.6 Hz, 2H, H^{D6}), 7.61 (dd, *J* = 5.8, 1.7 Hz, 2H, H^{D5}), 7.44 (dd, *J* = 5.6, 0.8 Hz, 2H, H^{A6}), 7.23 (ddd, *J* = 7.5, 5.6, 1.3 Hz, 2H, H^{A5}), 3.93 (s, 6H, H^{Me}). **^{13}C {^{1}H} NMR** (126 MHz, CD_3CN) δ/ppm 164.7 ($C^{C=O}$), 160.2 (C^{D2}), 158.6 (C^{A2}), 156.8 (C^{B2}), 156.5 (C^{B6}), 154.7 (C^{D6}), 153.6 (C^{A6}), 151.0 (C^{C2}), 146.6 (C^{C4}), 145.1 (C^{B4}), 140.0 (C^{D4}), 139.7 (C^{A4}), 128.9

(C^{A5}), 127.4 (C^{D5}), 126.0 (C^{A3}), 124.7 (C^{D3}), 123.6 (C^{C3+B5}), 123.3 (C^{B3}), 54.0 (C^{Me}). **ESI MS** (MeCN): *m/z* 983.0 $[M\text{-}PF_6]^+$ (12%, calc. 983.1), 419.1 $[M\text{-}2PF_6]^{2+}$ (100%, 419.1). **IR** (solid, ν/cm^{-1}) 3650 (w), 3076 (w), 1716 (m), 1700 (m), 1597 (m), 1471 (w), 1429 (w), 1404 (m), 1344 (w), 1313 (m), 1270 (m), 1254 (m), 1236 (w), 1118 (w), 1030 (m), 966 (w), 818 (s), 802 (s), 782 (m), 767 (m), 759 (m), 750 (m), 742 (m), 728 (m), 717 (w), 638 (w). **EA** found: C, 43.00; H, 3.03; N, 9.96%. $C_{44}H_{32}F_{12}N_8O_4P_2Ru{\cdot}H_2O{\cdot}0.5NH_4PF_6$ requires C, 43.06; H, 2.96; N, 9.70%. **UV/VIS** λ_{max}/nm (1.10 x 10^{-5}mol dm^{-3}, MeCN) 287 (ε/dm^3 mol^{-1} cm^{-1} 77000), 323 (59000), 497 (28000). **Luminescence** (MeCN, 1.10 x 10^{-5}mol dm^{-3}, λ_{ex} = 493 nm): λ_{em} = 662 nm.

$[Ru(\mathbf{L10})_2][PF_6]_2$ **(C28)**

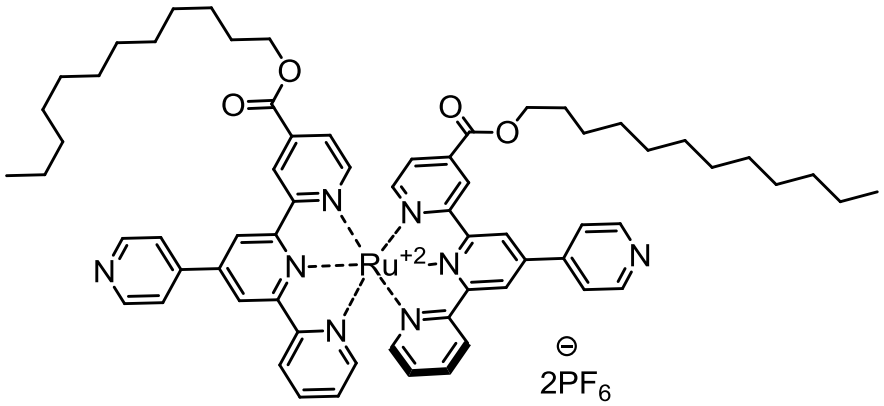

L10 (72 mg, 0.14 mmol) and $RuCl_3.3H_2O$ (36 mg, 0.14 mmol) were suspended in dry *N*,*N*-dimethylformamide (5 mL) in a microwave reactor vial. The reaction mixture was treated in a microwave reactor at 130 °C for 10 minutes. Silver hexafluorophosphate (103 mg, 0.41 mmol) was added and the black suspension was heated in a microwave reactor at 130 °C for 3 minutes. The ligand **L10** (72 mg, 0.14 mmol) and *N*-ethylmorpholine (3 drops) were added and the reaction mixture was treated in a microwave reactor at 160 °C for 15 minutes. The resulting dark red solution was poured into 250 mL of aqueous ammonium hexafluorophosphate to give a fine red precipitate, which was collected on Celite® and washed with cold water (250 mL) and diethyl ether (20 mL). The residue was redissolved in acetonitrile and solvent removed in vacuo to give a dark red solid, which was purified with column chromatography (SiO_2, eluted with MeCN/saturated aqueous KNO_3/H_2O = 10:0.5:0.5). The first red band was collected, aqueous ammonium hexafluorophosphate added and solvent evaporated until a red precipitate formed.

This was collected on Celite® and washed thoroughly with cold water (250 mL), cold ethanol (15 mL) and diethyl ether (15 mL). The residue was redissolved in acetonitrile and solvent removed in vacuo to give the product as a red powder (75 mg, 0.052 mmol, 38%).

^{1}H NMR (500 MHz, CD_3CN) δ/ppm 9.23 (d, *J* = 1.4 Hz, 2H, H^{B5}), 9.12 (d, *J* = 1.4 Hz, 4H, H^{B3+D3}), 8.97 (m, 4H, H^{C2}), 8.71 (d, *J* = 7.9 Hz, 2H, H^{A3}), 8.22 (dd, *J* = 4.5, 1.6 Hz, 4H, H^{C3}), 8.01 (m, 2H, H^{A4}), 7.63 (dd, *J* = 5.8, 0.7 Hz, 2H, H^{D6}), 7.60 (dd, *J* = 5.8, 1.7 Hz, 2H, H^{D5}), 7.45 (ddd, *J* = 5.6, 1.4, 0.6 Hz, 2H, H^{A6}), 7.23 (ddd, *J* = 7.5, 5.6, 1.3 Hz, 2H, H^{A5}), 4.33 (t, *J* = 6.6 Hz, 4H, H^{1}), 1.72 (m, 4H, H^{2}), 1.37 (m, 4H, H^{3}), 1.24 (m, 32H, H^{4-11}), 0.84 (t, *J* = 7.0 Hz, 6H, H^{12}). **^{13}C {^{1}H} NMR** (126 MHz, CD_3CN) δ/ppm 164.2 ($C^{C=O}$), 160.0 (C^{D2}), 158.6 (C^{A2}), 156.8 (C^{B2}), 156.3 (C^{B6}), 154.6 (C^{D6}), 153.6 (C^{A6}), 151.5 (C^{C2}), 146.8 (C^{B4}), 145.7 (C^{C4}), 140.2 (C^{D4}), 139.7 (C^{A4}), 128.9 (C^{A5}), 127.4 (C^{D5}), 126.0 (C^{A3}), 124.6 (C^{D3}), 123.5 (C^{B5}), 123.4 (C^{C3}), 123.3 (C^{B3}), 67.6 (C^{1}), 32.6 (C^{10}), 30.3, 30.2, 30.0 (C^{5-9}), 29.9 (C^{4}), 29.1 (C^{2}), 26.5 (C^{3}), 23.4 (C^{11}), 14.4 (C^{12}). **ESI MS** (MeCN): *m/z* 1291.3 $[M\text{-}PF_6]^+$ (2%, calc. 1291.5), 573.2 $[M\text{-}2PF_6]^{2+}$ (100%, 573.3). **IR** (solid, ν/cm^{-1}) 3087 (w), 2921 (m), 2851 (m), 1987 (w), 1706 (m), 1700 (m), 1635 (w), 1597 (m), 1464 (w), 1456 (w), 1423 (w), 1407 (m), 1307 (w), 1295 (w), 1265 (m), 1250 (m), 1237 (w), 1168 (w), 1117 (w), 1031 (w), 870 (w), 820 (s), 783 (m), 760 (m), 740 (m), 729 (m), 720 (w), 658 (w), 638 (w). **EA** found: C, 50.40; H, 4.97; N, 7.83%. $C_{66}H_{76}F_{12}N_8O_4P_2Ru{\cdot}0.8NH_4PF_6$ requires C, 50.60; H, 5.10; N, 7.87%. **UV/VIS** λ_{max}/nm (093 x 10^{-5}mol dm^{-3}, MeCN) 287 (ε/dm^3 mol^{-1} cm^{-1} 80000), 323 (62000), 497 (28000). **Luminescence** (MeCN, 1.13 x 10^{-5}mol dm^{-3}, λ_{ex} = 494 nm): λ_{em} = 663 nm.

$[Ru(HL11)_2][PF_6]_4$ **(C29)**

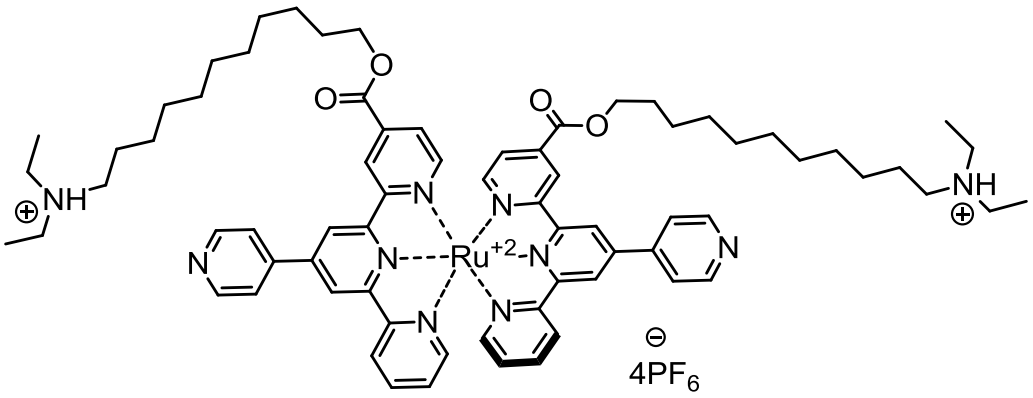

L11 (79 mg, 0.14 mmol) and $RuCl_3.3H_2O$ (36 mg, 0.14 mmol) were suspended in dry *N*,*N*-dimethylformamide (5 mL) in a microwave reactor vial. The reaction mixture was treated in a microwave reactor at 130 °C for 10 minutes. Silver hexafluorophosphate (103 mg, 0.41 mmol) was added and the black suspension was heated in a microwave reactor at 130 °C for 3 minutes. The ligand **L11** (79 mg, 0.14 mmol) and *N*-ethylmorpholine (3 drops) were added and the reaction mixture was treated in a microwave reactor at 160 °C for 15 minutes. The resulting dark red solution was poured into 250 mL of aqueous ammonium hexafluorophosphate to give a fine red precipitate, which was collected on Celite® and washed with cold water (250 mL) and diethyl ether (20 mL). The residue was redissolved in acetonitrile and solvent removed in vacuo to give a dark red solid, which was purified with column chromatography (SiO_2, eluted with MeCN/saturated aqueous KNO_3/H_2O = 10:0.5:1.5). The first red band was collected, aqueous ammonium hexafluorophosphate added and solvent evaporated until a red precipitate formed. This was collected on Celite® and washed thoroughly with cold water (250 mL), cold ethanol (15 mL) and diethyl ether (15 mL). The residue was redissolved in acetonitrile and solvent removed in vacuo to give the product as a red powder (91 mg, 0.049mmol, 37%).

^{1}H NMR (500 MHz, CD_3CN) δ/ppm 9.22 (d, *J* = 1.5 Hz, 2H, H^{B5}), 9.11 (d, *J* = 1.3 Hz, 2H, H^{B3}), 9.10 (br s, 2H, H^{D3}), 8.97 (br s, 4H, H^{C2}), 8.70 (d, *J* = 8.0 Hz, 2H, H^{A3}), 8.20 (d, *J* = 4.0 Hz, 4H, H^{C3}), 8.00 (td, *J* = 7.9, 1.5 Hz, 2H, H^{A4}), 7.62 (d, *J* = 5.9 Hz, 2H, H^{D6}), 7.60 (dd, *J* = 5.9, 1.7 Hz, 2H, H^{D5}), 7.44 (dd, *J* = 5.6, 0.7 Hz, 2H, H^{A6}), 7.23 (ddd, *J* = 7.2, 5.6, 1.3 Hz, 2H, H^{A5}), 4.33 (t, *J* = 6.7 Hz, 4H, H^1), 3.15 (m, 8H, H^{13}), 3.03 (m, 4H, H^{11}), 1.74 (m, 4H, H^2), 1.61 (m, 3H, H^{10}), 1.39 (m, 4H, H^3), 1.30 (m, 24H, H^{4-9}), 1.24 (t, *J* = 7.3 Hz, 12H, H^{14}). **^{13}C {^{1}H} NMR** (126 MHz, CD_3CN) δ/ppm 164.2 ($C^{C=O}$), 160.0 (C^{D2}), 158.7 (C^{A2}), 156.8 (C^{B2}), 156.3 (C^{B6}), 154.7 (C^{D6}), 153.5 (C^{A6}), 151.8 (C^{C2}), 146.9 (C^{B4}), 145.3 (C^{C4}), 140.2 (C^{D4}), 139.7 (C^{A4}), 128.9 (C^{A5}), 127.4 (C^{D5}), 125.9 (C^{A3}), 124.6 (C^{D3}), 123.5 (C^{B5}), 123.3 (C^{C3+B3}), 67.6 (C^1), 53.0 (C^{11}), 48.4 (C^{13}), 30.2, 30.1, 30.0 (C^{5-7}), 29.9 (C^4), 29.7 (C^8), 29.2 (C^2), 27.0 (C^9), 26.5 (C^3), 24.4 (C^{10}), 9.1 (C^{14}). **ESI MS** (MeCN): *m/z* 1697.5 $[M\text{-}PF_6]^+$ (2%, calc. 1697.5), 776.3 $[M\text{-}2PF_6]^{2+}$ (43%, 776.3). **IR** (solid, ν/cm^{-1}) 2928 (m), 2853 (w), 1994 (w), 1722 (m), 1595 (m), 1464 (w), 1406 (m), 1308 (m), 1293 (w), 1265 (m), 1248 (m), 1238 (m), 1165 (w), 1129 (w), 1031 (w), 819 (s), 800 (s), 782 (s), 776 (m), 765 (m), 758 (m), 751 (w), 738 (w), 730 (w), 711 (m), 601 (m). **EA** found: C, 45.23; H, 5.01; N, 8.07%. $C_{72}H_{92}F_{24}N_{10}O_4P_4Ru{\cdot}0.5NH_4PF_6$

requires C, 44.95; H, 4.92; N, 7.64%. **UV/VIS** λ_{max}/nm (0.97 x 10^{-5}mol dm^{-3}, MeCN) 287 (ε/dm^3 mol^{-1} cm^{-1} 80000), 323 (62000), 498 (29000). **Luminescence** (MeCN, 0.97 x 10^{-5}mol dm^{-3}, λ_{ex} = 494 nm): λ_{em} = 667 nm.

$[Ru(\mathbf{L17})_2][PF_6]_2$ **(C30)**

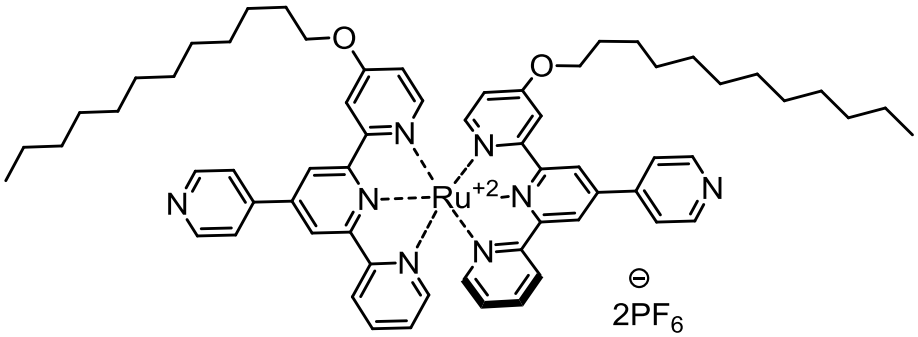

L17 (67 mg, 0.14 mmol) and $RuCl_3.3H_2O$ (36 mg, 0.14 mmol) were suspended in dry *N*,*N*-dimethylformamide (5 mL) in a microwave reactor vial. The reaction mixture was treated in a microwave reactor at 130 °C for 10 minutes. Silver hexafluorophosphate (103 mg, 0.41 mmol) was added and the black suspension was heated in a microwave reactor at 130 °C for 3 minutes. The ligand **L17** (67 mg, 0.14 mmol) and *N*-ethylmorpholine (3 drops) were added and the reaction mixture was treated in a microwave reactor at 160 °C for 15 minutes. The resulting dark red solution was poured into 250 mL of aqueous ammonium hexafluorophosphate to give a fine red precipitate, which was collected on Celite® and washed with cold water (250 mL) and diethyl ether (20 mL). The residue was redissolved in acetonitrile and solvent removed in vacuo to give a dark red solid, which was purified with column chromatography (SiO_2, eluted with MeCN/saturated aqueous KNO_3/H_2O = 10:0.5:1.5). The first red band was collected, aqueous ammonium hexafluorophosphate added and solvent evaporated until a red precipitate formed. This was collected on Celite® and washed thoroughly with cold water (250 mL), cold ethanol (15 mL) and diethyl ether (15 mL). The residue was redissolved in acetonitrile and solvent removed in vacuo to give the product as a red powder (110 mg, 0.080 mmol, 59%).

^{1}H NMR (500 MHz, CD_3CN) δ/ppm 9.05 (d, *J* = 0.8 Hz, 4H, H^{B3+B5}), 8.96 (br s, 4H, H^{C2}), 8.68 (d, *J* = 8.1 Hz, 2H, H^{A3}), 8.18 (m, 6H, H^{C3+D3}), 7.95 (td, *J* = 8.0, 1.4 Hz, 2H, H^{A4}), 7.43 (d, *J* = 5.0 Hz, 2H, H^{A6}), 7.20 (m, 4H, H^{A5+D6}), 6.74 (dd, *J* = 6.5, 2.7 Hz, 2H, H^{D5}), 4.14 (t, *J* = 6.6 Hz, 4H, H^1), 1.75 (m,

2H, H^2), 1.40 (m, 2H, H^3), 1.27 (m, 32H, H^{4-11}), 0.84 (t, *J* = 6.8 Hz, 6H, H^{12}). **^{13}C {^{1}H} NMR** (126 MHz, CD_3CN) δ/ppm 167.8 (C^{D4}), 159.9 (C^{D2}), 159.0 (C^{A2}), 156.7 (C^{B2+B6}), 153.8 (C^{D6}), 153.4 (C^{A6}), 151.8 (C^{C2}), 145.9 (C^{B4}), 145.4 (C^{C4}), 138.8 (C^{A4}), 128.5 (C^{A5}), 125.6 (C^{A3}), 123.0 (C^{C3}), 122.8 (C^{B5}), 122.7 (C^{B3}), 114.7 (C^{D5}), 113.1 (C^{D3}), 70.8 (C^1), 32.6 (C^{10}), 30.3, 30.2, 30.0 (C^{5-9}), 29.9 (C^4), 29.3 (C^2), 26.3 (C^3), 23.4 (C^{11}), 14.4 (C^{12}). **ESI MS** (MeCN): *m/z* 1235.3 $[M\text{-}PF_6]^+$ (47%, calc. 1235.5), 545.2 $[M\text{-}2PF_6]^{2+}$ (100%, 545.3). **IR** (solid, ν/cm^{-1}) 3076 (w), 2917 (m), 2850 (w), 1993 (w), 1609 (m), 1597 (m), 1464 (w), 1429 (w), 1408 (m), 1318 (m), 1262 (w), 1227 (m), 1026 (m), 822 (s), 818 (s), 782 (m), 757 (m), 739 (w), 601 (w). **EA** found: C, 53.95; H, 5.41; N, 8.25%. $C_{64}H_{76}F_{12}N_8O_2P_2Ru{\cdot}2H_2O$ requires C, 54.27; H, 5.69; N, 7.91%. **UV/VIS** λ_{max}/nm (0.97 x 10^{-5}mol dm^{-3}, MeCN) 274 (ε/dm^3 mol^{-1} cm^{-1} 60000), 311 (64000), 493 (29000). **Luminescence** (MeCN, 1.10 x 10^{-5}mol dm^{-3}, λ_{ex} = 497 nm): λ_{em} = 680 nm.

$[Ru(HL19)_2][PF_6]_4$ **(C32)**

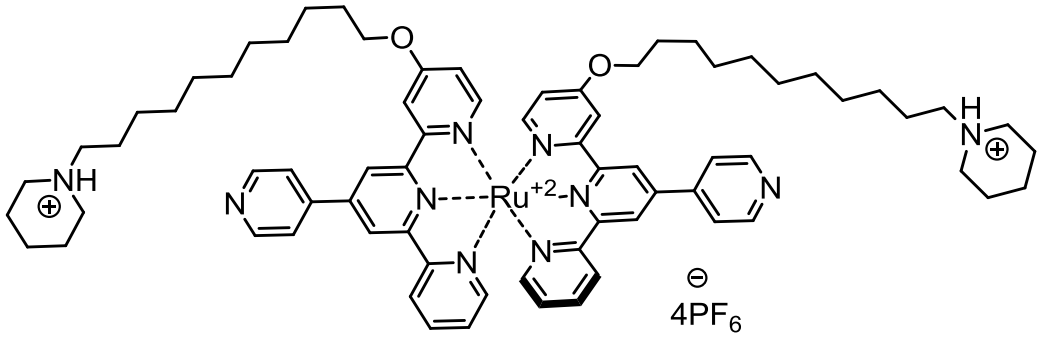

C32 was isolated in a trace amount as a side product of C24.

ESI MS (MeCN) bisprotonated form: *m/z* 760.3 $[M\text{-}2PF_6]^{2+}$ (26%, calc. 760.3), monoprotonated form: *m/z* 687.3 $[M\text{-}2PF_6]^{2+}$ (17%, 687.3), 410.0 $[M\text{-}3PF_6]^{3+}$ (37%, 409.9).

[Ru(**L23**)$_2$][PF$_6$]$_2$ **(C33)**

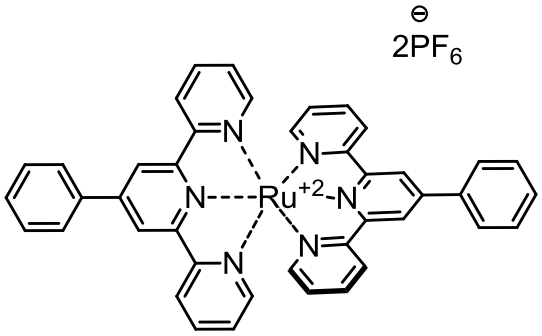

L23 (30 mg, 0.10 mmol) and $RuCl_3.3H_2O$ (25 mg, 0.10 mmol) were suspended in dry *N*,*N*-dimethylformamide (5 mL) in a microwave reactor vial. The reaction mixture was treated in a microwave reactor at 130 °C for 10 minutes. Silver hexafluorophosphate (74 mg, 0.29 mmol) was added and the black suspension was heated in a microwave reactor at 130 °C for 3 minutes. The ligand **L23** (30 mg, 0.10 mmol) and *N*-ethylmorpholine (3 drops) were added and the reaction mixture was treated in a microwave reactor at 160 °C for 15 minutes. The resulting dark red solution was poured into 250 mL of aqueous ammonium hexafluorophosphate to give a fine red precipitate, which was collected on Celite® and washed with cold water (250 mL) and diethyl ether (20 mL). The residue was redissolved in acetonitrile and solvent removed in vacuo to give a dark red solid, which was purified by recrystallization from MeCN-Et_2O. The product was obtained as a red powder (76 mg, 0.075 mmol, 78%).

^{1}H NMR (400 MHz, CD_3CN) δ/ppm 9.02 (s, 4H, H^{B3}), 8.66 (d, *J* = 8.1 Hz, 4H, H^{A3}), 8.21 (dd, *J* = 7.2, 1.3 Hz, 4H, H^{C2}), 7.95 (td, *J* = 7.9, 1.5 Hz, 4H, H^{A4}), 7.77 (t, *J* = 7.5 Hz, 4H, H^{C3}), 7.69 (m, 2H, H^{C4}), 7.44 (dd, *J* = 5.6, 0.7 Hz, 4H, H^{A6}), 7.18 (ddd, *J* = 7.4, 5.6, 1.2 Hz, 4H, H^{A5}). **UV/VIS** λ_{max}/nm (1.12 x 10^{-5}mol dm^{-3}, MeCN) 283 (ε/dm^3 mol^{-1} cm^{-1} 76000), 311 (62000), 488 (24000). **Luminescence** (MeCN, 0.64 x 10^{-5}mol dm^{-3}, λ_{ex} = 489 nm): λ_{em} = 644 nm.

[Ru(**L26**)(**L23**)][PF_6]$_2$ **(C34)**

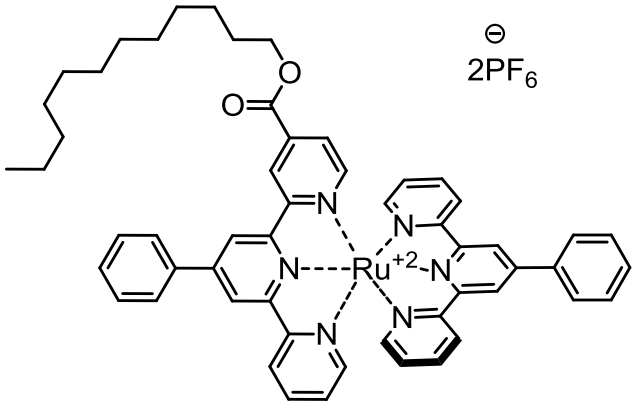

L26 (44 mg, 0.08 mmol) and $RuCl_3.3H_2O$ (22 mg, 0.08 mmol) were suspended in dry *N*,*N*-dimethylformamide (5 mL) in a microwave reactor vial. The reaction mixture was treated in a microwave reactor at 130 °C for 10 minutes. Silver hexafluorophosphate (64 mg, 0.25 mmol) was added and the black suspension was heated in a microwave reactor at 130 °C for 3 minutes. The ligand **L3** (26 mg, 0.08 mmol) and *N*-ethylmorpholine (3 drops) were added and the reaction mixture was treated in a microwave reactor at 160 °C for 15 minutes. The resulting dark red solution was poured into 250 mL of aqueous ammonium hexafluorophosphate to give a fine red precipitate, which was collected on Celite® and washed with cold water (250 mL) and diethyl ether (20 mL). The residue was redissolved in acetonitrile and solvent removed in vacuo to give a dark red solid, which was purified with column chromatography (SiO_2, eluted with MeCN/saturated aqueous KNO_3/H_2O = 10:0.5:0.5). The second red band was collected, aqueous ammonium hexafluorophosphate added and solvent evaporated until a red precipitate formed. This was collected on Celite® and washed thoroughly with cold water (250 mL), cold ethanol (15 mL) and diethyl ether (15 mL). The residue was redissolved in acetonitrile and solvent removed in vacuo to give the product as a red powder (42 mg, 0.034 mmol, 41%).

^{1}H NMR (500 MHz, CD_3CN) δ/ppm 9.17 (d, *J* = 1.5 Hz, 1H, H^{B5}), 9.08 (dd, *J* = 1.8, 0.7 Hz, 1H, H^{D3}), 9.06 (d, *J* = 1.5 Hz, 1H, H^{B3}), 9.04 (s, 2H, H^{F3}), 8.68 (m, 3H, H^{A3+E3}), 8.24 (m, 4H, H^{C2+G2}), 7.97 (ddd, *J* = 15.7, 7.7, 1.5 Hz, 3H, H^{A4+E4}), 7.78 (t, *J* = 7.8 Hz, 4H, H^{C3+G3}), 7.70 (t, *J* = 7.4 Hz, 2H, H^{C4+G4}), 7.64 (dd, *J* = 5.8, 0.6 Hz, 1H, H^{D6}), 7.59 (dd, *J* = 5.8, 1.7 Hz, 1H, H^{D5}), 7.47 (m, 1H, H^{A6}), 7.43 (m, 2H, H^{E6}), 7.20 (m, 3H, H^{A5+E5}), 4.33 (t, *J* = 6.6 Hz, 2H, H^1), 1.73 (m, 2H, H^2), 1.38 (m, 2H, H^3), 1.25 (m, 16H, H^{4-11}), 0.85 (t, *J* = 7.0 Hz, 3H, H^{12}). **^{13}C {^{1}H} NMR** (126 MHz, CD_3CN) δ/ppm 164.3 ($C^{C=O}$),

160.4 (C^{D2}), 159.1 (C^{A2+E2}), 156.5 (C^{B2}), 156.4 (C^{F2}), 156.1 (C^{B6}), 154.3 (C^{D6}), 153.6 (C^{E6}), 153.4 (C^{A6}), 149.7 (C^{F4}), 149.6 (C^{B4}), 139.4 (C^{D4}), 139.3 (C^{A4}), 139.2 (C^{E4}), 137.7 (C^{C1+G1}), 131.5 (C^{C4}), 131.4 (C^{G4}), 130.7 (C^{C3}), 130.6 (C^{G3}), 129.0 (C^{C2}), 128.8 (C^{G2}), 128.6 (C^{A5}), 128.5 (C^{E5}), 127.1 (C^{D5}), 125.6 (C^{A3+E3}), 124.3 (C^{D3}), 123.2 (C^{B5}), 123.0 (C^{B3}), 122.8 (C^{F3}), 67.5 (C^{1}), 32.6 (C^{10}), 30.3, 30.2, 30.0 (C^{5-9}), 29.9 (C^{4}), 29.1 (C^{2}), 26.5 (C^{3}), 23.4 (C^{11}), 14.4 (C^{12}). **ESI MS** (MeCN): *m/z* 1077.4 $[M\text{-}PF_6]^+$ (100%, calc. 1077.3). **IR** (solid, ν/cm^{-1}) 3094 (w), 2915 (m), 2844 (w), 1985 (w), 1722 (m), 1717 (m), 1609 (m), 1464 (w), 1404 (m), 1305 (w), 1260 (m), 1119 (w), 1034 (w), 826 (s), 763 (m), 730 (m), 695 (m), 512 (m). **EA** found: C, 52.36; H, 4.82; N, 7.00%. $C_{55}H_{54}F_{12}N_6O_2P_2Ru{\cdot}2H_2O$ requires C, 52.51; H, 4.65; N, 6.68%. **UV/VIS** λ_{max}/nm (1.20 x 10^{-5}mol dm^{-3}, MeCN) 285 ($\varepsilon/dm^3\ mol^{-1}\ cm^{-1}$ 71000), 311 (58000), 494 (22000). **Luminescence** (MeCN, 0.50 x 10^{-5}mol dm^{-3}, λ_{ex} = 494 nm): λ_{em} = 673 nm.

$[Ru(H\mathbf{L27})(\mathbf{L23})][PF_6]_3$ **(C35)**

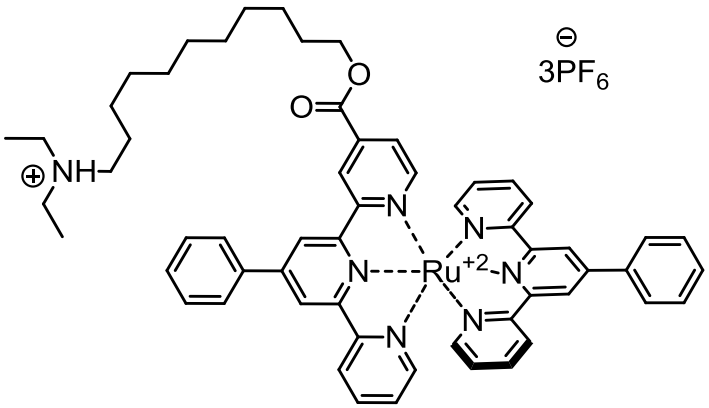

L27 (42 mg, 0.07 mmol) and $RuCl_3.3H_2O$ (19 mg, 0.07 mmol) were suspended in dry *N*,*N*-dimethylformamide (5 mL) in a microwave reactor vial. The reaction mixture was treated in a microwave reactor at 130 °C for 10 minutes. Silver hexafluorophosphate (55 mg, 0.22 mmol) was added and the black suspension was heated in a microwave reactor at 130 °C for 3 minutes. The ligand **L3** (23 mg, 0.07 mmol) and *N*-ethylmorpholine (3 drops) were added and the reaction mixture was treated in a microwave reactor at 160 °C for 15 minutes. The resulting dark red solution was poured into 250 mL of aqueous ammonium hexafluorophosphate to give a fine red precipitate, which was collected on Celite® and washed with cold water (250 mL) and diethyl ether (20 mL). The residue was redissolved in acetonitrile and solvent removed in vacuo

to give a dark red solid, which was purified with column chromatography (SiO_2, eluted with MeCN/saturated aqueous KNO_3/H_2O = 10:0.5:0.5). The second red band was collected, aqueous ammonium hexafluorophosphate added and solvent evaporated until a red precipitate formed. This was collected on Celite® and washed thoroughly with cold water (250 mL), cold ethanol (15 mL) and diethyl ether (15 mL). The residue was redissolved in acetonitrile and solvent removed in vacuo to give the product as a red powder (46 mg, 0.033 mmol, 45%).

^{1}H NMR (500 MHz, CD_3CN) δ/ppm 9.16 (d, *J* = 1.4 Hz, 1H, H^{B5}), 9.07 (dd, *J* = 1.7, 0.6 Hz, 1H, H^{D3}), 9.05 (d, *J* = 1.4 Hz, 1H, H^{B3}), 9.04 (s, 2H, H^{F3}), 8.67 (m, 3H, H^{A3+E3}), 8.24 (td, *J* = 8.3, 1.2 Hz, 4H, H^{C2+G2}), 7.96 (ddd, *J* = 15.7, 7.7, 1.5 Hz, 3H, H^{A4+E4}), 7.77 (t, *J* = 7.6 Hz, 4H, H^{C3+G3}), 7.69 (m, 2H, H^{C4+G4}), 7.65 (dd, *J* = 5.8, 0.6 Hz, 1H, H^{D6}), 7.59 (dd, *J* = 5.8, 1.7 Hz, 1H, H^{D5}), 7.47 (ddd, *J* = 5.6, 1.4, 0.6 Hz, 1H, H^{A6}), 7.43 (ddd, *J* = 5.6, 1.6, 0.7 Hz, 2H, H^{E6}), 7.20 (m, 3H, H^{A5+E5}), 4.32 (t, *J* = 6.7 Hz, 2H, H^1), 3.14 (m, 4H, H^{13}), 3.01 (m, 2H, H^{11}), 1.74 (m, 2H, H^2), 1.61 (m, 2H, H^{10}), 1.39 (m, 2H, H^3), 1.29 (m, 12H, H^{4-9}), 1.23 (t, *J* = 7.3 Hz, 6H, H^{14}). **^{13}C {^{1}H} NMR** (126 MHz, CD_3CN) δ/ppm 164.3 ($C^{C=O}$), 160.4 (C^{D2}), 159.1 (C^{A2+E2}), 156.6 (C^{B2}), 156.4 (C^{F2}), 156.1 (C^{B6}), 154.4 (C^{D6}), 153.6 (C^{E6}), 153.4 (C^{A6}), 149.7 (C^{F4}), 149.6 (C^{B4}), 139.8 (C^{D4}), 139.3 (C^{A4}), 139.2 (C^{E4}), 137.8 (C^{C1+G1}), 131.4 (C^{C4+G4}), 130.7 (C^{C3}), 130.6 (C^{G3}), 128.9 (C^{C2}), 128.8 (C^{G2}), 128.6 (C^{A5}), 128.5 (C^{E5}), 127.1 (C^{D5}), 125.6 (C^{A3+E3}), 124.3 (C^{D3}), 123.2 (C^{B5}), 123.0 (C^{B3}), 122.8 (C^{F3}), 67.5 (C^1), 53.0 (C^{11}), 48.2 (C^{13}), 30.2, 30.1, 30.0 (C^{5-7}), 29.9 (C^4), 29.7 (C^8), 29.2 (C^2), 27.0 (C^9), 26.5 (C^3), 24.4 (C^{10}), 9.1 (C^{14}). **ESI MS** (MeCN) deprotonated form: *m/z* 1280.4 $[M+H]^+$ (100%, calc. 1280.3), 1134.4 $[M\text{-}PF_6]^+$ (20%, 1134.4). **IR** (solid, ν/cm^{-1}) 3329 (w), 3207 (w), 2921 (m), 2852 (m), 1995 (w), 1717 (m), 1703 (w), 1610 (w), 1541 (w), 1463 (w), 1419 (m), 1404 (m), 1308 (w), 1269 (m), 1120 (w), 1012 (m), 820 (s), 763 (s), 753 (m), 740 (m), 728 (m), 720 (m), 702 (m), 682 (m), 555 (s), 513 (m), 505 (m). **EA** found: C, 38.02; H, 4.12; N, 7.46%. $C_{58}H_{62}F_{18}N_7O_2P_3Ru{\cdot}2.5NH_4PF_6$ requires C, 38.01; H, 3.96; N, 7.26%. **UV/VIS** λ_{max}/nm (1.17 x 10^{-5}mol dm^{-3}, MeCN) 285 (ε/dm^3 mol^{-1} cm^{-1} 68000), 311 (56000), 494 (22000). **Luminescence** (MeCN, 0.46 x 10^{-5}mol dm^{-3}, λ_{ex} = 494 nm): λ_{em} = 668 nm.

[Ru(**L29**)(**L23**)][PF_6]$_2$ **(C36)**

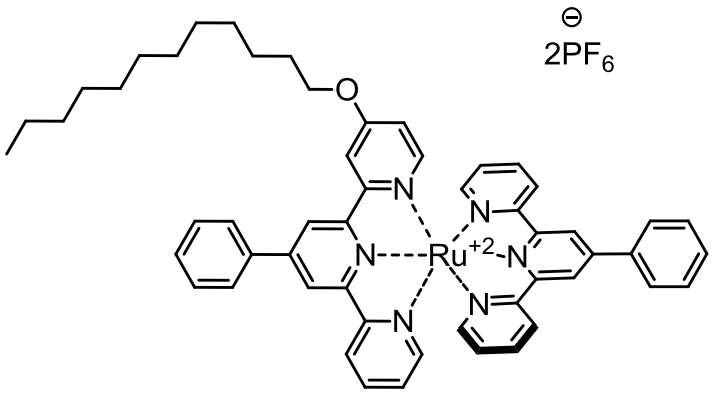

L29 (45 mg, 0.09 mmol) and $RuCl_3.3H_2O$ (24 mg, 0.09 mmol) were suspended in dry *N*,*N*-dimethylformamide (5 mL) in a microwave reactor vial. The reaction mixture was treated in a microwave reactor at 130 °C for 10 minutes. Silver hexafluorophosphate (69 mg, 0.27 mmol) was added and the black suspension was heated in a microwave reactor at 130 °C for 3 minutes. The ligand **L3** (28 mg, 0.09 mmol) and *N*-ethylmorpholine (3 drops) were added and the reaction mixture was treated in a microwave reactor at 160 °C for 15 minutes. The resulting dark red solution was poured into 250 mL of aqueous ammonium hexafluorophosphate to give a fine red precipitate, which was collected on Celite® and washed with cold water (250 mL) and diethyl ether (20 mL). The residue was redissolved in acetonitrile and solvent removed in vacuo to give a dark red solid, which was purified with column chromatography (SiO_2, eluted with MeCN/saturated aqueous KNO_3/H_2O = 10:0.5:0.5). The second red band was collected, aqueous ammonium hexafluorophosphate added and solvent evaporated until a red precipitate formed. This was collected on Celite® and washed thoroughly with cold water (250 mL), cold ethanol (15 mL) and diethyl ether (15 mL). The residue was redissolved in acetonitrile and solvent removed in vacuo to give the product as a red powder (55 mg, 0.046 mmol, 51%).

^{1}H NMR (500 MHz, CD_3CN) δ/ppm 9.02 (m, 4H, $H^{B3+B5+F3}$), 8.67 (m, 3H, H^{A3+E3}), 8.23 (m, 4H, H^{C2+G2}), 8.17 (d, *J* = 2.7 Hz, 1H, H^{D3}), 7.94 (m, 3H, H^{A4+E4}), 7.77 (td, *J* = 7.7, 1.6 Hz, 4H, H^{C3+G3}), 7.69 (m, 2H, H^{C4+G4}), 7.47 (m, 2H, H^{E6}), 7.42 (dd, *J* = 5.6, 0.7 Hz, 1H, H^{A6}), 7.19 (m, 4H, $H^{A5+E5+D6}$), 6.71 (dd, *J* = 6.5, 2.7 Hz, 1H, H^{D5}), 4.13 (t, *J* = 6.6 Hz, 2H, H^1), 1.75 (m, 2H, H^2), 1.40 (m, 2H, H^3), 1.27 (m, 16H, H^{4-11}), 0.85 (t, *J* = 6.9 Hz, 3H, H^{12}). **^{13}C {^{1}H} NMR** (126 MHz, CD_3CN) δ/ppm 167.8 (C^{D4}), 160.2 (C^{D2}), 159.2 (C^{A2+E2}), 156.5 (C^{F2}), 156.4 (C^{B2+B6}), 153.9 (C^{D6}), 153.4 (C^{A6}), 153.3 (C^{E6}),

149.3 (C^{F4}), 149.0 (C^{B4}), 138.9 (C^{E4}), 138.7 (C^{A4}), 137.9 (C^{C1+G1}), 131.3 (C^{C4+G4}), 130.6 (C^{C3+G3}), 128.8 (C^{C2+G2}), 128.4 (C^{E5}), 128.3 (C^{A5}), 125.5 (C^{A3}), 125.4 (C^{E3}), 122.8 (C^{B5}), 122.7 (C^{B3}), 122.6 (C^{F3}),114.6 (C^{D5}), 113.0 (C^{D3}), 70.7 (C^{1}), 32.6 (C^{10}), 30.3, 30.2, 30.0 (C^{5-9}), 29.8 (C^{4}), 29.4 (C^{2}), 26.3 (C^{3}), 23.4 (C^{11}), 14.4 (C^{12}). **ESI MS** (MeCN): *m/z* 1049.4 $[M\text{-}PF_6]^+$ (100%, calc. 1049.3). **IR** (solid, ν/cm^{-1}) 2924 (m), 2849 (w), 1996 (w), 1607 (m), 1464 (w), 1419 (m), 1407 (m), 1315 (w), 1222 (w), 1160 (w), 1032 (w), 875 (w), 823 (s), 789 (m), 761 (m), 754 (m), 740 (m), 690 (m), 553 (m), 521 (s). **EA** found: C, 50.41; H, 4.22; N, 7.49%. $C_{54}H_{54}F_{12}N_6O_2P_2Ru\cdot 0.5NH_4PF_6$ requires C, 50.85; H, 4.43; N, 7.14%. **UV/VIS** λ_{max}/nm (0.84 x 10^{-5}mol dm^{-3}, MeCN) 284 ($\varepsilon/dm^3\ mol^{-1}\ cm^{-1}$ 69000), 310 (63000), 490 (25000). **Luminescence** (MeCN, 0.46 x 10^{-5}mol dm^{-3}, λ_{ex} = 490 nm): λ_{em} = 652 nm.

Literature

1 Jameson, D. L.; Guise, L. E. *Tetrahedron Letters,* **1991**, *32 (18)*, 1999-2002.

2 Ishihara, M.; Tsuneya, T.; Shiga, M.; Kawashima, S.; Yamagishi, K.; Yoshida, S.; Sato, H.; Uneyama, K. *J. Agric. Food Chem.,* **1992**, *40*, 1647.

3 Busto, E.; Gotor-Fernández, V.; Gotor, V. *Tetrahedron: Asymmetry*, **2006**, *17*, 1007–1016.

4 Mikel, C.; Potvin, P. G. *Polyhedron,* **2002**, *21*, 49-54.

5 Eryazici, I.; Moorefield, C. N.; Durmus, S.; Newkome, G. R. *J. Org. Chem,.* **2006**, *71*, 1009.

6 Zhao, L.-X.; et all. *Bioorg. Med. Chem. Let.,* **2001**, *11*, 2659-2662.

7 Wetter, W. P.; De Witt Blanton, C. Jr. *J. Med. Chem.,* **1974**, *17*, 620-624.

8 Wang, J.; Hanan, G. S. *Synlett,* **2005**, *8*, 1251-1254.

9 Constable, E. C.; Housecroft, C. E.; Neuburger, M.; Phillips, D.; Raithby, P.R.; Schofield, E.; Tocher, D.A.; Zehnder, M.; Zimmermann, Y. *J. Chem. Soc., Dalton Trans.,* **2000**, 2219-2228.

Curriculum Vitae

Ing. Markéta Šmídková
Date of birth: 30th June, 1984. Sex: female. Nationality: Czech.
Permanent Home Address: Olbramovice 153, 259 01 Votice, Czech Republic
Swiss Home Address: Lothringerstr. 167, 4056 Basel, Switzerland
Tel: +420 608 317 999, +41 78 631 9652, email: marketa.smidkova@gmail.com

Education:

Sep 2009 – Sep 2013

PhD in inorganic and coordination chemistry, University of Basel, Switzerland
Supervisor: Prof. Edwin C. Constable, Prof. Catherine E. Housecroft
Ruthenium(II) complexes of amino-substituted polypyridine ligands: Synthesis and photophysical studies with a potential application for molecular switches

Sep 2007 – Jun 2009

MSc in organic chemistry, Institute of Chemical Technology Prague, Czech Republic
Supervisor: Prof. Dalimil Dvorak
Preparation of 6-halo- and 2,6-dihalo-7,8-dihydropurines and their reactivity in palladium catalysed Reactions, compounds with a potential biological activity

Sep 2003 – Jun 2007

BSc in organic chemistry, Institute of Chemical Technology Prague, Czech Republic
Supervisor: Prof. Dalimil Dvorak
Preparation and study of the reactivity of 9-substituted 2-chloro-6-(α-hydroxybenzyl)purines, compounds with a potential biological activity

Sep 1999 – Jun 2003

Grammar School in Sedlčany, Czech Republic

Professional experience and skills:

- Ten years of practical synthetic experience in organic, inorganic, organometallic and coordination chemistry, combinatorial chemistry, synthesis in small and large scales, strong experience in chromatography separation and purification methods, handling light, temperature and air sensitive materials (Schlenk line technique), microwave assisted reactions (Biotage)
- Measurement and data processing of: 1D and 2D NMR experiments, IR, electrochemistry (CV, DPV), UV/VIS and Fluorescence spectroscopy, LC-MS
- Computer skills: MS Office Word, Excel, PowerPoint; ChemBioDraw, OriginPro, MestReNova, Databases in chemistry: SciFinder, Reaxys
- Five semesters supervising of students in General and Inorganic chemistry practicum
- Regular oral and poster research presentations, weekly research reports
- Experiences in both working on self-dependent and team projects
- Years of working on multicultural environment

Sep 2009 – Present

University of Basel, Switzerland, PhD researcher in inorganic and coordination chemistry research group of Prof. Edwin C. Constable and Prof. Catherine E. Housecroft, mainly specialized in materials for OLED, LEC, DSSC.

Synthesis, photophysical and electrochemical studies of ruthenium(II) complexes with potential applications as molecular switches and dye-sensitized solar cells

International project collaboration and visiting researcher in the photochemistry laboratories of Prof. Alberto Credi, University of Bologna, Italy

Five semesters as an assistant and supervisor of BSc and MSc students at General chemistry practicum and at Inorganic and coordination chemistry practicum

Feb 2004 – Aug 2009

Institute of Chemical Technology Prague, Czech Republic

Member of organometallic research group of Prof. Dalimil Dvorak. Preparation and reactivity of purines and 7,8-didyhopurines in palladium catalysed reactions, compounds with a potential biological activity

Took part in the Student research activities competition at ICT Prague (SVK): 5th place award (November 2008) and 2nd place award and received an extra studentship from Zentiva company for a topic specialized in pharmaceuticals (November 2007)

June 2008 – July 2008

RE&D VÚFB Drug Research and Discovery Company (now Apigenex), Czech Republic

Practical training experience with a research project in combinatorial chemistry

Chemical Society Membership:

Since May 2012:	Member of the Royal Society of Chemistry
Since January 2010:	Member of the Swiss Chemical Society
Since November 2008:	Member of the Czech Chemical Society

Languages:

Native Language:	Czech
Other Languages:	English - fluent, working verbal and written level
	German – advanced, communication and written level
	Spanish, Russian and Slovak: basic-level

Conferences:

9th-13th September 2012

ICCC40 – Valencia, Spain, 40th International Conference on Coordination Chemistry.

Presented poster: Molecular computing, New ligand and Complex Paradigm for Molecular Switches

18th-22nd June 2012

RSC Dalton Division Summer School, State of the Art Instrumental and Electronic Structural methods in Inorganic Chemistry, University of Edinburgh, Scotland.

Took part in a week-long workshop and presented a poster entitled: Molecular computing, New ligand and Complex Paradigm for Molecular Switches

9th September 2011

SCS Fall meeting in the fields of Inorganic and Coordination Chemistry, EPFL Lausanne, Switzerland.

Presented poster: Molecular computing

14^{th}-20^{th} June 2011

International Krutyn Summer School 2011, Poland, „Frontiers in Organic, Dye-sensitised and Hybrid Solar Cells“

Presented poster: New ligand paradigm for Dye-sensitized solar cells

16^{th} September 2010

SCS Fall meeting in the fields of Inorganic and Coordination Chemistry, ETH Zürich, Switzerland.

Presented poster: Molecular computing

14^{th}-16^{th} November 2008

43^{rd} Conference on Organic, Bioorganic and Pharmaceutical Chemistry held by Czech Chemical Society, Nymburk, Czech Republic, Received 3^{rd} place award in poster section

Publications:

Acidity of Benzoic Acids Bearing the $(CO)_5Cr{:}CN(CH_3)_2$ Group

Parik, P.; Kulhanek, J.; Ludwig, M.; Wagner, R.; Rotrekl, I.; Drahonovsky, D.; Meca, L.; Smidkova, M.; Tobrman, T.; Dvorak, D. *Organometallics*, **2010**, *29*(18), 4135-4138.

Driving licence: B

References:

It is possible to get references from:

Prof. Dr. Edwin Constable (University of Basel, Switzerland)
e-mail: Edwin.Constable@unibas.ch

Prof. Dr. Catherine Housecroft (University of Basel, Switzerland)
e-mail: Catherine.Housecroft@unibas.ch

Prof. Alberto Credi (Universirty of Bologna, Italy)
e-mail: alberto.credi@unibo.it

Prof. Ing. Dalimil Dvorak, CSc. (Institute of Chemical Technology, Prague, Czech Rep.)
e-mail: Dalimil.Dvorak@vscht.cz

Ing. Miroslav Havranek, Ph.D. (Apigenex, formerly RE&D VÚFB Drug Research and Discovery Company, Prague, Czech Rep.)
e-mail: havranek@apigenex.cz